MATTIA STUCCHI / R10073

Multicomponent approaches to the synthesis of small bioactive molecules

CHIM/06 Organic Chemistry
Doctorate Course in Industrial Chemistry
XXVIII Cycle - A.Y. 2014/2015

Tutor: Dr. Alessandra SILVANI
Co-Tutor: Prof. Dr. Giordano LESMA
Coordinator: Prof. Dr. Dominique ROBERTO

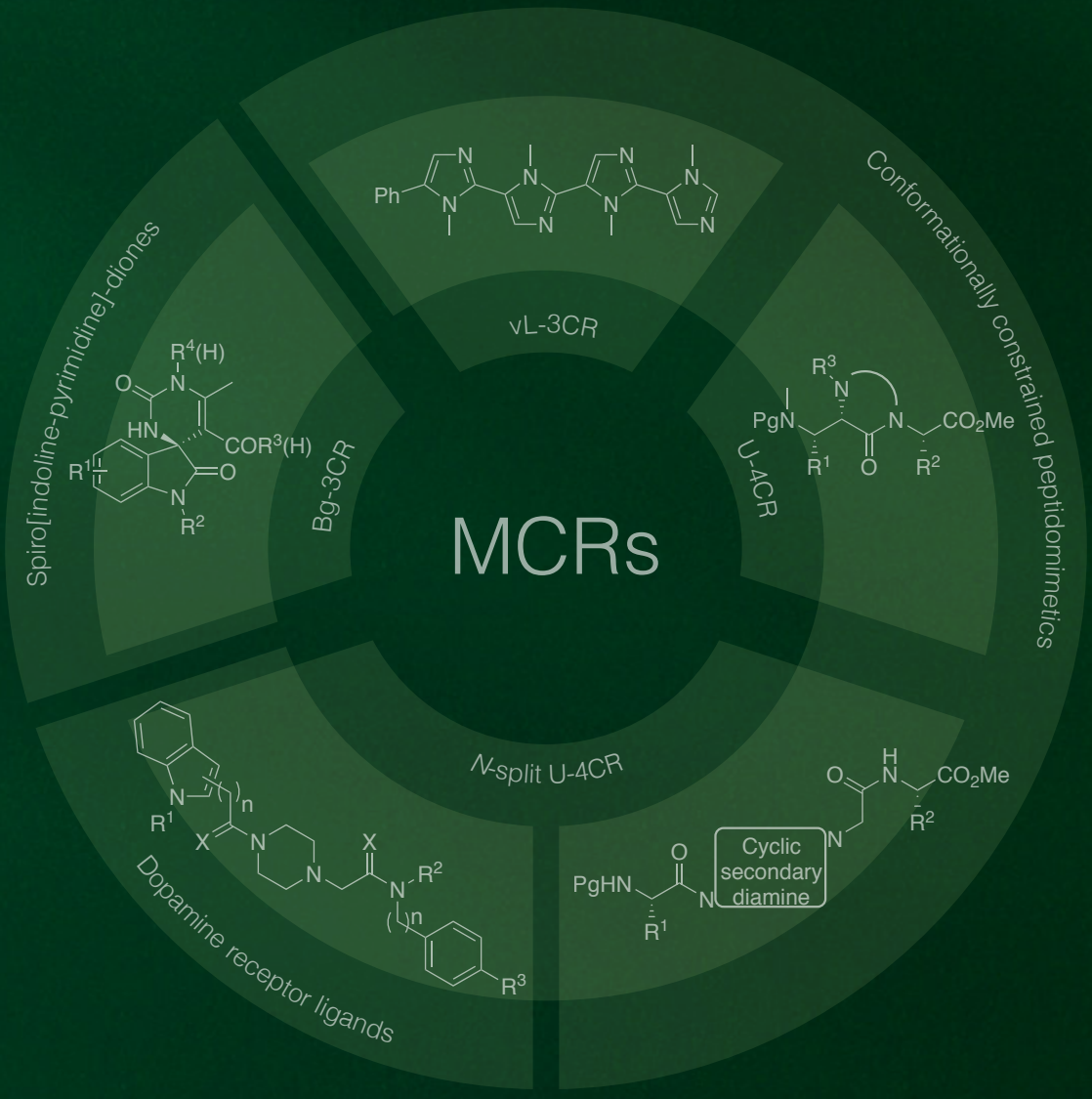

UNIVERSITÀ DEGLI STUDI DI MILANO
DIPARTIMENTO DI CHIMICA

MATTIA STUCCHI / R10073

Multicomponent approaches to the synthesis of small bioactive molecules

CHIM/06 Organic Chemistry
Doctorate Course in Industrial Chemistry
XXVIII Cycle - A.Y. 2014/2015

Tutor: Dr. Alessandra SILVANI
Co-Tutor: Prof. Dr. Giordano LESMA
Coordinator: Prof. Dr. Dominique ROBERTO

UNIVERSITÀ DEGLI STUDI DI MILANO
DIPARTIMENTO DI CHIMICA

Acknowledgements

Il primo e doveroso ringraziamento va sicuramente alla mia famiglia: senza il supporto dei miei genitori, Giovanna e Guido, per tutta la durata del mio percorso accademico, non avrei nemmeno potuto conseguire un titolo di dottorato. Una considerazione particolare spetta a mia sorella, Giulia, che con la sua allegria ha sempre reso le mie giornate meno monotone. Spero, inoltre, che il corso di studi scientifico che ha scelto le porti grandi soddisfazioni, come è stato per me con la chimica. Vorrei inoltre ringraziare enormemente la mia ragazza, Lucia, che mi ha accompagnato e mi è stata vicina per tutta la durata del mio dottorato, curando anche l'impostazione grafica di questa tesi.

Per quanto riguarda il contenuto scientifico, un grosso riconoscimento va a tutti coloro che hanno lavorato con me: i tesisti, tirocinanti e dottorandi, che hanno contribuito alla parte di sintesi, e i collaboratori citati lungo la tesi. Infine, nulla di tutto ciò che è presente in questa tesi sarebbe stato scritto senza il sostanziale aiuto della Dr.ssa Alessandra Silvani e del Prof. Giordano Lesma, che mi hanno permesso di lavorare per tre anni nel loro gruppo di ricerca e conseguire un titolo di dottorato, seguendomi e insegnandomi con passione, incentivandomi a seguire ogni mia idea e facendomi crescere come chimico, pur rimanendo un costante punto di riferimento professionale.

TABLE OF CONTENTS

Preface

Most of the drugs discovered in the last decades were small molecules, including those targeting novel biological targets. Although in recent years the number of biological drugs (e.g. antibodies, enzymes and fusion proteins) has been steadily increasing, small molecules remain an attractive research area, as outlined by the countless reports continuously published. Currently, only a small portion of the possible molecular scaffolds have been investigated, and expanding the number of potentially accessible small molecules is of great importance, with consequences in the potential treatment of "undruggable" diseases. Therefore, synthetic organic chemists hold major responsibility, and continuing efforts in the development of more efficient processes for obtaining improved small-molecule drugs are needed.

Although multicomponent reactions have been recognized by the synthetic community in industry and academia as a preferred method to design and discover new lead compounds, their limited scaffold-diversity and stereoselectivity remain as major drawbacks, limiting their widespread application. Recently, a renovated interest in this field greatly expanded the chemical space potentially accessible, leading to improved industrial processes and better drugs candidates.

In this context, I pursued the synthesis of libraries of small bioactive molecules, exploiting different multicomponent approaches. In most of them, the employment of chiral components or, alternatively, organocatalysis allowed me to address the hot issue of asymmetry.

INTRODUCTION

1. MULTICOMPONENT REACTIONS

Multicomponent reactions (MCRs) are usually defined as chemical transformations in which three or more components combine together to form a product in which most of the atoms are present. Strecker reported the first multicomponent reaction in 1850,[1] describing the synthesis of racemic α-amino cyanides, by means of a one-pot condensation between an aldehyde, ammonium chloride and potassium cyanide. Since then many MCRs were developed, finding applications in many relevant areas, such as natural product synthesis, polymer and agro chemistry, combinatorial chemistry and drug discovery programs. The broad applicability and success of MCRs arise from their atom economy,[2] convergent character, operational simplicity, and the structural diversity and complexity of the resulting molecules, which are intrinsic characteristics of this type of chemistry. The advantages of MCRs can be summarized as follows: (1) MCRs are one-pot reactions; if a structurally elaborated compound can be synthesized in one (or a few) step(s) this is advantageous in terms of effort, cost, and time. (2) MCR products are assembled by three or more starting materials; therefore, the complexity of the resulting products is higher than in a typical two-component process. (3) MCRs typically rely on a set of starting materials which are commercially available; the consequence is that a very large chemical space can be accessed.

Although there is still a lack in awareness, MCRs are indeed able to address industrial chemical problems in an eco-friendly matter, matching most of the principles of *green chemistry*[3] (**Figure 1**) and therefore especially suited for process design.

Figure 1. Principles of *green chemistry* (fig. from ref 4, pg. 2659).

One of the major ecologic and monetary problem during the design of a chemical process is for sure the amount of wastes generated. MCRs are able to overcome this problem by nature, being able to obtain the desired product in highly convergent and resource efficient way, reducing the synthetic and purification steps, with the beneficial effect of shortening the whole process. By looking at the single reaction, MCRs are usually high-yielding transformations, with excellent chemo- and regioselectivity, in which near stoichiometric amounts of reactants are used without any additives. Therefore, unreacted starting materials and by-products are usually present in small amounts, with the addition benefit of being simple molecules with low molecular weight, like amines, alcohols, water or common salts.

In almost any industrial process, the treatment of the solvents waste is one of the most costly entry in the business plan. In addition, they are usually burnt, with the side effect of increasing the *greenhouse effect*. The combined effect of few synthetic steps and the easy purification of simple by-products allows MCR-based processes to be usually less solvent consuming, compared to "classical" synthesis. In the recent past, the development of multiple one-pot processes was acknowledged as a viable green solution. For example, the improved industrial process for the synthesis of anticonvulsant drug candidate LY300164[5] and Pfizer's Zoloft®,[6] developed by Eli Lilly, received the prestigious US Presidential Green Chemistry Challenge Awards.

Barry Trost introduced the concept of atom economy (AE) in 1991, defining it as the amount of reactants present in the product,[7] and later was appointed as second among the principles of *green chemistry* (**Figure 1**). In this context, MCRs possess near no rivals, having almost a perfect atom economy. As an example, the Passerini three-component reaction (P-3CR)[8] scores an astonishing 100% of atom economy, with all the atoms of the reactants present in the final product.

Although atom economy is an important parameter, the reaction safety and the hazards associated with the chemicals are of primary importance during the development of a process. MCRs usually employ simple and not particularly hazardous reactants, and the air sensitivity is not usually an issue. Isocyanides are worth of a special digression, being the key component of a widely used class of MCRs, namely isocyanide-based multicomponent reactions (IMCRs). They are volatile compounds with a tedious smell, especially the low molecular weight ones, and their believed toxicity is usually associated to cyanides and nitriles. However, the most comprehensive investigation on the isocyanides safety, performed almost fifty years ago at Bayern AG, did not conclude a general toxicity for this class of compounds.[9] Indeed, isocyanides show toxicity comparable to that of other commonly used chemicals, and they can be stored, transported and handled with no particular precautions.

Another important aspect in the design of a chemical process is the energy efficiency, especially in large batch preparations. Although is difficult to make a general statement in such a heterogeneous class of reactions, MCRs usually proceed under mild conditions, without the need of high temperatures or pressures. This is because MCRs are sequences of elementary equilibrium steps, pushed towards the product side by a

thermodynamic driving force, usually in the later steps. Consequently, there is no need for harsh conditions or sophisticated equipment for heat transfer, thus lowering the process energy consumption.

The high chemoselectivity and functional groups tolerability of MCRs allow the formation of different chemical bonds in high purity and with fewer by-products. Protecting groups are usually used only to conceal the reactivity of portions of the molecules, triggered later for further transformations, like in the Ugi-deprotection-cyclization approach (UDC).[10]

Whenever is possible, the use of a catalytic version of the process is always preferred, because it allows to enhance the reactivity and to control the stereoselectivity, thus reducing wastes and by-products. Different catalytic MCRs examples are present in the literature, and special considerations will be given in **Chapter 1.4**.

Although the importance of the *green chemistry* principles is widely recognized, during the last few years the concept of "ideal synthesis" was proposed and explored by important names in the synthetic organic field.[11] An "ideal synthesis" could be defined as a process in which the desired product is obtained starting from readily available reactants, in a limited number of steps and in good overall yields. As the reader could note, this is more or less the dream goal of every industrial process, and the key concepts present in **Figure 2** are what every organic chemist hopes to achieve during the design of a new synthesis. Although MCRs possess some drawbacks, their characteristics make them suitable candidates for key transformations in "ideal synthesis" processes. They are by definition one-pot processes, in which multiple bonds are formed without isolating the intermediates, changing reaction conditions or adding further reagents, making them operationally simple. As explained above, they are atom economical and steps efficient transformations, saving time and energy with a high convergence character. Starting materials are usually readily available and they can be considered safe and environmentally friendly (see above). Although not always high-yielding, they proceed with high conversion and with the formation of limited amount of by-products.

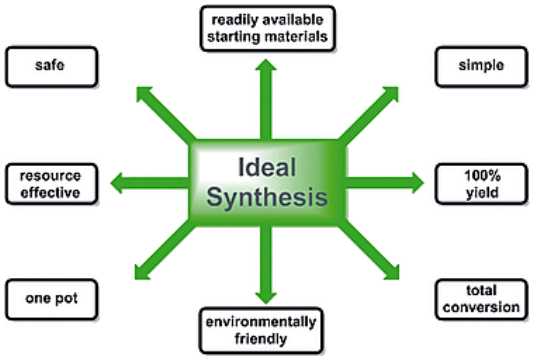

Figure 2. The "ideal synthesis" principles (fig. from ref 12, pg 666).

All the above-mentioned features of MCRs make them preferable to linear synthesis in industrial applications. In the recent literature, two examples clearly underline the potential of MCRs: Dömling's synthesis[13] of *Praziquantel* (PZQ) and Ruijter's synthesis[14] of *Telaprevir*.

Praziquantel is an anti-schistosomiasis generic drug present in the WHO list of essential medicines,[15] being one of the most important medications needed in a basic health system. The largest worldwide suppliers of PZQ employ a linear five-steps synthesis, with amide-bonding formation and the key intramolecular *N*-acyliminium Pictet-Spengler cyclization (**Scheme 1**). Although this process is robust and high-yielding, in 2010 Dömling and co-workers reported a multicomponent approach based on only two steps, an Ugi four-component reaction (U-4CR) followed by the same Pictet-Spengler cyclization (**Scheme 1**). Considering the high atom economy of the two stages, the operational simplicity and facile isolation of the products, the multicomponent approach is clearly superior, and is under development for scale-up for manufacturing PZQ on an industrial level.

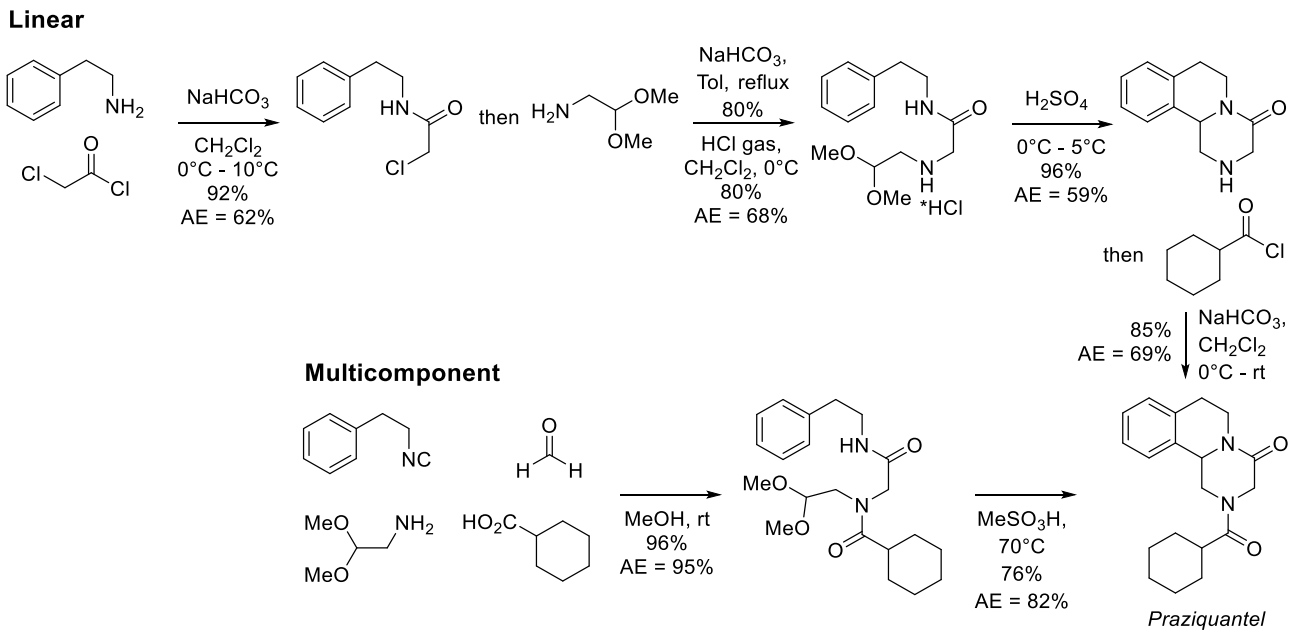

Scheme 1. Linear *vs.* multicomponent synthesis of *Praziquantel*.[13]

In the same year, Ruijter and co-workers[14] reported an improved synthesis for *Telaprevir*, the active pharmaceutical ingredient (API) sell by Vertex under the name of *Incivek*®, approved in 2013 by FDA for the treatment of hepatitis C (**Scheme 2**). Although the patent will expire in 2022, there is a huge interest in the generic market for this drug and many companies are making huge efforts for the development of efficient not-patented routes for its synthesis. Looking at the structure (**Scheme 2**), the molecule is composed by four different chiral non-racemic amino acidic residues, and the originator describes the synthesis using classical amide-formation chemistry with a final oxidation step using Dess-Martin periodinane (DMP). In the Ruijter's

synthesis the product is isolated in higher global yields and less synthetic and purification steps, thanks to two key multicomponent steps, a diastereoselective Ugi-type 3CR and a Passerini three-component reaction (P-3CR) (**Scheme 2**). In collaboration with Chemessentia, the reaction scale-up on an industrial level is currently underway.

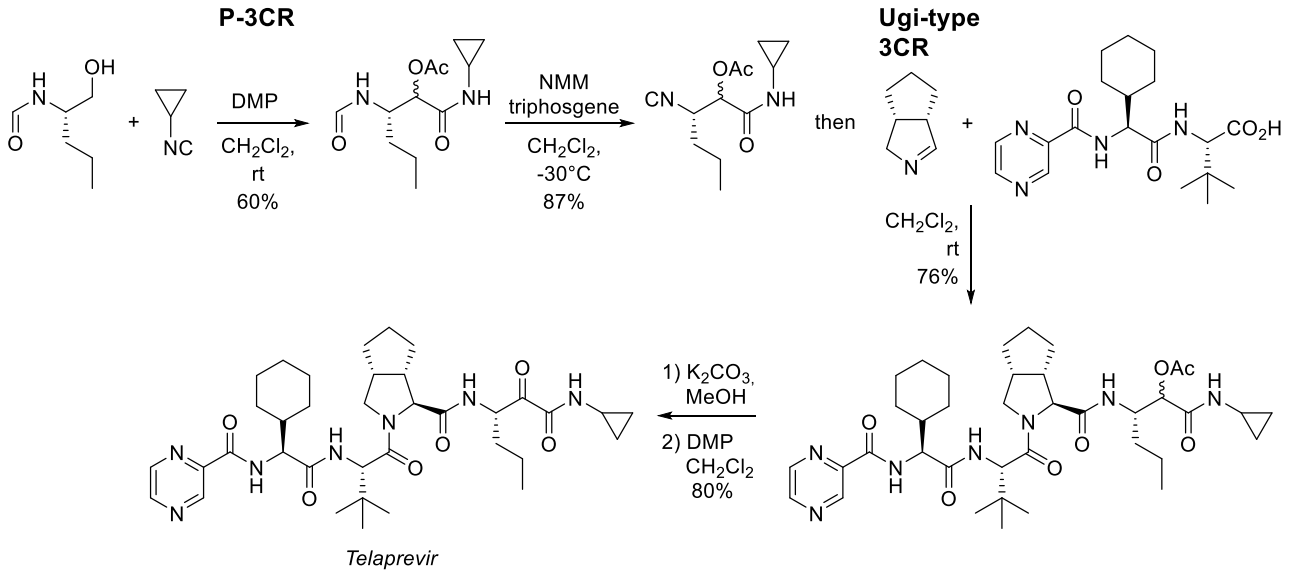

Scheme 2. Ruijter's multicomponent approach to the synthesis of *Telaprevir*.[14]

Although there are quite a few examples of successful industrial processes based on multicomponent approaches, the most important application of MCRs is, undoubtedly, library generation for drug discovery and design.[16]

In particular, MCRs have been used extensively to exploit the full potential of diversity-oriented synthesis (DOS)[17] and biology-oriented synthesis (BIOS),[18] being able to explore virgin areas of biologically relevant chemical space, defined as the 3D representation of molecules with descriptors other than molecular structure.[19] The major problem addressing the synthesis of a library of small molecules is indeed the probability of obtaining the desired biological effect, considering the impossibility to systematically explore such a huge number of molecules, calculated to be in the range from 10^{60} to 10^{200} for small molecules (MW < 500) containing biological recurring atoms (C, H, N, O, S).[20] Although biological active compounds are confined in a small portion of the chemical space ("biological activity space"),[21] there is a need for efficient synthetic tools to obtain high quality libraries able to address "undrugged" non-classical biological targets.[22] In this context, the ability of MCRs to form multiple chemical bonds, generating in a single step complex molecules with high regio- and chemoselectivity, makes them the ideal candidates. The ensemble of possible molecules which can be synthesized by MCRs, usually called "MCR chemical space", differs considerably from other scaffolds and

chemical spaces, as recently demonstrated by studying the topography-biased compound libraries accessible through MCR chemistry.[23]

Although MCRs have been recognized by the synthetic community in industry and academia as a preferred method to design and discover biologically active compounds,[24] they possess two major drawbacks, such as limited scaffold diversity and poor stereocontrol. The latter is a common industrial problem, and in MCRs is addressed in similar ways to other reaction classes, by developing diastereoselective transformations or suitable catalysts for enantioselective versions. On the contrary, the limited scaffold diversity is an intrinsic problem of MCRs, and can be overcome by discovering new MCRs or by combining existing MCRs with complexity generation reactions. Although serendipity has always played a key role in discovering new MCRs, lately the rationale design approach allowed to unearth new molecular scaffolds, especially heterocycles, with interesting biological activities (**Scheme 3**).

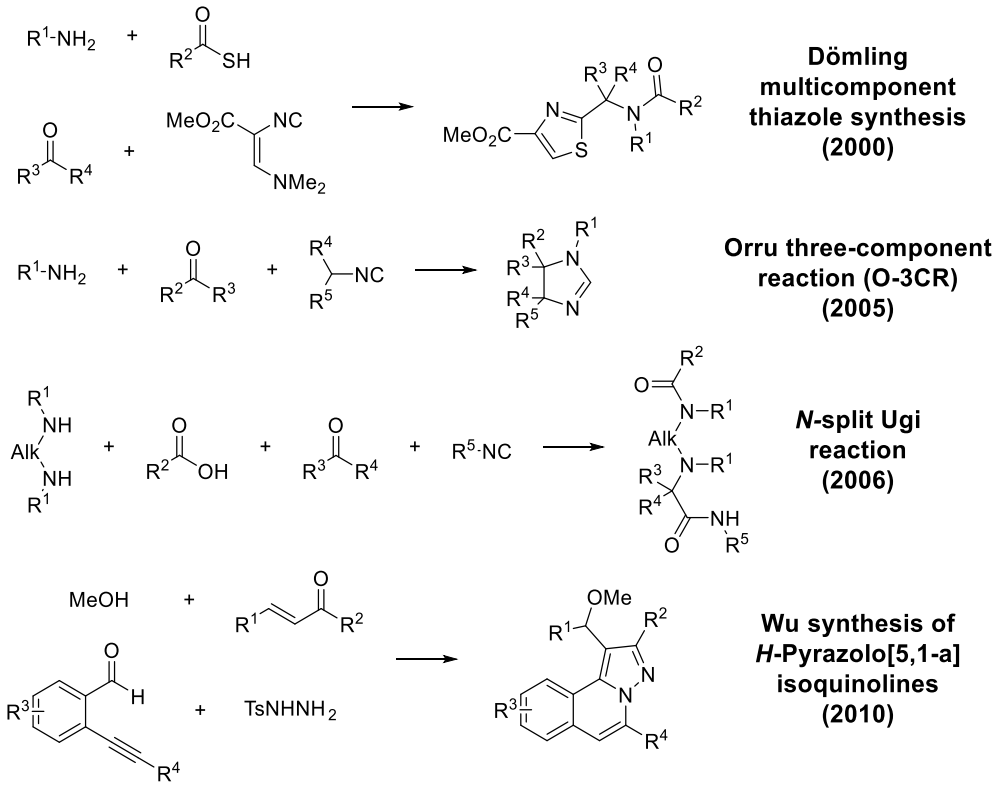

Scheme 3. Recent example of successful design of multicomponent reactions for the synthesis of small bioactive molecules.[25]

Combining MCRs with complexity generating reactions has proved to be a robust and effective methodology to overcome the limited scaffolds accessible through MCRs, with countless examples in the literature. In 2008, Schreibner and co-workers rationalize this synthetic approach giving the name build/couple/pair (B/D/P) strategy.[26] In this three-stage strategy, the initial asymmetric syntheses of chiral

bifunctional molecules, suitable for subsequent coupling and pairing steps, is identified as "build". Combined with the subsequent "couple" phase, it determines the basis for stereochemical diversity. In the "couple" phase, building blocks are joined by intermolecular coupling reactions, with (ideally) completely control on the stereochemistry. Lastly, the "pair" phase consist of intramolecular reactions able to regio- and chemoselectively join functional groups already present in the molecule, providing the basis for skeletal diversity. MCRs play a key role in this kind of approach, thanks to their high regio- and chemoselectivity and functional group tolerability, being one of the reaction of choice for the "couple" phase, able to generate highly densely functionalized templates. Although the stereochemical control is not always trivial, by strategic choice of functional groups it is possible to allow as many ring-closing modes as possible in the "pair" phase, increasing exponentially the size and quality of the final library (**Figure 3**).

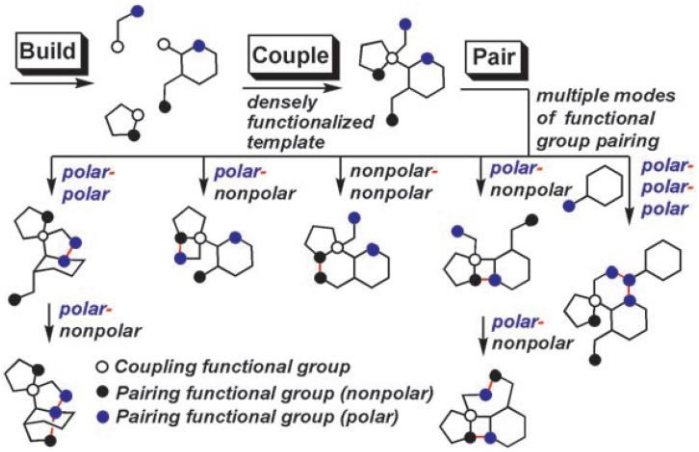

Figure 3. Build/couple/pairing multicomponent strategy for the synthesis of libraries of small bioactive molecules (fig. from ref 26, pg. 51).

In conclusion, MCRs are suitable for industrial application, matching most of the "green chemistry" principles. By applying them to an industrial process, it is possible to achieve an "ideal synthesis" by developing superior strategies for the synthesis of important APIs, like Dömling's synthesis of *Praziquantel* (PZQ) and Ruijter's synthesis of *Telaprevir*. MCRs express their full potential when applied to library generation for drug discovery and design, for both diversity-oriented synthesis (DOS) and biology-oriented synthesis (BIOS), being able to explore virgin areas of biologically relevant chemical space, in few synthetic and purification steps. Their major drawbacks, limited scaffold diversity and poor stereocontrol, can be overcome by developing new MCRs or by combining existing ones with complexity generation reactions, using the so called build/couple/pair strategy.

In the context of MCRs, we developed different multicomponent approaches for the synthesis of libraries of small bioactive molecules, in a stereocontrolled way. In particular, we exploited diastereoselective Ugi four-component reactions (U-4CRs) followed by ring closing reactions (**Chapter 1.1**), to generate a library of ketopiperazine-based *minimalist* peptidomimetics, employing chiral α-amino aldehydes and α-isocyanoacetates derived from natural amino acids (**Chapter 2.1**). By employing a modified U-4CR, namely the *N*-split Ugi reaction (**Chapter 1.2**), we developed an improved methodology for the synthesis of diamine-based peptidomimetics, using chiral reactants in a stereoconservative way (**Chapter 2.2**). We addressed the search for new piperazine-based dopamine receptor ligands, employing the same *N*-split Ugi reaction, conducting structure activity relationship (SAR) studies and rationalizing them with docking studies (**Chapter 3**). A new poly-imidazole β-strand peptidomimetic was smoothly obtained (**Chapter 2.3**), by means of an iterative van Leusen three-component reaction (vL-3CR) (**Chapter 1.3**). By employing 3,3'-disubstituted BINOL-based monophosphoric acids as catalysts, we developed the first organocatalytic enantioselective Biginelli reaction (**Chapter 1.3**) on a ketone, obtaining a library of enantioenriched spiro[indoline-pyrimidine]-diones derivatives with potential biological activities (**Chapter 4**).

1.1 Ugi four-component reaction (U-4CR)

On Christmas Eve in 1957, Cornelius Steinbrücker, a Ph.D. student working in the laboratories of Ivar Ugi, set up the first Ugi four-component reaction (U-4CR). Two years later, in 1959, the first publication on this reaction appeared in a peer-reviewed journal, leading the way for the four-component reaction class.[27] Since then, Ivar Ugi spent his entire life working in this field, reporting several variations of this useful transformation, relying on the mechanism that he proposed more than fifty years ago.[28] He hypothesized the initial formation of imine between the amine and carbonyl moieties, followed by protonation by carboxylic acid to form the highly electrophilic species iminium ion. The subsequent attack by the isocyanide allows the formation of the nitrilium ion, an electrophilic specie which rapidly reacts with the carboxylate to form the imino-anhydride intermediate (**Path A**, **Scheme 4**). The final intramolecular nucleophilic attack of the secondary amine affords the observed product. This last step was called Mumm rearrangement and considered the only thermodynamic driving force, being an irreversible step displacing all the equilibrium by forming an amide bond (**Scheme 4**). More recently, an alternative mechanism was postulated, involving the insertion of the isocyanide in the hemiaminal (**Path B**), allowing the formation of the imino-anhydride intermediate and the subsequent Mumm rearrangement (**Scheme 4**).[29]

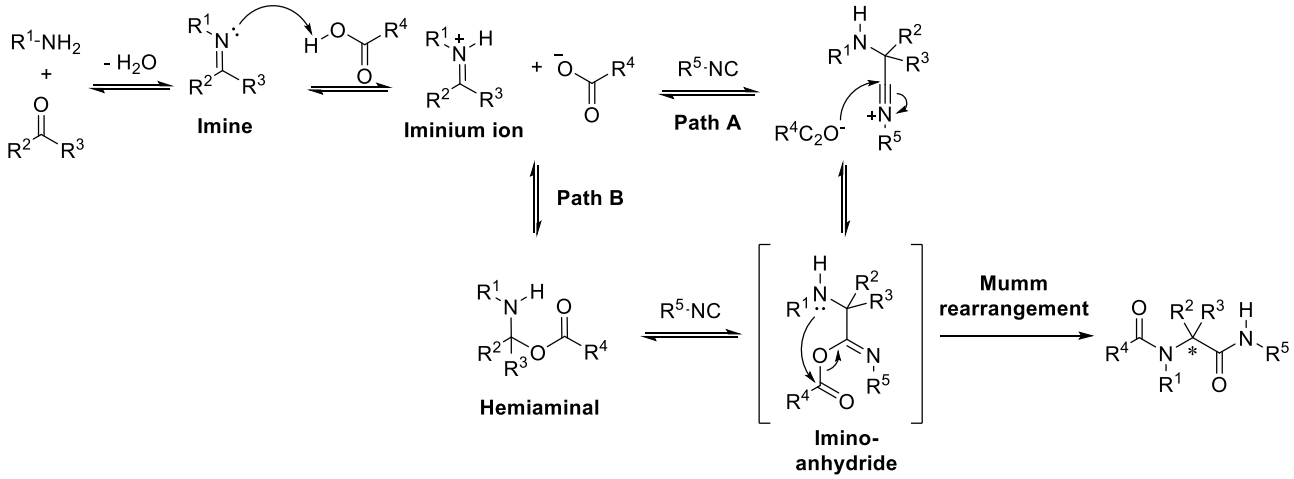

Scheme 4. Possible U-4CR mechanisms.[28]

In 2012, Fleurat-Lessard and coworkers[30] conducted a theoretical study on the U-4CR, with the aim to identify the privileged mechanistic pathway and to suggest alternatives to some commonly accepted assumptions, such as the reversibility of the intermediate steps and the rate determining step (RDS). Moreover, the study was conducted in the presence of two different solvents: a protic one, methanol, and toluene, an aprotic solvent; U-4CR can be performed in high yields in both of them.

Firstly, this study demonstrated that the path proposed by Ugi (**Path A**) is more plausible than **Path B** (**Scheme 4**). Secondly, the authors clarified the activation process of the imine to occur by a proton transfer, although this process is not feasible in aprotic solvents. Therefore, the authors computed mechanisms in both

methanol and toluene, showing that the activation of the imine arises from a hydrogen-bonded complex with the acidic substrate, which explains the reason why the reaction can be performed also in apolar solvents.

Contrary to Ugi's hypothesis, they proposed the formation of the imino-anhydride intermediate as the rate determining step and driving force of the reaction, being an irreversible and exothermic reaction. Indeed, the Mumm rearrangement occurs in different ways, depending on the type of solvent. In methanol, it is assisted by two molecules of solvent reducing the activation energy, thanks to the positive solvating interactions. On the contrary, in toluene a molecule of carboxylic acid assists the Mumm rearrangement, reducing the activation energy by complexing the imino-anhydride intermediate (**Scheme 5**).

The authors concluded that both formation of the imino-anhydride intermediate and the Mumm rearrangement are highly exothermic steps, thermodynamically driving the whole process to the final product in both polar and apolar solvents. Consequently, U-4CR should be no more considered as a sequence of equilibria displaced by a final irreversible step.

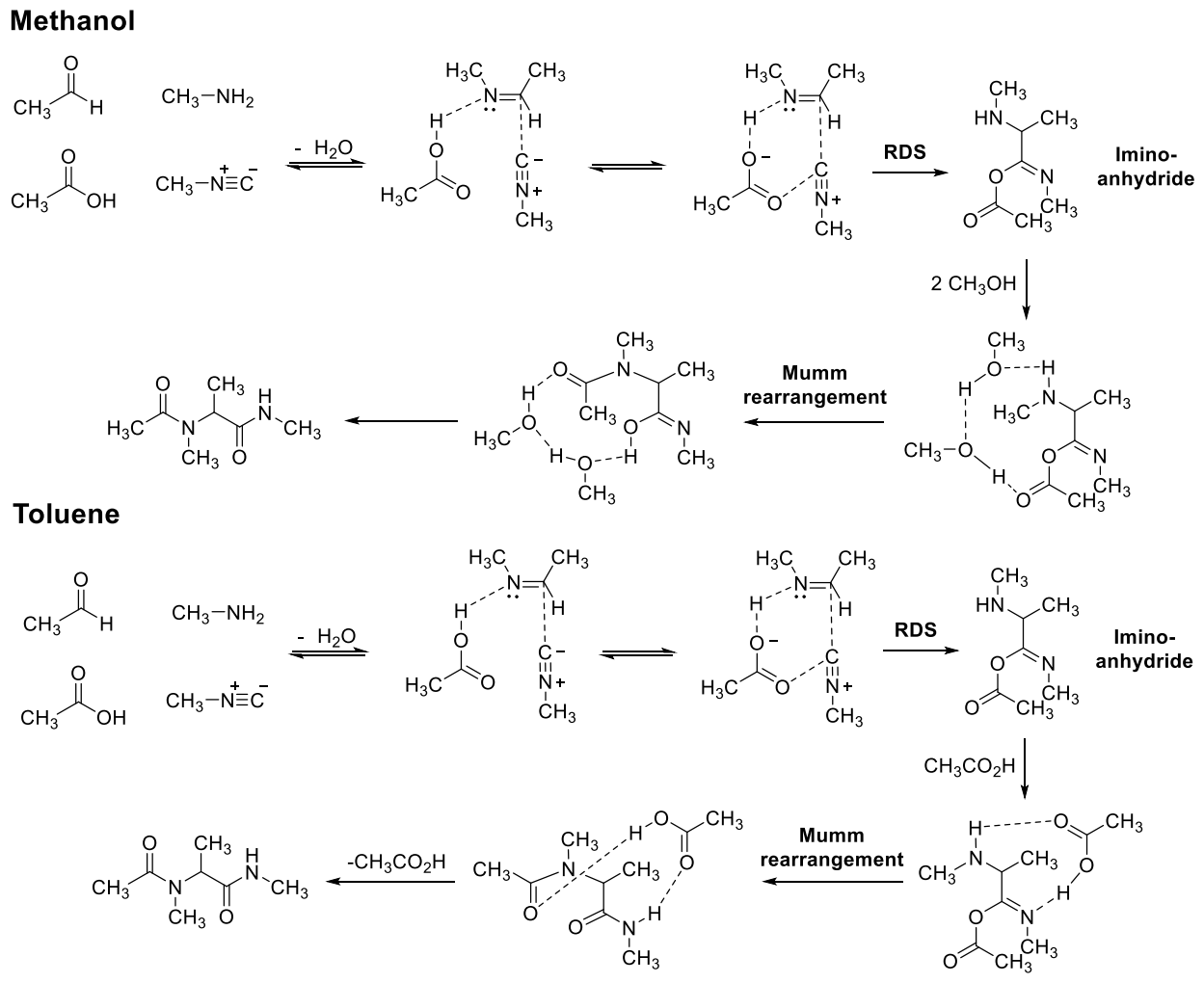

Scheme 5. U-4CR mechanism proposed through computational studies.[30]

Only two years later, Neto and Eberlin[31] proved the theoretical assumptions of Fleurat-Lessard and coworkers (**Scheme 5**) by employing charge-tagged reagents in the U-4CR, and analyzing them with ESI-MS(/MS).

Their aim was to isolate and characterize either the nitrilium ion or the hemiaminal, to support one of the two possible mechanisms (**Scheme 4**). To do that, they developed imidazolium-based carboxylic acid and amine, improving the sensitivity for ESI(+)-MS detection (**Scheme 6**).

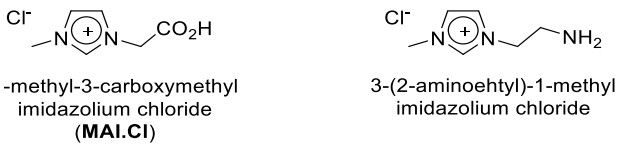

Scheme 6. Imidazolium-tagged reagents.

By reacting MAI.Cl (**Scheme 6**) with benzylamine, formaldehyde and *t*-butyl isocyanide in methanol, they observed the formation of the major ion of *m/z* 343 (**Figure 4**) in the ESI(+)-MS spectrum. The authors attributed the ion to either the imino-anhydride intermediate or the final Ugi-adduct, being unable to separate the possible isomeric mixture by TWIN-MS. The MS/MS fragmentation pattern of the ion of *m/z* 343 is much more coherent with the final Ugi-adduct, indicating therefore a very fast Mumm rearrangement, with no accumulation of the transient imino-anhydride (**Figure 4**).

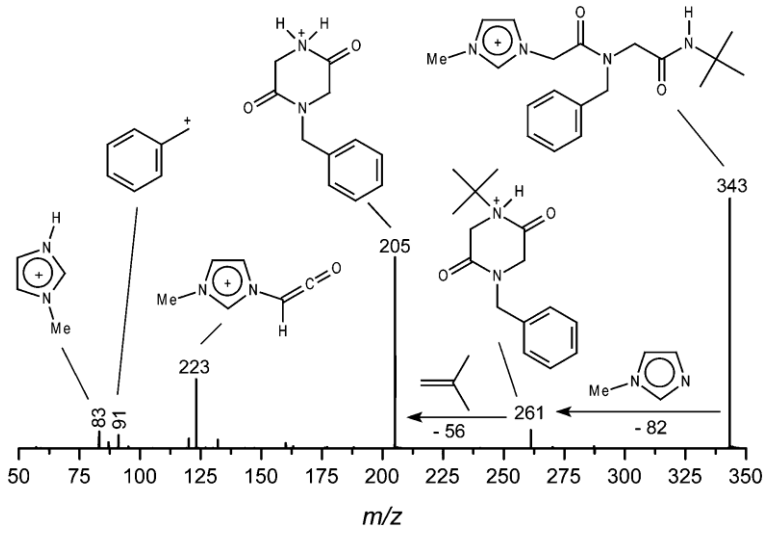

Figure 4. ESI(+)-MS/MS of the ion of m/z 343 (fig. from ref. 31, pg. 339).

However, by using the imidazolium-tagged amine (**Scheme 6**) in a similar reaction setup, the authors were able to detect and unambiguously characterize the ion of *m/z* 221, with an ESI(+)-MS/MS spectrum consistent with the nitrilium ion intermediate (**Figure 5**). In addition, in this case no sign of the hemiaminal intermediate

can be detected, confirming the previously findings and strongly indicating the reaction pathway proceeding *via* **Path A** (**Scheme 4**).

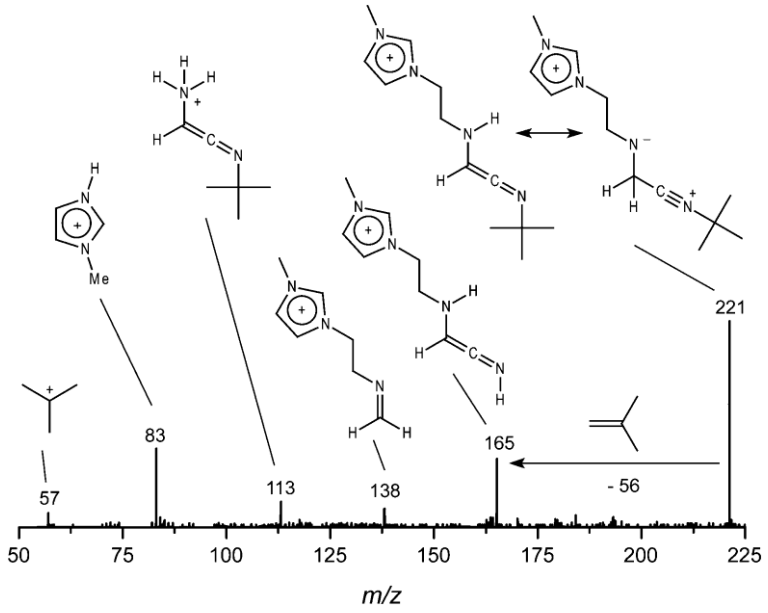

Figure 5. ESI(+)-MS/MS of the ion of *m/z* 221 (fig. from ref. 31, pg. 340).

Finally, the authors performed quantum-mechanical calculations to evaluate the kinetic of the Mumm rearrangement, observing high global activation energies without considering solvent effects, as previously stated by Fleurat-Lessard and coworkers.[30] Simply by including one molecule of methanol the Mumm rearrangement transition state, it becomes energetically favored, with a global activation energy of 7.20 kcal mol^{-1}, allowing the formation of the highly stable Ugi-adduct (**Figure 6**).

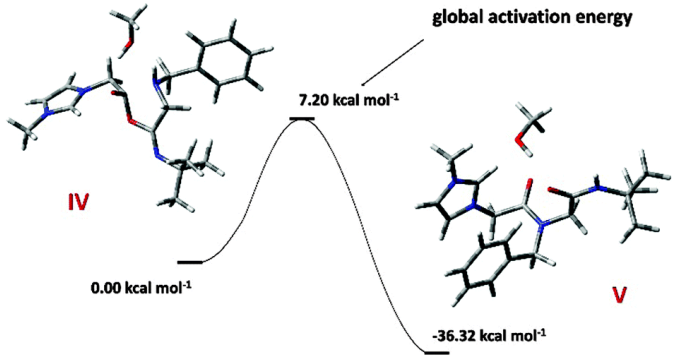

Figure 6. DFT calculation of the Mumm rearrangement with a molecule of methanol (fig. from ref. 31, pg. 342).

Both theoretical and experimental findings strongly suggested a reaction mechanism similar to the one proposed by Ugi (**Path A**, **Scheme 4**), with the initial reversible formation of the iminium ion, which evolves

to the transient imino-anhydride intermediate, followed by a final rapid Mumm rearrangement to form the thermodynamically favoured Ugi-adduct.

These mechanistic considerations are of great importance when trying to perform stereoselective U-4CR, giving the possibility to predict and explain the stereochemical outcome of the newly formed stereocenter. Although an enantioselective classical U-4CR is far from being developed, different high diastereoselective versions have been reported using optically pure components.

For example, by using chiral amines either as substrates or as chiral auxiliaries, high diastereoselectivities are observed. A widely used amine chiral auxiliary is α-methylbenzyl amine,[32] due to the easy removal by means of hydrogenolysis under mild conditions. Among the examples which are present in the literature, in our recent work[33] we were able to synthesize a library of optically active quaternary 3-aminooxindoles, *via* a U-4CR on ketimines, preformed between isatin derivatives and *S*-α-methylbenzyl amine. Good yields and excellent diastereoisomeric excesses were achieved using different carboxylic acids and isocyanides (**Scheme 7.a**), with the preferred *S* configuration for the newly formed stereocenter, as observed by X-ray diffraction. The stereochemical outcome can be explained taking into account the 1,3-allylic strain, which favours the shown conformation, with the delivery of the nucleophile from the less hindered *re* face of the imine double bond (**Scheme 7.b**).

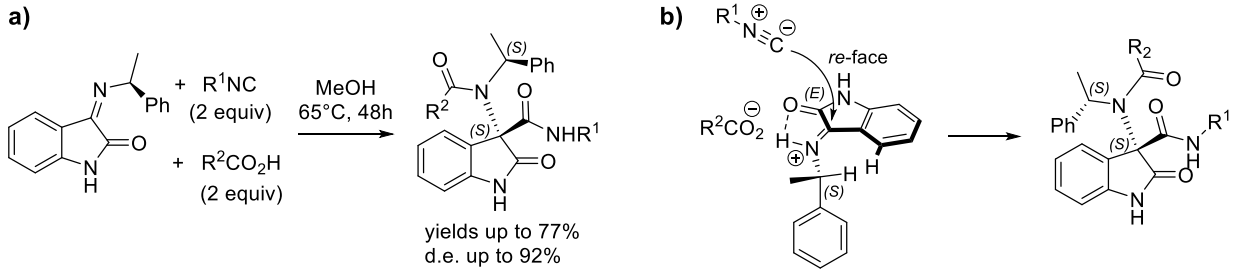

Scheme 7. Example of diastereoselective U-4CR using *S*-α-methylbenzyl amine as chiral auxiliary.[33]

On the contrary, the employment of chiral carbonyl compounds usually give low stereoselectivity. Good to excellent levels of diastereoselectivity are observed only when chiral cyclic imines are used, as in the Ruijter's synthesis of *Telaprevir* (**Scheme 2**).[14] The authors obtained the optically pure cyclic imine through a biocatalytic process, demonstrating the potentiality of biocatalysis combined with MCRs.[32]

Moreover, few examples of U-4CRs employing chiral carboxylic acids are present in the literature, with no significant control of the stereochemistry of the newly formed stereogenic center.[34] In addition, chiral isocyanides usually exert little or no stereocontrol,[35] in contrast with the related P-3CR.[29] The poor diastereoselectivity induced by these two components in the U-4CR is explainable by looking at the reaction mechanism. Indeed, the stereoinduction probably arises from a Felkin-Ahn attack mode, governed by the

stereocenters present on the imine, like in the classical Mannich reactions, with little or no effect of the other two components.

In general, when employing optically pure reactants, their configurational stability in the reaction conditions is a major problem, and the U-4CR makes no exception. Chiral amine and carboxylic acid moieties proved to be configurationally stable, and they are extensively employed without any appreciable loss in optical purity.[32] Unfortunately, this is not true for carbonyl compounds and isocyanides bearing a stereocenter in the α-position.

In his pioneering work,[36] Kelly noticed partial epimerization of α-chiral aldehydes under U-4CR conditions. Although their α-acidity is quite low (pK_a ~ 20) and no loss of optical purity is observed in similar imine-based reactions (e.g. Mannich reaction), Kelly hypothesized the racemization occurring through the imine/enamine equilibrium. By conducting deuterium-exchange experiments, the author demonstrated the hypothesis and observed that the configurational stability of α-chiral aldehydes under U-4CR conditions depends on their α-acidity, with no epimerization for α-oxygenated aldehydes.

A synthetically useful class of chiral α-substituted isocyanides, namely α-isocyanoacetates, deserves a specific dissertation. They are difficult to synthesize as optically pure compounds, and their believed configurational instability under U-4CR conditions has prevented their use for decades, even though interesting peptide-like structures could be in principle obtained, where the α-isocyanoacetates take the place of the *C-terminus*. Therefore, the feasibility of such a peptide coupling strategy strictly depends on the ability to generate enantiomerically pure α-isocyanoacetates, and preserving the stereochemistry under controlled U-4CR conditions. Danishefsky and coworkers solved the first problem, reporting a stereoconservative synthesis starting from optically pure α-amino acid ester hydrochlorides. In this two-step sequence, enantiomerically pure α-isocyanoacetates are smoothly obtained, with the initial formylation of the precursor followed by dehydration of the obtained α-*N*-formylamino acid esters, by means of triphosgene as a mild dehydrating agent and *N*-methyl morpholine at low temperature.[37] On the other hand, the believed, but surmountable, configurational instability under U-4CR conditions was extensively studies by Sello and coworkers.[38] Firstly, they proposed two different hypothetical mechanisms for isocyanoacetate epimerization, *via* enolate formation under basic conditions (α-carbon pK_a = 9-11[39]), or *via* oxazole formation, by means of reversible intramolecular cyclization and aromatization (**Scheme 8**). The authors showed that α-isocyanoacetates epimerization can be suppressed simply by preforming quantitatively the imine (longer time for ketones), prior to the addiction of the carboxylic acid and the optically pure isocyanide.[38]

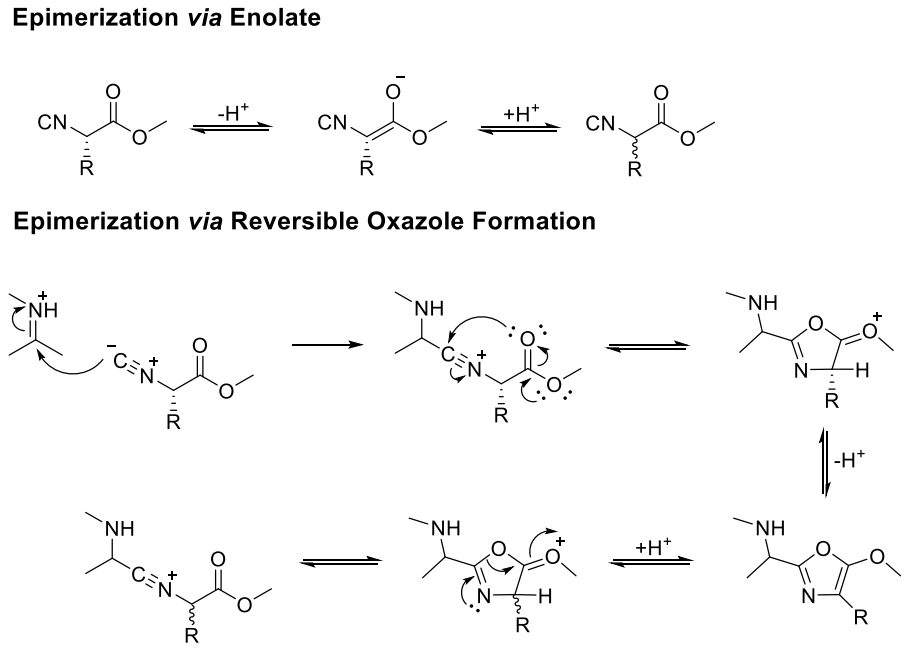

Scheme 8. Hypothetical mechanisms for isocyanoacetates epimerization.[38]

Although the above-mentioned stereochemical issues remain a major drawback, the U-4CR is undoubtedly the most used MCRs for the creation of libraries for drug design and discovery. In particular, U-4CR has found increasing application in the build/couple/pair strategy,[26] expanding the structural variability and exploring unmined regions of the biological active space.[40] The combination of appropriate chiral bifunctional molecules ("build" phase) in a diastereoselective U-4CR ("couple" phase), allows to conduct subsequent complexity-generating transformations ("pair" phase), producing a wide range of scaffolds in a highly more efficient way, with respect to classical linear synthesis (**Scheme 9**).

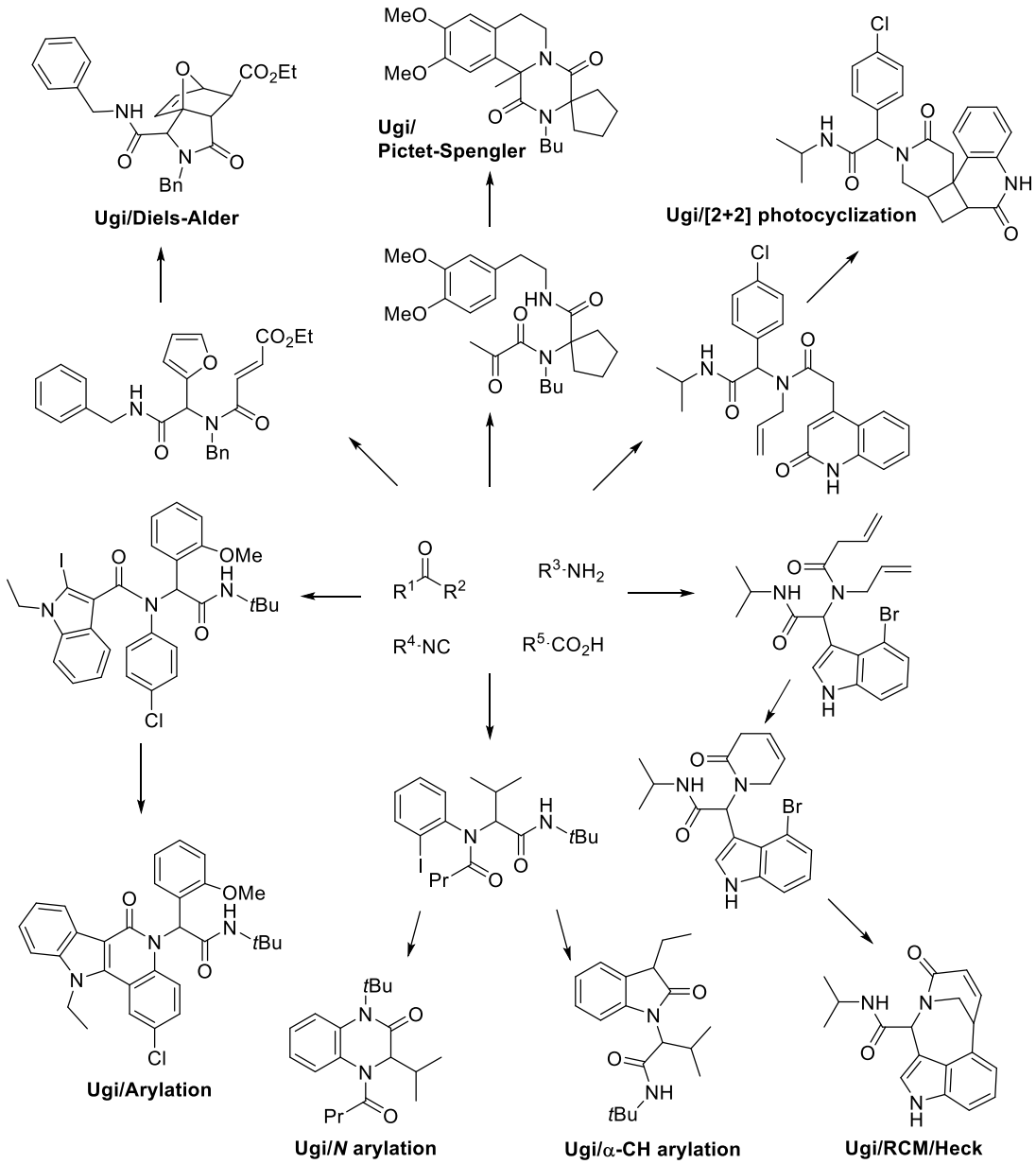

Scheme 9. Examples of build/couple/pair strategy applied to U-4CR.[40]

By exploiting the build/couple/pair strategy, we developed a methodology for the synthesis of a library of ketopiperazine-based *minimalist* peptidomimetics, by means of a diastereoselective U-4CR followed by different cyclization steps. In particular, by employing optically pure α-amino aldehydes and α-isocyanoacetates derived from natural amino acids, in combination with suited amine and carboxylic acid moieties, we were able to obtain the desired Ugi-adducts in good yields and high diastereoisomeric excess, introducing at the same time selected side chains in the final peptidomimetics. The final cyclization step smoothly afforded three different keto-piperazine scaffolds, able to mimic well-defined secondary structures (**Chapter 2.1**).

1.2 *N*-split Ugi reaction (*N*-split U-4CR)

U-4CR is a well-studied and applied MCR, but since its discovery many variations have been reported by simply changing one of the components, trying in this way to expand the structural variability by the so-called *single reactant replacement* (SRR) approach.[41] One of simplest and most obvious modification is the replacement of the primary amine by a secondary one. In this case, following the U-4CR mechanism (**Scheme 4**), the tertiary amine present in the imino-anhydride intermediate can no longer be acylated, preventing the thermodynamic favoured Mumm rearrangement. The first attempt to exploit the potentiality of using a secondary amine in a classical U-4CR was reported by Ugi himself,[42] who observed the formation of an α-aminoamide when methanol is used as solvent. The formation of the α-aminoamide probably arises from the nucleophilic attack of a molecule of methanol on the imino-anhydride intermediate, generating the methyl ester of starting carboxylic acid as secondary product. Despite the dismal atom economy, this reaction is sometimes used as an efficient esterification protocol in challenging substrates.[43]

Similar considerations were done by McFarland,[44] who observed different ratio between α-aminoamide and the P-3CR by-product depending on the equivalents of secondary amine used (**Scheme 10**). McFarland explained these experimental observations by taking into account the nucleophilic attack of a second molecule of secondary amine on the imino-anhydride intermediate, favouring the formation of an α-aminoamide and a tertiary amide.

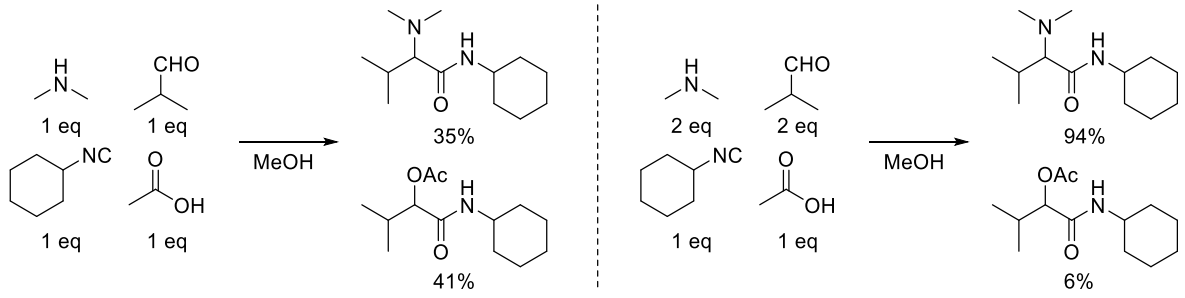

Scheme 10. McFarland's experiments that demonstrated the trapping of the imino-anhydride by the excess of secondary amine.[44]

McFarland's work passed unnoticed until 2006, when more than forty year later Giovenzana and co-workers reported a new isocyanide-based multicomponent reaction (IMCR), namely the *N*-split Ugi reaction (*N*-split U-4CR).[45] Instead of a simple secondary amine, the authors employed a symmetric secondary diamine, obtaining an α-aminoamide and a tertiary amide like in McFarland's experiments, although in this case in a single molecule. From a mechanistic point of view, Giovenzana and co-workers proposed the initial formation of an iminium ion between one of the two secondary amino groups and the carbonyl moiety, which is then

attacked by the isocyanide component, affording the nitrilium ion intermediate. Afterwards, the carboxylic acid reacts giving an imino anhydride intermediate, on which a final "remote" Mumm rearrangement occurs, thanks to the intervention of the remaining secondary amino group. The result is the differentiation of the two nitrogen atoms, achieving in this way the observed regiochemical desymmetrization of the diamine core in only one-step, without the need of protecting groups (**Scheme 11**).

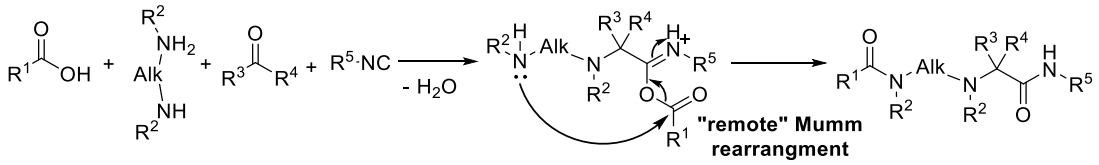

Scheme 11. *N*-split Ugi reaction proposed mechanism.[45]

The reaction proved to be quite general, leading to the desired products in moderate to good yields, employing aliphatic and alicyclic symmetrical secondary diamines as substrates. As stated by the authors, this new IMCR possesses huge synthetic advantages in addition to the intrinsic regiochemical desymmetrization. Indeed, it is possible to generate new molecular scaffolds, for examples cyclic structures, without the need for further reaction steps, like in the build/couple/pair strategy applied to the U-4CR (**Chapter 1.1**). Moreover, by choosing the proper symmetrical secondary diamine, it is possible to build molecular skeletons with different 3D shapes and biological properties. To prove the synthetic potential, the authors reported a high-yielding one-pot process for the synthesis of a known piperazine-based vasodilator (**Scheme 12.a**),[45] usually obtained in four steps starting from piperazine.[46] They also reported an improved methodology to afford polyamines, bioactive molecules with interesting anticancer activity, usually synthesised with many protection/deprotection steps. In particular, by employing the *N*-split Ugi methodology on a dibenzyl protected propyl diamine, followed by the subsequent amide-reduction and hydrogenolysis, different nonsymmetric alkyl polyamines can be obtained in a very straightforward manner (**Scheme 12.b**).[47] Recently, other applications in medicinal chemistry have been reported, like the synthesis of human neutrophil elastase inhibitors (**Scheme 12.c**), and the one-pot functionalization of the chelating agent *N*,*N*-dimethylcyclen (**Scheme 12.d**).[48]

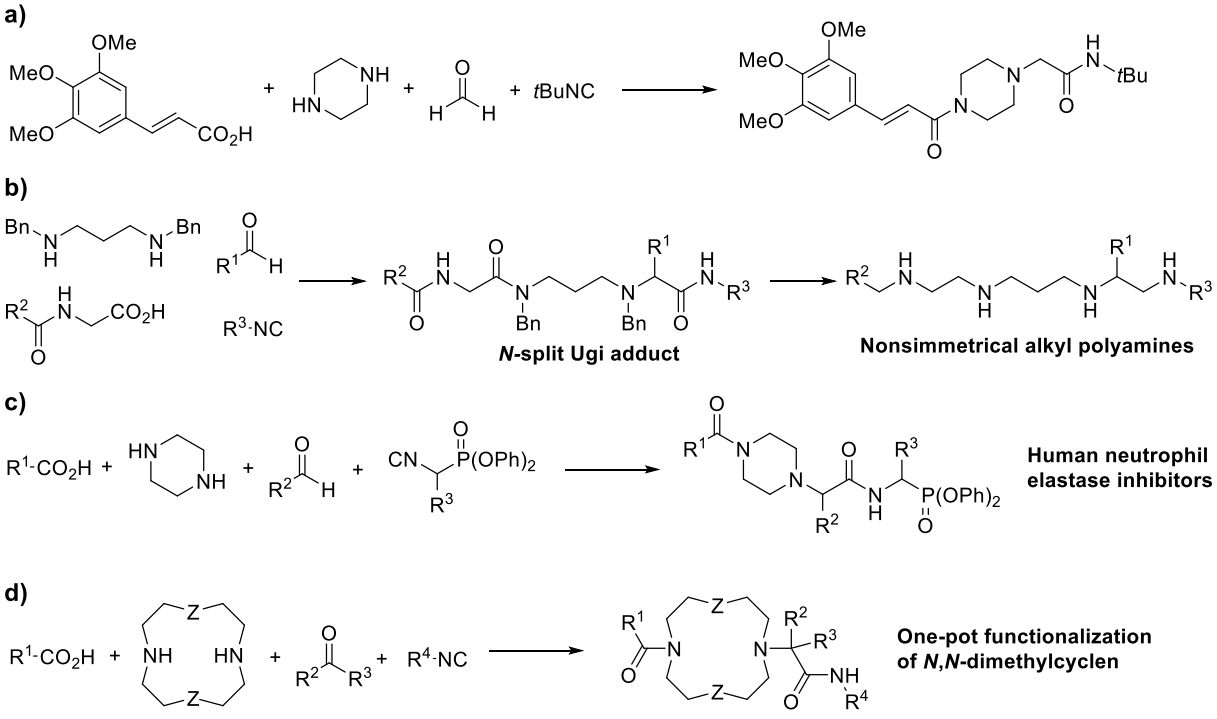

Scheme 12. *N*-split Ugi applications in medicinal chemistry.[49]

At the best of our knowledge, no efforts have been made to employ enantiopure chiral components in the *N*-split Ugi reaction, unlike in the related U-4CR.[50] We believe this a synthetic lack which reduces the applicability of this MCR. Therefore, we developed a synthetic methodology for obtaining diamine-based peptidomimetics in a one-pot process, simply by using *N*-protected natural amino acids and enantiopure α-substituted isocyanoacetates, without the need for protection/deprotection steps and expensive coupling agents (**Chapter 2.2**). We selected piperazine and bispidine (3,7-diazabicyclo[3.3.1]nonane) as substrates, because of the relevant biological activity of the related peptidomimetics, able to modulate specific protein-protein interactions (PPIs).

We also focused our attention on another important class of biological relevant diamine-based compounds, namely 1,4-disubstituted aromatic piperazines (1,4-DAP), mainly studied as dopamine receptors ligands for the potential treatment of Parkinson's disease, dyskinesia, schizophrenia, drug addiction, hyperprolactinemia and restless legs syndrome. Exploiting the potentiality of the *N*-split Ugi reaction, we carried out the synthesis of a library of piperazine-based D_2/D_3 receptors agonists, in few synthetic steps and high overall yields. Structure-activity relationship (SAR) and docking studies allowed us to explain their activity and increase the knowledge about this challenging biological target (**Chapter 3**).

1.3 van Leusen three-component reaction (vL-3CR)

Tosylmethyl isocyanide (TosMIC) is the only commercially available representative of a wide class of odourless, shelf-stable α-acidic isocyanides,[51] introduced and extensively studied by Van Leusen.[52] Its improved synthesis was reported by Van Leusen himself in a two steps process, starting from cheap commercially available reagents, by means of a Mannich condensation followed by classical formamide dehydration (**Scheme 13**). Analogues can be easily obtained, simply by changing sulfinate or aldehyde sources, or by base-induced α-alkylation under phase transfer catalysis (PTC) conditions.[52]

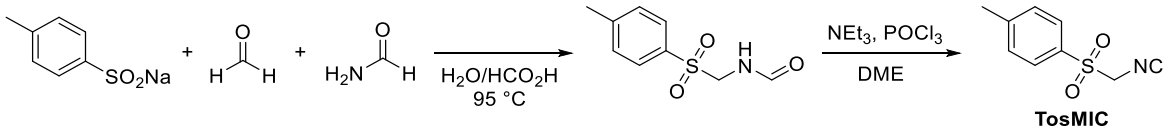

Scheme 13. Improved synthesis of tosylmethyl isocyanide (TosMIC).[52]

Thanks to its high α-acidity and to the moderate leaving nature of the tosyl moiety, TosMIC and derivatives have found increasing use in organic synthesis, establishing one of the most important application of isocyanides in MCRs, after the U-4CR and P-3CR. Possible transformations involving TosMIC are represented in **Scheme 14** and extensively covered in recent reviews and book chapters.[51,52]

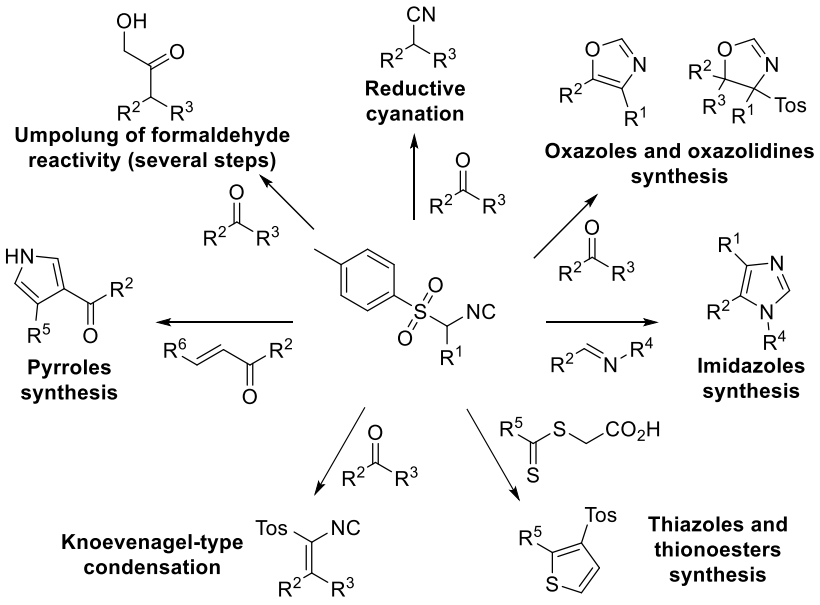

Scheme 14. Examples of transformations involving TosMIC as reagent. [51,52]

Although TosMIC is a multipurpose synthetic reagent, the synthesis of heterocycles is the most important application area, being able to afford different biologically relevant heterocyclic structures.[53] In this field, the major contribute of TosMIC is undoubtedly the synthesis of 1,4,5-trisubstituted imidazoles, otherwise not easily accessible. Van Leusen reported their synthesis for the first time in 1977, by means of base-induced reaction between an aldehyde, a primary amine and TosMIC,[54] nowadays known as the van Leusen three-component reaction (vL-3CR). After several experimental observations, the author proposed different plausible reaction pathways, depending on the base used and substrate reactivity. In particular, variable amounts of α-deprotonated TosMIC anion are present in the reaction mixture depending on the pK_b of the base of choice, and its nucleophilic addition on the imine formed between aldehyde and the primary amine, lead to the intermediate **I**. After a rapid intramolecular cyclization leading to intermediate **IIa** or **b**, a prototropic tautomerism can occur on the more acidic tosyl α-position (**IIIb**) or with the only available proton (**IIIa**), depending on the α-substitution of the starting TosMIC reagent. In the latter case, the intermediate evolves to the final 1,4,5-trisubstituted imidazole (**IVa**) with the loss of a molecule of sulfinate. Differently, intermediate **IIIb** is protonated by the reaction medium, as observed by deuterium-exchange experiments, leading to compound **IVb**. Although sufficiently stable to be isolated, this molecule is usually directly converted to the final product **VIb**, either by *cis* or *trans* elimination from the compound **IVb**, or through intermediate **Vb** (**Scheme 15**).[54]

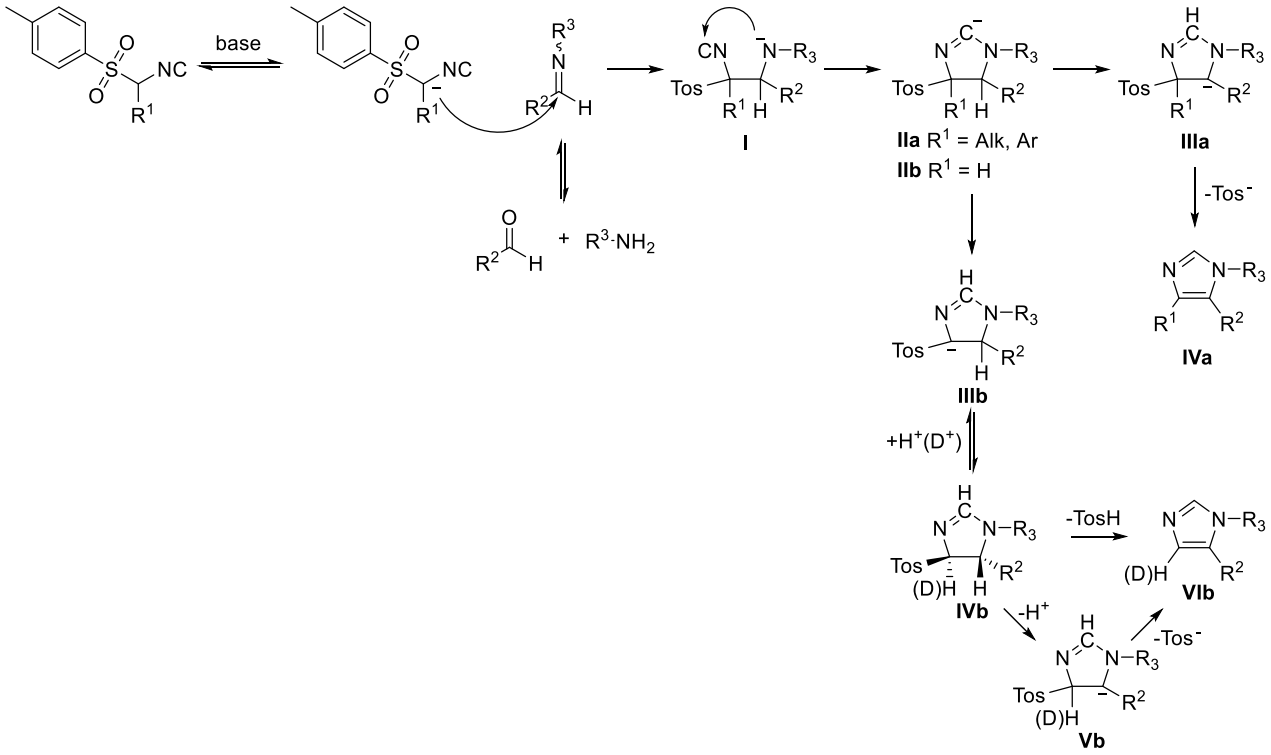

Scheme 15. Proposed mechanisms for the vL-3CR.[54]

This useful chemical transformation has found large application in medicinal chemistry, and recently Dömling and co-workers reported the parallel synthesis of arrays of 1,4,5-trisubstituted 1-(4-piperidyl)-imidazoles as a novel class of aspartyl protease inhibitors.[55] The easily multi grams scale synthesis of α-substituted TosMIC derivatives, combined with the advantages of the multicomponent approach, allowed the author to synthesized a vast library comprising thousands of 1,4,5-imidazoles, with interesting biological activities (**Scheme 16**).

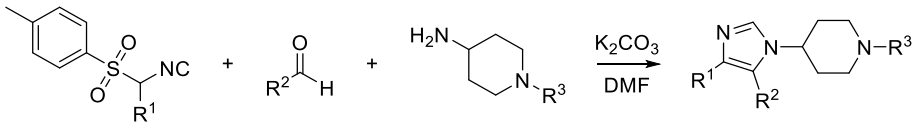

Scheme 16. Application of the vL-3CR for the rapid synthesis of 1,4,5-imidazoles as aspartyl protease inhibitors.[55]

Exploiting the chemistry of tosylmethyl isocyanide (TosMIC), we were able to obtain a β-strand peptidomimetic bearing a C2-C5' linked polyimidazoles scaffold, by means of an iterative vL-3CR. Its ability to mimic the *i*, *i*+1, *i*+2 and *i*+3 amino acid residues of a β-strand motif was assessed through NMR NOE contacts and molecular dynamics simulations (**Chapter 2.3**).

1.4 Biginelli three-component reaction (Bg-3CR)

The Biginelli three-component reaction (Bg-3CR),[56] discovered by the Italian chemist Pietro Biginelli in 1893, consists of the acid-catalysed condensation between an aldehyde, (thio)urea and a β-dicarbonyl compound to obtain 3,4-dihydropyrimidin-2(1*H*)-ones (DHPMs) as major products. Since its discovery, different possible reaction mechanisms have been proposed, involving various protonated intermediates (**Scheme 17**). The first and widely accepted one is the so called iminium route,[57] in which the initial condensation product between aldehyde and (thio)urea, activated either by protonation (acidic conditions) or hydrogen bonding, is attacked by the enol form of the β-dicarbonyl compound. Subsequently, intramolecular cyclization and elimination of a molecule of water affords the desired DHPM (**Scheme 17.a**). An alternative mechanism, proposed in the early 1930',[58] suggests the reaction proceeding through the formation of the enamine between (thio)urea and the β-dicarbonyl compound, which rapidly reacts with the aldehyde moiety. Finally, an intramolecular cyclization followed by dehydration afford the Biginelli-adduct (**Scheme 17.b**). The third proposed mechanism relies on a Knoevenagel type reaction, followed by a Michael-type 1,4-nucleophilic addition of the (thio)urea, affording the desired DHMP after the intramolecular cyclization/dehydration step (**Scheme 17.c**).

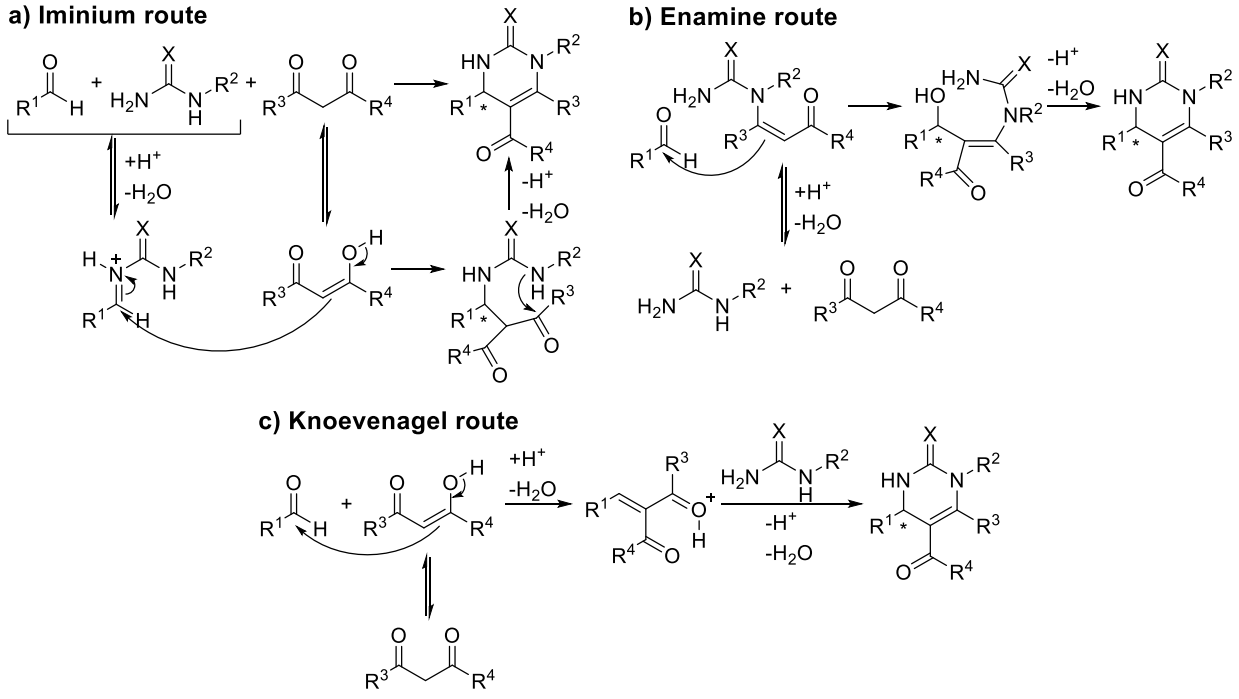

Scheme 17. Plausible Biginelli three-component reaction mechanisms.

Trying to evaluate the Biginelli reaction mechanism, many experimental and theoretical studies were reported in the literature, exploring the effects of different catalytic systems, solvents and reaction conditions.[59]

An extensive study on the classical acid-catalysed Biginelli condensation was recently reported by De Souza and co-workers, by means of infusion electrospray ionization mass spectrometry (ESI-MS) in combination with quantum-mechanical calculations.[60] Firstly, they incubated benzaldehyde and urea in the presence of a catalytic amount of formic acid, observing the formation of the protonated bisureide derivative **I**, the iminium ion **II** and its precursor **III** by ESI(+)-MS (**Figure 7**), confirming the structures by ESI(+)-MS/MS. Afterwards, they analysed an equimolar mixture of classical Biginelli reactants, in the presence of a catalytic amounts of formic acid, observing the formation of three novel ions with *m/z* of 191, 261 e 279 by ESI(+)-MS. The authors confidently attributed them to intermediate **IV**, protonated Biginelli adduct **V** and its precursor **VI** respectively (**Figure 7**). There was no evidence for the formation of the Knoevenagel product, even at prolonged reaction time, excluding the related possible mechanism (**Scheme 17**). Although it was possible to detect the enamine precursor **IV**, no sign of dehydrated product was observed. To verify the possibility of its transient nature, a mixture of ethyl acetoacetate and urea, under catalytic acidic conditions, was analysed by ESI(+)-MS, observing no formation of the enamine product, being intermediate **IV** the most abundant ion.

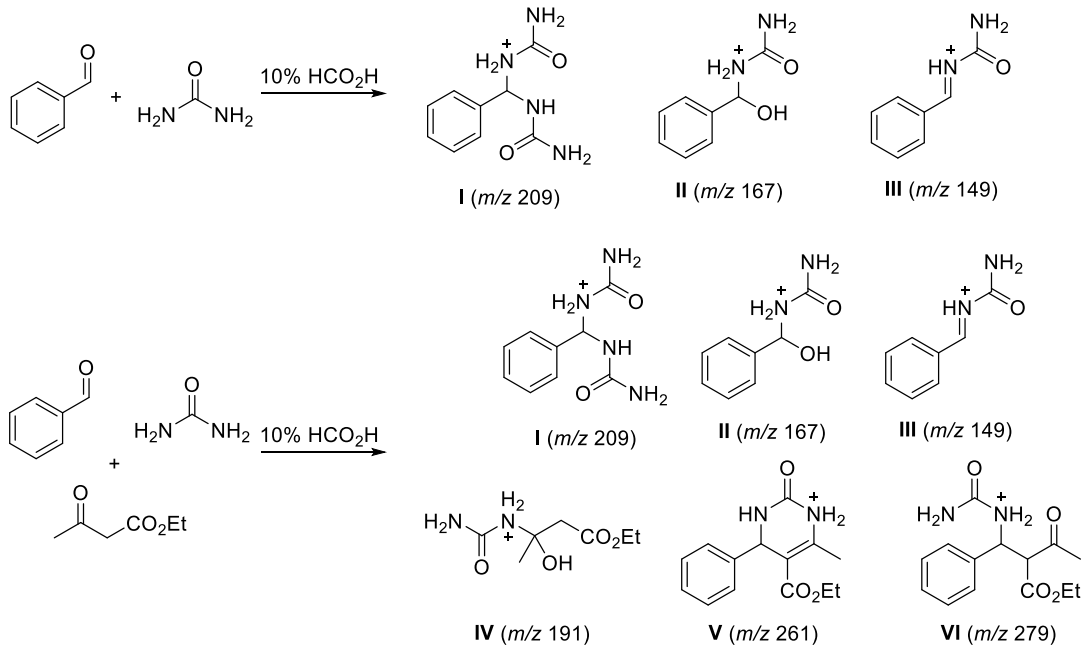

Figure 7. Ions detected by ESI(+)-MS for different mixtures of Biginelli reactants.[60]

To evaluate possible intermediates and transition states, and to compare the energy profiles of the possible mechanisms (**Scheme 17**), the authors perform quantum-mechanical calculations at the DFT level of theory, using the implicit solvent model IEFPCM.[60] Analysing the combined experimental and theoretical results, they concluded that the iminium ion mechanism (**Scheme 17.a**) is by far the kinetically and thermodynamically

favoured for the acid-catalysed Biginelli reaction, with the nucleophilic addition of the β-keto ester on the iminium ion being the rate determining step (RDS).[60]

In this context, Clark and co-workers[61] studied in deep the role of the catalyst and of the solvent in the tautomeric equilibrium of the β-keto ester, and how this affects the process efficiency. In particular, the quantity of enol form of the 1,3-dicarbonyl compound was found to be crucial for the successful formation of the Biginelli adduct in appreciable yields. The best catalyst choice was found to be hydrochloric acid, being inexpensive and effective at low concentrations. The replacement of the classical solvent of choice ethanol with non-polar alternatives (e.g. *p*-cymene), affected the reaction outcome in a beneficial way, thanks to the higher reaction temperature accessible. In addition, water was found to be a very favourable option as solvent, especially when acyclic β-dicarbonyl reactants are employed.[61]

The deep interest in studying the Biginelli reaction is driven by the great industrial profile of this MCR. Indeed, this condensation is the most effective process to obtain DHMPs, which are present in a wide range of chiral marketed drugs or lead candidates, targeting important diseases (**Figure 8**).[62]

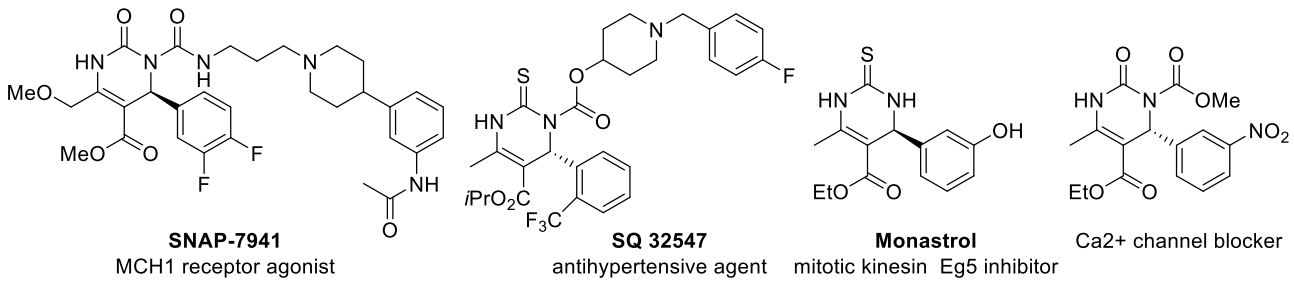

Figure 8. Examples of marketed drugs or lead compounds bearing a DHMP core.[62]

In design the synthesis of potentially bioactive chiral compounds, it is crucial to be able to access to their enantiopure form. Indeed, different biological activity, pharmacodynamics, pharmacokinetics and toxicity are usually observed for the two enantiomers.[63] In the pharmaceutical industry, the methods to access enantiomerically pure molecules can be divided in three main categories: the so-called "chiral pool" approach,[64] the resolution of a racemic mixture[65] and the asymmetric synthesis.[66] The latter is by far the most attractive method, with a better atom economy and less wastes generated. Although chiral auxiliary-controlled asymmetric reactions have been extensively studied in the recent past, reaching a high level of sophistication,[67] asymmetric catalysis is the ideal approach for the synthesis of enantiopure compounds.[68] Nowadays there are three main synthetic tools to perform enantioselective catalytic transformations: asymmetric metallic catalysis, enzymatic catalysis and asymmetric organocatalysis.[69]

It is not surprising that enantioselective catalytic versions of the Biginelli reaction have been extensively reported, and recently reviewed by Gong and co-workers.[70] In the last two decades, organocatalysis played a central role in developing asymmetric MCRs,[71] and proved to be quite fruitful for developing highly efficient and enantioselective Biginelli transformations, relying on different organocatalytic systems.[72] They can be divided in three categories, depending on the supposed activation mechanism (**Figure 9**). When employing enantiopure primary amines as catalysts, a chiral enamine species is probably formed with the β-keto esters, governing the stereochemistry of the nucleophilic attack on the iminium ion. Moreover, the presence either of a Lewis acidic specie, an additive or a bifunctional catalyst, rigidifies the system while increasing the electrophilicity of the iminium ion, enhancing the enantiomeric excess of the final product.[73] Proline-derived bifunctional catalysts follow a similar activation mechanism, although better enantioselectivity is usually observed.[74] A completely different catalysis is observed with 3,3'-disubstituted BINOL-derived monophosphoric acids,[75] which work by activation of the imine, formed from aldehyde and (thio)urea, in a well-studied way.[76]

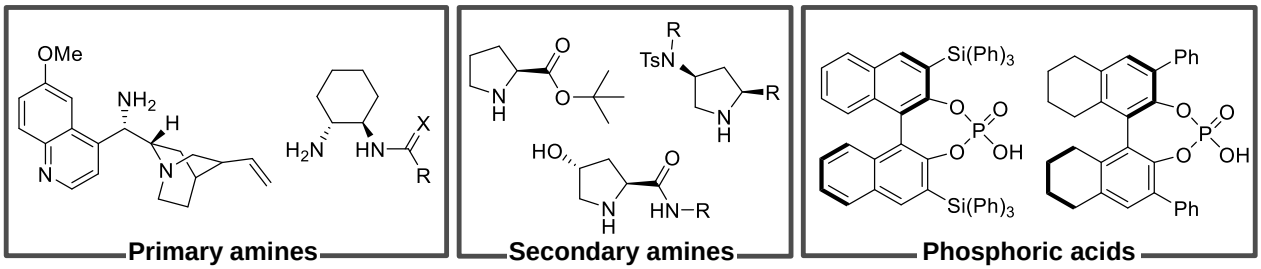

Figure 9. Recently reported organocatalytic systems for enantioselective Biginelli reactions.[72]

Going on with our interest in the asymmetric synthesis of 3,3-disubstituted oxindole derivatives and related spiro-compounds,[77] we looked at the potential application of BINOL-derived monophosphoric acids to the Biginelli-like reaction employing isatin as carbonyl components. A small library of potentially bioactive chiral spiro[indoline-pyrimidine]-diones derivatives was obtained in good yields and moderate enantioselectivity. Post-condensation reactions have been performed, increasing the number of potentially useful compounds. The assignment of the configuration at the new oxindole C-3 stereocenter was assessed through quantum-mechanical methods and NMR spectroscopy on diastereoisomeric derivatives. Computational studies on the transition state (TS) have been performed, which helped to rationalize the enantioselectivity and stereochemical outcome (**Chapter 4**).

References

[1] Strecker, A. *Annalen der Chemie und Pharmazie* **1850**, *75*, 27.
[2] (a) Eckert, H. *Molecules* **2012**, *17*, 1074. (b) Ganem, B. *Accounts of Chemical Research* **2009**, *42*, 463.
[3] Anastas, P. T.; Warner, J. C. *Green Chemistry: Theory and Practice*, Oxford University Press, New York, 1998.
[4] Cioc, R. C.; Ruijter, E.; Orru, R. V. A. *Green Chem.* **2014**, *16*, 2958.
[5] Anderson, A. B.; Hansen, B. B.; Harkness, A. R.; Henry, C. L.; Vicenzi, J. T.; Zmijewski, M. J. *J. Am. Chem. Soc.* **1995**, *117*, 12358.
[6] Taber, G. P.; Pfisterer, D. M.; Colberg, J. C. *Org. Process Res. Dev.* **2004**, *8*, 385.
[7] Trost, B. *Science* **1991**, *254*, 1471.
[8] Passerini, M.; Simone, L. *Gazz. Chim. Ital.* **1921**, *51*, 126.
[9] Ugi, I.; Fetzer, U.; Eholzer, U.; Knupfer, H.; Offerman, K. *Angew. Chem., Int. Ed. Engl.* **1965**, *4*, 472.
[10] Hulme, C.; Morrisette, M. M.; Volz, F. A.; Burns, C. J. *Tetrahedron Lett.* **1998**, *39*, 1113.
[11] (a) Sheldon, R. A. *Green Chem.* **2007**, *9*, 1273. (b) Wender, P. A.; Miller, B. L. *Nature (London)* **2009**, *460*, 197. (c) Gaich, T.; Baran, P. S. *J. Org. Chem.* **2010**, *75*, 4657.
[12] Van der Heijden, G.; Ruijter, E.; Orru, R. V. A. *Synlett* **2013**, *24*, 666.
[13] Cao, H.; Liu, H.; Dömling, A. *Chem. Eur. J.* **2010**, *16*, 12296.
[14] Znabet, A.; Polak, M. M.; Janssen, E.; de Kanter, F. J. J.; Turner, N. J.; Orru, R. V. A.; Ruijter, E. *Chem. Comm.* **2010**, *46*, 7918.
[15] W. H. Organization, *WHO Model List of Essential Medicines,* Geneva, 17th edn, **2011**.
[16] (a) Akritopoulou-Zanze, I. *Curr. Opin. Chem. Biol.* **2008**, *12*, 324. (b) Kalinski, C.; Umkehrer, M.; Weber, L.; Kolb, J.; Burdack, C.; Ross, G. *Mol. Diversity* **2010**, *14*, 513.
[17] Schreiber, S. L. *Science* **2000**, *287*, 1964.
[18] Van Hattum, H.; Waldmann, H. *J. Am. Chem. Soc.* **2014**, *136*, 11853.
[19] Dobson, C. M. *Nature* **2004**, *432*, 824.
[20] Lipinski, C. A.; Lombardo, F.; Dominy, B. W.; Feeney, P. J. *Adv. Drug Delivery Rev.* **2001**, *46*, 3.
[21] Lipinski, C. A.; Hopkins, A. *Nature* **2004**, *432*, 855.
[22] Schreiber, S. L. *Nature* **2009**, *457*, 153.
[23] Akritopoulou-Zanze, I.; Metz, J. T.; Djuric, S. W. *Drug Discovery Today* **2007**, *12*, 948.
[24] Dömling, A.; Wang, W.; Wang, K. *Chem. Rev.* **2012**, *112*, 3083.
[25] (a) Heck, S.; Dömling, A. *Synlett* **2000**, *3*, 424. (b) Bon, R. S.; van Vliet, B.; Sprenkels, N. E.; Schmitz, R. F.; de Kanter, F. J. J.; Stevens, C. V.; Swart, M.; Bickelhaupt, F. M.; Groen, M. B.; Orru, R. V. A. *J. Org. Chem.* **2005**, *70*, 3542. (c) Giovenzana, G. B.; Tron, G. C.; Di Paola, S.; Menegotto, I. G.; Pirali, T. *Angew. Chem. Int. Ed.* **2006**, *45*, 1099. (d) Chen, Z.; Wu, J. *Org. Lett.* **2010**, *12*, 4856.
[26] Nielsen, T. E.; Schreiber, S. L. *Angew. Chem. Int. Ed.* **2008**, *47*, 48.
[27] Ugi, I.; Meyr, U.; Fetzer, U.; Steinbrücker, C. *Angew. Chem.* **1959**, *71*, 386.
[28] Ugi, I.; Meyr, U. *Chem. Ber.* **1961**, *94*, 2229.
[29] Bock, H.; Ugi, I. *J. Prakt. Chem.* **1997**, *339*, 385.
[30] Chéron, N.; Ramozzi, R.; El Kaim, L.; Grimaud, L., Fleurat-Lessard, P. *J. Org. Chem.* **2012**, *77*, 1361.
[31] Medeiros, G. A.; da Silva, W. A.; Bataglion, G. A.; Ferreira, D. A. C.; de Oliveira, H. C. B.; Eberlin, M. N.; Neto, B. A. D. *Chem. Commun.* **2014**, *50*, 338.
[32] (a) Banfi, L.; Basso, A.; Guanti, G.; Riva, R. (**2005**) *Asymmetric Isocyanide-Based MCRs*, in *Multicomponent Reactions* (eds J. Zhu and H. Bienaymé), Wiley-VCH Verlag GmbH & Co. KGaA, Weinheim, FRG. (b) van Berkel, S. S.; Bögels, B. G. M.; Wijdeven, M. A.; Westermann, B.; Rutjes, F. P. J. T. *Eur. J. Org. Chem.* **2012**, 3543.
[33] Lesma G.; Meneghetti, F.; Sacchetti, A.; Stucchi, M.; Silvani, A. *Belstein J. Org. Chem.* **2014**, *10*, 1383.
[34] (a) Golebiowski, A.; Klopfenstein, S. R.; Shao, X.; Chen, J. J.; Colson, A. O.; Grieb, A. L.; Russell, A. F. *Org. Lett.* **2000**, *2*, 2615. (b) Golebiowski, A.; Jozwik, J.; Klopfemìnstein, S. R.; Colson, A. O.; Grieb, A. L.; Russell, A. F.; Rastogi, V. L.; Diven, C. F.; Portlock, D. E.; Chen, J. J. *J. Comb. Chem.* **2002**, *4*, 584.
[35] (a) Bayer, T.; Riemer, C.; Kessler, H. *J. Peptide Sci.* **2001**, *7*, 250. (b) Banfi, L.; Basso, A.; Guanti, G.; Riva, R. *Tetrahedron Lett.***2003**, *44*, 7655.
[36] Kelly, G. L.; Lawrie, K. W. M.; Morgan, P.; Willis, C. L. *Tetrahedron Lett.* **2000**, *41*, 8001.

[37] Zhu, J.; Wu, X.; Danishefsky, S. J. *Tetrahedron Lett.* **2009**, *50*, 577.
[38] Carney, D. W.; Troung, J. D.; J. K. Sello *J. Org. Chem.* **2011**, *76*, 10279.
[39] Zhdanko, A. G.; Nenajdenko, V. G. *J. Org. Chem.* **2009**, *74*, 884.
[40] Ruijter, E.; Scheffelaar, R.; Orru, R. V. A. *Angew. Chem. Int. Ed.* **2011**, *50*, 6234.
[41] Ganem, B. *Acc. Chem. Res.* **2009**, *42*, 463.
[42] *Isonitrile Chemistry* (Ed.: I. Ugi), Academic Press New York, **1971**.
[43] Ugi, I.; Skorna, G. *Chem. Ber.* **1979**, *112*, 776.
[44] McFarland, J. W. *J. Org. Chem.* **1963**, *28*, 2179.
[45] Giovenzana, G. B.; Tron, G. C.; Di Paola, S.; Menegotto, I. G.; Pirali, T. *Angew. Chem.* **2006**, *118*, 1117; *Angew. Chem. Int. Ed.* **2006**, *45*, 1099.
[46] Itho, Y.; Kato, H; Koshinaka, E.; Ogawa, N.; Kurata, S.; Yamagishi, K. US 4478838, **1984**.
[47] Pirali, T.; Callipari, G.; Ercolano, E.; Genazzani, A. A.; Giovenzana, G. B.; Tron, G. C. *Org. Lett.* **2008**, *10*, 4199.
[48] (a) Piersanti, G.; Remi, F.; Fusi, V.; Formica, M.; Luca, G.; Zappia, G. *Org. Lett.* **2009**, *11*, 417. (b) Sienczyk, M.; Podgorski, D.; Blazejewska, A.; Kulbacka, J.; Saczko, J.; Oleksyszyn, J. *Bioorg. Med. Chem.* **2011**, *19*, 1277.
[49] Tron, G. C. *Eur. J. Org. Chem.* **2013**, 1849.
[50] Dömling, A. *Chem. Rev.* **2006**, *106*, 17.
[51] Elders, N., Ruijter, E., Nenajdenko, V. G. and Orru, R. V. A. (**2012**) *α-Acidic Isocyanides in Multicomponent Chemistry,* in *Isocyanide Chemistry: Applications in Synthesis and Material Science* (ed V. G. Nenajdenko), Wiley-VCH Verlag GmbH & Co. KGaA, Weinheim, Germany.
[52] (a) van Leusen, A. M.; Strating, J. *Q. Rep. Sulfur Chem.* **1970**, *5*, 67. (b) van Leusen, D; van Leusen, A. M. *Org. React.* **2003**, *57*, 419.
[53] Kaur, T.; Wadhwa, P.; Sharma, A. *RSC Adv.* **2015**, *5*, 52769.
[54] van Leusen, A. M.; Wildeman, J.; Oldenziel, O. *J. Org. Chem.* **1977**, *42*, 1977.
[55] Dömling, A.; Beck, B.; Herdtweck, E.; Antuch, W.; Oefner, C.; Yehia, N.; Gracia-Marques, A. *ARKIVOC* **2007**, 99.
[56] Biginelli, P. Gazz. Chim. Ital. 1893, 23, 360.
[57] Kappe, C. O. *J. Org. Chem.* **1997**, *62*, 7201.
[58] Folkers, K.; Johnson, T. B. *J. Am. Chem. Soc.* **1933**, *55*, 3784.
[59] (a) Atwal, K. S.; Rovnyak, G. C.; Reilly, B. C. O.; Schwartz, J. *J. Org. Chem.* **1989**, *54*, 5898. (b) Cepanec, I.; Litvic, M.; Filipan-Litvic, M.; Grungold, I. *Tetrahedron* **2007**, *63*, 11822. (c) Shen, Z. L.; Xu, X. P.; Ji, S. J. *J. Org. Chem.* **2010**, *75*, 1162. (d) Litvic, M.; Vecenaj, I.; Ladisič, Z. M.; Lovric´ , M.; Vinkovic´ , V.; Filipan Litvic, M. *Tetrahedron* **2010**, *66*, 3463. (e) Kamal Raj, M.; Rao, H. S. P.; Manjunatha, S. G.; Sridharan, R.; Nambiar, S.; Keshwan, J.; Rappai, J.; Bhagat, S.; Shwetha, B. S.; Hegde, D.; Santhosh, U. *Tetrahedron Lett.* **2011**, *52*, 3605. (f) Ramos, L. M.; Ponce, A. Y.; Leon, D.; Santos, M. R.; Oliveira, H. C. B.; De Gomes, A. F.; Gozzo, F. C.; Oliveira, A. L.; De Neto, B. A. D. *J. Org. Chem.* **2012**, *77*, 10184. (g) Ramos, L. M.; Guido, B. C.; Nobrega, C. C.; Correa, J. R.; Silva, R. G.; Oliveira, Heibbe C. B. de; Gomes, A. F.; Gozzo, F. C.; Neto, B. A. D. *Chem. Eur. J.* **2013**, *19*, 4156. (h) Alvim, H. G. O.; Lima, T. B.; de Oliveira, H. C. B.; de Gozzo, F. C.; Macedo, J. L.; de Abdelnur, P. V.; Silva, W. A.; Neto, B. A. D. *ACS Catal.* **2013**, *3*, 1420. (i) Alvim, H. G. O.; da Silva Junior, E. N.; Neto, B. A. D.´ *RSC Adv.* **2014**, *4*, 54282. (j) Alvim, H. G. O.; Lima, T. B.; de Oliveira, A. L.; de Oliveira, H. C. B.; Silva, F. M.; Gozzo, F. C.; Souza, R. Y.; da Silva, W. A.; Neto, B. A. D. *J. Org. Chem.* **2014**, *79*, 3383. (k) Puripat, M.; Ramozzi, R.; Hatanaka, M.; Parasuk, W.; Parasuk, V.; Marokuma, K. *J. Org. Chem.* **2015**, *80*, 6959.
[60] De Souza, R. O. M. A.; da Penha, E. T.; Milagre, H. M. S.; Garden, S. J.; Esteves, P. M.; Eberlin, M. N.; Antunes, O. A. C. *Chem. Eur. J.* **2009**, *15*, 9799.
[61] Clark, J. H.; Macquarrie, D. J.; Sherwood, J. *Chem. Eur. J.* **2013**, *19*, 5174.
[62] (a) Kappe, C. O. *Tetrahedron* **1993**, *49*, 6937. (b) Kappe, C. O. *Eur. J. Med. Chem.* **2000**, *35*, 1043. (c)Tron, G. C.; Minassi, A.; Appendino, G. *Eur. J. Org. Chem.* **2011**, *2011*, 5541. (d) De Fatima, A.; Braga, T.C.; Da S. Neto, L.; Terra, B.S.; Oliveira, B.G.F.; Da Silva, D.L.; Modolo, L.V. J. *Adv. Res.* **2014**, http://dx.doi.org/ 10.1016/j.jare.2014.10.006.
[63] Rouf, A.; Taneja, S. C. *Chirality* **2014**, *26*, 23.
[64] Breuer, M.; Ditrick, K.; Habicher, T.; Hauer, B.; Kesseler, M.; Sturmer, R.; Zelinski, T. *Angew. Chem. Int. Ed.* **2004**, *43*, 788.
[65] Fogassy, E.; Nogradi, M.; Kozma, D.; Egri, G.; Palovics, E.; Kiss, V. *Org. Biomol. Chem.* **2006**, *4*, 3011.
[66] Farina, V.; Reeves, J. T.; Senanayake, C. H.; Song, J. J. *Chem. Rev.* **2006**, *106*, 2734.
[67] Seyden-Penne, J. *Chiral Auxiliaries and Ligands in Asymmetric Synthesis*; John Wiley: New York, **1995**.

[68] Blaser, H. U.; Schmidt, E. *Asymmetric Catalysis on Industrial Scale: Challenges, Approaches and Solutions*; WileyVCH: Weinheim, **2004**.
[69] Ricci, A. *ISRN Organic Chemistry* **2014**, *2014*, http://dx.doi.org/10.1155/2014/531695.
[70] Gong, L. Z.; Chen, X. H.; Xu, X. Y. *Chem. Eur. J.* **2007**, *13*, 8920.
[71] (a) Guillena, G.; Ramon, D. J.; Yus, M. *Tetrahedron Asymmetry* **2007**, *18*, 693. (b) de Graff, C.; Ruijter, E.; Orru, R. V. A. *Chem. Soc. Rev.* **2012**, *41*, 3969.
[72] Heravi, M. M.; Asadi, S.; Lashkariani, B. M. *Mol. Divers.* **2013**, *17*, 389.
[73] (a) Wang, Y. Y.; Yu, J.; Miao, Z.; Chena, R. *Adv. Synth. Catal.* **2009**, *351*, 3057. (b) Ding, D.; Zhao, C. G. *Eur. J. Org. Chem.* **2010**, *2010*, 3802. (c) Xu, D. Z.; Li, H.; Wang, Y. *Tetrahedron* **2012**, *68*, 7867.
[74] (a) Sohn, J. H. C.; Lee, H. M.; Joung, S.; Lee, S. H. Y. *Eur. J. Org. Chem.* **2009**, *2009*, 3858. (b) Saha, S.; Moorthy, J. N. *J. Org. Chem.* **2011**, *76*, 396.
[75] (a) Chen, X.U.; Xu, X.Y.; Liu, H.; Cun, L.F.; Gong, L.Z. J. Am. Chem. Soc. 2006, 128, 14802. (b) Li, N.; Chen, X.H.; Song, J.; Luo, S.W.; Fan, W.; Gong, L.Z. J. Am. Chem. Soc. 2009, 131, 15301.
[76] Simon, L.; Goodman, J. M. *J. Org. Chem.* **2011**, *76*, 1775.
[77] G. Lesma, F. Meneghetti, A. Sacchetti, M. Stucchi, A. Silvani *Belstein J. Org. Chem.* **2014**, *10*, 1383.

RESULTS *and* DISCUSSION

2. CONFORMATIONALLY CONSTRAINED PEPTIDOMIMETICS AS INHIBITORS OF PPIs

Protein-protein interactions (PPIs) determine the biological role of the relative proteins, and only in the last decade have begun to gain attention as viable targets for therapeutic intervention, being dysregulation of PPIs the subject of many therapeutic areas, such as cancer, diabetes, neurodegeneration and HIV.[1] Indeed, the different interaction patterns are at least as important as the intrinsic biochemical activity status of the protein itself, expanding the "druggable genome" initially estimated to comprise only 1500 single proteins targets.[2] Although this number is significantly higher than the 266 human protein targets of currently approved drugs,[3] adding the number of PPIs the possible therapeutic targets increase drastically to 130000-650000.[4] Therefore, successfully addressing PPIs will greatly expand the opportunities for pharmacological intervention, considering their huge number and different roles in the human physiology (**Figure 10**), extensively surveyed in recent reviews and books.[5]

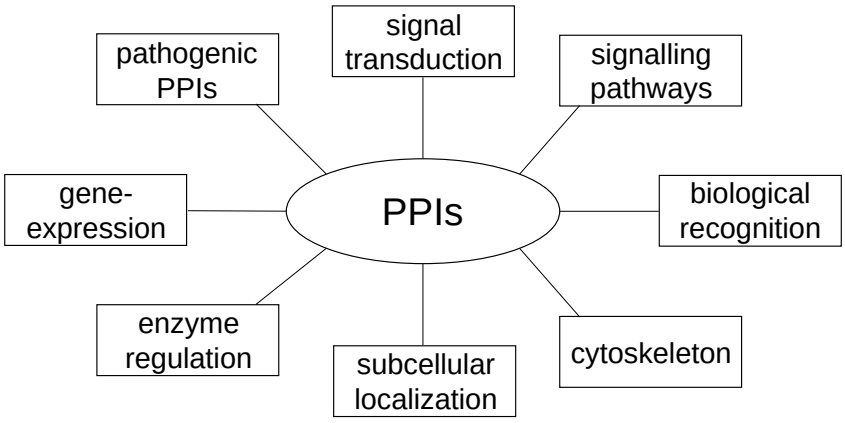

Figure 10. Examples of the role of PPIs in human physiology.[5]

Although therapeutic targeting of PPIs has been in the past largely the domain of biotech industries employing large biomolecules, in recent years synthetic organic chemists are playing a key role in this field. Indeed, large biomolecules have intrinsic disadvantages like lack of oral bioavailability, high cost of goods and they can only target extracellular structures. Small bioactive molecules can easily overcome these drawbacks, and their advance into clinical trials clearly underlines their increasing role in targeting PPIs.

Recent literature regarding the use of small molecules in disrupting PPIs is covered by a large number of reviews and books chapters,[6] and therefore will be no further discuss in this thesis.

Among the possible classes of small molecules able to disrupt PPIs, peptidomimetics deserve a special consideration. They are usually referred as compounds that mimic the action or active conformation of a peptide by incorporating non-peptidic structural features that imitate those of the related peptide, with improved biological and pharmacological properties. Because PPIs are usually restricted to small protein portions with well-defined secondary structures motifs, the design of suitable conformationally constrained peptidomimetics have attracted lot of interests, using different approaches and methodologies, as depicted by the increasing number of publications on the topic.[7]

The design and synthesis of conformationally constrained peptidomimetics have been usually performed by employing multistep processes along with a variety of protection/deprotection steps. Furthermore, this kind of approach often limits the structural diversity accessible in a set of peptidomimetics, reducing the possibility to incorporate slight modifications to improve their activity and the biological active space covered (*for further details see* **Chapter 1**). In this context, multicomponent reactions (MCRs) represent a valid alternative, being able to generate high level of complexity in a very straightforward and robust way. In particular, isocyanide-based multicomponent reactions (IMCRs) able to generate peptide-like structures have been extensively employed, and by combining them with complexity generating reactions (*for further details see* **Chapter 1.1**) different conformationally constrained cyclic peptidomimetics have become easily accessible.[8]

In the rapidly growing field of conformationally constrained peptidomimetics as inhibitors of PPIs, we have further expanded the potential scaffolds accessible through IMCRs by developing three different approaches able to generate heterocyclic compounds with well-defined secondary structures. In particular, we recently reported the synthesis of a library of ketopiperazine-based *minimalist* peptidomimetics,[9] by means of a diastereoselective Ugi four-component reaction (U-4CR) (*for further details see* **Chapter 1.1**), followed by different cyclization steps. We employed amino acid derived chiral α-amino aldehydes and α-isocyanoacetates as key components (**Chapter 2.1**). Exploiting the ability of the *N*-split Ugi reaction (*N*-split U-4CR) (*for further details see* **Chapter 1.2**) to regioselectively functionalize a symmetric secondary diamine, we developed an improved methodology for the synthesis of piperazine- and bispidine-based peptidomimetics. In this case, *N*-protected natural amino acids, chiral α-isocyanoacetates and formaldehyde, in combination with the desired preformed cyclic diamine, were employed in a one-pot process (**Chapter 2.2**). Finally, a novel C2-C5' linked polyimidazole scaffold mimicking a β-strand secondary structure was smoothly obtained (**Chapter 2.3**), by means of an iterative van Leusen three-component reaction (vL-3CR) employing the commercially available tosylmethyl isocyanide (TosMIC) (*for further details see* **Chapter 1.3**).

2.1 Ketopiperazine-based *minimalist* peptidomimetics

Introduction

Peptidomimetics design can be divided in three main categories, depending on which key structural feature is retained from the parent peptide. For instance, peptidomimetics can be designed to resemble only peptide main-chains, by substituting one or all amide bonds with esters or thioesters linkages, without incorporating the side chains. The resulting compounds can hardly be called peptidomimetics, because of their inability to form specific intermolecular interactions and limited H-bonds. On the other hand, the combination of amide bonds and/or their mimics with appropriate side chains has proved to be a successful design strategy, being able to produce small molecules inhibitors of specific enzymes, by mimicking the structural features of the natural substrate.[10] Unfortunately, this peptidomimetics design completely fails when the therapeutical target is a PPI, with usually no known natural small inhibitors. Moreover, statistical analyses of structurally characterized protein–protein interfaces have shown side-chain substituents account for about 80% of the interactions, while the backbone accounts for much less.[11] Therefore, designing a peptidomimetic in which only the side chains are retained will lead to a more proteolytically stable and orally bioavailable compound, and likely to be most useful for targets where exact binding conformations are unknown, like for PPIs. Compounds that present only selected side-chains to resemble peptide secondary structures are referred for the first time as *minimalist* peptidomimetics by Burgess in 2011.[12]

Although this concept is quite general, Burgess established some fundamental criteria to better define them and to give indications for their good design.[12] In particular, a rigid scaffold with a strongly thermodynamic preferred conformation is not important; instead, the rotation around a few degrees of freedom should allow the interconversion between relevant conformations, with energies similar to the global minima. Moreover, the transition-state energy barriers must be easily surmountable at ambient temperature, allowing the interaction between *minimalist* peptidomimetics and protein-protein interfaces *via* the so-called induced fit.[13] On the other hand, scaffolds must possess limited degrees of freedom, reducing the unfavourable loss of entropic free energy during the interactions with the proper protein-protein interface. Finally, another important criterion is the possibility to smoothly introduce selected amino acid side chains, affording *minimalist* peptidomimetics able to interact with a specific PPI.

Early examples of *minimalist* peptidomimetics shown in **Figure 11** clearly underline the above-mentioned criteria. Hirschmann and Smith designed β-turn mimetics by using different cyclic scaffolds,[14] in which challenging side chains can be easily introduced (**Figure 11.a**). Achiral terphenyl compounds reported by Hamilton and co-workers clearly demonstrated the induced fit concept, possessing few degrees of freedom, which allow them to reach a helical conformation with no unsurmountable thermodynamic or kinetic

obstacles (**Figure 11.b**).[15] Latest reports on *minimalist* peptidomimetics have been extensively surveyed in recent reviews and books.[16]

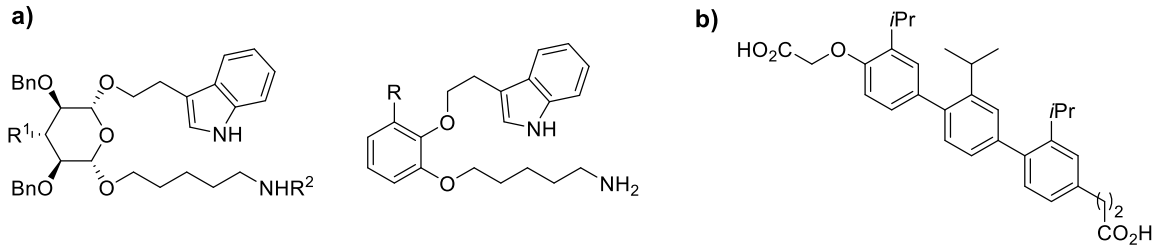

Figure 11. Early examples of *minimalist* peptidomimetics.[14,15]

Determine which secondary structure can be mimicked is another fundamental criterion in the design of a *minimalist* peptidomimetics. Although different experimental methods are available, such as NMR or circular dichroism (CD), applying them to *minimalist* peptidomimetics often give no conclusive results, due to the rapid interconversion between low energy conformations. Therefore, the comparison between thermodynamically and kinetically accessible conformations of *minimalist* peptidomimetics and common secondary structures can be performed by using three different parameters: C^{α}-atoms separation, C^{α}-C^{β} vector and C^{β}-C^{β} separation. The former, introduced by Garland and Dean for the analysis of β-turns,[17] represents the spatial separation between two α-carbons in a peptide sequence. Although it is computationally inexpensive, the β-carbon orientation are not taken into account, thus preventing a safe application to the mobile side chains of a *minimalist* peptidomimetic. The same authors proposed a better indicator, namely the C^{α}-C^{β} vector parameter,[18] in which vectors between α- and β-carbons describe the orientation of the side chains. Its application to *minimalist* peptidomimetics requires computer overlay and clustering techniques, making it not quick and easy to use. Therefore, Burgess introduced the C^{β}-C^{β} separation[12] as a good compromise between the previously reported parameters, for correlating *minimalist* peptidomimetics with common secondary structures (**Figure 12**). Indeed, calculating the spatial separation between β-carbons is as easy as for C^{α}-atoms separation, while it takes into account the side chains flexibility and their projection into space, as well as C^{α}-C^{β} vector.

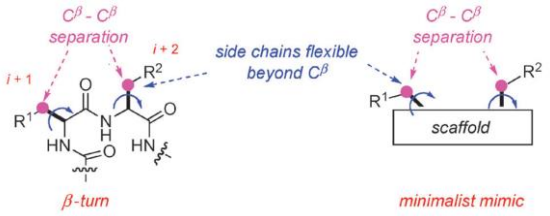

Figure 12. Comparison between C^{β}-C^{β} separation between a β-turn and a minimalist peptidomimetic (fig. from ref 12a, pg. 4414).

In this context, we recently reported[9] the design of a library of ketopiperazine-based *minimalist* peptidomimetics, by means of a diastereoselective U-4CR/post-cyclization approach in a build/couple/pair strategy (*for further details see* **Chapter 1**). In particular, amino acids-derived chiral α-amino aldehydes and α-isocyanoacetates were obtained following literature procedures ("build" phase), and employed with suitable bifunctional amine and carboxylic acid moieties in a U-4CR ("couple" phase) followed by the final cyclization step ("pair" phase), affording the desired ketopiperazine-based peptidomimetics (**Scheme 18**). Finally, we also accomplished a computational evaluation of their secondary structure mimicking properties and subjected the whole library to biological screening against different resistant cancer-cell lines.

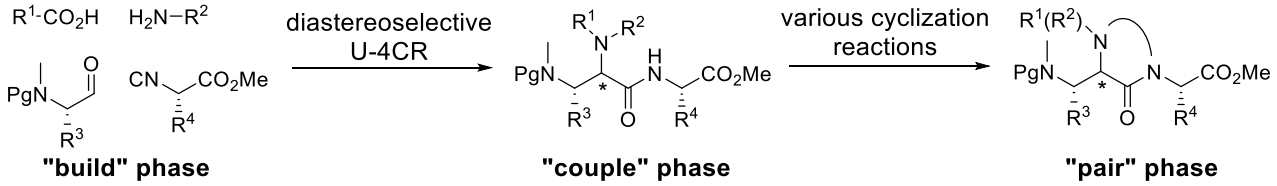

Scheme 18. Build/couple/pair strategy applied to the synthesis of a library of ketopiperazine-based *minimalist* peptidomimetics.

Results and discussion

To demonstrate the methodological feasibility, we selected L-alanine and L-phenylalanine as representative amino acids, employed as starting materials for the synthesis of both the carbonyl and isocyanide moieties. In particular, among the reported procedures for the synthesis of optically pure *N*-methyl-*N*-protected α-amino aldehydes, we selected a three-step sequence starting from the commercially available *N*-Boc or *N*-Cbz protected amino acids. After the initial *N*-alkylation under standard conditions, reduction of the carboxylic groups afforded the corresponding alcohols in good yields with no need for further purifications. A final IBX(2-iodoxybenzoic acid)-mediated oxidation followed by column chromatography purification allowed us to prepare compounds **1-4** in a very straightforward manner (**Scheme 19a**). On the other hand, optically pure methyl α-isocyanoacetates **5** and **6** were obtained in a two-step sequence, with the initial formylation of

the corresponding commercially available L-amino acid methyl ester hydrochlorides, by means of trimethyl orthoformate without the use of a solvent, followed by mild dehydration under Danishefsky's conditions[19] (**Scheme 19b**).

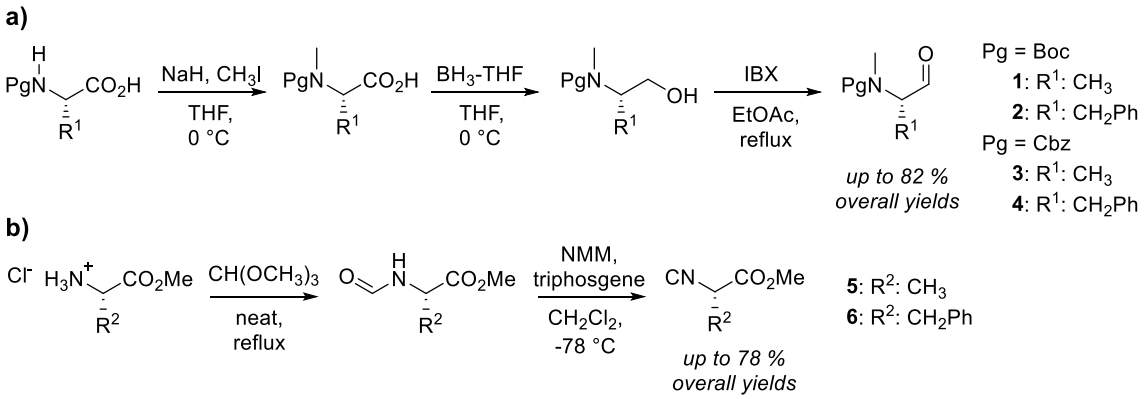

Scheme 19. Synthesis of optically pure *N*-methyl-*N*-protected α-amino aldehydes **1**-**4** and methyl α-isocyanoacetates **5**-**6**.

Firstly, we focused our attention on the synthesis of a small family of 2,5-diketopiperazine-based peptidomimetics, employing *p*-anisidine and the bifunctional chloroacetic acid as the amine and carboxylic acid components in the U-4CR step (**Scheme 20**). In particular, the Ugi condensation was performed after a precondensation time of two hours between *p*-anisidine and α-amino aldehyde **1** or **2**, in order to avoid the risk of epimerization of chiral α-isocyanoacetates[20] (*for further details see* **Chapter 1.1**), followed by the subsequent addition of chloroacetic acid and isocyanoacetates **5** or **6**. Although all the desired Ugi-adducts **7**-**10** were obtained in good yields and moderate diastereoisomeric excess (from ^{1}H NMR), only for compound **7** it was possible to separate the two diastereoisomers by flash chromatography. Therefore, separated cyclization were performed on compounds **7a** and **7b**, by means of cesium carbonate in anhydrous acetonitrile,[21] leading to 2,5-diketopiperazines **11a** and **11b** (**Scheme 20**) with an overall stereochemistry determined by computational-assisted NMR and CD studies (*vide infra*). While compound **7b** smoothly afforded the corresponding product **11b** in good yields, slower reaction rate was observed for **7a** even at higher temperature. Evidently, the cyclization leading to crowded 2,5-ketopiperazine ring is strongly influenced by steric factors, favouring the Ugi major diastereoisomer **7b** instead of **7a**. This observation was confirmed when 2,5-diketopiperazine compounds **12**-**14** were obtained in moderate yields as single stereoisomers, starting from the corresponding diastereoisomeric mixtures **8**-**10** (**Scheme 20**).

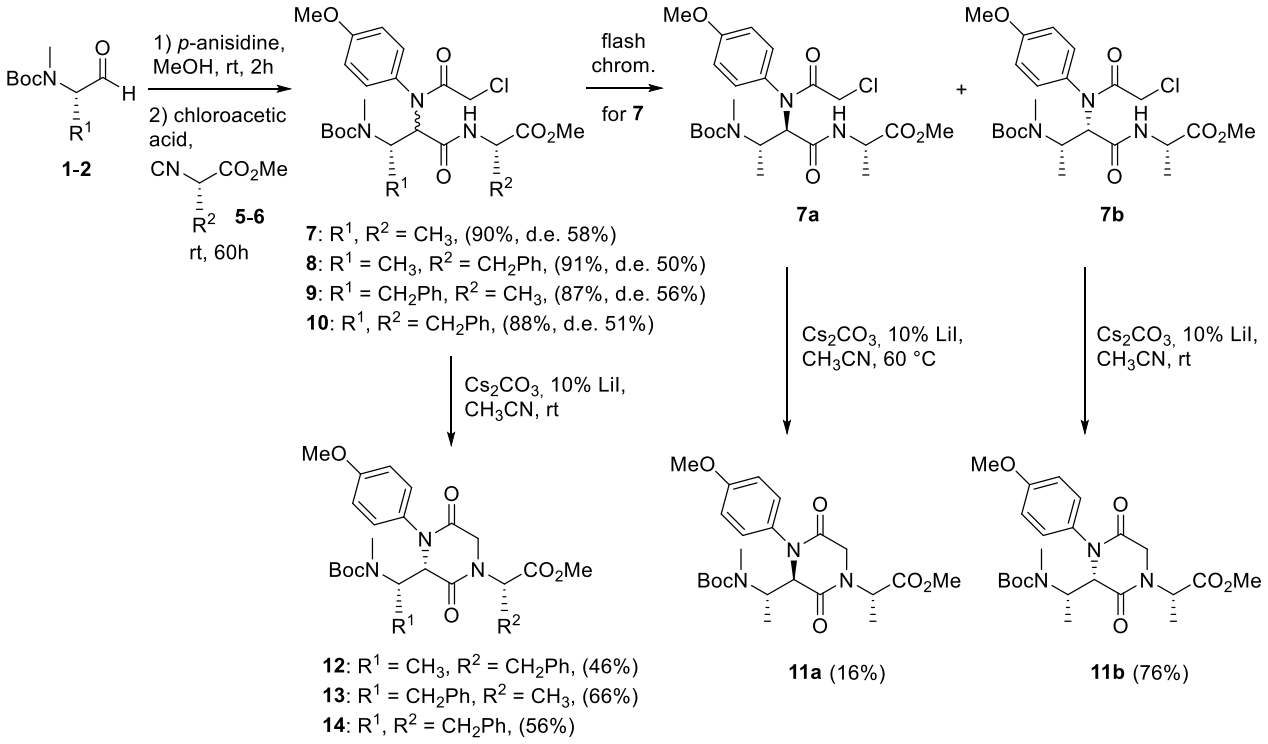

Scheme 20. Synthesis of 2,5-diketopiperazine-based peptidomimetics **11-14**.

Starting again from aldehydes **1** and **2** and isocyanoacetates **5** and **6**, we could also obtained 2,6-diketopiperazine based peptidomimetics **19**-**22,** simply varying the acid and amine components in the initial U-4CR (**Scheme 21**). Indeed, employing acetic acid and glycine benzylester in a similar U-4CR set up, intermediates **15**-**18** were easily obtained in high yields and diastereoisomeric excesses (from ^{1}H NMR), even though only for compound **15** chromatographic separation was successful. Therefore, diastereoisomers **15a** and **15b** were separately cyclized to afforded **19a** and **19b** respectively, by means of catalytic hydrogenolysis of the benzylester group, followed by activation with 1,1'-carbonyldiimidazole (CDI) in tetrahydrofuran.[22] As expected, different reaction kinetics were observed, with a trend similar to the above-mentioned case of 2,5-diketopiperazine. Finally, applying the same two-step cyclization strategy to diastereoisomeric mixtures **16**-**18**, 2,6-ketopiperazines **20**-**22** were obtained in good yields and high diastereoisomeric excesses (from ^{1}H NMR) (**Scheme 21**).

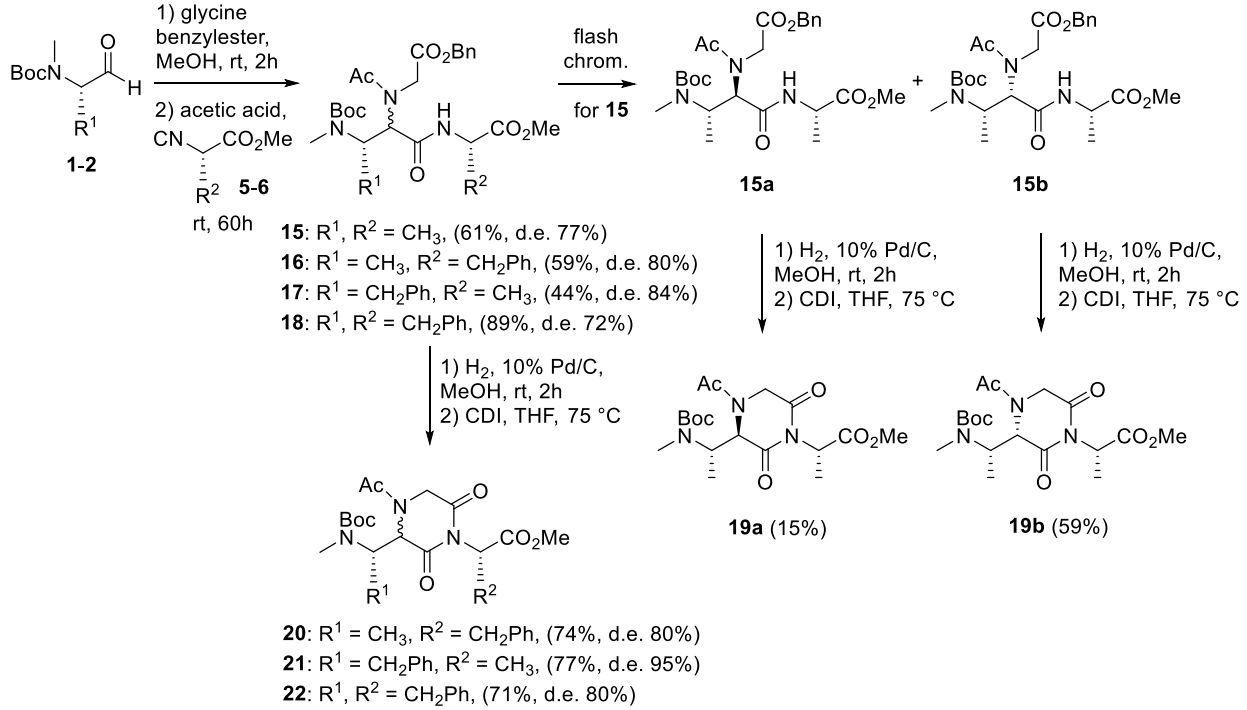

Scheme 21. Synthesis of 2,6-diketopiperazine-based peptidomimetics **19-22**.

Finally, starting from *N*-Cbz α-amino aldehydes **3-4** we also accomplished the synthesis of 3,4-dihydropyrazin-2(1*H*)-one-based peptidomimetics, employing 2,2-diethoxy amine as the key bifunctional component (**Scheme 22**). Performing the initial U-4CR under usual conditions, the corresponding highly unstable intermediates were directly treated with trifluoroacetic acid to give final cyclic compounds **23-26** in good overall yields. In this case, diastereoisomeric compounds **23a-26a** and **23b-26b** could be easily separated by flash chromatography, with an overall high diastereoisomeric ratios, up to **b:a** = 93:7.

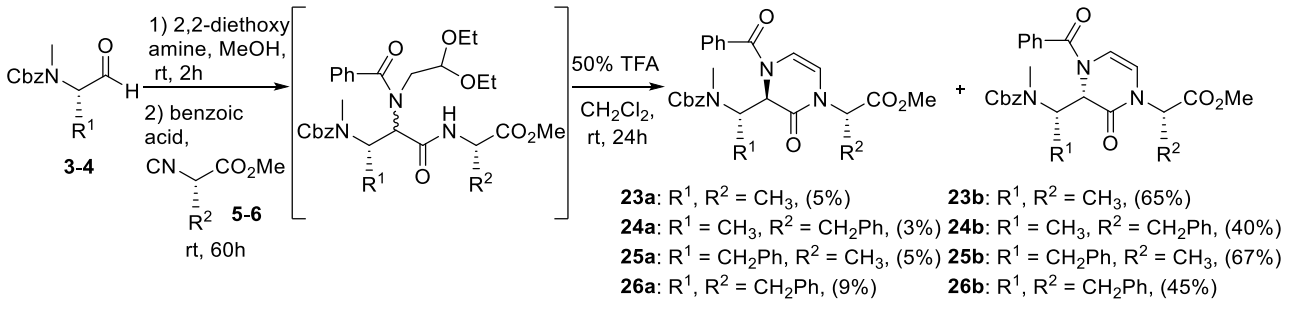

Scheme 22. Synthesis of 3,4-dihydropyrazin-2(1*H*)-one-based peptidomimetics **23-26**.

Unfortunately, any attempt to obtain crystals suitable for X-ray diffraction analysis proved to be unfruitful, for both the open Ugi-adducts and the cyclized products, in a wide range of solvents and

crystallization conditions. Therefore, in collaboration with Dr. Pescitelli,[23] we relied on theoretical conformational analysis, in combination with NMR and CD spectra, to rationalize the stereochemical outcome of the U-4CR/cyclization approaches. We focused our attention on the more rigid cyclic products, and in particular on the separated diastereoisomers **11a** and **11b**. Conformer distribution analysis was performed independently for the C-2(*S*) and C-2(*R*) isomers of **11** (for atom numerations, see the structure in **Figure 13a**), employing Monte-Carlo algorithm and molecular mechanics (MMFF force field) and including all rotable bonds and the puckering of 6-membered ring atoms. The geometries of all the obtained conformers were optimized with the DFT method at the B3LYP/6-31G(d) level of theory, without considering solvent effects. Single-point calculation using the same quantum-mechanical approach allowed us to compute the Bolztmann distribution at room temperature, and all the structures with population <1% were not further considered.

Almost all the populated structures for the C-2(*R*) isomer showed a consistent conformation around the C-2/C-15 bond, with *anti* orientation between H-2 and H-15 and a pseudo-axial position of the C-2 appendage. Therefore, aromatic *ortho* hydrogens are expected to give NOE contacts only with the *t*Bu group of the Boc moiety and the *N*-methyl, and not with CH_3-17 (**Figure 13a**).

On the other hand, the conformational situation for the C-2(*S*) isomer is less clear around the C-2/C-15 bond. Although the C-2 appendage occupies again a pseudo-axial position, there are at least two main conformational families regarding the situation between H-2 and H-15, with either a *gauche* or an *anti* orientations. In this case the NOE analysis is less straightforward, but we confidently could predict a strong NOE contact between aromatic *ortho* hydrogens and CH_3-17, while smaller or no NOE with the Boc moiety and *N*-methyl should be observed (**Figure 13a**).

The comparison between the theoretical NOEs and the experimental ones from ROESY correlation peaks strongly suggested a C-2(*S*) configuration for the major diastereoisomer **11b** and a C-2(*R*) one for the minor diastereoisomer **11a** (**Figure 13a**) (*for further details see* **Appendix A.2**).

To further confirm the stereochemical assignment, the experimental CD spectrum of the major diastereoisomer **11b** was compared to theoretical ones, obtained with the TDDFT method on DFT-optimized input structures for both the C-2(*S*) and the C-2(*R*) isomers. Unfortunately, the two isomers led to similar theoretical sequence of bands, in accordance with the experimental CD spectrum of **11b**, and a safe discrimination based only on CD spectra was not possible. However, since CD spectroscopy did not contradict the NMR results, we could confidently confirm the above reported stereochemical assignment (*for further details see* **Appendix A.2**).

Moreover, the observed stereochemical outcome can be rationalized by considering a Felkin-Ahn model for the irreversible nucleophilic attack of the isocyanoacetate on the iminium ion in the U-4CR step (*for further details on the U-4CR mechanism see* **Chapter 1.1**). By employing optically pure (*S*)-α-amino aldehyde

1, the steric hindrance of the *N*-methyl-*N*-Boc moiety shields the *si* face, leading to a preferred attack on the *re* face by the isocyanoacetate **5**, affording the final Ugi-adduct with a *S* configuration for the newly formed stereocenter of the major diastereoisomer **11b** (**Figure 13b**).

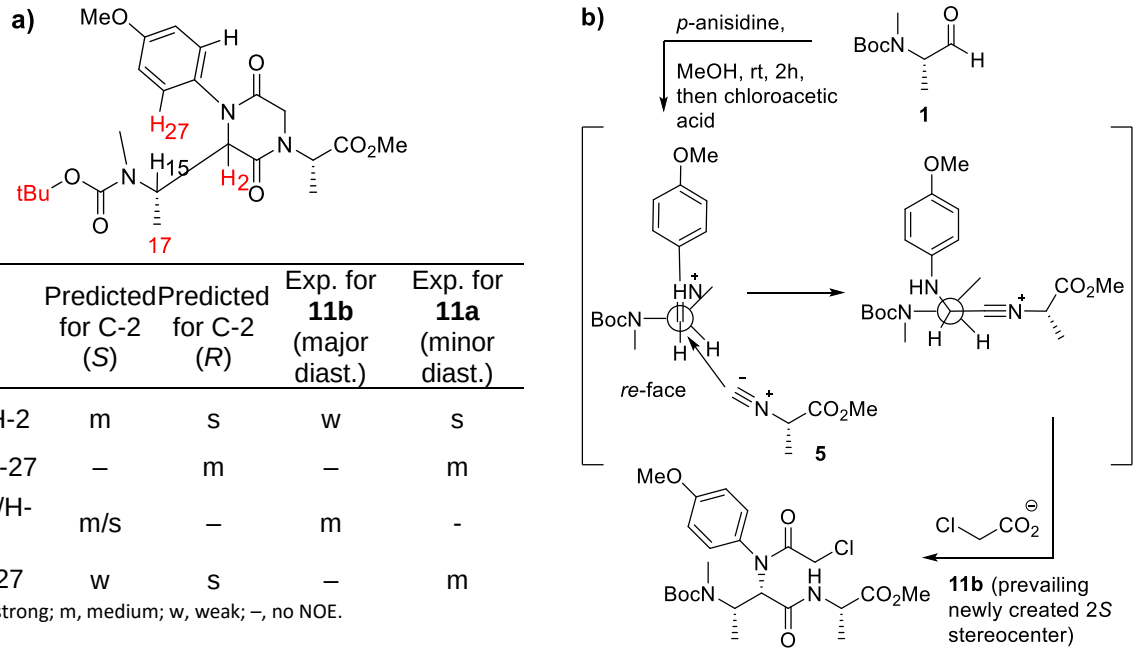

NOE	Predicted for C-2 (*S*)	Predicted for C-2 (*R*)	Exp. for **11b** (major diast.)	Exp. for **11a** (minor diast.)
NCH_3/H-2	m	s	w	s
NCH_3/H-27	–	m	–	m
CH_3-17/H-27	m/s	–	m	-
*t*Bu/H-27	w	s	–	m

Legend: s, strong; m, medium; w, weak; –, no NOE.

Figure 13. a) Predicted and experimentally observed diagnostic NOE's.
b) Felkin-Ahn attack mode proposed for the observed stereochemistry.

In order to properly defined our compounds as *minimalist* peptidomimetics, a computational study was performed on structures **a**, **b** and **c** as representative models of compounds **11b**, **19b** and **23b** respectively. Models **a**, **b** and **c** possess the *S* stereochemistry at the ketopiperazine-ring and L-Ala-derived side-chains, with *N*-Ac and CO-$NHCH_3$ terminal groups, aimed to mimic the insertion of the peptidomimetic into a putative peptide.

In collaboration with Dr. Grazioso,[24] molecular dynamics simulations were performed on the three models using the algorithm of the AMBER12 package,[25] with the GB implicit water solvent model and acquisitions every 10 ps. In particular, they were analysed by minimizing, equilibrating and heating up the starting conformations to 300 K, 700 K and 1000 K for a short period (2 ns). After an intermediate equilibrium step at 700 K, 20 ns of molecular dynamics (MD) simulations at 300 K were performed,[26] acquiring 2800 conformational states of each models. Dihedral angle fluctuations (arrows in **Figure 14**) were analysed over the obtained trajectories, obtaining different families of conformations for models **a**, **b** and **c**.

Furthermore, geometry optimization for each families were performed using GAUSSIAN09[27] at the quantum-mechanics DFT/B3LYP/6-31g(d)/CPCM-water level of calculation. Finally, application of the Boltzmann equation provided the conformers distribution percentage of the model compounds representing our ketopiperazine-based *minimalist* peptidomimetics (tables in **Figure 14**).

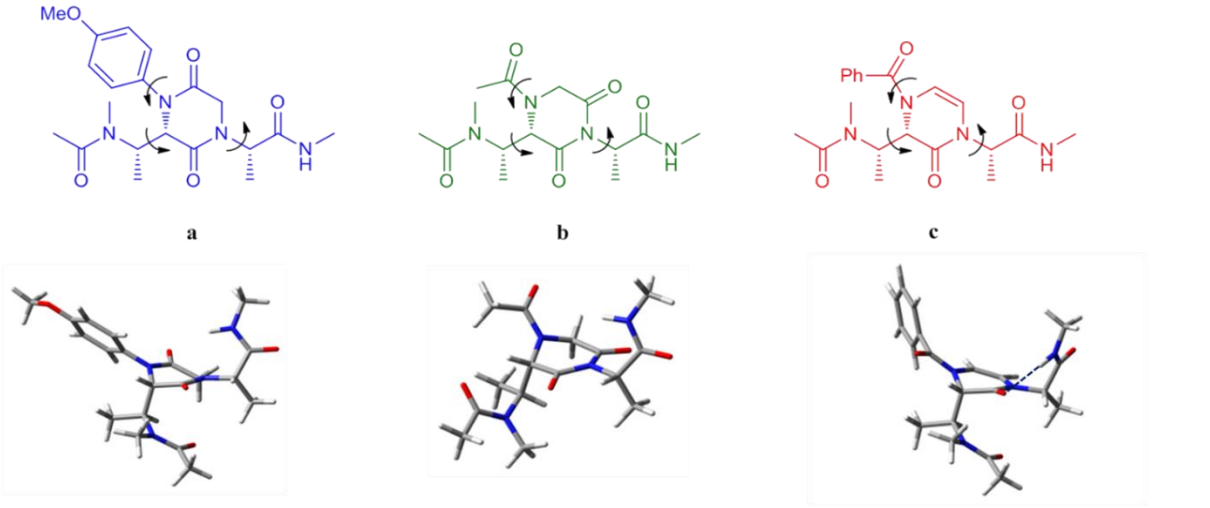

Conformer	ΔE (Kcal/mol)	Boltzmann distribution (%)	C^{β}-C^{β} distances (Å)
1	0	72	6,6
2	0,57	27	6
3	2,93	1	4,6

Conformer	ΔE (Kcal/mol)	Boltzmann distribution (%)	C^{β}-C^{β} distances (Å)
1	0	39	6,4
2	0,16	30	5,8
3	0,27	25	6,7
4	1,16	6	5,7
5	1,88	2	4,6

Conformer	ΔE (Kcal/mol)	Boltzmann distribution (%)	C^{β}-C^{β} distances (Å)
1	0	85	6,5
2	1,22	11	6,3
3	1,97	3	6,1
4	2,38	2	4,9

Figure 14. Above: 2D structures of models **a**, **b** and **c** with their low energy conformers 3D images. Blue dotted line on model **c** represents the internal hydrogen-bond.
Below: tables reporting the Boltzmann distributions and the C^{β}-C^{β} distances.

To determine which secondary structures can be mimicked, distances between β-carbons were measured on the quantum-mechanical optimized lowest energy conformers. Therefore, by comparing the obtained C^{β}-C^{β} distances to the ones reported by Burgess and coworkers[12] for typical secondary structures (**Table 1**), we were able to predict the secondary structure potentially mimicked by our compounds. In particular, model compounds **a** and **c** can assume conformations compatible with α-helix, β-sheet (anti-parallel) and γ-turn (classic) secondary structures. On the other hand, the more flexible model **b** may mimic all the secondary structures reported in **Table 1**.

Table 1. Correspondence of C^{β}- C^{β} distances for model **a**, **b** and **c** with those reported for the most common peptide secondary structures. Numbers highlighted by color represent the conformer percentage showing that specific C^{β}- C^{β} distance/secondary structure. They were retrieved from the Boltzmann distribution showed on **Figure 14**.

Structure	Sequence	C^{β}-C^{β} distances (Å)	a	b	C
α-Helix	*i-i+3*	5,6		6	
	i-i+4	6,5	72	64	96
β-Sheet (parallel)	*i-i+1*	5,8		36	
	i-i'	5,5		36	
β-Sheet (anti-parallel)	*i-i+1*	5,8		36	
	i-i+2	6,5	72	64	96
	i-i'	4,5	1	2	
γ-Turn (type-1)	*i-i+1*	5,7		36	
	i+2-i+3	5,6		36	
γ-Turn (classic)	*i-i+1*	4,7	1	2	2
γ-Turn (inverse)	*i-i+1*	5,7		36	
	i+1-i+2	6,2	27	64	13

All compounds were preliminary evaluated for their antiproliferative effects on two different hepatocellylar carcinoma (HCC) cellular lines, namely Huh7 (weel differentiated cells) and Mahlavu (PTEN deficient poorly differentiated cells), in which the differentiation *versus* resistance ability seems to be strongly correlated with well-defined types of PPIs.[28] A significant antiproliferative effect, in the micromolar range, has been observed for **14** and **25b** and deserves further studies, which are currently in progress (*for further details see* **Appendix A.3**).

Conclusions

We developed a novel class of complex ketopiperazine-based *minimalist* peptidomimetics, by means of a high diastereoselective two-step process involving a U-4CR/cyclization sequence, employing both amino acid-derived chiral α-amino aldehydes and α-isocyanoacetates in a stereoconservative way. All compounds are characterized by the presence of L-Ala and/or L-Phe amino acid side chains, and their ability to act as *minimalist* peptidomimetics mimicking well-defined secondary structures was assessed. Preliminary biological evaluation on cancer resistant cellular lines has revealed a promising antiproliferative activity for selected compounds, underlining their ability to act as small molecules PPIs modulators.

Experimental section

GENERAL INFORMATION

All commercial materials (Aldrich, Fluka) were used without further purification. All solvents were of reagent grade or HPLC grade. All reactions were carried out under a nitrogen atmosphere unless otherwise noted. All reactions were monitored by thin layer chromatography (TLC) on precoated silica gel 60 F254; spots were visualized with UV light or by treatment with a 1% aqueous $KMnO_4$ solution. Products were purified by flash chromatography on silica gel 60 (230–400 mesh). ^{1}H NMR spectra and ^{13}C NMR spectra were recorded on 300 and 400 MHz spectrometers. Chemical shifts are reported in parts per million relative to the residual solvent. ^{13}C NMR spectra have been recorded using the APT pulse sequence (*for further details see* **Appendix A.1**). Multiplicities in ^{1}H NMR are reported as follows: s = singlet, d = doublet, t = triplet, m = multiplet, br s = broad singlet. High-resolution MS spectra were recorded with an FT-ICR (Fourier Transform Ion Cyclotron Resonance) instrument, equipped with an ESI source. CD spectra were obtained with JASCO J-715 spectropolarimeter.

GENERAL PROCEDURE FOR THE SYNTHESIS OF COMPOUNDS **7-10**

Aldehyde (**1** or **2**) (1.0 mmol, 1 eq) was dissolved in 1 mL of dry methanol under nitrogen, 4-methoxy aniline (1.0 mmol, 123 mg, 1 eq) was added and the resulting mixture was kept under stirring for 2h at room temperature. 2-Chloroacetic acid (1.0 mmol, 94.5 mg, 1 eq) and isocyanide (**5** or **6**) (1.2 mmol, 1.2 eq) were sequentially added and the reaction was stirred for additional 60h at room temperature. The resulting mixture was then concentrated under reduced pressure, to give a residue which was purified by flash chromatography (FC) as indicated below.

(S)-methyl-2-((2R,3S)-3-((tert-butoxycarbonyl)(methyl)amino)-2-(2-chloro-N-(4-ethoxyphenyl)acetamido)butanamido)propanoate, 5a and (S)-methyl-2-((2S,3S)-3-((tert-butoxycarbonyl)(methyl)amino)-2-(2-chloro-N-(4-methoxyphenyl)acetamido)butanamido)propanoate (**7b**)

Prepared according to the above general procedure from aldehyde **1** and isocyanide **5**; FC: ethyl acetate:*n*-hexane, 1:1.5; yield: **7a** (97 mg, 19%), **7b** (356 mg, 71%). **7a**: colorless oil; R_f 0.21 (1.5:1 *n*-hexane/EtOAc); $[\alpha]^{30}_D$ - 16.3 (*c* 0.5, $CHCl_3$); ^{1}H NMR (300 MHz, CD_3CN, 1:1 mixture of rotamers) δ 7.38-7.08 (m, 3H), 6.95 (d, *J* = 8.8 Hz, 2H), 4.45-4.09 (br, s, 1H), 3.85 (br, s , 2H), 3.81 (s, 3H), 3.82-3.75 (m, 1H), 3.69 (s, 1.5H), 3.71-3.63 (m, 1H), 3.67 (br, s, 1.5H), 2.65 (s, 3H), 1.46-1.31 (m,12H), 1.27 (br, d, *J* = 6.8 Hz, 3H); ^{13}C NMR (75 MHz, CD_3CN) δ 178.1, 173.0 (2C), 165.4, 160.2, 136.5, 136.2, 135.5, 120.0, 119.8, 84.8 and 84.6 (1C), 60.6, 60.5, 57.2, 53.5, 53.4, 48.5, 48.3, 34.3, 33.0 (3C), 22.2 and 21.9 (1C), 19.7 and 19.6 (1C); HRMS (ESI) calcd for $C_{23}H_{34}ClN_3NaO_7^+$ $[MNa]^+$ 522.1977, found 522.1983. **7b**: colorless oil; R_f 0.18 (1.5:1 *n*-hexane/EtOAc); $[\alpha]^{30}_D$ + 8.5 (*c* 0.5, $CHCl_3$); ^{1}H NMR (300 MHz, CD_3CN, 1:1 mixture of rotamers) δ 7.40-7.08 (br, m, 1H), 7.20 (m, 2H), 6.95 (d, *J* = 9.1 Hz, 2H), 4.41-4.12 (br, m, 1H), 3.86 (br, s, 2H), 3.81 (s, 3H), 3.79 (m, 1H), 3.67 (br, s, 1.5H), 3.65 (m, 1H), 3.64 (s, 1.5H), 2.67 (s, 3H), 1.38 (s, 9H), 1.32 (m, 3H), 1.27 (br, d, *J* = 6.8 Hz, 3H); ^{13}C NMR (100 MHz, $CDCl_3$) δ 173.5 and 173.4 (1C), 169.4-168.7 (2C), 160.6, 157.0 and 156.8 (1C), 131.4, 130.8, 130.2, 115.7, 115.5, 81.0 and 80.6 (1C), 56.1 (2C), 53.0, 52.9, 48.9 (2C), 43.1 and 43.0 (1C), 29.1 (4C), 18.2, 16.1; HRMS (ESI) calcd for $C_{23}H_{34}ClN_3NaO_7^+$ $[MNa]^+$ 522.1977, found 522.1961.

(2S)-methyl 2-((3S)-3-((tert-butoxycarbonyl)(methyl)amino)-2-(2-chloro-N-(4-methoxyphenyl)acetamido)butanamido)-3-phenylpropanoate (**8**)

Prepared according to the above general procedure from aldehyde **1** and isocyanide **6**; FC: ethyl acetate:*n*-hexane, 1:1.5; yield 524 mg, (91%) as an inseparable mixture of diastereoisomers (*d.e.* 50%, NMR analysis): pale yellow oil; R_f 0.24 (1.5:1 *n*-hexane/EtOAc); ^{1}H NMR (300 MHz, CD_3CN, rotameric mixture of a mixture of diastereoisomers) δ 7.47-6.99 (m, 8H), 6.89 (br, d, *J* = 8.8 Hz, 2H), 4.80-4.40 (br, m, 1H), 3.81 (br, s , 2H), 3.80-3.74 (m, 4H), 3.69 (s, 0.5H), 3.69-3.63 (m, 3.5H), 3.24-3.05 (br, m, 1H), 3.03-2.80 (br, m, 1H), 2.62 (s, 2.75H), 2.58 (s, 0.25H), 1.36 (s,9H), 1.28-1.21 (m, 3H); HRMS (ESI) calcd for $C_{29}H_{38}ClN_3NaO_7^+$ $[MNa]^+$ 598.2290, found 598.2305.

(2S)-methyl 2-((3S)-3-((tert-butoxycarbonyl)(methyl)amino)-2-(2-chloro-N-(4-methoxyphenyl)acetamido)-4-phenylbutanamido)propanoate (**9**)

Prepared according to the above general procedure from aldehyde **2** and isocyanide **5**; FC: ethyl acetate:*n*-hexane, 1:1.5; yield 501 mg, (87%) as an inseparable mixture of diastereoisomers (*d.e.* 56%, NMR analysis): pale yellow oil; R_f 0.22 (1.5:1 *n*-hexane/EtOAc); ^{1}H NMR (300 MHz, CD_3CN, rotameric mixture of a mixture of diastereoisomers) δ 7.40-7.04 (m, 8.4H), 6.96 (br, d, *J* = 8.4 Hz, 1.6H), 4.59-4.40 (br, m, 1H), 3.93-3.64 (m , 10H), 3.33-2.87 (m, 1H), 2.80 (s, 0.66H), 2.76 (s, 2.34H), 2.64 (m, 1H), 1.52-1.26 (m, 12H); HRMS (ESI) calcd for $C_{29}H_{38}ClN_3NaO_7^+$ $[MNa]^+$ 598.2290, found 598.2305.

(2S)-methyl 2-((3S)-3-((tert-butoxycarbonyl)(methyl)amino)-2-(2-chloro-N-(4-methoxyphenyl)acetamido)-4-phenylbutanamido)-3-phenylpropanoate (**10**)

Prepared according to the above general procedure from aldehyde **2** and isocyanide **6**; FC: ethyl acetate:*n*-hexane, 1:1.5; yield 573 mg, (88%) as an inseparable mixture of diastereoisomers (*d.e.* 51%, NMR analysis): oil; R_f 0.44 (1.5:1 *n*-hexane/EtOAc); ^{1}H NMR (400 MHz, $CDCl_3$, rotameric mixture of a mixture of diastereoisomers) δ 7.38-7.06 (m, 11.4H), 7.02-6.80 (br, m, 3.6H), 5.05-4.67 (br, m, 1H), 3.93-3.58 (m , 10H), 3.32-3.18 (m, 1H), 3.05-2.86 (m, 2H), 2.78 (s, 0.75H), 2.75 (s, 2.25H), 2.65 (m, 1H), 1.40 (m, 9H); HRMS (ESI) calcd for $C_{35}H_{42}ClN_3NaO_7^+$ $[MNa]^+$ 674.2603, found 674.2622.

GENERAL PROCEDURE FOR THE SYNTHESIS OF COMPOUNDS **11-14**

To a solution of the Ugi product (**7a**, **7b**, **8**, **9** or **10**) (0.5 mmol, 1 eq) in dry acetonitrile (4.5 mL) under nitrogen, cesium carbonate (1 mmol, 326 mg, 4 eq) and LiI (0.05 mmol, 7 mg, 0.1 eq) were added, and the mixture was stirred for 20h, at room temperature (or at 60 °C, for **7a**). The mixture was quenched with satd aq NH_4Cl (20 mL) and extracted with EtOAc (3 x 20 mL). The combined organic layers were washed with brine, dried by Na_2SO_4 and concentrated under reduced pressure, to give a residue, which was purified by flash chromatography (FC) as indicated below.

(S)-methyl 2-((R)-3-((S)-1-((tert-butoxycarbonyl)(methyl)amino)ethyl)-4-(4-methoxyphenyl)-2,5-dioxopiperazin-1-yl)propanoate (**11a**)

Prepared according to the above general procedure from **7a**; FC: ethyl acetate:*n*-hexane, 1:1.5; yield: 37 mg (16%); colorless oil; R_f 0.18 (1.5:1 *n*-hexane/EtOAc); $[\alpha]^{30}_D$ - 12.7 (*c* 0.5, $CHCl_3$); ^{1}H NMR (300 MHz, CD_3CN) δ 7.43 (br, m, 2H), 6.98 (d, *J* = 8.8 Hz, 2H), 5.03 (q, *J* = 7.0 Hz, 1H), 4.63 (br, m, 1H), 4.34 (br, m, 1H), 4.30 (br, d, *J* = 16.6 Hz, 1H), 3.88 (d, *J* = 16.7 Hz, 1H), 3.83 (s, 3H), 3.73 (s, 3H), 2.67 (s, 3H), 1.45 (s, 9H), 1.44 (d, *J* = 7.0 Hz, 3H), 1.24 (br, d, *J* = 7.5 Hz, 3H); ^{13}C NMR (100 MHz, CD_3CN) δ 172.2, 168.4, 165.0 (2C), 160.7, 133.9, 131.4 (2C), 130.0, 115.3 (2C), 80.9, 68.5, 55.8, 52.5 (2C), 49.1 and 48.9 (1C), 48.0, 28.3 (3C), 17.4, 14.2; HRMS (ESI) calcd for $C_{23}H_{33}N_3NaO_7^+$ $[MNa]^+$ 486.2211, found 486.2227.

(S)-methyl 2-((S)-3-((S)-1-((tert-butoxycarbonyl)(methyl)amino)ethyl)-4-(4-methoxyphenyl)-2,5-dioxopiperazin-1-yl)propanoate (**11b**)

Prepared according to the above general procedure from **7b**; FC: ethyl acetate:*n*-hexane, 1:1.5; yield: 176 mg (76%); colorless oil; R_f 0.16 (1.5:1 *n*-hexane/EtOAc); $[\alpha]^{30}_D$ + 24.2 (*c* 1.0, MeOH); ^{1}H NMR (400 MHz, CD_3CN) δ 7.36 (br, d, *J* = 8.9 Hz, 2H), 6.98 (d, *J* = 9.2 Hz, 2H), 5.12 (q, *J* = 7.3 Hz, 1H), 4.73 (br, m, 1H), 4.29 (d, *J* = 16.7 Hz, 1H), 4.27 (br, m, 1H), 3.88 (br, d, *J* = 16.7 Hz, 1H), 3.83 (s, 3H), 3.69 (s, 3H), 2.68 (s, 3H), 1.46 (d, *J* = 7.3 Hz, 3H), 1.45 (s, 9H), 1.16 (br, d, *J* = 7.0 Hz, 3H); ^{13}C NMR (100 MHz, CD_3CN) δ 172.2, 165.9, 164.9, 159.1, 133.9, 130.0, 129.2 (2C), 114.6 (2C), 80.2, 68.4, 55.9, 52.7, 52.1, 51.5, 48.0, 29.5, 28.3 (3C), 16.5, 13.8; HRMS (ESI) calcd for $C_{23}H_{33}N_3NaO_7^+$ $[MNa]^+$ 486.2211, found 486.2216.

(S)-methyl-2-((S)3-((S)-1-((tert-butoxycarbonyl)(methyl)amino)ethyl)-4-(4-ethoxyphenyl)- 2,5-dioxopiperazin-1-yl)-3-phenylpropanoate (**12**)

Prepared according to the above general procedure from **8**; FC: ethyl acetate:*n*-hexane, 3:7; yield: 124 mg (46%); wax; R_f 0.15 (7:3 *n*-hexane/EtOAc); $[\alpha]^{22}_D$ - 55.2 (*c* 1.0, $CHCl_3$); ^{1}H NMR (400 MHz, $CDCl_3$) δ 7.34-7.23 (m, 3H), 7.21-7.16 (m, 2H), 7.14-7.05 (m, 2H), 6.90 (d, *J* = 8.9 Hz, 2H), 5.68 (dd, *J* = 11.4, 5.1 Hz, 1H), 4.70 (br, m, 1H), 4.41 (d, *J* = 17.3

Hz, 1H), 4.03 (d, *J* = 17.3 Hz, 1H), 3.88 (br, m, 1H), 3.81 (s, 3H), 3.80 (s, 3H) 3.40 (dd, *J* = 14.4 and 5.1 Hz, 1H), 2.99 (dd, *J* = 14.4, 11.4 Hz, 1H), 2.68 (s, 3H), 1.46 (s, 9H), 1.17 (d, *J* = 7.1 Hz, 3H); ^{13}C NMR (100 MHz, $CDCl_3$) δ 170.7, 166.8, 164.7, 159.3, 156.7, 136.1, 133.0, 129.8 (2C), 129.4 (2C), 129.2 (2C), 127.7, 115.0 (2C), 80.9, 69.0, 56.6, 56.1, 53.0, 51.9, 47.6, 35.5, 29.9, 29.1 (3C), 17.1; HRMS (ESI) calcd for $C_{29}H_{37}N_3NaO_7^+$ $[MNa]^+$ 562.2524, found 562.2509.

(S)-methyl-2-((S)3-((S)-1-((tert-butoxycarbonyl)(methyl)amino)-2-phenylethyl)-4-(4-methoxyphenyl)-2,5-dioxopiperazin-1-yl)propanoate (**13**)

Prepared according to the above general procedure from **9**; FC: ethyl acetate:*n*-hexane, 1:1.5; yield: 178 mg (66%); pale yellow oil; R_f 0.15 (1.5:1 *n*-hexane/EtOAc); $[\alpha]^{30}_D$ + 2.2 (*c* 0.5, $CHCl_3$); ^{1}H NMR (400 MHz, $CDCl_3$) δ 7.35-7.24 (m, 2H), 7.24-7.12 (m, 3H), 7.12-7.05 (m, 2H), 6.92 (d, *J* = 8.6 Hz, 2H), 5.29 (q, *J* = 7.1 Hz, 1H), 4.97 (br, m, 1H), 4.43-4.30 (m, 2H), 3.99 (d, *J* = 16.7 Hz, 1H), 3.83 (s, 3H), 3.74 (s, 3H) 3.08 (br, m, 1H), 2.77 (br, m, 2H), 2.67 (s, 3H), 1.47 (d, *J* = 7.1 Hz, 3H), 1.44 (s, 9H); ^{13}C NMR (100 MHz, $CDCl_3$) δ 171.8, 166.0, 164.7, 159.3, 157.1, 137.7, 132.9, 129.6 (2C), 129.1 (2C), 128.8 (2C), 127.2, 115.1 (2C), 81.0, 67.3, 57.7, 56.1, 52.3, 51.7, 47.6, 36.9, 30.8, 28.9 (3C), 14.5; HRMS (ESI) calcd for $C_{29}H_{37}N_3NaO_7^+$ $[MNa]^+$ 562.2524, found 562.2536.

(2S)-methyl-2-((S)3-((S)-1-((tert-butoxycarbonyl)(methyl)amino)-2-phenylethyl)-4-(4-methoxyphenyl)-2,5-dioxopiperazin-1-yl)-3-phenylpropanoate (**14**)

Prepared according to the above general procedure from **10**; FC: ethyl acetate:*n*-hexane, 3:7; yield: 151 mg (56%); yellow oil; R_f 0.21 (7:3 *n*-hexane/EtOAc); $[\alpha]^{31}_D$ = - 74.7 (*c* 1.0, MeOH); ^{1}H NMR (400 MHz, $CDCl_3$) δ 7.35-7.23 (m, 4H), 7.23-7.18 (m, 2H), 7.18-7.11 (m, 2H), 7.10-6.99 (m, 4H), 6.88 (d, *J* = 8.8 Hz, 2H), 5.73 (dd, *J* = 11.3 and 5.3 Hz, 1H), 4.94 (br, m, 1H), 4.40 (d, *J* = 17.2 Hz, 1H), 4.05 (d, *J* = 17.2 Hz, 1H), 4.03 (br, m, 1H), 3.83 (s, 3H), 3.81 (s, 3H), 3.44 (dd, *J* = 14.4 and 5.3 Hz, 1H), 3.03 (dd, *J* = 14.4 and 11.3 Hz, 1H), 3.05-2.77 (m, 2H), 2.64 (s, 3H), 1.40 (s, 9H); ^{13}C NMR (100 MHz, $CDCl_3$) δ 170.6, 166.8, 164.7, 159.5, 157.0, 137.5, 136.1, 132.2, 129.7 (2C), 129.4-129.0 (8C), 127.8, 127.1 (2C), 115.1, 80.9, 67.1, 56.7, 56.1 (2C), 53.1, 47.4, 36.7, 35.4, 30.3, 28.9 (3C); HRMS (ESI) calcd for $C_{35}H_{41}N_3NaO_7^+$ $[MNa]^+$ 638.2837, found 638.2847.

GENERAL PROCEDURE FOR THE SYNTHESIS OF COMPOUNDS **15-18**

Aldehyde (**1** or **2**) (1.0 mmol, 1 eq) was dissolved in 1 mL of dry methanol under nitrogen, *O*-benzyl glycine (1.0 mmol, 165 mg, 1 eq) was added and the resulting mixture was kept under stirring for 2h at room temperature. Acetic acid (1.0 mmol, 60 mg, 1 eq) and isocyanide (**5** or **6**) (1.2 mmol, 1.2 eq) were sequentially added and the reaction was stirred for additional 60h at room temperature. The resulting mixture was diluted with water (10 mL) and extracted with EtOAc (3 x 5 mL). The combined organic layers were dried over Na_2SO_4 and the solvent removed under reduced pressure to afford the crude Ugi product, which was purified by flash chromatography (FC) as indicated below.

(S)-methyl 2-((2R,3S)-2-(N-(2-(benzyloxy)-2-oxoethyl)acetamido)-3-((tert-butoxycarbonyl)(methyl)amino)butanamido)propanoate, 13a and (S)-methyl 2-((2S,3S)-2-(N-(2-(benzyloxy)-2-oxoethyl)acetamido)-3-((tert-butoxycarbonyl)(methyl)amino)butanamido)propanoate (**15b**)

Prepared according to the above general procedure from aldehyde **1** and isocyanide **5**; FC: ethyl acetate:*n*-hexane, 1:1.5; yield: **15a** (35 mg, 7%), **15b** (276 mg, 54%). **15a**: amber oil; R_f 0.18 (1:1.5 *n*-hexane/EtOAc); $[\alpha]^{30}_D$ - 3.4 (*c* 0.5, $CHCl_3$); ^{1}H NMR (300 MHz, $CDCl_3$, 1:1 mixture of rotamers) δ 7.34 (br, m, 5H), 6.62-6.27 (br, m, 1H), 5.16-5.08 (m, 2H), 5.06 (br, m, 1H), 4.79-4.61 (br, m, 1H), 4.47 (d, *J* = 19.5 Hz, 0.5H), 4.45 (d, *J* = 19.5 Hz, 0.5H), 4.23 (br, m, 1H), 4.01 (br, d, *J* = 19.5 Hz, 1H), 3.72 (s, 1.5), 3.71 (s, 1.5), 2.62 (br, s, 3H), 1.98 (br, s, 1.5), 1.95 (s, 1.5), 1.42 (s, 9H), 1.36 (d, *J* = 6.8 Hz 3H), 1.14 (br, m, 3H); ^{13}C NMR (75 MHz, $CDCl_3$, mixture of rotamers) δ 173.0 and 172.9 (1C), 172.6 and 172.4 (1C), 168.2 and 168.1 (1C), 167.8, 155.8, 135.4, 128.6-128.2 (5C), 79.4, 66.9, 57.4-56.0 (br, 1C), 52.3, 48.4, 48.1, 47.1 and 46.7 (br, 1C), 28.7, 28.4 (3C), 21.6, 18.0, 15.2 and 14.8 (1C); HRMS (ESI) calcd for $C_{25}H_{37}N_3Na\ O_8^+$ $[MNa]^+$ 530.2473, found 530.2455. **15b**: R_f 0.15 (1:1.5 *n*-hexane/EtOAc); $[\alpha]^{30}_D$ + 8.8 (*c* 0.5, $CHCl_3$); ^{1}H NMR (300 MHz, $CDCl_3$, 1:1 mixture of conformers) δ 7.35 (br, m, 5H), 6.65-6.28 (br, m, 1H), 5.17 (br, m, 3H), 4.51-4.19 (br, m, 4H), 3.70 (s, 1.5), 3.68 (s, 1.5), 2.81 (s, 3H), 2.03 (br, s, 3H), 1.42 (s, 9H), 1.32 (d, *J* = 6.8 Hz 3H), 1.15 (d, *J* = 6.8 Hz 1.5H), 1.12 (d, *J* = 6.8 Hz 1.5H), ; ^{13}C NMR (75 MHz, $CDCl_3$, mixture of rotamers) δ 172.4-172.0 (2C), 169.6, 168.9 and 168.8 (1C), 155.4 and 155.2 (1C), 135.4 and 135.2 (1C), 129.1-128.0 (5C), 80.3, 67.4 and 67.2 (1C), 59.6, 52.6,

48.5, 48.1, 47.8, 29.7, 28.4 (3C), 21.6, 17.6, 15.7 and 15.3 (1C); HRMS (ESI) calcd for $C_{25}H_{37}N_3Na\ O_8^+$ $[MNa]^+$ 530.2473, found 530.2482.

(2S)-methyl-2-((3S)-2-(N-(2-(benzyloxy)-2-oxoethyl)acetamido)-3-((tert-butoxycarbonyl)(methyl)amino)butanamido)-3-phenylpropanoate, (**16**)

Prepared according to the above general procedure from aldehyde **1** and isocyanide **6**; FC: ethyl acetate:*n*-hexane, 1:1; yield: 344 mg (59%), as an inseparable mixture of diastereoisomers (*d.e.* 80%, NMR analysis): pale yellow oil; R_f 0.27 (1:1 *n*-hexane/EtOAc); ^{1}H NMR (300 MHz, $CDCl_3$, rotameric mixture of two diastereoisomers) δ 7.41-7.03 (m, 11H), 5.28-5.10 (m, 3H), 4.78 (br, m, 0.9H), 4.78-3.93 (m, 3.1H), 3.68 (s, 0.3H), 3.65 (s, 2.7H), 3.09 (br, m, 1H), 3.01 (m, 1H), 2.75 (br, s, 2.7H), 2.58 (s, 0.3H), 1.97 (br, m, 3H), 1.42 (s, 0.9H), 1.39 (s, 8.1H), 1.09 (br, d, J = 6.8 Hz 3H); HRMS (ESI) calcd for $C_{31}H_{41}N_3NaO_8^+$ $[MNa]^+$ 606.2786, found 606.2800.

(2S)-methyl-2-((3S)-2-(N-(2-(benzyloxy)-2-oxoethyl)acetamido)-3-((tert- butoxycarbonyl)(methyl)amino)-4-phenylbutanamido)propanoate (**17**)

Prepared according to the above general procedure from aldehyde **2** and isocyanide **5**; FC: ethyl acetate:*n*-hexane, 1.5:1; yield: 256 mg (44%), as an inseparable mixture of diastereoisomers (*d.e.* 84%, NMR analysis): pale yellow oil; R_f 0.20 (1:.5 *n*-hexane/EtOAc); ^{1}H NMR (300 MHz, $CDCl_3$, rotameric mixture of two diastereoisomers) δ 7.46-7.04 (m, 11H), 5.34-5.10 (m, 3H), 4.88 (br, m, 0.9H), 4.62-3.91 (m, 3.1H), 3.73 (s, 0.24H), 3.65 (s, 2.76H), 3.32 (br, m, 1H), 3.07 (br, m, 1H), 2.81 (br, s, 2.76H), 2.65 (s, 0.24H), 2.00 (br, s, 2.76H), 1.97 (s, 0.24H), 1.43 (br, s, 9H), 1.36 (br, m, 3H); HRMS (ESI) calcd for $C_{31}H_{41}N_3NaO_8^+$ $[MNa]^+$ 606.2786, found 606.2761.

(2S)-methyl-2-((3S)-2-(N-(2-(benzyloxy)-2-oxoethyl)acetamido)-3-((tert-butoxycarbonyl)(methyl)amino)-4-phenylbutanamido)-3-phenylpropanoate (**18**)

Prepared according to the above general procedure from aldehyde **2** and isocyanide **6**; FC: ethyl acetate:*n*-hexane, 1:1.5; yield: 587 mg (89%), as an inseparable mixture of diastereoisomers (*d.e.* 72%, NMR analysis): colorless oil; R_f 0.18 (1.5:1 *n*-hexane/EtOAc); ^{1}H NMR (300 MHz, $CDCl_3$, rotameric mixture of two diastereoisomers) δ 7.43-7.01 (m, 16H), 5.29-5.09 (m, 3H), 4.88 (m, 0.86H), 4.74 (m, 0.14H), 4.64-4.43 (m, 1.86H), 4.29 (m, 0.14H), 4.01 (br, d, J = 16.6 Hz, 1H), 3.74 (s, 0.24H), 3.67 (s, 1.26H), 3.65 (s, 1.5H), 3.54-2.84 (m, 4H), 2.70 (s, 2.52H), 2.63 (s, 0.48H), 2.07 (s, 0.24H), 1.98 (s, 1.5H), 1.95 (s, 1.26H), 1.41 (s, 9H); HRMS (ESI) calcd for $C_{37}H_{45}N_3NaO_8^+$ $[MNa]^+$ 682.3099, found 682.3114.

GENERAL PROCEDURE FOR THE SYNTHESIS OF COMPOUNDS **19-22**

Palladium (10 wt.% on carbon, 70 mg) was added to a solution of the Ugi product (**15a**, **15b**, **16**, **17** or **18**) (0.30 mmol, 1 eq) in methanol (3 mL). The reaction mixture was degassed *in vacuo*, placed under an atmosphere of H_2 (g), and stirred in the dark at rt for 2h. The mixture was filtered through a pad of Celite eluting with methanol (10 mL), and the combined organic layers were concentrated *in vacuo* to give the crude carboxylic acid intermediate, which was directly used in the next step, as follows. 1,1'- Carbonyl diimidazole (0.30 mmol, 127 mg, 1 eq) was added to a solution of the crude carboxylic acid in dry tetrahydrofuran (3 mL), under nitrogen, and the resulting mixture was refluxed for 60 min and then stirred for additional 3h at room temperature. The solvent was removed under reduced pressure to give a residue which was partitioned between $CHCl_3$ (10 mL) and 1M HCl, (10 mL). The aqueous phase was extracted with $CHCl_3$ (3 x 10 mL) and the combined organic layers were washed with H_2O, dried over Na_2SO_4 and concentrated *in vacuo* to afford the crude product, which was purified by flash chromatography (FC), as indicated below.

(S)-methyl 2-((R)-4-acetyl-3-((S)-1-((tert-butoxycarbonyl)(methyl)amino)ethyl)-2,6-dioxopiperazin-1-yl)propanoate (**19a**)

Prepared according to the above general procedure from **15a**; FC: ethyl acetate:*n*-hexane, 7:3; yield: 18 mg (15%); colorless oil; R_f 0.33 (3:7 *n*-hexane/EtOAc); $[\alpha]^{30}_D$ - 15.6 (*c* 0.5, $CHCl_3$); ^{1}H NMR (300 MHz, $CDCl_3$) δ 4.63-3.90 (m, 5H), 3.72 (br, s, 3H), 2.82 (br, s, 3H), 2.08 (br, s, 3H), 1.45 (s, 9H), 1.37 (br, d, J = 6.8 Hz, 3H), 1.12 (br, d, J = 6.8 Hz, 3H); ^{13}C NMR (100 MHz, $CDCl_3$) δ 170.1, 169.1, 167.0, 166.5 and 166.4 (1C), 155.9, 80.5, 55.0, 52.5, 49.5, 48.8, 46.5, 29.0, 28.3 (3C), 21.1, 15.5 and 15.4 (1C), 14.2 and 13.9 (1C); HRMS (ESI) calcd for $C_{18}H_{29}N_3NaO_7^+$ $[MNa]^+$ 422.1898, found 422.1924.

(S)-methyl 2-((S)-4-acetyl-3-((S)-1-((tert-butoxycarbonyl)(methyl)amino)ethyl)-2,6-dioxopiperazin-1-yl)propanoate (**19b**)

Prepared according to the above general procedure from **15b**; FC: ethyl acetate:*n*-hexane, 7:3; yield: 71 mg (59%); colorless oil; R_f 0.29 (3:7 *n*-hexane/EtOAc); $[\alpha]^{30}_D$ + 39.9 (*c* 0.5, $CHCl_3$); ^{1}H NMR (400 MHz, $CDCl_3$, mixture of conformers 1.5:1) δ 5.36 (br, d, *J* = 9.9 Hz, 1H), 5.19 (m, 1H), 4.72 (m, 1H), 4.57 (d, *J* = 18.7 Hz, 0.6H), 4.52 (d, *J* = 18.7 Hz, 0.4H), 4.29 (d, *J* = 18.7 Hz, 0.4H), 4.24 (d, *J* = 18.7 Hz, 0.6H), 3.68 (s, 1.8H), 3.67 (s, 1.2H), 2.82 (br, s, 1.8H), 2.80 (s, 1.2H), 2.23-2.15 (m, 3H), 1.52 (d, *J* = 7.0 Hz, 1.8H), 1.45 (d, *J* = 7.0 Hz, 1.2H), 1.44-1.38 (m, 9H), 1.19 (br, d, *J* = 6.5 Hz, 3H); ^{13}C NMR (100 MHz, $CDCl_3$) δ 169.9, 169.0, 167.0, 166.4, 156.1, 80.2, 54.7, 52.4, 49.4, 48.7, 46.8, 28.9, 28.3 (3C), 21.4, 15.5, 14.1; HRMS (ESI) calcd for $C_{18}H_{29}N_3NaO_7^+$ $[MNa]^+$ 422.1898, found 422.1917.

(2S)-methyl-2-(4-acetyl-3-((S)-1-((tert-butoxycarbonyl)(methyl)amino)ethyl)-2,6-dioxopiperazin-1-yl)-3-phenylpropanoate (**20**)

Prepared according to the above general procedure from **16**; FC: ethyl acetate:*n*-hexane, 1.5:1; yield: 105 mg (74%), as an inseparable mixture of diastereoisomers (*d.e.* 80%, NMR analysis); foam; R_f 0.36 (1:1.5 *n*-hexane/EtOAc); ^{1}H NMR (400 MHz, CD_3CN, mixture of two diastereoisomers) δ 7.34-7.03 (m, 5H), 5.56-5.37 (br, m, 1.9H), 4.59 (br, m, 1H), 4.57 (d, *J* = 18.7 Hz, 1H), 4.83-4.11 (m, 2H), 3.66 (br, s, 3H), 3.43 (m, 1H), 3.17-2.99 (m, 1H), 2.79 (s, 0.3H), 2.77 (s, 2.7H), 2.23 (s, 2.7H), 2.14 (s, 0.3H), 1.42 (s, 9H), 1.14 (m, 3H); ^{13}C NMR (101 MHz, CD_3CN), δ 170.2-167.8 (4C), 156.3 and 156.0 (1C), 138.2, 129.8 (2C), 129.0 (2C), 127.3 (1C), 80.4, 54.2-53.8 (2C), 52.8, 51.4 and 50.9 (1C), 47.1 and 46.9 (1C), 34.7, 30.4, 28.4 (3C), 21.3, 15.2 and 14.8 (1C); HRMS (ESI) calcd for $C_{24}H_{33}N_3NaO_7^+$ $[MNa]^+$ 498.5239, found 498.5223.

(2S)-methyl-2-(4-acetyl-3-((S)-1-((tert-butoxycarbonyl)(methyl)amino)-2-phenylethyl)-2,6-dioxopiperazin-1-yl)propanoate (**21**)

Prepared according to the above general procedure from **17**; FC: ethyl acetate:*n*-hexane, 1:1.5; yield: 110 mg (77%), as an inseparable mixture of diastereoisomers (*d.e.* 95%, NMR analysis); foam; R_f 0.13 (1.5:1 *n*-hexane/EtOAc); ^{1}H NMR (400 MHz, CD_3CN,1:1 rotameric mixture) δ 7.37-7.19 (m, 5H), 5.50(m, 1H), 5.25 (m, 1H), 5.02-4.58 (m, 2H), 4.41 (d, *J* = 18.6 Hz, 1H), 3.66 (s, 1.5H), 3.65 (s, 1.5H), 3.04-2.77 (br, m, 2H), 2.79 (s, 3H), 2.18 (s, 3H), 1.45 (d, *J* = 6.9 Hz, 1.5H), 1.44 (d, *J* = 6.9 Hz, 1.5H), 1.35 (br, m, 9H); ^{13}C NMR (100 MHz, CD_3CN), δ 170.7 and 170.1 (1C), 170.0-169.7 (1C), 169.1, 167.5, 156.2 and 156.1 (1C), 137.8, 129.1, 128.9, 128.3 (2C), 126.5 and 126.4 (1C), 79.7 and 79.4 (1C), 56.4, 54.9 and 54.5 (1C), 52.0, 48.3, 46.7, 34.4 and 34.3 (1C), 27.9, 27.5 (3C), 20.9, 13.6 and 13.4 (1C); HRMS (ESI) calcd for $C_{24}H_{33}N_3NaO_7^+$ $[MNa]^+$ 498.2211, found 498.2225.

(2S)-methyl-2-(4-acetyl-3-((S)-1-((tert-butoxycarbonyl)(methyl)amino)-2-phenylethyl)-2,6-dioxopiperazin-1-yl)-3-phenylpropanoate, (**22**)

Prepared according to general procedure above from **18**; FC: ethyl acetate:*n*-hexane, 1:1.5; yield: 117 mg (71%), as an inseparable mixture of diastereoisomers (*d.e.* 80%, NMR analysis); thick oil; R_f 0.39 (1.5:1 *n*-hexane/EtOAc); ^{1}H NMR (400 MHz, CD_3CN, rotameric mixture of two distereoisomers) δ 7.36-7.07 (m, 10H), 5.56-5.40 (m, 1H), 5.14 (d, *J* = 9.3 Hz, 0.9H), 5.03 (d, *J* = 10.5 Hz, 0.1H), 4.95-4.80 (m, 0.9H), 4.65 (d, *J* = 18.5 Hz, 0.1H), 4.62 (d, *J* = 18.6 Hz, 0.9H), 4.42 (m, 0.1H), 4.33 (d, *J* = 18.5 Hz, 1H), 3.71 (s, 0.3H), 3.66 (s, 2.7H), 3.59-3.38 (m, 1H), 3.19-3.03 (m, 1H), 2.92-2.80 (m, 1H), 2.80-2.67 (m, 1H), 2.67 (s, 2.7H), 2.58 (s, 0.3H), 2.10 (s, 2.7H), 2.08 (s, 0.3H), 1.45 (br, s, 9H); ^{13}C NMR (101 MHz, CD_3CN), δ 169.7-168.5 (3C), 167.8 and 167.6 (1C), 154.7 and 154.6 (1C), 138.3-137.8 (1C), 137.2-137.0 (1C), 129.1 (4C), 128.4 and 128.3 (4C), 126.7-126.4 (2C), 79.7-79.4 (1C), 56.2, 54.9-54.6 (1C), 53.8, 52.1 and 52.0 (1C), 46.8 and 46.5 (1C), 34.4-34.2 (2C), 27.9, 27.7 (3C), 21.0 and 20.8 (1C); HRMS (ESI) calcd for $C_{30}H_{37}N_3NaO_7^+$ $[MNa]^+$ 574.2524, found 574.2506.

GENERAL PROCEDURE FOR THE SYNTHESIS OF COMPOUNDS **23-26**

Aldehyde (**3** or **4**) (1.0 mmol, 1 eq) was dissolved in 1 mL of dry methanol under nitrogen, 2,2-diethoxyethanamine (1.0 mmol, 133 mg, 1 eq) was added and the resulting mixture was kept stirring for 2h at room temperature. Benzoic acid (1.0 mmol, 122 mg, 1 eq) and isocyanide (**5** or 6) (1.2 mmol, 1.2 eq) were sequentially added and the reaction was stirred for additional 24h at room temperature. The solvent was removed under reduced pressure, to afford the unstable crude Ugi product, which was directly used in the next step. The crude was dissolved in 4.5 mL of 50% trifluoroacetic acid in dichloromethane, and the resulting solution was kept under stirring for 24h. The solvent was removed under reduced pressure to give a residue which was dissolved in EtOAc (10 mL) and washed with satd aq $NaHCO_3$ (2 x 10 mL). The organic layer was dried over Na_2SO_4 and concentrated *in vacuo*, to afford the crude

product, which was purified by flash chromatography (FC) as indicated below.

(S)-methyl 2-((R)-4-benzoyl-3-((S)-1-(((benzyloxy)carbonyl)(methyl)amino)ethyl)-2-oxo-3,4-dihydropyrazin-1(2H)-yl)propanoate, 23a and (S)-methyl 2-((S)-4-benzoyl-3-((S)-1-(((benzyloxy)carbonyl)(methyl)amino)ethyl)-2-oxo-3,4-dihydropyrazin-1(2H)-yl)propanoate (**23b**)

Prepared according to the above general procedure from aldehyde **3** and isocyanide **5**; FC: ethyl acetate:*n*-hexane, 7:3; yield: **23a** (24 mg, 5%), **23b** (311 mg, 65%). **23a**: thick oil; R_f 0.30 (7:3 *n*-hexane/ EtOAc); $[\alpha]^{30}_D$ - 22.4 (*c* 0.5, $CHCl_3$); ^{1}H NMR (300 MHz, $CDCl_3$) δ 7.60-7.20 (m, 10H), 6.04 (br, d, *J* = 5.9 Hz, 1H), 5.68 (d, *J* = 5.9 Hz, 1H), 5.28 (br, d, *J* = 9.2 Hz, 1H), 5.20-4.61 (m, 4H), 3.74 (s, 3H), 2.92 (s, 3H), 1.52 (d, *J* = 7.0 Hz, 3H), 1.24 (br, m, 3H); ^{13}C NMR (75 MHz, $CDCl_3$) δ 170.9, 168.1, 162.9, 155.0, 136.7, 132.3, 130.8, 128.5-127.7 (9C), 112.3, 110.6, 67.2, 56.8, 52.6, 52.0, 48.0, 29.7, 15.2, 14.9; HRMS (ESI) calcd for $C_{26}H_{29}N_3NaO_6^+$ $[MNa]^+$ 502.1949, found 502.1953. **23b**: foam; R_f 0.37 (7:3 *n*-hexane/ EtOAc); $[\alpha]^{20}_D$ + 27.6 (*c* 1.0, $CHCl_3$); ^{1}H NMR (400 MHz, $CDCl_3$, 1:1 mixture of rotamers) *δ* 7.61-7.40 (m, 5H), 7.39-7.27 (m, 5H), 5.96 (br, m, 0.5H), 5.88 (br, d, *J* = 5.4 Hz, 0.5H), 5.73 (m, 1H), 5.42-5.29 (m, 1H), 5.20-4.95 (m, 3H), 4.93-4.74 (m, 1H), 3.77 (s, 1.5H), 3.74 (s, 1.5H), 3.00 (s, 1.5H), 2.94 (s, 1.5H), 1.50 (d, *J* = 7.1 Hz, 1.5H), 1.38 (d, *J* = 7.3 Hz, 1.5H), 1.35-1.24 (m, 3H); ^{13}C NMR (100 MHz, $CDCl_3$) *δ* 171.6 and 170.9 (1C), 168.7 and 168.6 (1C), 163.1 and 162.9 (1C), 156.6, 137.0, 134.0 and 133.9 (1C), 131.1 and 131.0 (1C), 128.6-127.4 (9C), 111.9 and 111.0 (1C), 111.4 and 110.3 (1C), 67.3 and 67.0 (1C), 57.9 and 57.1 (1C), 52.5, 52.0 and 50.3 (1C), 50.1 and 49.0 (1C), 29.1 and 28.8 (1C), 15.9-14.4 (2C); HRMS (ESI) calcd for $C_{26}H_{29}N_3NaO_6^+$ $[MNa]^+$ 502.1949, found 502.1961.

(S)-methyl 2-((R)-4-benzoyl-3-((S)-1-(((benzyloxy)carbonyl)(methyl)amino)ethyl)-2-oxo-3,4-dihydropyrazin-1(2H)-yl)-3-phenylpropanoate, 24a and (S)-methyl 2-((S)-4-benzoyl-3-((S)-1-(((benzyloxy)carbonyl)(methyl)amino)ethyl)-2-oxo-3,4-dihydropyrazin-1(2H)-yl)-3-phenylpropanoate (**24b**)

Prepared according to the above general procedure from aldehyde **3** and isocyanide **6**; FC: ethyl acetate:*n*-hexane, 3:7; yield: **24a** (16 mg, 3%), **24b** (223 mg, 40%). **24a**: colorless oil; R_f 0.23 (7:3 *n*-hexane/ EtOAc); $[\alpha]^{20}_D$ - 13.6 (*c* 0.9, $CHCl_3$); ^{1}H NMR (300 MHz, $CDCl_3$) *δ* 7.61- 7.08 (m, 15H), 5.93 (br, d, *J* = 5.9 Hz, 0.7H), 5.75 (br, d, *J* = 5.9 Hz, 0.3H), 5.66 (d, *J* = 5.9 Hz, 0.7H), 5.60 (d, *J* = 5.9 Hz, 0.3H), 5.36-4.97 (m, 4H), 4.72 (m, 0.3H), 4.33 (dq, *J* = 10.7 and 6.8 Hz, 0.7H), 3.82 (s, 2.1H), 3.80 (s, 0.9H), 3.48 (dd, *J* = 14.7 and 4.9 Hz, 0.7H), 3.43 (dd, *J* = 14.7 and 4.9 Hz, 0.3H), 3.17 (dd, *J* = 14.7 and 12.7 Hz, 0.7H), 3.04 (dd, *J* = 13.8 and 11.7 Hz, 0.3H), 2.92 (s, 0.9H), 2.85 (s, 2.1H), 0.73 (d, *J* = 6.8 Hz, 2.1H), 0.64 (d, *J* = 6.8 Hz, 0.9H); ^{13}C NMR (75 MHz, $CDCl_3$) *δ* 170.0, 168.7, 163.7 and 163.2 (1C), 155.9, 136.0, 135.7, 133.8, 130.8, 129.1-127.2 (14C), 111.8 and 111.3 (1C), 111.0 and 110.0 (1C), 67.4 and 67.0 (1C), 57.7, 56.7, 55.0, 52.7, 34.8, 28.5, 14.6 and 14.3 (1C); HRMS (ESI) calcd for $C_{32}H_{33}N_3NaO_6^+$ $[MNa]^+$ 578.2262, found 578.2250. **24b**: oil; R_f 0.27 (7:3 *n*-hexane/ EtOAc); $[\alpha]^{20}_D$ + 34.5 (*c* 1.0, $CHCl_3$); ^{1}H NMR (400 MHz, $CDCl_3$) *δ* 7.56- 7.18 (m, 15H), 5.90 (d, *J* = 5.9 Hz, 0.7H), 5.78 (br, d, J = 5.7 Hz, 1H), 5.72 (dd, J = 11.3 and 5.4 Hz, 0.3H), 5.59 (m, 1H), 5.38 (br, d, J = 9.3 Hz, 0.7H), 5.23-5.01 (m, 2.3H), 4.83 (br, m, 1H), 3.73 (s, 2.1H), 3.70 (s, 0.9H), 3.45 (dd, *J* = 14.4 and 5.4 Hz, 0.3H), 3.40 (dd, *J* = 14.4 and 5.7 Hz, 0.7H), 3.02 (dd, *J* = 14.4 and 10.8 Hz, 1H), 2.90 (s, 2.1H), 2.86 (s, 0.9H), 1.25 (m, 3H); ^{13}C NMR (100 MHz, $CDCl_3$) δ 170.2, 168.6, 163.7 and 163.3 (1C), 156.6 and 156.0 (1C), 137.0 and 136.6 (1C), 135.7, 133.9, 131.0, 129.3-126.9 (14C), 112.7 and 111.6 (1C), 111.4 and 110.4 (1C), 67.0 and 66.9 (1C), 57.8 and 57.4 (1C), 54.6 and 54.4 (1C), 52.5, 49.9 and 49.7 (1C), 36.7, 28.9, 15.2 and 15.1 (1C); HRMS (ESI) calcd for $C_{32}H_{33}N_3NaO_6^+$ $[MNa]^+$ 578.2262, found 578.2248.

(S)-methyl 2-((R)-4-benzoyl-3-((S)-1-(((benzyloxy)carbonyl)(methyl)amino)-2-phenylethyl)-2-oxo-3,4dihydropyrazin-1(2H)-yl)propanoate, 25a and (S)-methyl 2-((S)-4-benzoyl-3-((S)-1-(((benzyloxy)carbonyl)(methyl)amino)-2-phenylethyl)-2-oxo-3,4-dihydropyrazin-1(2H)-yl)propanoate (**25b**)

Prepared according to the above general procedure from aldehyde **4** and isocyanide **5**; FC: ethyl acetate:*n*-hexane, 1:1.5; yield: **25a** (27 mg, 5%), **25b** (372 mg, 67%). **25a**: colorless oil; R_f 0.19 (1.5:1 *n*-hexane/ EtOAc); $[\alpha]^{20}_D$ - 5.9 (*c* 0.5, $CHCl_3$); ^{1}H NMR (300 MHz, $CDCl_3$) *δ* 7.74-6.96 (m, 15 H), 6.47 (d, *J* = 6.8 Hz, 0.5H), 6.32 (d, *J* = 6.8 Hz, 0.5H), 6.09-6.01 (m, 0.5H), 5.93-5.84 (m, 0.5H), 5.36-4.83 (m, 4.5H), 4.49 (m, 0.5H), 3.75 (s, 1.5H), 3.70 (s, 1.5H), 3.18-2.69 (m, 5H), 1.32 (d, *J* = 7.8 Hz, 3H); ^{13}C NMR (75 MHz, $CDCl_3$) *δ* 173.0, 167.4, 162.8, 160.2 and 159.6 (1C), 137.2, 136.2, 133.0, 131.8, 129.4-127.1 (14C), 112.1-112.3 (2C), 68.1 and 66.8 (1C), 53.4, 52.8, 52.5, 48.3, 37.9 and 37.6 (1C), 29.1, 18.2; HRMS (ESI) calcd for $C_{32}H_{33}N_3NaO_6^+$ $[MNa]^+$ 578.2262, found 578.2270. **25b**: pale yellow oil; R_f 0.35 (1.5:1 *n*-hexane/ EtOAc); $[\alpha]^{20}_D$ - 72.1 (*c* 0.5, $CHCl_3$); ^{1}H NMR (400 MHz, $CDCl_3$) *δ* 7.61- 7.11 (m, 15H), 5.91 (br, d, *J* = 5.6 Hz, 0.6H), 5.82-5.74 (m, 1H), 5.70 (d, *J* = 5.8 Hz, 0.4H), 5.51 (d, *J* = 9.8 Hz, 0.6H), 5.42 (d, *J* = 7.6 Hz, 0.4H), 5.13 (m, 1H), 5.06-4.90 (m, 2.6H), 4.81 (d, *J* = 13.0 Hz, 0.4H), 3.77 (s, 1.8H), 3.74 (s, 1.2H), 3.17-2.92 (m, 1.6H), 2.97 (s, 1.8H),

2.87 (s, 1.2H), 2.78 (dd, *J* = 13.9 and 8.1 Hz, 0.4H), 1.49 (d, *J* = 7.2 Hz, 1.2H), *J* = 7.5 Hz, 1.8H); ^{13}C NMR (100 MHz, $CDCl_3$) δ 170.7, 169.3, 163.3, 157.5 and 157.0 (1C), 138.0 and 137.8 (1C), 137.3 and 137.1 (1C), 134.5 and 134.3 (1C), 132.0 and 131.7 (1C), 129.4-127.1 (14C), 113.4-111.1 (2C), 67.9 and 67.5 (1C), 59.3 and 58.4 (1C), 57.4 and 54.1 (1C), 53.2 and 52.9 (1C), 51.3 and 51.0 (1C), 36.2 and 35.6 (1C), 29.9 and 29.8 (1C), 15.5 and 15.0 (1C); HRMS (ESI) calcd for $C_{32}H_{33}N_3NaO_6^+$ $[MNa]^+$ 578.2262, found 578.2268.

(S)-methyl 2-((R)-4-benzoyl-3-((S)-1-(((benzyloxy)carbonyl)(methyl)amino)-2-phenylethyl)-2-oxo-3,4-dihydropyrazin-1(2H)-yl)-3-phenylpropanoate, 26a and (S)-methyl 2-((S)-4-benzoyl-3-((S)-1-(((benzyloxy)carbonyl)(methyl)amino)-2-phenylethyl)-2-oxo-3,4-dihydropyrazin-1(2H)-yl)-3-phenylpropanoate (**26b**)

Prepared according to the above general procedure from aldehyde **4** and isocyanide **6**; FC: ethyl acetate:*n*-hexane, 3:7; yield: **26a** (56 mg, 9%), **26b** (284 mg, 45%). **26a**: colorless oil; R_f 0.22 (7:3 *n*-hexane/ EtOAc); $[\alpha]^{30}_D$ - 11.1 (*c* 0.5, $CHCl_3$); ^{1}H NMR (300 MHz, $CDCl_3$, complex mixture of conformers) δ 7.68-6.81 (m, 20H), 6.38 (d, *J* = 5.8 Hz, 0.1H), 5.94-5.80 (m, 0.7H), 5.79-5.72 (m. 0.2H), 5.72-5.54 (m, 1H), 5.51-5.37 (m, 0.5H), 5.31-4.65 (m, 4.5H), 3.74 (s, 0.3H), 3.70 (s, 2H), 3.67 (s, 0.7H), 3.49-3.18 (m, 1H), 3.16-2.87 (m, 3H), 2.83 (s, 0.7H), 2.80 (s, 2H), 2.72 (s, 0.3H); ^{13}C NMR (75 MHz, $CDCl_3$) δ 170.2-169.6 (1C), 168.9-168.4 (1C), 163.6 and 163.1 (1C), 157.0 and 156.8 (1C), 137.3-135.7 (4C), 131.8-130.9 (1C), 129.3-126.5 (19C), 112.5-106.7 (2C), 68.1-66.8 (1C), 58.0 and 57.7 (1C), 57.3-57.0 (1C), 55.8-55.3 (1C), 54.1-52.2 (2C), 38.0-37.6 (1C), 35.3-34.7 (1C), 29.4 and 29.0 (1C); HRMS (ESI) calcd for $C_{38}H_{37}N_3NaO_6^+$ $[MNa]^+$ 654.2575, found 654.2561. **26b**: foam; R_f 0.30 (7:3 *n*-hexane/ EtOAc); $[\alpha]^{20}_D$ - 139.8 (*c* 1.0, $CHCl_3$); ^{1}H NMR (400 MHz, CD_3CN, mixture of two conformers 1.5:1) δ 7.64-7.01 (m, 20H), 6.01 (m, 0.8H), 5.96 (d, *J* = 5.9 Hz, 0.6H), 5.79 (d, *J* = 5.4 Hz, 0.6H), 5.63 (dd, *J* = 11.1 and 5.4 Hz, 0.4H), 5.53 (dd, *J* = 10.8 and 5.4 Hz, 0.6H), 5.15-4.87 (m, 3.6H), 4.69 (d, *J* = 12.9 Hz, 0.4H), 3.71 (s, 3H), 3.43 (dd, *J* = 14.7 and 5.4 Hz, 0.4H), 3.37 (dd, *J* = 14.7 and 5.4 Hz, 0.6H), 3.08 (dd, *J* = 14.7 and 11.1 Hz, 0.4H), 3.07 (dd, *J* = 14.7 and 0.81 Hz, 0.6H), 3.04-2.87 (m, 2H), 2.83 (s, 3H); ^{13}C NMR (100 MHz, CD_3CN) δ 170.1 and 169.9 (1C), 168.5 and 168.4 (1C), 163.6 and 163.3 (1C), 156.6 and 155.8 (1C), 138.0 and 137.4 (1C), 136.5 and 136.4 (2C), 134.2 and 133.8 (1C), 131.1 and 130.9 (1C), 129.1-126.4 (19C), 112.0-111.5 (2C), 66.5 and 66.3 (1C), 57.2 and 57.1 (1C), 56.0, 55.1-54.8 (2C), 52.2 and 52.1 (1C), 36.1 and 35.9 (1C), 34.9 and 34.6 (1C), 29.0 and 28.8 (1C); HRMS (ESI) calcd for $C_{38}H_{37}N_3NaO_6^+$ $[MNa]^+$ 654.2575, found 654.2558.

COMPUTATIONAL STUDIES

Conformational analysis on compound 11.

MMFF and DFT calculations were run with Spartan'10 (Wavefunction, Inc., Irvine CA, 2010), with standard parameters and convergence criteria. TDDFT calculations were run with Gaussian'09,[27] with default grids and convergence criteria. Conformational searches were run with the Monte Carlo algorithm implemented in Spartan'10 using Merck molecular force field (MMFF) in vacuo. All structures thus obtained were optimized with DFT method using B3LYP functional and 6-31G(d) basis set in vacuo. TDDFT calculations were run using CAM-B3LYP functional and SVP basis set, including 36 excited states (roots). On some representative structures, we verified the consistency with the results obtained with the larger TZVP basis set. CD spectra were generated using the program SpecDis[29] by applying a Gaussian band shape with 0.3 eV exponential half-width, from dipole-length rotational strengths. The difference with dipole-velocity values was checked to be minimal for all relevant transitions.

Computational studies on models a, b and c.

The starting geometries of compounds **a**, **b** and **c** (**Figure 14**), created by GaussView,[27] were energy minimized by the conjugate gradient algorithm implemented in Gaussion09.[27] Thus, The optimized geometries were subjected to heating, equilibration, and molecular dynamics simulation by *sander* module of AMBER 12.[25] GAFF force field were used for the parametrization of the molecules, modeled as neutral compounds in an implicit GB solvent model and a dielectric continuum of 80 (simulating water).[26] With a time step 2 fs, each peptidomimetic was heated to 300 K, 700 K and then to 1000 K over 20 ps. After an equilibration phase of 2 ns, each model were frozen to 700 K and then to 300 K, over 20 ps. The production run of the MD simulations were performed for a total time of 20 ns with trajectories saved every 10 ps. The resulting structures in the trajectories were visually analyzed by VMD.[30] In this stage, the fluctuation of the diverse torsion angles were analyzed and the different families of conformers were identified. They were then minimized by Gasussian09 at DFT/B3LYP/6-31g(d) level of theory and the lowest energy conformation and the Boltzmann equation was applied to calculate the conformers percentage distribution (**Figure**

14). C^6-C^6 distances were measured by GaussView.

BIOLOGICAL EVALUATION

Cytotoxicities of compounds **11-14**, **19-22** *and* **23-26**.

Cytotoxic activities were investigated using the NCI-SRB method on epithelial-like (Huh7) and PTEN deficient mesenchymal like Mahlavu cells.[31] Cytotoxic effects of the compounds were observed after 72 hours (see Supporting Information). Human liver cancer cells (Huh7 and Mahlavu,) were grown in Dulbecco's Modified Eagle Medium **(**DMEM), with 10% fetal bovine serum, 1% non-essential amino acids and 1% penicillin/streptomycin (GIBCO, Invitrogen) at 37 °C under 5% CO_2.

NCI-60 Sulforhodamine B (SRB) assay.

Huh7 and Mahlavu liver cancer cells were grown in 96-well plates (2000-cells/well in 150 µl). After 24hr one plate for each cell line was fixed with 100µl 10% ice-cold trichloroacetic acid (TCA). This plate represents the behavior of the cells just prior to drug treatment and is accepted as the time-zero plate (T_z). Then they were treated with serial dilution concentrations of the compounds (40, 20, 10, 5, 2.5 µM) dissolved in Dimethyl sulfoxide (DMSO). Corresponding DMSO vehicle were also applied to Huh7 and Mahlavu cells as negative controls. DMSO concentrations were always below 0.01%. After 72h, cells were washed with 1xPBS ($CaCl_2$-, $MgCl_2$-free) (Gibco, Invitrogen), and then fixed with cold 10% (v/v) trichloroacetic acid (MERCK). Microplates were left for 1h at 4°C, then washed with water and left to dry. The plates were then stained with 100µl of 0.4% sulphorhodamine B (SRB) (Sigma Aldrich) in 1% acetic acid solution for 10min. The unbound SRB was washed with 1% acetic acid. SRB was then solubilized in 200µl of 10mM Tris-base solution. The absorbance was read at 515 nm. The experiment was performed in duplicate and the absorbance values were normalized to DMSO controls and T_z values. Standard deviations were less than 10%.

2.2 Diamine-based peptidomimetics

Introduction

A widely recognized and successful method to develop new peptidomimetics is to modify the backbone by replacing an amino acid unit within a peptide sequence with an organic fragment. This strategy is called single amino acid modification and, by selecting the appropriate constraining element, it is possible to reduce the conformational flexibility, improving the target specificity and pharmacokinetic properties of the parental peptide.[29]

Among the possible modifications, few reports are present in the literature on the introduction of a cyclic symmetric secondary diamine in the amino acid sequence.[30,31] This class of conformationally constrained peptidomimetics able to disrupt protein-protein interactions (PPIs) will be referred as diamine based-peptidomimetics in the present thesis.

In particular, Haridas and co-workers[32] employed bispidine (3,7-diazabicyclo[3.3.1]nonane) as a secondary structure nucleator. Indeed, when both the nitrogens of this peculiar bicyclic symmetric secondary diamine are alkylated an open-turn is observed, while a β-sheet conformation is induced when both nitrogens are acylated. On the other hand, a helical conformation can be obtained if one nitrogen is alkylated and the other one acylated (**Figure 15a**).[30] Helix is one of the most common peptide secondary structures and a major recognition motif of PPIs, currently a compelling therapeutic target for small molecules-based drug discovery.[33]

Dutta and co-workers reported the introduction of a piperazine moiety in a cyclic peptide containing the Ile-Leu-Asp-Val sequence to be beneficial for its activity against the specific PPI VLA-4-mediated MOLT-4 adhesion. In particular, this peptidomimetic (**Figure 15b**) shows promising results both *in vitro* and *in vivo* targeting, and represents therefore an important lead compound for the development of new treatments for inflammatory and autoimmune diseases.[31]

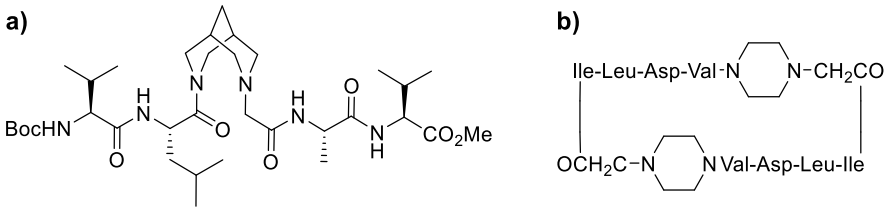

Figure 15. Examples of diamine-based peptidomimetics able to disrupt PPIs.[30,31]

We believe such unexplored class of potential PPIs modulators virtually accessible through the *N*-split Ugi methodology (*for further details see* **Chapter 1.2**), in a very straightforward manner. Therefore, by employing amino acid-derived chiral reactants, such as *N*-protected amino acids and α-isocyanoacetates, we developed a stereoconservative protocol for obtaining diamine-based peptidomimetics in a one-pot process (**Scheme 23**). Moreover, we choose piperazine and bispidine as diamine substrates, being able to induce a certain conformation or to increase the activity in the related biological relevant diamine-based peptidomimetics.

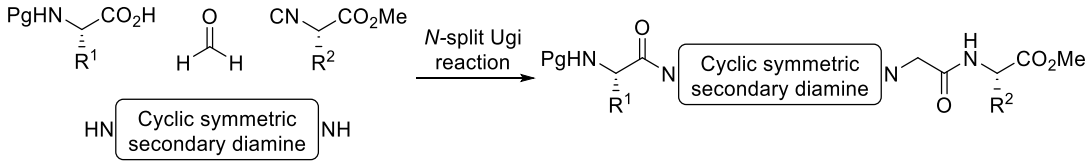

Scheme 23. Multicomponent approach for the synthesis of diamine-based peptidomimetics through *N*-split Ugi reaction.

Results and discussion

Firstly, we evaluated the compatibility of *N*-protected amino acids in the *N*-split Ugi reaction conditions, by employing the commercially available *N*-Boc-L-alanine in combination with the well-studied piperazine as the secondary diamine component (*for further details see* **Chapter 1.2**). Paraformaldehyde was chosen as the carbonyl source, being easy-to-handle polymeric form of the simplest not prochiral aldehyde.

Although the believed, but surmountable, configurational instability of chiral α-substituted isocyanoacetates was extensively studied in the parental U-4CR (*for further details see* **Chapter 1.1**), as far as we know no such efforts have been done in the *N*-split Ugi reaction. Therefore, we slightly modified the conditions reported by Sello and coworkers,[20] and successfully applied by us[9] (*for further details see* **Chapter 2.1**), by adding the carboxylic acid component *N*-Boc-L-alanine **27a** in the initial preformation step, with the aim to counteract the basicity of the second nitrogen of the piperazine **28a**, and by increasing the temperature to depolymerize the paraformaldehyde. The subsequent addition of isocyanides **29a-c** or optically pure methyl (*S*)-2-isocyanopropanoate **5**, at room temperature, smoothly afforded the desired *N*-split Ugi adducts **30a-d** (**Scheme 24**).

In particular, bulky *tert*-butyl isocyanide **29a** and 2-isocyano-2,4,4-trimethylpentane **29b** can be successfully employed, affording the corresponding products **30a**-**b** in moderate to good yields. By using commercially available methyl isocyanoacetate **29c**, the first piperazine-based peptidomimetic **30c** can be obtained in good yields, bearing L-Ala and Gly amino acids residues. As expected, no appreciable loss of optical purity was observed when methyl (*S*)-2-isocyanopropanoate **5** was employed as reactant. Compound **5** was prepared following the Danishefsky's procedure[19] as shown in **Scheme 19** (**Chapter 2.1**). Indeed,

piperazine-based peptidomimetic **30d** was isolated in good yield and excellent diastereoisomeric purity (from ^{1}H-NMR and ^{13}C-NMR).

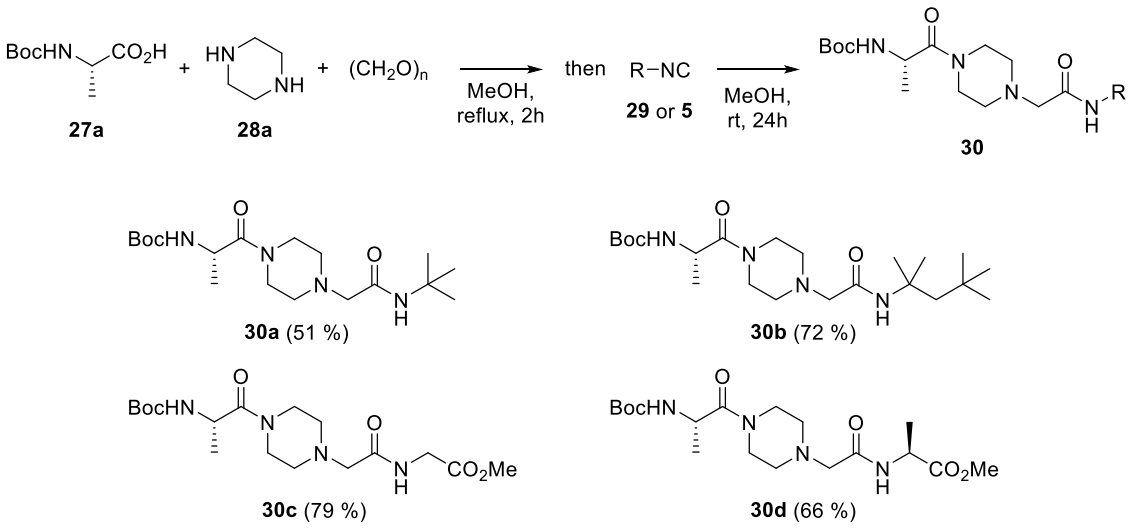

Scheme 24. One-pot synthesis of piperazine-based peptidomimetics **30a-d** *via N*-split Ugi reaction employing chiral components.

At the best of our knowledge, bicyclic symmetric secondary diamines were never reported as viable substrates in the *N*-split Ugi reaction (*for further details see* **Chapter 1.2**). In particular, the conformationally constrained bispidine was supposed to be a less trivial substrate, with respect to piperazine. First of all, we applied the same reaction conditions described above, using benzoic acid **27b** and 1-(isocyanomethyl)-4-methoxybenzene **29d**. We observed the formation of the desired *N*-split Ugi adduct in low yields, being 1,3-diazaadamantane (1,3-diazatricyclo[3.3.1.1^{3,7}]decane) **32** the major product (detected by ^{1}H NMR) (**Scheme 25**). Although its formation can be due to intramolecular cyclization during the precondensation step, we hypothesized 1,3-diazaadamantane **32** should be an unreactive by-product, and not a suitable electrophilic specie. To prove our hypothesis, we separately obtained **32** by treating bispidine with paraformaldehyde under acidic dry conditions at high temperature.[34] By mixing it with benzoic acid **27b** and 1-(isocyanomethyl)-4-methoxybenzene **29d** no formation of the *N*-split Ugi adduct **31** was observed, recovering only starting materials, even at prolonged reaction time (**Scheme 25**). Therefore, we could confidently confirm 1,3-diazamantane **32** to be an unreactive by-product, whose formation is facilitated by the high temperature employed (**Scheme 24**).

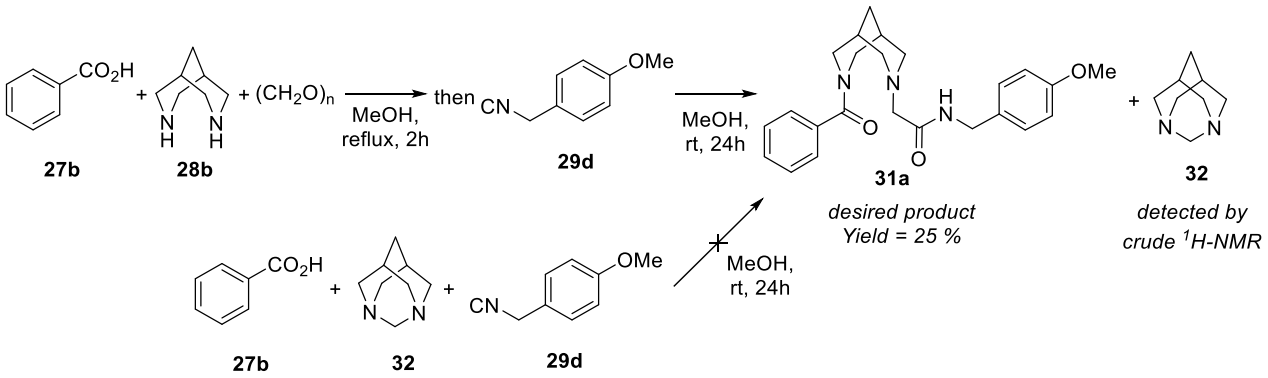

Scheme 25. *N*-split Ugi reaction involving bispidine **28b** with the formation of the desired product **31a** in combination with 1,3-diazaadamantane **32**. Determination of the role of 1,3-diazaadamantane.

Therefore, we replaced paraformaldehyde with the highly reactive aqueous formaldehyde and, simply by mixing the reactants at room temperature (**Scheme 26**), we observed a drastic increase in the product yields with no sign of by-product **32**. This result could arise from the combined effect of a lower reaction temperature and a little amount of water, which reduces the kinetic of the intramolecular cyclization leading to by-product **32**, allowing the formation of the thermodynamic *N*-split Ugi adduct. Under these milder conditions, only small amounts of classical U-4CR and *N*-split Ugi by-products have been isolated, like the Passerini-adduct and the formamide derived from hydration of the isocyanide.

The reaction proceeded smoothly either with benzoic acid **27b** or acetic acid **27c**, allowing the formation of desired *N*-split Ugi adducts **31a**-**b** in good yields, with no significant influence of the steric hindrance, electronic properties and acidity of the carboxylic acid components. Although benzyl isocyanide **29d** performed well in the reaction conditions, aromatic isocyanides 1-bromo-4-isocyanobenzene and 1-isocyano-4-methoxybenzene afforded only complex mixtures, from which *N*-split Ugi adducts could not be isolated. Finally, the combination of differently *N*-protected L-alanines with methyl (*S*)-2-isocyanopropanoate **5** smoothly afforded the bispidine-based peptidomimetics **31c**-**e** in moderate yields, with no evidence of loss of optical purity nor deprotection (from ^{1}H-NMR and ^{13}C-NMR), even with the labile 9-fluorenylmethoxycarbonyl (Fmoc) protecting group (**Scheme 26**).

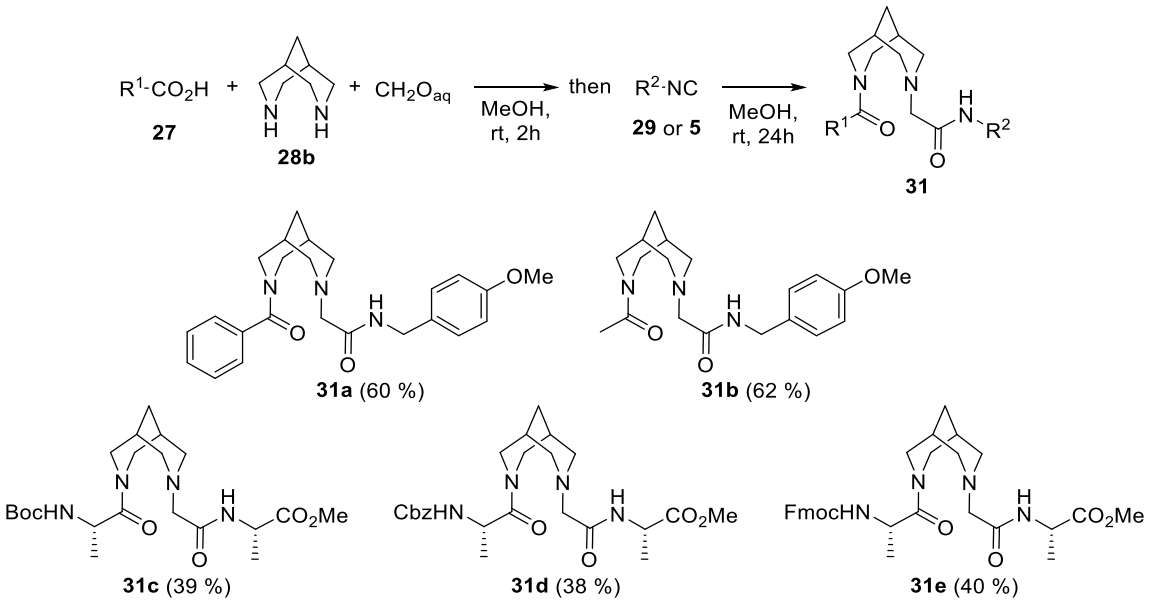

Scheme 26. One-pot synthesis of bispidine-containing *N*-split Ugi adducts **31a-b** and bispidine-based peptidomimetics **31c-e**.

Conclusions

We developed a novel multicomponent approach for the synthesis of biologically relevant diamine-based peptidomimetics, by means of a stereoconservative *N*-split Ugi reaction employing amino acid-derived chiral carboxylic and isocyanide components. The regiochemical desymmetrization of cyclic and bicyclic secondary diamines was achieved in a one-pot process, without the use of expensive coupling agents and protection/deprotection steps. In particular, a constrained bicyclic diamine, namely bispidine, was successfully employed in the *N*-split Ugi reaction for the first time, with moderate to good yields under mild conditions. The corresponding peptidomimetics were synthesized, bearing different *N*-protecting groups, which make them suitable for incorporation into peptide sequences, as α-helix nucleators.

Experimental section

GENERAL INFORMATION

All commercial materials (Aldrich, Fluka) were used without further purification. All solvents were of reagent grade or HPLC grade. Compound **28b** was synthesized through a slightly modified reported procedure[35] and stored as a perchlorate salt. All reactions were carried out under a nitrogen atmosphere unless otherwise noted. All reactions were monitored by thin layer chromatography (TLC) on precoated silica gel 60 F254; spots were visualized with UV light or by treatment with a 1% aqueous KMnO4 solution. Products were purified by flash chromatography on silica gel 60 (230–400 mesh). ^{1}H NMR spectra and ^{13}C NMR spectra were recorded on 300 and 400 MHz spectrometers. Chemical shifts are reported in parts per million relative to the residual solvent. ^{13}C NMR spectra have been recorded using the APT pulse sequence (*for further details see* **Appendix A.1**). Multiplicities in ^{1}H NMR are reported as follows: s = singlet, d = doublet, t = triplet, m = multiplet, br s = broad singlet. High resolution MS spectra were recorded with an FT-ICR (Fourier Transform Ion Cyclotron Resonance) instrument, equipped with an ESI source. CD spectra were recorded with a JASCO J-715 spectropolarimeter.

GENERAL PROCEDURE FOR PIPERAZINE-BASED COMPOUNDS **30a-d**

To a solution of piperazine **28a** (0.8 mmol, 1 eq) in 2 ml of dry MeOH under nitrogen was added *N*-Boc-L-Alanine **27a** (0.87 mmol, 1.1 eq) and paraformaldehyde (0.95 mmol, 1.2 eq). The solution was heated to reflux and stirred for 2 h. After cooling to r.t., isocyanide **29** or **5** (0.95 mmol, 1.2 eq) was added and stirring was allowed to continue for 48 h. The solvent was evaporated in vacuo and the crude reaction mixture was purified by flash chromatography on silica gel (EtOAc) to afford the pure product **30**.

(S)-tert-butyl (1-(4-(2-(tert-butylamino)-2-oxoethyl)piperazin-1-yl)-1-oxopropan-2-yl)carbamate (**30a**)

White solid, 0.136 g (51%); $[\alpha]^{20}_{D}$ +8.3 (*c* 0.1.0, $CHCl_3$); ^{1}H NMR (400 MHz, $CDCl_3$): δ 6.87 (s, 1H), 5.49 (d, J = 7.8 Hz, 1H), 4.65-4.60 (m, 1H), 3.70-3.45 (m, 4H), 2.95 (s, 2H), 2.64-2.49 (m, 4H), 1.46 (s, 9H), 1.39 (s, 9H), 1.32 (d, J=6,9 Hz ,3H); ^{13}C NMR (100 MHz, $CDCl_3$): δ 171.3, 168.4, 155.1, 79.6, 62.1, 53.3, 53.0, 50.7, 46.0, 45.4, 42.0, 28.8 (3C), 28.4 (3C), 19.38; HRMS (ESI): calcd for $[C_{18}H_{35}N_4O_4]^+$ 371.2653, found 371.2661 [MH^+].

(S)-tert-butyl(1-oxo-1-(4-(2-oxo-2-((2,2,3,3-tetramethylbutyl)amino)ethyl)piperazin-1-yl)propan-2-yl)carbamate (**30b**)

White solid, 0.243 g (72%); $[\alpha]^{20}_{D}$ +7.19 (*c* 0.9, $CHCl_3$); ^{1}H NMR (400 MHz, $CDCl_3$): δ 7.02 (s, 1H), 5.49 (d, *J* = 7.5 Hz 1H), 4.62 (m, 1H), 3.82-3.43 (m, 4H), 2.94 (s, 2H), 2.54 (m, 4H), 1.72 (s, 2H), 1.45 (s, 15H), 1.31 (d, *J* = 6.8 Hz, 3H), 1.04 (s, 9H); ^{13}C NMR (100 MHz, $CDCl_3$): δ 171.9, 168.9, 155.7, 80.3, 63.1, 55.4, 54.1, 53.7, 53.4, 46.7, 46.0, 42.7 (2C), 32.2 (3C), 29.5 (2C), 29.0 (3C), 20.1; HRMS (ESI): calcd for $[C_{22}H_{43}N_4O_4]^+$ 427.3279, found 427,3271[MH^+].

(S)-methyl-2-(2-(4-(2-((tert-butoxycarbonyl)amino)propanoyl)piperazin-1-yl)acetamido)acetate (**30c**)

Yellowish oil, 0.242 g (79%); $[\alpha]^{20}_{D}$ +5.2 (*c* 0.3, $CHCl_3$); ^{1}H NMR (400 MHz, $CDCl_3$): δ 7.54 (br, 1H), 5.48 (d, *J* = 7.7 Hz, 1H), 4.59 (m, 1H), 4.08 (d, *J* = 5.7 Hz, 2H), 3.75 (s, 3H), 3.74-3.43 (m, 4H), 3.09 (s, 2H), 2.58 (m, 4H), 1.42 (s, 9H), 1.29 (d, *J* = 6.9 Hz, 3H); ^{13}C NMR (100 MHz, $CDCl_3$): δ 171.8, 170.6, 169.7, 155.5, 80.2, 60.8, 53.4, 53.2, 52.9, 46.4, 45.0, 41.2, 40.8, 28.8 (3C), 19.6; HRMS (ESI): calcd for $[C_{17}H_{31}N_4NaO_6]^+$ 409.2058, found 409.2071 [MNa^+].

(S)-methyl2-(2-(4-((S)-2-((tert-butoxycarbonyl)amino)propanoyl)piperazin-1-yl)acetamido)propanoate (**30d**)

Yellowish oil, 0.210 g (66%); $[\alpha]^{20}_{D}$ +4.1 (*c* 0.6, $CHCl_3$); ^{1}H NMR (400 MHz, DMSO-d_6, 80°C): δ 7.57 (br, 1H), 5.51 (d, *J* = 7.7 Hz, 1H), 4.63 (m, 2H), 3.77 (s, 3H), 3.76-3.49 (m, 4H), 3.13 (d, *J* = 16.2 Hz, 1H), 3.03 (d, *J* = 16.2 Hz, 1H), 2.78-2.47 (m, 4H), 1.47-1.42 (m, 12H), 1.31 (d, *J* = 6.9 Hz, 3H); ^{13}C NMR (100 MHz, DMSO-d_6, 80°C): δ 174.0, 171.9, 169.8, 155.7, 80.3, 61.9, 54.0, 53.6, 53.2, 48.1, 46.7, 46.0, 42.7, 29.0 (3C), 20.0, 19.1; HRMS (ESI): calcd for $[C_{18}H_{32}N_4NaO_6]^+$ 423.2214, found 423.2209 [MNa^+].

GENERAL PROCEDURE FOR BISPIDINE-BASED COMPOUNDS **31a-e**

To a solution of bispidine **28b** (0.8 mmol, 1 eq) in 1.6 mL of MeOH was added benzoic acid **27b** (or **27**, 0.950 mmol, 1.2 eq) and aqueous formaldehyde solution 37 wt % (1.6 mmol, 2 eq). After 2h, isocyanide **29** or **5** (0.950 mmol, 1.2 eq) was added and stirring was allowed to continue for 48 h. The solvent was evaporated in vacuo and the crude reaction mixture was purified by flash chromatography on silica gel (EtOAc) to afford pure product **31**.

2-(7-benzoyl-3,7-diazabicyclo[3.3.1]nonan-3-yl)-N-(4-methoxybenzyl)acetamide (**31a**)

Yellowish solid, 0.194 g (60%); ^{1}H NMR (300 MHz, $CDCl_3$, rotameric mixture): δ 8.70 (m, 0.5H), 8.33 (m, 0.5H), 7.67-7.24 (m, 5H), 7.17 (d, *J* = 8.7 Hz, 2H), 6.87 – 6.71 (m, 2H), 4.94 (br, d, *J* = 13.7 Hz, 1H), 4.45 (br, t, *J* = 6.4 Hz, 1H), 4.33 (br, d, *J* = 5.5 Hz 2H), 3.81-3.50 (m, 6H), 3.40 (m, 1H), 3.25 (br, d, *J* = 11.2 Hz, 1H), 3.15 (m, 1H), 2.99 (d, *J* = 12.0 Hz, 1H), 2.65 (m, 1H), 2.48-1.57 (m, 4H); ^{13}C NMR (75 MHz, $CDCl_3$): δ 172.2, 169.6, 158.5, 136.6, 131.9, 129.8 (2C), 129.5, 128.5 (2C), 126.8 (2C), 113.6 (2C), 63.3, 58.7 (2C), 55.2, 53.4, 46.0, 42.2, 32.2, 29.7, 28.8; HRMS (ESI): calcd for $[C_{24}H_{30}N_3O_3]^+$ 408.2282, found 408.2286 $[MH^+]$.

2-(7-acetyl-3,7-diazabicyclo[3.3.1]nonan-3-yl)-N-(4-methoxybenzyl)acetamide (**31b**)

Yellowish solid, 0.164 g (62%); ^{1}H NMR (400 MHz, $CDCl_3$): δ 7.74 (br, m, 1H), 7.36 (d, *J* = 8.2 Hz, 2H), 6.86 (d, *J* = 8.2 Hz, 2H), 4.75 (br, d, *J* = 12.9 Hz, 1H), 4.47 (br, dd, *J* = 14.0, 6.7 Hz, 1H), 4.29 (br, dd, *J* = 14.0, 5.2 Hz, 1H) 3.86 (br, d, *J* = 11.7 Hz, 1H), 3.80 (s, 3H), 3.40 (br, d, J = 12.6 Hz, 1H), 3.15-2.97 (br, m, 2H), 2.93 (br, d, *J* = 9.5 Hz, 1 H), 2.83 (br, d, J = 13.1 Hz, 1H), 2.70 (br, d, *J* = 15.8 Hz, 1H), 2.55 (br, d, *J* = 8.5 Hz, 1H), 2.20 (br, d, *J* = 9.5 Hz, 1H), 2.05-1.85 (br, m, 5H), 1.83-1.63 (br, m, 2H); ^{13}C NMR (100 MHz, $CDCl_3$): δ 172.0, 169.5, 158.6, 131.6, 129.5 (2C), 113.7 (2C), 61.6, 59.2, 58.7, 51.3, 45.8 (2C), 42.2, 29.7, 28.8 (2C), 22.1; HRMS (ESI): calcd for $[C_{19}H_{27}N_3NaO_3]^+$ 368.1945, found 368.1954 $[MNa^+]$.

methyl (2-(7-((tert-butoxycarbonyl)-L-alanyl)-3,7-diazabicyclo[3.3.1]nonan-3-yl)acetyl)-L-alaninate (**31c**)

White solid, 0.136 g (39%); $[\alpha]^{20}_D$ -17.6 (*c* 0.95, $CHCl_3$); ^{1}H NMR (400 MHz, $CDCl_3$, rotameric mixture): δ 7.7 (m, 0.5H), 7.6 (br, d, *J* = 9.5, 1H), 6.3 (m, 0.5H), 5.11-4.73 (m, 2H), 4.7-4.5 (m, 1H), 4.4 (br, d, *J* = 10.3, 0.75H), 4.20-4.07 (m, 0.25), 3.8-3.7 (m, 3H), 3.5-3.3 (m, 1H), 3.2-3.0 (m, 1H), 3.0-2.8 (m, 1H), 2.7-2.5 (m, 1H), 2.5-2.35 (m, 1H), 2.2-2.1 (m, 1H), 2.0-1.9 (m, 2H), 1.9-1.7 (m, 2H), 1.6-1.3 (m, 15H); ^{13}C NMR (100 MHz, $CDCl_3$): δ 174.5-173.2 (2C), 171.2, 156.0, 80.1, 63.9-62.6, 59.0-58.3 (2C), 53.0-52.6, 51.0-50.7, 48.4-47.8, 47.2-46.6, 45.8, 34.5-32.0, 29.5-28.7 (5C), 19.2-17.5 (2C); HRMS (ESI): calcd for $[C_{21}H_{36}N_4NaO_6]^+$ 463.2527, found 463.2516 $[MNa^+]$.

methyl (2-(7-(((benzyloxy)carbonyl)-L-alanyl)-3,7-diazabicyclo[3.3.1]nonan-3-yl)acetyl)-L-alaninate (**31d**)

White solid, 0.143 g (38%); $[\alpha]^{20}_D$ -10.2 (*c* 0.8, $CHCl_3$); ^{1}H NMR (400 MHz, $CDCl_3$, rotameric mixture): δ 7.61 (br, d, *J* = 9.0 Hz, 1H), 7.45-7.23 (m, 5H), 6.78 (br, d, *J* = 9.3 Hz, 1H), 5.20-4.98 (m, 2H), 4.91 (m, 1H), 4.87-4.75 (m, 2H), 4.39-3.95 (m, 1H), 3.75 – 3.72 (m, 3H), 3.55 - 2.77 (m, 3H), 2.82 – 2.45 (m, 2H), 2.45 (d, *J* = 16.1Hz, 1H), 2.28-2.07 (m, 2H), 2.07-1.60 (m, 4H), 1.58-1.44 (m, 3H), 1.36-1.29 (m, 3H); ^{13}C NMR (100 MHz, $CDCl_3$): δ 174.2-172.0 (2C), 169.4, 155.9, 136.5, 128.5-128.1 (2C), 66.6, 62.7, 59.0-58.3 (2C), 52.4-52.1 (2C), 50.3, 47.2, 46.2-46 (2C), 45.8, 32.1, 28.9 (2C), 18.7, 17.4; HRMS (ESI): calcd for $[C_{24}H_{35}N_4O_6]^+$ 475.2551, found 475.2562 $[MH^+]$.

methyl (2-(7-((((9H-fluoren-9-yl)methoxy)carbonyl)-L-alanyl)-3,7-diazabicyclo[3.3.1]nonan-3-yl)acetyl)-L-alaninate (**31e**)

White solid, 0.178 g (40%); $[\alpha]^{20}_D$ -6.8 (*c* 1, $CHCl_3$); ^{1}H NMR (400 MHz, $CDCl_3$, rotameric mixture): δ 7.77 (br, 2d, *J* = 6.9 Hz, 2H), 7.69 (br, d, *J* = 9.4 Hz, 1H), 7.65-7.58 (m, 2H), 7.41 (br, 2d, *J* = 7.3 Hz, 2H), 7.37-7.29 (m, 2H), 6.98 (br, d, *J* = 9.5, 1H), 4.97 (m, 1H), 4.92-4.78 (m, 1.5H), 4.71 (m, 0.5H), 4.54-4.30 (m, 2H), 4.30-4.13 (m, 1.5H), 4.13-3.93 (m, 0.5), 3.84-3.69 (m, 3H), 3.58-3.35 (m, 1.5H), 3.20-3.03 (m, 1.5H), 3.01-2.93 (m, 1.5H), 2.92-2.82 (m, 1H), 2.66-2.42 (m, 1.5H), 2.39 (br, d, *J* = 11.2 Hz, 1H), 2.10-1.92 (m, 2H), 1.90-1.65 (m, 2H), 1.62-1.44 (m, 3H), 1.44-1.34 (m, 3H); ^{13}C NMR (100 MHz, $CDCl_3$): δ 174.2-171.0 (2C), 169.4, 155.9, 143.9 (2C), 141.2 (2C), 127.7 (2C), 127.2-127.0 (2C), 125.2 (2C), 119.9 (2C), 67.1, 62.6, 58.6-58.1 (2C), 52.3, 50.2, 47.4-47.0 (2C), 46.3, 46, 32.2, 29.0-28.5 (2C), 18.8, 17.5; HRMS (ESI): calcd for $[C_{31}H_{39}N_4O_6]^+$ 563.2864, found 563.2868 $[MH^+]$.

2.3 Polyimidazole-based β-strand peptidomimetics

Introduction

The majority of protein-protein interfaces are characterized by three main recognition motifs (α-helix, β-turn, or β-strand), and the design of small molecules mimetics of these recognition motifs is an attractive way to disrupt protein-protein interactions (PPIs).[36] Helical domain is one of the most common peptide secondary structure and a major recognition motif of PPIs.[33] By mimicking it, many successful inhibitors of believed "undruggable" PPIs were recently reported.[37] β-Turn peptidomimetics are usually obtained either through cyclization of the related peptides or by introducing constraining elements in the peptide sequence, and their use as PPI inhibitors have been extensively reported in the literature.[38]

On the other hand, only in the last decade synthetic organic chemists focused their attention on the simpler β-strand motif,[39] reporting small molecules mimics of this underestimated secondary structure with relevant therapeutic activities.[40] Last year, Arora and co-workers[41] extensively studied β-strand protein-protein interfaces whose structures are available in the Protein Data Bank (PDB), identifying roughly 15000 high affinity β-strands mediated PPIs. Therefore, there is a need for novel β-strand peptidomimetics, which could lead to better treatment for nowadays incurable diseases, by exploiting this largely undermined PPIs area.

In this context, Hamilton and co-workers[42] recently reported non-peptidic β-strand mimics, relying on different linear *minimalist* frameworks (*for further details see* **Chapter 2.1**). In their earlier report,[42a] alkyne-linked 2,2-disubstituted-indolin-3-one oligomers were able to mimic the residues of a β-strand, stabilizing the conformation by intramolecular hydrogen bonds (**Figure 16a**). In 2012,[42b] the same authors reported an efficient iterative process for obtaining 1,3-phenyl-linked hydantoin oligomers, able to mimic the *i*, *i*+2 and *i*+4 alanine residues of an antiparallel β-strand motif (**Figure 16b**). By replacing hydantoin with an imidazolidin-2-one ring,[42c] they were able to incorporate other amino acid side-chains in a similar non peptidic-scaffold, retaining the ability to mimic the same β-strand motif (**Figure 16c**). In this case, the conformation is stabilized by dipolar repulsion, as observed by extensive computation as well as solid- and solution-phase studies.[42d] Again exploiting dipolar repulsion to exert conformational control, they recently designed[42e] a novel oligomer consisting of alternating pyridyl and six-membered cyclic urea groups (**Figure 16d**), able to mimic the same residues of the previously reported scaffolds.

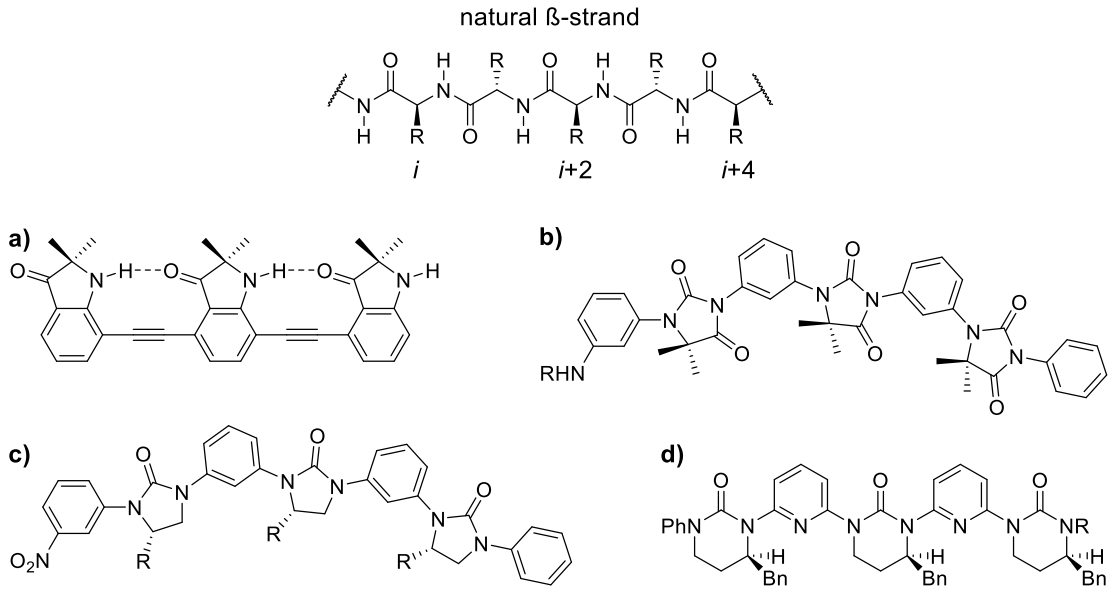

Figure 16. Hamilton's β-strand non-peptidic scaffolds.[42]

Inspired by Hamilton's works, we designed a novel C2-C5' linked polyimidazole minimalist framework, able to mimic *i*, *i*+1, *i*+2 and *i*+3 amino acid side chains of a β-strand motif, smoothly obtained by means of an iterative van Leusen three-component reaction (vL-3CR) (*for further details see* **Chapter 1.3**). In particular, by employing commercially available aromatic aldehydes as starting substrates, in combination with methylamine and tosylmethyl isocyanide (TosMIC), the expected *N*-substituted imidazole rings can be easily obtained. Afterwards, the formylation of the C-2 position under classical conditions smoothly afforded the corresponding carbonyl derivative, readily available for the next vL-3CR/formylation cycle (**Scheme 27**). The ability to mimic a β-strand structure was assessed through NMR and computational studies.

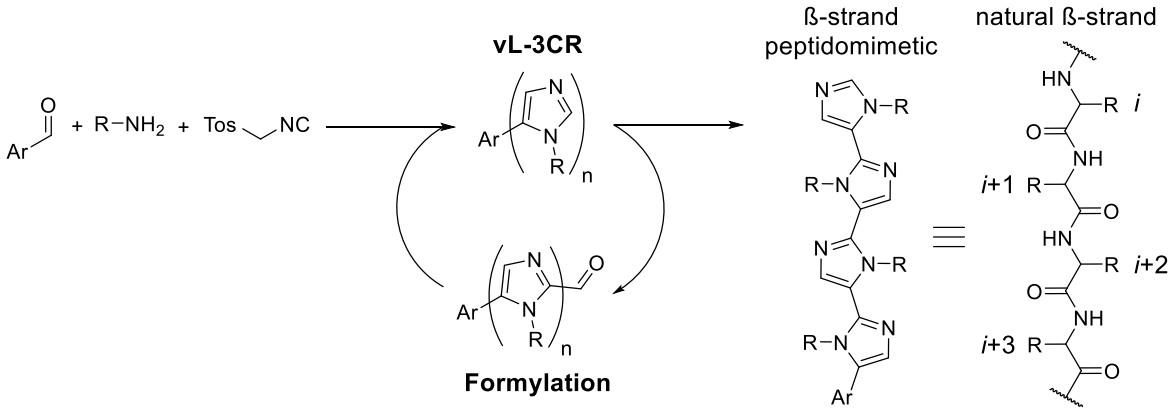

Scheme 27. Polyimidazole-based β-strand peptidomimetic obtained through an iterative van Leusen three-component reaction (vL-3CR).

Results and discussion

Firstly, we investigated the reactivity of different commercially available benzaldehydes in the vL-3CR (**Scheme 28**). Although diverse reaction conditions have been reported for the vL-3CR,[43] aromatic aldehydes are usually converted to the corresponding imidazoles employing potassium carbonate as base, and conducting the reaction in methanol, ethanol or dimethylformamide (DMF).[44] Therefore, we selected the high-boiling DMF as solvent, and introduced a precondensation time of two hours between benzaldehydes and methylamine aqueous solution, in order to allow the *in-situ* formation of the corresponding imines. The subsequent addition of potassium carbonate (K_2CO_3) and tosylmethyl isocyanide (TosMIC), followed by a reaction time of 24h at 50 °C afforded the desired 1-methyl-5-aryl imidazoles **33**, **34a** and **35-36**, in a one-pot process (**Scheme 28**). Under these conditions, when the high electrophilic 4-nitrobenzaldehyde was employed as substrate, a complex reaction mixture was observed, with the desired product **33** isolable only in low yield. On the other hand, electron rich 4-methoxybenzaldehyde and 4-(dimethylamino)benzaldehyde performed better, affording the corresponding products **35** and **36** in moderate to good yields. Benzaldehyde proved to be the substrate of choice, leading to imidazole **34a** in high yield (**Scheme 28**).

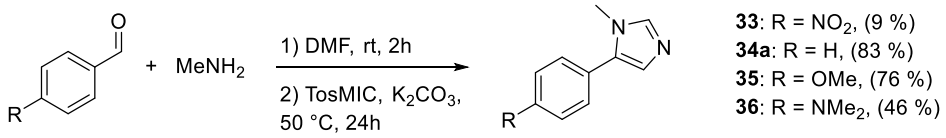

Scheme 28. Screening of *p*-substituted benzaldehydes in the vL-3CR.

Starting from monomer **34a**, elongation to the corresponding oligomers was easily performed, affording the β-strand mimics **34b**-**d** in moderate to good yields (**Scheme 29**), by means of vL-3CR employing the formyl derivatives **37a**-**c** as substrates. These intermediates could be obtained by classical conditions, using butyl lithium as strong base and dimethylformamide as formylating agent at low temperature (**Scheme 29**). Starting from monomer **34a** and dimer **34b**, the corresponding aldehydes **37a**-**b** were smoothly obtained in moderate to good yields. On the contrary, no appreciable formation of the formylated trimer **37c** could be observed, due to the low solubility of the lithiated derivative of compound **34c**. However, by combining the chelating properties of *N*,*N*,*N*′,*N*′-tetramethylethylenediamine (TMEDA) with a lower reaction concentration, we were able to obtain the formyl derivative **37c** in moderate yield (**Scheme 29**).

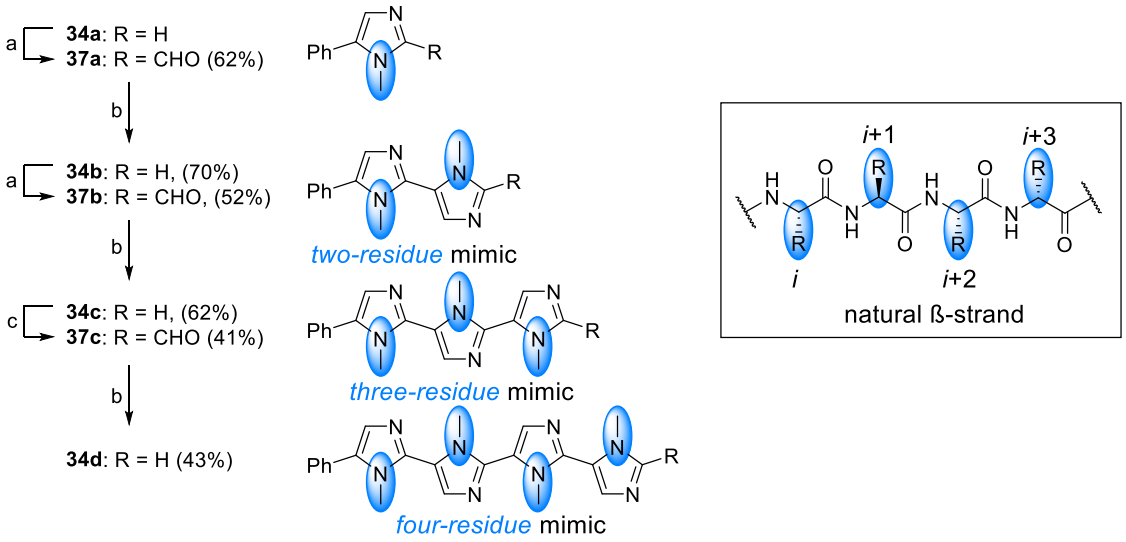

Scheme 29. Iterative synthesis of β-strand polyimidazole-based peptidomimetics, bearing two (**34b**), three (**34c**) and four (**34d**) side-chain residues. Reagents and conditions: (a) BuLI, THF, 2h, -78 °C; then DMF, -78 to rt, 24h. (b) $MeNH_2$, DMF, 2h, rt; then K_2CO_3, TosMIC, 24h, 50 °C. (c) BuLI, TMEDA, THF, 2h, -78 °C; then DMF, -78 to rt, 24h.

Solution-phase conformational behaviour was probed through NOESY NMR experiments in $CDCl_3$ on both the three-residue mimic **34c** and the four-residue mimic **34d** (**Figure 17**). NOE signals between *N*-Me groups, for examples H10↔H16 and H16↔H22 for trimer **34c** (**Figure 17a**), were not observed for compounds **34c-d**. On the other hand, strong correlations between *N*-Me groups and the proton of the vicinal aromatic rings, for examples H10↔H3, H10↔H15 and H16↔H21, could be detected, clearly indicating a *N*-Me alternate conformation for both polyimidazoles **34c-d** (**Figure 17**).

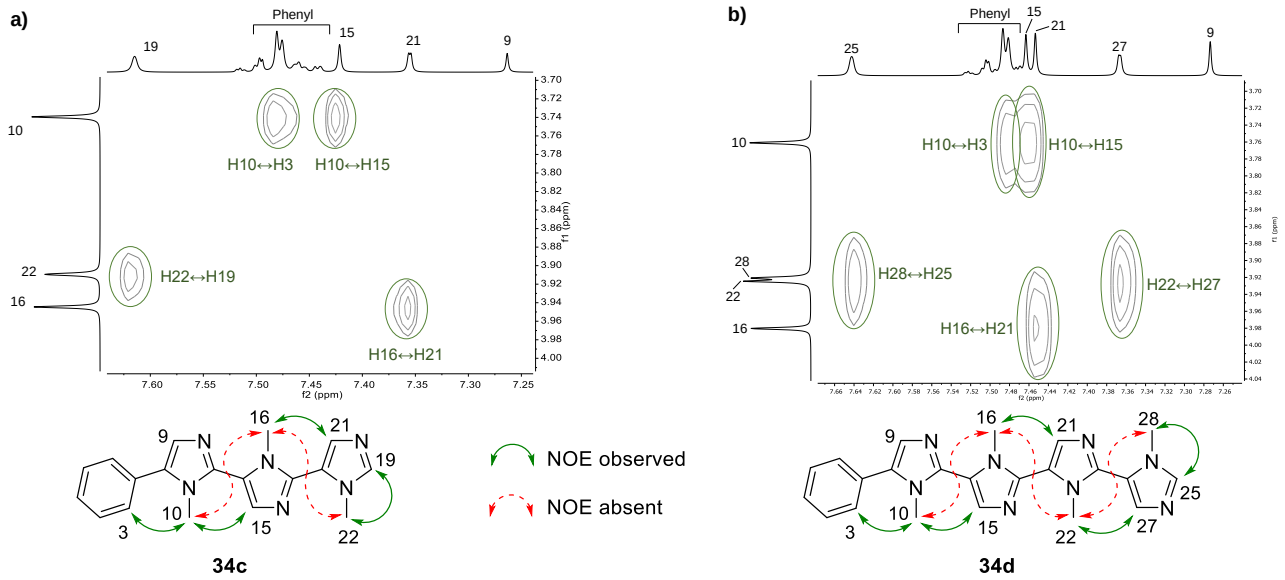

Figure 17. Solution-phase analysis of trimer **34c** (a) and tetramer **34d** (b). Selected regions of the NOESY NMR spectrum focusing on cross-peaks between *N*-Me and aromatic protons. Key observed (*green*) and absent (*red*) NOE correlations are indicated ($CDCl_3$, 400 MHz, 298 K).

In collaboration with Dr. Grazioso,[24] we applied the same computational procedure previously described for the ketopiperazine-based minimalist peptidomimetics (**Chapter 2.1**). Analysing the fluctuation of the dihedral angles connecting the imidazole rings, we were able to confirm that compound **34d** assumes the conformation verified by NOESY NMR studies, with the most populated values in the range from 180° to 150° and from -150° to -180° (**Figure 18a**).

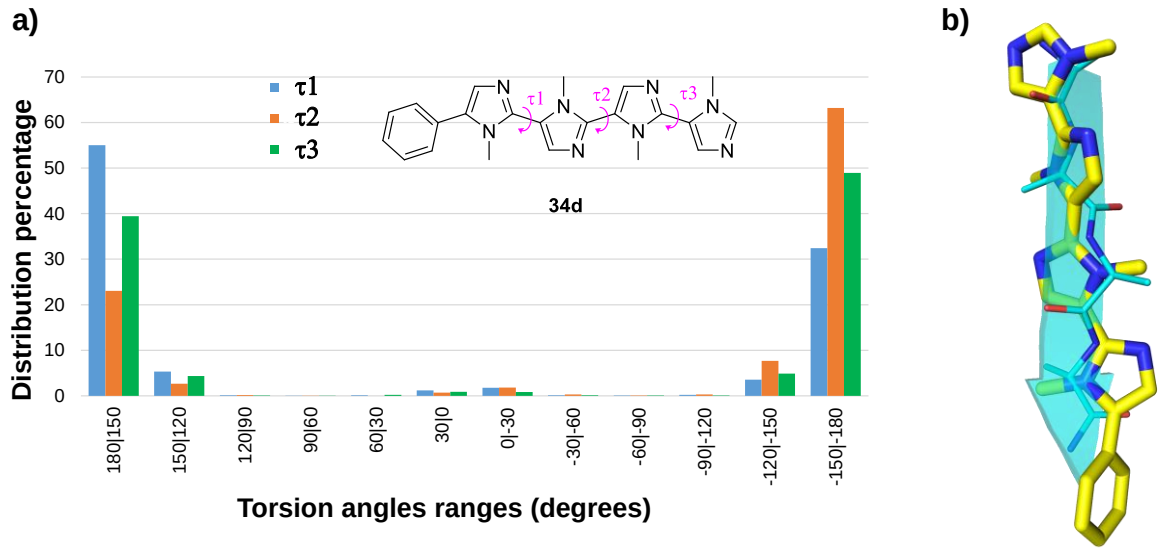

Figure 18. a) Torsion angle distributions derived from the MD simulations of **34d**. b) Superimposition between **34d** (*yellow*) and a hypothetical protein β-strand (*cyan*).

To determine which protein secondary structures are mimicked by compound **34d**, distances between methyl groups were measured on the DFT optimized lowest energy conformers. Therefore, by comparing them to the ones reported by Burgess and coworkers[12] for typical secondary structures, we were able to predict that **34d** mimics almost perfectly the β-strand motif. Moreover, superimposing our compound with a hypothetical β-strand found in a protein reported in Protein Data Bank, we observed a very good overlying (**Figure 18b**), with distance between the *N*-methyl groups of **34d** and the side chains of alanine residues lower than 0.5 Å.

Conclusions

We developed a synthetic route to an oligomer consisting of C2-C5' linked polyimidazole, by means of an iterative vL-3CR/formylation protocol. The solution-phase conformation behaviour of the resulting foldamer was investigated through experimental NOESY NMR studies and molecular dynamics calculations, demonstrating its ability to mimic *i*, *i*+1, *i*+2 and *i*+3 amino acid residues of a β-strand motif.

Experimental section

GENERAL INFORMATION

All commercial materials (Aldrich, Fluka) were used without further purification. All solvents were of reagent grade or HPLC grade. All reactions were carried out under a nitrogen atmosphere unless otherwise noted. All reactions were monitored by thin layer chromatography (TLC) on precoated silica gel 60 F254; spots were visualized with UV light or by treatment with a 1% aqueous $KMnO_4$ solution. Products were purified by flash chromatography on silica gel 60 (230–400 mesh). ^1H NMR spectra and ^{13}C NMR spectra were recorded on 300 and 400 MHz spectrometers. Chemical shifts are reported in parts per million relative to the residual solvent. ^{13}C NMR spectra have been recorded using the APT pulse sequence (*for further details see* **Appendix A.1**). Multiplicities in ^1H NMR are reported as follows: s = singlet, d = doublet, t = triplet, m = multiplet, br s = broad singlet. High-resolution MS spectra were recorded with an FT-ICR (Fourier Transform Ion Cyclotron Resonance) instrument, equipped with an ESI source. UV-Vis spectra were obtained with Jasco V-650 spectrophotometer. CD spectra were obtained with JASCO J-715 spectropolarimeter.

GENERAL PROCEDURE FOR THE SYNTHESIS OF COMPOUNDS **33**, **34a-d**, **35** AND **36**

Aldehyde (4-nitrobenzaldehyde, benzaldehyde, 4-methoxybenzaldehyde, 4-(dimethylamino)benzaldehyde or **37a-c**) (1 eq) was dissolved in DMF (Conc. as indicated below). Methylamine aqueous solution 40 wt. % (2 eq) was added and the resulting mixture was kept under stirring for 2h at room temperature. Potassium carbonate (1.5 eq) and tosylmethyl isocyanide (1.2 eq) were sequentially added and the reaction was stirred for additional 24h at 50 °C. The resulting mixture was then partitioned between ethyl acetate/water, and the organic phase was washed with brine (x5), dried over Na_2SO_4 and concentrated under reduced pressure, to give a residue that was purified by flash chromatography (FC) as indicated below.

1-methyl-5-(4-nitrophenyl)-1H-imidazole (**33**)

Prepared according to the above general procedure from 4-nitrobenzaldehyde (0.6 mmol, 91 mg); Conc: 1 M; FC: ethyl acetate; yellowish solid (11 mg); yield: 9%; spectroscopic data are in agreement with literature.[45]

1-methyl-5-phenyl-1H-imidazole (**34a**)

Prepared according to the above general procedure from benzaldehyde (9.8 mmol, 1040 mg); Conc: 1 M; FC: ethyl acetate; yellowish solid (1285 mg); yield: 83%; spectroscopic data in agreement with literature.[46]

1,3'-dimethyl-5-phenyl-1H,3'H-2,4'-biimidazole (**34b**)

Prepared according to the above general procedure from **37a** (3.8 mmol, 700 mg); Conc: 1 M; FC: CH_2Cl_2:methanol 98:2 to 90:10; yellowish solid (633 mg); yield: 70%; ^1H NMR (400 MHz, $CDCl_3$) δ 7.60 (s, 1H), 7.51 – 7.48 (m, 1H), 7.48 – 7.45 (m, 4H), 7.32 (br, d, J = 1.0 Hz, 1H), 7.23 (s, 1H), 3.93 (s, 3H), 3.71 (s, 3H); ^{13}C NMR (100 MHz,) δ 139.8, 139.6, 134.9, 130.0, 129.9, 128.8 (2C), 128.7 (2C), 128.1, 127.7, 122.9, 33.4, 33.2; HRMS (ESI) calcd for $C_{14}H_{15}N_4^+$ $[MH]^+$ 239.1291, found 239.1279.

1,3',3''-trimethyl-5-phenyl-1H,3'H,3''H-2,4':2',4''-terimidazole (**34c**)

Prepared according to the above general procedure from **37b** (1.1 mmol, 292 mg); Conc: 0.5 M; FC: ethyl acetate:methanol 96:4 to 90:10 + 1% Et_3N; yellowish solid (217 mg); yield: 62%; ^1H NMR (400 MHz, $CDCl_3$) δ 7.61 (s, 1H), 7.54 – 7.43 (m, 5H), 7.42 (s, 1H), 7.36 (d, J = 0.8 Hz, 1H), 7.26 (s, 1H), 3.94 (s, 3H), 3.91 (s, 3H), 3.74 (s, 3H); ^{13}C NMR (100 MHz, $CDCl_3$) δ 140.4, 140.0, 139.5, 135.1, 130.7, 130.0, 129.8, 128.8 (2C), 128.7 (2C), 128.2, 128.0, 123.9, 122.4, 33.5, 33.4, 33.2; HRMS (ESI) calcd for $C_{18}H_{19}N_6^+$ $[MH]^+$ 319.1666, found 319.1659.

1,3',3",3"'-tetramethyl-5-phenyl-1H,3'H,3"H,3"'H-2,4':2',4":2",4"'-quaterimidazole (**34d**)

Prepared according to the above general procedure from **37c** (0.12 mmol, 42 mg); Conc: 0.25 M; FC: ethyl acetate:methanol 85:15 + 1 % Et_3N; yellowish solid (20 mg); yield: 43%; ^{1}H NMR (400 MHz, $CDCl_3$) δ 7.64 (s, 1H), 7.54 – 7.49 (m, 1H), 7.48 (d, J = 2.2 Hz, 4H), 7.46 (s, 1H), 7.45 (s, 1H), 7.39 – 7.34 (br, m, 1H), 7.27 (s, 1H), 3.98 (s, 3H), 3.93 (s, 3H), 3.92 (s, 3H), 3.76 (s, 3H); 13C NMR (101 MHz,) δ 140.6, 140.3, 140.0, 139.4, 135.1, 130.5, 130.1, 129.7, 128.9 (2C), 128.7 (2C), 128.3 (2C), 127.9, 124.1, 123.4, 122.3, 33.6, 33.5, 33.4, 33.3; HRMS (ESI) calcd for $C_{22}H_{23}N_8^+$ $[MH]^+$ 399.2040, found 399.2046.

5-(4-methoxyphenyl)-1-methyl-1H-imidazole (**35**)

Prepared according to the above general procedure from 4-methoxybenzaldehyde (0.6 mmol, 82 mg); Conc: 1 M; FC: ethyl acetate; yellowish solid (86 mg); yield: 76%; spectroscopic data are in agreement with literature.[46]

N,N-dimethyl-4-(1-methyl-1H-imidazol-5-yl)aniline (**36**)

Prepared according to the above general procedure from 4-(dimethylamino)benzaldehyde (0.6 mmol, 88 mg); Conc: 1 M; FC: ethyl acetate; yellowish solid (56 mg); yield: 46%; 1H NMR (400 MHz, $CDCl_3$) δ 7.48 (s, 1H), 7.25 (d, J = 8.4 Hz, 2H), 7.00 (s, 1H), 6.77 (d, J = 8.4 Hz, 2H), 3.62 (s, 3H), 3.00 (s, 6H); ^{13}C NMR (100 MHz, $CDCl_3$) δ 150.8, 138.8, 134.5, 130.2 (2C), 127.5, 118.0, 112.9 (2C), 41.0 (2C), 33.0; HRMS (ESI) calcd for $C_{12}H_{16}N_3^+$ $[MH]^+$ 202.1339, found 202.1330.

GENERAL PROCEDURE FOR THE SYNTHESIS OF COMPOUNDS **37a-b**

To a solution of compound **34a** (or **34b**) (1 eq) in dry THF under nitrogen atmosphere (Conc. as indicated below) cooled to -78 °C, was added dropwise a solution of *n*-butyl lithium in hexane(1.5 eq), and the resulting mixture was kept under stirring for 2h at the same temperature. Freshly distilled DMF (2eq) was added and the reaction was stirred for additional 24h at room temperature. The resulting mixture was then quenched with ice-water and extracted with ethyl acetate (x2). The organic phase was washed with brine (x4), dried over Na_2SO_4 and concentrated under reduced pressure, to give a residue that was purified by flash chromatography (FC) as indicated below.

1-methyl-5-phenyl-1H-imidazole-2-carbaldehyde (**37a**)

Prepared according to the above general procedure from **34a** (6.3 mmol, 997 mg); Conc: 0.5 M; FC: ethyl acetate:*n*-hexane 4:6; yellowish solid (727 mg); yield: 62%; ^{1}H NMR (400 MHz, $CDCl_3$) δ 9.87 (s, 1H), 7.56 – 7.46 (m, 3H), 7.44 (dd, J = 7.7, 1.7 Hz, 2H), 7.36 (s, 1H), 4.00 (s, 3H); ^{13}C NMR (100 MHz, $CDCl_3$) δ 182.9, 145.2, 140.5, 131.7, 130.0, 129.7 (2C), 129.7 (2C), 128.5, 33.8; HRMS (ESI) calcd for $C_{11}H_{11}N_2O^+$ $[MH]^+$ 187.0866, found 187.0874.

1,3'-dimethyl-5-phenyl-1H,3'H-[2,4'-biimidazole]-2'-carbaldehyde (**37b**)

Prepared according to the above general procedure from **34b** (2.5 mmol, 595 mg); Conc: 0.25 M; FC: ethyl acetate:*n*-hexane 6:4; yellowish solid (345 mg); yield: 52%; ^{1}H NMR (300 MHz, $CDCl_3$) δ 9.88 (s, 1H), 7.51 (s, 1H), 7.50 – 7.40 (m, 5H), 7.28 (s, 1H), 4.23 (s, 3H), 3.70 (s, 3H); ^{13}C NMR (75 MHz, $CDCl_3$) δ 182.2, 144.6, 137.6, 135.9, 132.0, 129.3 (2C), 128.9 (2C), 128.8 (2C), 128.5, 33.7, 33.3 (1 quaternary carbon is missed); HRMS (ESI) calcd for $C_{15}H_{15}N_4O^+$ $[MH]^+$ 267.1240, found 267.1245.

PROCEDURE FOR THE SYNTHESIS OF *1,3',3"-trimethyl-5-phenyl-1H,3'H,3"H-[2,4':2',4"-terimidazole]-2"-carbaldehyde* (**37c**)

To a solution of compound **34c** (0.37 mmol, 118 mg, 1 eq) and TMEDA (0.74 mmol, 86 mg, 2 eq) in dry THF under nitrogen atmosphere (0.05 M) cooled to -78 °C, was added dropwise a solution of *n*-butyl lithium in hexane (0.55 mmol, 1.5 eq), and the resulting mixture was kept under stirring for 2h at the same temperature. Freshly distilled DMF (0.74 mmol, 54 mg, 2eq) was added and the reaction was stirred for additional 24h at room temperature. The resulting mixture was then quenched with ice-water and extracted with ethyl acetate (x2). The organic phase was washed with brine (x4), dried over Na_2SO_4 and concentrated under reduced pressure, to give a residue that was purified by flash chromatography (ethyl acetate:methanol 97.5:2.5 to 95:5), affording the desired product **37c** (52 mg,

yield: 41%) as a yellowish solid. ^{1}H NMR (400 MHz, $CDCl_3$) δ 9.89 (s, 1H), 7.53 (s, 1H), 7.51 – 7.32 (m, 6H), 7.24 (s, 1H), 4.19 (s, 3H), 3.94 (s, 3H), 3.72 (s, 3H); ^{13}C NMR (100 MHz, $CDCl_3$) δ 182.91, 145.47, 139.18, 135.77, 133.18, 131.12, 130.30, 129.52 (2C), 129.42 (2C), 128.99, 128.88, 34.34, 34.15, 33.88 (3 quaternary carbons are missed); HRMS (ESI) calcd for $C_{19}H_{19}N_6O^+$ $[MH]^+$ 347.1615, found 347.1608.

COMPUTATIONAL STUDIES

Conformational studies on compound **34d**

The starting geometries of **34d,** created by GaussView,[27] were energy minimized by the conjugate gradient algorithm implemented in Gaussion09.[27] Thus, The optimized geometries were subjected to heating, equilibration, and molecular dynamics simulation by *sander* module of AMBER 12.[25] GAFF force field were used for the parametrization of the molecules, modeled as neutral compounds in an implicit GB solvent model and a dielectric continuum of 80 (simulating water).[26] With a time step 2 fs, each peptidomimetic was heated to 300 K, 700 K and then to 1000 K over 20 ps. After an equilibration phase of 2 ns, each model were frozen to 700 K and then to 300 K, over 20 ps. The production run of the MD simulations were performed for a total time of 20 ns with trajectories saved every 10 ps. The resulting structures in the trajectories were visually analyzed by VMD.[30] In this stage, the fluctuation of the diverse torsion angles were analyzed and the different families of conformers were identified. They were then minimized by Gasussian09 at DFT/B3LYP/6-31g(d) level of theory and the lowest energy conformation and the Boltzmann equation was applied to calculate the conformers percentage distribution. C^{β}-C^{β} distances were measured by GaussView.

References

[1] Garner, L.; Janda, K. D. *Curr. Top. Med. Chem.* **2011**, *11*, 258; Villoutreix, B. O.; Kuenemann, M. A.; Poyet, J.; Bruzzoni-Giovanelli, H.; Labbé, C.; Lagorce, D.; Sperandio, O.; Miteva, M. A. *Mol. Inf.* **2014**, *33*, 414; Nero, T. L.; Morton, C. J.; Holien, J. K.; Wielens, J.; Parker, M. W. *Nature Reviews Cancer* **2014**, *14*, 248.
[2] Hopkins, A. L.; Groom, C. R. *Nature Reviews Drug Discovery* **2002**, *9*, 727.
[3] Overington, J. P.; Al-Lazikani, B.; Hopkins, A. L. *Nature Reviews Drug Discovery* **2006**, *5*, 993.
[4] (a) Stumpf, M.P.; Thorne, T.; de Silva, E.; Stewart, R.; An, H.J.; Lappe, M.; Wiuf, C. *Proc. Natl. Acad. Sci. U. S. A* **2008**, *105*, 6959. (b) Venkatesan, K.; Rual, J.F.; Vazquez, A.; Stelzl, U.; Lemmens, I.; Hirozane-Kishikawa, T.; Hao, T.; Zenkner, M.; Xin, X.; Goh, K.I.; Yildirim, M.A.; Simonis, N.; Heinzmann, K.; Gebreab, F.; Sahalie, J.M.; Cevik, S.; Simon, C.; de Smet, A.S.; Dann, E.; Smolyar, A.; Vinayagam, A.; Yu, H.; Szeto, D.; Borick, H.; Dricot, A.; Klitgord, N.; Murray, R.R.; Lin, C.; Lalowski, M.; Timm, J.; Rau, K.; Boone, C.; Braun, P.; Cusick, M.E.; Roth, F.P.; Hill, D.E.; Tavernier, J.;Wanker, E.E.; Barabasi, A.L.; Vidal, M. *Nature Methods* **2009**, *6*, 83.
[5] (a) Wilson, A. J. *Chem. Soc. Rev.* **2009**, *38*, 3289. (b) Ottman, C. (**2013**) *Protein–Protein Interactions: An Overview, in Protein-Protein Interactions in Drug Discovery* (ed A. Dömling), Wiley-VCH Verlag GmbH & Co. KGaA, Weinheim, Germany.
[6] (a) Arkin, M. R.; Wells, J. A. *Nature Reviews in Drug Discovery* **2004**, *3*, 301. (b) Yin, H.; Hamilton, A. D. *Angew. Chem. Int. Ed.* **2005**, *44*, 4130. (c) *Small-Molecule Inhibitors of Protein-Protein Interactions* (ed Vassilev, L.; Fry, D.), Springer-Verlag Berlin Heidelberg **2011**, Berlin, Germany. (d) Falchi, F.; Caporuscio, F.; Recanatini, M. *Future Med. Chem.* **2014**, *6*, 343. (e) Zhang, X.; Betzi, S.; Morelli, X.; Roche, P. *Future Med. Chem.* **2014**, *6*, 1291. (f) Milroy, L.; Grossmann, T. N.; Hennig, S.; Brunsveld, L.; Ottmann, C. *Chem. Soc. Rev.* **2014**, *114*, 4695. (g) Rognan, D. *Med. Chem. Comm.* **2015**, *6*, 51. (h) Sheng, C.; Dong, G.; Miao, Z.; Zhang, W.; Wang, W. *Chem. Soc. Rev.* **2015**, 10.1039/c5cs00252d.
[7] (a) Ross, N. T.; Katt, W. P.; Hamilton, A. D. *Phil. Trans. R. Soc. A* **2010**, *368*, 989. (b) Glas, A.; Bier, D.; Hahne, G.; Rademacher, C.; Ottmann, C.; Grossmann, T. N. *Angew. Chem. Int. Ed.* **2014**, *53*, 2489. (c) Lao, B. B.; Drew, K.; Guarracino, D. A.; Brewer, T. F.; Heindel, D. W.; Bonneau, R.; Arora, P. S. *J. Am. Chem. Soc.* **2014**, *136*, 7877. (d) Akram, O. N.; DeGraff, D. J.; Sheehan, J. H.; Tilley, W. D.; Matusik, R. J.; Ahn, J.; Raj, G. V. *Mol. Cancer Res.* **2014**, *12*, 967. (e) Wilson, A. J. *Progress in Biophysics and Molecular Biology* **2015**, *111*, 33. (f) Moon, H.; Lim, H. *Curr. Op. Chem. Biol.* **2015**, *24*, 38. (g) Watkins, A. M.; Arora, P. S. *Eur. J. Med. Chem.* **2015**, *94*, 480. (h) Tsomaia, N. *Eur. J. Med. Chem.* **2015**, *94*, 459. (i) Lanning, M. E.; Fletcher, S. *Biology* **2015**, *4*, 540. (j) Pelay-Gimeno, M.; Glas, A.; Koch, O.; Grossmann, T. N. *Angew. Chem. Int. Ed.* **2015**, *54*, 8896. (k) Watkins, A. M.; Wuo, M. G.; Arora, P. S *J. Am. Chem. Soc.* **2015**, *137*, 11622.
[8] (a) Weissjohann, L. A.; Rhoden, C. R. B.; Rivera, D. G.; Vercillo, O. E. (**2010**) *Cyclic Peptidomimetics and Pseudopeptides from Multicomponent Reactions, in Synthesis of Heterocycles via Multicomponent Reactions I* (ed Orru, R. V. A.; Ruijter, E.) Springer-Verlag Berlin Heidelberg, Berlin, Germany. (b) *Isocyanide Chemistry: Applications in Synthesis and Material Science* (ed Nenajdenko, V. G.), Wiley-VCH Verlag GmbH & Co. KGaA (**2012**), Weinheim, Germany. (c) Koopmanschap, G.; Ruijter, E.; Orru, R. V. A. *Beilstein J. Org. Chem.* **2014**, *10*, 544.
[9] Stucchi, M.; Cairati, S.; Cetin-Atalay, R.; Christodoulou, M. S.; Grazioso, G.; Pescitelli, G.; Silvani, A.; Yildirim, D. C.; Lesma, G. *Org. Biomol. Chem.* **2015**, *13*, 4993.
[10] Ghosh, A. K. *Aspartic Acid Protease as Therapeutic Agents*, Wiley-VCH, Weinheim, **2010**.
[11] (a) I. S. Moreira, P. A. Fernandes and M. J. Ramos, *Proteins: Struct., Funct., Bioinf.*, **2007**, 68, 803–812. (b) S. Jones and J. M. Thornton, *Proc. Natl. Acad. Sci. U. S. A.*, **1996**, 93, 13–20.
[12] (a) Ko E., Liu J., Burgess K., *Chem. Soc. Rev.*, **2011**, *40*, 4411-4421. (b) Ko E., Liu J., Perez L. M., Lu G., Schaefer A., Burgess K., *J. Am. Chem. Soc.*, **2011**, *133*, 462-477.
[13] Koshland, D. E. *Proc. Natl. Acad. Sci. U. S. A* **1958**, *44*, 98.
[14] (a) Hirshmann, R.; Nicolau, K. C.; Pietranico, S.; Salvino, J.; Leahy, E. M.; Sprengler, P. A.; Furst, G.; Smith III, A. B. *J. Am. Chem. Soc.* **1992**, *114*, 9217. (b) Hirshmann, R.; Nicolau, K. C.; Pietranico, S.; Salvino, J.; Leahy, E. M.; Arison, B.; Cichy, M. A.; Spoors, P. G.; Shakespeare, W. C.; Sprengler, P. A.; Hamley, P.; Smith III, A. B.; Reisine, T.; Raynor, L.; Maechler, L.; Donaldson, C.; Vale, W.; Freidinger, R. M.; Cascieri, M. R.; Strader, C. D. *J. Am. Chem. Soc.* **1993**, *115*, 12550. (c) Mowery, B. P.; Prasad, V.; Kenesky, C. S.; Angeles, A. R.; Taylor, L. L.; Feng, J. J.; Chen, W. L.; Lin, A.; Cheng, F. C.; Smith III, A. B.; Hirshmann, R. *Org. Lett.* **2006**, *8*, 4397.

[15] Yin, H.; Lee, G.; Sedey, K. A.; Kutzki, O.; Park, H. S.; Orner, B. P.; Ernst, J. T.; Wang, H. G.; Sebti, S. M.; Hamilton, A. D. *J. Am. Chem. Soc.* **2005**, *127*, 10191.
[16] (a) Xin, D.; Ko, E.; Perez, L. M.; Iorger, T. R.; Burgess, K. *Org. Biomol. Chem.* **2013**, *11*, 7789. (b) Sable, R.; Jois, S. *Moleculesi* **2015**, *20*, 11569. (c) Watkins, A. M. Wuo, M. G.; Arora P. S. *J. Am. Chem. Soc.* **2015**, *137*, 11622. (d) *Small Molecule Medicinal Chemistry: Strategies and Technologies* (ed Czechtizky, W.; Hamley, P.), Wiley-VCH Verlag GmbH & Co. KGaA (**2015**), Weinheim, Germany.
[17] Garland, S. L.; Dean, P. M. *J. Comput.-Aided Mol. Des.* **1999**, *13*, 469.
[18] Garland, S. L.; Dean, P. M. *J. Comput.-Aided Mol. Des.* **1999**, *13*, 485.
[19] Zhu, J.; Wu, X.; Danishefsky, S. J. *Tetrahedron Lett.* **2009**, *50*, 577.
[20] Carney, D. W.; Troung, J. D.; J. K. Sello *J. Org. Chem.* **2011**, *76*, 10279.
[21]Gerona-Navarro, G.; Bonache, M. A.; Herranz, R.; García-López, M. T.; González-Muñiz, R. *J. Org. Chem.*, **2001**, *66*, 3538.
[22] Harfenist, M.; Hoerr, D. C.; Crouch,, R. *J. Org. Chem.*, **1985**, *50*, 1356.
[23] *Dipartimento di Chimica e Chimica Industriale*, Università di Pisa, via Moruzzi 3, 56124 Pisa, Italy.
[24] *Dipartimento di Scienze Farmaceutiche*, Università degli Studi di Milano, via L. Mangiagalli 25, 20133 Milano, Italy.
[25] Case, D. A; Darden, T. A.; Cheatham III, T. E.; Simmerling, C. L.; Wang, J.; Duke, R. E.; Luo, R.; Walker, R. C.; Zhang, W.; Merz, K. M.; Roberts, B.; Hayik, S.; Roitberg, A.; Seabra, G.; Swails, J.; Götz, A. W.; Kolossváry, I.; Wong, K. F.; Paesani, F.; Vanicek, J.; Wolf, R. M.; Liu, J.; Wu, X.; Brozell, S. R.; Steinbrecher, T.; Gohlke, H.; Cai, Q.; Ye, X.; Wang, J.; Hsieh, M.-J.; Cui, G.; Roe, D. R.; Mathews, D. H.; Seetin, M. G.; Salomon-Ferrer, R.; Sagui, C.; Babin, V.; Luchko, T.; Gusarov, S.; Kovalenko, A.; Kollman, P. A. (**2012**), *AMBER 12*, University of California, San Francisco.
[26] Ko, E.; Liu, J.; Perez, L. M.; Lu, G.; Schaefer, A.; Burgess, K. *J. Am. Chem. Soc.*, **2011**, *133*, 462.
[27] Frisch, M. J.; Trucks, G. W.; Schlegel, H. B.; Scuseria, G. E.; Robb, M. A.; Cheeseman, J. R.; Scalmani, G.; Barone, V.; Mennucci, B.; Petersson, G. A.; Nakatsuji, H.; Caricato, M.; Li, X.; Hratchian, H. P.; Izmaylov, A. F.; Bloino, J.; Zheng, G.; Sonnenberg, J. L.; Hada, M.; Ehara, M.; Toyota, K.; Fukuda, R.; Hasegawa, J.; Ishida, M.; Nakajima, T.; Honda, Y.; Kitao, O.; Nakai, H.; Vreven, T.; Montgomery, J. A., Jr.; Peralta, J. E.; Ogliaro, F.; Bearpark, M.; Heyd, J. J.; Brothers, E.; Kudin, K. N.; Staroverov, V. N.; Kobayashi, R.; Normand, J.; Raghavachari, K.; Rendell, A.; Burant, J. C.; Iyengar, S. S.; Tomasi, J.; Cossi, M.; Rega, N.; Millam, J. M.; Klene, M.; Knox, J. E.; Cross, J. B.; Bakken, V.; Adamo, C.; Jaramillo, J.; Gomperts, R.; Stratmann, R. E.; Yazyev, O.; Austin, A. J.; Cammi, R.; Pomelli, C.; Ochterski, J. W.; Martin, R. L.; Morokuma, K.; Zakrzewski, V. G.; Voth, G. A.; Salvador, P.; Dannenberg, J. J.; Dapprich, S.; Daniels, A. D.; Farkas, Ö.; Foresman, J. B.; Ortiz, J. V.; Cioslowski, J.; Fox, D. J. *Gaussian 09, Revision A.02*, Gaussian, Inc., Wallingford, CT, **2009**.
[28] Liu, C.-H.; Chen, T.-C.; Chau, G.-Y.; Jan, Y.-H.; Chen, C. H.; Hsu, C.-N.; Lin, K.-T.; Juang, Y.-L.; Lu, P.-J.; Cheng, H.-C.; Chen, M.-H.; Chang, C.-F.; Ting, Y.-S.; Kao, C.-Y.; Hsiao, M.; Huang, C.-Y. F. *Mol. Cell. Proteomics*, **2013**, *12*, 1335.
[29] (a) Avan, I.; Hall, D.; Katritzky, A. R. *Chem. Soc. Rev.* **2014**, *43*, 3575. (b) Trabocchi, A.; Guarna, A. (**2014**) *The Basics of Peptidomimetics, in Peptidomimetics in Organic and Medicinal Chemistry: The Art of Transforming Peptides in Drugs*, John Wiley & Sons, Ltd, Chichester, UK.
[30] Haridas, V.; Sadanandan, S.; Gopalakrishna, M. V. S.; Bijesh, M. B.; Verma, R. P.; Chinthalapalli, S.; Shandilya, A. *Chem. Comm.* **2013**, *49*, 10980.
[31] Dutta, A. S.; Crowther, M.; Gormley, J. J.; Hassall, L.; Hayward, C. F.; Gellert, P. R.; Kittlety, R. S.; Alcock, P. J.; Jamieson, A.; Moores, J. M.; Rees, A.; Wood, L. J.; Reilly, C. F.; Haworth, D. *J. Peptide Sci.* **2000**, *6*, 321.
[32] Haridas, V.; Sadanandan, S.; Sharma, Y. K.; Chinthalapalli, S.; Shandilya, A. *Tetrahedron. Lett.* **2012**, *53*, 623.
[33] Cummings, C. G.; Hamilton, A. D. *Curr. Opin. Chem. Biol.* **2010**, *14*, 341.
[34] Smissman, E. E.; Weis, J. A. *J. Het. Chem.* **1968**, *5*, 405.
[35] Spieler, J.; Huttenloch, O.; Waldmann, H. *Eur. J. Org. Chem.* **2000**, 391.
[36] (a) Jones, S.; Thornton, J. M. *Proc. Natl. Acad. Sci. U. S. A.*, **1996**, *93*, 13. (b) Moreira, I. S.; Fernandes, P. A.; Ramos, M. J. *Proteins: Struct., Funct., Bioinf.*, **2007**, *68*, 803. (c) Garner, L.; Janda, K. D. *Curr. Top. Med. Chem.*, **2011**, *11*, 258.
[37] (a) Harrison, R. S.; Shepherd, N. E.; Hoang, H. N.; Ruiz-Gomez, G.; Hill, T. A.; Driver, R. W.; Desai, V. S.; Young, P. R.; Abbenante, G.; Fairlie, D. P. *Proc. Natl. Acad. Sci. U.S.A.* **2010**, *107*, 11686. (b) Verdine, G. L.; Hilinski, G. J. *Methods Enzymol.* **2012**, 503, 3. (c) Boersma, M. D.; Haase, H. S.; Peterson-Kaufman, K. J.; Lee, E. F.; Clarke, O. B.; Colman, P. M.; Smith, B. J.; Horne, W. S.; Fairlie, W. D.; and Gellman, S. H. *J. Am. Chem. Soc.* **2012**, *134*, 315. (d) Azzarito, V.; Long, K.; Murphy, N. S.; Wilson, A. J. *Nat. Chem.* **2013**, *5*, 161.

[38] Hill, T. A.; Shepherd, N. E.; Diness, F.; Fairlie, D. P. *Angew. Chem. Int. Ed.* **2014**, *53*, 13020.
[39] Remaut, H.; Waksman, G. *TRENDS in Biochem. Sci.* **2006**, *31*, 436.
[40] (a) W. A. Loughlin, J. D. A. Tyndall, M. P. Glenn, T. A. Hill, D. P. Fairlie, *Chem. Rev.* **2010**, *110*, PR32. (b) Ross, N. T.; Katt, W. P.; Hamilton, A. D. *Phil. Trans. R. Soc. A* **2010**, *368*, 989.
[41] Arora, P. S.; Watkins, A. M. *ACS Chem. Biol.* **2014**, *9*, 1747.
[42] (a) Wyrembak, P. N.; Hamilton, A. D. *J. Am. Chem. Soc.* **2009**, *131*, 4566. (b) Jamieson, A. G.; Russell, D.; Hamilton, A. D. *Chem. Commun.* **2012**, *48*, 3709. (c) Sutherell, C. L.; Thompson, S.; Scott, R. T. W.; Hamilton, A. D. *Chem. Commun.*, **2012**, *48*, 9834. (d) German, E. A.; Ross, J. E.; Knipe, P. C.; Don, M. F.; Thompson, S.; Hamilton, A. D. *Angew. Chem. Int. Ed.* **2015**, *54*, 2649. (e) Yamashita, T.; Knipe, P. C.; Busschaert, N.; Thompson, S.; Hamilton, A. D. *Chem. Eur. J.* **2015**, *21*, 1.
[43] a) van Leusen, A. M.; Strating, J. *Q. Rep. Sulfur Chem.* **1970**, *5*, 67. (b) van Leusen, A. M.; Wildeman, J.; Oldenziel, O. *J. Org. Chem.* **1977**, *42*, 1977. (c) van Leusen, D; van Leusen, A. M. *Org. React.* **2003**, *57*, 419.
[44] (a) Che, H.; Tuyen, T. N.; Kim, H. P.; Park, H. *Bioorg. Med. Chem. Lett.* **2010**, *20*, 4035. (b) Zhang, Z.; Lippert, K. M.; Hausmann, H.; Kotke, M.; Schreiner, P. R. *J. Org. Chem.* **2011**, *76*, 9764. (c) Lamberth, C.; Dumeunier, R.; Trah, S.; Wendeborn, S.; Godwin, J.; Schneiter, P.; Corran, A. *Bioorg. Med. Chem.* **2013**, *21*, 127.
[45] Baghbanzadeh, M.; Pilger, C.; Kappe, O. C. *J. Org. Chem.* **2011**, *76*, 8138.
[46] Bellina, F.; Cauteruccio, S.; Di Fiore, A.; Rossi, R. *Eur. J. Org. Chem.* **2008**, *2008*, 5436.

3. PIPERAZINE-BASED DOPAMINE RECEPTORS LIGANDS

Introduction

Dopamine receptors belong to the rhodopsin family and have been classified in five subtypes, usually divided into two families: D_1-like and D_2-like, depending on which G-proteins are coupled and the activity of these latter. In the first class are present the D_1 and the less abundant D_5 receptor, which are coupled with G_s-proteins responsible for the activation of adenylyl cyclase and the stimulation of cyclic-AMP. The receptors D_2, D_3 and D_4 belong to the second class and are coupled with $G_{i/o}$-proteins, which inhibit adenylyl cyclase, suppress Ca^{2+} currents and activate receptor-gated K^+ currents.[1] The most abundant receptors in this last class are D_2 and D_3, which possess a high structural homology, sharing about 50% overall amino acid sequence and 78% in their agonist binding sites. They are targeted for the treatment of Parkinson's disease, dyskinesia, schizophrenia, drug addiction, hyperprolactinemia and restless legs syndrome,[1] with slightly different effects on each diseases. Only recently, the X-ray structure of a chimeric D_3 receptor was resolved,[2] but computational models failed to predict selective molecules for one of the two receptors.

In this context, the symmetric secondary diamine piperazine is a privileged scaffold, and in particular the 1,4-disubstituted aromatic piperazine (1,4-DAP) framework is widely present in a number of dopamine receptors ligands.[3] Although presently commercial drugs are not selective, recent papers reported selective agonists for both D_2 and D_3 receptors (**Figure 19**).[4] It is indeed sure that even moderately D_3/D_2 selective compounds might offer a favorable profile compared to currently available drugs. Therefore, the design of selective ligands is a notable and challenging task.[1]

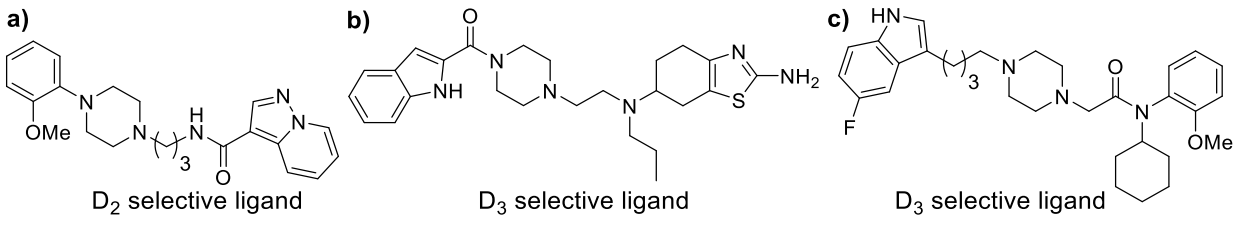

Figure 19. Recently developed D_3/D_2 selective 1,4-DAP ligands.[4]

Despite disparate chemical structures, currently available structure activity relationship (SAR) studies on piperazine and piperidine-based D_2/D_3 receptor ligands indicate that some key features are always present in most relevant bioactive compounds. In particular, all structures present an aromatic head group that ensures

the overall activity (*red*), a linker usually involved in the subtype selectivity among dopamine receptors, and a lipophilic appendage (*green*) able to control the affinity (**Figure 20**).[3]

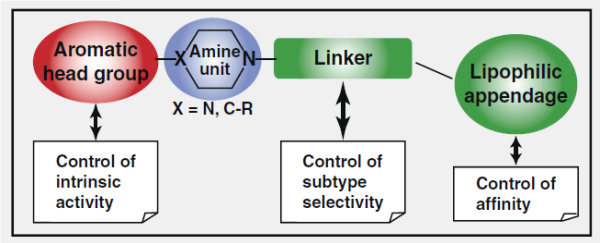

Figure 20. Results of SAR (Structure-Activity Relationship) studies on 1,4-DAP dopaminergic drugs (fig. from ref. 3, pg. 152).

Being aware that even minor structural modifications of these three key elements would be able to deeply affect the biological action, we decided to exploit the potentiality of the *N*-split Ugi reaction (*for further details see* **Chapter 1.2**) to rapidly generate great diversity around few assessed key elements. Focusing our attention on the binding mode of the most D_3 selective agonists known to date (**Figure 19b-c**),[4] we recently reported[5] the design of a new family of piperazine-based potential agonists, with the aim to investigate the effect of various chemical elements on bioactivity and, possibly, on selectivity. In particular, we achieved a library of new 1,4-disubstituted aromatic piperazines (1,4-DAP), which are characterized by a variety of lipophilic appendages and linker's lengths (**Scheme 30**).

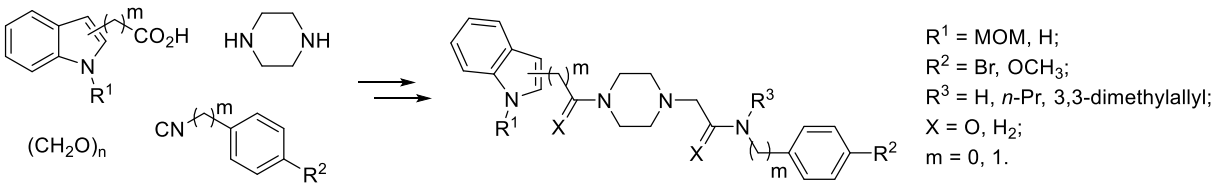

Scheme 30. Synthesis of a library of novel D_2/D_3 receptors agonists, employing the *N*-split Ugi reaction as the key diversity-generation step.

Results and discussion

To mimic the aromatic head group of the D_3 selective compound reported in **Figure 19b**, we selected 1*H*-indole-2-carboxylic acid or the corresponding *N*-methoxymethyl (*N*-MOM) protected derivative as acidic component, and in combination with piperazine, paraformaldehyde and different aromatic and benzylic isocyanides we carried out the *N*-split Ugi reaction in methanol at reflux. In particular, employing aromatic

1-isocyano-4-methoxybenzene or 1-isocyano-4-bromobenzene and benzylic 1-(isocyanomethyl)-4-methoxybenzene or 1-bromo-4-(isocyanomethyl)benzene as isocyanide moieties we were able to smoothly obtain the corresponding *N*-split Ugi adducts **38-44** in good yields (**Scheme 31**), with different linker lengths and lipophilic properties, important parameters for the biological activity (**Figure 20**). To further investigate the biological behaviour of a higher flexible and more basic scaffold, we considered to reduce the amide carbonyl groups of selected compounds, by means of a double reductions using $LiAlH_4$, affording quantitatively the corresponding triamines derivatives **45-48**. Moreover, compounds **49-52** with increased lipophilicity could be easily obtained by reductive amination with propionaldehyde (**Scheme 31**). On the other hand, starting from *N*-MOM protected compounds **40-41** and **44**, a regioselective alkylation of the secondary amide was achieved, employing either 1-bromopropane or 3,3-dimethylallyl bromide as electrophilic species. Starting from the obtained compounds **53-57**, the corresponding NH-indole derivatives **58-62** could be easily achieved under classical deprotection conditions (**Scheme 31**).

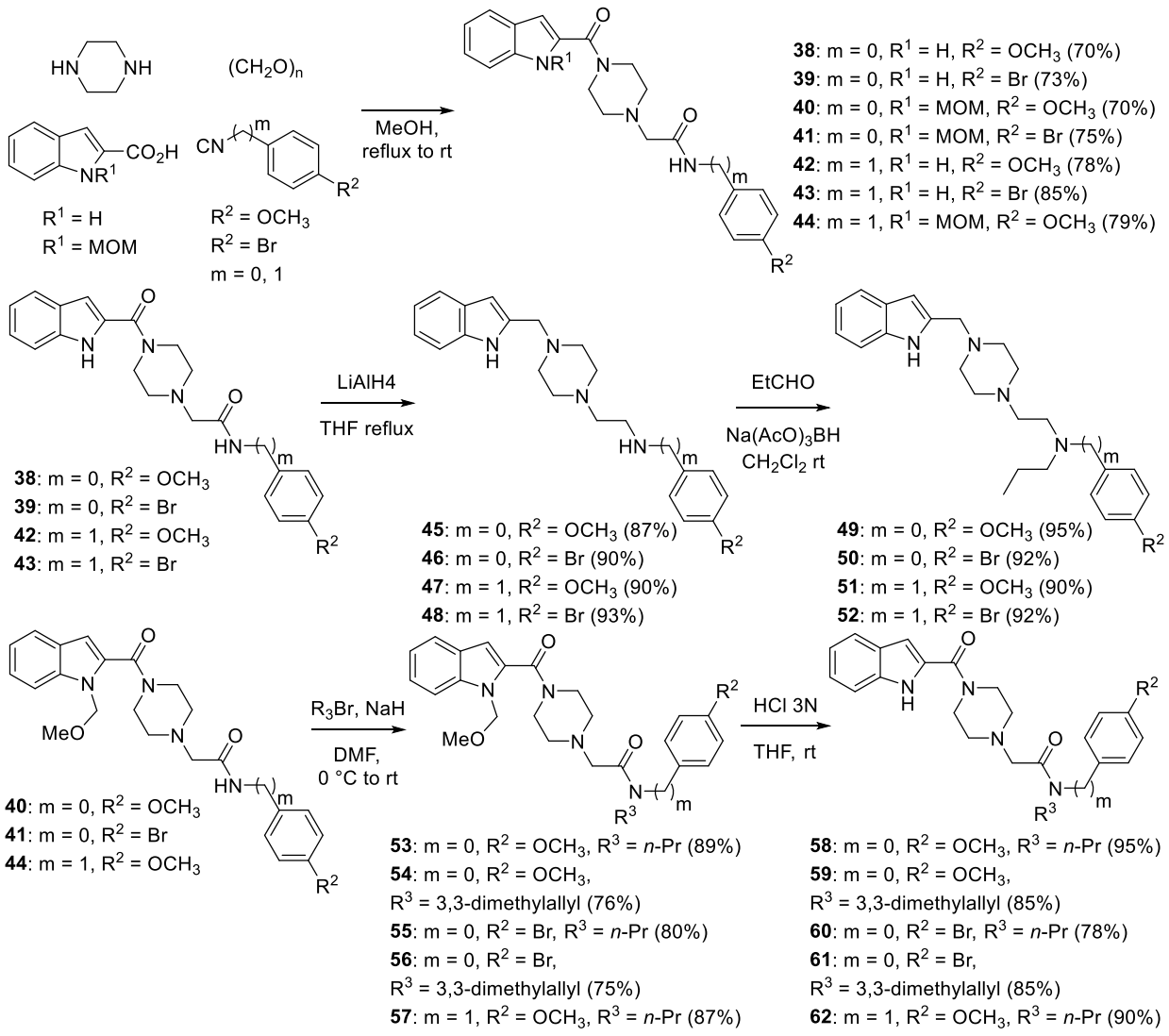

Scheme 31. General scheme for the synthesis of compounds **38-62**.

Employing 2-(1*H*-indol-3-yl)acetic acid and the corresponding *N*-MOM protected derivative as acid component in a similar *N*-split Ugi reaction protocol, we were able to increase the distance between the piperazine core and the aromatic indolyl head group. In this case, only aromatic 1-isocyano-4-methoxybenzene or 1-isocyano-4-bromobenzene were employed as isocyanide moieties, affording compounds **63**-**66** in comparable yields (**Scheme 32**). Reactions conducted on **63**-**64** allowed to obtain triamines **67**-**68** and the corresponding *N*-propyl derivatives **69**-**70**. Starting from *N*-MOM protected *N*-split Ugi adducts **65**-**66**, direct alkylation smoothly afforded compounds **71**-**72** (**Scheme 32**).

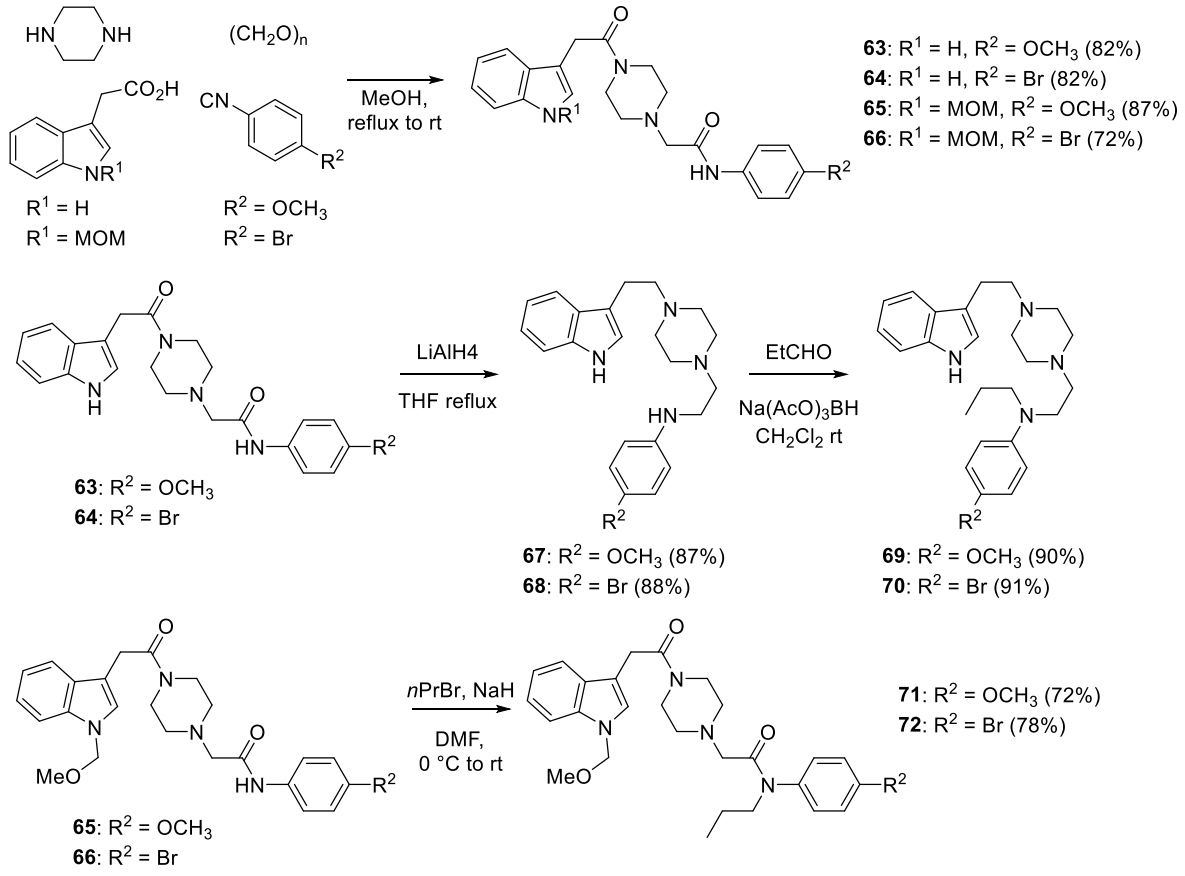

Scheme 32. General scheme for the synthesis of compounds **63**-**72**.

In collaboration with by Prof. Gmeiner and Dr. Hubner,[6] compounds **38**–**72** have been evaluated for their affinity and selectivity through competitive binding assay for the dopamine D_2 and D_3 receptors, against the standard tritiated spiperone.[7] Although no significant D_2/D_3 selectivity was observed, the more active compounds are characterized by the triamine scaffold (**45**-**52** and **67**-**70**), with different behaviour depending on the elongation between piperazine and indolyl moieties. In order to better formulate our structure-activity relationship (SAR) considerations, we divided the set of more active compounds into two families: 2-indolyl methyl derivatives (**45**-**52**) and 3-indolyl ethyl ones (**67**-**70**). In particular, in the 2-indolyl methyl series,

compound **50** was the most active one, with a D_2 affinity of 220 nM, while the steric hindrance of *p*-OMe-substituent (**49**) affected negatively the activity. In addition, the basicity and substitutions of the linear amine seem to be important, with worst result for the benzylic compound **52** and not substituted one **46** (**Graphic 1**). On the other hand, in the 3-indolyl ethyl series (**67**-**70**) *p*-Br substituted compounds **68** and **70** proved to be the the most active, showing the best D_2 affinities of 53 and 58 nM respectively. Again, the steric hindrance of the methoxyl groups was detrimental, and no significant improvement in the activity was observed for the *N*-propyl derivative **70** (**Graphic 1**) (*for further details see* **Appendix A.3**).

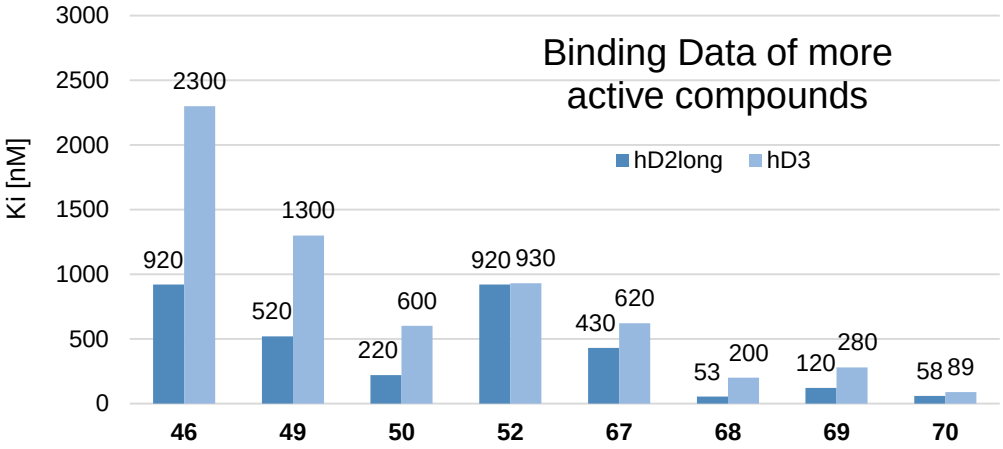

Graphic 1. Selected radioligand binding data for the most promising 2-indolyl methyl derivatives **46**, **49**, **50**, **52** and the 3-indolyl ethyl ones **68**, **70** employing the Human D_{2L} and D_3 receptors.

For the most promising compounds **68** and **70** binding selectivity within the dopamine receptors family was determined. They display affinities for D_{2S} (48 nM, 51 nM) similar to D_{2L} (**Graphic 1**), while reduced binding data was observed for the D_1-like (D_1 480 nM, 250 nM; D_5 3600 nM, 1300 nM). Surprisingly, best affinities among the D_2-like family could be determined towards D_4, with 20 nM for **68** and even 0.72 nM for **70**. Furthermore, compounds **68** and **70** were also tested on D_{2S} receptor activation properties showing antagonist effects in a cAMP accumulation assay.

Finally, in collaboration with Dr. Sacchetti,[8] we performed molecular docking with Autodock 4.2[9] for compounds **68** and **70** on D_2 and D_3 homology models (prepared with YASARA software,[10] starting from the X-ray structure of human D_3 receptor (PDB code: 3BPL); *for further details see* **Appendix A.2**), with the aim to guide the future structure optimization of the *N*-split Ugi primary scaffold. The best docking conformations were further optimized with molecular dynamics in a membrane model with YASARA. The two compounds presented both piperazine nitrogens protonated at physiological *p*H, while the less basic aniline nitrogen is present as a free base. In the D_3 receptor homology model, both compounds showed a strong hydrogen bond between N_a^+H hydrogen and the key residue Asp110$^{3.32}$, thus anchoring the ligands to the receptor binding site, as reported for similar structures.[11] The aromatic indole headgroup is disposed in a

more internal region, and it is involved in π-π interactions with Phe345, Phe346 and His349, with additional cation-π interaction for compound **70**. Moreover, compound **70** shows lipophilic interactions between the *n*-propyl residue and Val86, Leu89 and Glu90, combined with a stronger π-π interaction of the bromoaryl group with Tyr365. From these computational studies, the presence of the *n*-propyl group seems to force the indole ring to go deeper in the receptor pocket thus enabling a further H-bond between NH and Ser192 (**Figure 21**). This observation could explain the slightly higher affinity of **70** for the D_3 receptor (**Figure 21**). The contribution of individual amino acid residues of the dopamine receptor D_3 cited above has been recently highlighted using accurate QM/MM calculations.[12]

Similar results were observed for docking studies on the D_2 model receptor, explaining the low levels of D_2/D_3 selectivity experimentally observed. On the other hand, the presence of an additional H-bond between the NH-indole for both compounds could explain their similar affinities for the D_{2L} (53 nM and 58 nM, **Graphic 1**).

The lower activity of *p*-OMe substituted compounds **67** and **69** (**Graphic 1**) can be ascribed to a reorganization of the entire molecule, due to the different position of the *p*-OMe substituted phenyl ring in the binding site.

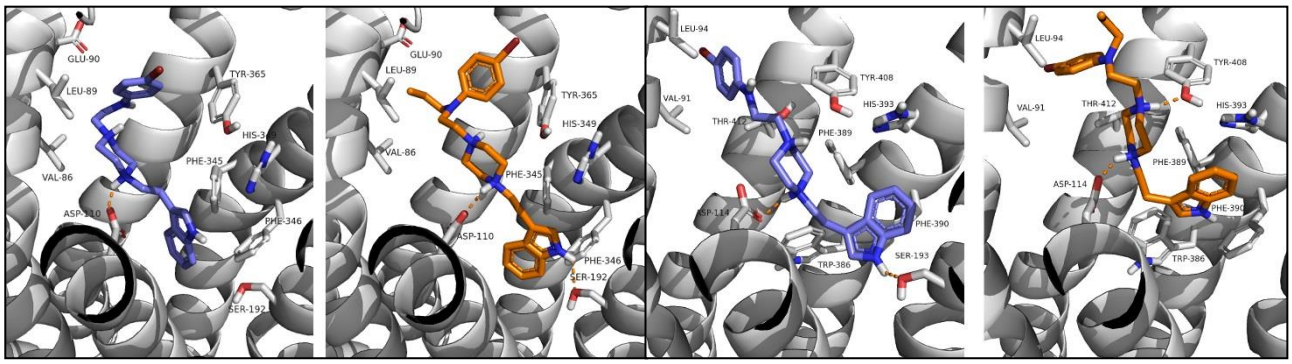

Figure 21. Left: docking poses for **68** (*cyan*) and **70** (*orange*) on the D_3 receptor model.
Right: docking poses for **68** (*cyan*) and **70** (*orange*) on the D_2 receptor model.

Conclusions

We developed a novel approach for the synthesis of piperazine-based dopamine receptor ligands, by means of the key *N*-split Ugi multicomponent reaction. The resulting initial scaffolds were successfully modified to enhance the potentiality of this approach, being able to adjust almost every key pharmacophoric elements, such as the indole head, the linker to the aromatic moiety and the global flexibility and basicity of the molecule. Biological evaluation on D_2 and D_3 receptors resulted in the identification of a novel piperazine-based framework, for which docking studies allowed to pinpoint the key interactions, with useful indications to extend the *N*-split Ugi library and possibly to improve the present poor D_2/D_3 selectivity.

Experimental section

GENERAL INFORMATION

All solvents were distilled and properly dried, when necessary, prior to use. All chemicals were purchased from commercial sources and used directly, unless indicated otherwise. All reactions were run under N_2, unless otherwise indicated. All reactions were monitored by thin layer chromatography (TLC) on precoated silica gel 60 F254; spots were visualized with UV light or by treatment with 1% aqueous $KMnO_4$ solution. Products were purified by flash chromatography on silica gel 60 (230 - 400 mesh).

NMR spectra were recorded with 300 or 400 MHz spectrometers. Chemical shifts (δ) are expressed in ppm relative to TMS at δ = 0 ppm for ^{1}H NMR and relative to CDCl3 at δ = 77.16 ppm for ^{13}C NMR. ^{13}C NMR spectra have been recorded using the APT pulse sequence; the signals of CH and CH_3 are positive while CH_2 and quarternary carbons are negative (*for further details see* **Appendix A.1**). High-resolution MS spectra were recorded with a Waters Micromass Q-ToF micro TM mass spectrometer, equipped with an ESI source. Formamides,[13] isocyanides[14] and *N*-MOM protected indoles[15] were prepared according to the literature.

GENERAL PROCEDURE FOR THE SYNTHESIS OF COMPOUNDS **38-44**, **63-66**

To a solution of piperazine (3 mmol, 1.0 eq.) in 3 mL of methanol, paraformaldehyde (4.5 mmol, 1.5 eq.), carboxylic acid (3 mmol, 1.0 eq.) and isocyanide (3 mmol, 1.0 eq.) were added. The mixture was refluxed for 15 minutes, then cooled to room temperature and stirred for 1 hour. The resulting mixture was then concentrated under reduced pressure, to give a residue which was purified as indicated below.

2-(4-(1H-indole-2-carbonyl)piperazin-1-yl)-N-(4-methoxyphenyl)acetamide (**38**)

2-carboxy indole and 1-isocyano-4-methoxybenzene were used. The product was collected by filtration (70% yield). ^{1}H NMR (300 MHz, $CDCl_3$): δ 9.37 (br, m, 1H), 8.86 (br, m, 1H), 7.64 (br, d, *J* = 7.8 Hz, 1H), 7.48 (d, *J* = 8.9 Hz, 2H), 7.42 (br, d, *J* = 7.8 Hz, 1H), 7.28 (br, t, *J* = 7.5 Hz, 1H), 7.13 (br, t, *J* = 7.5 Hz, 1H), 6.89 (d, *J* = 8.9 Hz, 2H), 6.77 (s, 1H), 4.01 (br, m, 4H), 3.80 (s, 3H), 3.20 (s, 2H), 2.72 (br, t, *J* = 4.9 Hz, 4H). ^{13}C NMR (75 MHz, $CDCl_3$): δ 167.4, 162.6, 156.4, 135.7, 130.5, 128.8, 127.4, 124.5, 121.9, 121.3 (2C), 120.7, 114.2 (2C), 111.8, 105.3, 61.9, 55.4, 53.5 (2C), 43.6 (2C). HRMS (ESI): calcd for $[C_{22}H_{25}N_4O_3]^+$ 393.1921, found 393.1933 [MH^+].

2-(4-(1H-indole-2-carbonyl)piperazin-1-yl)-N-(4-bromophenyl)acetamide (**39**)

2-carboxy indole and 1-bromo-4-isocyanobenzene were used. The product was collected by filtration (73% yield). ^{1}H NMR (300 MHz, $CDCl_3$): δ 9.31 (br, m, 1H), 9.02 (br, m, 1H), 7.64 (br, d *J* = 7.7 Hz, 1H), 7.55 – 7.38 (m, 5H), 7.29 (br, t, *J* = 7.6 Hz, 1H), 7.14 (br, t, *J* = 7.5 Hz, 1H), 6.77 (s, 1H), 4.02 (br, m, 4H), 3.22 (s, 2H), (br, m, 4H).^{13}C NMR (75 MHz, DMF-d_7): δ 169.3, 162.9, 138.6, 136.7, 131.9 (2C), 130.7, 127.6, 123.5, 121.9 (3C), 120.2, 115.4, 112.3, 104.6, 62.1, 53.4 (2C), 45.8 (2C). HRMS (ESI): calcd for $[C_{21}H_{21}BrN_4NaO_2]^+$ 463.0740, found 463.0734 [MNa^+].

2-(4-(1-(methoxymethyl)-1H-indole-2-carbonyl)piperazin-1-yl)-N-(4-methoxyphenyl)acetamide (**40**)

1-(methoxymethyl)-indole-2-carboxylic acid and 1-isocyano-4-methoxybenzene were used. The solvent was evaporated under reduced pressure and the residue was purified by flash chromatography (EtOAc/Hex 8/2) (70% yield). ^{1}H NMR (300 MHz, $CDCl_3$): δ 8.90 (br, m, 1H), 7.62 (br, d, *J* = 7.7 Hz, 1H), 7.51 (br, d, *J* = 7.8 Hz, 1H), 7.47 (d, *J* = 8.9 Hz, 2H), 7.32 (br, t, *J* = 7.6 Hz, 1H), 7.18 (br, t, *J* = 7.5 Hz, 1H), 6.87 (d, *J* = 8.9 Hz, 2H), 6.65 (s, 1H), 5.65 (s, 2H), 3.87 (br, m, 4H), 3.79 (s, 3H), 3.24 (s, 3H), 3.22 (s, 2H), 2.70 (br, m, 4H). ^{13}C NMR (75 MHz, $CDCl_3$): δ 163.0 (2C), 156.6, 137.9, 130.4 (2C), 126.5, 124.1, 121.5, 121.0 (3C), 114.0 (2C), 110.3, 105.5, 74.7, 61.5, 56.0, 55.5, 53.4 (2C), 49.0, 43.6. HRMS (ESI): calcd for $[C_{24}H_{28}N_4NaO_4]^+$ 459.2003, found 459.2014 [MNa^+].

N-(4-bromophenyl)-2-(4-(1-(methoxymethyl)-1H-indole-2-carbonyl)piperazin-1-yl)acetamide (**41**)

1-(methoxymethyl)-indole-2-carboxylic acid and 1-bromo-4-isocyanobenzene were used. The solvent was evaporated under reduced pressure and the residue was purified by flash chromatography (EtOAc/Hex 8/2) (75% yield). ^{1}H NMR

(400 MHz, $CDCl_3$): δ 9.06 (br, m, 1H), 7.66 (br, d, *J* = 7.7 Hz, 1H), 7.55 (br, d, *J* = 7.8 Hz, 1H), 7.51 (d, *J* = 8.9 Hz, 2H), 7.47 (d, *J* = 8.9 Hz, 2H), 7.35 (t, *J* = 7.7 Hz, 1H), 7.22 (t, *J* = 7.5 Hz, 1H), 6.68 (s, 1H), 5.68 (s, 2H), 3.91 (br, m, 4H), 3.25 (br, s, 2H), 3.27 (s, 3H), 2.74 (br, m, 4H). ^{13}C NMR (100 MHz, $CDCl_3$): δ 167.6, 163.8, 137.3, 135.2, 132.7 (2C), 127.5, 124.7, 122.2, 121.8 (3C), 117.7, 111.1, 107.0, 106.0, 75.7, 62.6, 56.6, 54.2 (2C), 45.5 (2C). HRMS (ESI): calcd for $[C_{23}H_{25}BrN_4NaO_3]^+$ 507.1002, found 506.9987 [MNa^+].

2-(4-(1H-indole-2-carbonyl)piperazin-1-yl)-N-(4-methoxybenzyl)acetamide (**42**)

2-carboxy indole and 1-(isocyanomethyl)-4-methoxybenzene were used. The solvent was evaporated under reduced pressure and the residue was purified by flash chromatography (CH_2Cl_2/CH_3OH/Et_3N 98/1/1) (78% yield). ^{1}H NMR (300 MHz, $CDCl_3$): δ 9.51 (br, m, 1H), 7.63 (br, d, *J* = 7.7 Hz, 1H), 7.41 (br, d, *J* = 7.8 Hz, 1H), 7.35 (br, m, 1H), 7.27 (br, t, *J* = 7.6 Hz, 1H), 7.22 (d, *J* = 8.6 Hz, 2H), 7.12 (br, t, *J* = 7.6 Hz, 1H), 6.88 (d, *J* = 8.6 Hz, 2H), 6.73 (s, 1H), 4.43 (d, *J* = 5.9 Hz, 2H), 3.92 (br, m, 4H), 3.79 (s, 3H), 3.14 (s, 2H), 2.63 (br, m, 4H). ^{13}C NMR (75 MHz, $CDCl_3$): δ 162.5 (2C), 159.0, 135.8, 130.3, 129.1 (2C), 128.7, 127.1, 124.4, 121.9, 120.7, 114.0 (2C), 111.7, 105.4, 61.3, 55.2, 53.3 (2C), 46.8, 42.6, 43.1. HRMS (ESI): calcd for $[C_{23}H_{26}N_4NaO_3]^+$ 429.1897, found 429.1891 [MNa^+].

2-(4-(1H-indole-2-carbonyl)piperazin-1-yl)-N-(4-bromobenzyl)acetamide (**43**)

2-carboxy indole and 1-bromo-4-(isocyanomethyl)benzene were used. The solvent was evaporated under reduced pressure and the residue was purified by flash chromatography (CH_2Cl_2/CH_3OH/Et_3N 98/1/1) (85% yield). ^{1}H NMR (300 MHz, $CDCl_3$): δ 9.50 (br, m, 1H), 7.63 (br, d, *J* = 7.8 Hz, 1H), 7.54 – 7.34 (m, 4H), 7.27 (br, t, *J* = 7.6 Hz, 1H), 7.18 – 7.03 (m, 3H), 6.74 (s, 1H), 4.45 (d, *J* = 6.1 Hz, 2H), 3.92 (br, m, 4H), 3.13 (s, 2H), 2.61 (br, m, 4H). ^{13}C NMR (75 MHz, $CDCl_3$): δ 167.6, 162.5, 137.4, 135.6, 131.8, 129.5 (2C), 129.0, 127.4, 124.5 (2C), 122.0, 121.8, 120.7, 111.7, 105.3, 61.4, 53.5 (2C), 46.1, 42.5, 43.3. HRMS (ESI): calcd for $[C_{22}H_{23}N_4NaO_2]^+$ 477.0897, found 477.0884 [MNa^+].

N-(4-methoxybenzyl)-2-(4-(1-(methoxymethyl)-1H-indole-2-carbonyl)piperazin-1-yl)acetamide (**44**)

1-(methoxymethyl)-indole-2-carboxylic acid and 1-(isocyanomethyl)-4-methoxybenzene were used. The solvent was evaporated under reduced pressure and the residue was purified by flash chromatography (EtOAc/Et_3N 99/1) (79% yield). ^{1}H NMR (300 MHz, $CDCl_3$): δ 7.61 (br, d, *J* = 7.9 Hz, 1H), 7.50 (br, d, *J* = 7.8 Hz, 1H), 7.31 (br, t, *J* = 7.7 Hz, 1H), 7.20 (d, *J* = 8.6 Hz, 2H), 7.17 (br, t, *J* = 7.7 Hz, 1H), 6.86 (d, *J* = 8.6 Hz, 2H), 6.60 (s, 1H), 5.62 (s, 2H), 4.41 (d, *J* = 5.9 Hz, 2H), 3.79 (s, 3H), 3.77 (br, m, 4H), 3.21 (s, 3H), 3.13 (br, s, 2H), 2.59 (br, m, 4H). ^{13}C NMR (75 MHz, $CDCl_3$): δ 163.1 (2C), 159.1, 137.8, 130.8, 130.2, 129.1 (2C), 126.7, 124.2, 121.6, 121.2, 114.3 (2C), 110.4, 105.5, 75.0, 61.3, 56.1, 55.3, 53.3 (2C), 46.9, 42.6, 41.8. HRMS (ESI): calcd for $[C_{25}H_{30}N_4NaO_4]^+$ 473.2159, found 473.2152 [MNa^+].

2-(4-(2-(1H-indol-3-yl)acetyl)piperazin-1-yl)-N-(4-methoxyphenyl)acetamide (**63**)

2-(1H-indol-3-yl)acetic acid and 1-isocyano-4-methoxybenzene were used. The solvent was evaporated under reduced pressure and the residue was purified by flash chromatography (CH_2Cl_2/CH_3OH/Et_3N 98/1/1) (82% yield). ^{1}H NMR (300 MHz, $CDCl_3$): δ 8.77 (br, m, 1H), 8.35 (br, m, 1H), 7.61 (br, d, *J* = 7.8 Hz, 1H), 7.42 (d, *J* = 8.9 Hz, 2H), 7.36 (br, d, *J* = 7.8 Hz, 1H), 7.20 (br, t, *J* = 7.6 Hz, 1H), 7.12 (br, t, *J* = 7.6 Hz, 1H), 7.08 (s, 1H), 6.84 (d, *J* = 8.9 Hz, 2H), 3.85 (s, 2H), 3.77 (s, 3H), 3.70 (br, m, 2H), 3.53 (br, m, 2H), 3.05 (s, 2H), 2.55 (br, m, 2H), 2.36 (br, m, 2H). ^{13}C NMR (75 MHz, $CDCl_3$): δ 170.3, 167.4, 156.1, 136.1, 130.6, 126.7, 122.5, 122.2, 121.3 (2C), 119.6, 118.6, 114.1 (2C), 111.5, 108.7, 61.8, 55.5, 53.3, 53.2, 46.1, 41.8, 31.5. HRMS (ESI): calcd for $[C_{23}H_{27}N_4O_3]^+$ 407.2078, found 407.2076 [MH^+].

2-(4-(2-(1H-indol-3-yl)acetyl)piperazin-1-yl)-N-(4-bromophenyl)acetamide (**64**)

2-(1H-indol-3-yl)acetic acid and 1-bromo-4-isocyanobenzene were used. The solvent was evaporated under reduced pressure and the residue was purified by flash chromatography (CH_2Cl_2/CH_3OH/Et_3N 98/1/1) (82% yield). ^{1}H NMR (300 MHz, $CDCl_3$): δ 8.92 (br, m, 1H), 8.30 (br, m, 1H), 7.61 (br, d, *J* = 7.7 Hz, 1H), 7.41 (br, m, 4H), 7.36 (br, d, *J* = 7.8 Hz, 1H), 7.21 (br, t, *J* = 7.6 Hz, 1H), 7.12 (br, t, *J* = 7.6 Hz, 1H), 7.09 (br, s, 1H), 3.85 (s, 2H), 3.72 (br, m, 2H), 3.53 (br, m, 2H), 3.06 (s, 2H), 2.55 (br, m, 2H), 2.37 (br, m, 2H). ^{13}C NMR (75 MHz, $CDCl_3$): δ 170.5 (2C), 136.8, 136.5, 132.4 (2C), 127.3, 122.8, 121.5 (2C), 120.1 (2C), 119.0, 117.4, 111.8, 109.2, 61.9, 53.6, 53.5, 46.1, 41.9, 31.7. HRMS (ESI): calcd for $[C_{22}H_{23}BrN_4NaO_2]^+$ 478.3368, found 478.3364 [MNa^+].

2-(4-(2-(1-(methoxymethyl)-1H-indol-3-yl)acetyl)piperazin-1-yl)-N-(4-methoxyphenyl)acetamide (**65**)

2-(1-(methoxymethyl)-indol-3-yl)acetic acid and 1-isocyano-4-methoxybenzene were used. The solvent was evaporated under reduced pressure and the residue was purified by flash chromatography (CH_2Cl_2/CH_3OH/Et_3N

98/1/1) (87% yield). ^{1}H NMR (300 MHz, $CDCl_3$): δ 8.78 (br, m, 1H), 7.60 (br, d, *J* = 7.9 Hz, 1H), 7.46 (br, d, *J* = 7.8 Hz, 1H), 7.42 (d, *J* = 9.0 Hz, 2H), 7.26 (br, t, *J* = 7.6 Hz, 1H), 7.16 (br, t, *J* = 7.5 Hz, 1H), 7.10 (s, 1H), 6.85 (d, *J* = 9.0 Hz, 2H), 5.41 (s, 2H), 3.84 (s, 2H), 3.78 (s, 3H), 3.73 (br, m, 2H), 3.56 (br, m, 2H), 3.23 (s, 3H), 3.08 (s, 2H), 2.56 (br, m, 2H), 2.39 (br, m, 2H). ^{13}C NMR (75 MHz, $CDCl_3$): δ 169.7, 167.2, 156.4, 136.5, 130.5, 128.0, 126.1, 122.8, 121.2 (2C), 120.3, 118.8, 114.3 (2C), 110.0, 109.2, 77.2, 61.8, 56.0, 55.4, 53.4, 53.2, 46.1, 41.7, 31.1. HRMS (ESI): calcd for $[C_{25}H_{30}N_4NaO_4]^+$ 473.2159, found 473.2126 [MNa^+].

N-(4-bromophenyl)-2-(4-(2-(1-(methoxymethyl)-1H-indol-3-yl)acetyl)piperazin-1-yl)acetamide (**66**)

2-(1-(methoxymethyl)-indol-3-yl)acetic acid and 1-bromo-4-isocyanobenzene were used. The solvent was evaporated under reduced pressure and the residue was purified by flash chromatography (CH_2Cl_2/CH_3OH/Et_3N 98/1/1) (72% yield). ^{1}H NMR (300 MHz, $CDCl_3$): δ 9.01 (br, m, 1H), 7.59 (br, d, *J* = 7.8 Hz, 1H), 7.52 – 7.37 (m, 5H), 7.26 (br, t, *J* = 7.4 Hz, 1H), 7.16 (br, t, *J* = 7.4 Hz, 1H), 7.09 (s, 1H), 5.40 (s, 2H), 3.84 (s, 2H), 3.74 (br, m, 2H), 3.60 (br, m, 2H), 3.22 (s, 3H), 3.19 (br, s, 2H), 2.67 (br, m, 2H), 2.49 (br, m, 2H). ^{13}C NMR (75 MHz, $CDCl_3$): δ 170.2 (2C), 137.0, 136.6, 132.3 (2C), 128.4, 126.5, 123.1, 121.4 (2C), 120.7, 119.2, 117.3, 110.4, 109.3, 76.9, 62.2 and 61.8 (1C), 56.3, 53.7 (2C), 46.4 and 46.1 (1C), 42.0 and 41.8 (1C), 31.5. HRMS (ESI): calcd for $[C_{24}H_{27}BrN_4NaO_3]^+$ 521.1159, found 521.1141 [MNa^+].

GENERAL PROCEDURE FOR THE SYNTHESIS OF COMPOUNDS **45-48**, **67-68**

$LiAlH_4$ (1M in THF, 1.95 mmol) was dissolved in anhydrous THF (2 mL) at 40 °C under N_2 atmosphere and a solution of compound **38** (or **39-43**, **63-64**) (0.65 mmol) in anhydrous THF (10 mL) was slowly added. After 15 minutes, the solution was refluxed until full conversion (monitored by TLC). Then the reaction was cooled to room temperature, quenched with H_2O, NaOH 15% and H_2O (n. g of $LiAlH_4$ require n. mL of H_2O, n. mL of NaOH 15%, and 3n. mL of H_2O added in succession) and stirred vigorously overnight. The precipitate was removed by filtration over celite and the solvent was evaporated under reduced pressure. The resulting residue was purified by flash chromatography (FC) as indicated below.

N-(2-(4-((1H-indol-2-yl)methyl)piperazin-1-yl)ethyl)-4-methoxyaniline (**45**)

FC: CH_2Cl_2/CH_3OH 98/2 (87% yield). ^{1}H NMR (300 MHz, $CDCl_3$): δ 8.65 (br, m, 1H), 7.55 (br, d, *J* = 7.7 Hz, 1H), 7.33 (br, d, d, *J* = 7.8 Hz, 1H), 7.14 (br, t, *J* = 7.5 Hz, 1H), 7.07 (br, t, *J* = 7.6 Hz, 1H), 6.79 (d, *J* = 8.8 Hz, 2H), 6.61 (d, *J* = 8.8 Hz, 2H), 6.36 (s, 1H), 3.74 (s, 3H), 3.68 (s, 2H), 3.11 (t, *J* = 5.9 Hz, 2H), 2.62 (t, *J* = 5.9 Hz, 2H), 2.52 (br, m, 9H). ^{13}C NMR (75 MHz, $CDCl_3$): δ 148.1, 138.7, 132.1, 131.2, 124.3, 117.6, 116.2, 115.7, 111.0 (2C), 110.3 (2C), 106.8, 97.7, 52.93, 52.1, 51.7, 49.1 (2C), 48.6 (2C), 37.3. HRMS (ESI): calcd for $[C_{22}H_{29}N_4O]^+$ 365.2336, found 365.2322 [MH^+].

N-(2-(4-((1H-indol-2-yl)methyl)piperazin-1-yl)ethyl)-4-bromoaniline (**46**)

FC: CH_2Cl_2/CH_3OH 98/2 (90% yield). ^{1}H NMR (300 MHz, $CDCl_3$): δ 8.60 (br, m, 1H), 7.55 (br, d, *J* = 7.7 Hz, 1H), 7.33 (br, d, *J* = 7.8 Hz, 1H), 7.24 (d, *J* = 8.8 Hz, 2H), 7.15 (br, t, *J* = 7.4 Hz, 1H), 7.07 (br, t, *J* = 7.4 Hz, 1H), 6.49 (d, *J* = 8.8 Hz, 2H), 6.36 (s, 1H), 4.31 (br, m, 1H), 3.70 (s, 2H), 3.10 (br, q, *J* = 5.5 Hz, 2H), 2.62 (t, *J* = 5.7 Hz, 2H), 2.53 (br, m, 8H). ^{13}C NMR (75 MHz, $CDCl_3$): δ 147.3, 136.0, 135.0, 132.0 (2C), 128.3, 121.7, 120.2, 119.6, 114.5 (2C), 110.8, 108.8, 101.9, 56.3, 55.7, 52.9 (2C), 52.5 (2C), 40.2. HRMS (ESI): calcd for $[C_{21}H_{26}BrN_4]^+$ 413.1335, found 413.1342 [MH^+].

2-(4-((1H-indol-2-yl)methyl)piperazin-1-yl)-N-(4-methoxybenzyl)ethan-1-amine (**47**)

FC: EtOAc/CH_3OH/Et_3N 90/9/1 (90% yield). ^{1}H NMR (300 MHz, $CDCl_3$): δ 8.80 (br, m, 1H), 7.53 (br, d, *J* = 7.6 Hz, 1H), 7.32 (br, d, *J* = 7.8 Hz, 1H), 7.26 (d, *J* = 8.6 Hz, 2H), 7.13 (br, t, *J* = 7.6 Hz, 1H), 7.06 (br, t, *J* = 7.6 Hz, 1H), 6.85 (d, *J* = 8.6 Hz, 2H), 6.34 (s, 1H), 3.75 (s, 3H), 3.66 (s, 2H), 3.46 (s, 2H), 2.78 (br, m, 4H), 2.72 (t, *J* = 6.8 Hz, 2H), 2.64 (t, *J* = 6.8 Hz, 2H), 2.49 (br, m, 5H). ^{13}C NMR (75 MHz, $CDCl_3$): δ 159.2, 136.2, 135.2, 130.4, 129.9 (2C), 128.2, 121.6, 120.2, 119.6, 114.1 (2C), 110.8, 101.9, 56.7, 55.7, 55.3, 53.1 (2C), 52.9 (2C), 52.7, 44.7. HRMS (ESI): calcd for $[C_{23}H_{31}N_4O]^+$ 379.2492, found 379.2481 [MH^+].

2-(4-((1H-indol-2-yl)methyl)piperazin-1-yl)-N-(4-bromobenzyl)ethan-1-amine (**48**)

FC: EtOAc/CH3OH/Et3N 90/9/1 (93% yield). 1H NMR (300 MHz, CDCl3): δ 8.69 (br, m, 1H), 7.54 (br, d, J = 7.6 Hz, 1H), 7.44 – 7.19 (m, 5H), 7.14 (br, t, J = 7.4 Hz, 1H), 7.06 (br, t, J = 7.4 Hz, 1H), 6.35 (s, 1H), 3.86 (s, 2H), 3.69 (s, 2H), 3.64 (br, m, 1H), 2.74 (t, J = 6.0 Hz, 2H), 2.66 - 2.39 (m, 10H). 13C NMR (75 MHz, CDCl3): δ 139.4, 136.1, 135.3 (2C), 128.4, 128.2, 127.1, 121.4 (2C), 120.0, 119.5, 111.3, 110.7, 101.7, 57.2, 55.7, 53.6, 53.1 (2C), 53.0 (2C), 45.2. HRMS (ESI): calcd for [C22H28BrN4]+ 427.1492, found 427.1481 [MH+].

N-(2-(4-(2-(1H-indol-3-yl)ethyl)piperazin-1-yl)ethyl)-4-methoxyaniline (**67**)

FC: $CH_2Cl_2/CH_3OH/Et_3N$ 97/2/1 (87% yield). ^{1}H NMR (300 MHz, $CDCl_3$): δ 8.09 (br, m, 1H), 7.61 (br, d, *J* = 7.7 Hz, 1H), 7.35 (br, d, *J* = 7.8 Hz, 1H), 7.18 (br, t, *J* = 7.4 Hz, 1H), 7.11 (br, t, *J* = 7.5 Hz, 1H), 7.04 (br, s, 1H), 6.79 (d, *J* = 8.9 Hz, 2H), 6.61 (d, *J* = 8.9 Hz, 2H), 3.74 (s, 3H), 3.14 (t, *J* = 5.9 Hz, 2H), 3.02 (m, 2H), 2.78 (m, 2H), 2.67 (t, *J* = 5.9 Hz, 2H), 2.63 (br, m, 9H). ^{13}C NMR (75 MHz, $CDCl_3$): δ 152.4, 143.1, 136.5, 127.9, 122.4, 122.1, 119.7, 119.2, 115.4 (2C), 114.7 (2C), 114.3, 111.6, 59.6, 57.2, 56.3, 53.6 (2C), 53.1 (2C), 41.7, 23.2. HRMS (ESI): calcd for $[C_{23}H_{31}N_4O]^+$ 379.2492, found 379.2483 [MH^+].

N-(2-(4-(2-(1H-indol-3-yl)ethyl)piperazin-1-yl)ethyl)-4-bromoaniline (**68**)

FC: $CH_2Cl_2/CH_3OH/Et_3N$ 97/2/1 (88% yield). ^{1}H NMR (300 MHz, $CDCl_3$): δ 8.15 (br, m, 1H), 7.61 (br, d, *J* = 7.7 Hz, 1H), 7.35 (br, d, *J* = 7.8 Hz, 1H), 7.25 (d, *J* = 8.8 Hz, 2H), 7.18 (br, t, *J* = 7.5 Hz, 1H), 7.10 (br, t, *J* = 7.5 Hz, 1H), 7.01 (s, 1H), 6.50 (d, *J* = 8.8 Hz, 2H), 4.36 (br, m, 1H), 3.12 (m, 2H), 3.04 – 2.89 (m, 2H), 2.74 (m, 2H), 2.70 – 2.44 (m, 10H). ^{13}C NMR (75 MHz, $CDCl_3$): δ 147.3, 136.1, 132.0 (2C), 127.4, 122.0, 121.7, 119.2, 118.7, 114.5 (2C), 113.8, 111.2, 108.8, 59.0, 56.3, 52.9 (2C), 52.4 (2C), 40.2, 22.6. HRMS (ESI): calcd for $[C_{22}H_{28}BrN_4]^+$ 427.1492, found 427.1478 [MH^+].

GENERAL PROCEDURE FOR THE SYNTHESIS OF COMPOUNDS **49-52**, **69-70**

To a solution of compound **45** (or **46-48**, **67-68**) (0.26 mmol) in CH_2Cl_2 (1.5 mL) sodium triacetoxyboronhydride (0.31 mmol, 1.2 eq.) and propionaldehyde (0.29 mmol, 1.1 eq.) were added. The resulting mixture was stirred at room temperature until full conversion (monitored by TLC). The reaction was quenched with saturated aq. $NaHCO_3$ (5 mL) and the organic layer was separated. The aqueous phase was then extracted with CH_2Cl_2 (3 x 5 mL), the combined organic layer was dried over anhydrous Na_2SO_4 and the solvent was evaporated under reduced pressure to give the desired product with no need for further purification.

N-(2-(4-((1H-indol-2-yl)methyl)piperazin-1-yl)ethyl)-4-methoxy-N-propylaniline (**49**)

95% yield. ^{1}H NMR (300 MHz, $CDCl_3$): δ 8.61 (br, m, 1H), 7.54 (br, d, *J* = 7.7 Hz, 1H), 7.33 (br, d, *J* = 7.8 Hz, 1H), 7.15 (br, t, *J* = 7.5 Hz, 1H), 7.07 (br, t, *J* = 7.4 Hz, 1H), 6.80 (d, *J* = 8.9 Hz, 2H), 6.65 (d, *J* = 8.9 Hz, 2H), 6.36 (s, 1H), 3.74 (s, 3H), 3.68 (s, 2H), 3.40 (t, *J* = 7.5 Hz, 2H), 3.14 (t, *J* = 7.5 Hz, 2H), 2.66 – 2.40 (m, 10H), 1.55 (br, sext, *J* = 7.4 Hz, 2H), 0.89 (t, *J* = 7.4 Hz, 3H). ^{13}C NMR (75 MHZ, $CDCl_3$): δ 151.3, 143.1, 136.4, 135.5, 128.5, 121.8, 120.3, 119.6, 115.1 (2C), 114.5 (2C), 110.9, 101.9, 56.0, 55.9, 55.7, 54.2, 53.7 (2C), 53.3 (2C), 49.7, 20.6, 11.7. HRMS (ESI): calcd for $[C_{25}H_{35}N_4O]^+$ 407.2805, found 407.2788 [MH^+].

N-(2-(4-((1H-indol-2-yl)methyl)piperazin-1-yl)ethyl)-4-bromo-N-propylaniline (**50**)

92% yield. ^{1}H NMR (400 MHz, $CDCl_3$): δ 8.73 (br, m, 1H), 7.60 (br, d, *J* = 7.8 Hz, 1H), 7.37 (br, d, *J* = 7.8 Hz, 1H), 7.29 (d, *J* = 9.0 Hz, 2H), 7.19 (br, t, *J* = 7.5 Hz, 1H), 7.12 (br, t, *J* = 7.4 Hz, 1H), 6.56 (d, *J* = 9.0 Hz, 2H), 6.41 (s, 1H), 3.72 (s, 2H), 3.45 (t, *J* = 7.5 Hz, 2H), 3.24 (t, *J* = 7.5 Hz, 2H), 2.68 – 2.42 (m, 10H), 1.63 (br, sext, *J* = 7.4 Hz, 2H), 0.96 (t, *J* = 7.4 Hz, 3H). ^{13}C NMR (100 MHZ, $CDCl_3$): δ 147.0, 136.3, 135.3, 131.9 (2C), 128.3, 121.7, 120.2, 119.7, 113.4 (2C), 110.8, 107.3, 101.9, 55.8, 55.0, 53.5 (2C), 53.1 (3C), 48.9, 20.3, 11.4. HRMS (ESI): calcd for $[C_{24}H_{32}BrN_4]^+$ 455.1805, found 455.1806 [MH^+].

N-(2-(4-((1H-indol-2-yl)methyl)piperazin-1-yl)ethyl)-N-(4-methoxybenzyl)propan-1-amine (**51**)

90% yield. ^{1}H NMR (400 MHz, $CDCl_3$): δ 8.63 (br, m, 1H), 7.57 (br, d, *J* = 7.7 Hz, 1H), 7.35 (br, d, *J* = 7.8 Hz, 1H), 7.25 (d, *J* = 8.5 Hz, 2H), 7.17 (br, t, *J* = 7.6 Hz, 1H), 7.10 (br, t, *J* = 7.6 Hz, 1H), 6.86 (d, *J* = 8.5 Hz, 2H), 6.38 (s, 1H), 3.82 (s, 3H), 3.68 (s, 2H), 3.56 (s, 2H), 2.71 – 2.36 (m, 14H), 1.51 (br, sext, *J* = 7.4 Hz, 2H), 0.88 (t, *J* = 7.4 Hz, 3H). ^{13}C

NMR (100 MHZ, $CDCl_3$): δ 159.5, 137.0, 136.5, 133.0, 130.4 (2C), 129.3, 122.2, 120.8, 120.3, 114.4 (2C), 111.2, 102.2, 59.3, 57.3, 57.2, 56.4, 55.9, 54.1 (2C), 53.9 (2C), 52.1, 21.1, 12.2. HRMS (ESI): calcd for $[C_{26}H_{37}N_4O]^+$ 421.2962, found 421.2977 $[MH^+]$.

N-(2-(4-((1H-indol-2-yl)methyl)piperazin-1-yl)ethyl)-N-(4-bromobenzyl)propan-1-amine (**52**)

92% yield. ^{1}H NMR (400 MHz, $CDCl_3$): δ 8.93 (br, m, 1H), 7.62 (br, d, *J* = 7.8 Hz, 1H), 7.42 – 7.25 (m, 5H), 7.20 (br, td, *J* = 7.6 and 1.2 Hz, 1H), 7.14 (br, td, *J* = 7.7 and 1.2 Hz, 1H), 6.41 (br, s, 1H), 3.67 (s, 2H), 3.65 (s, 2H), 2.70 – 2.45 (m, 14H), 1.55 (br, sext, *J* = 7.4 Hz, 2H), 0.93 (t, *J* = 7.5 Hz, 3H). ^{13}C NMR (100 MHZ, $CDCl_3$): δ 140.1, 136.4, 135.6, 128.9 (2C), 128.5 (2C), 128.2 (2C), 121.6, 120.3, 119.7, 110.9, 101.9, 59.2, 56.7, 56.5, 55.9, 53.6 (2C), 53.3 (2C), 51.3, 20.4, 12.0. HRMS (ESI): calcd for $[C_{25}H_{34}BrN_4]^+$ 469.1961, found 469.1945 $[MH^+]$.

N-(2-(4-(2-(1H-indol-3-yl)ethyl)piperazin-1-yl)ethyl)-4-methoxy-N-propylaniline (**69**)

90% yield. ^{1}H NMR (400 MHz, $CDCl_3$): δ 8.45 (br, m, 1H), 7.67 (br, d, *J* = 7.8 Hz, 1H), 7.36 (br, d, *J* = 7.7 Hz, 1H), 7.23 (br, t, *J* = 7.5 Hz, 1H), 7.17 (br, t, *J* = 7.5 Hz, 1H), 7.03 (s, 1H), 6.88 (d, *J* = 8.9 Hz, 2H), 6.73 (d, *J* = 8.9 Hz, 2H), 3.81 (s, 3H), 3.48 (t, *J* = 7.5 Hz, 2H), 3.24 (t, *J* = 7.5 Hz, 2H), 3.01 (m, 2H), 2.79 (m, 2H), 2.69(br, m, 8H), 2.61 (m, 2H), 1.63 (br, sext, *J* = 7.4 Hz, 2H), 0.97 (t, *J* = 7.4 Hz, 3H). ^{13}C NMR (100 MHZ, $CDCl_3$): δ 151.3, 143.1, 136.3, 127.5, 121.9, 121.7, 119.2, 118.8, 115.0 (2C), 114.4 (2C), 114.2, 111.2, 59.3, 55.9, 55.6, 54.1, 53.7 (2C), 53.2 (2C), 49.5, 22.9, 20.6, 11.6. HRMS (ESI): calcd for $[C_{26}H_{37}N_4O]^+$ 421.2962, found 421.2950 $[MH^+]$.

N-(2-(4-(2-(1H-indol-3-yl)ethyl)piperazin-1-yl)ethyl)-4-bromo-N-propylaniline (**70**)

91% yield. ^{1}H NMR (300 MHz, $CDCl_3$): δ 8.06 (br, m, 1H), 7.61 (br, d, *J* = 7.7 Hz, 1H), 7.35 (br, d, *J* = 7.7 Hz, 1H), 7.25 (d, *J* = 8.9 Hz, 2H), 7.18 (br, t, *J* = 7.4 Hz, 1H), 7.11 (br, t, *J* = 7.5 Hz, 1H), 7.04 (s, 1H), 6.52 (d, *J* = 8.9 Hz, 2H), 3.43 (t, *J* = 8.0 Hz, 2H), 3.19 (t, *J* = 7.9 Hz, 2H), 3.03 (m, 2H), 2.88 – 2.47 (m, 12H), 1.58 (br, sext, *J* = 7.7 Hz, 2H), 0.91 (t, *J* = 7.7 Hz, 3H). ^{13}C NMR (75 MHZ, $CDCl_3$): δ 147.3, 136.3, 132.0 (2C), 127.6, 122.1 and 121.8 (1C), 119.4, 119.0, 114.3, 113.6 (2C), 112.0, 111.4, 107.5, 59.4, 55.3, 53.8 (2C), 53.3 (3C), 49.0, 23.0, 20.5, 11.6. HRMS (ESI): calcd for $[C_{25}H_{34}BrN_4]^+$ 469.961, found 469.1982 $[MH^+]$.

GENERAL PROCEDURE FOR THE SYNTHESIS OF COMPOUNDS **53-57**, **71-72**

To a suspension of NaH (80% in mineral oil, 5.5 mmol, 1.1 eq.) in anhydrous DMF (3 mL), cooled to 0 °C under N_2 atmosphere, a solution of compound **40** (or **41**, **44**, **65-66**) (5 mmol) in anhydrous DMF (7 mL) was added and the mixture was stirred for 15 minutes. After dropwise addition of the alkylating agent (6 mmol, 1.2 eq.), the solution was warmed to room temperature and stirred until full conversion (monitored by TLC). The reaction was quenched with H_2O (10 mL), and the aqueous phase was extracted with EtOAc (3 x 10 mL). The combined organic phases were washed with saturated aq. NaCl (5 x 10 mL) and dried over anhydrous Na_2SO_4. The resulting mixture was then concentrated under reduced pressure, to give a residue which was purified by flash chromatography (FC) as indicated below.

2-(4-(1-(methoxymethyl)-1H-indole-2-carbonyl)piperazin-1-yl)-N-(4-methoxyphenyl)-N-propylacetamide (**53**)

FC: EtOAc (89% yield). ^{1}H NMR (400 MHz, $CDCl_3$): δ 7.63 (d, *J* = 7.7 Hz, 1H), 7.53 (br, d, *J* = 7.8 Hz, 1H), 7.32 (br, t, *J* = 7.7 Hz, 1H), 7.19 (br, t, *J* = 7.5 Hz, 1H), 7.09 (d, *J* = 8.8 Hz, 2H), 6.95 (d, *J* = 8.8 Hz, 2H), 6.63 (s, 1H), 5.65 (s, 2H), 3.86 (s, 3H), 3.83 (br, m, 4H), 3.63 (m, 2H), 3.24 (s, 3H), 2.99 (br, s, 2H), 2.62 (br, m, 4H), 1.56 (br, sext, *J* = 7.6 Hz, 2H), 0.91 (t, *J* = 7.6 Hz, 3H). ^{13}C NMR (100 MHz, $CDCl_3$): δ 168.5, 162.9, 159.3, 137.8, 134.2, 131.3, 129.3 (2C), 127.0, 123.9, 121.6, 121.1, 114.9 (2C), 110.6, 105.2, 74.9, 59.1, 56.0, 55.5, 53.1 (2C), 51.1, 47.5, 41.8, 20.9, 11.2. HRMS (ESI): calcd for $[C_{27}H_{34}N_4NaO_4]^+$ 501.2472, found 501.2488 $[MNa^+]$.

2-(4-(1-(methoxymethyl)-1H-indole-2-carbonyl)piperazin-1-yl)-N-(4-methoxyphenyl)-N-(3-methylbut-2-en-1-yl)acetamide (**54**)

FC: EtOAc (76% yield). ^{1}H NMR (400 MHz, $CDCl_3$): δ 7.63 (d, *J* = 7.8 Hz, 1H), 7.53 (d, *J* = 7.8 Hz, 1H), 7.32 (br, t, *J* = 7.7 Hz, 1H), 7.19 (t, *J* = 7.6 Hz, 1H), 7.06 (d, *J* = 8.8 Hz, 2H), 6.92 (d, *J* = 8.8 Hz, 2H), 6.62 (s, 1H), 5.64 (s, 2H), 5.23 (br, t, *J* = 7.3 Hz, 1H), 4.26 (d, *J* = 7.3 Hz, 2H), 3.85 (s, 3H), 3.82 (br, m, 4H), 3.23 (s, 3H), 2.98 (s, 2H), 2.59 (br, m, 4H), 1.69 (s, 3H), 1.46 (s, 3H). ^{13}C NMR (100 MHz, $CDCl_3$): δ 168.4, 162.9, 159.2, 138.1, 136.6, 134.2, 131.4, 129.4 (2C), 126.6, 123.9, 121.6, 121.1, 119.0, 114.7 (2C), 110.6, 105.2, 75.2, 59.1, 55.9, 55.5, 53.2 (2C), 47.5, 47.2, 42.0, 25.7,

17.7. HRMS (ESI): calcd for $[C_{29}H_{36}N_4NaO_4]^+$ 527.2629, found 527.2637 [MNa^+].

N-(4-bromophenyl)-2-(4-(1-(methoxymethyl)-1H-indole-2-carbonyl)piperazin-1-yl)-N-propylacetamide (**55**)

FC: EtOAc (80% yield). ^{1}H NMR (300 MHz, $CDCl_3$): δ 7.60 (br, d, *J* = 7.8 Hz, 1H), 7.55 (d, *J* = 8.6 Hz, 2H), 7.49 (br, d, *J* = 7.8 Hz, 1H), 7.29 (br, t, *J* = 7.5 Hz, 1H), 7.16 (br, t, *J* = 7.7 Hz, 1H), 7.05 (d, *J* = 8.6 Hz, 2H), 6.59 (s, 1H), 5.61 (s, 2H), 3.79 (br, m, 4H), 3.60 (m, 2H), 3.20 (s, 3H), 2.95 (br, s, 2H), 2.56 (br, m, 4H), 1.50 (br, sext, *J* = 7.4 Hz, 2H), 0.87 (t, *J* = 7.4 Hz, 3H). ^{13}C NMR (75 MHz, $CDCl_3$): δ 163.3 (2C), 138.0, 136.4, 132.1 (2C), 126.7, 124.2, 121.7, 121.3, 121.1 (2C), 117.1, 111.4, 110.4, 105.6, 74.8, 61.7, 56.1, 53.4 (2C), 47.3, 41.0, 29.7, 20.1, 11.0. HRMS (ESI): calcd for $[C_{26}H_{31}BrN_4NaO_3]^+$ 549.1472, found 549.1479 [MNa^+].

N-(4-bromophenyl)-2-(4-(1-(methoxymethyl)-1H-indole-2-carbonyl)piperazin-1-yl)-N-(3-methylbut-2-en-1-yl)acetamide (**56**)

FC: EtOAc (75% yield). ^{1}H NMR (300 MHz, $CDCl_3$): δ 7.59 (br, d, *J* = 7.8 Hz, 1H), 7.53 – 7.42 (m, 3H), 7.28 (br, t, *J* = 7.6 Hz, 1H), 7.15 (t, *J* = 7.6 Hz, 1H), 7.02 (d, *J* = 8.4 Hz, 2H), 6.59 (s, 1H), 5.61 (s, 2H), 5.17 (br, t, *J* = 7.8 Hz, 1H), 4.24 (br, d, *J* = 7.8 Hz, 2H), 3.76 (br, m, 4H), 3.19 (s, 3H), 2.91 (s, 2H), 2.51 (br, m, 4H), 1.65 (s, 3H), 1.42 (s, 3H). ^{13}C NMR (75 MHz, $CDCl_3$): δ 167.9, 162.7, 140.6, 138.0, 137.1, 132.9 (2C), 131.5, 130.1 (2C), 126.7, 123.9, 121.8, 121.6, 121.1, 118.7, 110.7, 105.3, 75.0, 59.5, 55.9, 53.3 (2C), 47.2, 44.2, 40.6, 25.8, 17.8. HRMS (ESI): calcd for $[C_{28}H_{33}BrN_4NaO_3]^+$ 575.1628, found 575.1636 [MNa^+].

N-(4-methoxybenzyl)-2-(4-(1-(methoxymethyl)-1H-indole-2-carbonyl)piperazin-1-yl)-N-propylacetamide (**57**)

FC: EtOAc/Hex 9/1 (87% yield). ^{1}H NMR (300 MHz, $CDCl_3$, mixture of 2 conformers in ratio 1:1): δ 7.62 (br, d, *J* = 7.8 Hz, 1H), 7.51 (br, d, *J* = 7.8 Hz, 1H), 7.30 (br, t, *J* = 7.7 Hz, 1H), 7.25 – 7.13 (m, 2H), 7.08 (d, *J* = 8.6 Hz, 1H), 6.88 (d, *J* = 8.6 Hz, 1H), 6.83 (d, *J* = 8.6 Hz, 1H), 6.64 (s, 0,5H), 6.62 (s, 0.5H), 5.64 (s, 1H), 5.62 (s, 1H), 4.54 (s, 1H), 4.52 (s, 1H), 3.97 – 3.72 (br, m, 4H), 3.80 (s, 1.5H), 3.78 (s, 1.5H), 3.42 – 3.11 (m, 7H), 2.85 – 2.61 (br, m, 4H), 1.56 (m, 2H), 0.98 – 0.81 (m, 3H). ^{13}C NMR (75 MHz, $CDCl_3$): δ 168.8 and 168.5 (1C), 162.9, 159.1 and 159.0 (1C), 137.8, 131.2, 129.5, 128.8, 127.5, 126.8, 124.0, 121.6, 121.2, 114.3, 113.7, 110.5, 105.3, 74.9, 60.3 and 59.8 (1C), 56.0, 55.2, 53.5 (2C), 50.2 and 48.0 (1C), 47.7 and 47.5 (1C), 47.1, 42.6, 21.7 and 20.7 (1C), 11.3. HRMS (ESI): calcd for $[C_{28}H_{36}N_4NaO_4]^+$ 515.2629, found 515.2610 [MNa^+].

2-(4-(2-(1-(methoxymethyl)-1H-indol-3-yl)acetyl)piperazin-1-yl)-N-(4-methoxyphenyl)-N-propylacetamide (**71**)

FC: CH_2Cl_2/CH_3OH/Et_3N 98/1/1 (72% yield). ^{1}H NMR (400 MHz, $CDCl_3$): δ 7.60 (br, d, *J* = 7.8 Hz, 1H), 7.47 (br, d, *J* = 7.8 Hz, 1H), 7.26 (br, t, *J* = 7.5 Hz, 1H), 7.17 (br, t, *J* = 7.8 Hz, 1H), 7.10 (s, 1H), 7.05 (d, *J* = 8.5 Hz, 2H), 6.92 (d, *J* = 8.5 Hz, 2H), 5.42 (s, 2H), 3.84 (s, 3H), 3.81 (s, 2H), 3.73 (br, m, 2H), 3.60 (m, 2H), 3.55 (br, m, 2H), 3.22 (s, 3H), 2.91 (br, s, 2H), 2.53 (br, m, 2H), 2.44 (br, m, 2H), 1.52 (br, sext, *J* = 7.6 Hz, 2H), 0.89 (t, *J* = 7.6 Hz, 3H). ^{13}C NMR (100 MHz, $CDCl_3$): δ 169.4, 167.9, 158.9, 136.3, 133.8, 129.0 (2C), 127.7, 126.0, 122.3, 119.9, 118.6, 114.6 (2C), 109.7, 109.0, 77.1, 58.6, 55.6, 55.2, 52.6, 52.4, 50.8, 45.5, 41.0, 30.7, 20.5, 10.9. HRMS (ESI): calcd for $[C_{28}H_{37}N_4O_4]^+$ 493.2809, found 493.3707 [MH^+].

N-(4-bromophenyl)-2-(4-(2-(1-(methoxymethyl)-1H-indol-3-yl)acetyl)piperazin-1-yl)-N-propylacetamide (**72**)

FC: CH_2Cl_2/CH_3OH/Et_3N 98/1/1 (78% yield). ^{1}H NMR (400 MHz, $CDCl_3$): δ 7.60 (br, d, *J* = 7.8 Hz, 1H), 7.55 (d, *J* = 8.5 Hz, 2H), 7.46 (br, d, *J* = 7.7 Hz, 1H), 7.26 (br, t, *J* = 7.5 Hz, 1H), 7.17 (br, t, *J* = 7.5 Hz, 1H), 7.09 (s, 1H), 7.04 (d, *J* = 8.5 Hz, 2H), 5.42 (s, 2H), 3.81 (s, 2H), 3.69 (br, m, 2H), 3.61 (br, t, *J* = 7.6 Hz, 2H), 3.51 (br, m, 2H), 3.22 (s, 3H), 2.87 (s, 2H), 2.46 (br, m, 2H), 2.35 (br, m, 2H), 1.50 (sext, *J* = 7.6 Hz, 2H), 0.88 (t, *J* = 7.6 Hz, 3H). ^{13}C NMR (100 MHz, $CDCl_3$): δ 170.4, 168.6, 141.4, 137.3, 133.6 (2C), 130.6 (2C), 128.9, 126.9, 123.2, 122.7, 120.9, 119.6, 110.7, 109.7, 78.0, 60.0, 56.6, 53.6, 53.4, 51.7, 46.5, 42.1, 31.6, 21.5, 11.8. HRMS (ESI): calcd for $[C_{27}H_{33}BrN_4NaO_3]^+$ 563.1628, found 563.1624 [MNa^+].

GENERAL PROCEDURE FOR THE SYNTHESIS OF COMPOUNDS **58-62**

To a solution of **53** (or **54-57**) (0.26 mmol) in THF (2 mL) HCl 3N (10 mL) was added and the solution was stirred at room temperature until full conversion (monitored by TLC). The solution was made basic (pH>12) with KOH 20% and then the aqueous phase was extracted with CH_2Cl_2 (3 x 10 mL). The reunited organic phases were washed with brine (10 mL) and dried over anhydrous Na_2SO_4. The resulting mixture was then concentrated under reduced

pressure, to give a residue which was purified by flash chromatography (FC) as indicated below.

2-(4-(1H-indole-2-carbonyl)piperazin-1-yl)-N-(4-methoxyphenyl)-N-propylacetamide (**58**)

FC: CH_2Cl_2/CH_3OH 98.5/1.5 (95% yield). ^1H NMR (300 MHz, $CDCl_3$): δ 9.43 (br, m, 1H), 7.61 (br, d, *J* = 7.8 Hz, 1H), 7.36 (br, d, *J* = 7.8 Hz, 1H), 7.25 (br, t, *J* = 7.8 Hz, 1H), 7.11 (br, t, *J* = 7.8 Hz, 1H), 7.07 (br, d, *J* = 8.7 Hz, 2H), 6.91 (br, d, *J* = 8.7 Hz, 2H), 6.71 (s, 1H), 4.04 (br, m, 4H), 3.82 (s, 3H), 3.61 (dd, *J* = 7.8 and 5.8 Hz, 2H), 2.95 (s, 2H), 2.60 (br, m, 4H), 1.53 (m, 2H), 0.92 (t, 7.4 Hz, 3H). ^{13}C NMR (75 MHz, $CDCl_3$): δ 168.5, 162.1, 159.1, 135.6, 134.2, 129.4 (2C), 127.4, 124.4, 121.9, 120.4, 114.6 (2C), 111.9, 111.4, 104.9, 59.2, 55.5, 53.1 (2C), 51.1, 41.8, 39.9, 20.8, 11.2. HRMS (ESI): calcd for $[C_{25}H_{31}N_4O_3]^+$ 435.2391, found 435.2409 [MH^+].

2-(4-(1H-indole-2-carbonyl)piperazin-1-yl)-N-(4-methoxyphenyl)-N-(3-methylbut-2-en-1-yl)acetamide (**59**)

FC: $CH_2Cl_2/CH_3OH/Et_3N$ 98/1/1 (85% yield). ^1H NMR (300 MHz, $CDCl_3$): δ 9.76 (br, m, 1H), 7.60 (br, d, *J* = 7.8 Hz, 1H), 7.40 (br, d, *J* = 7.8 Hz, 1H), 7.23 (br, t, *J* = 7.5 Hz, 1H), 7.08 (br, t, *J* = 7.5 Hz, 1H), 7.02 (d, *J* = 8.7 Hz, 2H), 6.87 (d, *J* = 8.7 Hz, 2H), 6.70 (br, s, 1H), 5.21 (br, t, *J* = 7.7 Hz, 1H), 4.22 (d, *J* = 7.7 Hz, 2H), 3.93 (br, m, 4H), 3.80 (s, 3H), 2.93 (s, 2H), 2.57 (br, m, 4H), 1.65 (s, 3H), 1.42 (s, 3H). ^{13}C NMR (75 MHz, $CDCl_3$): δ 168.6, 162.2, 159.1, 136.4, 135.7, 134.0, 129.5 (2C), 127.3, 124.2, 121.8, 120.3, 118.8, 114.7 (2C), 111.9, 111.5, 105.1, 59.3, 55.3, 53.2 (2C), 47.1, 42.9 (2C), 25.6, 17.7. HRMS (ESI): calcd for $[C_{27}H_{32}N_4NaO_3]^+$ 483.2367, found 483.2343 [MNa^+].

2-(4-(1H-indole-2-carbonyl)piperazin-1-yl)-N-(4-bromophenyl)-N-propylacetamide (**60**)

FC: $CH_2Cl_2/CH_3OH/Et_3N$ 98/1/1 (78% yield). ^1H NMR (300 MHz, $CDCl_3$): δ 9.41 (br, m, 1H), 7.61 (br, d, *J* = 7.8 Hz, 1H), 7.55 (d, *J* = 8.5 Hz, 2H), 7.40 (br, d, *J* = 7.8 Hz, 1H), 7.25 (br, t, *J* = 7.8 Hz, 1H), 7.11 (br, t, *J* = 7.6 Hz, 1H), 7.06 (d, *J* = 8.5 Hz, 2H), 6.72 (br, s, 1H), 3.92 (br, m, 4H), 3.62 (br, t, *J* = 7.8 Hz, 2H), 2.94 (s, 2H), 2.56 (br, m, 4H), 1.52 (sext, *J* = 7.8 Hz, 2H), 0.88 (t, *J* = 7.8 Hz, 3H). ^{13}C NMR (75 MHz, $CDCl_3$): δ 168.1, 162.5, 140.8, 135.5, 132.9, 129.9 (2C), 129.0, 127.3, 124.4, 122.1, 121.9 (2C), 120.6, 111.9, 105.3, 59.6, 52.7 (2C), 51.4, 42.8, 40.0, 20.7, 10.9. HRMS (ESI): calcd for $[C_{24}H_{28}BrN_4O_2]^+$ 483.1390, found 483.1377 [MH^+].

2-(4-(1H-indole-2-carbonyl)piperazin-1-yl)-N-(4-bromophenyl)-N-(3-methylbut-2-en-1-yl)acetamide (**61**)

FC: $EtOAc/CH_3OH/Et_3N$ 98/1/1 (85% yield). ^1H NMR (300 MHz, $CDCl_3$): δ 9.69 (br, m, 1H), 7.61 (br, d, *J* = 7.8 Hz, 1H), 7.51 (d, *J* = 8.4 Hz, 2H), 7.40 (br, d, *J* = 7.8 Hz, 1H), 7.24 (br, t, *J* = 7.8 Hz, 1H), 7.10 (br,t, *J* = 7.5 Hz, 1H), 7.02 (d, *J* = 8.4 Hz, 2H), 6.72 (br, s, 1H), 5.19 (br, t, *J* = 7.8 Hz, 1H), 4.25 (br, d, *J* = 7.8 Hz, 2H), 3.93 (br, m, 4H), 2.94 (s, 2H), 2.58 (br, m, 4H), 1.66 (s, 3H), 1.43 (br, s, 3H). ^{13}C NMR (75 MHz, $CDCl_3$): δ 167.4, 162.4, 140.4, 137.2, 135.7, 132.9 (2C), 130.0, 129.0, 127.3, 124.4, 122.2, 121.8 (2C), 120.5, 118.5, 111.8, 105.3, 59.0, 52.9 (2C), 47.1, 45.8, 40.0, 25.7, 17.7. HRMS (ESI): calcd for $[C_{26}H_{29}BrN_4NaO_2]^+$ 531.1366, found 531.1341 [MNa^+].

2-(4-(1H-indole-2-carbonyl)piperazin-1-yl)-N-(4-methoxybenzyl)-N-propylacetamide (**62**)

FC: $CH_2Cl_2/CH_3OH/Et_3N$ 98/1/1 (90% yield). ^1H NMR (400 MHz, $CDCl_3$, mixture of 2 conformers in ratio 1:1): δ 9.88 (br, m, 0.5H), 9.86 (br, m, 0.5H), 7.65 (dd, *J* = 8.2 and 2.4 Hz, 1H), 7.45 (dd, *J* = 8.2 and 2.6 Hz, 1H), 7.27 (br, t, *J* = 7.7 Hz, 1H), 7.23 – 7.08 (m, 3H), 6.95 – 6.83 (m, 2H), 6.78 (br, s, 0.5H), 6.76 (br, s, 0.5H), 4.58 (s, 1H), 4.56 (s, 1H), 4.02 (br, m, 2H), 3.97 (br, m, 2H), 3.82 (br, s, 3H), 3.40 – 3.29 (m, 3H), 3.20 (br, t, *J* = 7.6 Hz, 1H), 2.76 (br, m, 2H), 2.69 (br, m, 2H), 1.59 (m, 2H), 0.90 (m, 3H). ^{13}C NMR (100 MHz, $CDCl_3$): δ 167.5, 163.1, 159.1, 136.6, 131.2, 125.0 (2C), 124.6, 122.4, 121.7, 121.2, 120.0, 116.1 (2C), 112.4 and 110.7 (1C), 106.9 and 105.8 (1C), 60.8 and 60.4 (1C), 55.9, 53.8 (2C), 48.9 and 48.6 (1C), 48.1*, 43.0*, 45.5, 21.6, 11.8. HRMS (ESI): calcd for $[C_{26}H_{33}N_4O_3]^+$ 449.2547, found 449.2535 [MH^+].

COMPUTATIONAL STUDIES

Docking studies

The selected ligands were first submitted to a Monte Carlo conformational search with the MMFF94 force field in vacuo with Spartan '08.[16] The obtained conformers were used for docking studies. Docking was performed using AutoDock[9] using the default docking parameters supplied with AutoDock in the 'examples' subdirectory, and point charges initially assigned according to the AMBER03 force field,[17] and then damped to mimic the less polar Gasteiger charges used to optimize the AutoDock scoring function. The setup was done with the YASARA molecular modeling

program[10] (Krieger E et al, 2002). For each ligands 50 Autodock LGA runs were executed. Results, were sorted by binding energy (more positive energies indicate stronger binding, and negative energies mean no binding). After clustering the 50 runs, the resulting complex conformations were originated (they all differ by at least 5.0 A heavy atom RMSD).

Molecular dynamics studies

The highest binding energy complex of each ligand was then submitted to molecular dynamics studies. Simulations were run at 298K and 1 bar in a protein membrane of phosphatidyl-ethanolamine (PEA) with the AMBER03 ForceField. The protein was scanned for secondary structure elements with hydrophobic surface residues and oriented accordingly and embedded in the membrane. Water was then added as 0.9% NaCl physiological solution. A 250 ps restrained equilibration simulation was run, which ensures that the membrane can adapt to the newly embedded protein. Then a simulation was run for 15 ns (5 fs timestep, simulation snapshots saved every 250000 fs). For each compound, the lowest energy complex from MD simulations was further minimized with the same force field.

BIOLOGICAL EVALUATION

Receptor Binding Studies

Dopamine receptor binding was determined by competition binding experiments with membranes from CHO cells stably expressing the human D_{2L}, D_{2S}, D_3 and D_4 receptor displacing the radioligand [^{3}H]spiperone. Affinities for the D_1 and D_5 receptor were performed using transiently transfected HEK cells expressing the appropriate receptor and the radioligand [^{3}H]SCH23390.

Receptor binding studies were carried out as described previously.[18] In brief, competition binding experiments with the human D_{2L},[19] D_{2S},[19] D_3[20] and D_4[21] receptor were done with preparations of membranes from CHO cells stably expressing the corresponding receptor and the radioligand [^{3}H]spiperone (specific activity = 81 Ci/mmol, PerkinElmer, Rodgau, Germany) at a final concentration of 0.10 nM, 0.15 nM, 0.20-0.50 nM and 0.30 nM for D_{2L}, D_{2S}, D_3 and D_4 binding, respectively. The assays were carried out at a protein concentration of 1-6 µg/assay tube, KD values of 0.058 nM, 0.032 nM, 0.20-0.50 nM and 0.25 nM and corresponding Bmax values of 910 fmol/mg, 8500 fmol/mg, 4200-5000 fmol/mg and 1300 fmol/mg for D_{2L}, D_{2S}, D_3 and D_4, respectively. Human D_1 and D_5 binding was achieved using homogenates of membranes from HEK 293 cells, which were transiently transfected with the pcDNA3.1 vector containing the appropriate human gene (from Missouri S&T cDNA Resource Center (UMR), Rolla, MO) by the calcium phosphate method[22] and worked up as described.[18] Binding assays were performed using the radioligand [^{3}H]SCH23390 (specific activity 80 Ci/mmol; Biotrend, Cologne, Germany) at 0.40 nM and 0.50 nM with membranes expressing the receptors at a density of 4500 fmol/mg and 2300 fmol/mg, a protein content of 3 µg/well and 6 µg/well and K_D values of 0.34 nM and 0.43 nM for D_1 and D_5, respectively. Unspecific binding was determined for all receptors in the presence of haloperidol (10 µM). Protein concentration was established by the method of Lowry using bovine serum albumin as standard.[23] The resulting competition curves of the receptor binding experiments were analyzed by nonlinear regression using the algorithms in PRISM 5.0 (GraphPad Software, San Diego, CA). The data were initially fit using a sigmoid model to provide an IC_{50} value, representing the concentration corresponding to 50% of maximal inhibition. IC_{50} values were transformed to K_i values according to the equation of Cheng and Prusoff.[24]

cAMP BRET Assay

HEK293T cells were transiently co-transfected with pcDNA3L-His-CAMYEL (purchased from ATCC via LGC Standards, Wesel, Germany) and D_{2S}, respectively. Twenty-four hours after transfection cells were split into white half-area 96-well plates at 20 x 104 cells/well and grown overnight. On the following day phenol red free medium was removed and replaced by phosphate buffered saline (PBS) and cells were serum starved for 1 hour before treatment. The assay was started by adding 10 µl coelenterazine-h (Promega, Mannheim, Germany) to each well at a final concentration of 5 µM. After 5 minutes incubation time compounds were added containing 50µM forskolin (final concentration 10µM). Determination of BRET signals started 15 minutes after agonist addition using a CLARIOstar plate reader (BMG LabTech, Ortenberg, Germany). Emission signals from Renilla Luciferase and YFP were measured simultaneously using a BRET filter set (475-30nm/535-30nm).[25]

References

[1] (a) Micheli, F.; Heidbreder, C. *Dopamine D3 Receptor Antagonists: a Patent Review (2007–2012). Expert Opin. Ther. Pat.* **2013**, *23*, 363. (b) Ye, N.; Neumeryer, J. L.; Baldessarini, R. J.; Zhen, X.; Zhang, A. *Chem. Rev.*, **2013**, 113, PR123.
[2] Chien, E. Y. T. *Science*, **2010**, *330*, 1091.
[3] Lober, S.; Hubner, H.; Tschammer, N.; Gmeiner, P. *T. Phar. Sci.*, **2011**, *32*, 148.
[4] (a) Johnson, M.; Antonio, T.; Reith, E. A. M.; Dutta, K. A. *J. Med. Chem.*, **2012**, *55*, 5826; (b) Du, P.; Xu, L.; Huang, J.; Yu, K.; Zhao, R.; Gao, B.; Jiang, H.; Zhao, W.; Zhen, X.; Fu, W. *Chem. Biol. Drug Des.*, **2013**, *82*, 326.
[5] Stucchi, M.; Gmeiner, P.; Huebner, H.; Rainoldi, G.; Sacchetti, A.; Silvani, A.; Lesma, G. *ACS Med.Chem. Lett.* **2015**, *6*, 882.
[6] Department of Chemistry and Pharmacy Emil Fischer Center, Friedrich Alexander University, Schuhstrabe 19, D-91052 Erlangen, Germany
[7] Möller D., Kling R. C., Skultety M., Leuner K:, Hübner H., Gmeiner P., *J. Med. Chem.,* **2014**, *57*, 4861−4875.
[8] *Dipartimento di Chimica, Materiali ed Ing.Chimica 'Giulio Natta', Politecnico di Milano, p.zza Leonardo da Vinci 32, 20133, Milano, Italy.*
[9] Morris, G.M.; Huey, R.; Lindstrom, W.; Sanner, M.F.; Belew, R.K.; Goodsell, D.S.; Olson, A.J. *J.Comput.Chem.* **209**, *30*, 2785.
[10] (a) Krieger, E.; Vriend, G.; *Bioinformatics* **2014**, *30*, 2981. (b) Krieger, E.; Darden, T.; Nabuurs, S.; Finkelstein, A.; Vriend, G. *Proteins* **2004**, *57*, 678.
[11] (a) Trumpp-Kallmeyer, S.; Hoflack, J.; Bruinvels, A.; Hibert, M. *J. Med. Chem.* **1992**, *35*, 3448. (b) Malmberg, A.; Nordvall, G.; Johansson, A. M.; Mohell, N.; Hacksell, U. *Mol. Pharmacol.* **1994**, *46*, 299.
[12] Zanatta, G.; Nunes, G.; Bezerra, E. M.; da Costa, R. F.; Martins, A.; Caetano, E. W. S.; Freire, V. N.; Gottfried, C. *ACS Chem. Neurosci.* **2014**, *5*, 1041.
[13] (a) Elders, N.; Schmitz, R.; de Kanter, F.; Ruijter, E.; Groen, B. M.; Orru, R. V. A. *J. Org. Chem.* **2007**, *72*, 6135-6142. (b) Shekhar, A. C.; Kumar, A. R.; Sathaiah, G.; Paul, V. L.; Sridhar, M.; Rao, P. S. *Tetrahedron Lett.* **2009**, *50*, 7099-7101.
[14] Ugi, I.; Meyr, R. *Angew. Chem.* **1958**, *70*, 702.
[15] Putey, A.; Joucla, L.; Picot, L.; Besson, T.; Joseph, B. *Tetrahedron Letters* **2007**, *63*, 867-879.
[16] *Spartan*'08. Wavefunction, Inc. Irvine, CA.
[17] Duan, Y.; Wu, C.; Chowdhury, S.; Lee, M.C.; Xiong, G.; Zhang, W.; Yang, R.; Cieplak, P.; Luo, R.; Lee, T. *J.Comput.Chem.* **2003**, *24*, 1999.
[18] Huebner, H.; Haubmann, C.; Utz, W.; Gmeiner, P. *J. Med. Chem.* **2000,** *43*, 756.
[19] Hayes, G.; Biden, T. J.; Selbie, L. A.; Shine, J. *Mol. Endocrinol.* **1992,** *6*, 920.
[20] Sokoloff, P.; Giros, B.; Martres, M. P.; Bouthenet, M. L.; Schwartz, J. C. *Nature* **1990,** *347*, 146.
[21] Asghari, V.; Sanyal, S.; Buchwaldt, S.; Paterson, A.; Jovanovic, V.; Van Tol, H. H. *J. Neurochem.***1995,** *65*, 1157.
[22] Jordan, M.; Schallhorn, A.; Wurm, F. M. *Nucleic. Acids Res.* **1996,** *24*, 596.
[23] Lowry, O. H.; Rosebrough, N. J.; Farr, A. L.; Randall, R. J. **1951,** *193*, 265.
[24] Cheng, Y.-C.; Prusoff, W. H. *Biochem. Pharmacol.* **1973,** *22*, 3099.
[25] Jiang, L.I.; Collins, J.; Davis, R.; Lin, K.-M.; DeCamp, D.; Roach, T.; Hsueh, R.; Rebres, R.A.; Ross, E.M.; Taussig, R.; Fraser, I.; Sternweis, P.C. *J. Biol. Chem.* **2007,** *282*, 10576.

4. ENANTIOENRICHED SPIRO[INDOLINE-PYRIMIDINE]-DIONES DERIVATIVES

Introduction

Isatin (1*H*-indole-2,3-dione) was first discovered by Erdmann and Laurent in 1840[1] as a product arising from the oxidation of indigo using nitric and chromic acids, and its current structure was later proposed by Kekulé.[2] The compound was considered synthetic for almost 140 years, until it was found to be widely present in the vegetable and animal kingdoms.[3] In humans and other mammals, isatin is found as an endogenous molecule. Although the metabolic pathways of isatin have not yet been fully elucidated, recently it has been isolated as a metabolic derivative of adrenaline.[4]

Isatin is a versatile molecule and its analogues display a wide range of biological activities, acting as inhibitors of various protein kinase families, like receptor tyrosine kinases and serine/threonine-specific protein kinases,[5] as intercalating agents between DNA base pairs and inhibitors of the ribonucleoprotein telomerase.[6] These and other biological activities are extensively surveyed by recent reviews.[7]

In particular, isatin derived 3,3'-disubstituted or spiro-fused 2-oxindoles have drawn tremendous interest of researchers in the area of synthetic organic chemistry and medicinal chemistry worldwide because they occur in many natural or pharmaceutical products such as spirotryprostatins, horsfiline, gelsemine, gelseverine, rhynchophylline, and elacomine, and have been reported to have various types of bioactivity (**Figure 22**).[8]

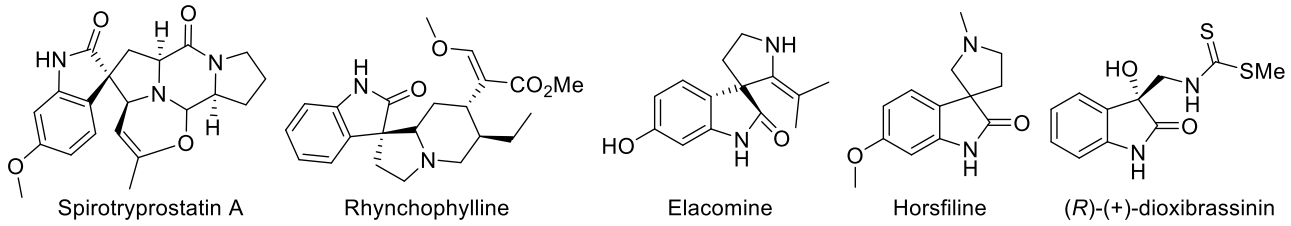

Figure 22. Selected examples of small bioactive molecules based on 3,3'-disubstituted or spiro-fused 2-oxindole motifs.

At the best of our knowledge, only two examples of synthetic methodologies for obtaining racemic 2-oxindoles spiro-fused with 3,4-dihydropyrimidine-2(1H)-ones (DHPMs) are present in the literature, relying on the acid-catalyzed Biginelli reaction.[9] Although DHPMs are prominent pharmacologically active molecules and have found increasing applications,[10] only few asymmetric versions of the Biginelli reaction have been reported,[11] using different organocatalytic systems, including primary and secondary amines, chiral ionic liquids and BINOL-derived phosphoric acids[12] (*for further details see* **Chapter 1.4**).

The stereochemistry of a small bioactive molecule usually affects its activity, absorption, distribution, metabolism, excretion, and toxicity. Moreover, two different enantiomers of a chiral drug may work differently in the body, making the development of stereoselective methodologies a notable and challenging task.

Therefore, going on with our interest in the asymmetric synthesis of 3,3'-disubstituted oxindole derivatives and related spiro-compounds,[5] we looked at the potential application of BINOL-derived monophosphoric acids as organocatalyst in the Biginelli-like reaction employing isatins as carbonyl components (**Scheme 33**). We obtained a small library of chiral enantioenriched spiro[indoline-pyrimidine]-diones, which was further expanded through post-condensation reactions. The configuration at the new oxindole C-3 quaternary stereocenter was assessed through quantum mechanical methods and NMR spectroscopy on diastereoisomeric derivatives. Computational studies on the reaction transition state (TS) were performed in order to explain the experimentally observed enantioselectivity and stereochemical outcome.

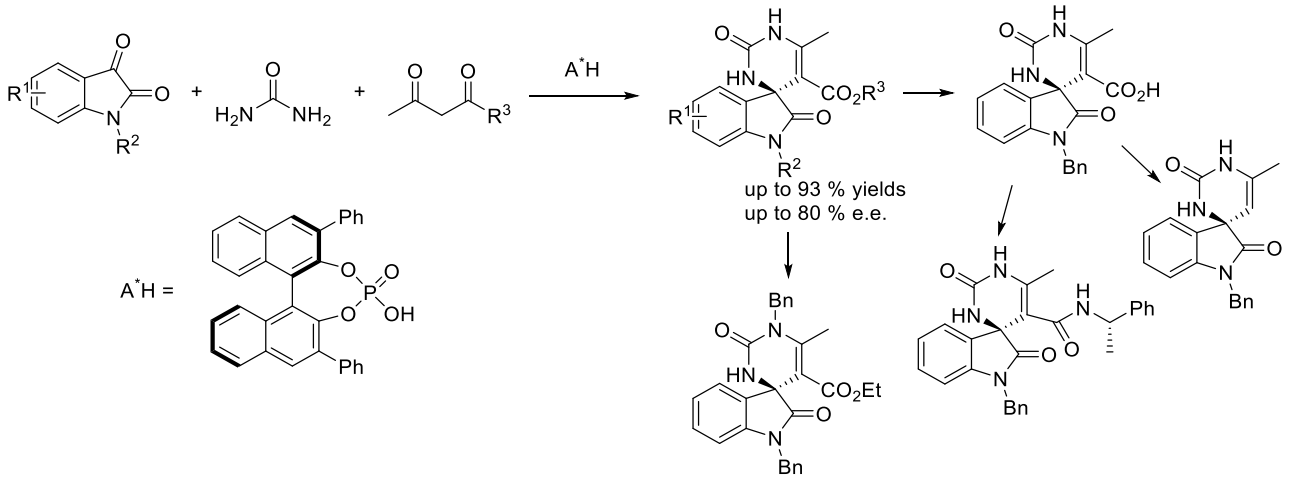

Scheme 33. Synthesis of a library of enantioenriched spiro[indoline-pyrimidine]-diones derivatives by means of a BINOL-derived monophosphoric acids catalyzed Biginelli-like reaction.

Results and discussion

Our initial studies were performed employing *N*-benzyl isatin **73a** as substrate, in combination with urea and ethyl acetoacetate, taking into account the BINOL-derived phosphoric acid catalysed protocol reported by Gong[13] for the true, aldehyde involving, Biginelli reaction.

At room temperature, with catalyst (*R*)-**74a**, the reaction proceeded slowly either in CH_2Cl_2 or in toluene (entries 1 and 2 **Table 2**), with the desired product **75a** isolated by flash chromatography only in trace amounts, even at prolonged reaction time (96 hours). Although aldehydes have been reported to smoothly react at room temperature, the unsatisfying results obtained employing isatin as substrate could be ascribed to the lower reactivity of the C-3 carbonyl, along with its higher steric demand. To our delight, conducting the reaction at 50 °C (entry 3 and 4 **Table 2**) had a beneficial effect on the chemical conversion, and in particular toluene proved to be the solvent of choice, affording compound **75a** in moderate yields and good enantioselectivity. Aiming to evaluate the impact of the phosphoric acid catalyst (*R*)-**74** on the reaction, screening of more hindered (*R*)-**74b-f** and of the reduced one (*R*)-**74g** was performed (entries 5-10 **Table 2**). In all cases, increasing the size of substitution resulted detrimental for the chemical conversion, with only catalysts (*R*)-**74c** and (*R*)-**74d** able to afford product **75a**, with maintenance of the same level of enantioselectivity as (*R*)-**74a**, but in definitely decreased yields (entry 5-10 **Table 2**). After we established (*R*)-**74a** as the catalyst of choice, further screening of the reaction conditions were performed. Some improvement in the yield without sacrificing the stereoselectivity could be achieved by prolonging the reaction time until 96 hours (entry 11 **Table 2**). More prolonged times are not convenient for the balance among yield and *ee* (entry 12 **Table 2**). Increasing the reaction temperature or the concentration deeply eroded the enantioselectivity, albeit with better yield (entry 13 and 14 **Table 2**). On the other hand, lowering the reactant concentration or the catalyst loading led to a significant decrease in yield.

Table 2. Asymmetric Biginelli-like condensation of N-benzyl isatin **73a**, urea and ethyl acetoacetate, catalyzed by chiral phosphoric acids (*R*)-**74**.

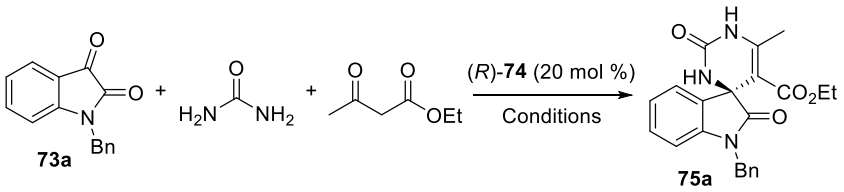

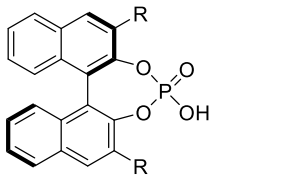

(*R*)-**74a**: R = Ph;
(*R*)-**74b**: R = 4-NO_2-C_6H_4;
(*R*)-**74c**: R = 4-Ph-C_6H_4;
(*R*)-**74d**: R = 9-Anthracenyl;
(*R*)-**74e**: R = 2,5,6-(*i*Pr)$_3$-C_6H_2;
(*R*)-**74f**: R = $SiPh_3$.

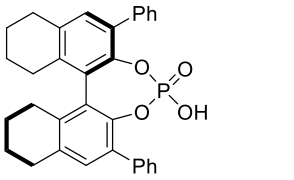

(*R*)-**74g**

entry	catalyst	solvent	conc. [mol/L]	temp. [°C], time [h]	yield[a] [%]	*ee*[b] [%]
1	**74a**	CH_2Cl_2	0.2	rt, 96	trace	/
2	**74a**	Tol	0.2	rt, 96	trace	/
3	**74a**	CH_2Cl_2	0.2	50, 48	32	75
4	**74a**	Tol	0.2	50, 48	51	80
5	**74b**	Tol	0.2	50, 48	trace	/
6	**74c**	Tol	0.2	50, 48	30	79
7	**74d**	Tol	0.2	50, 48	31	81
8	**74e**	Tol	0.2	50, 48	trace	/
9	**74f**	Tol	0.2	50, 48	trace	/
10	**74g**	Tol	0.2	50, 48	26	79
11	**74a**	Tol	0.2	50, 96	60	80
12	**74a**	Tol	0.2	50, 240	66	77
13	**74a**	Tol	0.2	70, 96	65	48
14	**74a**	Tol	0.4	50, 96	62	66

[a]Isolated yield. [b]Determined by chiral HPLC analysis.

After establishing the optimal conditions, the Biginelli-like reaction of a series of isatins was examined, using (*R*)-**74a** as catalyst, in toluene at 50 °C for 96 h (**Scheme 34**). The substrate scope of isatins was surveyed, by evaluating differently *N*-substituted isatins and the presence of substituents at 5- or 6-position. In general, all isatins readily undergo this reaction, to afford the desired products **75a-h** in moderate to high yields with a good degree of enantioselectivity (**Scheme 34**). Only the sterically demanding *N*-trityl isatin failed to participate in the reaction and the corresponding Biginelli-like adduct could not be detected. The *N*-Me isatin gave a better result than the corresponding *N*-Bn, *N*-*p*NO_2-Bn and *N*-PMB ones in terms of yield (93% in comparison to up to 63%), but at the price of a drop in *ee* (50% in comparison to up to 80%).

The presence of various halogen substituents at the aryl ring has almost no effect on both yield and *ee*. Variations at the ester moiety of the β-ketoester component were also evaluated, with methyl and benzyl acetoacetates participating at the reaction efficiently to provide adducts **75i-j** in good yields and moderate *ee*'s (**Scheme 34**).

Finally, to our surprise, neither thiourea in place of urea, nor various linear or cyclic β-diketones in place of alkyl acetoacetates, showed to react efficiently, together with *N*-benzyl-isatin, in this kind of reaction.

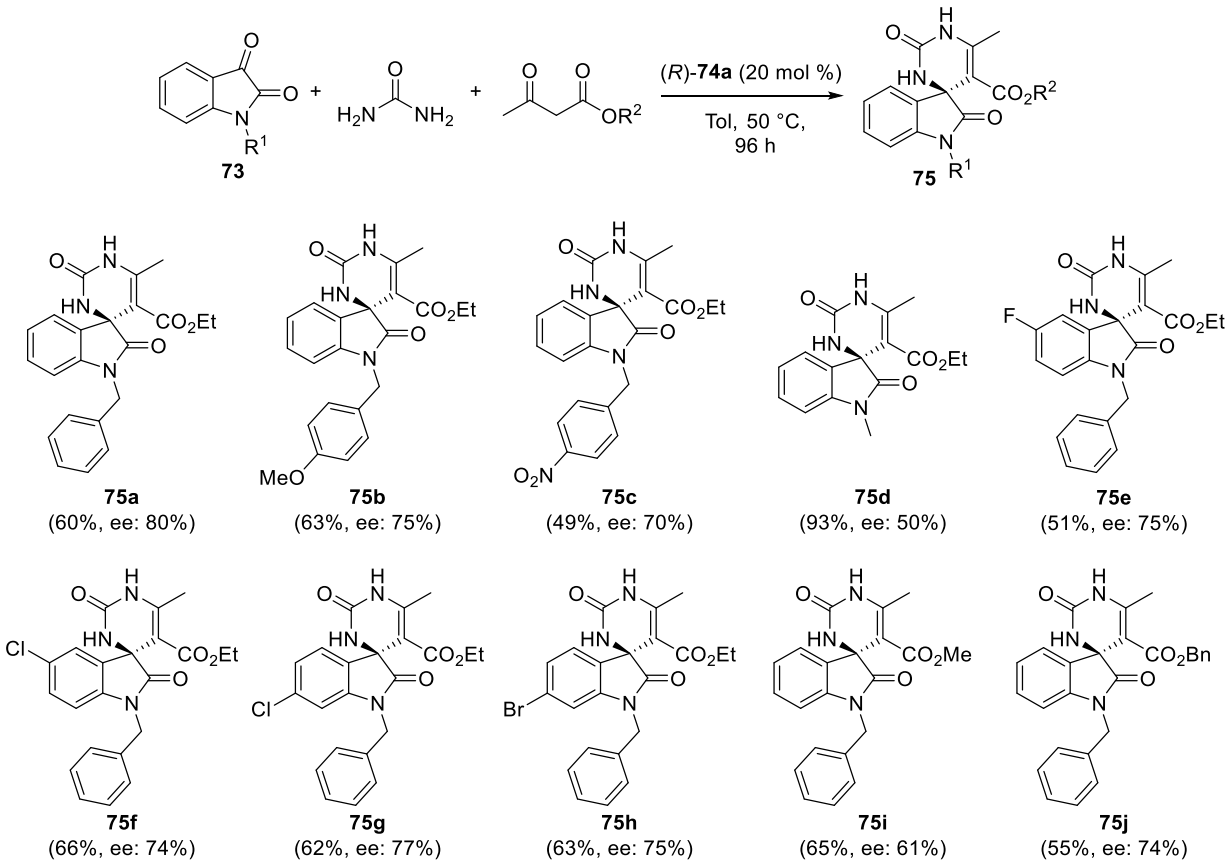

Scheme 34. Substrate scope of the Biginelli-like reaction catalyzed by (*R*)-**74a**.

We next examined some transformations of the products, first of all the facile regioselective mono-*N*-alkylation of the dihydropyrimidin-2-one ring. Starting from the Biginelli-like compound **75a**, the corresponding *N*-benzyl derivative **76** was achieved in high yield, by reaction with benzyl bromide and cesium carbonate, in DMF at room temperature (**Scheme 35**).

Further, catalytic hydrogenolysis of the benzyl ester moiety of compound **75j** allowed to easily obtain the carboxylic acid derivative **77**, that can be regarded as a useful key intermediate toward the synthesis of peptidomimetic compounds. The carboxylic acid functional group of **77** can also be quantitatively removed to give **78**, by heating in acidic conditions. Moreover, by reaction with (*S*)-(−)-α-methylbenzylamine in the presence of the condensing agent HATU, acid **77** was cleanly converted into diastereoisomeric amides **79a** and **79b**, which could be efficiently separated by flash chromatography (**Scheme 35**).

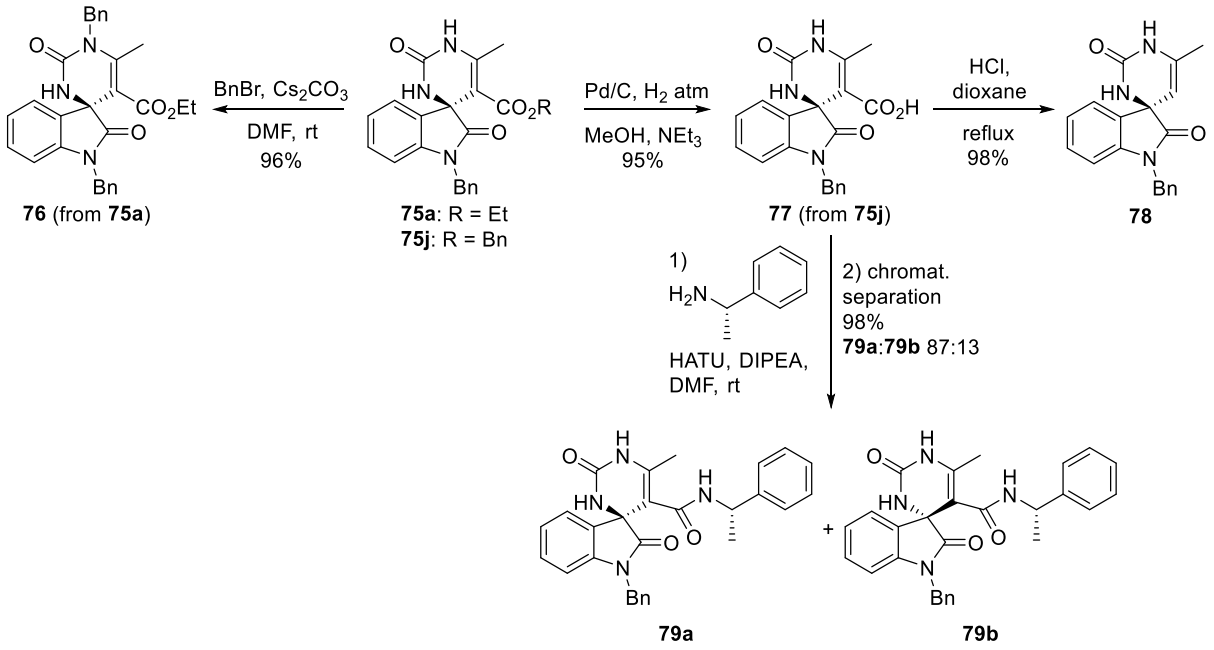

Scheme 35. Synthetic transformations on compounds **75a** and **75j**.

Although it was not possible to obtain suitable crystals for X-ray diffraction, we were able to determine the stereochemistry of the newly formed C-3 quaternary stereocenter through *ab initio* calculation of NMR shifts, a technique pioneered by Bifulco.[14] We considered the differences in both ^{1}H NMR and ^{13}C spectra for the two diastereoisomers **79a** and **79b** (**Figure 23**). In particular, a theoretical conformational search was performed on both possible stereoisomers with (3*S*,1'*S*) and (3*R*,1'*S*) absolute configurations, employing the Monte Carlo algorithm and molecular mechanics (MMFF force field). All structures obtained with population > 1% were further optimized with GAUSSIAN09[15] at quantum-mechanics DFT/B3LYP/6-31g(d,p) in gas phase. All conformations were subjected to single-point *ab initio* calculation of energy (DFT/B3LYP/6-31g(d,p)) and GIAO shielding constants at the DFT/6-311+G(2d,p)/SCRF-dmso level. To calculate ^{1}H and ^{13}C NMR chemical shifts for each diastereoisomer **79a** and **79b**, the shielding constants were subjected to Boltzmann averaging over the conformers, followed by linear regression, as reported by Pierens.[16] From a qualitative point of view, we observed a strong correspondence between the experimental ^{1}H chemical shifts of the major diastereoisomer **79a** and the calculated ones for the (3*S*,1'*S*) absolute configuration, especially in the high fields region (**Figure 23**).

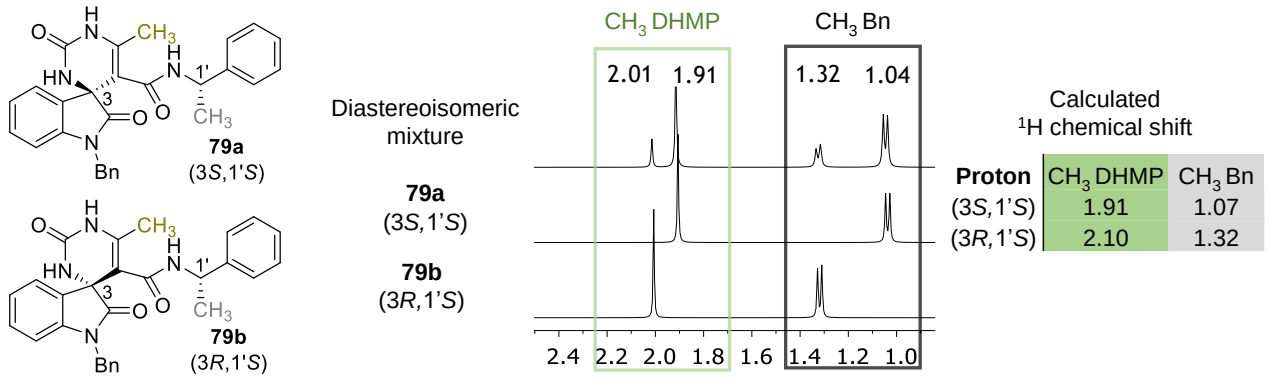

Figure 23. Experimental ^{1}H NMR spectra and calculated chemical shifts for selected protons of diastereoisomers **79a** and **79b**.

To give a quantitative assignment of the stereochemistry, the comparison between the chemical shifts of the possible computed stereoisomers and the experimental data is usually performed by using the correlation coefficient *R*, the mean absolute error (MAE), the correct MAE (CMAE), the root mean square deviation (RMSD) or other methods.[17] Among them, the comparison parameter (CP3) was especially designed by Goodman[18] for the assignment of the stereochemistry of pairs of diastereoisomers, in which only the configuration of one stereocenter is unknown. CP3 compares the differences in calculated shifts with differences in experimental shifts.[18] Therefore we applied the equation reported by the author, computing the CP3 for ^{1}H, ^{13}C and on the global data for both the possible assignments (**79a**→3*S*,1'*S* **79b**→3*R*,1'*S* and **79a**→3*R*,1'*S* **79b**→3*S*,1'*S*). Finally, applying the Bayes' theorem as reported by Goodman,[18] the stereochemical assignment can be made with quantifiable confidence, determining the configuration of the C-3 quaternary stereocenter for the major diastereoisomer **79a** to be *S* with a 100% confidence, confirming the previous qualitative supposition.

In collaboration with Dr. Sacchetti,[19] quantum-mechanical studies on the transition states were performed, in order to gather information about the stereochemical outcome of the reaction. The mechanism of the acid-catalyzed Biginelli reaction has been previously investigated by means of computational tools, indicating the iminium path as the most favourable (*for further details see* **Chapter 1.4**). Therefore, we decided to investigate the initial addition of the enol form of ethyl acetoacetate on the imine formed between isatin and urea, in the presence of (*R*)-**74a**, since in this step the final configuration of **75a** is determined (**Scheme 36**).

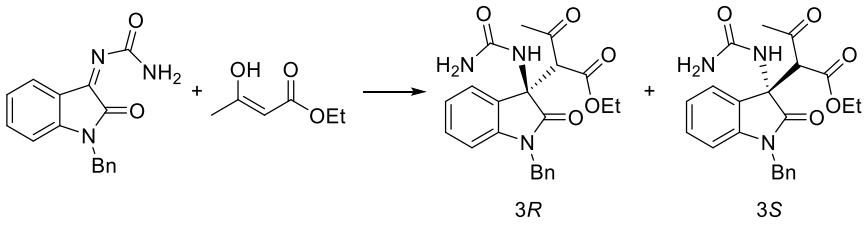

Scheme 36. Possible stereoisomers formed in the initial step of the acid-catalyzed Biginelli-like reaction.

Therefore, DFT study at the B3LYP/6-31G(d,p) level of theory were performed taking into account the two possible spatial arrangement of the more stable *Z*-imine in the reagents-catalyst complex,[20] leading to the diastereoisomeric transition state models **TS-A** and **TS-B** (**Figure 24a**). The energy profiles for both **TS-A** (path A) and **TS-B** (path B) clearly indicate a strong preference for **TS-A**, with a $\Delta\Delta G^{\ddagger}$ = 2.27 Kcal/mol at T=323K (**Figure 24b**), from which an *ee* = 92% could be calculated in favor of intermediate with a 3*R* configuration (**Scheme 36**). These results are in agreement with the experimental observed enantiomeric excesses, and further support the previously predicted *S* configuration for major diastereoisomer **79a**.

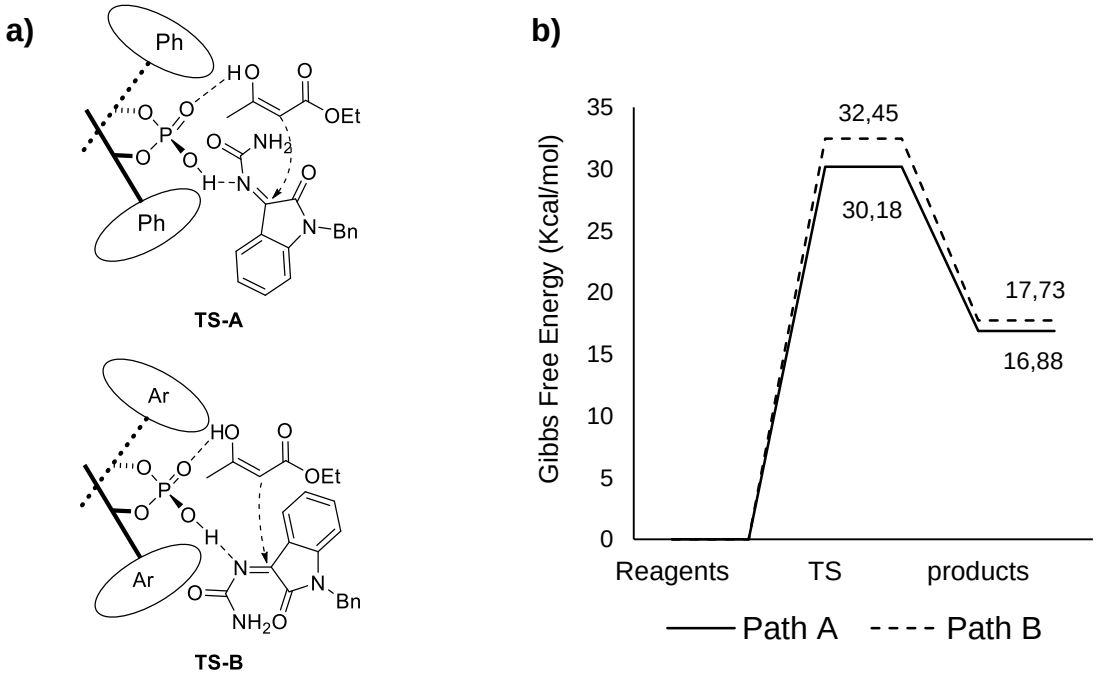

Figure 24. a) Proposed transition states of the BINOL-derived phosphoric acid catalyzed Biginelli-like reaction. b) Gibbs free energy profiles for both the two possible transition states.

Looking at the transition states 3D structures, the steric hindrance between the (*R*)-**74a** phenyl substituent and the urea residue in **TS-B** could explain its higher activation energy (**Figure 25**), favouring the nucleophilic attack on the *si*-face of the imine (**TS-A**).

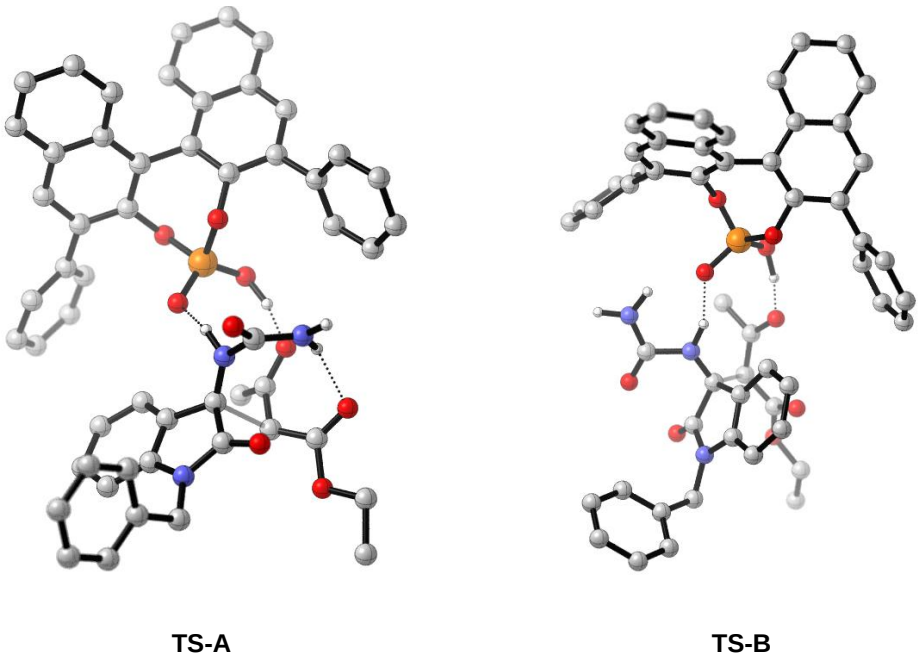

Figure 25. 3D structures of the two possible transition states **TS-A** and **TS-B**.

Conclusions

We developed the first enantioselective organocatalyzed Biginelli-like reaction applied to a ketone, namely isatin, with good yields and enantioselectivity. Different isatins and alkyl acetoacetates were successfully employed, obtaining a small library of enantioenriched spiro[indoline-pyrimidine]-dione derivatives. Post-condensation reactions have been performed, increasing the number of potentially useful compounds. The absolute configuration at the newly formed oxindole C-3 quaternary stereocenter was assessed to be *S* for the major enantiomer, by means of quantum mechanical methods and NMR spectroscopy on diastereoisomeric derivatives. Computational studies on the reaction transition state (TS) allowed us to explain the experimentally observed enantioselectivity and stereochemical outcome.

Experimental section

GENERAL INFORMATION

All commercial materials (Aldrich, Fluka) were used without further purification. All solvents were of reagent grade or HPLC grade. All reactions were carried out under a nitrogen atmosphere unless otherwise noted. All reactions were monitored by thin layer chromatography (TLC) on precoated silica gel 60 F254; spots were visualized with UV light or by treatment with a 1% aqueous $KMnO_4$ solution. Products were purified by flash chromatography on silica gel 60 (230–400 mesh). 1H NMR spectra and ^{13}C NMR spectra were recorded on 300 and 400 MHz spectrometers. Chemical shifts are reported in parts per million relative to the residual solvent. ^{13}C NMR spectra have been recorded using the APT pulse sequence (*for further details see* **Appendix A.1**). Multiplicities in ^{1}H NMR are reported as follows: s = singlet, d = doublet, t = triplet, m = multiplet, br s = broad singlet. High-resolution MS spectra were recorded with a Waters Micromass Q-ToF micro TM mass spectrometer, equipped with an ESI source. HPLC analysis was performed on Jasco PU-2080 (UV Detector and binary HPLC pump) at 254 nm. Chiralcel OD column were purchased from Daicel Chemical Industries®. Optical rotator power $[\alpha]^{T}_{D}$ was measured with a Jasco P-1030 polarimeter, endowed with a cell of 1 dm pathlength and 1 mL capacity. The light used has a wavelength of 589 nm (Sodium D line). *N*-substituted isatins[21] and BINOL-phosphoric acids[22] were synthetized according to reported literature.

GENERAL PROCEDURE FOR THE SYNTHESIS OF COMPOUNDS **75a-j**

Substituted isatin **73** (0.16 mmol, 1 eq), urea (0.19 mmol, 1.2 eq), alkyl acetoacetate (0.48 mmol, 3 eq) and (*R*)-**74a** catalyst (0.03 mmol, 0.2 eq) were dissolved in toluene (0.800 mL, 0.2 M). The reaction was stirrer at 50 °C for 96h. The resulting mixture was then concentrated under reduced pressure, to give a residue which was purified by flash chromatography (FC) as indicated below.

(S)-ethyl 1-benzyl-6'-methyl-2,2'-dioxo-2',3'-dihydro-1'H-spiro[indoline-3,4'-pyrimidine]-5'-carboxylate (**75a**)

Prepared according to general procedure starting from *N*-benzyl isatin and ethyl acetoacetate; FC: dichlorometane:methanol, 97.5:2.5; yield: 60%; white solid; $[\alpha]^{20}_{D}$ – 45.5 (*c* 0.2, $CHCl_3$); ^{1}H NMR (400 MHz, $CDCl_3$) δ 8.50 (br, m, 1H), 7.42 (d, J = 7.4 Hz, 2H), 7.38 – 7.24 (m, 4H), 7.21 (t, J = 7.5 Hz, 1H), 7.03 (t, J = 7.5 Hz, 1H), 6.76 (d, J = 7.8 Hz, 1H), 5.69 (br, m, 1H), 4.99 (d, J = 15.5 Hz, 1H), 4.80 (d, J = 15.5 Hz, 1H), 3.99 – 3.86 (m, 1H), 3.70 – 3.55 (m, 1H), 2.38 (s, 3H), 0.71 (t, J = 7.1 Hz, 3H). 13C NMR (100 MHz, CDCl3) δ 176.5, 165.2, 151.9, 149.9, 143.2, 136.3, 132.9, 130.5, 129.5 (2C), 128.5 (3C), 124.6, 124.0, 109.9, 99.4, 64.2, 60.6, 45.0, 20.1, 14.1; HRMS (ESI) calcd for C22H21N3NaO4+ [MNa]+ 414.1434, found 414.1442; enantiomeric excess: 80%, determined by chiral HPLC (n-hexane:isopropanol = 80:20, flow rate 1.0 mL/min): tR = 14.98 min (major), tR = 33.78 min (minor).

(S)-ethyl 1-(4-methoxybenzyl)-6'-methyl-2,2'-dioxo-2',3'-dihydro-1'H-spiro[indoline-3,4'-pyrimidine]-5'-carboxylate (**75b**)

Prepared according to general procedure starting from *N*-(4-methoxybenzyl) isatin and ethyl acetoacetate; FC: dichlorometane:methanol, 97.5:2.5; yield: 63%; white solid; $[\alpha]^{20}_{D}$ 4.5 (*c* 0.35, $CHCl_3$); ^{1}H NMR (300 MHz, $CDCl_3$, mixture of conformers 6:1) δ 8.87 (br, m, 0.15H), 8.74 (br, m, 0.85H), 7.33 (d, *J* = 8.7 Hz, 2H), 7.26 (d, *J* = 8.2 Hz, 1H), 7.17 (t, *J* = 7.7 Hz, 1H), 6.98 (t, *J* = 7.3 Hz, 1H), 6.88 – 6.70 (m, 3H), 6.01 (br, m, 0.86H), 5.81 (br, m, 0.14H), 4.85 (d, *J* = 15.3 Hz, 1H), 4.71 (d, *J* = 15.3 Hz, 1H), 3.96 – 3.78 (m, 1H), 3.74 (s, 0.43H), 3.71 (s, 2.57H), 3.64 – 3.43 (m, 1H), 2.33 (s, 0.44H), 2.27 (s, 2.56H), 0.64 (t, *J* = 7.1 Hz, 3H). ^{13}C NMR (75 MHz, $CDCl_3$, mixture of conformers 6:1) δ 175.9, 164.6, 159.1, 152.1, 149.5, 142.6, 132.5, 129.7, 129.2 (2C), 127.8, 123.9, 123.2, 114.1 (2C), 109.2, 98.5, 63.4, 59.8, 55.2, 43.7, 19.1, 13.5; HRMS (ESI) calcd for $C_{23}H_{23}N_3NaO_5^+$ $[MNa]^+$ 444.1530, found 444.1519; enantiomeric excess: 75%, determined by chiral HPLC (*n*-hexane:isopropanol = 65:35, flow rate 1.0 mL/min): t_R = 9.85 min (major), t_R = 27.96 min (minor).

(S)-ethyl 6'-methyl-1-(4-nitrobenzyl)-2,2'-dioxo-2',3'-dihydro-1'H-spiro[indoline-3,4'-pyrimidine]-5'-carboxylate (**75c**)

Prepared according to general procedure starting from *N*-(4-nitrobenzyl) isatin and ethyl acetoacetate; FC: dichlorometane:methanol, 97.5:2.5; yield: 49%; white solid; $[\alpha]^{20}_{D}$ – 8.2 (*c* 0.3, $CHCl_3$); ^{1}H NMR (300 MHz, $CDCl_3$, mixture of conformers 5:1) δ 8.48 (br, m, 0.17H), 8.40 (br, m, 0.83H), 8.21 – 8.08 (m, 2H), 7.65 – 7.54 (m, 2H), 7.30 (d,

J = 7.3 Hz, 1H), 7.19 (t, *J* = 7.3 Hz, 1H), 7.03 (t, *J* = 7.5 Hz, 1H), 6.62 (d, *J* = 7.6 Hz, 1H), 6.28 (br, m, 0.84H), 6.12 (br, m, 0.16H), 5.09 – 4.87 (m, 2H), 4.07 – 3.89 (m, 1H), 3.86 – 3.68 (m, 1H), 2.34 (s, 0.5H), 2.30 (s, 2.5H), 0.88 (m, 3H). ^{13}C NMR (75 MHz, $CDCl_3$, mixture of conformers 5:1) δ 176.0, 164.6, 151.8, 149.0, 147.5, 143.0, 141.9, 132.2, 130.0, 128.4 (2C), 124.1, 124.0 (2C), 123.8, 109.0, 98.9, 63.51, 60.3, 43.7, 19.5, 13.8; HRMS (ESI) calcd for $C_{22}H_{20}N_4NaO_6^+$ $[MNa]^+$ 459.1275, found 459.1268. enantiomeric excess: 70%, determined by chiral HPLC (*n*-hexane:isopropanol = 50:50, flow rate 1.0 mL/min): t_R = 10.05 min (major), t_R = 45.50 min (minor).

(S)-ethyl 1,6'-dimethyl-2,2'-dioxo-2',3'-dihydro-1'H-spiro[indoline-3,4'-pyrimidine]-5'-carboxylate (**75d**)

Prepared according to general procedure starting from *N*-methyl isatin and ethyl acetoacetate; FC: dichlorometane:methanol, 95:5; yield: 93%; white solid; $[\alpha]^{20}_D$ – 1.6 (*c* 0.35, $CHCl_3$); ^{1}H NMR (400 MHz, DMSO-d_6) δ 9.45 (br, m, 1H), 7.75 (br, m, 1H), 7.30 (t, *J* = 7.7 Hz, 1H), 7.18 (d, *J* = 7.3 Hz, 1H), 7.01 (t, *J* = 7.4 Hz, 1H), 6.97 (d, *J* = 7.8 Hz, 1H), 3.68 (q, *J* = 7.1 Hz, 2H), 3.10 (s, 3H), 2.26 (s, 3H), 0.75 (t, *J* = 7.1 Hz, 3H). ^{13}C NMR (100 MHz, DMSO-d_6) δ 176.2, 164.8, 150.9 (2C), 144.0, 134.0, 129.6, 123.4, 122.8, 108.7, 97.1, 63.1, 59.5, 26.6, 18.7, 13.8; HRMS (ESI) calcd for $C_{16}H_{17}N_3NaO_4^+$ $[MNa]^+$ 338.1111, found 338.1123. enantiomeric excess: 50%, determined by chiral HPLC (*n*-hexane:isopropanol = 65:35, flow rate 1.0 mL/min): t_R = 7.25 min (major), t_R = 38.20 min (minor).

(S)-ethyl 1-benzyl-5-fluoro-6'-methyl-2,2'-dioxo-2',3'-dihydro-1'H-spiro[indoline-3,4'-pyrimidine]-5'-carboxylate (**75e**)

Prepared according to general procedure starting from 5-fluoro-*N*-benzyl isatin and ethyl acetoacetate; FC: dichlorometane:methanol, 97.5:2.5; yield: 51%; white solid; $[\alpha]^{20}_D$ 3.8 (*c* 0.3, $CHCl_3$); ^{1}H NMR (300 MHz, $CDCl_3$, mixture of conformers 5:1) δ 8.76 – 8.49 (br, m, 1H), 7.38 (d, *J* = 7.2 Hz, 2H), 7.34 – 7.16 (m, 3H), 7.03 (dd, *J* = 7.3, 2.5 Hz, 1H), 6.88 (td, *J* = 8.8, 2.4 Hz, 1H), 6.67 (dd, *J* = 8.5, 3.8 Hz, 1H), 6.13 – 5.88 (br, m, 1H), 4.92 (d, *J* = 15.5 Hz, 1H), 4.76 (d, *J* = 15.5 Hz, 1H), 4.04 – 3.83 (m, 1H), 3.74 – 3.52 (m, 1H), 2.35 (s, 0.5H), 2.30 (s, 2.5H), 0.83 – 0.68 (m, 3H). ^{13}C NMR (75 MHz, $CDCl_3$, mixture of conformers 5:1) δ 175.7, 164.4, 161.1, 157.9, 151.80, 149.75, 138.42, 135.34, 128.77 (2C), 127.81, 127.74 (2C), 116.17 and 115.86 (1C), 112.19 and 111.9 (1C), 110.0 and 109.9 (1C), 98.2, 63.6, 60.1, 44.4, 19.3, 13.6; HRMS (ESI) calcd for $C_{22}H_{20}FN_3NaO_4^+$ $[MNa]^+$ 432.1330, found 432.1326. enantiomeric excess: 75%, determined by chiral HPLC (*n*-hexane:isopropanol = 70:30, flow rate 1.0 mL/min): t_R = 8.15 min (major), t_R = 16.35 min (minor).

(S)-ethyl 1-benzyl-5-chloro-6'-methyl-2,2'-dioxo-2',3'-dihydro-1'H-spiro[indoline-3,4'-pyrimidine]-5'-carboxylate (**75f**)

Prepared according to general procedure starting from 5-chloro-*N*-benzyl isatin and ethyl acetoacetate; FC: dichlorometane:methanol, 97.5:2.5; yield: 66%; white solid; $[\alpha]^{20}_D$ 33.6 (*c* 0.2, $CHCl_3$); ^{1}H NMR (300 MHz, $CDCl_3$, mixture of conformers 5:1) δ 8.76 (br, m, 0.16H), 8.69 (br, m, 0.84H), 7.37 (d, *J* = 7.1 Hz, 2H), 7.33 – 7.18 (m, 4H), 7.14 (d, *J* = 8.3, 1H), 6.67 (d, *J* = 8.3 Hz, 1H), 6.24 (br, m, 0.83H), 6.18 (br, m, 0.17H), 4.90 (d, *J* = 15.6 Hz, 1H), 4.77 (d, *J* = 15.7 Hz, 1H), 4.01 – 3.84 (m, 1H), 3.75 – 3.56 (m, 1H), 2.34 (s, 0.5H), 2.29 (s, 2.5H), 0.83 – 0.68 (m, 3H). ^{13}C NMR (75 MHz, $CDCl_3$) δ 175.5, 164.4, 151.9, 149.8, 141.1, 135.2, 134.0, 129.7, 128.8 (2C), 128.5, 127.8, 127.7 (2C), 124.3, 110.3, 98.1, 63.4, 60.1, 44.4, 19.3, 13.6; HRMS (ESI) calcd for $C_{22}H_{20}ClN_3NaO_4^+$ $[MNa]^+$ 448.1035, found 448.1049. enantiomeric excess: 74%, determined by chiral HPLC (*n*-hexane:isopropanol = 70:30, flow rate 1.0 mL/min): t_R = 9.05 min (major), t_R = 16.45 min (minor).

(S)-ethyl 1-benzyl-6-chloro-6'-methyl-2,2'-dioxo-2',3'-dihydro-1'H-spiro[indoline-3,4'-pyrimidine]-5'-carboxylate (**75g**)

Prepared according to general procedure starting from 6-chloro-*N*-benzyl isatin and ethyl acetoacetate; FC: dichlorometane:methanol, 97.5:2.5; yield: 62%; white solid; $[\alpha]^{20}_D$ – 1.0 (*c* 0.3, $CHCl_3$); ^{1}H NMR (300 MHz, $CDCl_3$) δ 8.44 (br, m, 1H), 7.39 (d, *J* = 7.0 Hz, 2H), 7.35 – 7.22 (m, 3H), 7.19 (d, *J* = 7.7 Hz, 1H), 6.98 (d, *J* = 7.6 Hz, 1H), 6.79 (s, 1H), 6.14 (br, m, 1H), 4.90 (d, *J* = 15.5 Hz, 1H), 4.75 (d, *J* = 15.5 Hz, 1H), 3.90 (m, 1H), 3.60 (m, 1H), 2.29 (s, 3H), 0.74 (t, *J* = 6.8 Hz, 3H). ^{13}C NMR (75 MHz, $CDCl_3$) δ 175.8, 164.4, 151.9, 149.4, 143.9, 135.6, 135.1, 130.7, 128.8 (2C), 127.9, 127.8 (2C), 124.8, 123.1, 109.9, 98.4, 63.0, 60.1, 44.4, 19.2, 13.6; HRMS (ESI) calcd for $C_{22}H_{20}ClN_3NaO_4^+$ $[MNa]^+$ 448.1035, found 448.1039; enantiomeric excess: 77%, determined by chiral HPLC (*n*-hexane:isopropanol = 65:35, flow rate 1.0 mL/min): t_R = 8.65 min (major), t_R = 15.35 min (minor).

(S)-ethyl 1-benzyl-6-bromo-6'-methyl-2,2'-dioxo-2',3'-dihydro-1'H-spiro[indoline-3,4'-pyrimidine]-5'-carboxylate (**75h**)

Prepared according to general procedure starting from 6-bromo-*N*-benzyl isatin and ethyl acetoacetate; FC: dichlorometane:methanol, 97.5:2.5; yield: 63%; white solid; $[\alpha]^{20}_D$ 7.6 (*c* 0.55, $CHCl_3$); ^{1}H NMR (300 MHz, $CDCl_3$) δ 8.52 (br, m, 1H), 7.39 (d, *J* = 7.3 Hz, 2H), 7.26 (m, 3H), 7.18 – 7.06 (m, 2H), 6.95 (s, 1H), 6.22 (m, 1H), 4.87 (d, *J* = 15.6 Hz, 1H), 4.75 (d, *J* = 15.6 Hz, 1H), 4.00 – 3.77 (m, 1H), 3.70 – 3.49 (m, 1H), 2.27 (s, 3H), 0.72 (t, *J* = 7.1 Hz, 3H). ^{13}C NMR

(75 MHz, $CDCl_3$) δ 175.7, 164.4, 152.0, 149.5, 144.0, 135.1, 131.3, 128.8 (2C), 127.9, 127.8 (2C), 126.1, 125.2, 123.4, 112.6, 98.3, 63.1, 60.1, 44.1, 19.2, 13.6; HRMS (ESI) calcd for $C_{22}H_{20}BrN_3NaO_4^+$ $[MNa]^+$ 492.0529, found 492.0518; enantiomeric excess: 75%, determined by chiral HPLC (*n*-hexane:isopropanol = 70:30, flow rate 1.0 mL/min): t_R = 9.35 min (major), t_R = 16.50 min (minor).

(S)-methyl 1-benzyl-6'-methyl-2,2'-dioxo-2',3'-dihydro-1'H-spiro[indoline-3,4'-pyrimidine]-5'-carboxylate (**75i**)

Prepared according to general procedure starting from *N*-benzyl isatin and methyl acetoacetate; FC: dichlorometane:methanol, 97.5:2.5; yield: 65%; white solid; $[\alpha]^{20}_D$ – 6.8 (*c* 0.35, $CHCl_3$); ^{1}H NMR (300 MHz, $CDCl_3$) δ 7.77 (br, m, 1H), 7.40 (d, *J* = 7.7 Hz, 2H), 7.36 – 7.23 (m, 4H), 7.20 (td, *J* = 7.8, 1.2 Hz, 1H), 7.01 (t, *J* = 7.5 Hz, 1H), 6.75 (d, *J* = 7.7 Hz, 1H), 5.29 (br, m, 1H), 4.94 (d, *J* = 15.5 Hz, 1H), 4.83 (d, *J* = 15.4 Hz, 1H), 3.20 (s, 3H), 2.37 (s, 3H). ^{13}C NMR (75 MHz, $CDCl_3$) δ 175.8, 165.0, 151.3, 149.2, 142.3, 135.6, 132.1, 129.9, 128.8 (2C), 127.9 (2C), 127.8, 123.8, 123.3, 109.2, 98.7, 63.5, 51.0, 44.3, 19.4; HRMS (ESI) calcd for $C_{21}H_{19}N_3NaO_4^+$ $[MNa]^+$ 400.1268, found 400.1257; enantiomeric excess: 61%, determined by chiral HPLC (*n*-hexane:isopropanol = 70:30, flow rate 1.0 mL/min): t_R = 9.15 min (major), t_R = 18.30 min (minor).

(S)-benzyl 1-benzyl-6'-methyl-2,2'-dioxo-2',3'-dihydro-1'H-spiro[indoline-3,4'-pyrimidine]-5'-carboxylate (**75j**)

Prepared according to general procedure starting from *N*-benzyl isatin and benzyl acetoacetate; FC: dichlorometane:methanol, 97.5:2.5; yield: 55%; white solid; $[\alpha]^{20}_D$ 17.2 (*c* 0.5, dioxane); ^{1}H NMR (300 MHz, $CDCl_3$) δ 8.15 (m, 1H), 7.41 – 7.17 (m, 10H), 7.18 – 7.09 (m, 1H), 6.98 (t, *J* = 7.5 Hz, 1H), 6.85 (d, *J* = 6.5 Hz, 1H), 6.44 (d, *J* = 7.8 Hz, 1H), 5.39 (br, m, 1H), 4.85 – 4.70 (m, 2H), 4.63 (d, *J* = 12.0 Hz, 1H), 3.81 (d, *J* = 15.6 Hz, 1H), 2.39 (s, 3H). ^{13}C NMR (75 MHz,) δ 175.8, 164.4, 162.2, 150.2, 142.3, 135.8, 132.2, 129.9, 128.9 (4C), 128.6 (2C), 128.3, 127.8, 127.7 (2C), 124.0, 123.4, 109.8, 66.5, 43.8, 19.6 (3 quaternary carbons are missed); HRMS (ESI) calcd for $C_{27}H_{23}N_3NaO_4^+$ $[MNa]^+$ 476.1581, found 476.1589. enantiomeric excess: 74%, determined by chiral HPLC (*n*-hexane:isopropanol = 80:20, flow rate 1.0 mL/min): t_R = 13.50 min (major), t_R = 28.20 min (minor).

PROCEDURE FOR THE SYNTHESIS OF ethyl *(S)-1,1'-dibenzyl-6'-methyl-2,2'-dioxo-2',3'-dihydro-1'H-spiro[indoline-3,4'-pyrimidine]-5'-carboxylate* (**76**)

To a solution of compound **75a** (0.25 mmol, 1 eq) in anhydrous dimethylformamide (0.830 mL, 0.3 M), $CsCO_3$ (0.33 mmol, 1.3 eq) was added, then the mixture was stirred for 1 hour at room temperature. Benzyl bromide (0.38 mmol, 1.5 eq) was slowly added and the mixture was stirred overnight. After the completion of reaction (monitored by TLC), saturated aq. NaCl (1 mL) was added. The reaction mixture was extracted with ethyl acetate (3 x 2 mL). The combined organic layer was washed with water (2 x 6 mL), followed by brine (2 x 6 mL). the organic phase was dried over anhydrous Na_2SO_4 and concentrated *in vacuo* to afford the crude product, which was purified by FC (*n*-hexane:ethyl acetate, 7:3), affording the desired product **76** (115 mg, 96%) as a white solid. $[\alpha]^{20}_D$ – 32.4 (*c* 0.5, $CHCl_3$); ^{1}H NMR (300 MHz, $CDCl_3$) δ 7.51 – 7.24 (m, 11H), 7.21 (d, *J* = 7.7 Hz, 1H), 7.02 (t, *J* = 7.4 Hz, 1H), 6.75 (d, *J* = 7.8 Hz, 1H), 5.32 (d, *J* = 17.0 Hz, 1H), 5.16 (br, m, 1H), 4.93 (d, *J* = 15.2 Hz, 2H), 4.83 (d, *J* = 15.4 Hz, 1H), 3.91 – 3.73 (m, 1H), 3.57 – 3.42 (m, 1H), 2.40 (s, 3H), 0.52 (t, *J* = 7.1 Hz, 3H); ^{13}C NMR (75 MHz, $CDCl_3$) δ 175.9, 165.1, 152.2, 150.7, 142.9, 137.7, 135.6, 131.7, 129.8, 128.9 (2C), 128.7 (2C), 127.8 (3C), 127.1, 126.0 (2C), 123.9, 123.2, 109.1, 101.9, 62.3, 60.0, 46.0, 44.2, 16.8, 13.2; HRMS (ESI) calcd for $C_{29}H_{27}N_3NaO_4^+$ $[MNa]^+$ 504.1894, found 504.1898.

PROCEDURE FOR THE SYNTHESIS OF *(S)-1-benzyl-6'-methyl-2,2'-dioxo-2',3'-dihydro-1'H-spiro[indoline-3,4'-pyrimidine]-5'-carboxylic acid* (**77**)

Palladium (10 wt.% on carbon, 0.025 mmol, 0.05 eq) was added to a solution of Biginelli-adduct **75j** (0.50 mmol, 1 eq) and Et_3N (0.50 mmol, 1 eq) in 7.5 mL of dioxane/methanol (2:1). The reaction mixture was degassed *in vacuo*, placed under an atmosphere of H_2 (g), and stirred in the dark at rt for 3h. The mixture was filtered through a pad of Celite eluting with methanol (10 mL), and the combined organic layers were concentrated *in vacuo* to give the crude carboxylic acid derivative **77** (173 mg, 95%) as a white solid, sufficiently pure to be directly used in the next step. $[\alpha]^{20}_D$ – 19.2 (*c* 0.25, $CHCl_3$); ^{1}H NMR (300 MHz, DMSO-d_6) δ 11.97 (br, s, 1H), 9.39 (br, m, 1H), 7.89 (br, m, 1H), 7.47 (d, *J* = 6.7 Hz, 2H), 7.39 – 7.25 (m, 3H), 7.23 (d, *J* = 7.2 Hz, 1H), 7.16 (t, *J* = 7.7 Hz, 1H), 6.98 (t, *J* = 7.4 Hz, 1H), 6.62 (d, *J* = 7.7 Hz,

1H), 4.96 (d, *J* = 16.3 Hz, 1H), 4.70 (d, *J* = 16.3 Hz, 1H), 2.29 (s, 3H); ^{13}C NMR (75 MHz, DMSO-d_6) δ 176.1, 166.4, 150.7, 149.4, 142.7, 136.3, 133.9, 128.8, 128.3 (2C), 127.1 (2C), 127.0, 123.0, 122.3, 108.9, 97.8, 63.0, 43.4, 18.5; HRMS (ESI) calcd for $C_{20}H_{17}N_3NaO_4^+$ $[MNa]^+$ 386.1111, found 386.1121.

PROCEDURE FOR THE SYNTHESIS OF *(R)-1-benzyl-6'-methyl-1'H-spiro[indoline-3,4'-pyrimidine]-2,2'(3'H)-dione* (**78**)

To a solution of the carboxylic acid derivative **77** (0.1 mmol, 1 eq) in 1 mL of dioxane/methanol (1:1), hydrochloric acid in dioxane (4 M, 0.4 mmol, 4 eq) was added, and the reaction was stirred at 90 °C for 0.5h. The solvent was removed under reduced pressure to afford compound **78** (31 mg, 98%) in high purity as a white solid, with no need for further purifications. $[\alpha]^{20}_D$ – 25.6 (*c* 0.5, $CHCl_3$); ^{1}H NMR (400 MHz, $CDCl_3$) δ 7.82 (br, m, 1H), 7.40 (d, *J* = 7.3 Hz, 1H), 7.37 – 7.23 (m, 5H), 7.18 (t, *J* = 7.7 Hz, 1H), 7.06 (t, *J* = 7.5 Hz, 1H), 6.71 (d, *J* = 7.8 Hz, 1H), 5.72 (br, m, 1H), 4.93 (d, *J* = 15.6 Hz, 1H), 4.79 (d, *J* = 15.6 Hz, 1H), 4.24 (s, 1H), 1.86 (s, 3H). ^{13}C NMR (100 MHz, $CDCl_3$) δ 177.2, 154.4, 142.0, 136.4, 136.1, 132.6, 130.5, 129.5 (2C), 128.4, 128.0 (2C), 125.7, 124.2, 110.2, 95.4, 64.3, 44.7, 19.4; HRMS (ESI) calcd for $C_{19}H_{17}N_3NaO_2^+$ $[MNa]^+$ 342.1213, found 342.1206.

PROCEDURE FOR THE SYNTHESIS OF DIASTEREOISOMERS *(S)-1-benzyl-6'-methyl-2,2'-dioxo-N-((S)-1-phenylethyl)-2',3'-dihydro-1'H-spiro[indoline-3,4'-pyrimidine]-5'-carboxamide* (**79a**) *AND (R)-1-benzyl-6'-methyl-2,2'-dioxo-N-((S)-1-phenylethyl)-2',3'-dihydro-1'H-spiro[indoline-3,4'-pyrimidine]-5'-carboxamide* (**79b**)

To a solution of carboxylic acid derivative **78** (0.9 mmol, 1 eq) and DIPEA (1.8 mmol, 2 eq) in 9.4 mL of anhydrous dimethylformamide, HATU (1.4 mmol, 1.5 eq) was added. After 5 min, (*S*)-(−)-α-methylbenzylamine (0.9 mmol, 1 eq) and DIPEA (1.8 mmol, 2 eq) were added, and the reaction was stirred at room temperature for 24 hours. The resulting mixture was partitioned between ethyl acetate (20 mL) and water (20 mL). The organic phase was washed with brine (6 x 10 mL), dried over Na_2SO_4 and concentrated *in vacuo* to afford the crude diastereoisomeric mixture **79**, which was purified by flash chromatography (ethyl acetate:*n*-hexane, 95:5), obtaining the two isolated stereoisomers **79a** (358 mg, 86%) and **79b** (54 mg, 12%).

79a: white solid; $[\alpha]^{20}_D$ 16.5 (*c* 0.9, $CHCl_3$); ^{1}H NMR (400 MHz, DMSO-d_6) δ 8.79 (br, m, 1H), 8.18 (d, *J* = 8.4 Hz, 1H), 7.62 (br, m, 1H), 7.46 (d, *J* = 7.3 Hz, 2H), 7.33 (d, *J* = 7.4 Hz, 1H), 7.32 – 7.22 (m, 7H), 7.18 (q, *J* = 8.4, 7.8 Hz, 2H), 7.00 (t, *J* = 7.5 Hz, 1H), 6.63 (d, *J* = 7.8 Hz, 1H), 4.78 (s, 2H), 4.71 – 4.59 (m, 1H), 1.91 (s, 3H), 1.04 (d, *J* = 7.0 Hz, 3H). ^{13}C NMR (100 MHz, DMSO-d_6) δ 177.4, 165.6, 153.2, 145.3, 144.4, 138.0, 137.3, 132.4, 130.2, 129.4 (2C), 129.3 (2C), 128.3 (2C), 128.1, 127.6, 127.2 (2C), 125.3, 123.0, 109.9, 105.1, 64.3, 48.6, 44.2, 23.0, 18.3. HRMS (ESI) calcd for $C_{28}H_{26}N_4NaO_3^+$ $[MNa]^+$ 489.1897, found 489.1905.

79b: white solid; $[\alpha]^{20}_D$ – 89.5 (*c* 1, $CHCl_3$); ^{1}H NMR (400 MHz, DMSO-d_6) δ 8.81 (br, m, 1H), 8.13 (d, *J* = 8.3 Hz, 1H), 7.62 (br, m, 1H), 7.42 (d, *J* = 6.4 Hz, 2H), 7.31 (d, *J* = 7.2 Hz, 1H), 7.29 – 7.19 (m, 3H), 7.17 (t, *J* = 7.6 Hz, 1H), 7.11 (m, 3H), 7.00 (t, *J* = 7.4 Hz, 1H), 6.83 (d, *J* = 7.4 Hz, 2H), 6.57 (d, *J* = 7.8 Hz, 1H), 4.88 – 4.67 (m, 3H), 2.01 (s, 3H), 1.32 (d, *J* = 7.0 Hz, 3H). ^{13}C NMR (100 MHz, DMSO-d_6) δ 177.4, 165.6, 153.0, 144.9, 144.32, 138.3, 137.3, 132.7, 130.1, 129.4 (2C), 128.9 (2C), 128.2 (2C), 128.07, 127.1, 126.8 (2C), 125.3, 123.2, 110.0, 105.12, 64.4, 48.1, 44.2, 22.5, 18.4. HRMS (ESI) calcd for $C_{28}H_{26}N_4NaO_3^+$ $[MNa]^+$ 489.1897, found 489.1909.

COMPUTATIONAL STUDIES

Determination of the stereochemistry of the C-3 quaternary stereocenter

Mono- and bidimensional NMR analysis on both diastereoisomers **79a** and **79b** allowed to assign each proton and carbon to experimental chemical shifts, although NH protons chemical shifts were not futher considered. Monte Carlo conformational search was run with Spartan '08[23] using MMFF forcefield on both possible stereoisomers with (3*S*,1'*S*) and (3*R*,1'*S*) absolute configurations, with standard parameters and convergence criteria. All structures with population

> 1% were further optimized with GAUSSIAN09[24] at quantum-mechanics DFT/B3LYP/6-31g(d,p) in gas phase, followed by single-point *ab initio* calculations of energy (DFT/B3LYP/6-31g(d,p)) and GIAO shielding constants at the DFT/6-311+G(2d,p)/SCRF-dmso level. Boltzmann averaging over the conformers, followed by linear regression employing reported[25] ^{1}H and ^{13}C NMR scaling factors afforded theoretical NMR chemical shift for the two possible (3*S*,1'*S*) and (3*R*,1'*S*) absolute configurations. Comparison parameters 3 (CP3) were computed for protons, carbons and all data. Application of the Bayes' theorem afforded the percentage probability for each assignment.[26]

Transition-state calculation

All the structures were first submitted to a Monte Carlo conformational search with MM (MMFF94 force field) minimization. The global minima were then submitted to a geometry optimization with DFT at the B3LYP/6-31G(d,p) level. All the minima were confirmed by frequency calculation. Transition state (TS) search was first attempted with HF/3-21G on a simplified model and then refined with DFT B3LYP/6-31G. Single point calculation at the B3LYP/6-31G(d,p) level was then performed on the complete TS structures. TS were confirmed by analysis of the imaginary frequencies.

References

[1] Erdmann, O.L. et al. (1980) Untersuchungen über den Indigo. J. Prakt. Chem., 19(1), 321-362. Laurent, A. et al. (1840) Recherches sur l'indigo. Ann. Chim. Phys., 3(3), 393-434.
[2] Kekule, A. *Chem. Ber.* **1869**, *2*, 748.
[3] (a) Bergman, J.; Lindström, J.-O; Tilstam, U. *Tetrahedron* **1985**, *41*, 2879. (b) Guo, Y.; Chen, F.; *Zhongcaoyao* **1986**, *17*, 8. (c) da Silva, J. F. M.; Garden, S. J.; Pinto, A. C. *J. Braz. Chem. Soc.* **2001**, *12*, 273.
[4] (a) Chiyanzu, I.; Hansell, E.; Gut, J.; Rosenthal, P. J.; McKerrowb, J. H.; Chibale, K. *Bioorg. Med. Chem. Lett.* **2003**, *13*, 3527. (b) Almeida, M. R.; Leitão, G. G.; Silva, B. V.; Barbosa, J. P.; Pinto, A. C. *J. Braz. Chem. Soc.* **2010**, *21*, 764.
[5] Hanahan, D.; Weinberg, R. A. *Cell* **2000**, *100*, 57.
[6] Gaeta, F.C.A.; Galan, A. A.; Kraynack, E. A. PCT/US99/13523 **1999**.
[7] (a) Vine, K. L.; Matesic, L.; Locke, J. M.; Ranson, M.; Skropeta, D. *Anti-Cancer Agents in Medicinal Chemistry* **2009**, *9*, 397. (b) Liu, Y.-C.; Zhang, R.; Wu, Q.-Y.; Chen, Q.; Yang, G.-F. *Organic Preparations and Procedures International* **2014**, *46*, 317.
[8] (a) Singh, G. S.; Desta, Z. Y. *Chem. Rev.* **2012**, *112*, 6104. (b) Babu, S. A.; Padmavathi, R.; Aslam, N. A.; Rajkumar, V. *Studies in Natural product Chemistry, Chapter 8 – Recent Developments on the Synthesis and Applications of Natural Products-Inspired Spirooxindole Frameworks* **2015**, *46*, 227.
[9] (a) Kefayati, H.; Rad-Moghadam, K.; Zamani, M.; Hosseyni, S. *Lett. Org. Chem.* **2010**, *7*, 277.. (b) Lahsasni, S.; Mohamed, M. A. A.; El-Saghier, A. M. M. *Res. J. Chem. Env.* **2014**, *18*, 38.
[10] De Fatima, A.; Braga, T.C.; Da S. Neto, L.; Terra, B.S.; Oliveira, B.G.F.; Da Silva, D.L.; Modolo, L.V. *J. Adv. Res.* **2014**, http://dx.doi.org/ 10.1016/j.jare.2014.10.006.
[11] Heravi, M.M.; Asadi, S.; Lashkariani, B.M. *Mol. Divers.* **2013**, *17*, 389.
[12] a) Chen, X.U.; Xu, X.Y.; Liu, H.; Cun, L.F.; Gong, L.Z. *J. Am. Chem. Soc.* **2006**, *128*, 14802. b) Li, N.; Chen, X.H.; Song, J.; Luo, S.W.; Fan, W.; Gong, L.Z. *J. Am. Chem. Soc.* **2009**, *131*, 15301.
[13] Chen, X.-H.; Xu, X.-Y.; Liu, H.; Cun, L.-F.; Gong, L.-Z. *J. Am. Chem. Soc.* **2006**, *128*, 14802.
[14] a) Barone, G.; Gomez-Paloma, L.; Duca, D.; Silvestri, A.; Riccio, R.; Bifulco, G. *Chem. Eur. J.* **2002**, *8*, 3233; b) Barone, G.; Gomez-Paloma, L.; Duca, D.; Silvestri, A.; Riccio, R.; Bifulco, G. *Chem. Eur. J.* **2002**, *8*, 3240.
[15] Frisch, M. J.; Trucks, G. W.; Schlegel, H. B.; Scuseria, G. E.; Robb, M. A.; Cheeseman, J. R.; Scalmani, G.; Barone, V.; Mennucci, B.; Petersson, G. A.; Nakatsuji, H.; Caricato, M.; Li, X.; Hratchian, H. P.; Izmaylov, A. F.; Bloino, J.; Zheng, G.; Sonnenberg, J. L.; Hada, M.; Ehara, M.; Toyota, K.; Fukuda, R.; Hasegawa, J.; Ishida, M.; Nakajima, T.; Honda, Y.; Kitao, O.; Nakai, H.; Vreven, T.; Montgomery, J. A., Jr.; Peralta, J. E.; Ogliaro, F.; Bearpark, M.; Heyd, J. J.; Brothers, E.; Kudin, K. N.; Staroverov, V. N.; Kobayashi, R.; Normand, J.; Raghavachari, K.; Rendell, A.; Burant, J. C.; Iyengar, S. S.; Tomasi, J.; Cossi, M.; Rega, N.; Millam, J. M.; Klene, M.; Knox, J. E.; Cross, J. B.; Bakken, V.; Adamo, C.; Jaramillo, J.; Gomperts, R.; Stratmann, R. E.; Yazyev, O.; Austin, A. J.; Cammi, R.; Pomelli, C.; Ochterski, J. W.; Martin, R. L.; Morokuma, K.; Zakrzewski, V. G.; Voth, G. A.; Salvador, P.; Dannenberg, J. J.; Dapprich, S.; Daniels, A. D.; Farkas, Ö.; Foresman, J. B.; Ortiz, J. V.; Cioslowski, J.; Fox, D. J. *Gaussian 09, Revision A.02*, Gaussian, Inc., Wallingford, CT, **2009**.
[16] Pierens, G. K. *J. Comp. Chem.* **2014**, *35*, 1388.
[17] a) G. Bifulco, P. Dambruoso, L. Gomez-Paloma, R. Riccio, *Chem. Rev.* **2007**, *107*, 3744–3779; b) S. Di Micco, M. G. Chini, R. Riccio, G. Bifulco, *Eur. J. Org. Chem.* **2010**, *8*, 1411–1434.
[18] Smith, S. G.; Goodman, J. M. *J. Org. Chem.* **2009**, *74*, 4597.
[19] *Dipartimento di Chimica, Materiali ed Ing.Chimica 'Giulio Natta'*, Politecnico di Milano, p.zza Leonardo da Vinci 32, 20133, Milano, Italy.
[20] Simón, L.; Goodman, J. M. J. Org. Chem. 2011, 76 (6), 1775–1788.
[21] Lu, S.; BeiPoh, S.; Siau, W.-Y.; Zhao, Y. *Angew. Chem. Inter. Ed.*, **2013**, *52*, 1731.
[22] Simonsen, K. B.; Gothelf, K. V.; Jørgensen, K. A. *J. Org. Chem.*, **1998**, *63*, 7536.
[23] *Spartan*'08. Wavefunction, Inc. Irvine, CA.
[24] Frisch, M. J.; Trucks, G. W.; Schlegel, H. B.; Scuseria, G. E.; Robb, M. A.; Cheeseman, J. R.; Scalmani, G.; Barone, V.; Mennucci, B.; Petersson, G. A.; Nakatsuji, H.; Caricato, M.; Li, X.; Hratchian, H. P.; Izmaylov, A. F.; Bloino, J.; Zheng, G.; Sonnenberg, J. L.; Hada, M.; Ehara, M.; Toyota, K.; Fukuda, R.; Hasegawa, J.; Ishida, M.; Nakajima, T.; Honda, Y.; Kitao, O.; Nakai, H.; Vreven, T.; Montgomery, J. A., Jr.; Peralta, J. E.; Ogliaro, F.; Bearpark, M.; Heyd, J. J.; Brothers, E.; Kudin, K. N.; Staroverov, V. N.; Kobayashi, R.; Normand, J.; Raghavachari, K.; Rendell, A.; Burant, J. C.; Iyengar, S. S.; Tomasi, J.; Cossi, M.; Rega, N.; Millam, J. M.; Klene, M.; Knox, J. E.; Cross, J. B.; Bakken, V.; Adamo, C.; Jaramillo, J.; Gomperts,

R.; Stratmann, R. E.; Yazyev, O.; Austin, A. J.; Cammi, R.; Pomelli, C.; Ochterski, J. W.; Martin, R. L.; Morokuma, K.; Zakrzewski, V. G.; Voth, G. A.; Salvador, P.; Dannenberg, J. J.; Dapprich, S.; Daniels, A. D.; Farkas, Ö.; Foresman, J. B.; Ortiz, J. V.; Cioslowski, J.; Fox, D. J. *Gaussian 09, Revision A.02*, Gaussian, Inc., Wallingford, CT, **2009**.
[25] Pierens, G. K. *J. Comp. Chem.* **2014**, *35*, 1388.
[26] Smith, S. G.; Goodman, J. M. *J. Org. Chem.* **2009**, *74*, 4597.

CONCLUSIONS

5. GENERAL CONCLUSIONS AND FUTURE PERSPECTIVES

In conclusion, we exploited the potentialities of four different multicomponent reactions (MCRs), namely Ugi four-component reaction (U-4CR), *N*-split Ugi reaction (*N*-split U-4CR), van Leusen three-component reaction (vl-3CR) and Biginelli reaction (Bg-3CR), developing five different approaches to the synthesis of small bioactive molecules.

In particular, we successfully applied the build/couple/pair strategy obtaining a small library of ketopiperazine-based *minimalist* peptidomimetics, by means of diastereoselective U-4CR/post-cyclization sequences, employing optically pure amino acid-derived α-amino aldehydes and α-isocyanoacetates as starting materials. Computer-assisted NMR NOE analysis allowed us to determine the configuration of the newly formed stereocenters, while molecular dynamics simulation and biological evaluation clearly underlined the potentiality of selected compounds to interfere with protein-protein interactions (PPIs). Although many successful attempts in combining MCRs with complexity generation reactions have been reported, the introduction of multiple amino-acid derived components easily afforded conformationally constrained peptidomimetics in a stereocontrolled way. Simply by changing such components in the initial U-4CR, countless similar structures should be accessible, greatly expanding this biologically relevant class of compounds.

We also focused our attention on another class of peptide-like compounds, namely diamine-based peptidomimetics, by carefully optimizing the *N*-split U-4CR conditions for the introduction of *N*-protected amino acids and α-isocyanoacetates components, in a stereoconservative way. This methodology largely simplifies the synthesis of such compounds, opening the way to the use of more complex secondary diamines, able to induce well-defined secondary structures in the related peptidomimetic and hopefully targeting novel PPIs.

Furthermore, by combining the same *N*-split U-4CR with common transformations, a library of dopamine receptor agonists was rapidly obtained, with biological activities in the nanomolar range. Although the desired D_2/D_3 selectivity was not achieved, structure-activity relationship (SAR) and docking studies allowed us to understand the key pharmacophoric elements in these novel structures, leading the way to the design of improved molecular scaffolds.

By employing the vL-3CR in an iterative way, we designed a novel C2-C5' linked polyimidazole-based *minimalist* framework, able to mimic the *i*, *i*+1, *i*+2 and *i*+3 amino acid residues of a β-strand motif. Its conformational behaviour was investigated through solution-phase NMR and molecular dynamics studies, allowing to demonstrate its ability to mimic a poly-alanine β-strand. Further work is currently underway in order to introduce selected side chains, affording polyimidazole-based β-strand peptidomimetics specially designed to disrupt specific PPIs.

Finally, we explored the possibility to combine MCRs with organocatalysis, developing the first BINOL-derived phosphoric acid catalysed Biginelli-like reaction on a ketone. In particular, employing *N*-substituted isatins as carbonyl substrates, we achieved the synthesis of a small library of biologically relevant enantioenriched spiro[indoline-pyrimidine]-diones derivatives. The assignment of the configuration at the new oxindole C-3 stereocenter was assessed through quantum-mechanical methods and NMR spectroscopy, while computational studies on the reaction transition state allowed us to explain the enantioselectivity and the stereochemical outcome. Further studies on organocatalyzed MCRs on the isatin core are currently underway in our laboratories, with the aim to obtain novel 3,3'-disubstituted oxindole derivatives and related spiro-compounds in a stereocontrolled way.

Our results clearly highlight the potentiality of the multicomponent approach, when applied to the synthesis of small bioactive molecules. In particular, the discovery of novel MCRs or their combination with complexity generation reactions in a stereocontrolled way will be the key points in the near future of this rapidly growing research area.

APPENDIX

A.1 NMR SPECTRA

Chapter 2.1

Compound **7a**: ^{1}H NMR (300 MHz, CD_3CN)

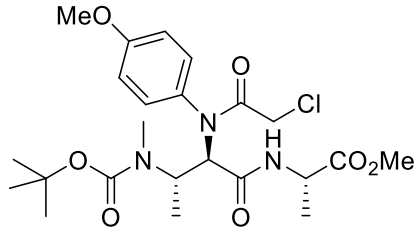

7a

Compound **7a**: ^{13}C NMR (75 MHz, CD_3CN)

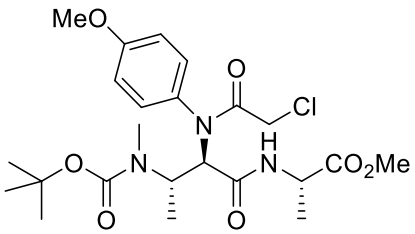

7a

Compound **7b**: ^{1}H NMR (300 MHz, CD_3CN)

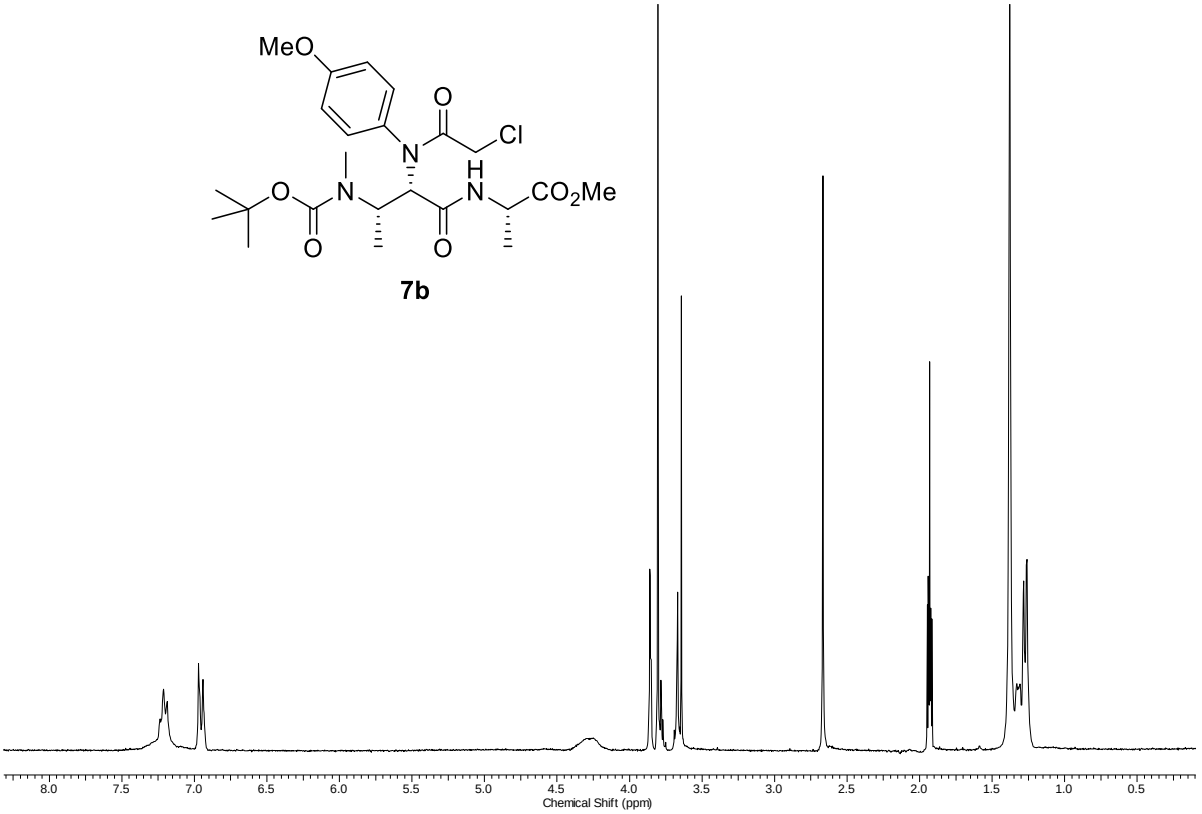

Compound **7b**: ^{13}C NMR (100 MHz, $CDCl_3$)

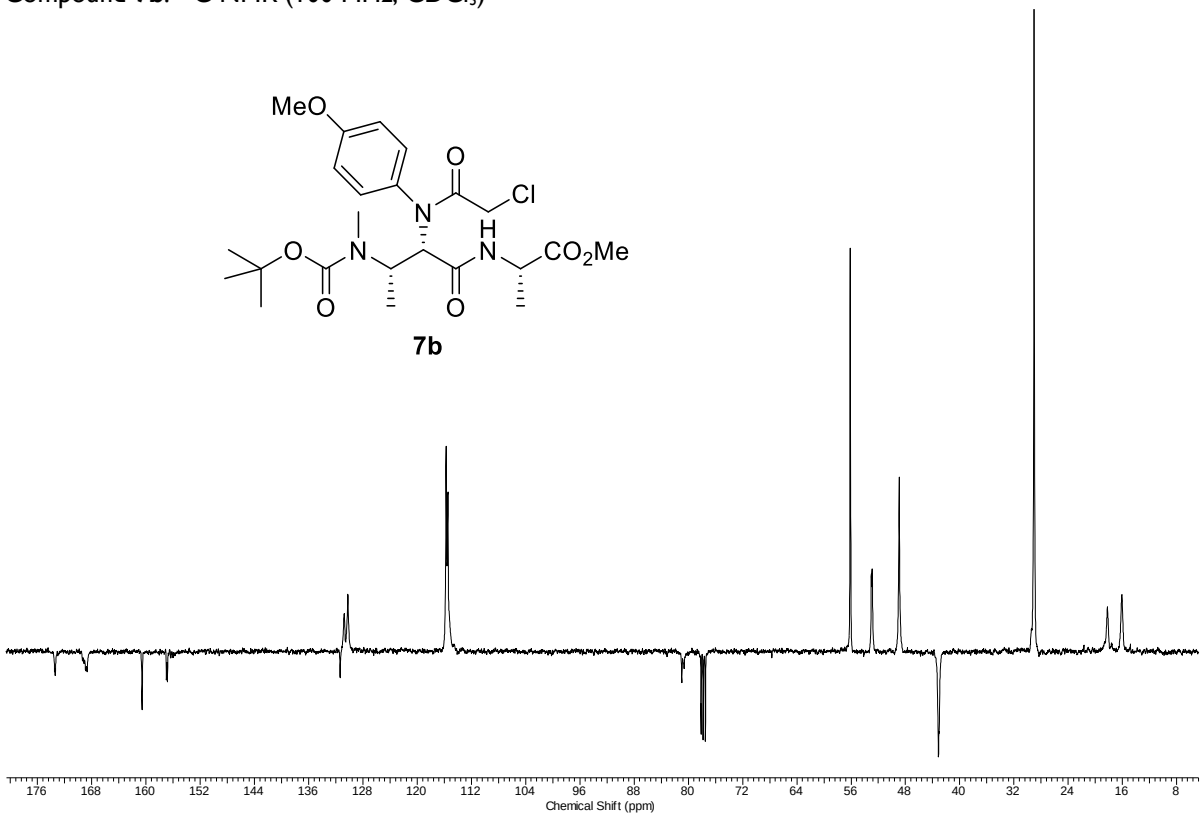

Compound **8**: ^{1}H NMR (300 MHz, CD_3CN)

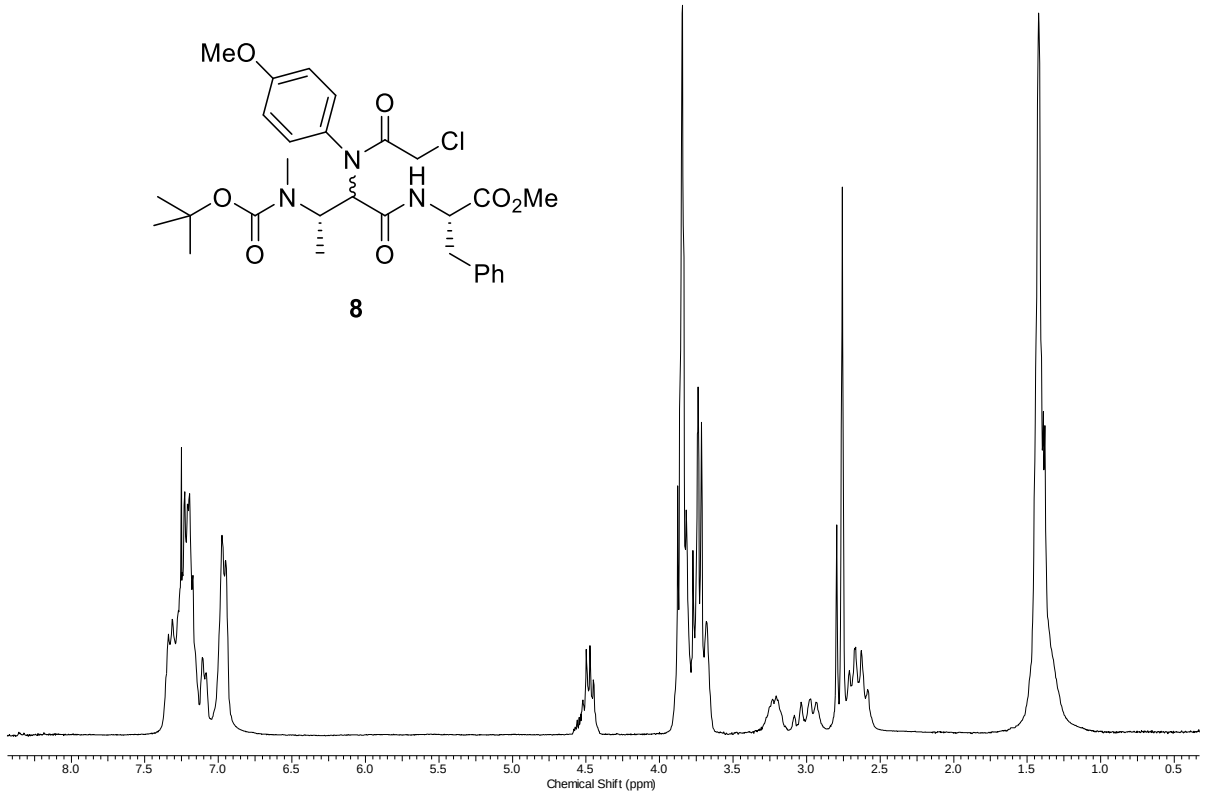

8

Compound **9**: ^{1}H NMR (300 MHz, CD_3CN)

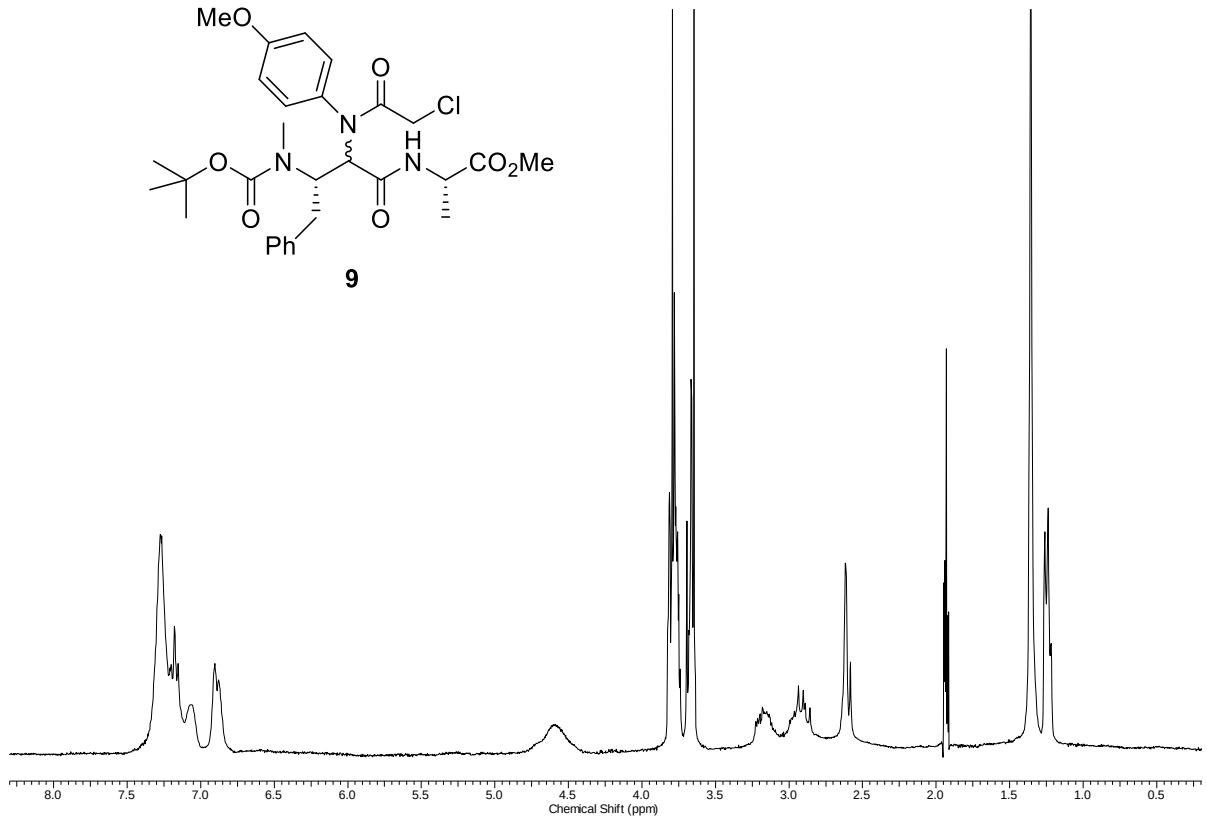

9

Compound **10**: ^{1}H NMR (400 MHz, $CDCl_3$)

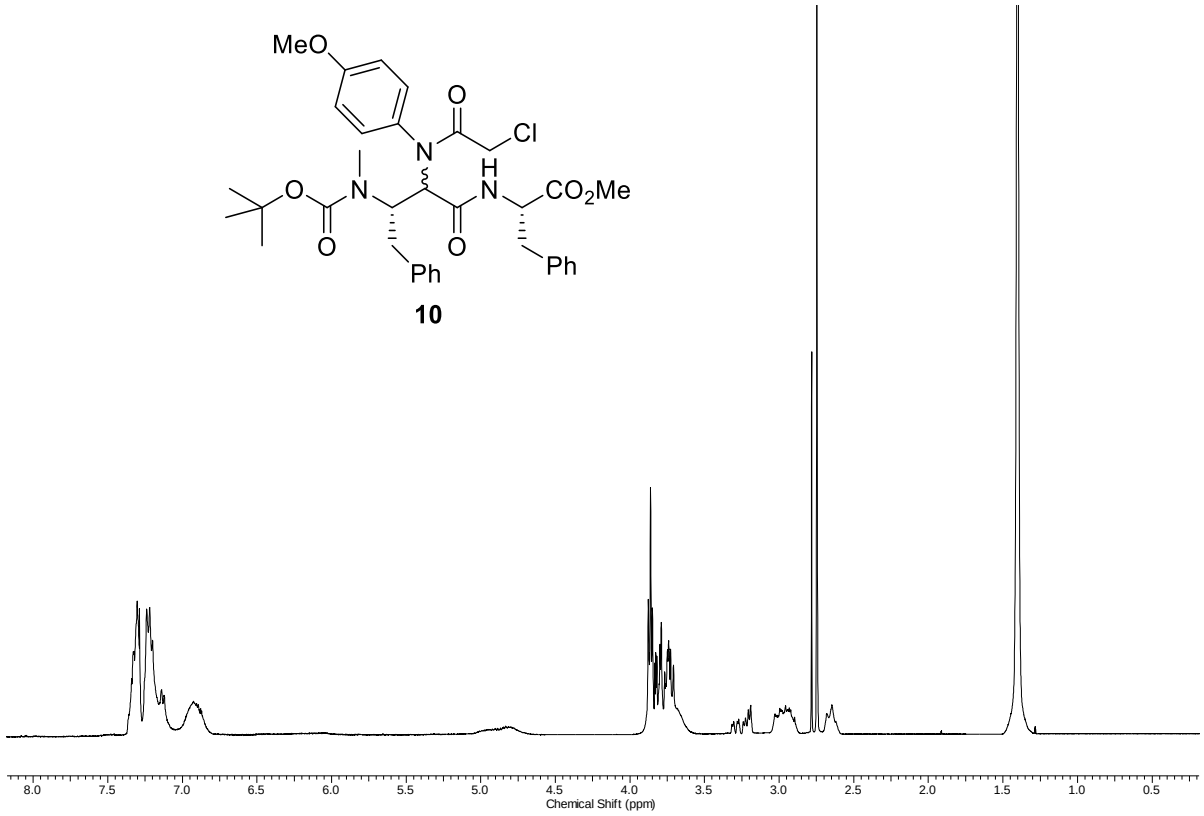

Compound **11a**: ^{1}H NMR (300 MHz, CD_3CN)

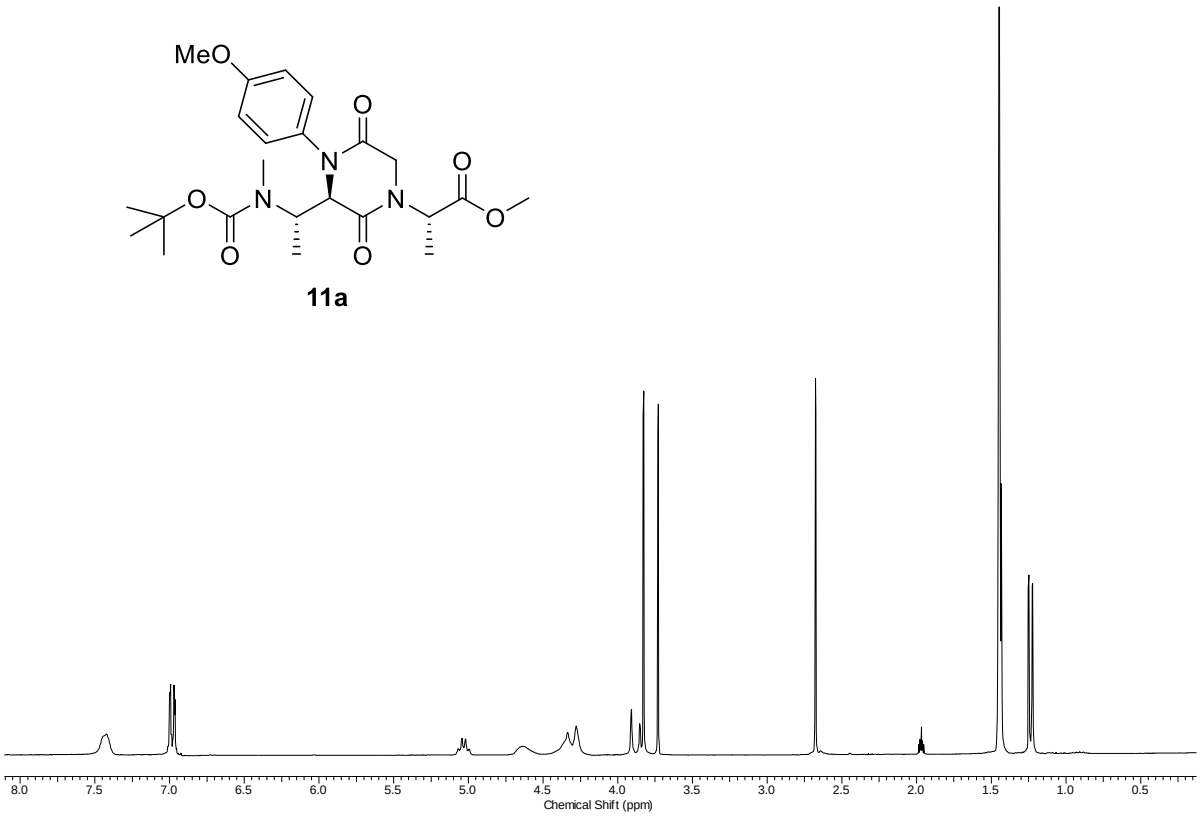

Compound **11a**: ^{13}C NMR (100 MHz, CD_3CN)

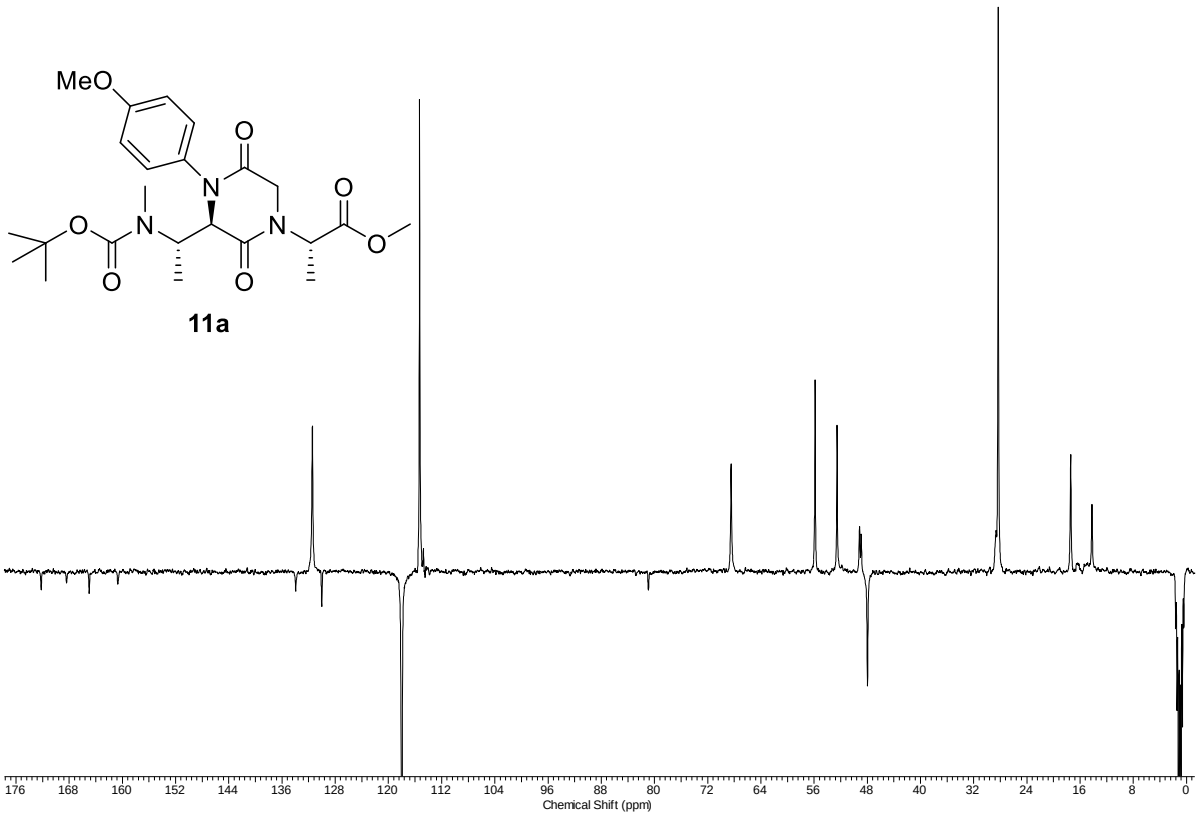

Compound **11b**: ^{1}H NMR (400 MHz, CD_3CN)

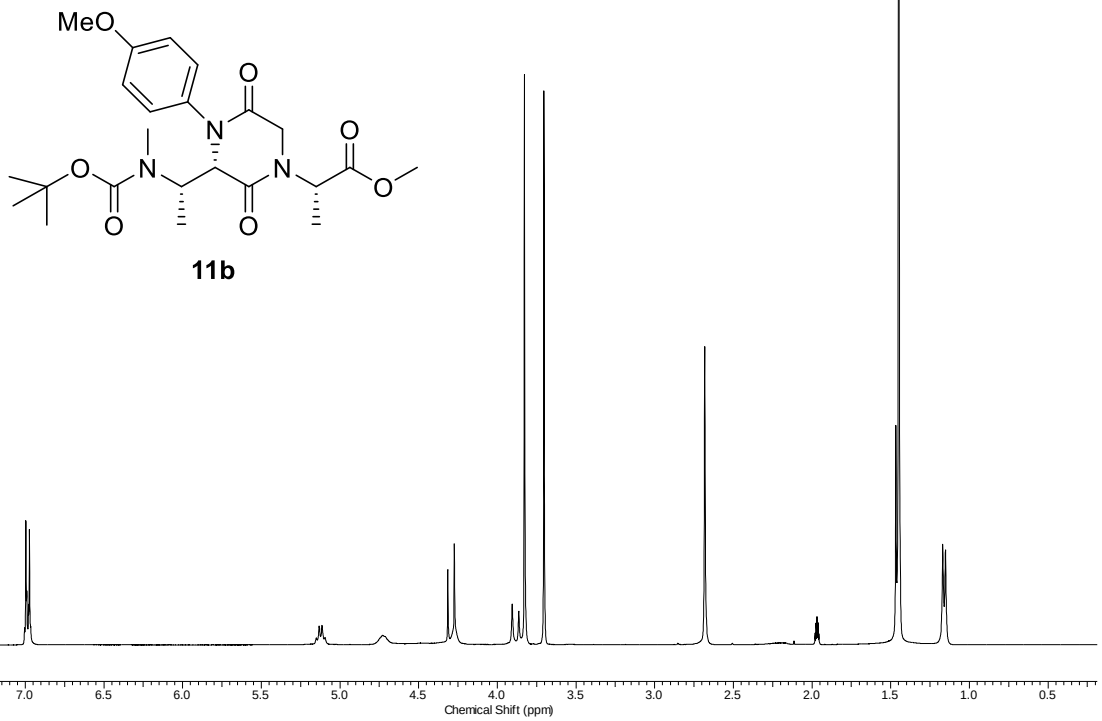

Compound **11b**: ^{13}C NMR (100 MHz, CD_3CN)

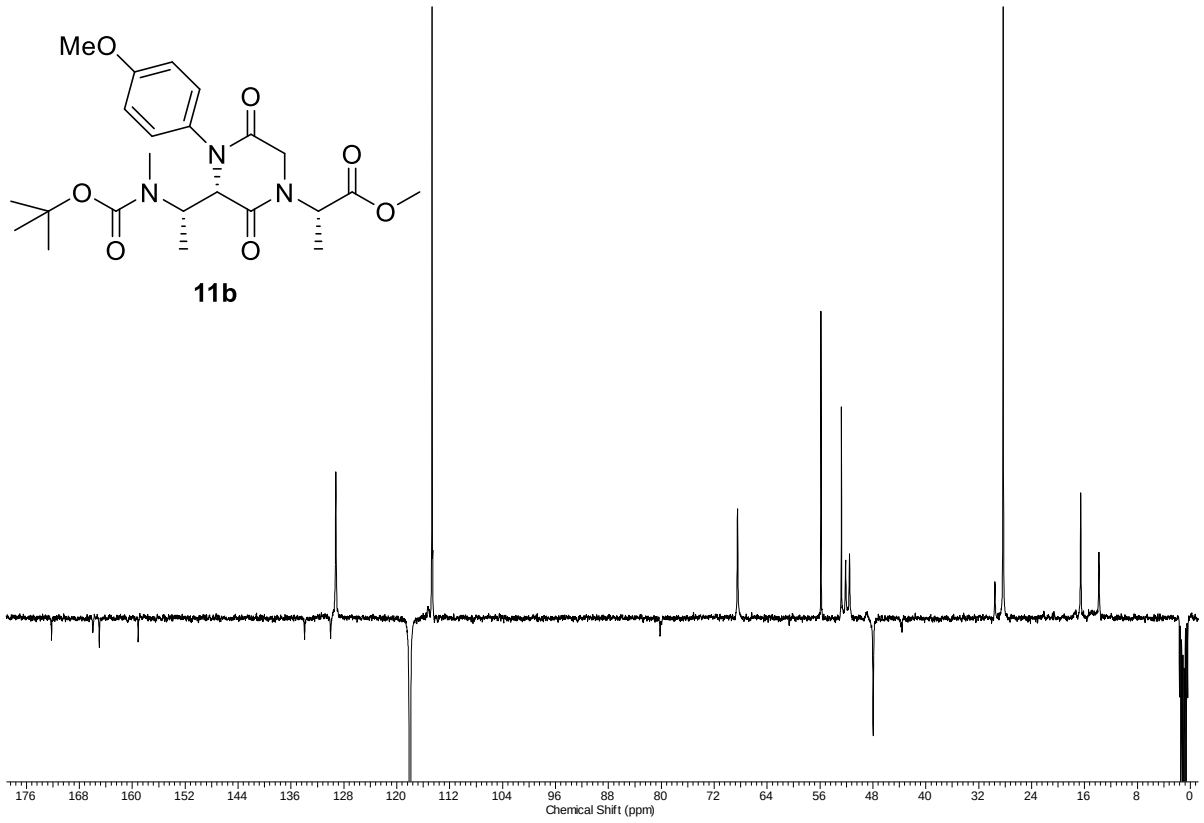

Compound **12**: ^{1}H NMR (400 MHz, $CDCl_3$)

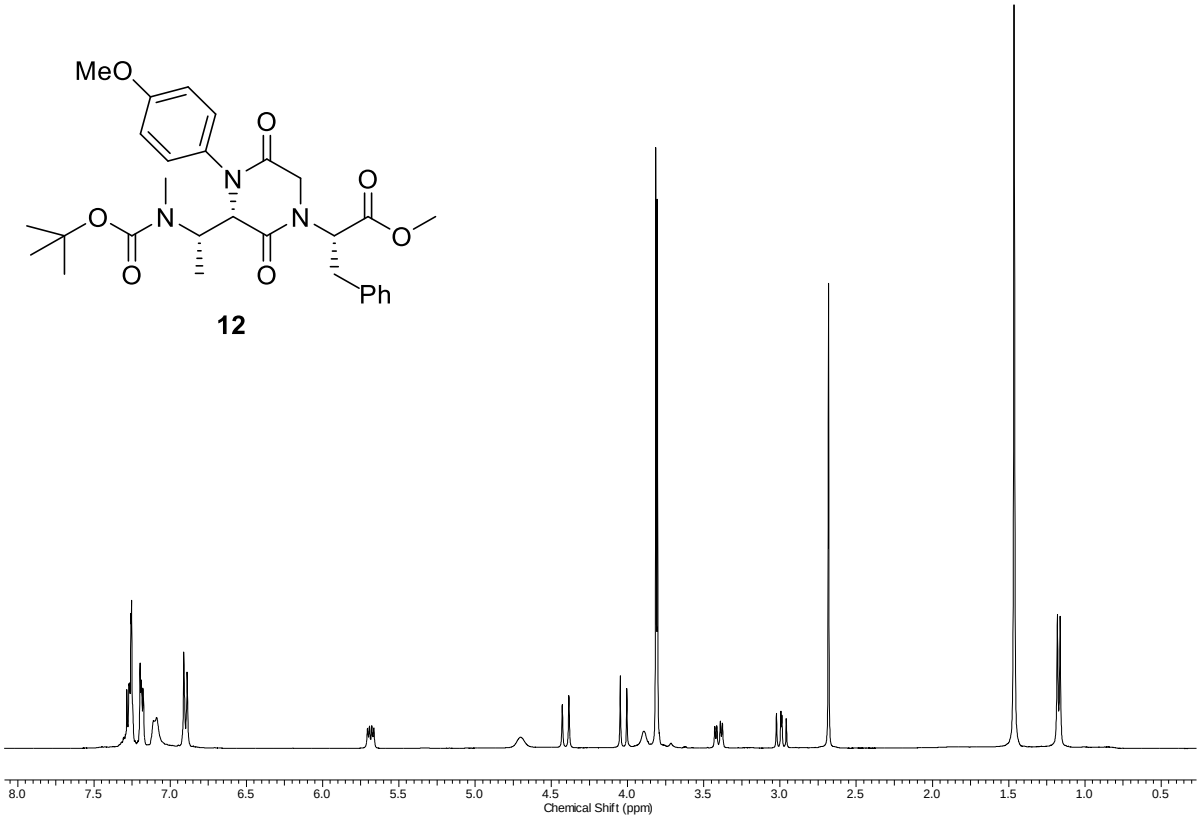

Compound **12**: ^{13}C NMR (100 MHz, $CDCl_3$)

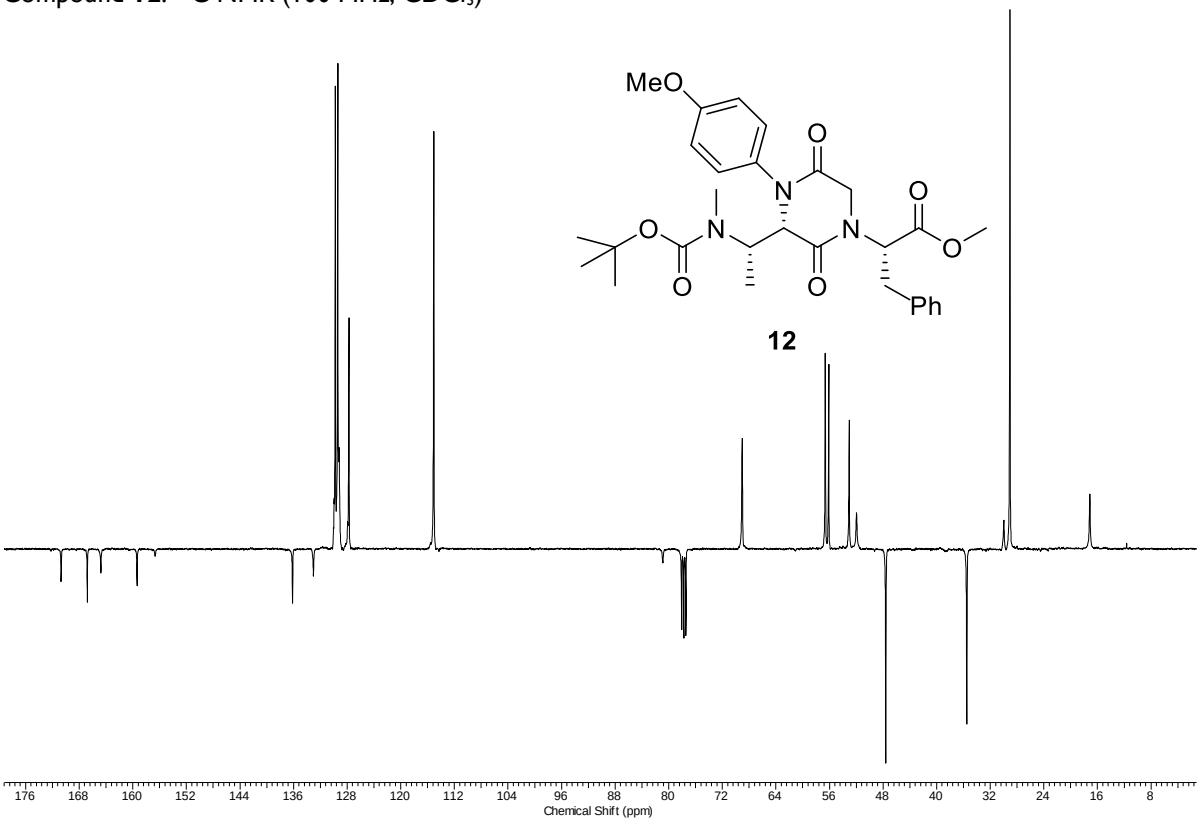

Compound **13**: ^{1}H NMR (400 MHz, $CDCl_3$)

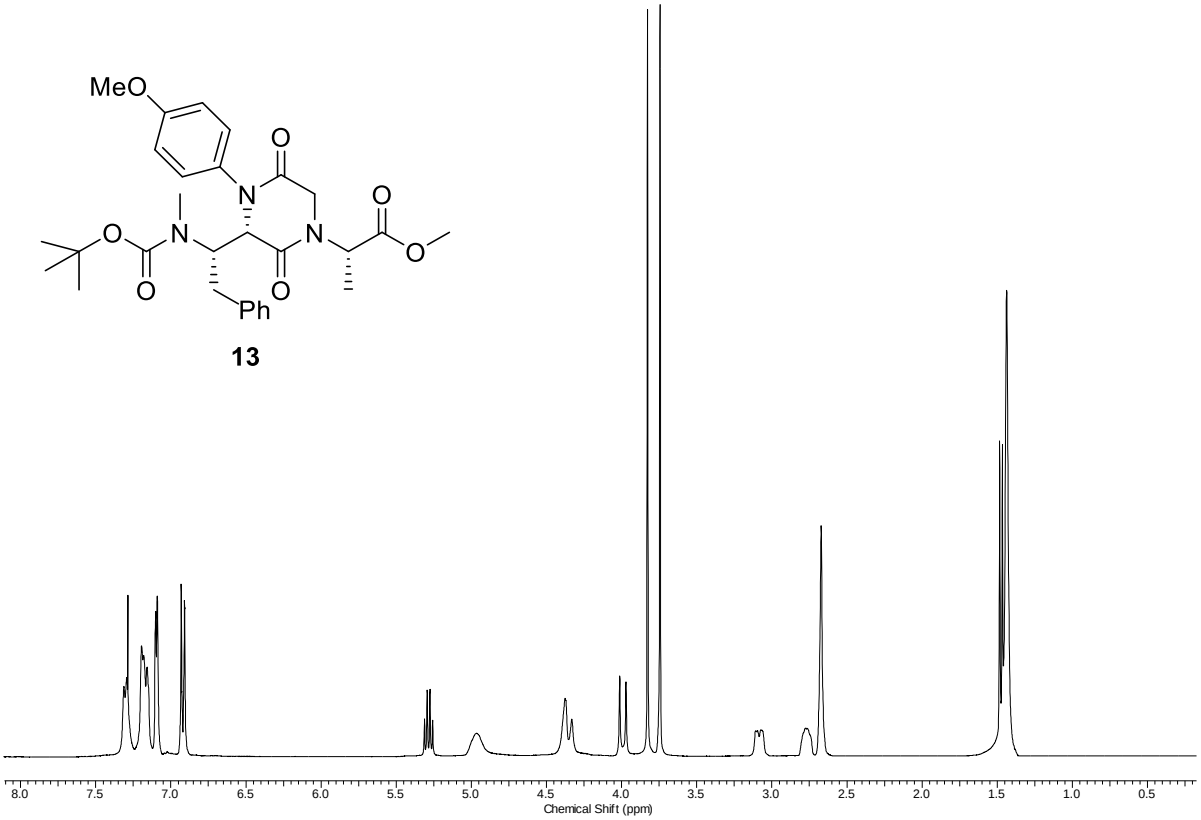

Compound **13**: ^{13}C NMR (100 MHz, $CDCl_3$)

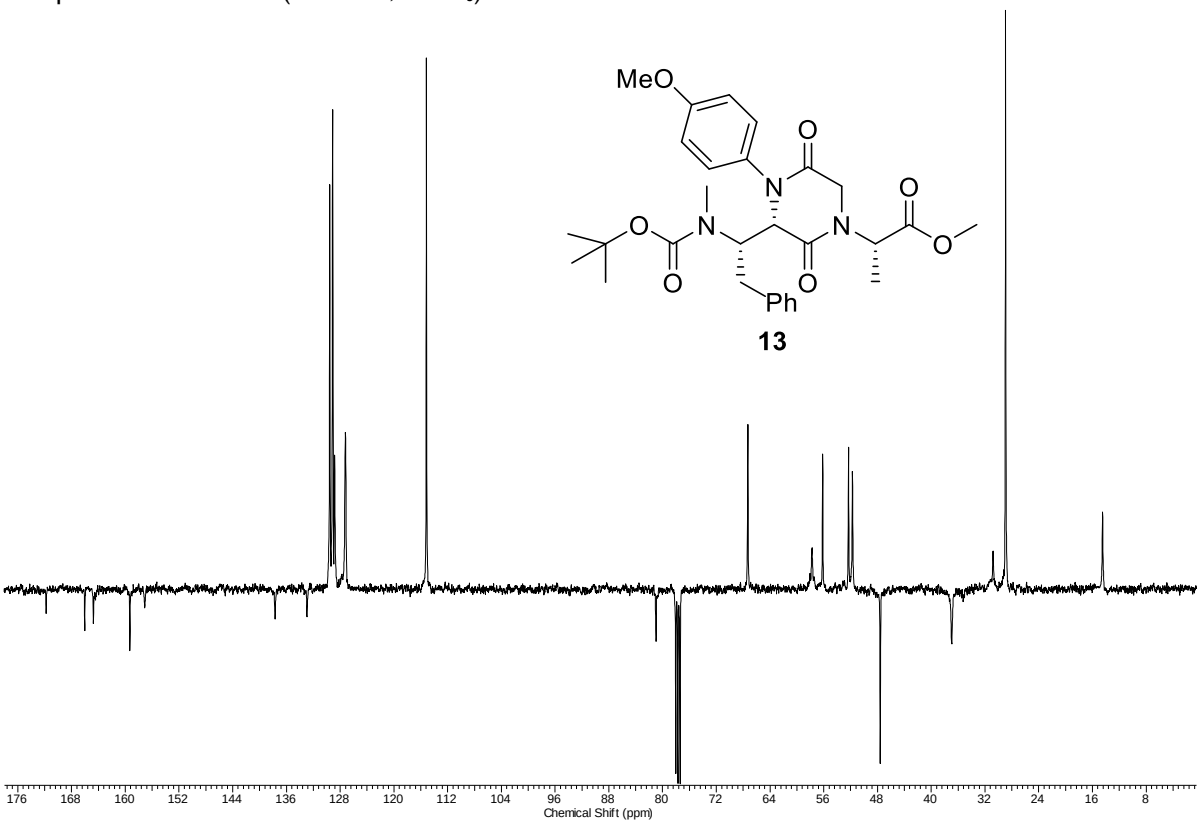

Compound **14**: ^{1}H NMR (400 MHz, $CDCl_3$)

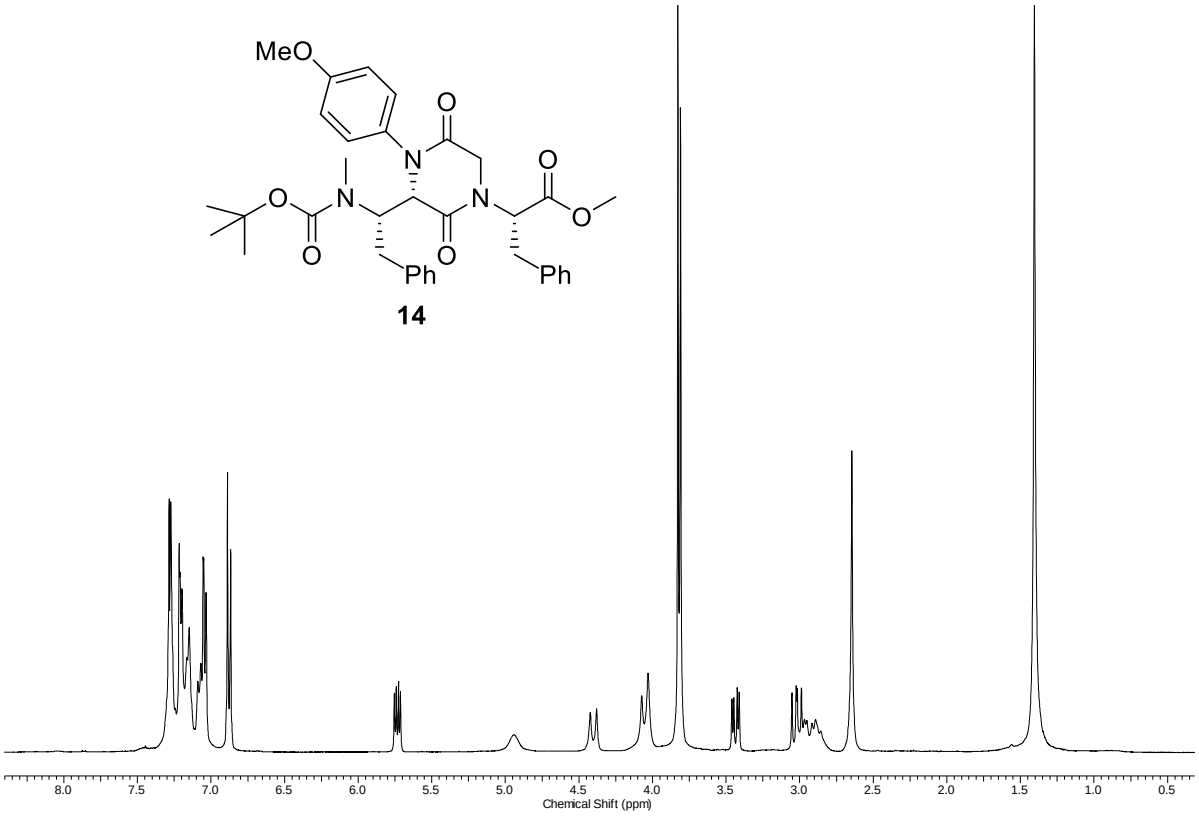

Compound **14**: ^{13}C NMR (100 MHz, $CDCl_3$)

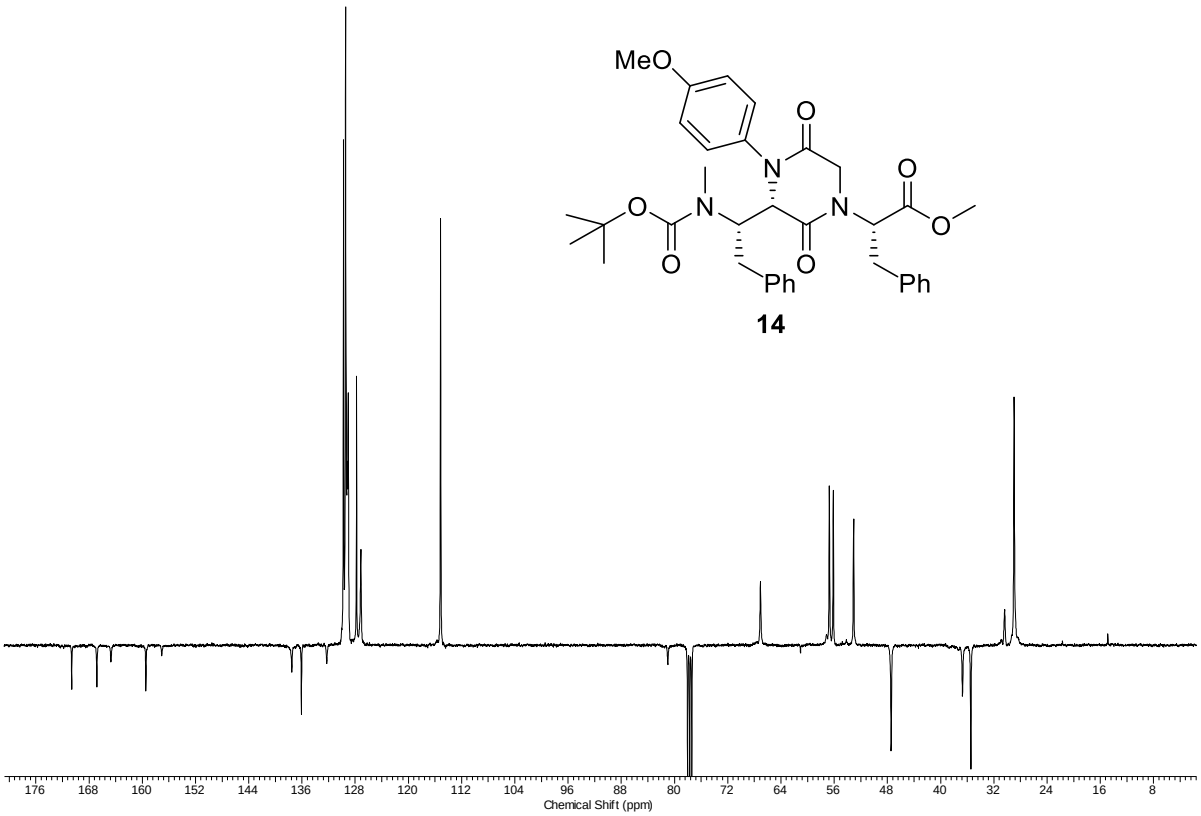

Compound **15a**: ^{1}H NMR (300 MHz, $CDCl_3$)

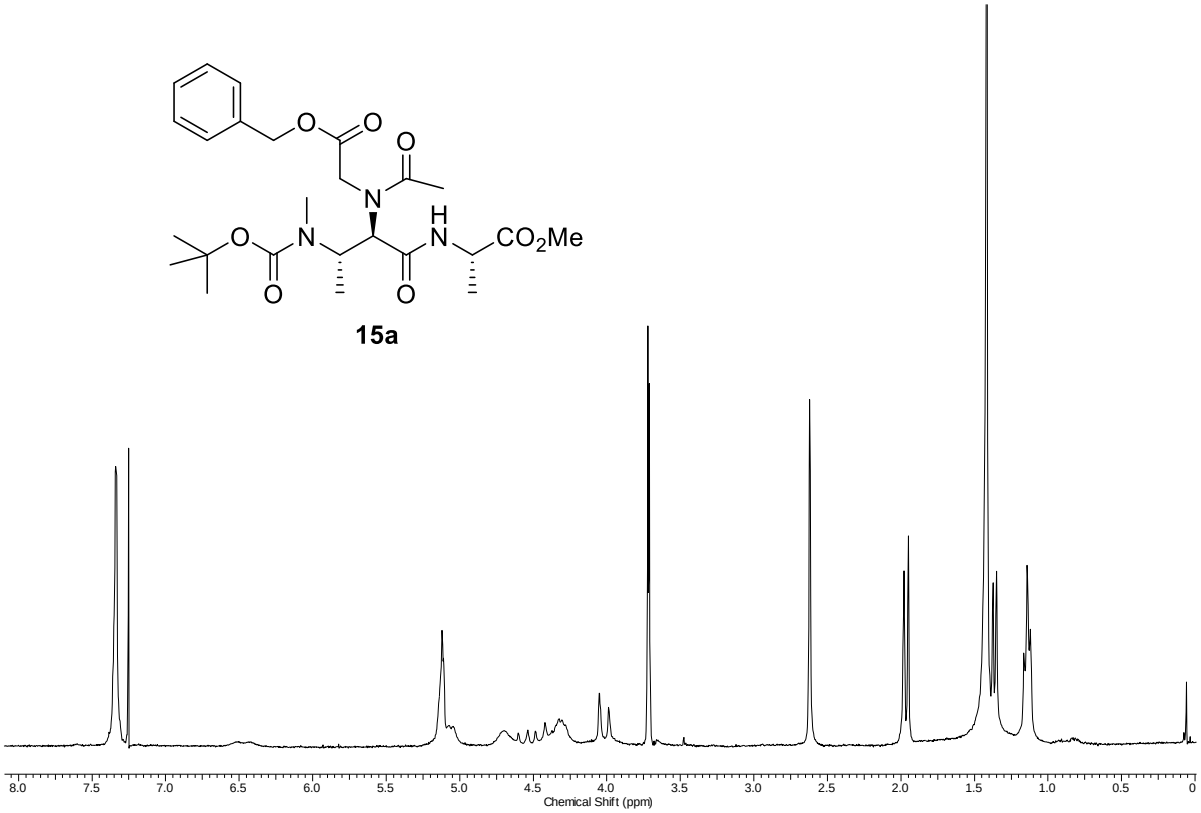

Compound **15a**: ^{13}C NMR (75 MHz, $CDCl_3$)

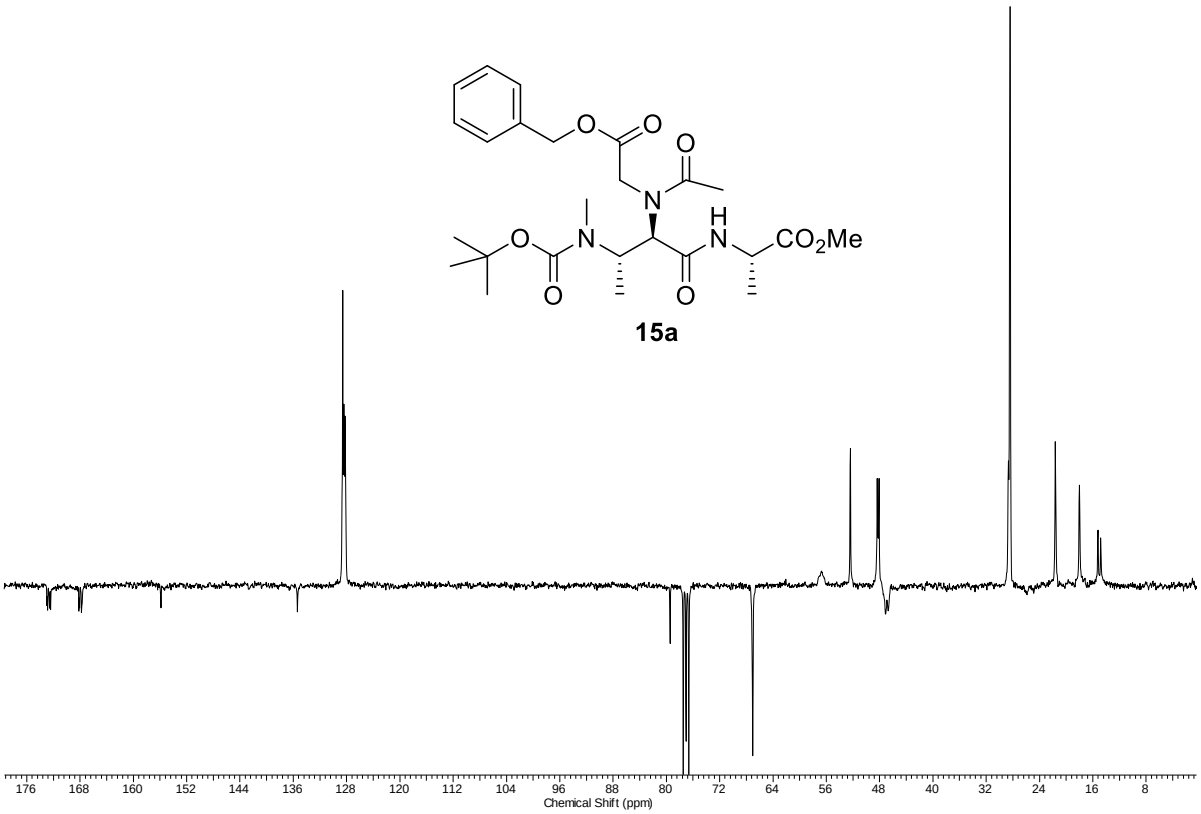

Compound **15b**: ^{1}H NMR (300 MHz, $CDCl_3$)

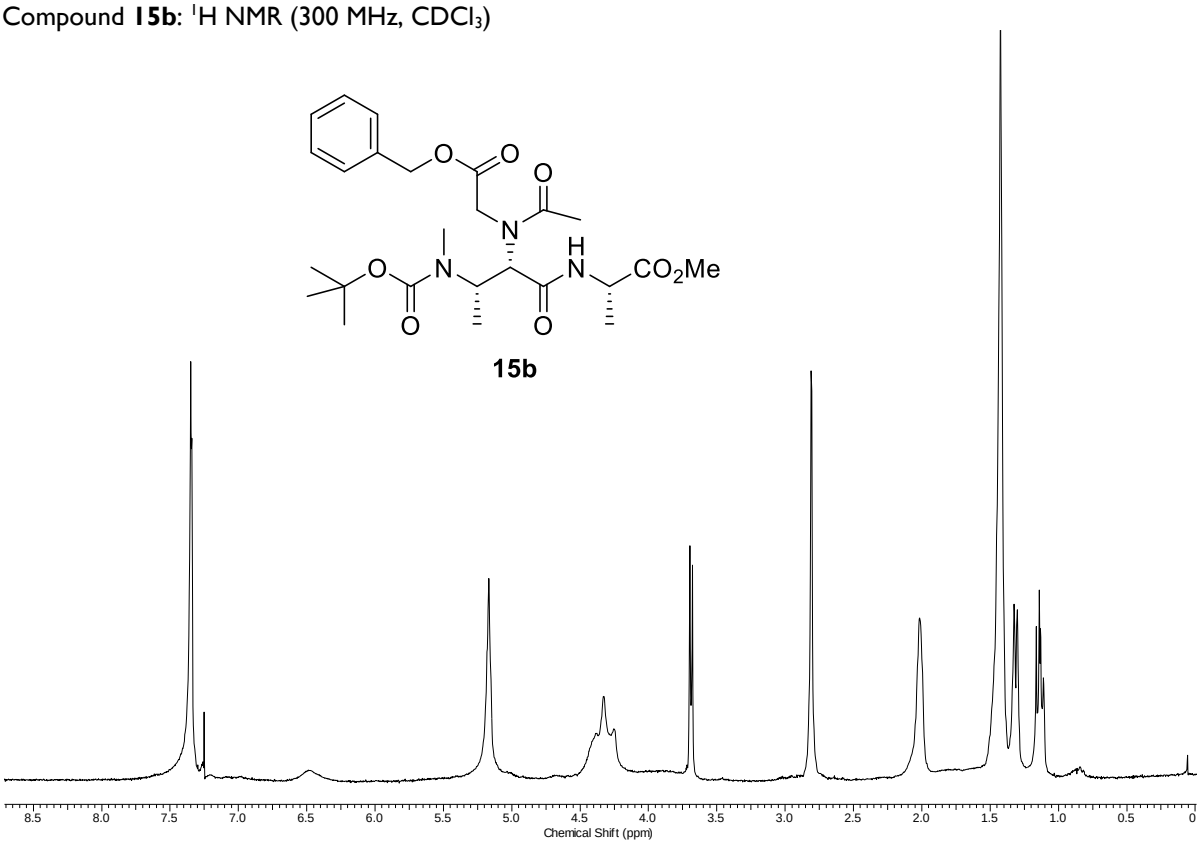

Compound **15b**: ^{13}C NMR (75 MHz, $CDCl_3$)

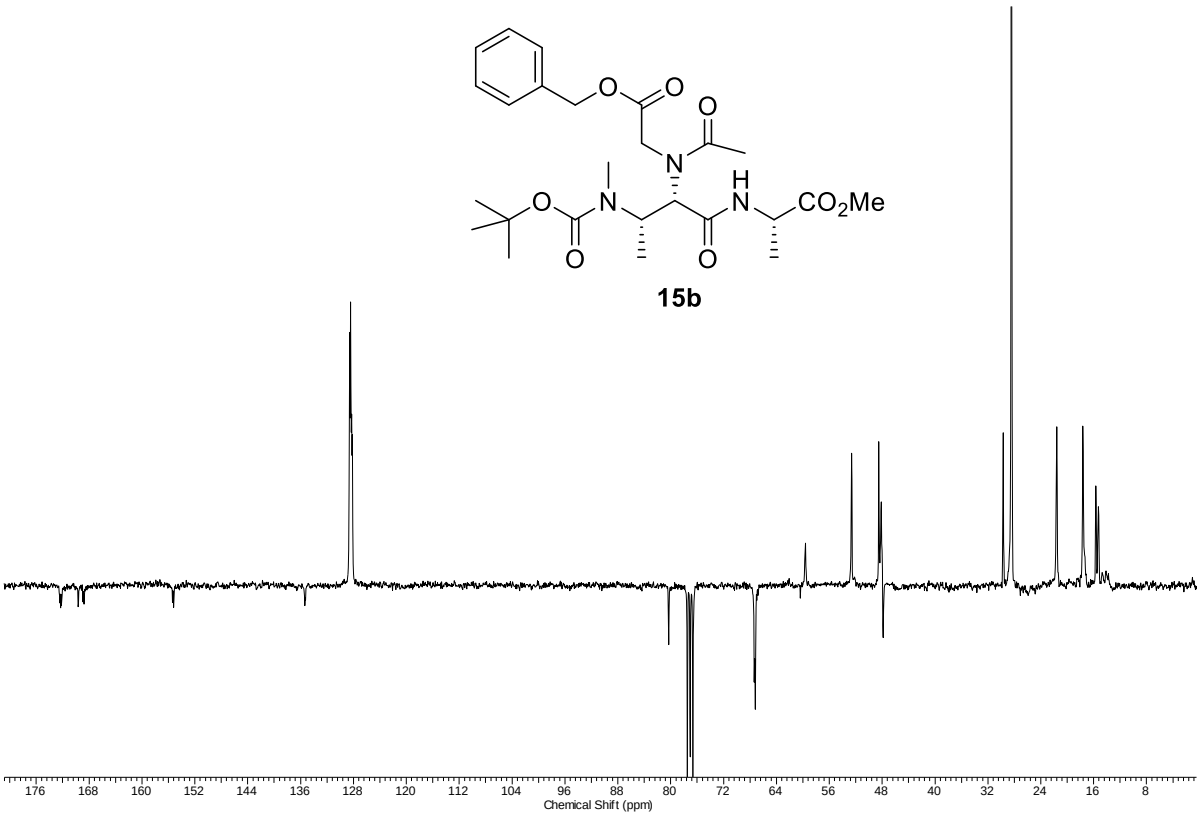

Compound **16**: ^{1}H NMR (300 MHz, $CDCl_3$)

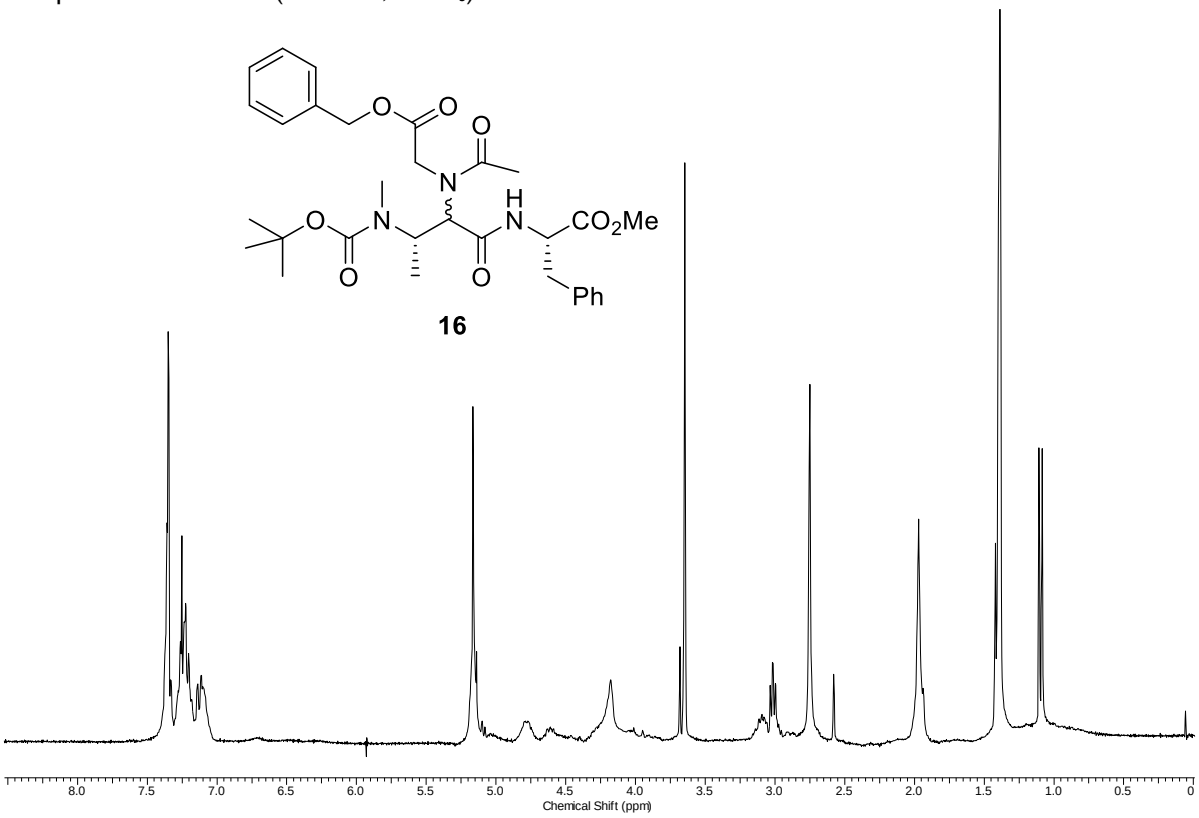

Compound **17**: ^{1}H NMR (300 MHz, $CDCl_3$)

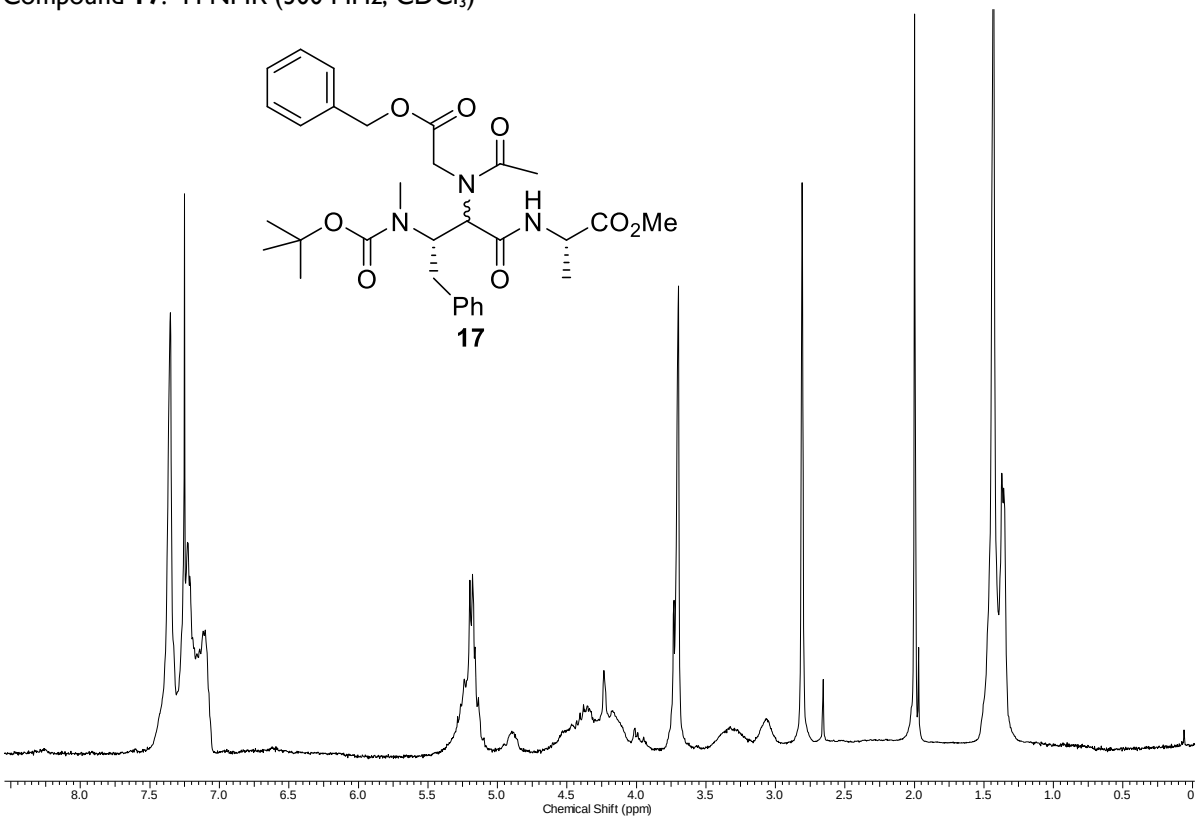

Compound **18**: ^{1}H NMR (300 MHz, $CDCl_3$)

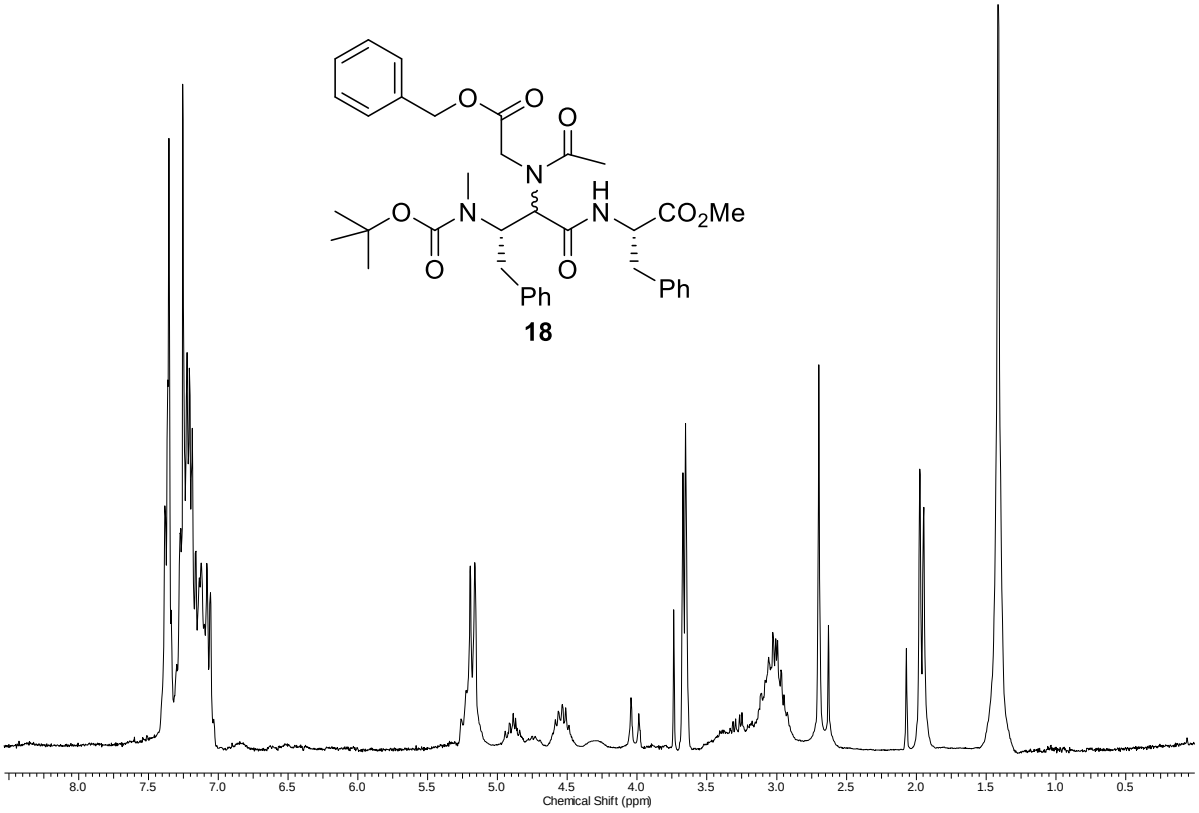

Compound **19a**: ^{1}H NMR (300 MHz, $CDCl_3$)

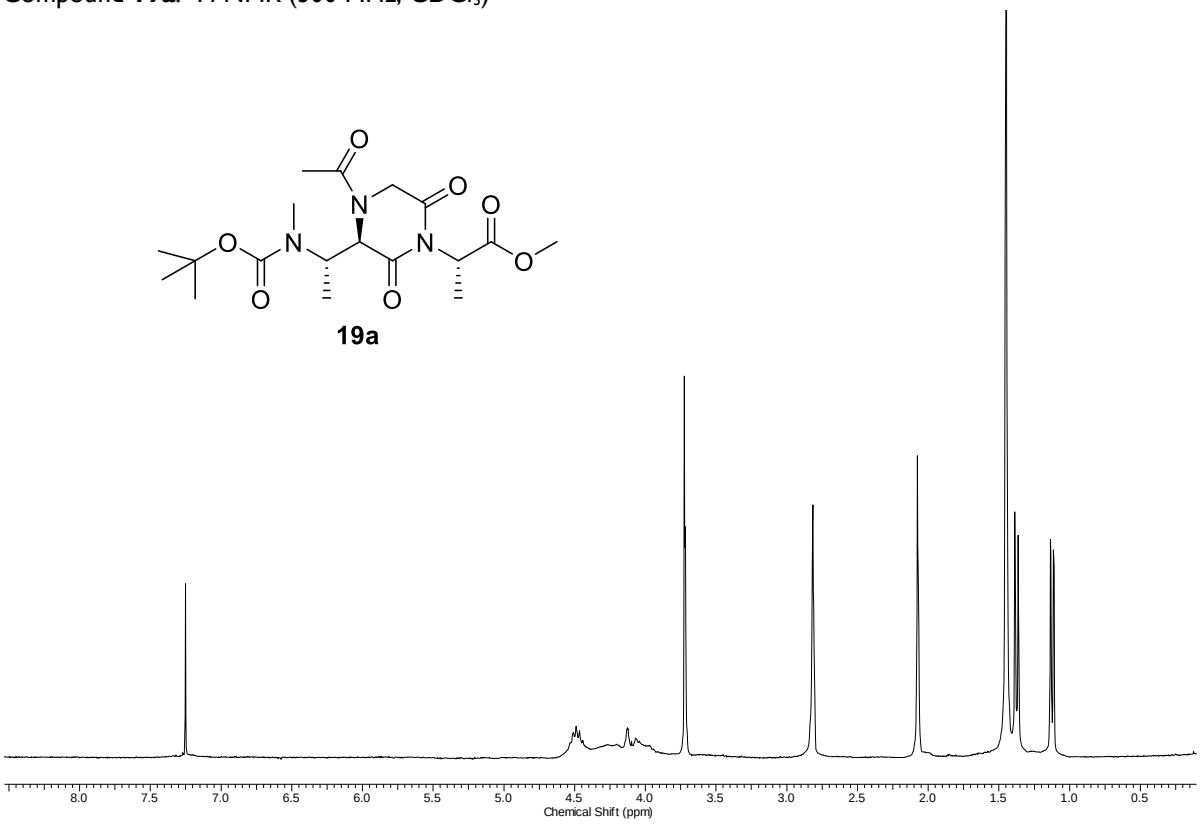

Compound **19a**: ^{13}C NMR (100 MHz, $CDCl_3$)

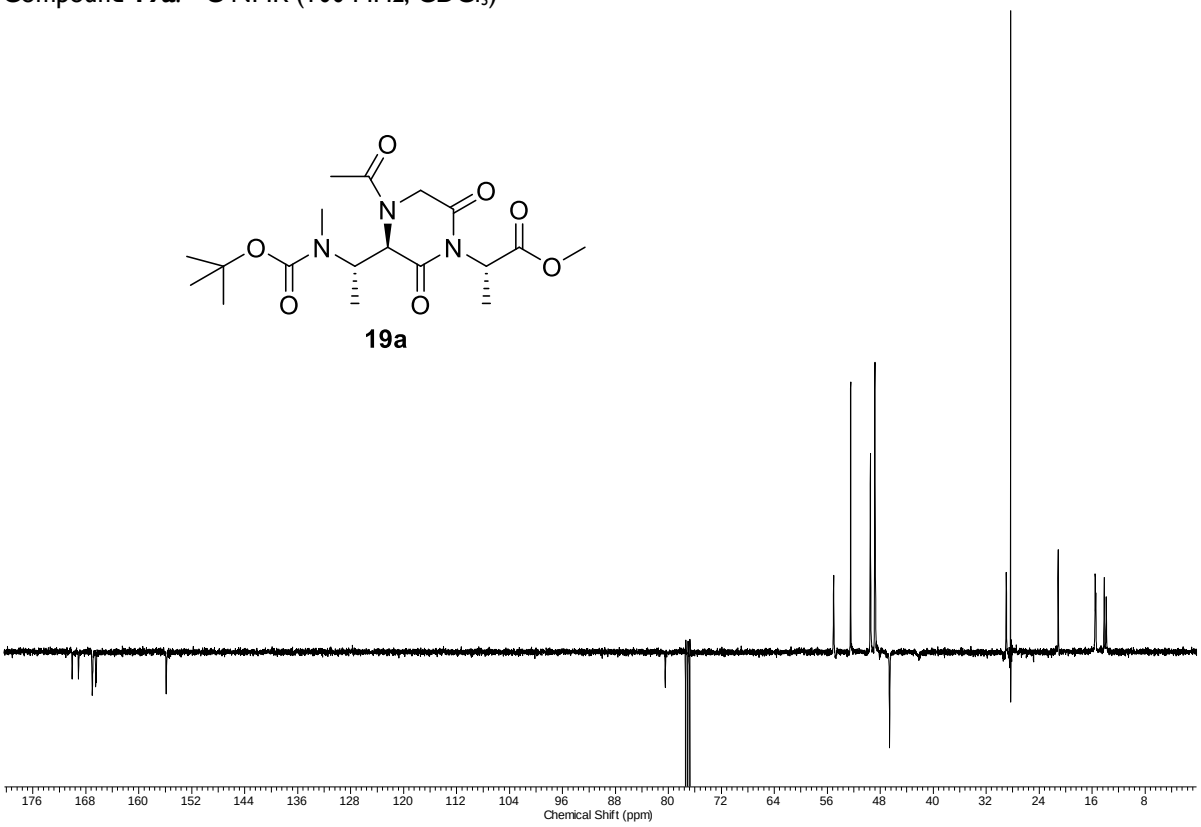

Compound **19b**: ^{1}H NMR (400 MHz, $CDCl_3$)

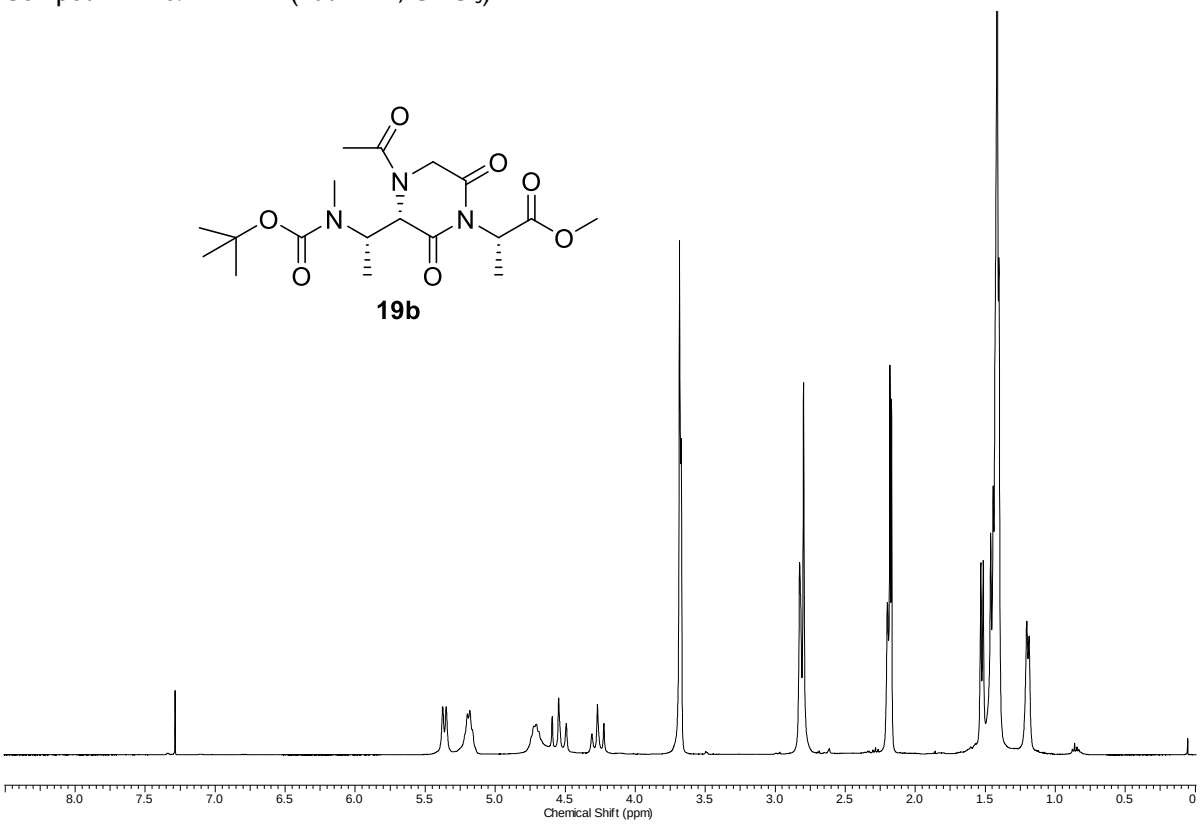

Compound **19b**: ^{13}C NMR (100 MHz, $CDCl_3$)

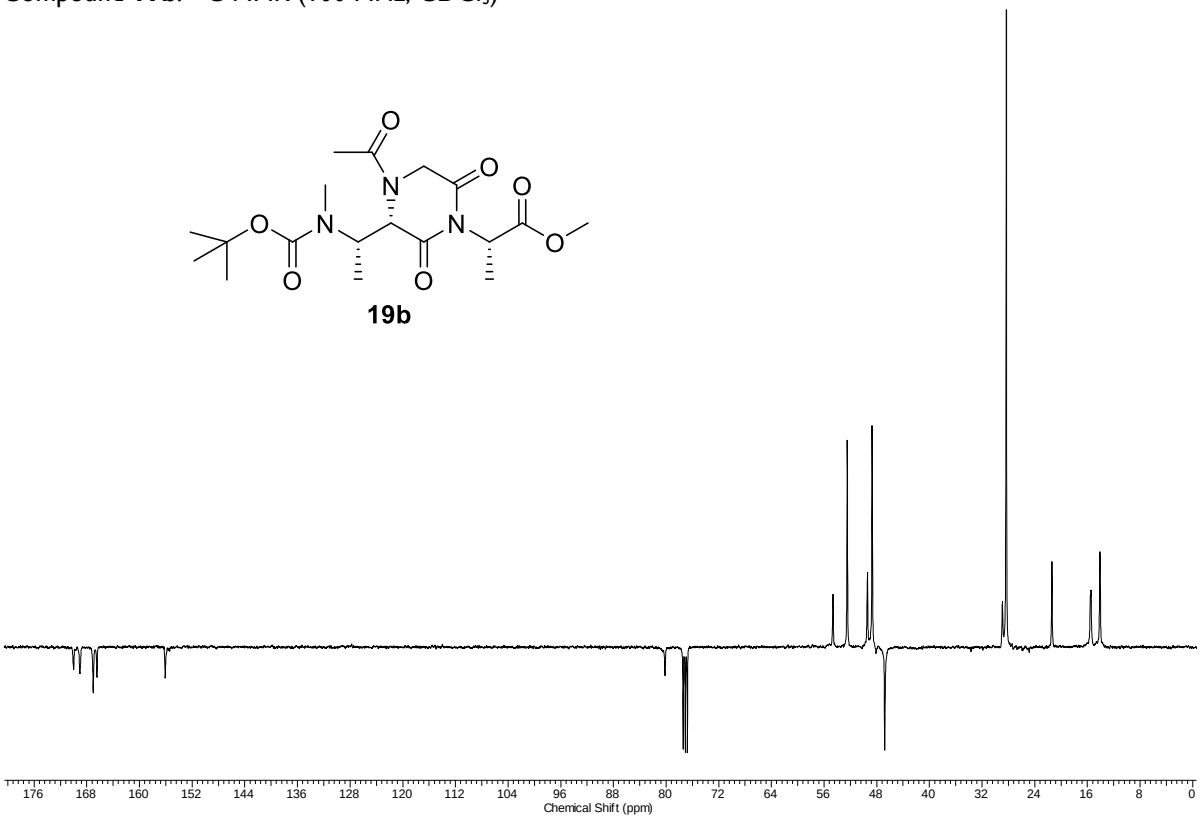

Compound **20**: ^{1}H NMR (400 MHz, CD_3CN)

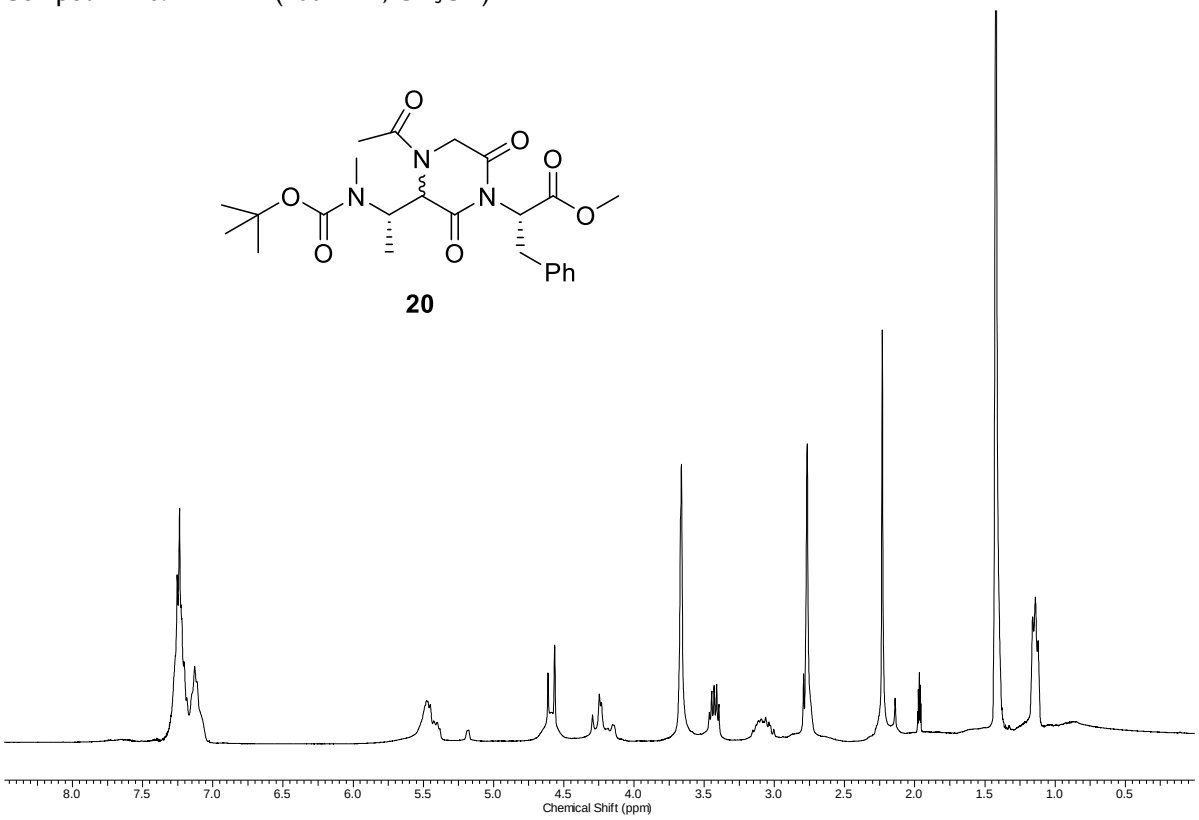

Compound **20**: ^{13}C NMR (100 MHz, CD_3CN)

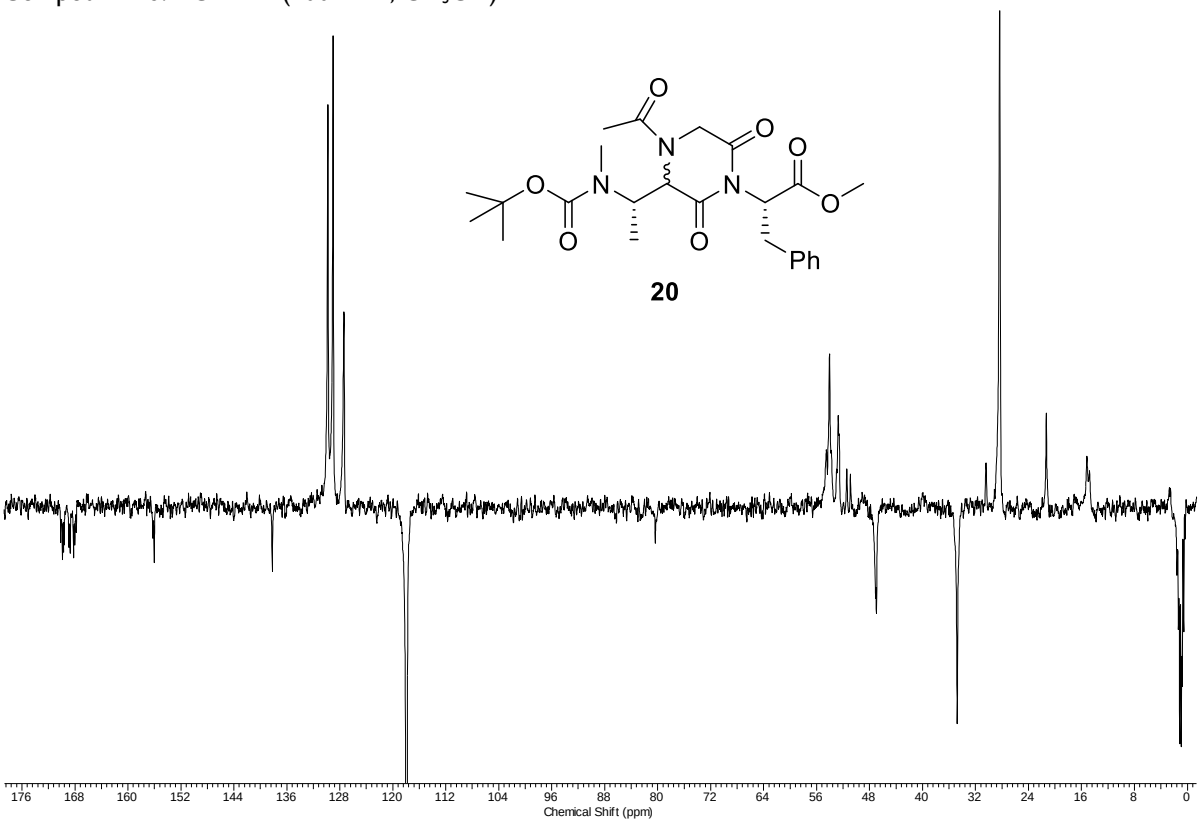

Compound **21**: ^{1}H NMR (400 MHz, CD_3CN)

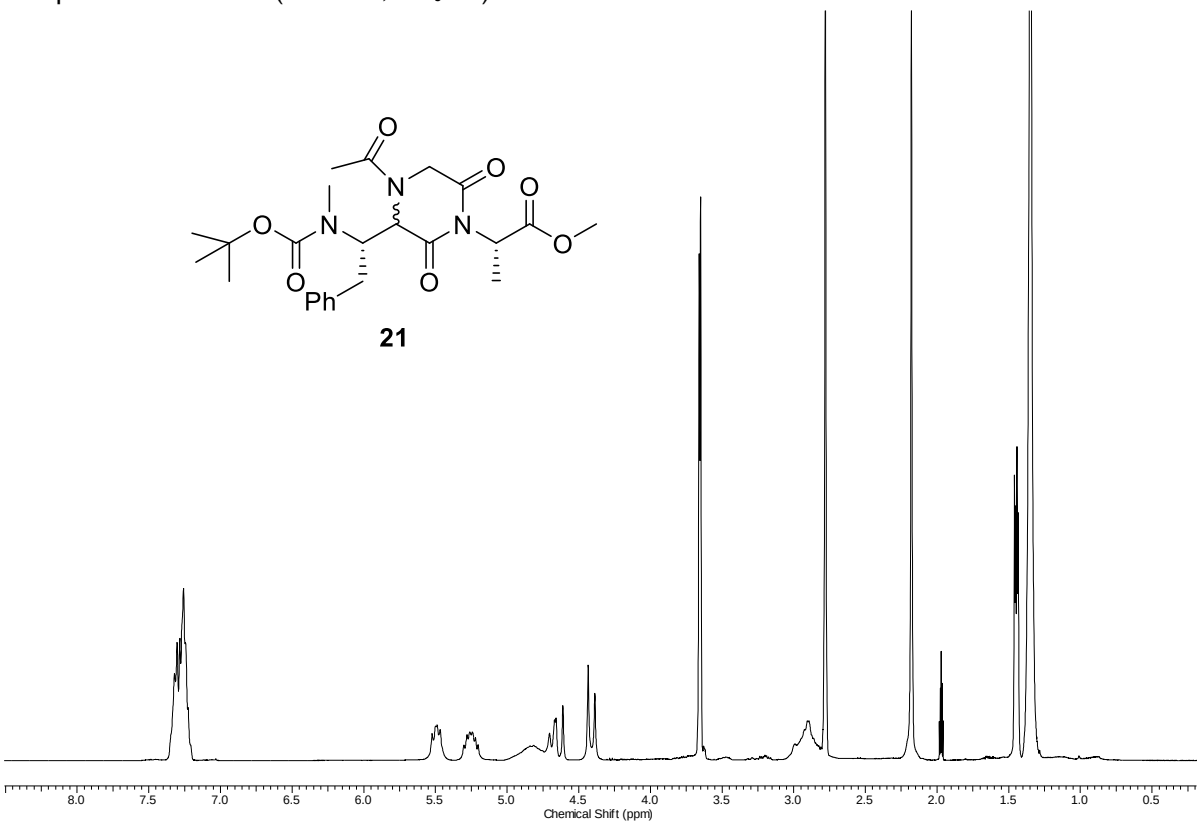

Compound **21**: ^{13}C NMR (100 MHz, CD_3CN)

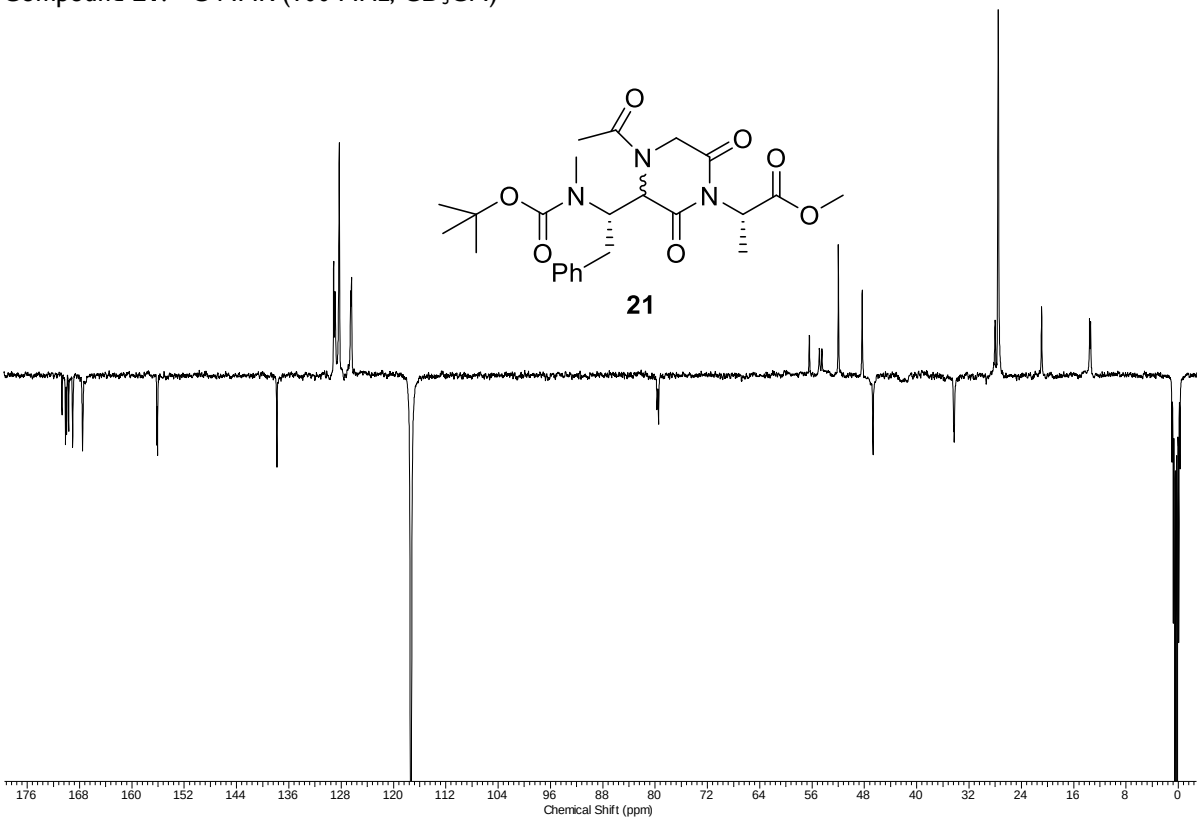

Compound **22**: ^{1}H NMR (400 MHz, CD_3CN)

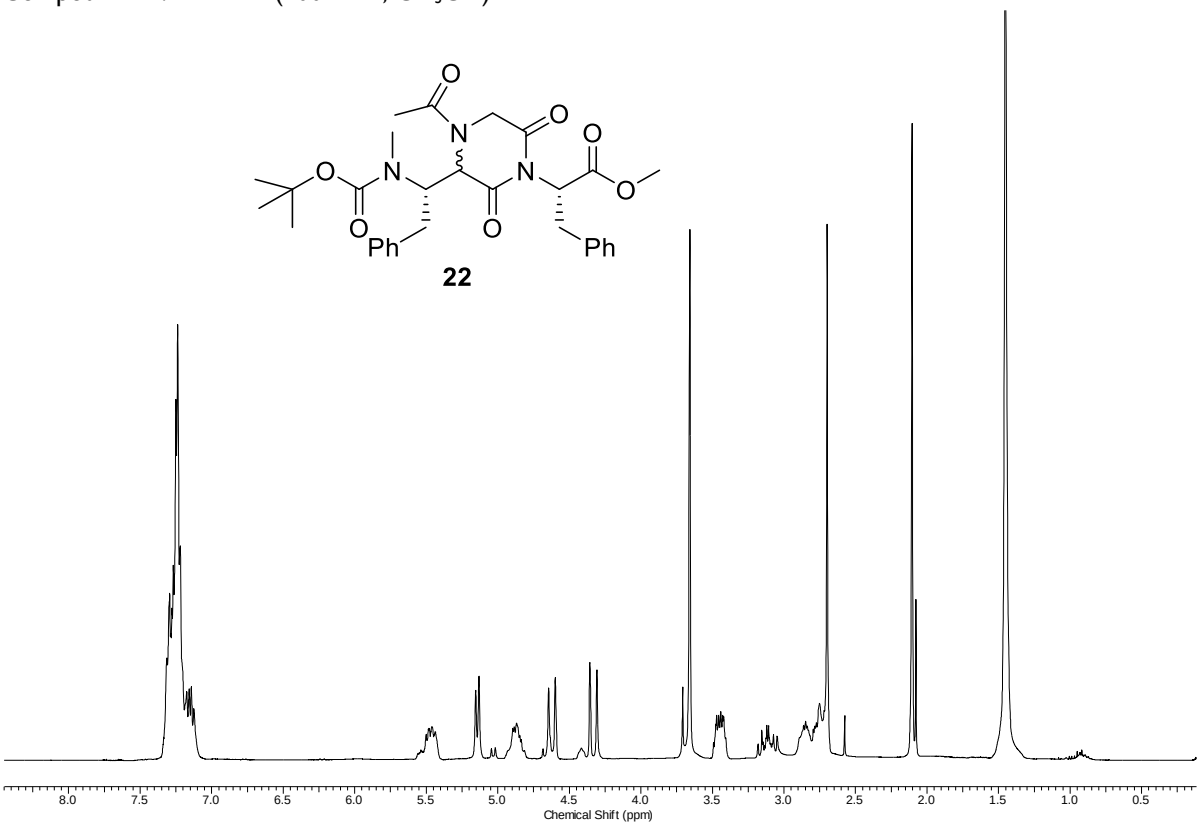

Compound **22**: ^{13}C NMR (100 MHz, CD_3CN)

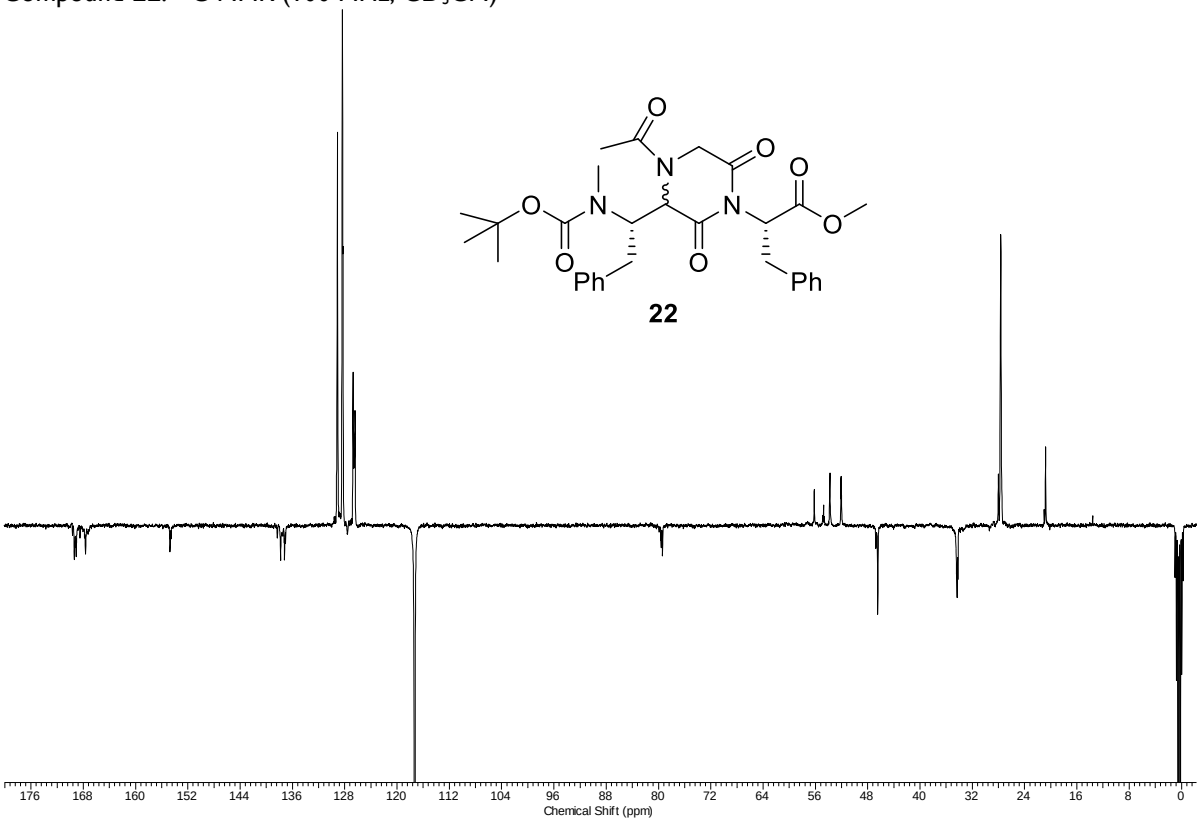

Compound **23a**: ^{1}H NMR (300 MHz, $CDCl_3$)

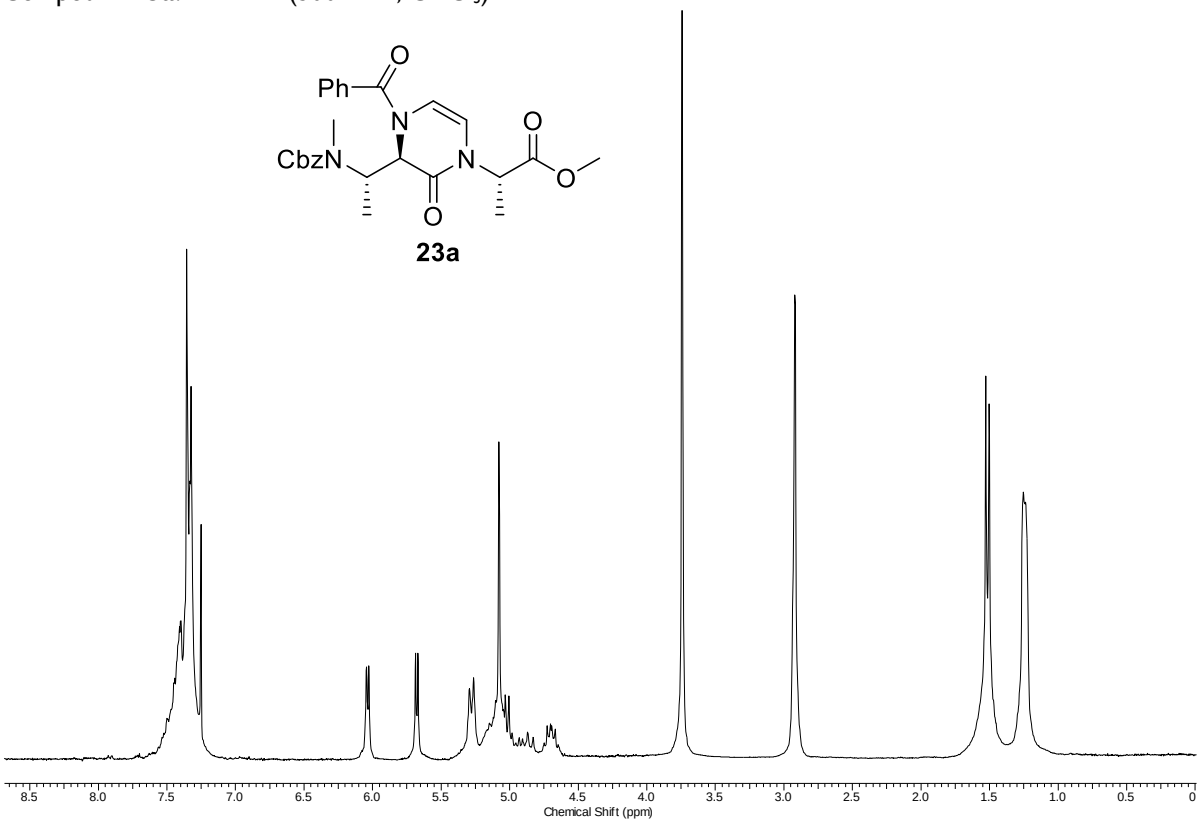

Compound **23a**: ^{13}C NMR (75 MHz, $CDCl_3$)

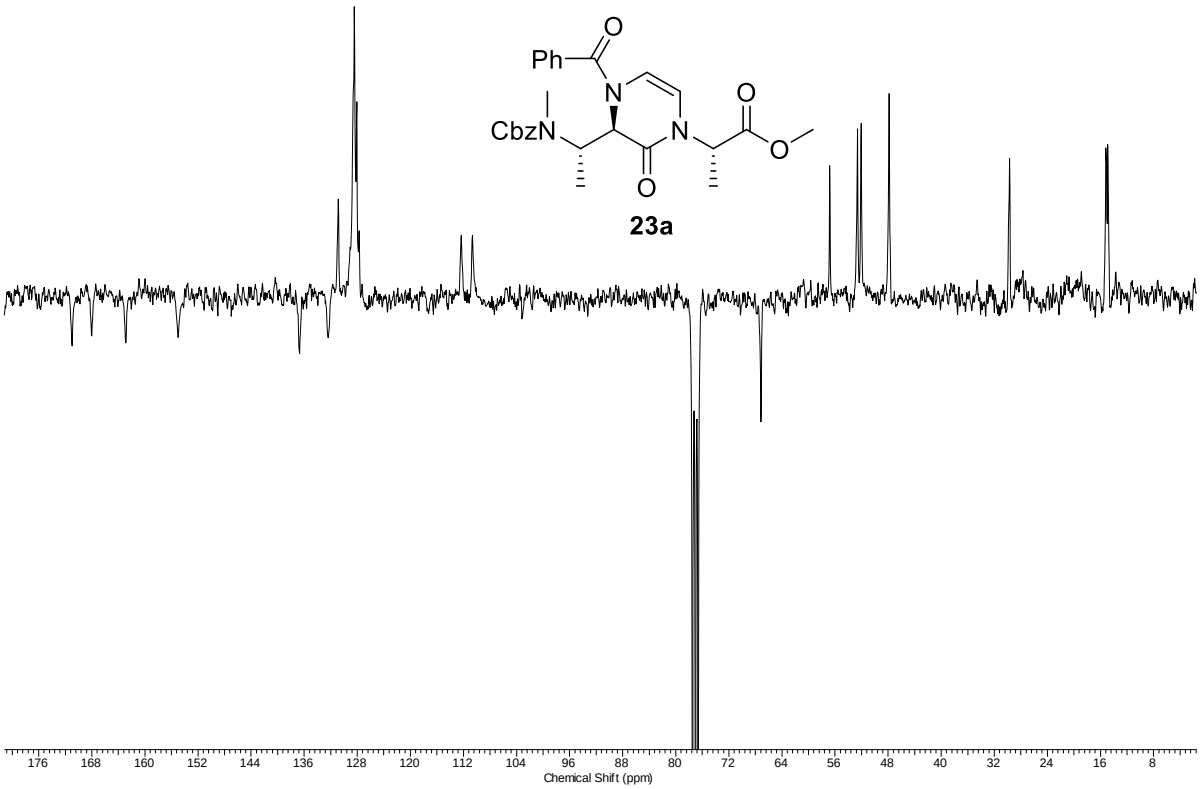

Compound **23b**: ^{1}H NMR (400 MHz, $CDCl_3$)

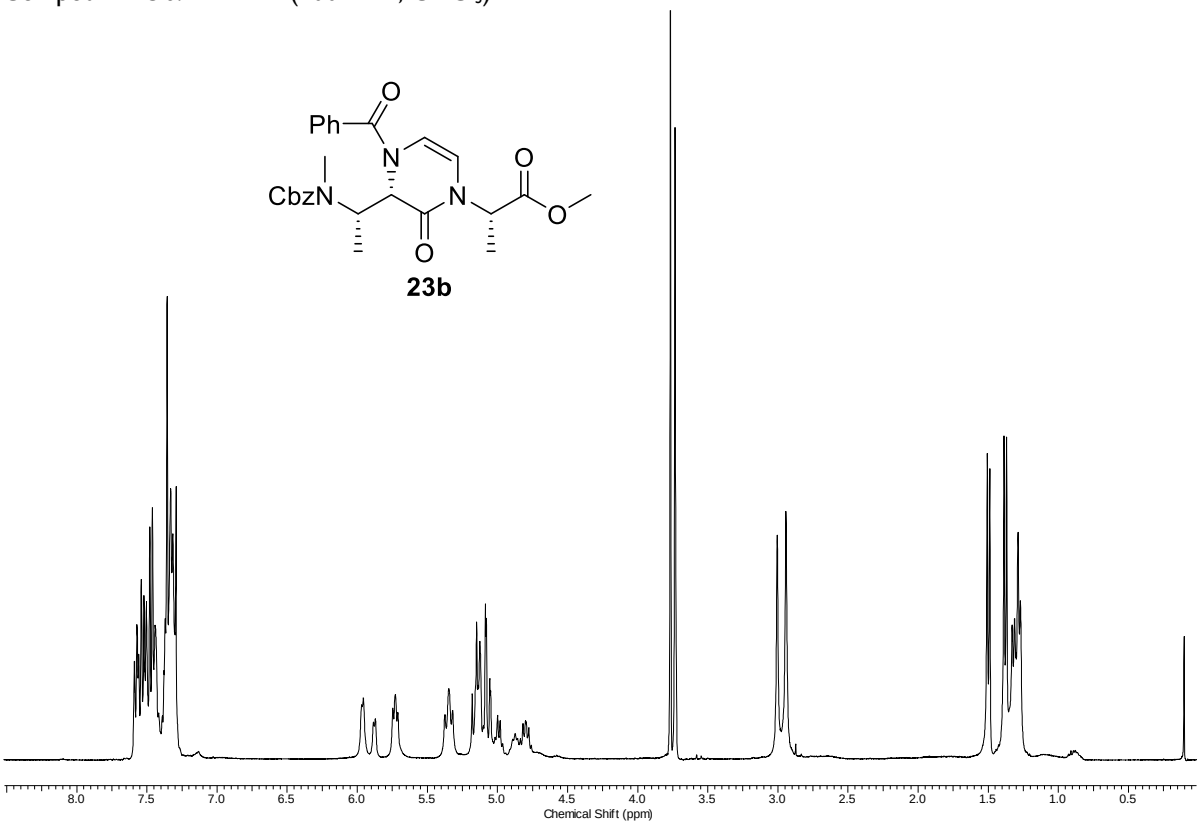

23b

Compound **23b**: ^{13}C NMR (100 MHz, $CDCl_3$)

23b

Compound **24a**: ^{1}H NMR (300 MHz, $CDCl_3$)

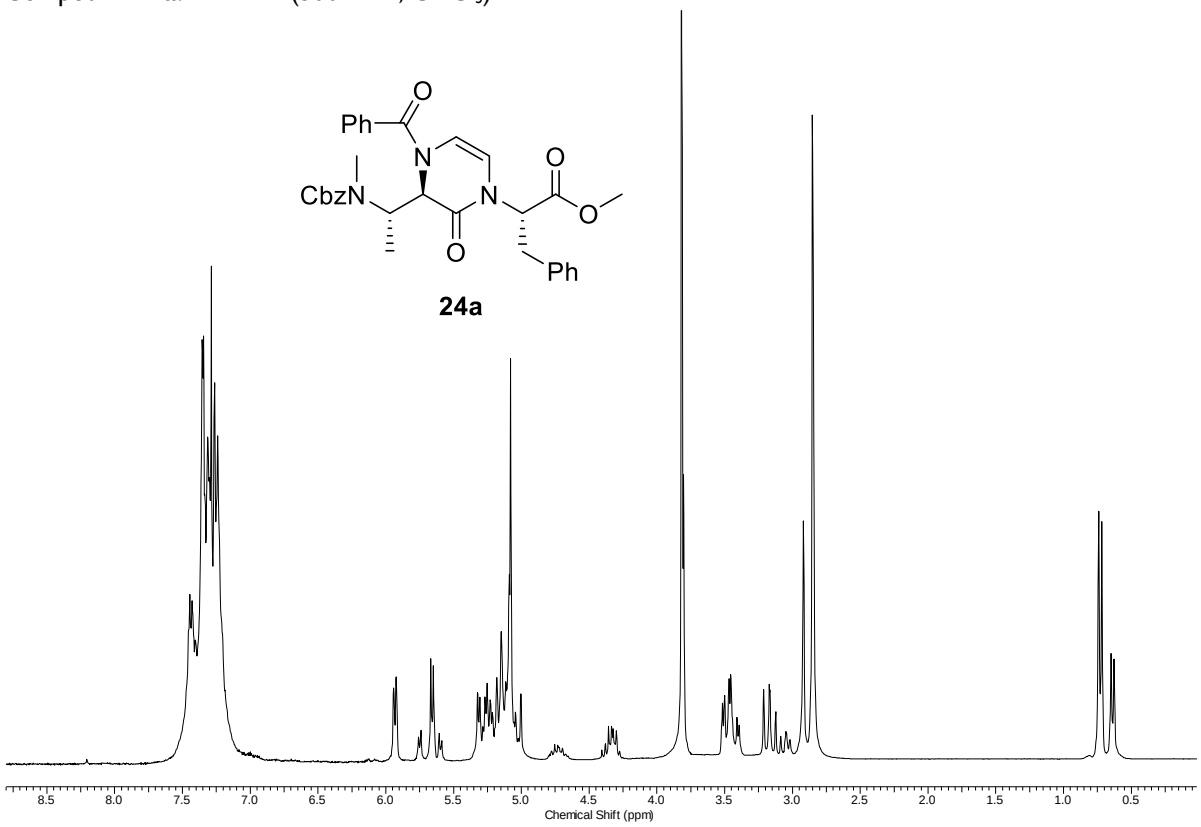

Compound **24a**: ^{13}C NMR (75 MHz, $CDCl_3$)

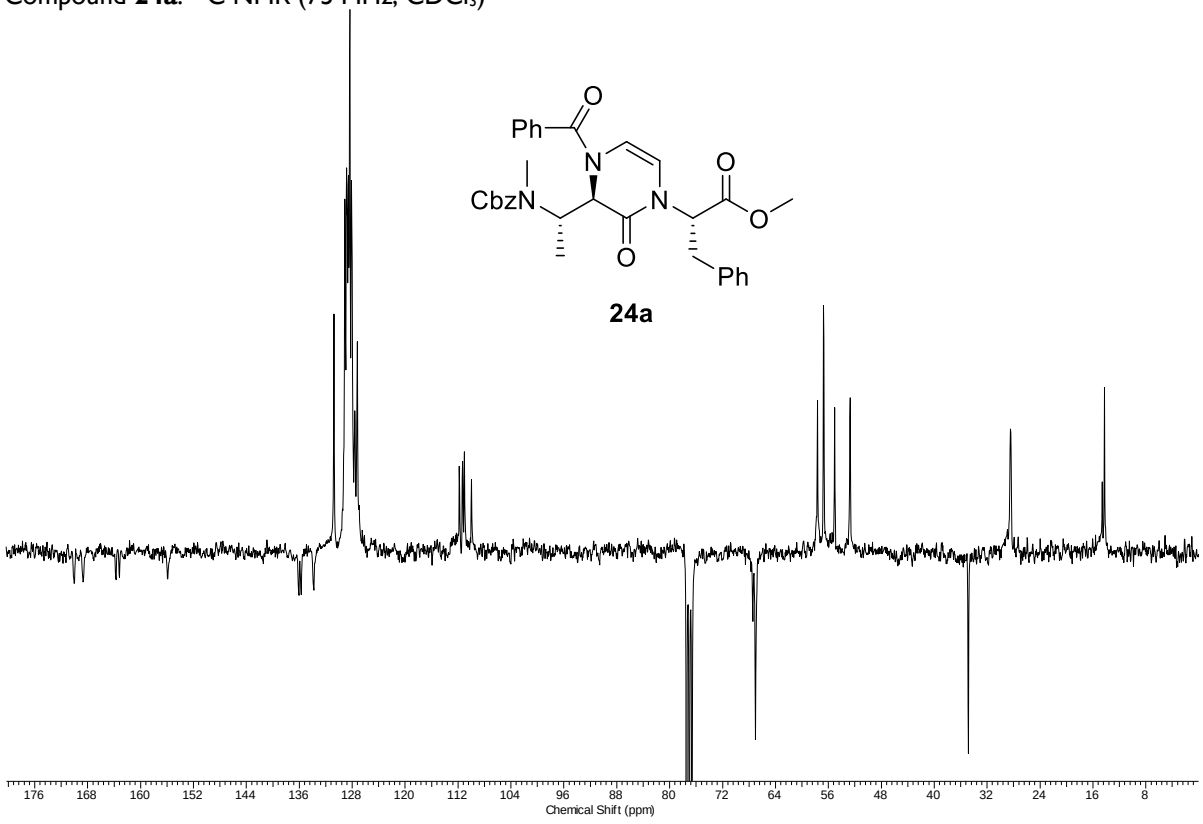

Compound **24b**: ^{1}H NMR (400 MHz, $CDCl_3$)

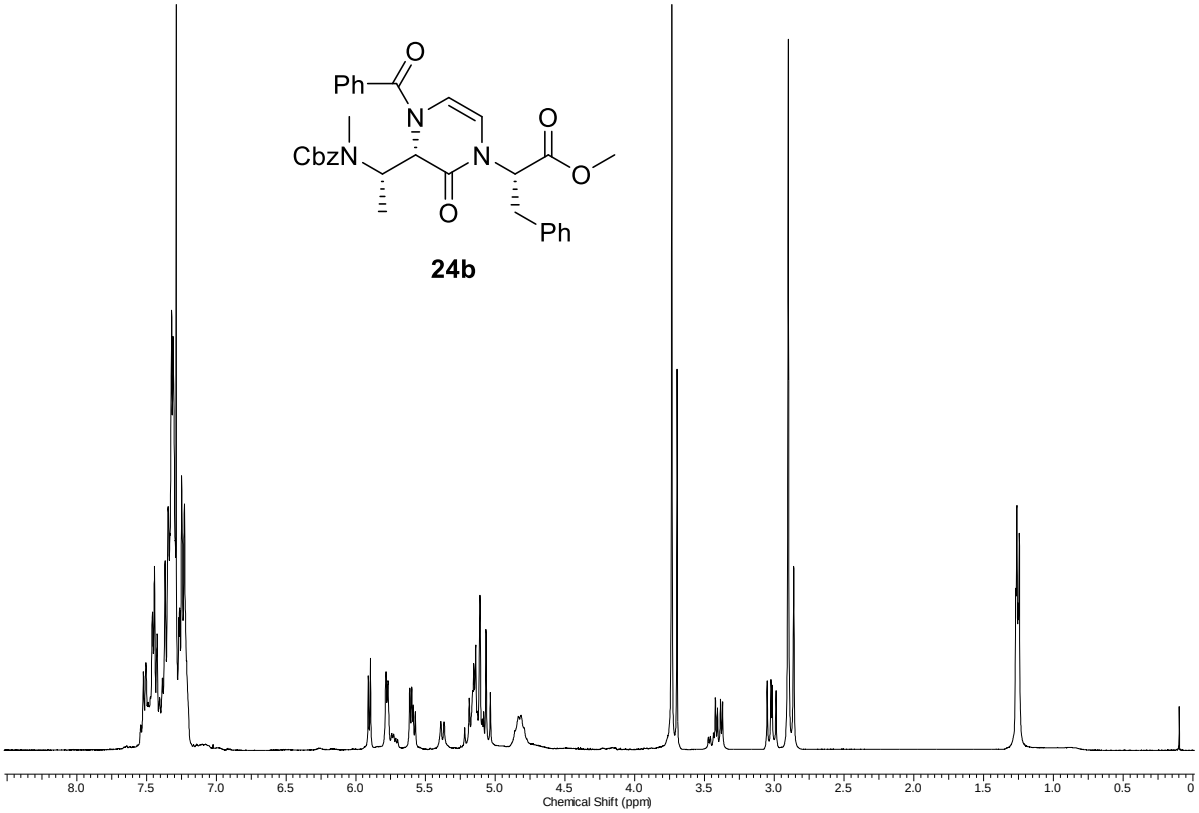

Compound **24b**: ^{13}C NMR (100 MHz, $CDCl_3$)

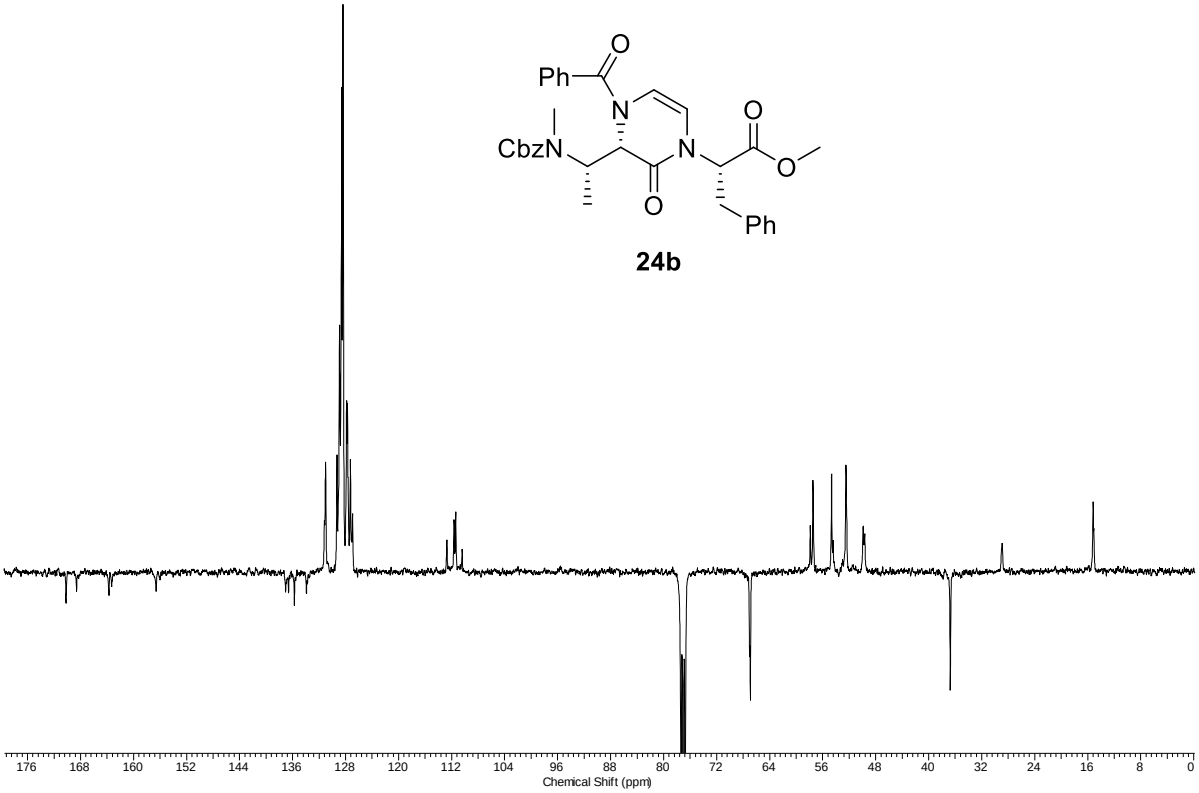

Compound **25a**: ^{1}H NMR (300 MHz, $CDCl_3$)

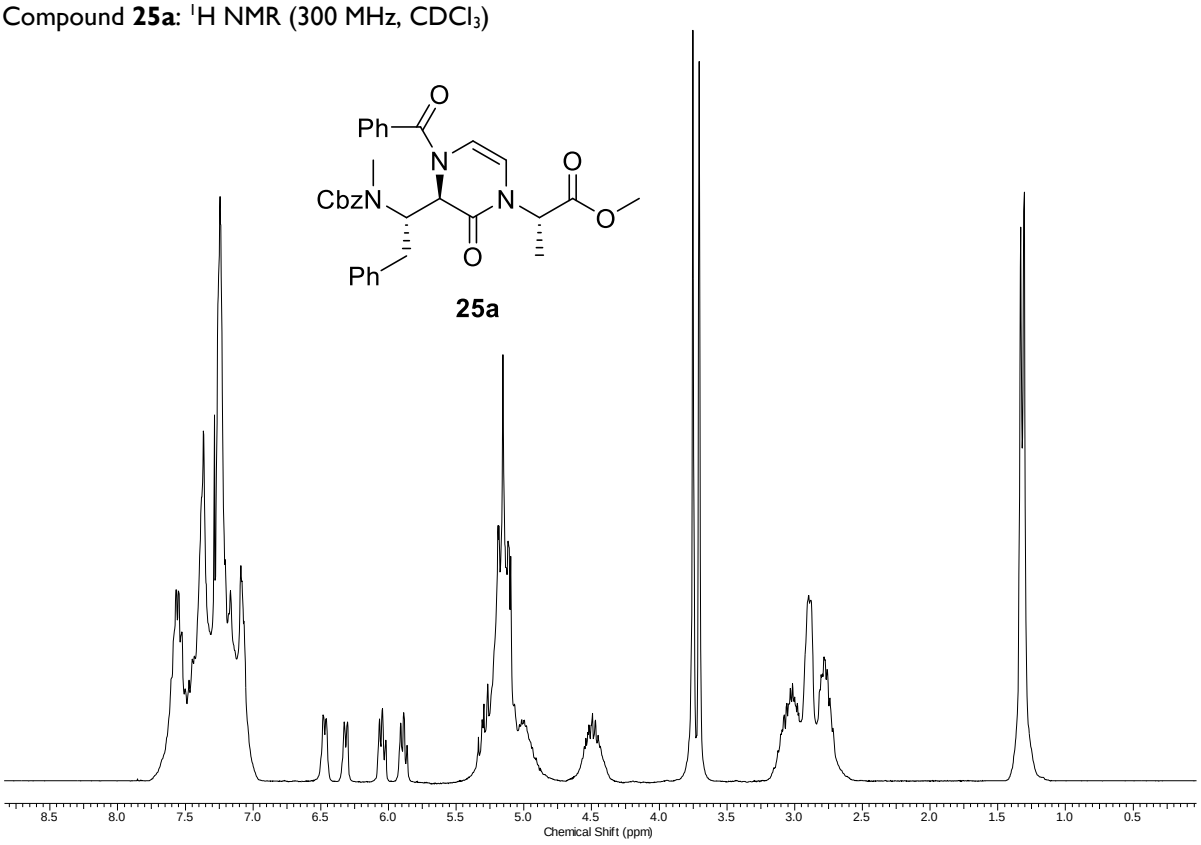

Compound **25a**: ^{13}C NMR (75 MHz, $CDCl_3$)

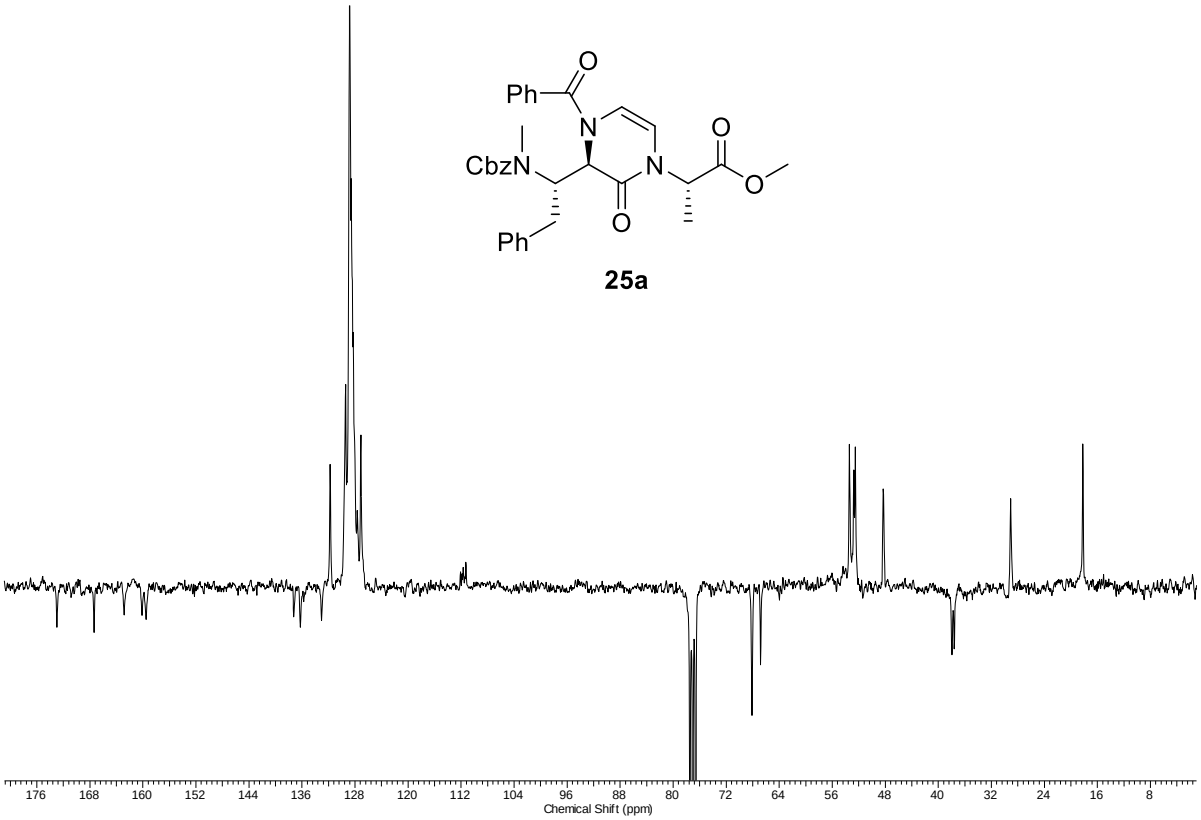

Compound **25b**: ^{1}H NMR (400 MHz, $CDCl_3$)

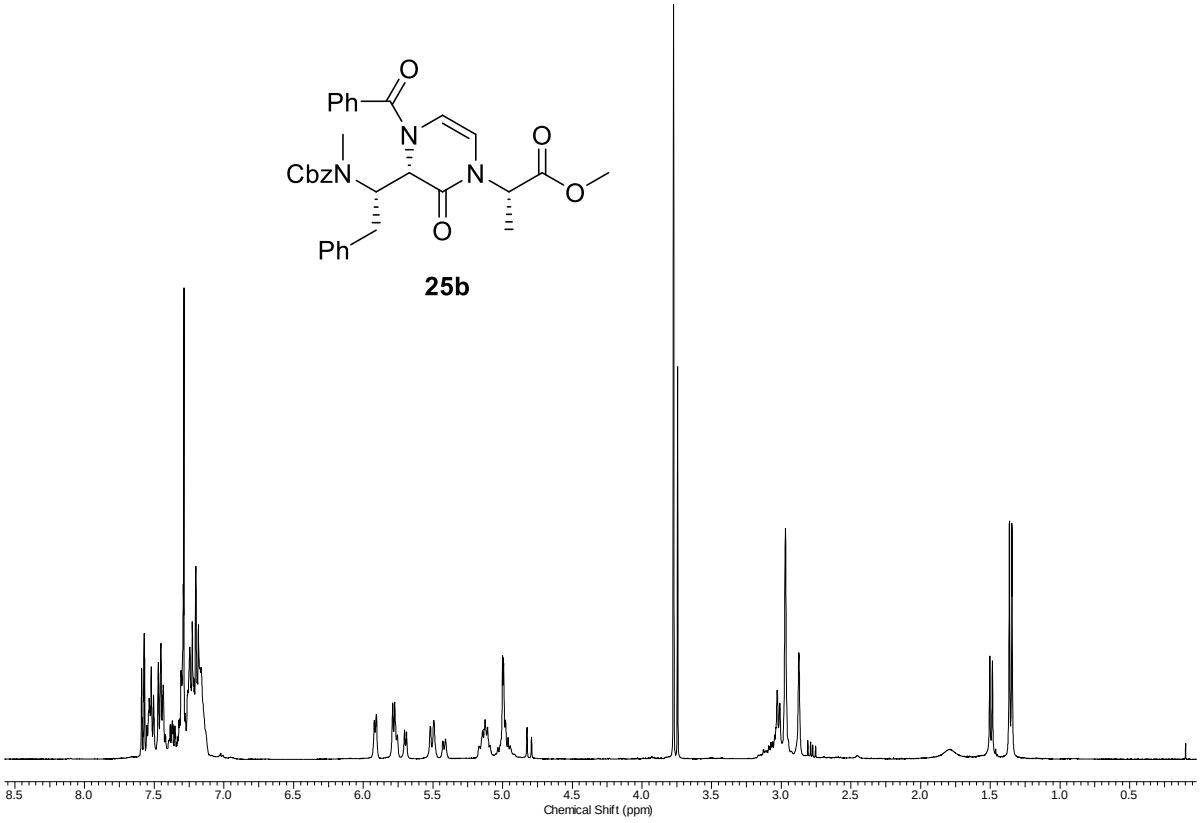

25b

Compound **25b**: ^{13}C NMR (100 MHz, $CDCl_3$)

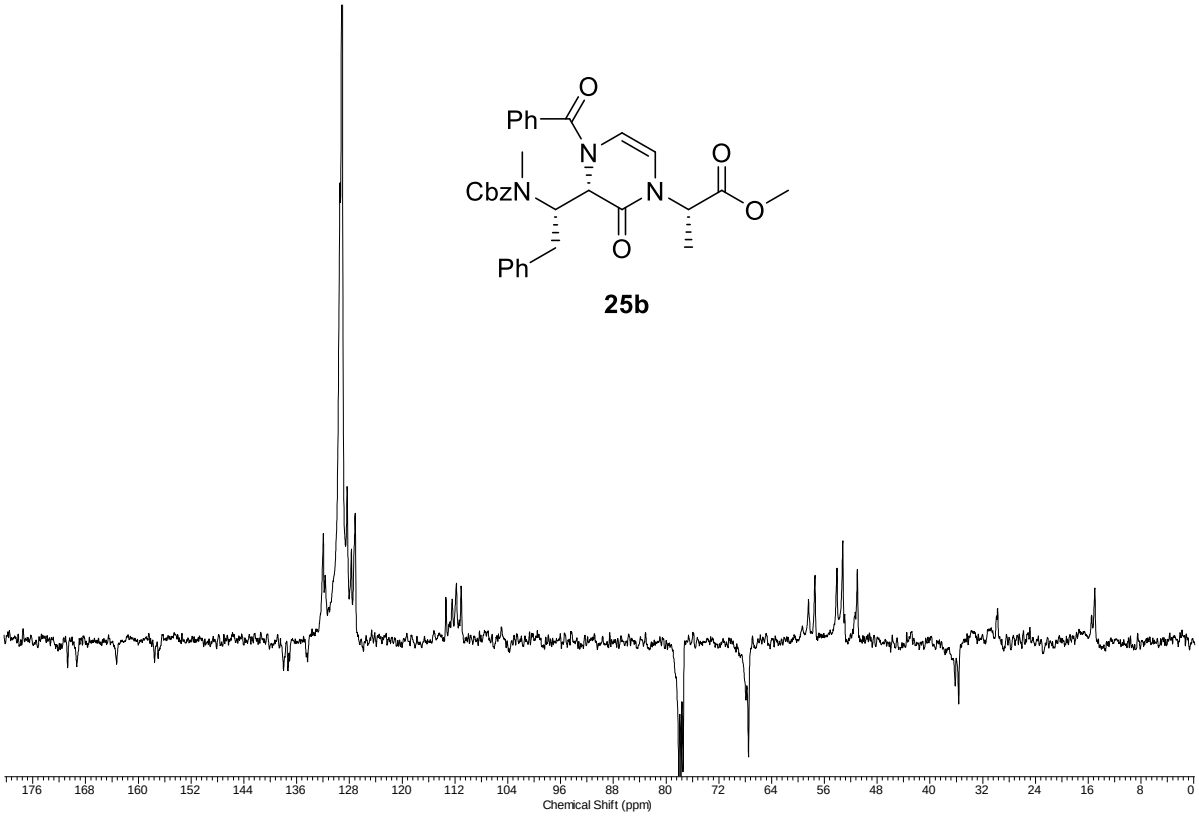

25b

Compound **26a**: ^{1}H NMR (300 MHz, $CDCl_3$)

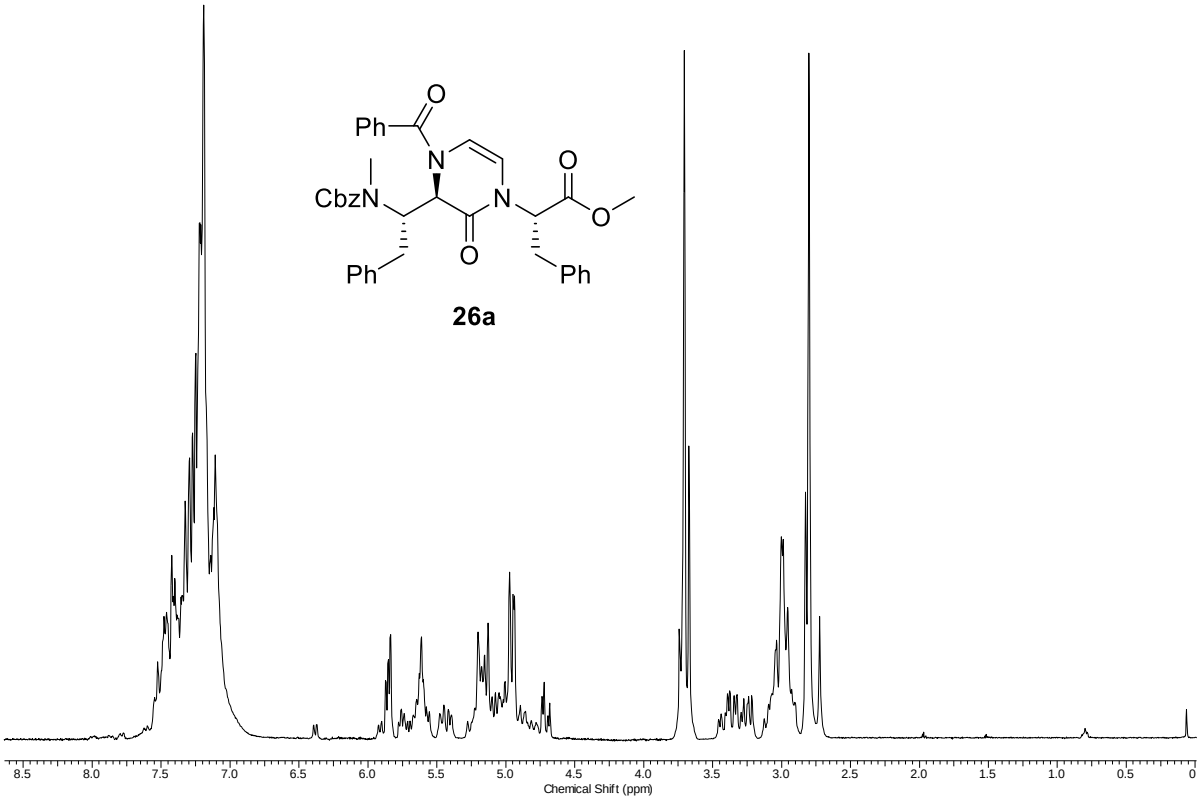

Compound **26a**: ^{13}C NMR (75 MHz, $CDCl_3$)

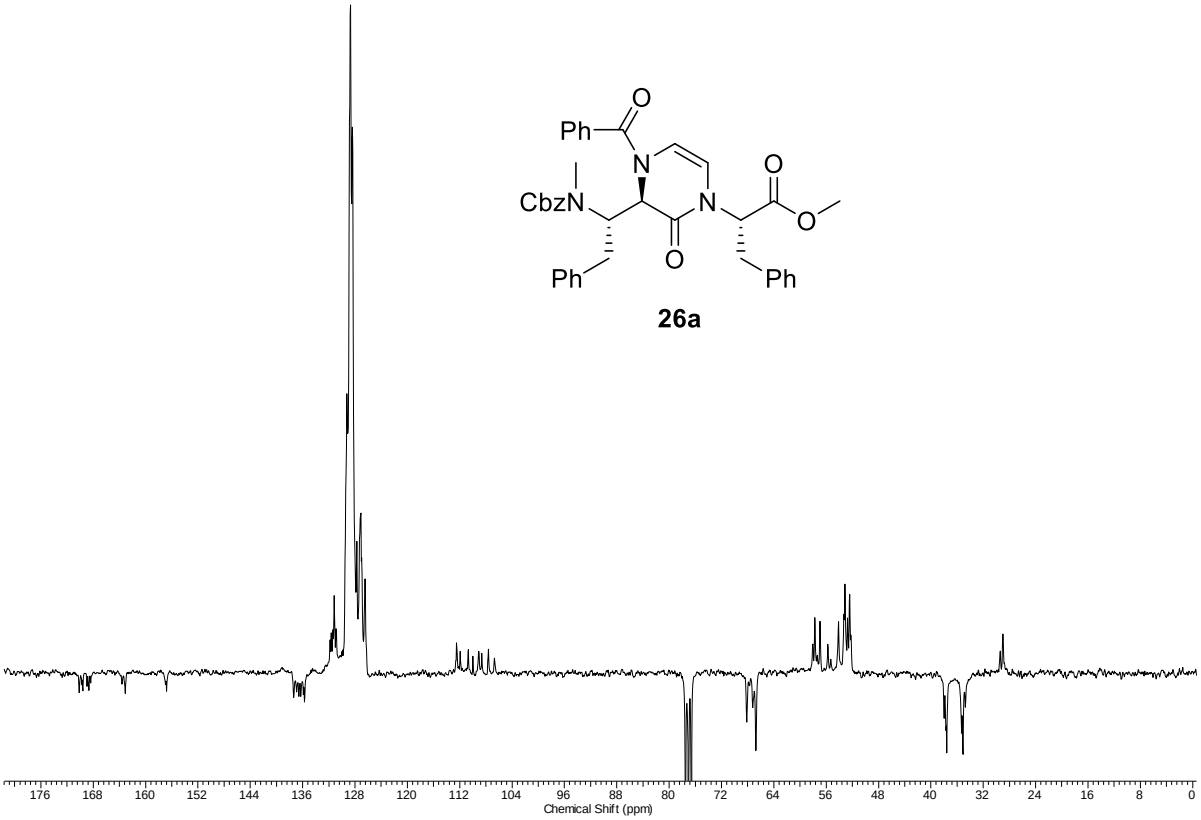

Compound **26b**: ^{1}H NMR (400 MHz, CD_3CN)

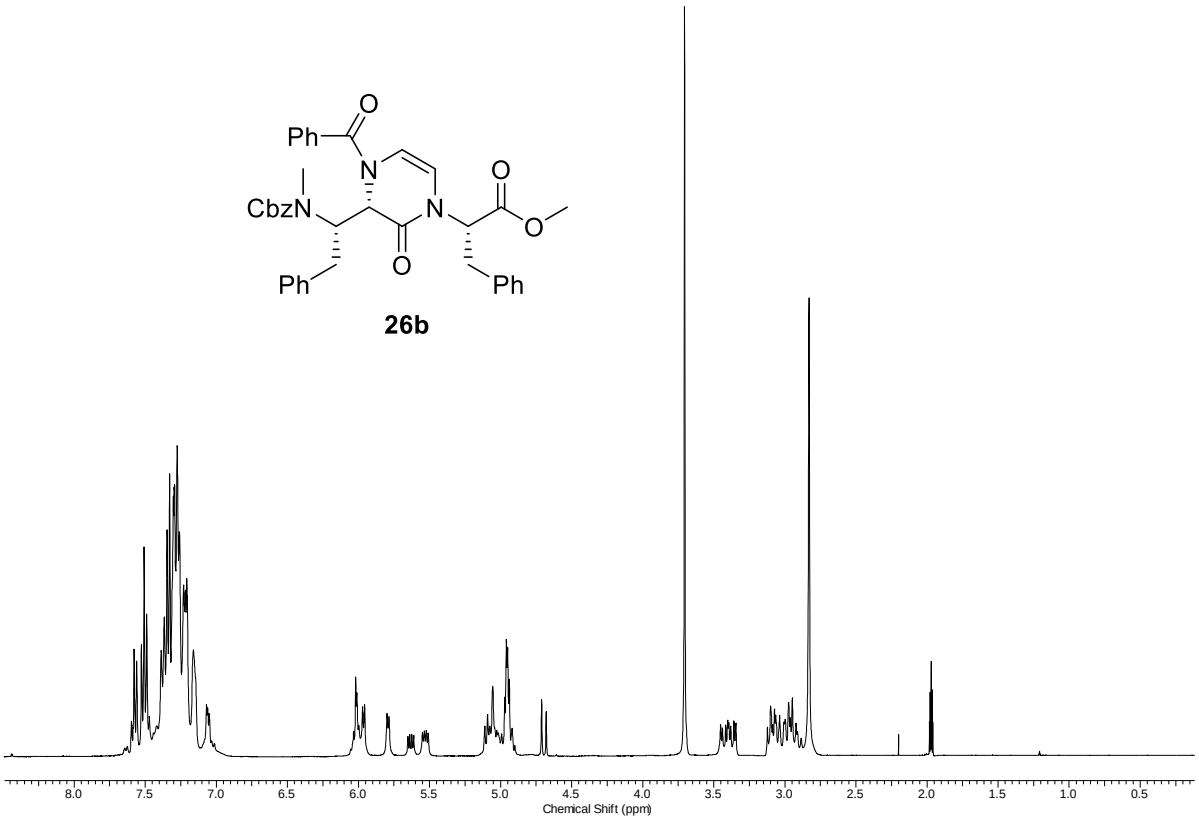

26b

Compound **26b**: ^{13}C NMR (100 MHz, CD_3CN)

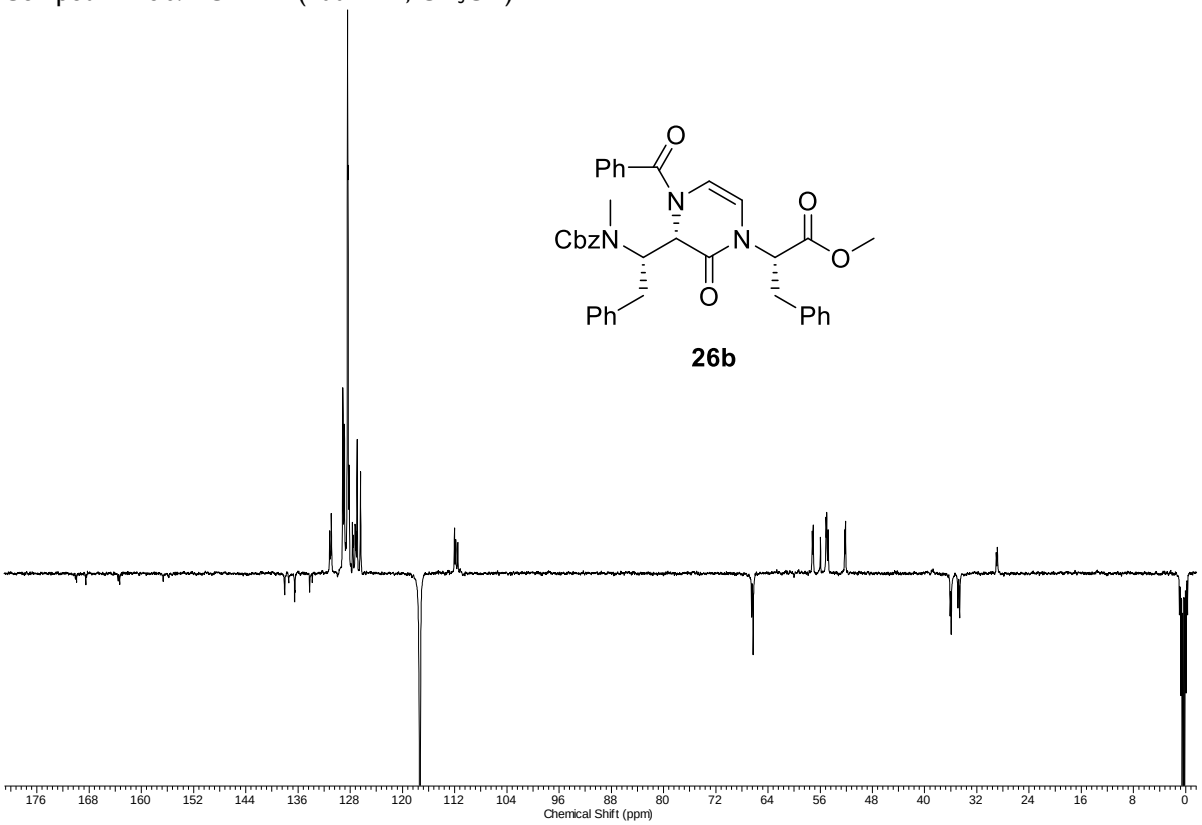

26b

Chapter 2.2

Compound **30a**: ^{1}H NMR (400 MHz, $CDCl_3$)

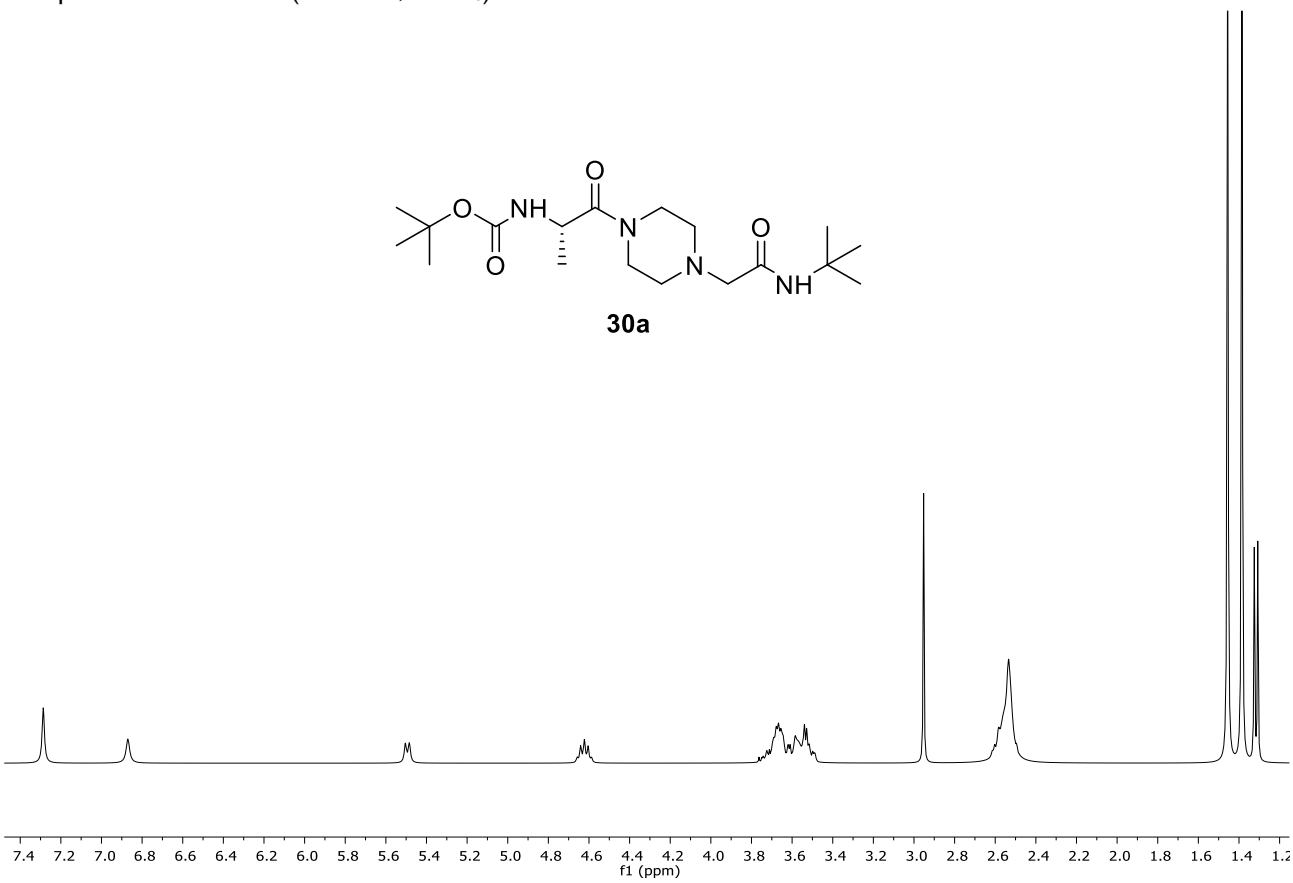

30a

Compound **30a**: ^{13}C NMR (100 MHz, $CDCl_3$)

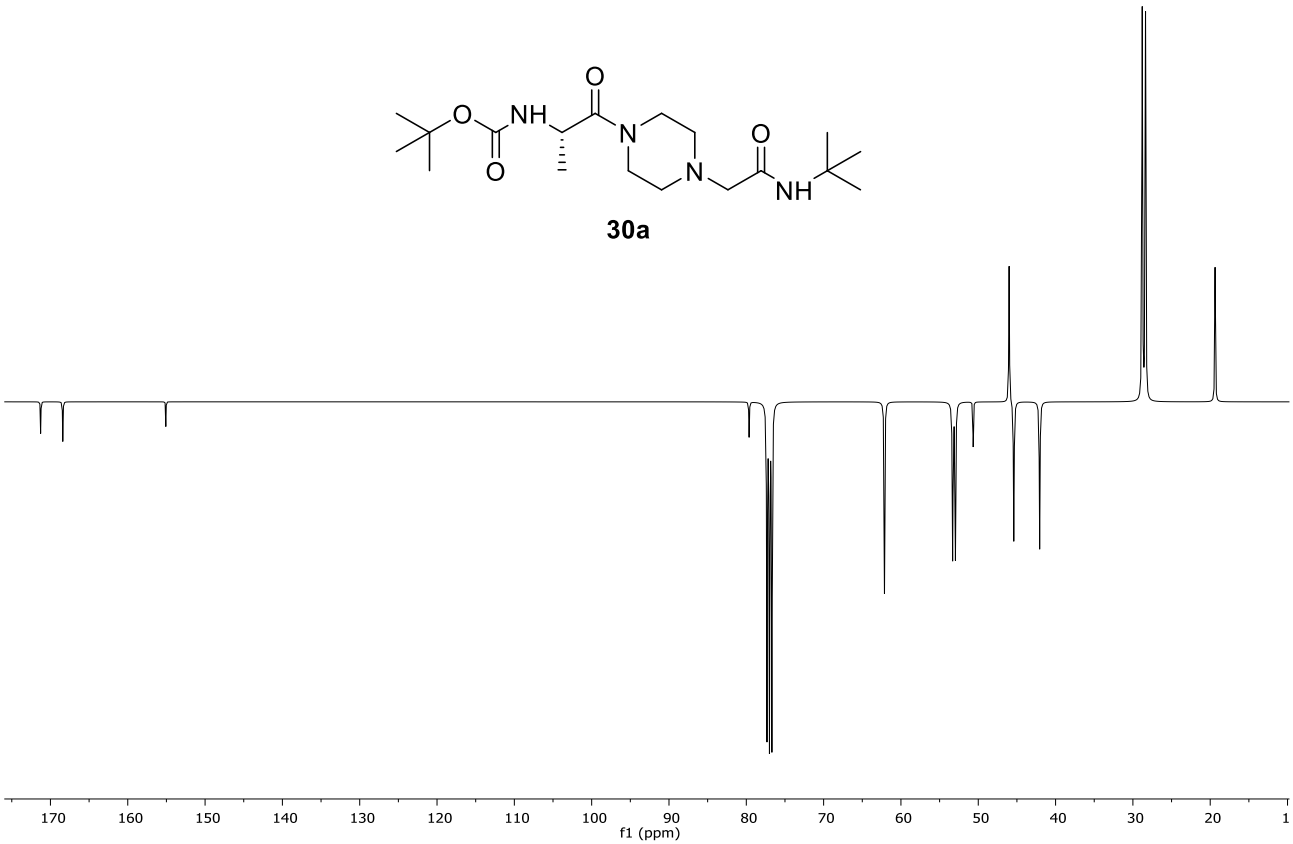

30a

Compound **30b**: ^{1}H NMR (400 MHz, $CDCl_3$)

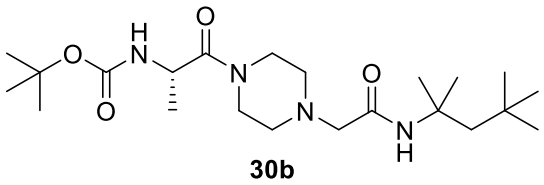

30b

Compound **30b**: ^{13}C NMR (100 MHz, $CDCl_3$)

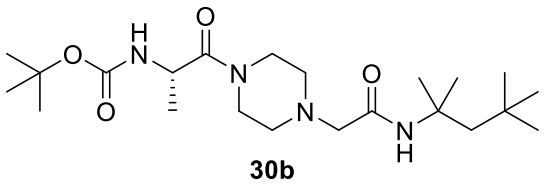

30b

Compound **30c**: ^{1}H NMR (400 MHz, $CDCl_3$)

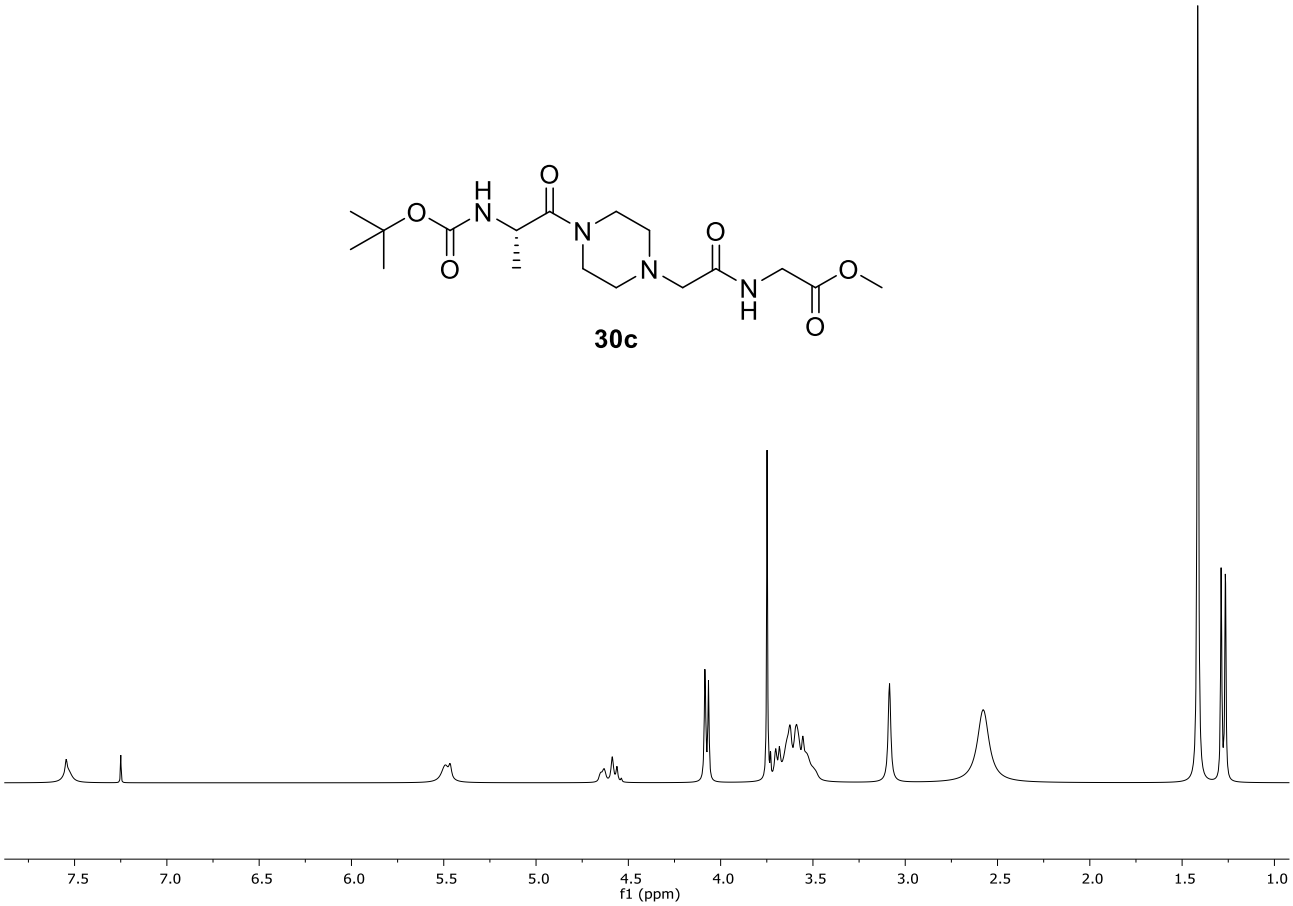

Compound **30c**: ^{13}C NMR (100 MHz, $CDCl_3$)

Compound **30d**: ^{1}H NMR (400 MHz, DMSO-d_6, 80 °C)

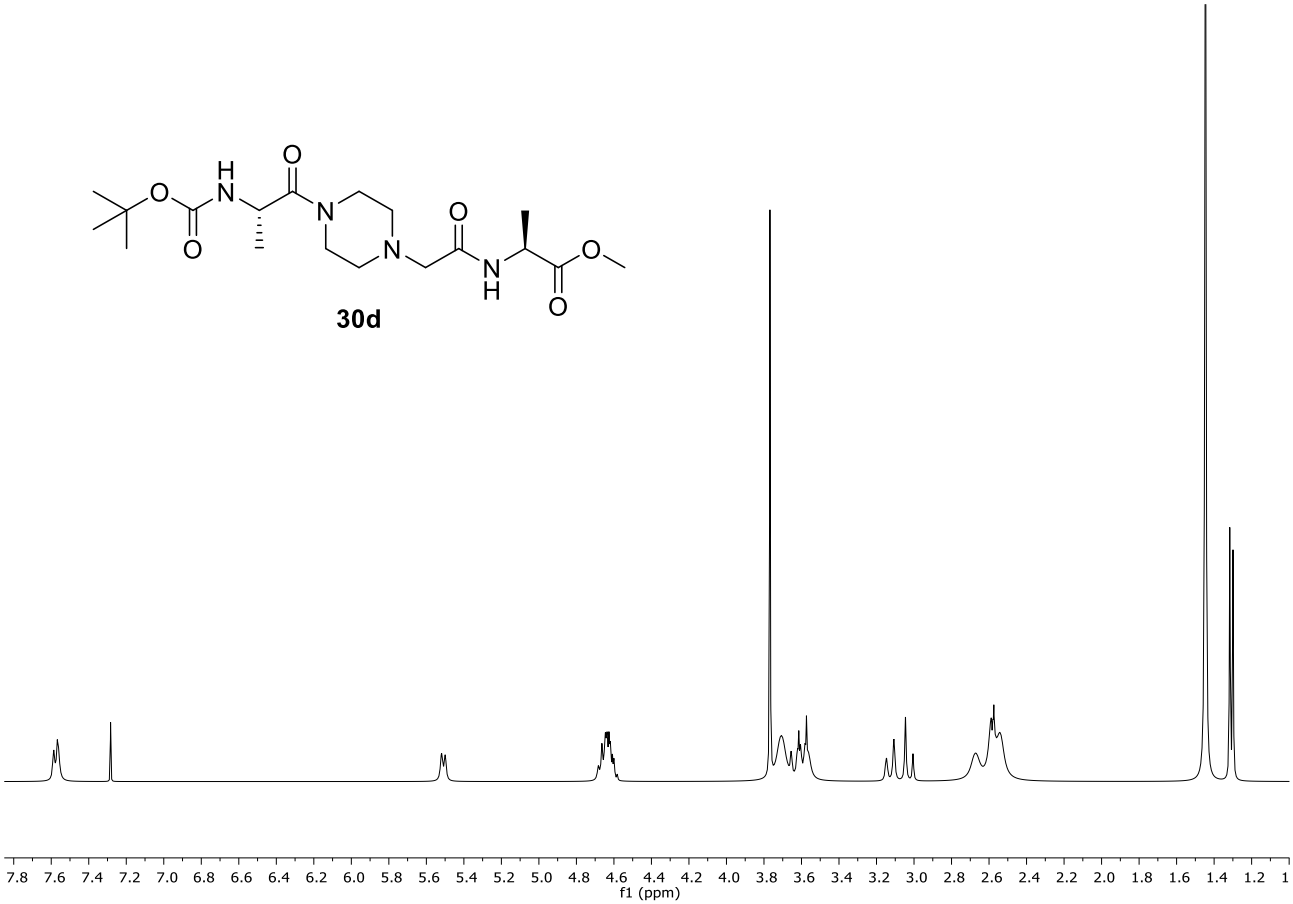

Compound **30d**: ^{13}C NMR (100 MHz, DMSO-d_6, 80 °C)

Compound **31a**: ^{1}H NMR (300 MHz, $CDCl_3$)

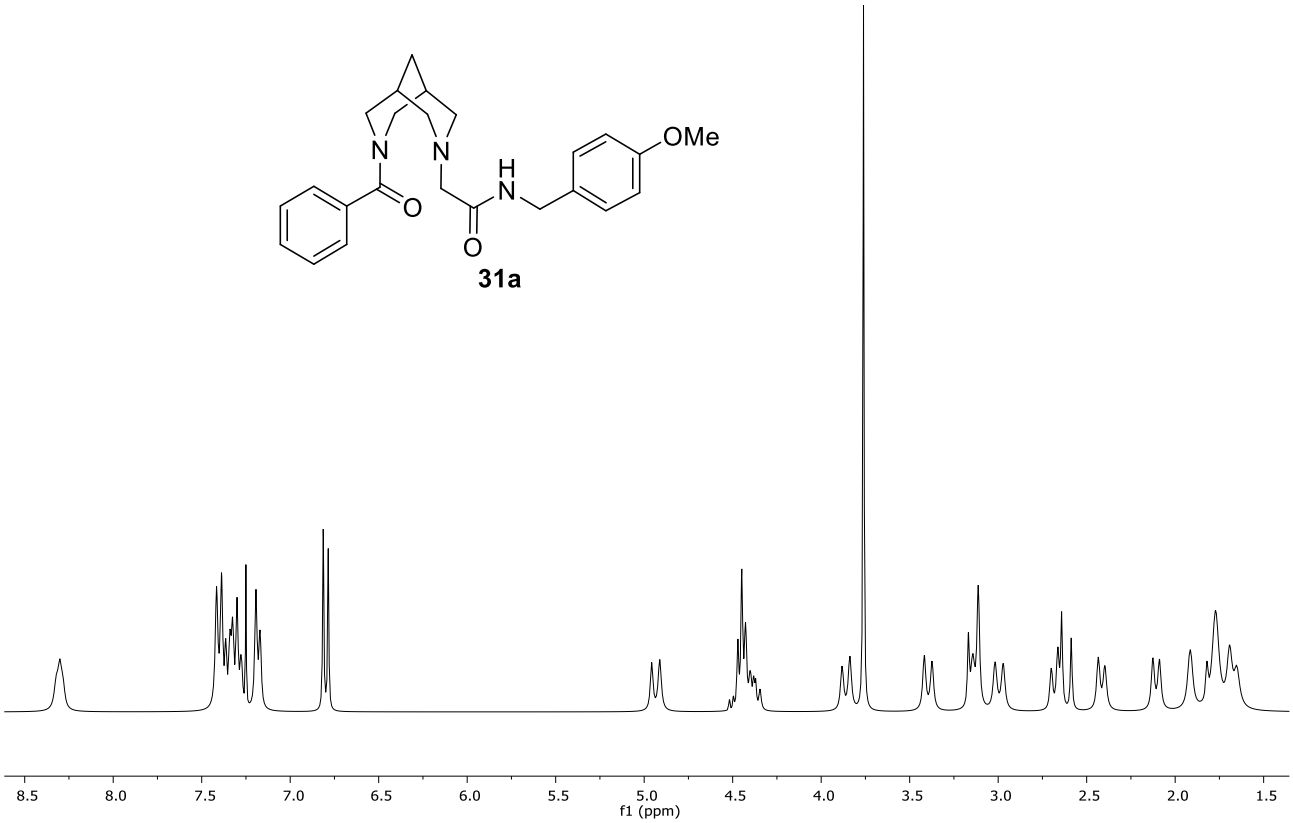

Compound **31a**: ^{13}C NMR (75 MHz, $CDCl_3$)

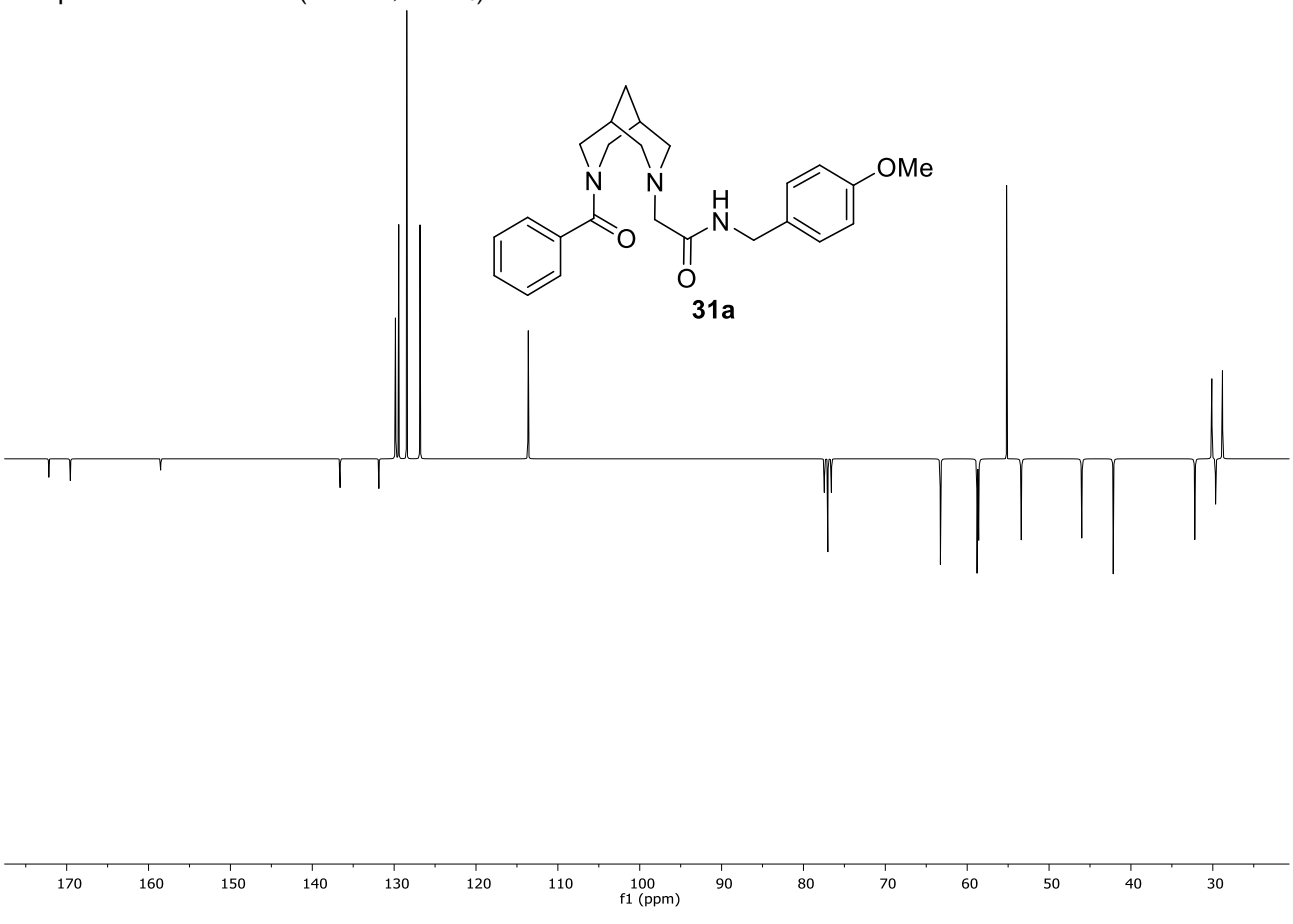

Compound **31b**: ^{1}H NMR (400 MHz, $CDCl_3$)

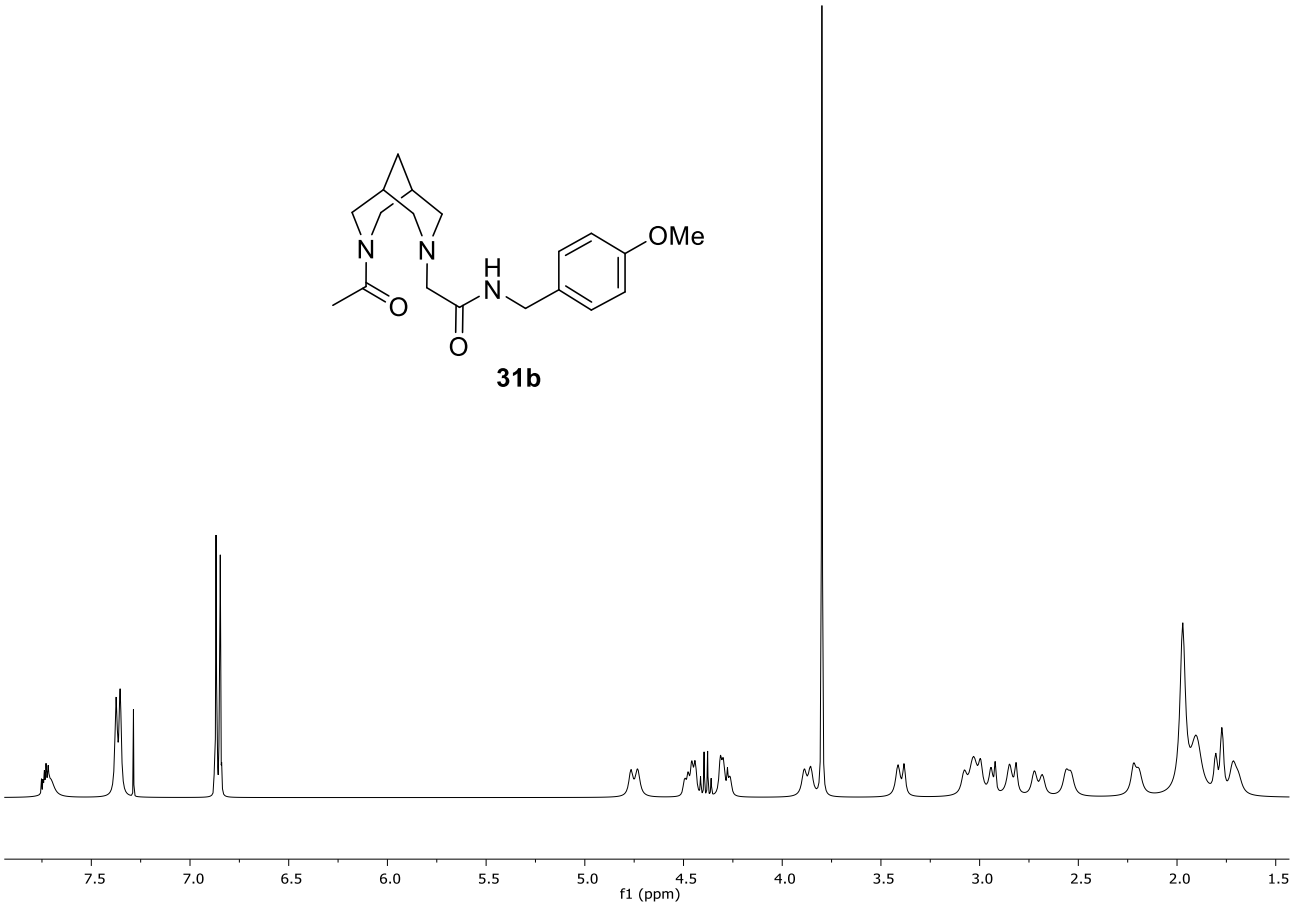

Compound **31b**: ^{13}C NMR (100 MHz, $CDCl_3$)

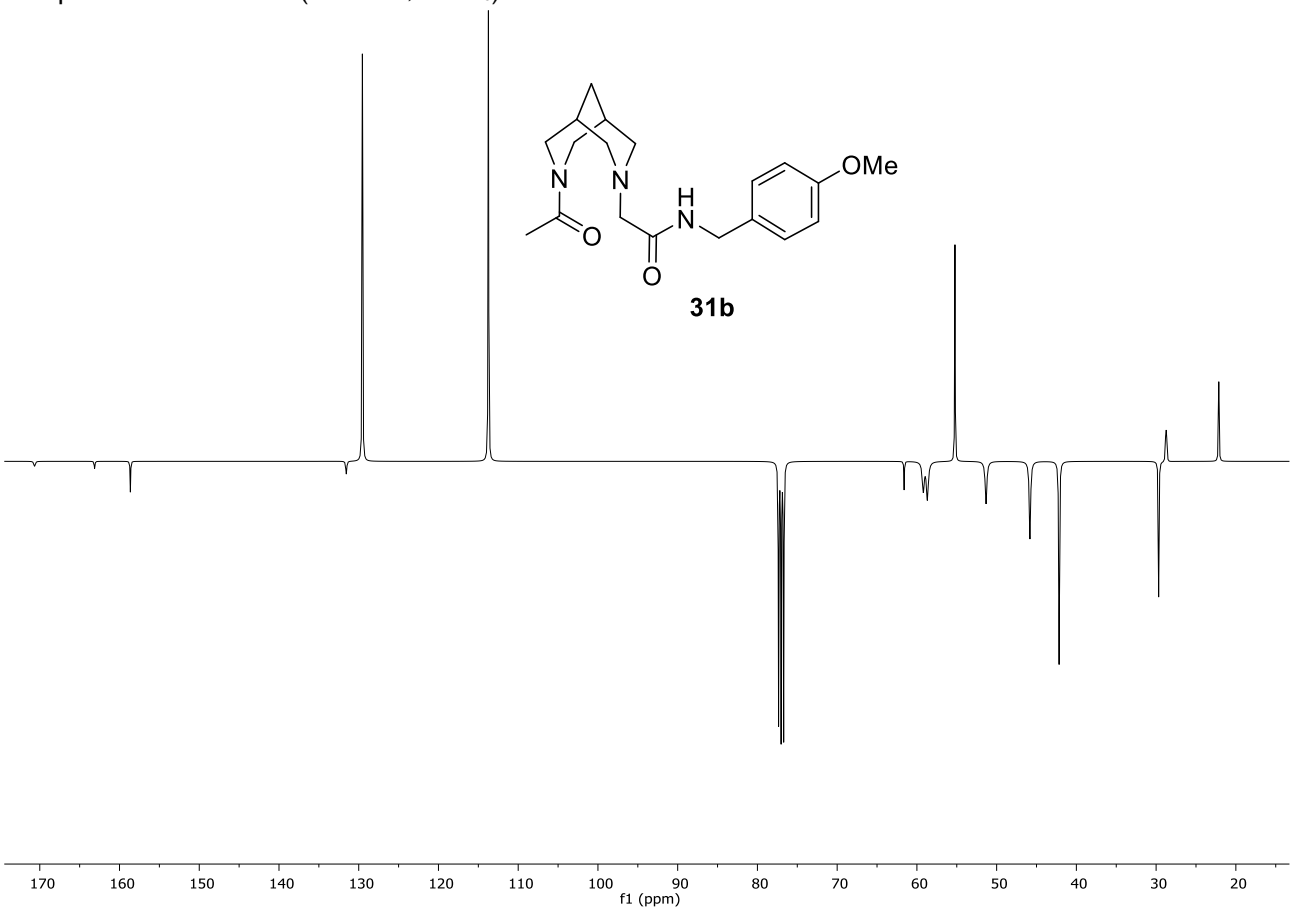

Compound **31c**: ^{1}H NMR (400 MHz, $CDCl_3$)

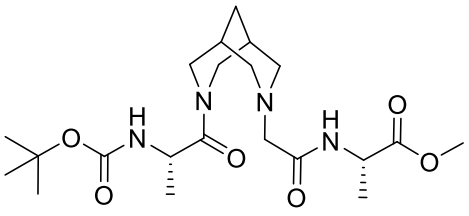

31c

Compound **31c**: ^{13}C NMR (100 MHz, $CDCl_3$)

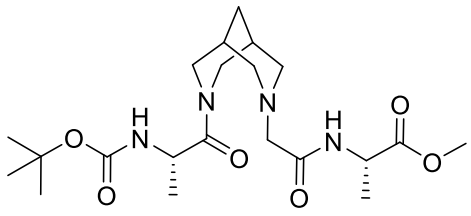

31c

Compound **31d**: ^{1}H NMR (400 MHz, $CDCl_3$)

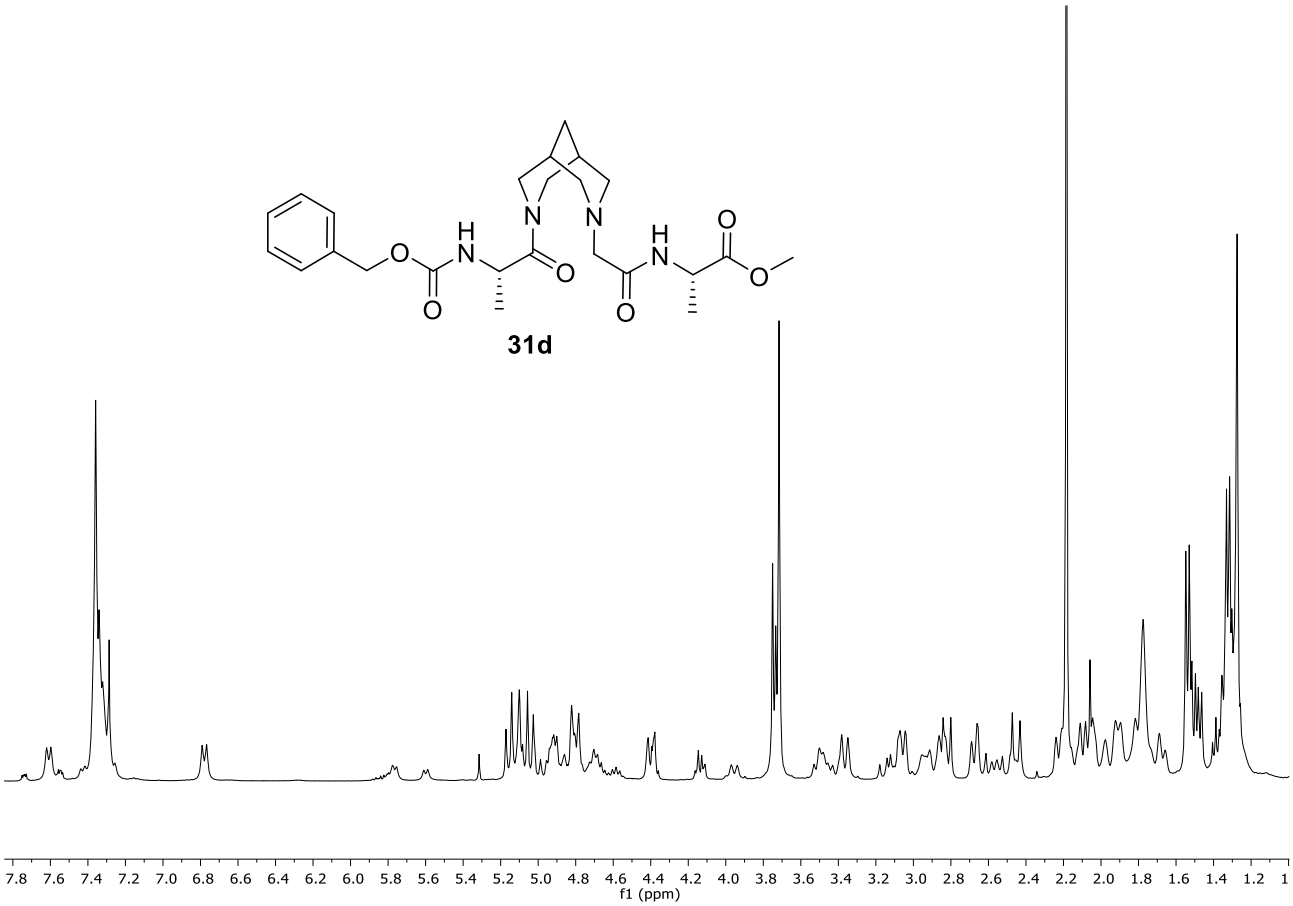

Compound **31d**: ^{13}C NMR (100 MHz, $CDCl_3$)

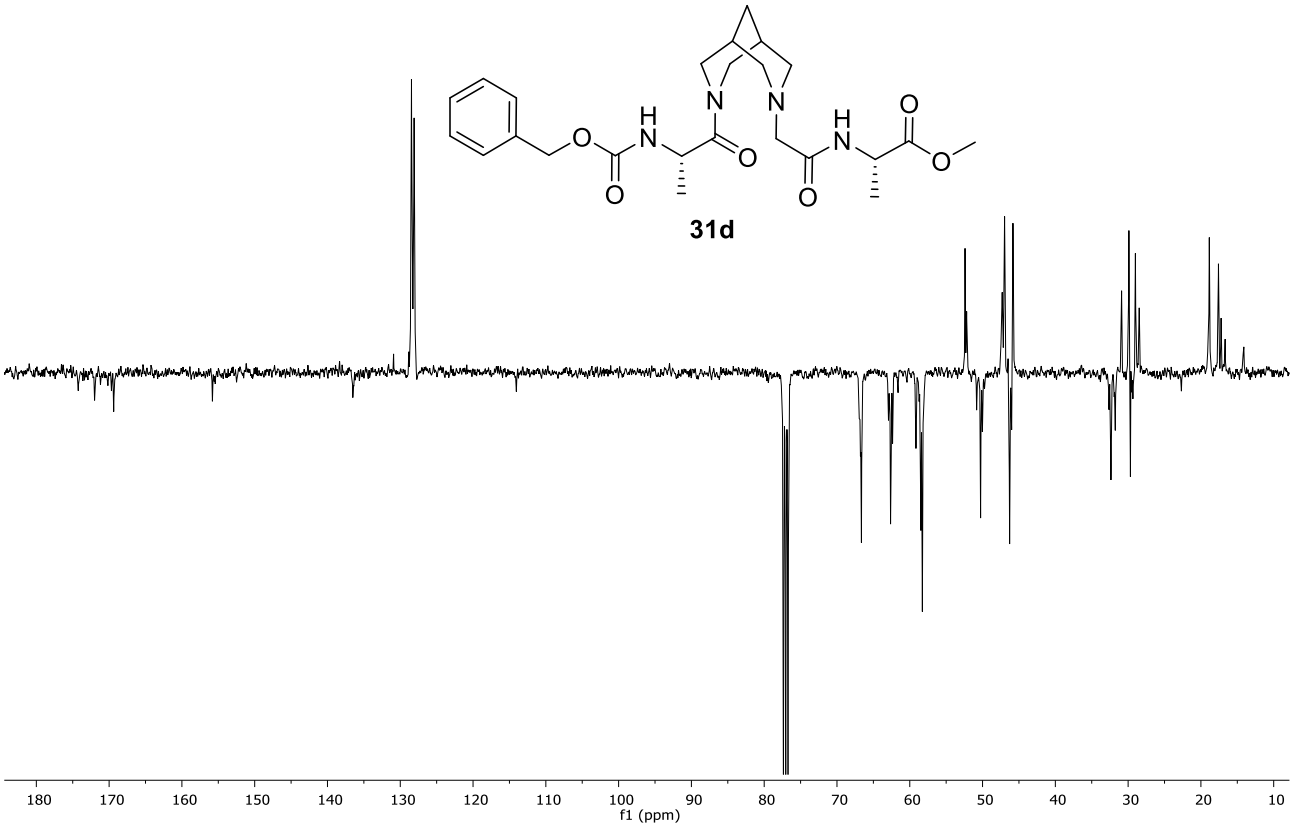

Compound **31e**: ^{1}H NMR (400 MHz, $CDCl_3$)

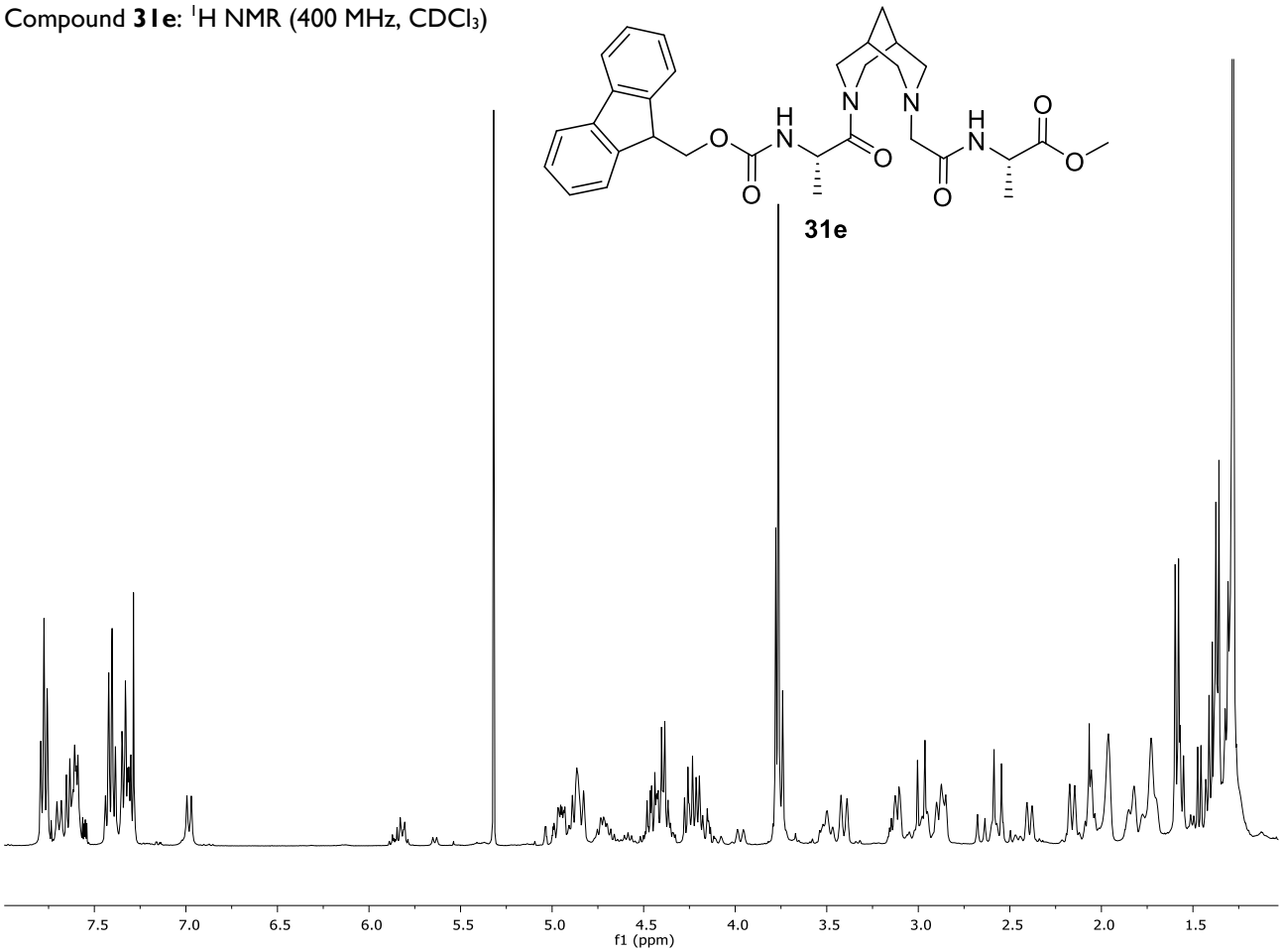

Compound **31e**: ^{13}C NMR (100 MHz, $CDCl_3$)

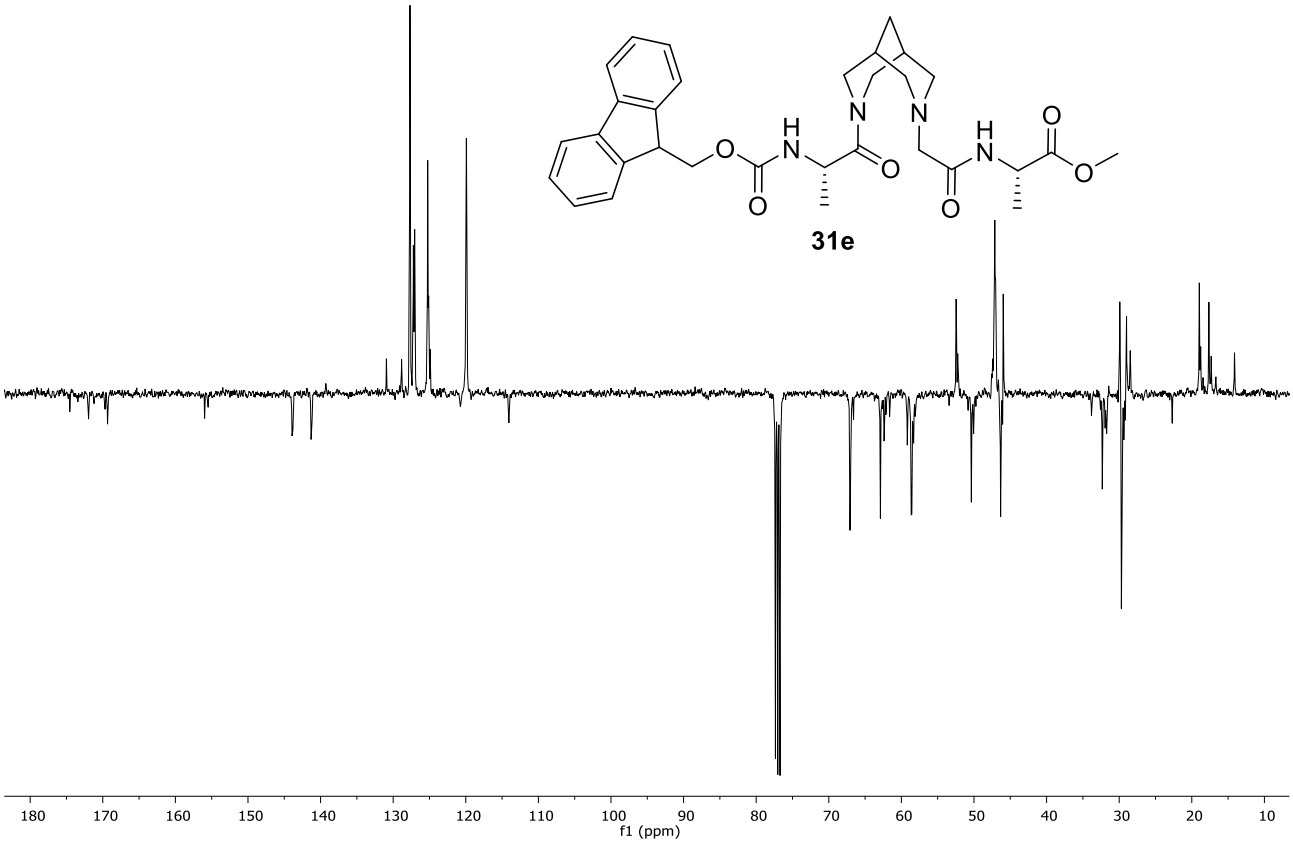

Chapter 2.3

Compound **34b**: ^{1}H NMR (400 MHz, $CDCl_3$)

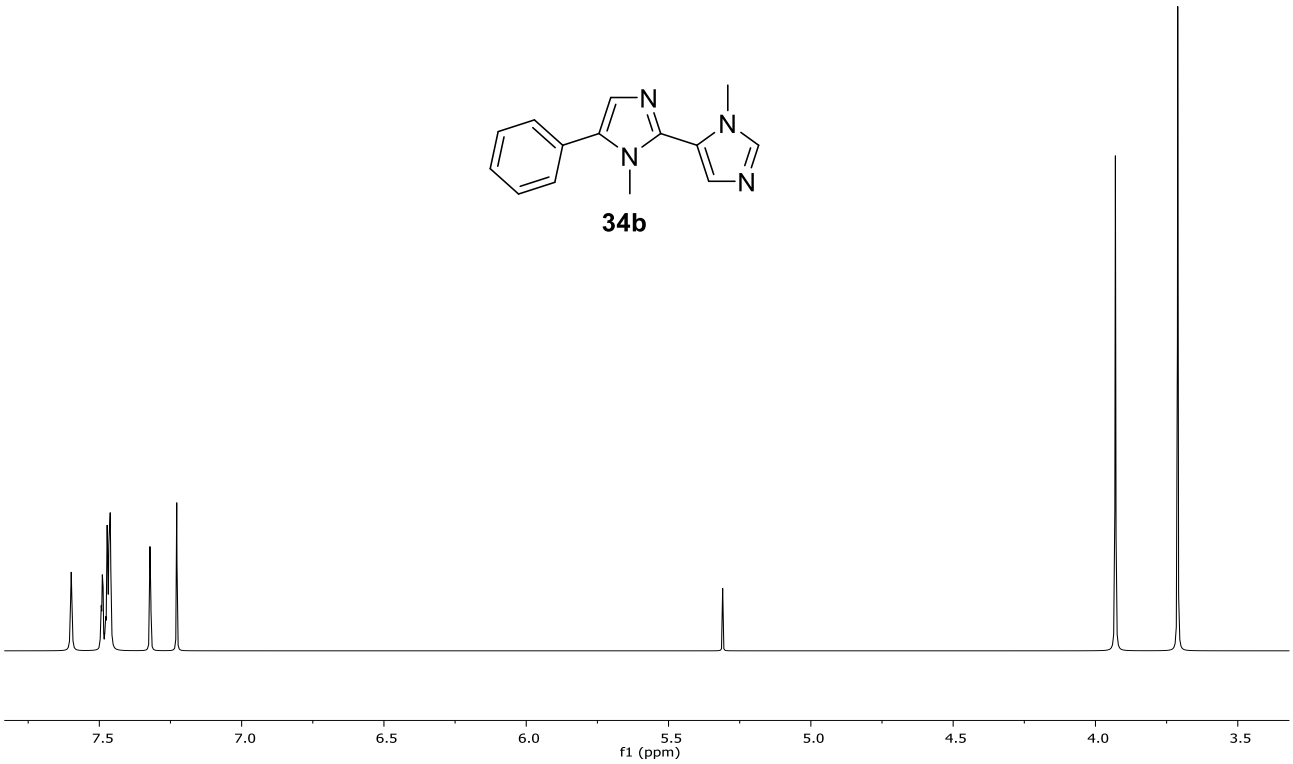

Compound **34b**: ^{13}C NMR (100 MHz, $CDCl_3$)

Compound **34c**: ^{1}H NMR (400 MHz, $CDCl_3$)

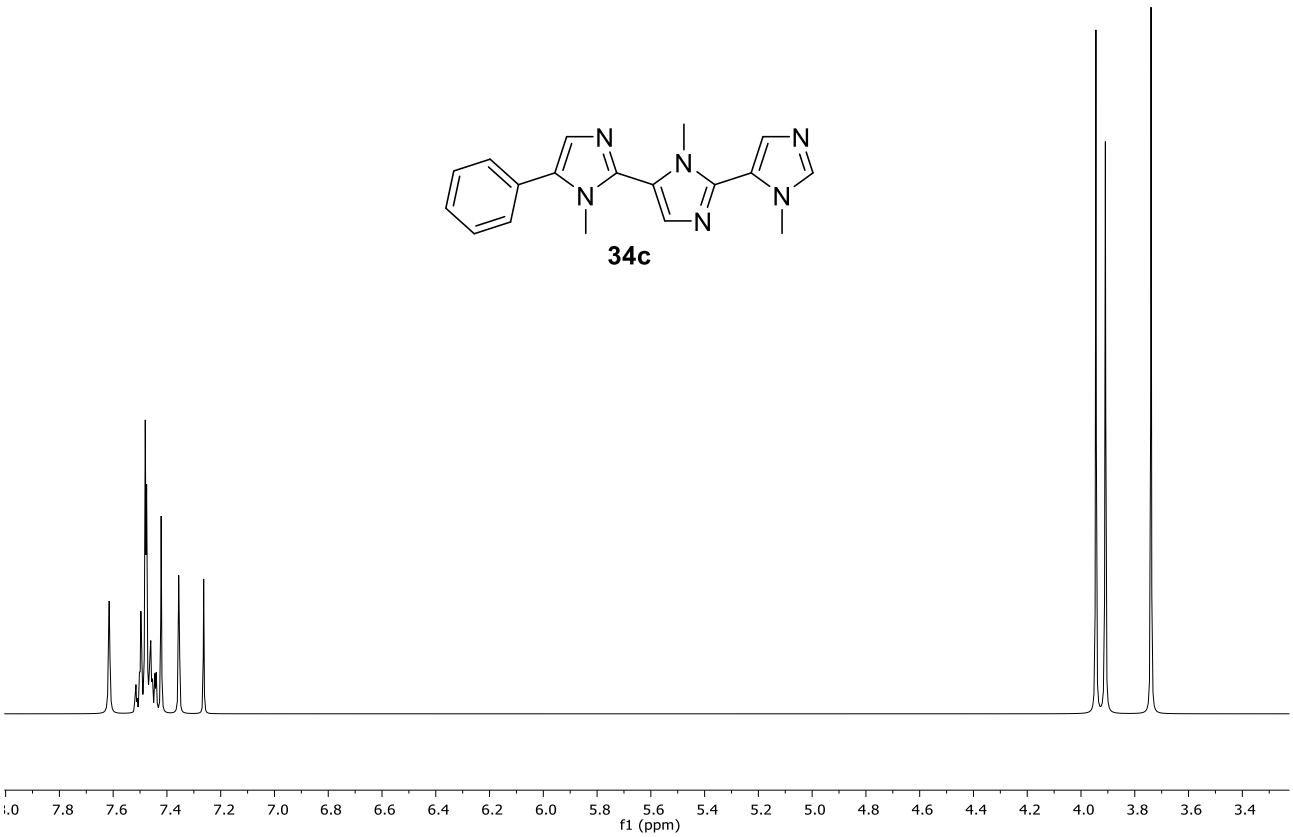

Compound **34c**: ^{13}C NMR (100 MHz, $CDCl_3$)

Compound **34c**: ^{1}H-^{1}H NOESY NMR (400, 400 MHz, $CDCl_3$)

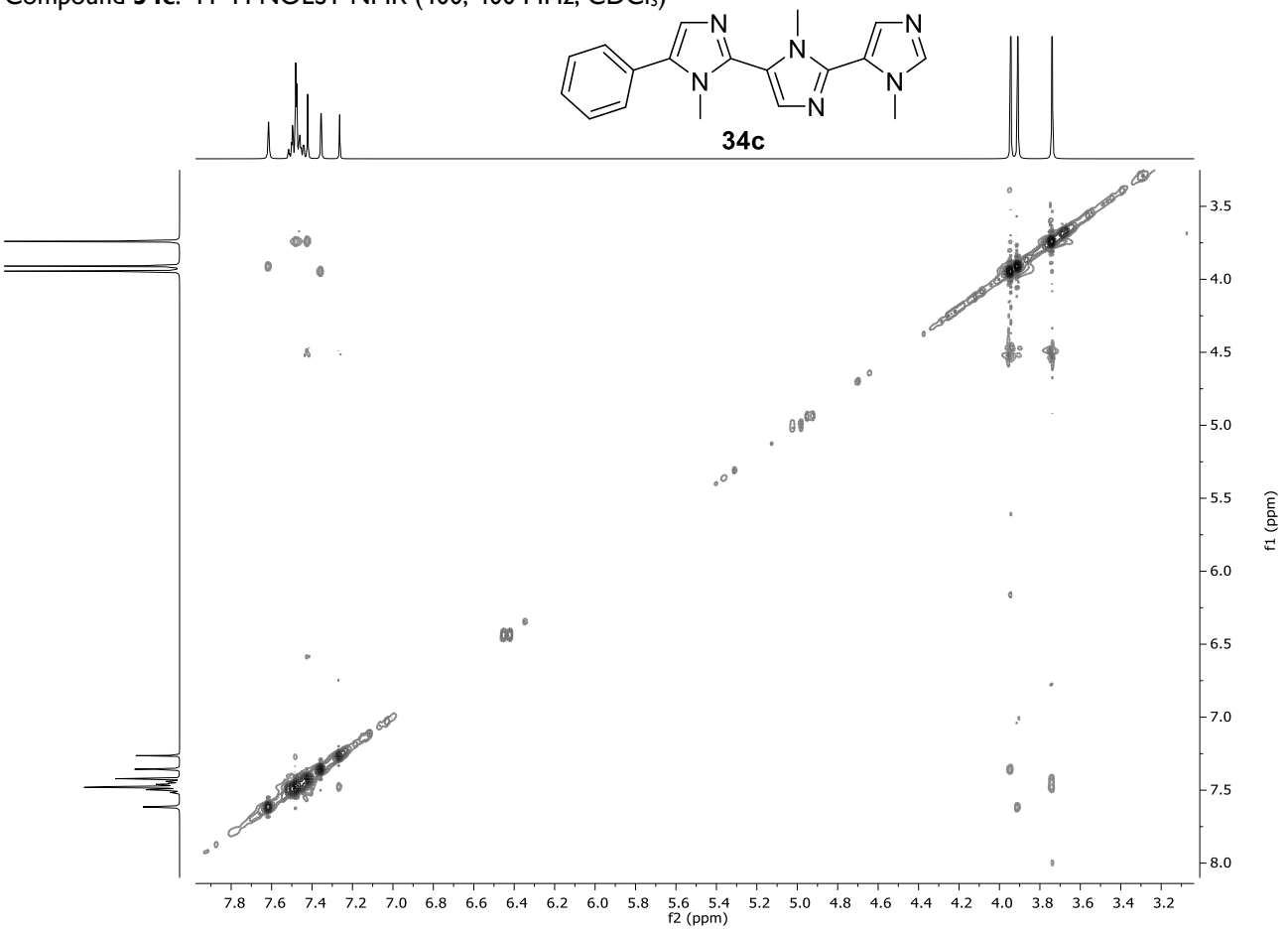

Compound **34d**: ^{1}H NMR (400 MHz, $CDCl_3$)

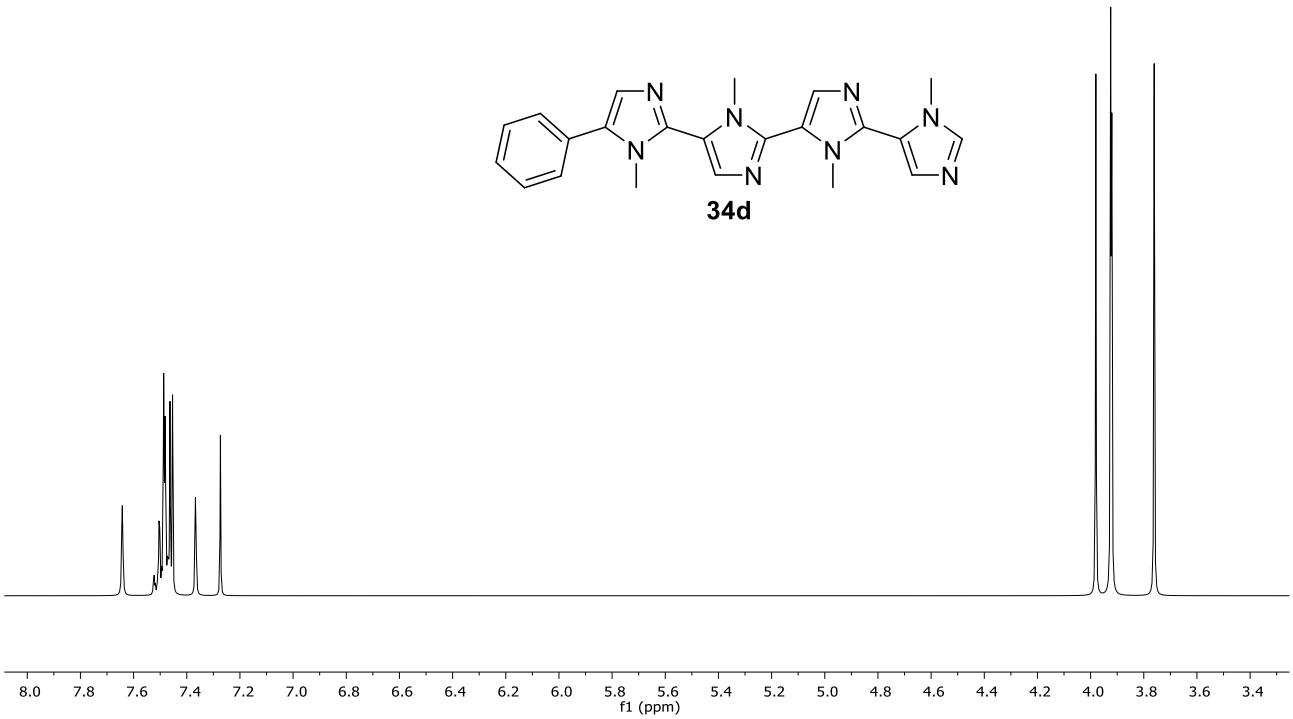

Compound **34d**: ^{13}C NMR (100 MHz, $CDCl_3$)

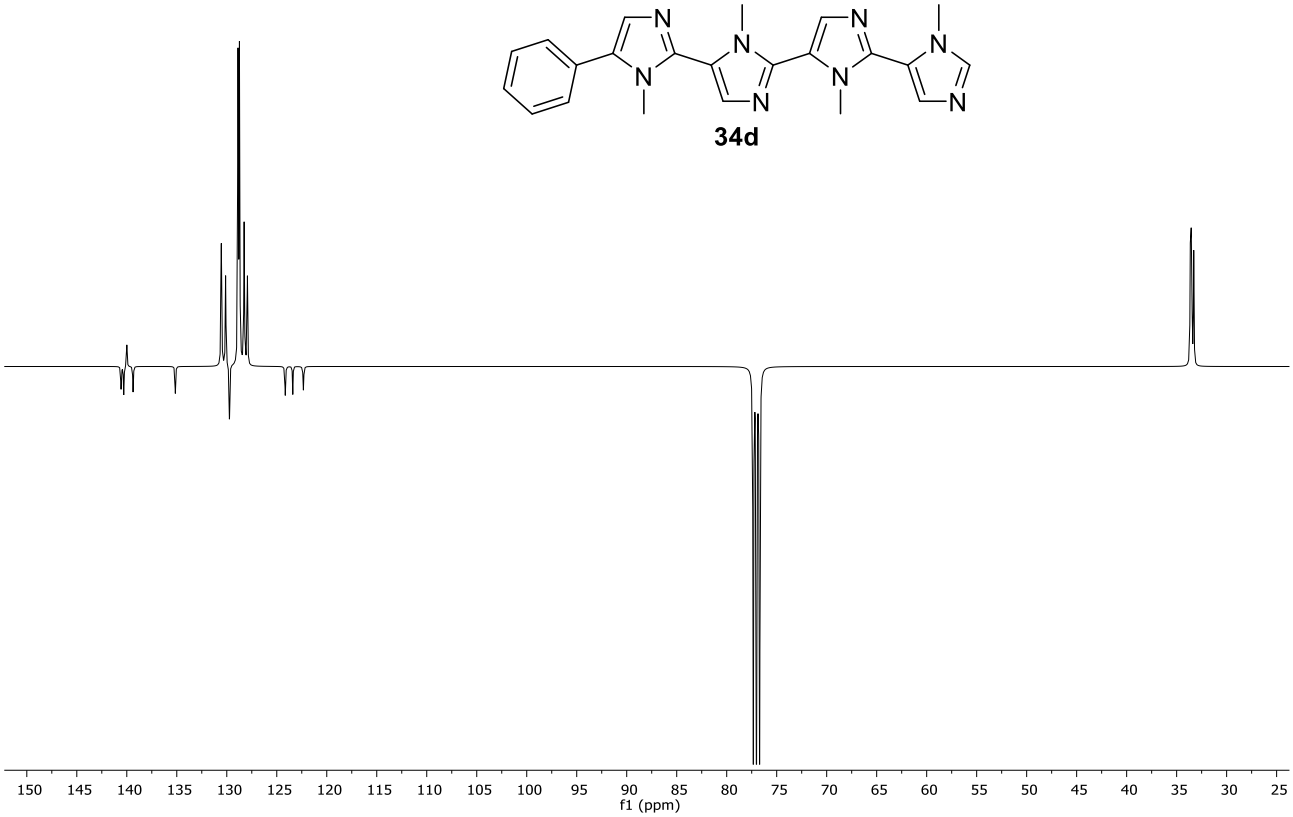

Compound **34d**: ^{1}H-^{1}H NOESY NMR (400, 400 MHz, $CDCl_3$)

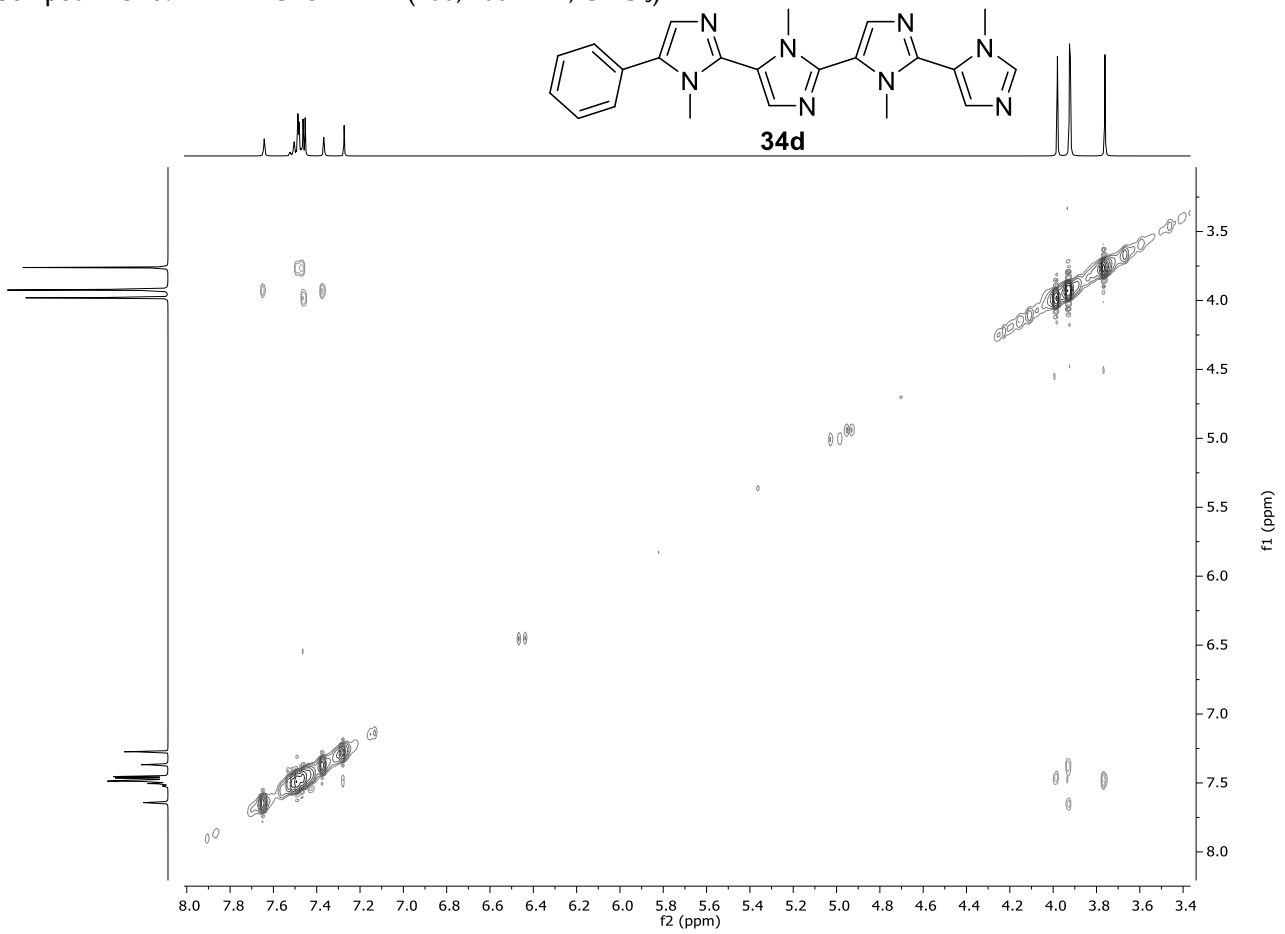

Compound **36**: ^{1}H NMR (300 MHz, $CDCl_3$)

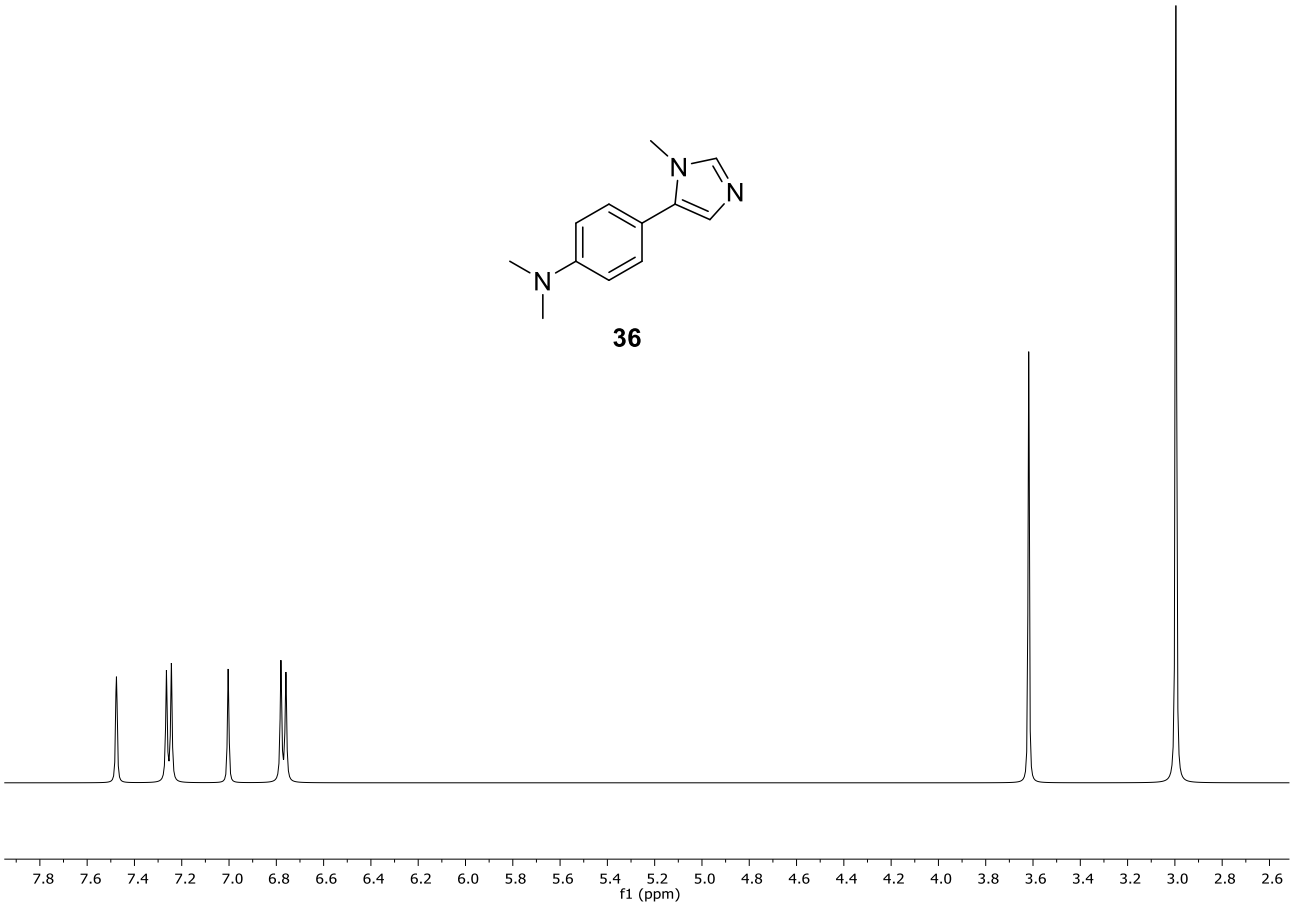

Compound **36**: ^{13}C NMR (75 MHz, $CDCl_3$)

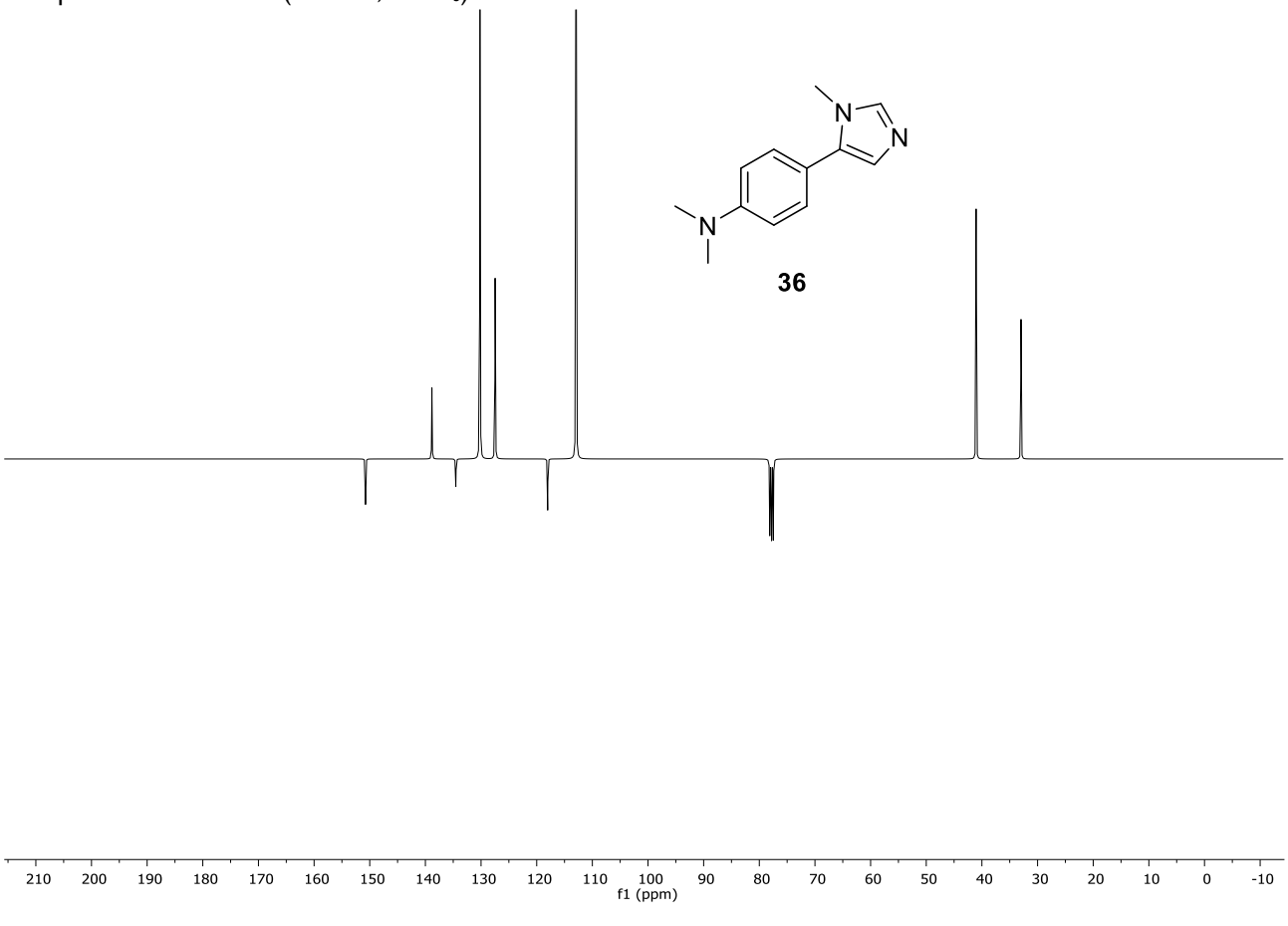

Compound **37a**: ^{1}H NMR (400 MHz, $CDCl_3$)

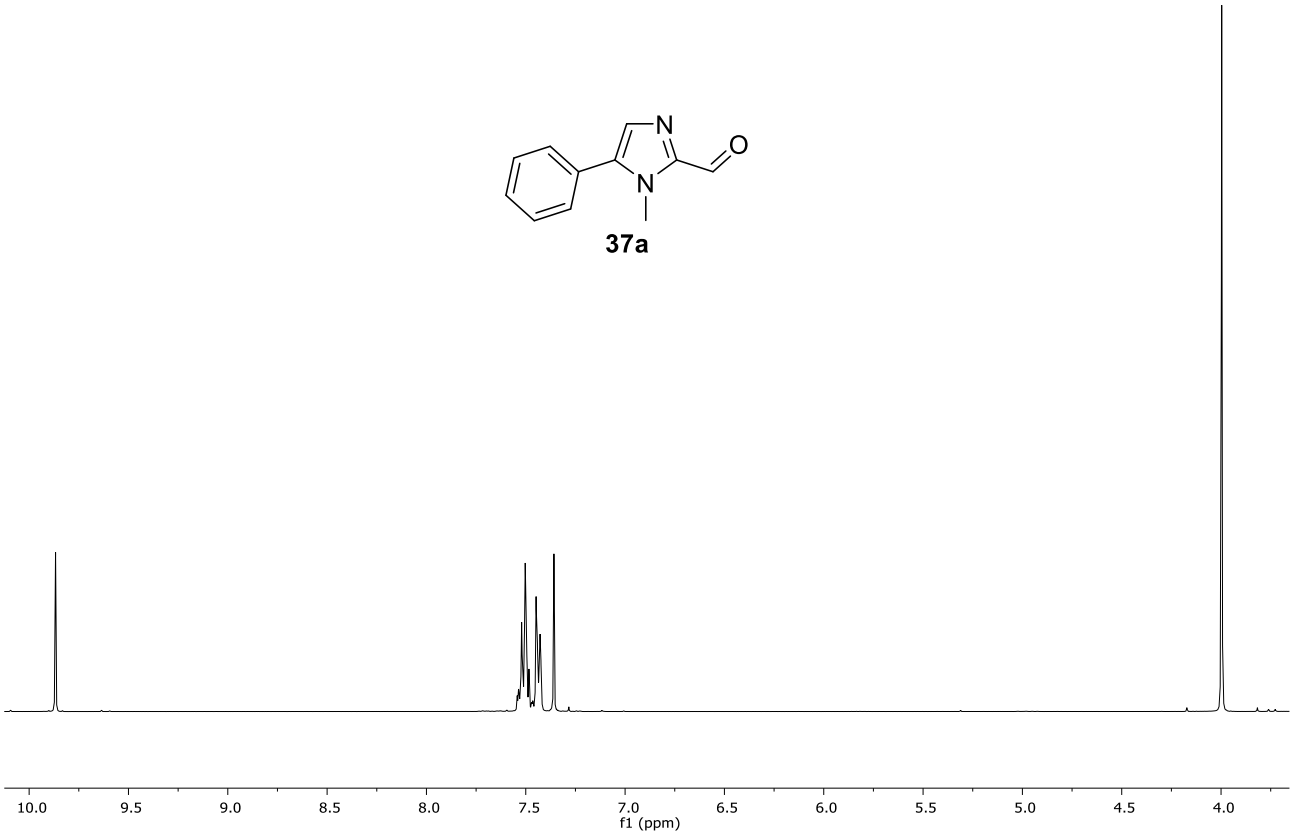

Compound **37a**: ^{13}C NMR (100 MHz, $CDCl_3$)

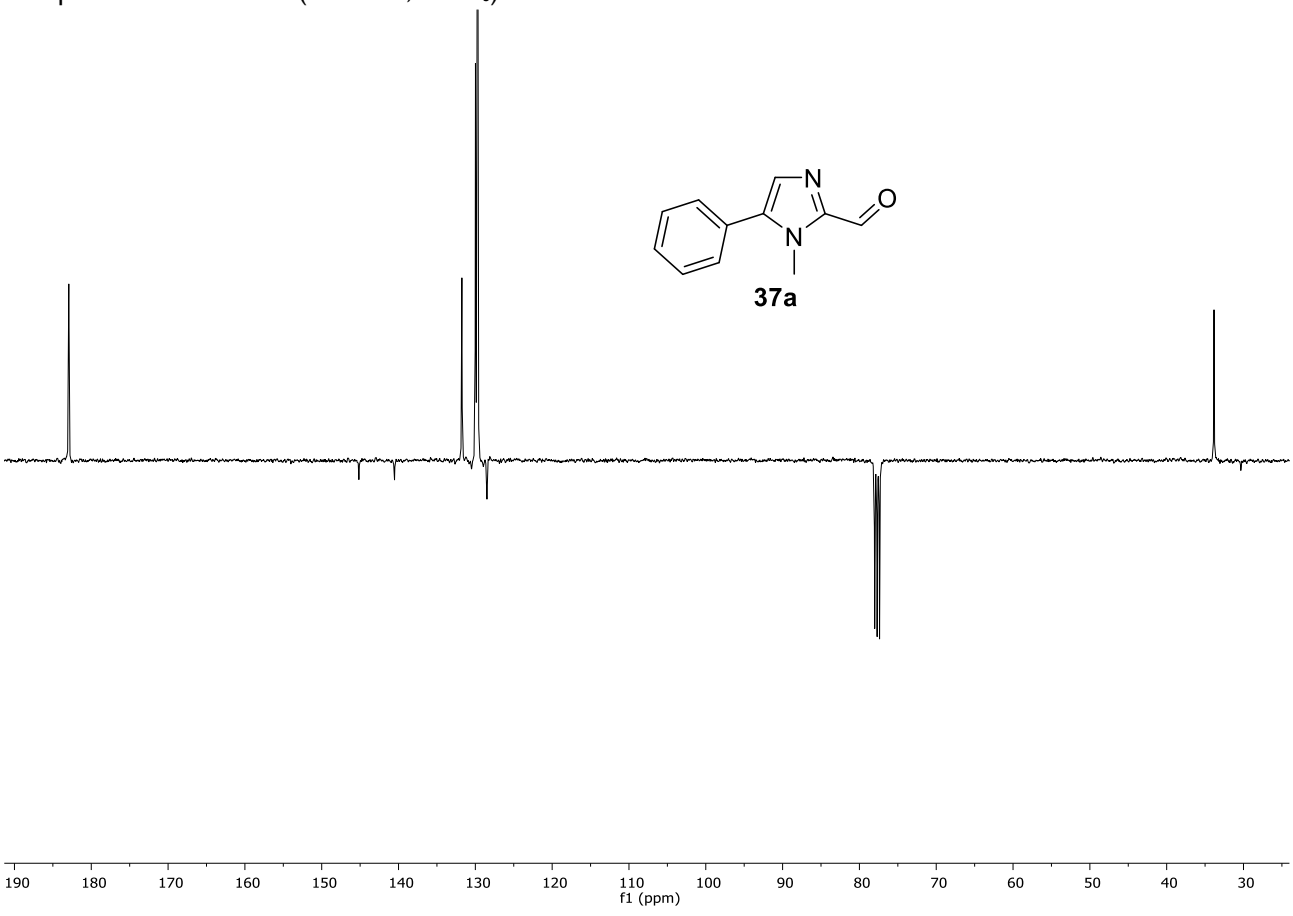

Compound **37b**: ^{1}H NMR (300 MHz, $CDCl_3$)

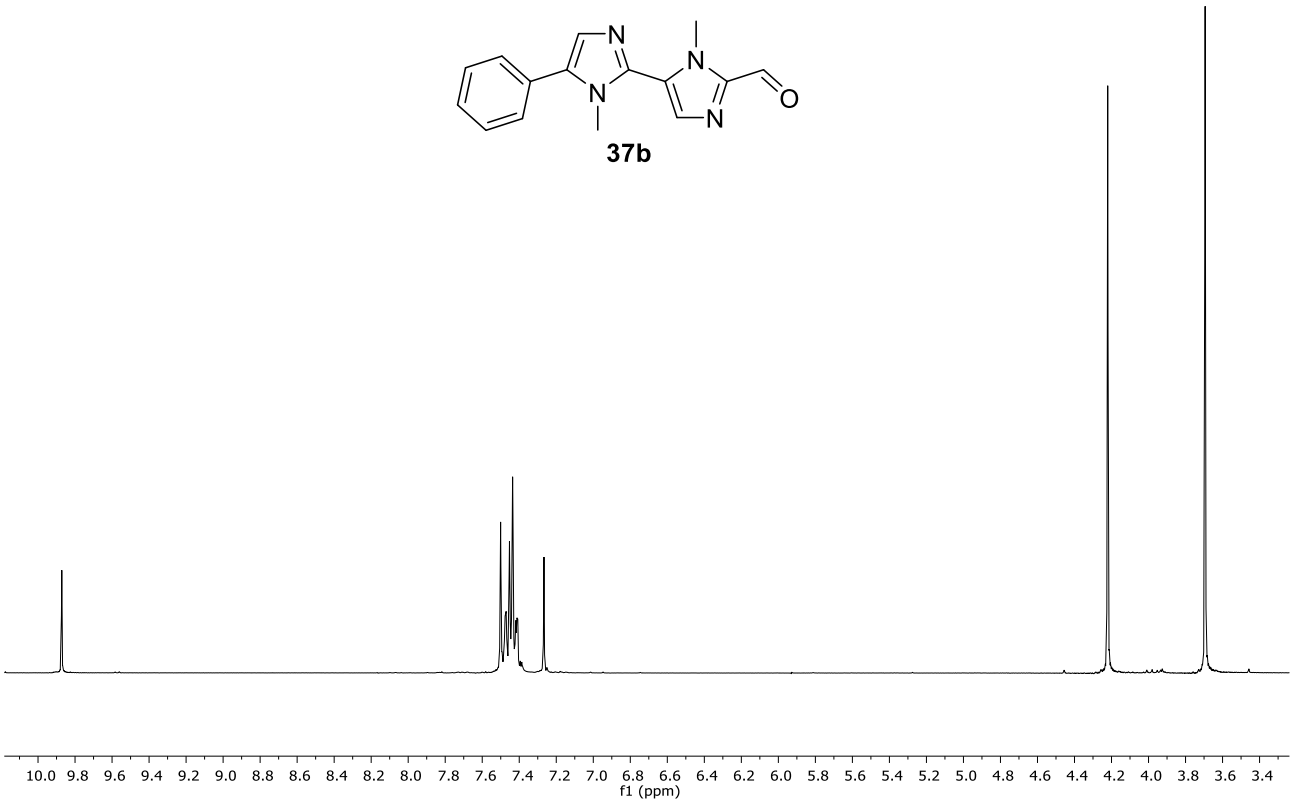

Compound **37b**: ^{13}C NMR (75 MHz, $CDCl_3$)

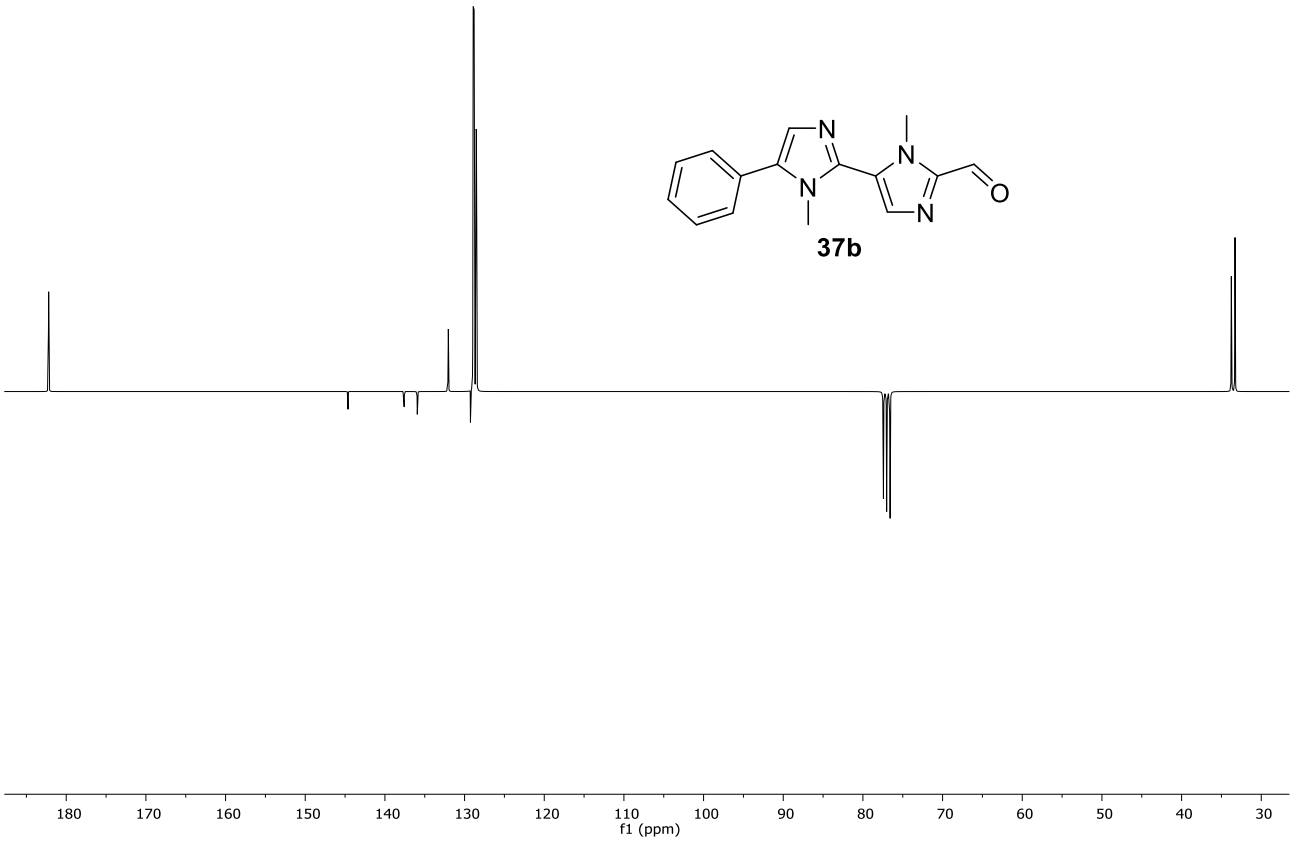

Compound **37c**: ^{1}H NMR (400 MHz, $CDCl_3$)

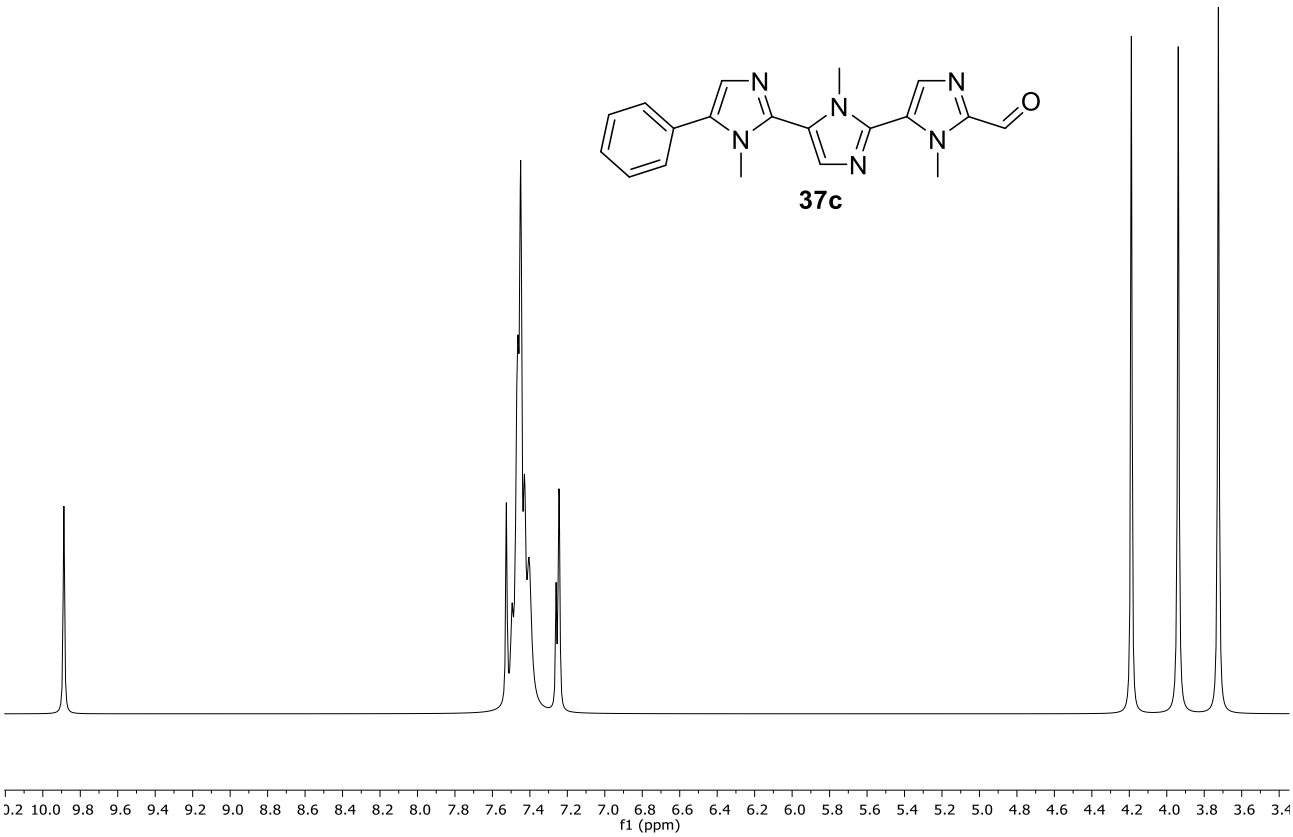

Compound **37c**: ^{13}C NMR (100 MHz, $CDCl_3$)

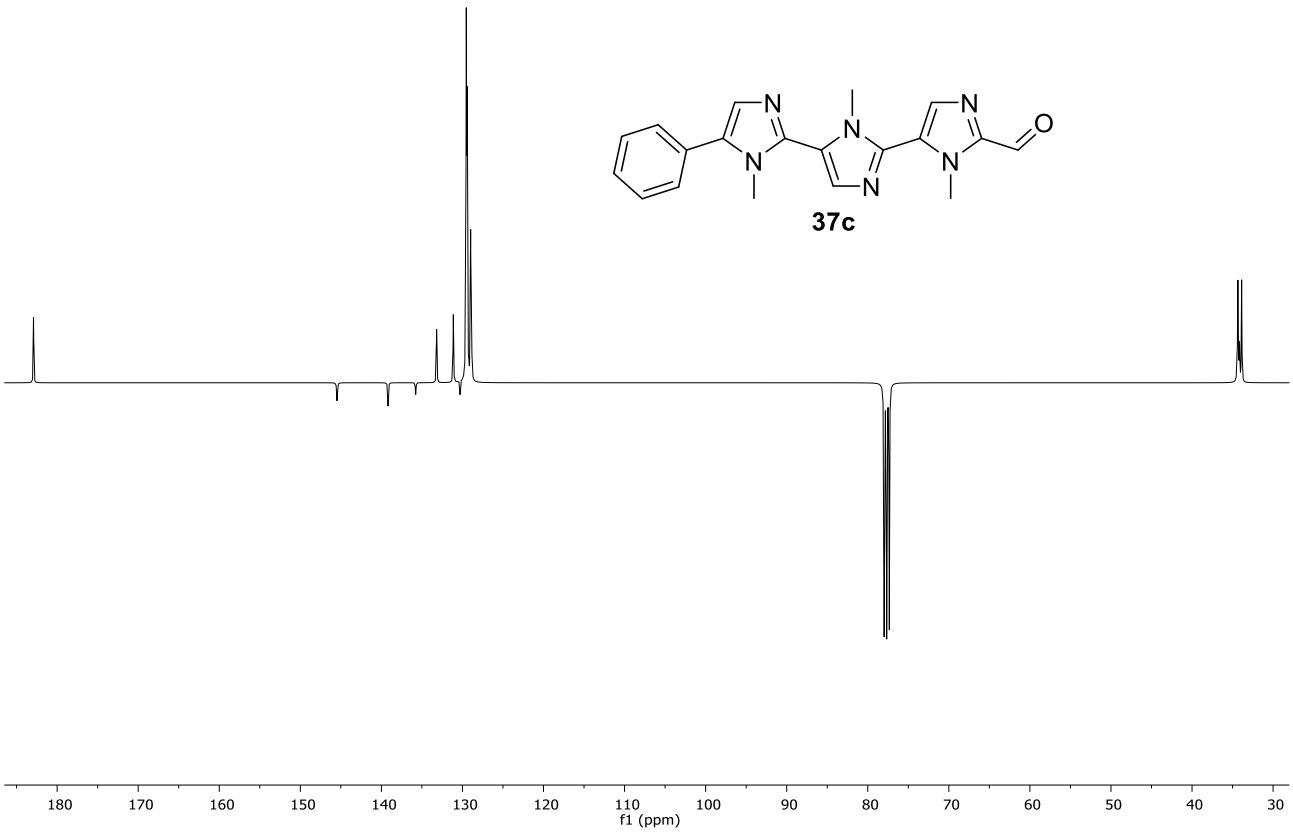

Chapter 3

Compound **38**: ^{1}H NMR (300 MHz, $CDCl_3$)

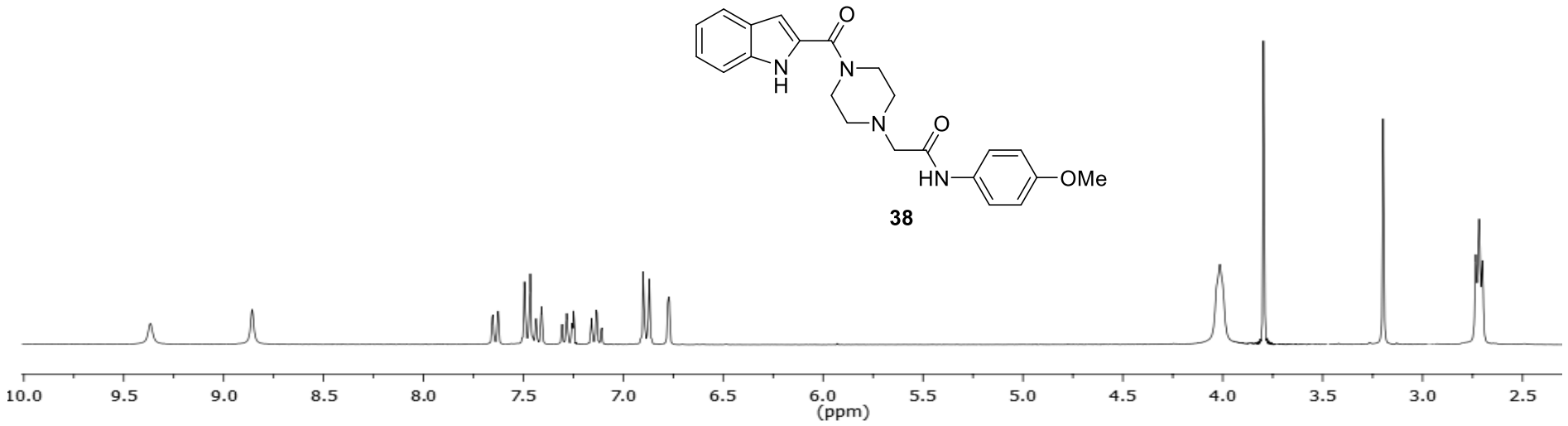

Compound **38**: ^{13}C NMR (75 MHz, $CDCl_3$)

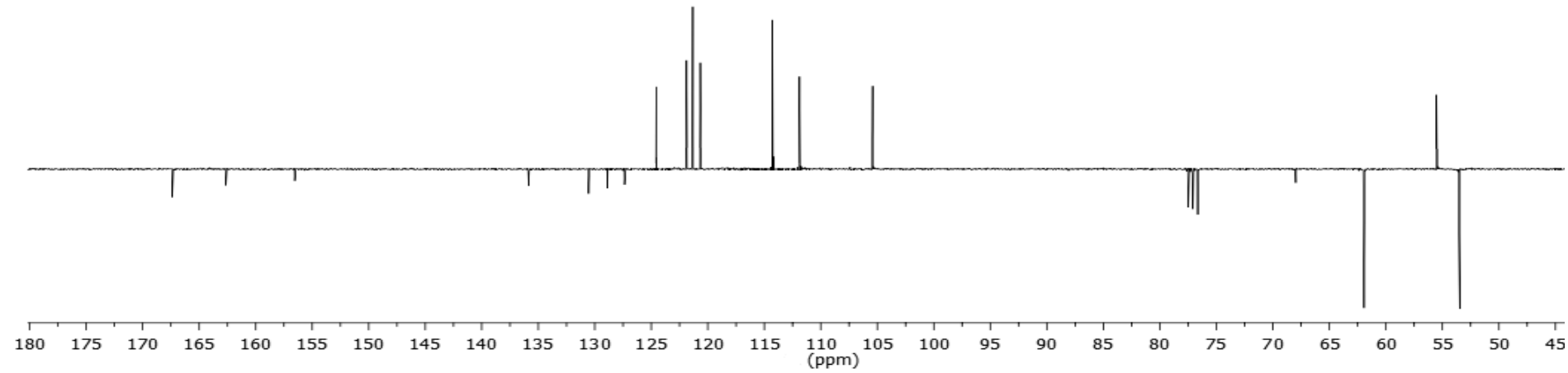

Compound **39**: ^{1}H NMR (300 MHz, $CDCl_3$)

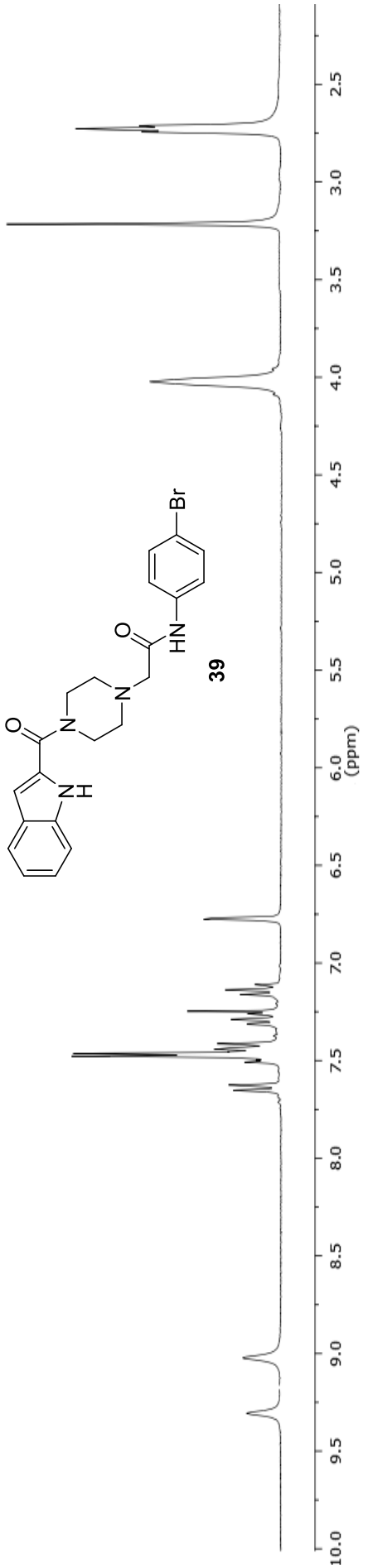

Compound **39**: ^{13}C NMR (75 MHz, DMF-d_7)

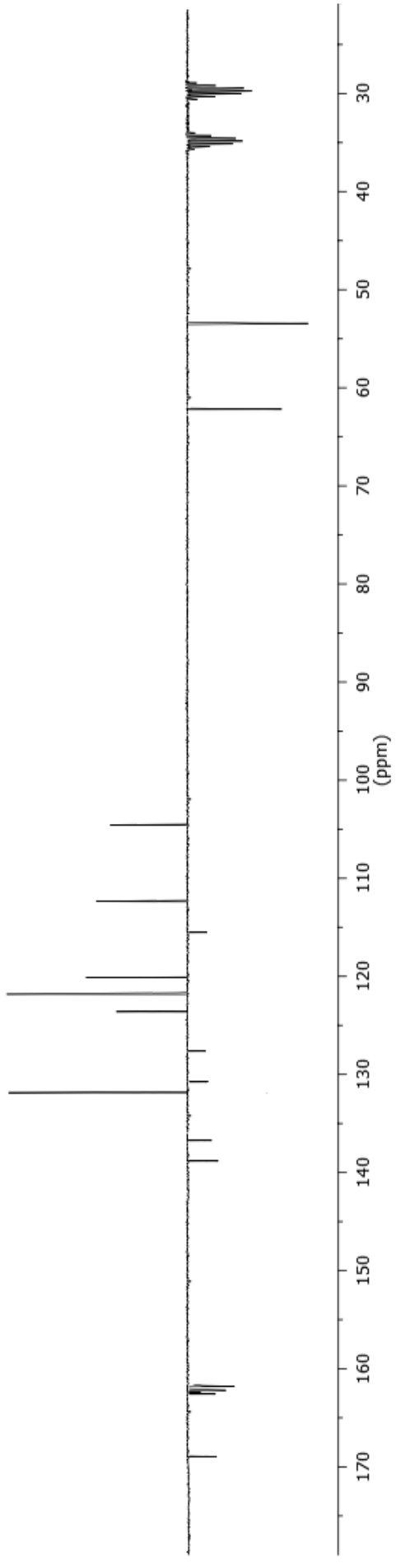

Compound **40**: ^{1}H NMR (300 MHz, $CDCl_3$)

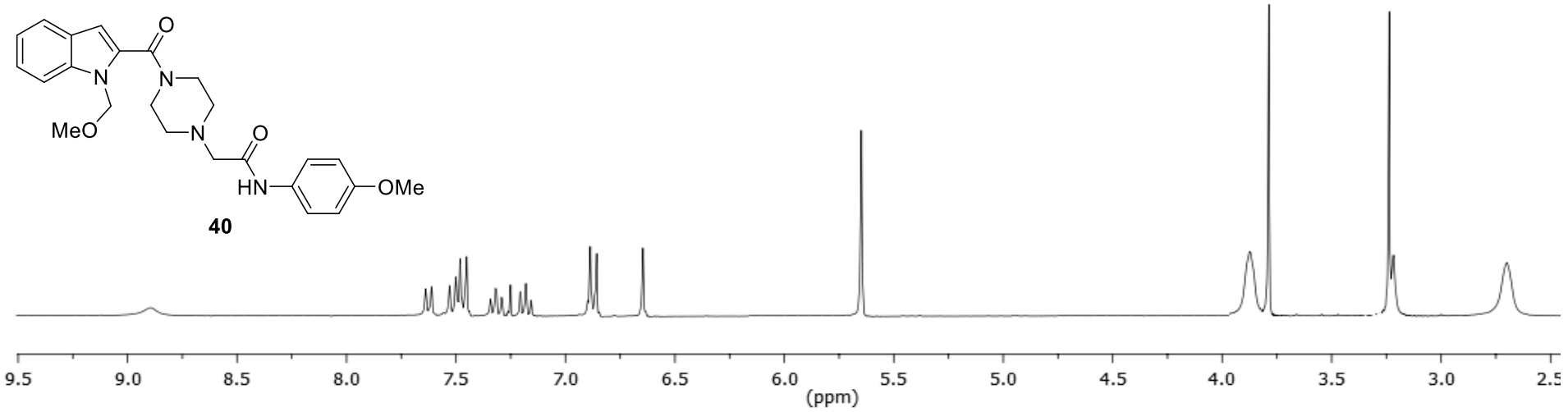

Compound **40**: ^{13}C NMR (75 MHz, $CDCl_3$)

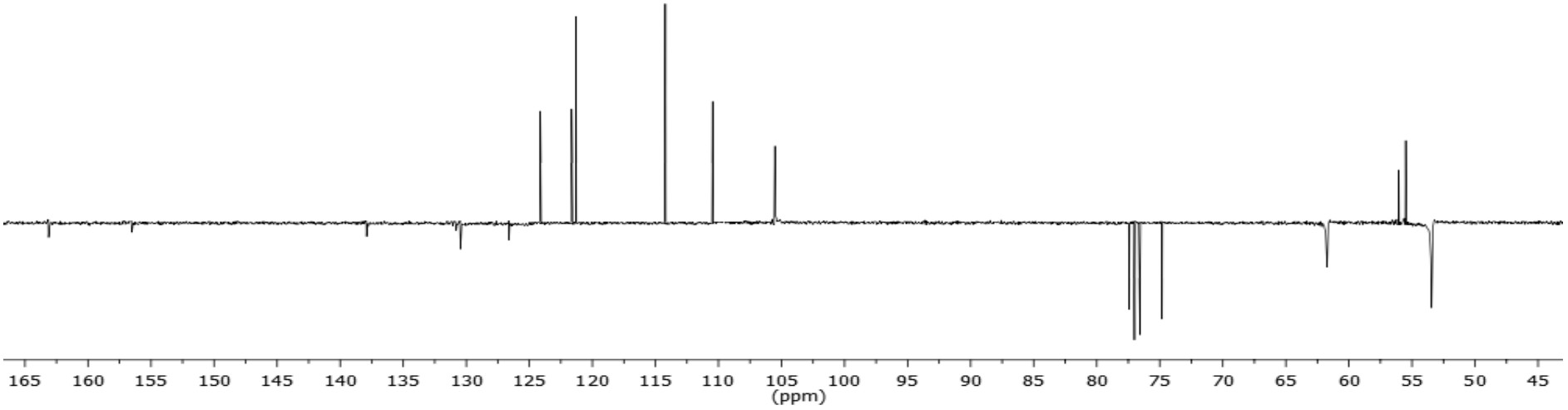

Compound **41**: ^{1}H NMR (400 MHz, $CDCl_3$)

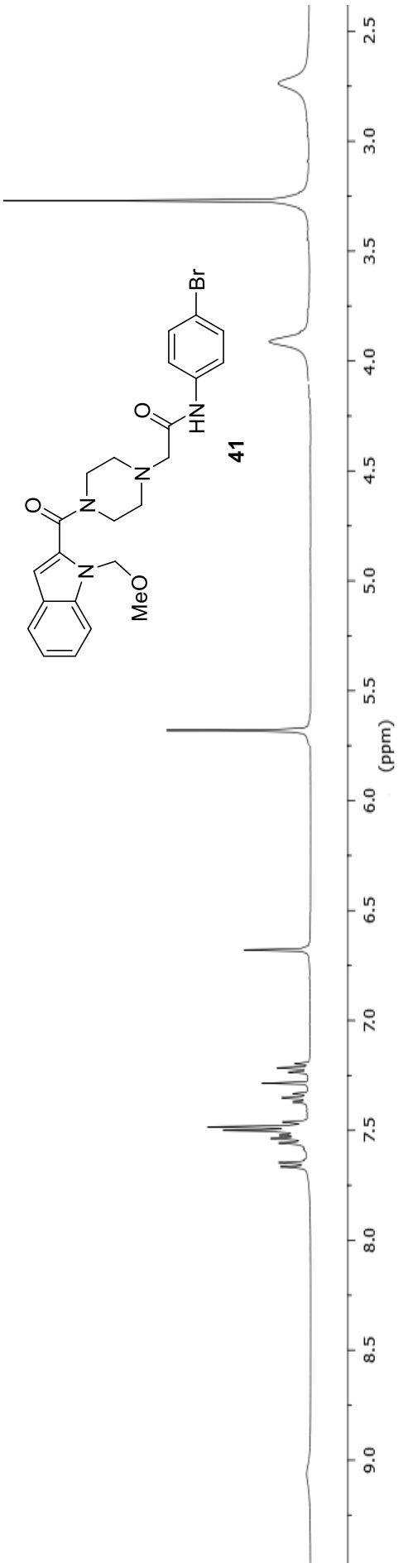

Compound **41**: ^{13}C NMR (100 MHz, $CDCl_3$)

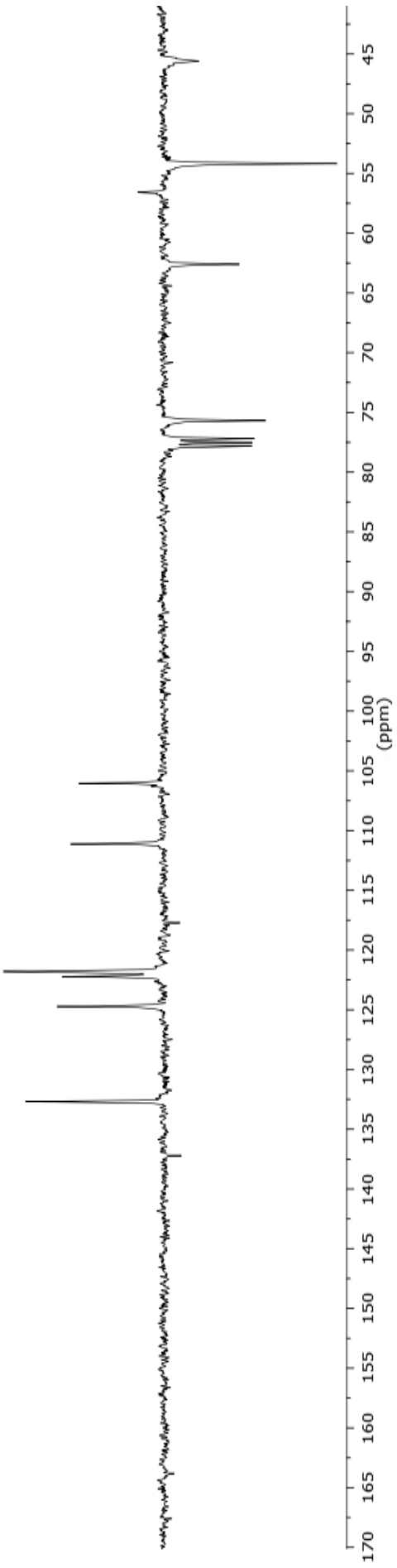

Compound **42**: ^{1}H NMR (300 MHz, $CDCl_3$)

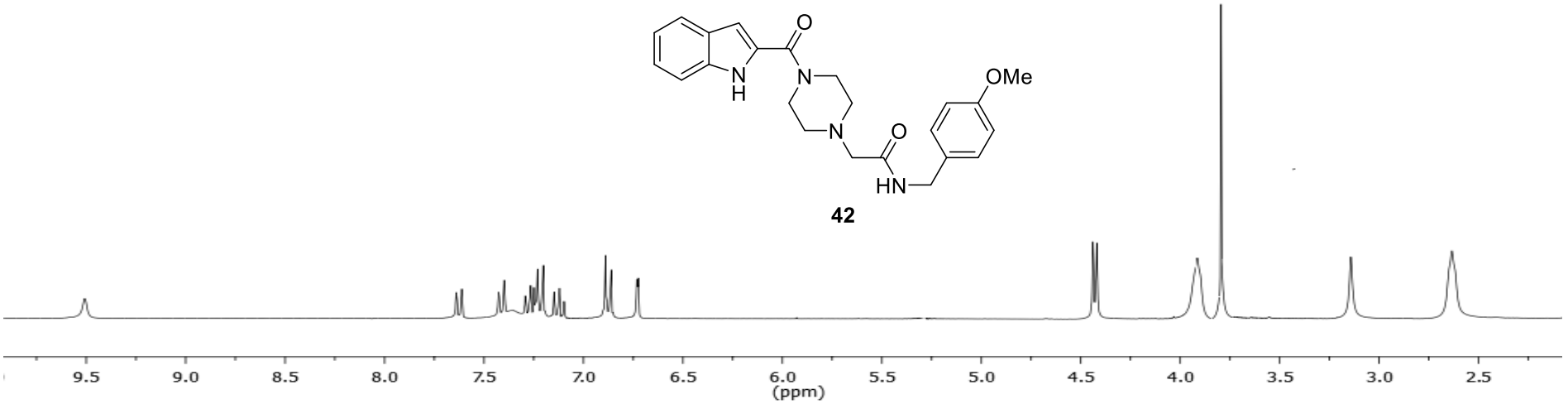

42

Compound **42**: ^{13}C NMR (75 MHz, $CDCl_3$)

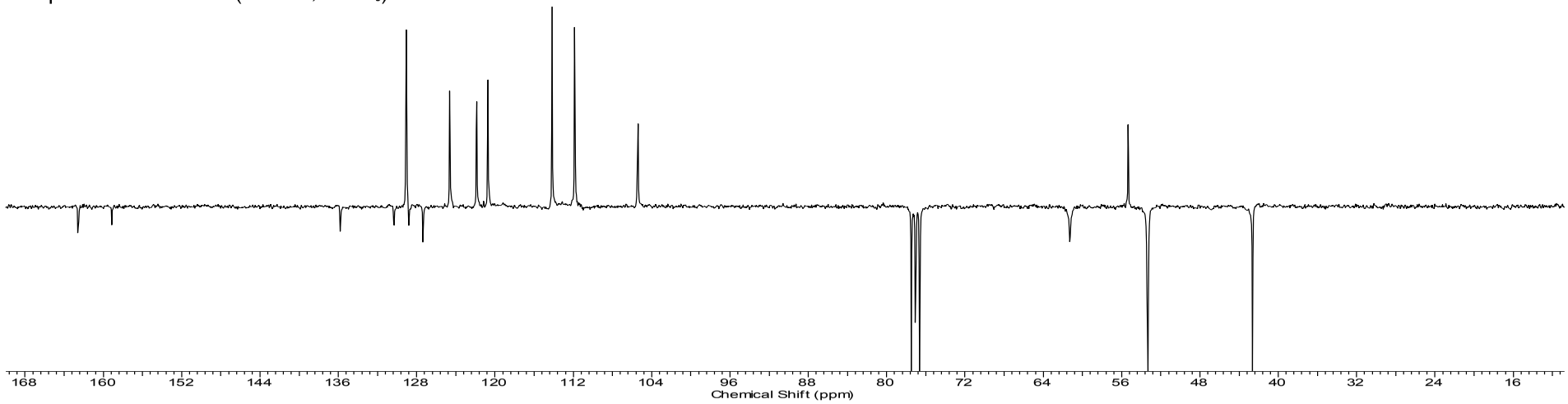

Compound **43**: ^{1}H NMR (300 MHz, $CDCl_3$)

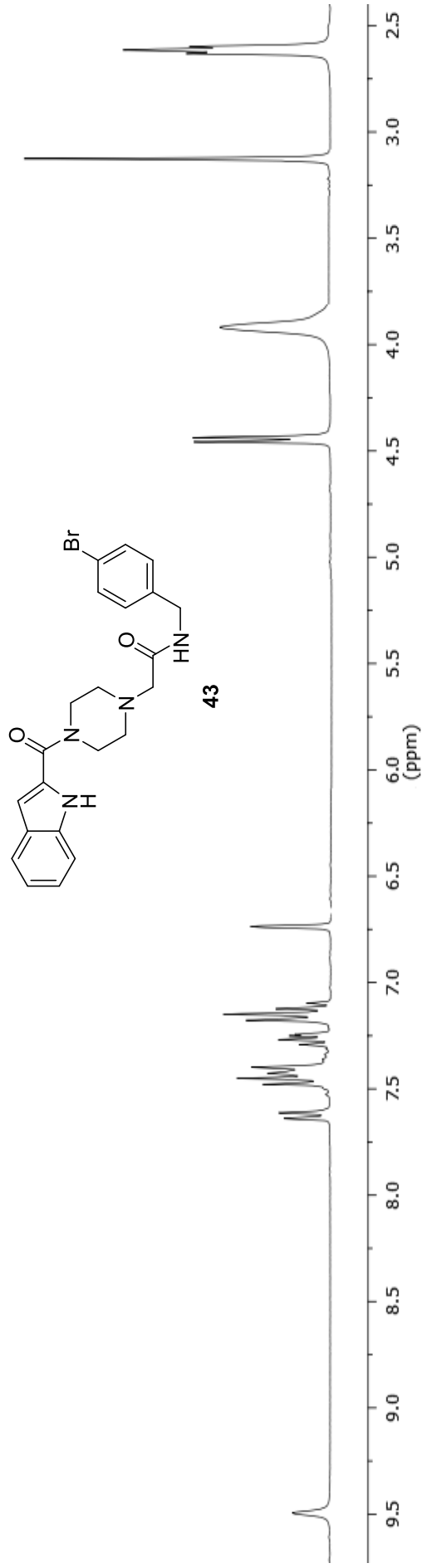

Compound **43**: ^{13}C NMR (75 MHz, $CDCl_3$)

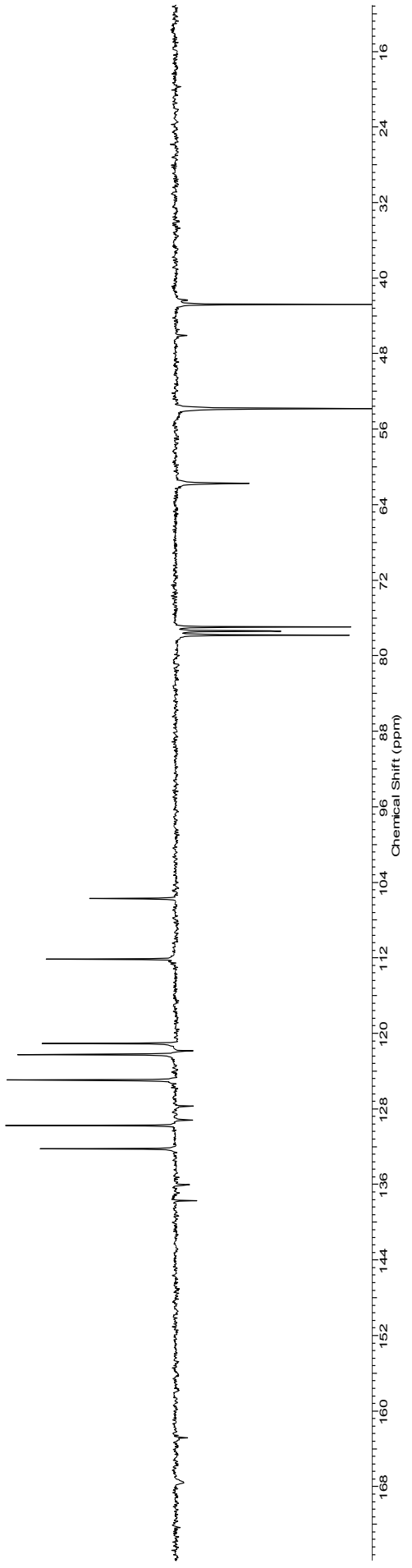

Compound **44**: ^{1}H NMR (300 MHz, $CDCl_3$)

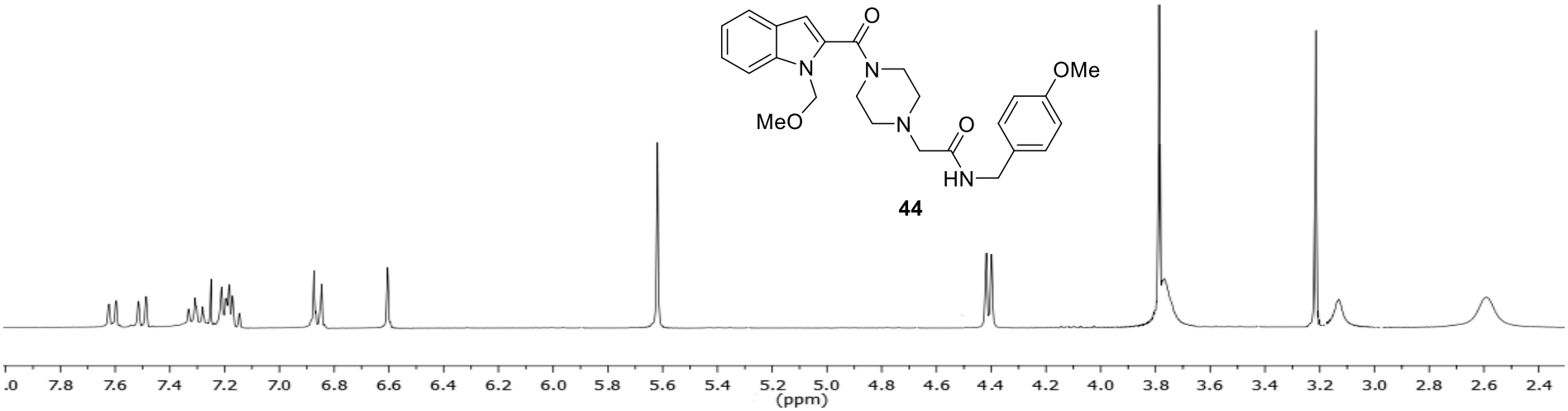

Compound **44**: ^{13}C NMR (75 MHz, $CDCl_3$)

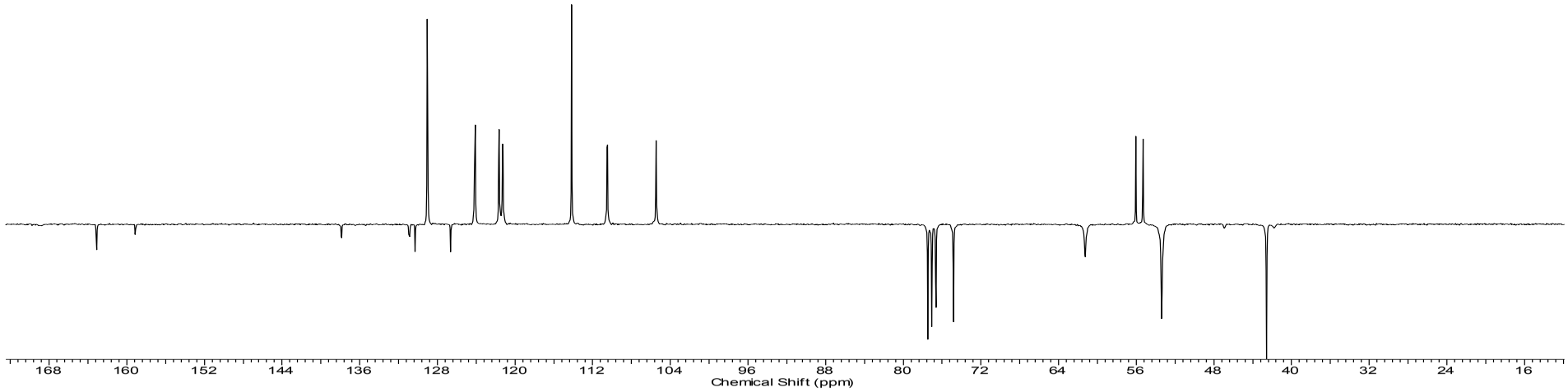

Compound **45**: ^{1}H NMR (300 MHz, $CDCl_3$)

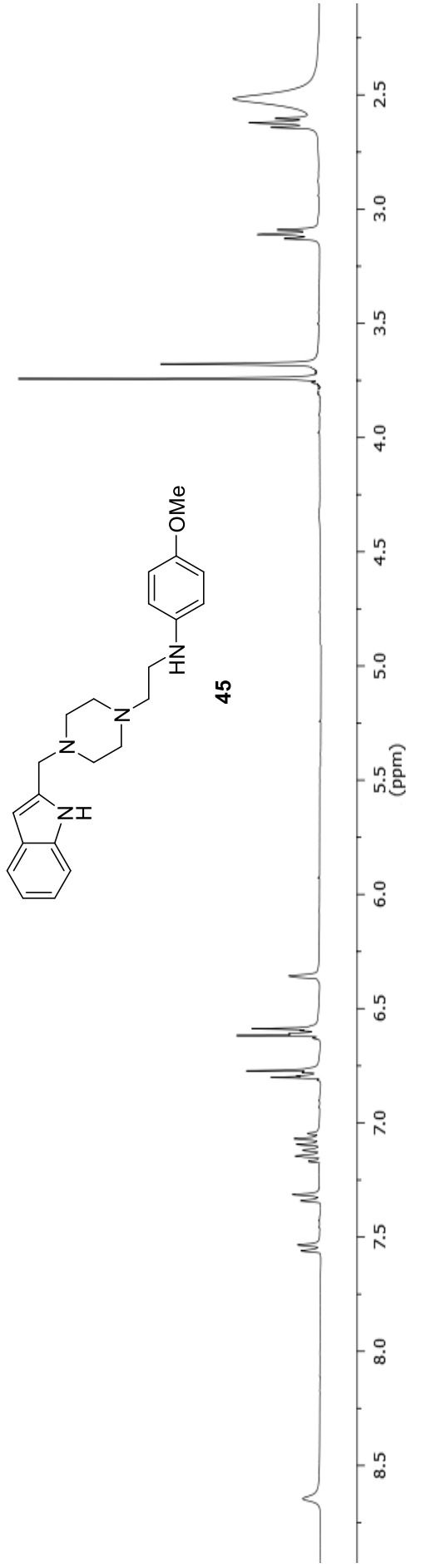

Compound **45**: ^{13}C NMR (75 MHz, $CDCl_3$)

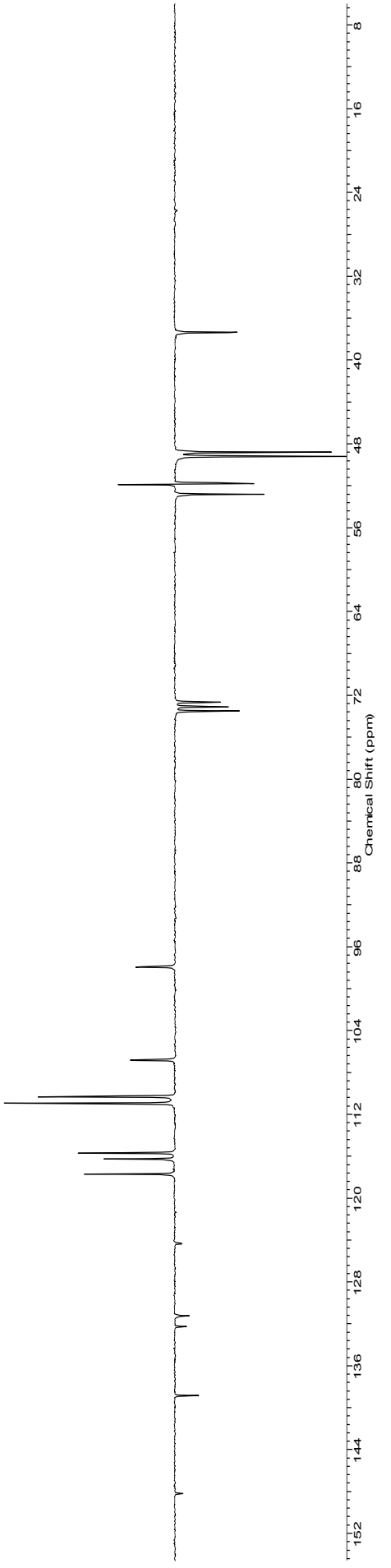

Compound **46**: ^{1}H NMR (300 MHz, $CDCl_3$)

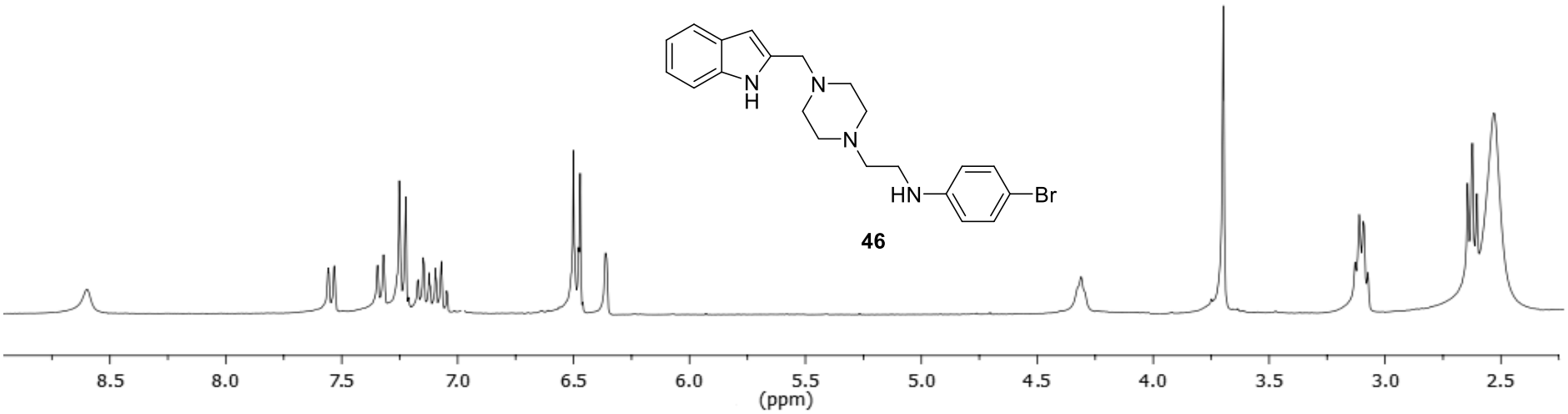

Compound **46**: ^{13}C NMR (75 MHz, $CDCl_3$)

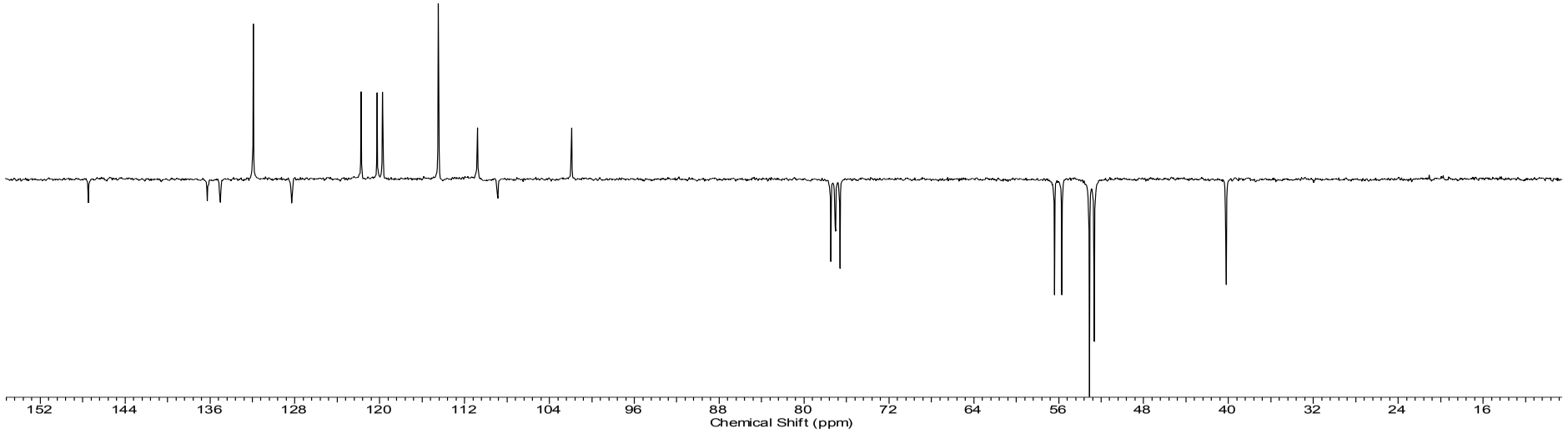

Compound **47**: ^{1}H NMR (300 MHz, $CDCl_3$)

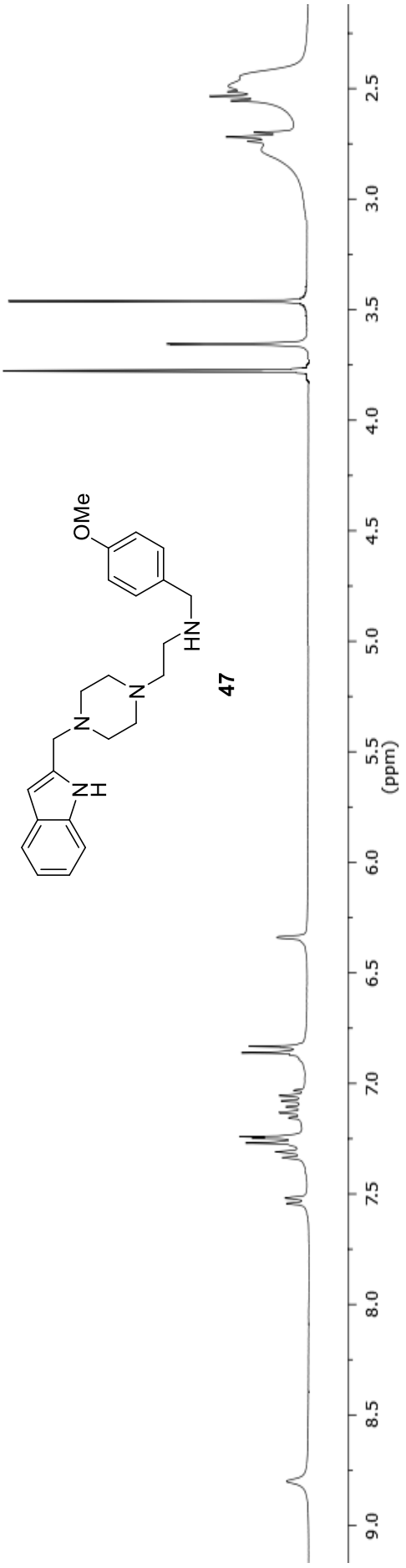

Compound **47**: ^{13}C NMR (75 MHz, $CDCl_3$)

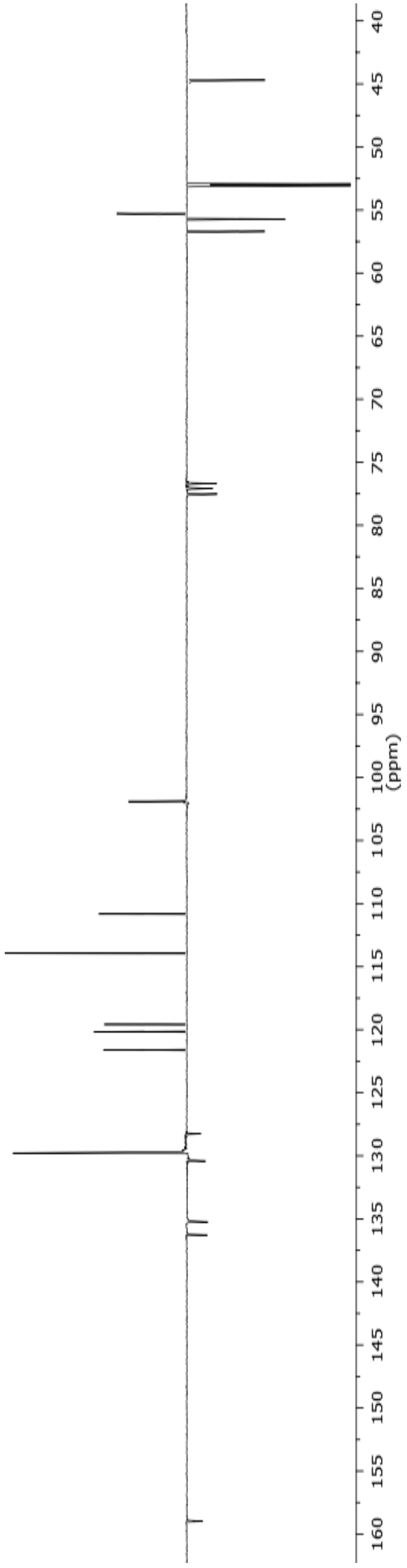

Compound **48**: ^{1}H NMR (300 MHz, $CDCl_3$)

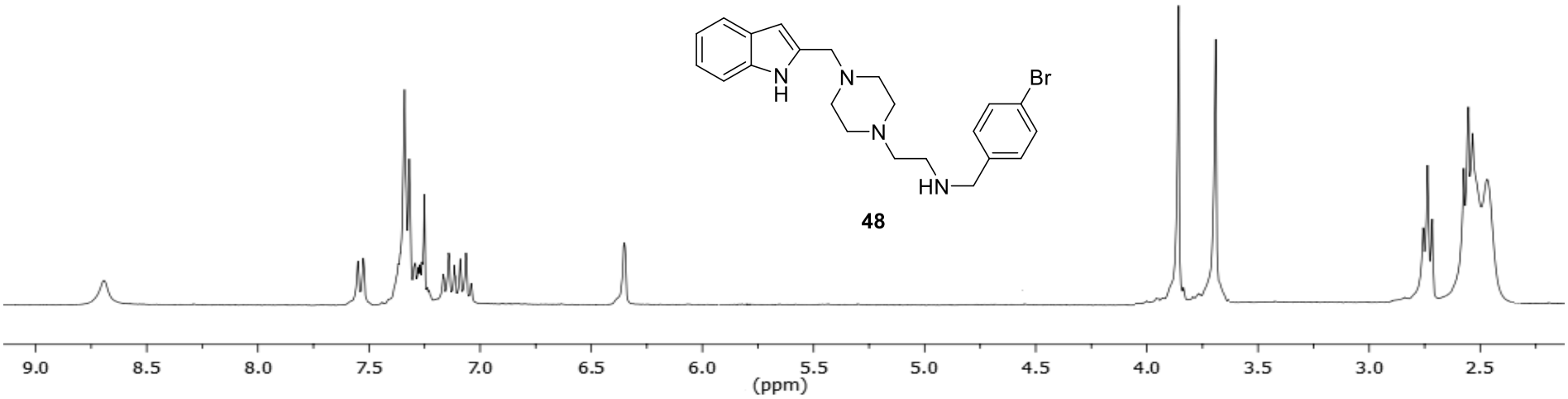

48

Compound **48**: ^{13}C NMR (75 MHz, $CDCl_3$)

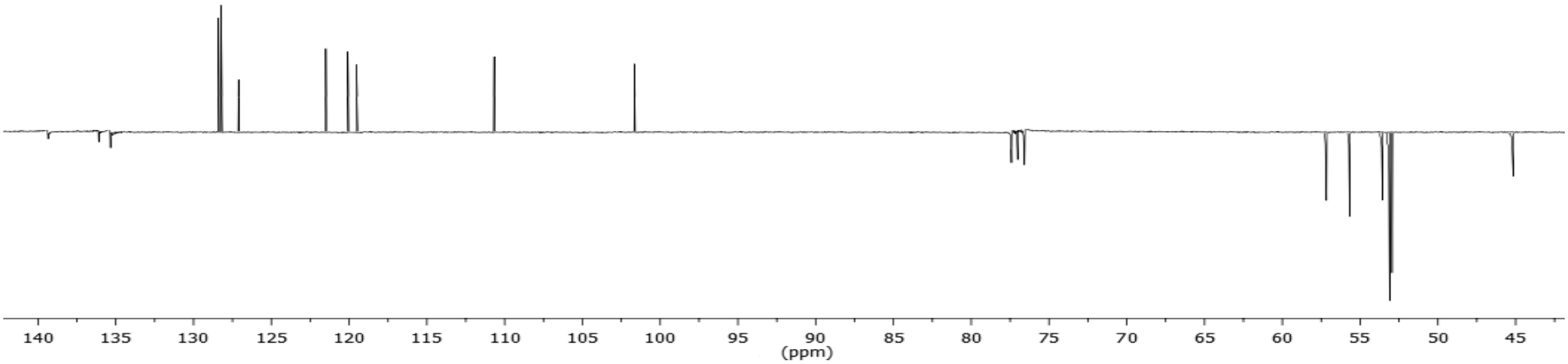

Compound **49**: ^{1}H NMR (300 MHz, $CDCl_3$)

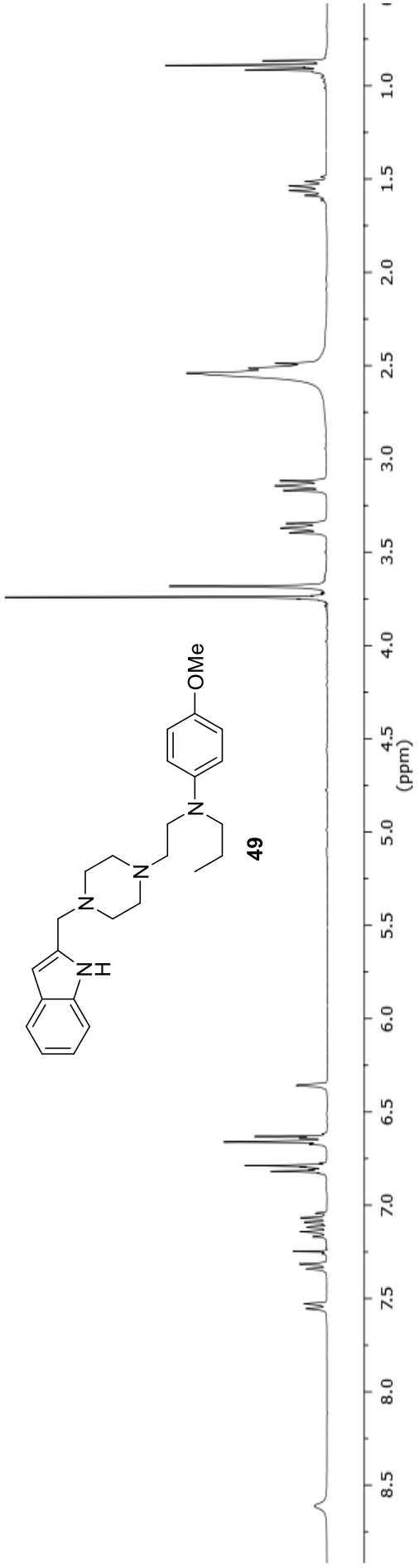

Compound **49**: ^{13}C NMR (75 MHz, $CDCl_3$)

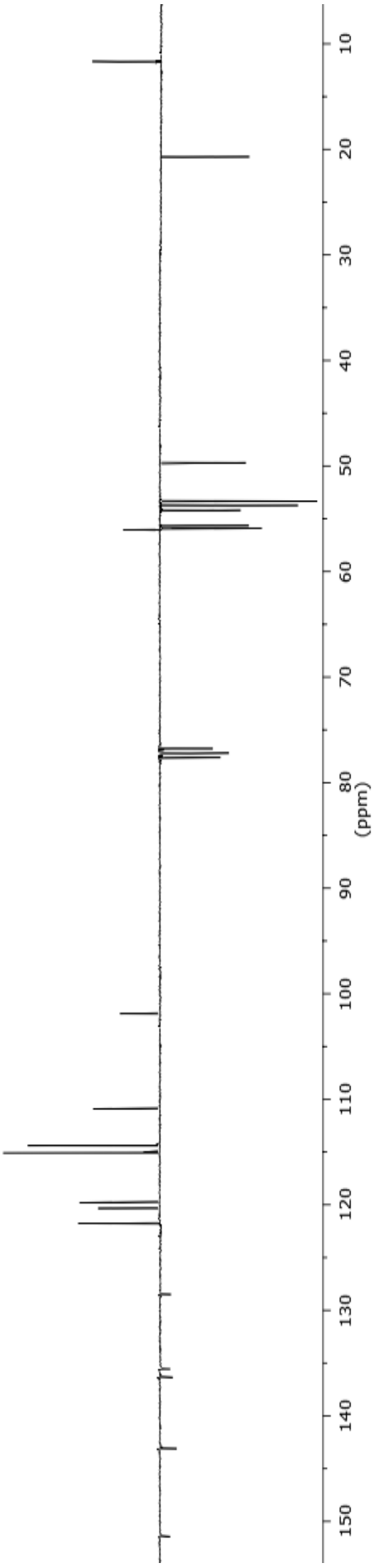

Compound **50**: ^{1}H NMR (400 MHz, $CDCl_3$)

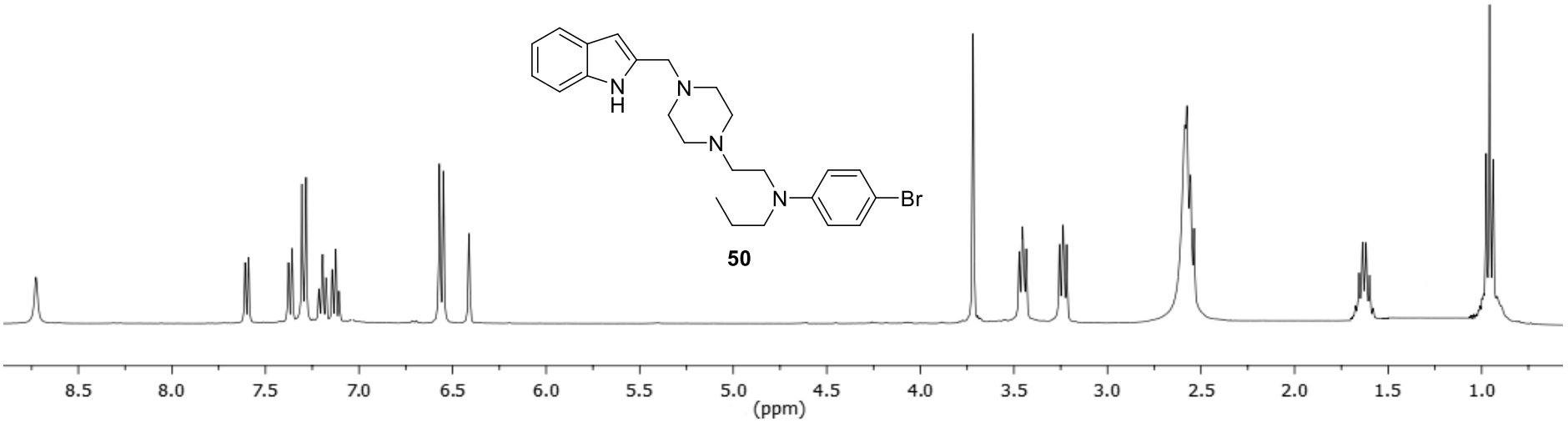

50

Compound **50**: ^{13}C NMR (100 MHz, $CDCl_3$)

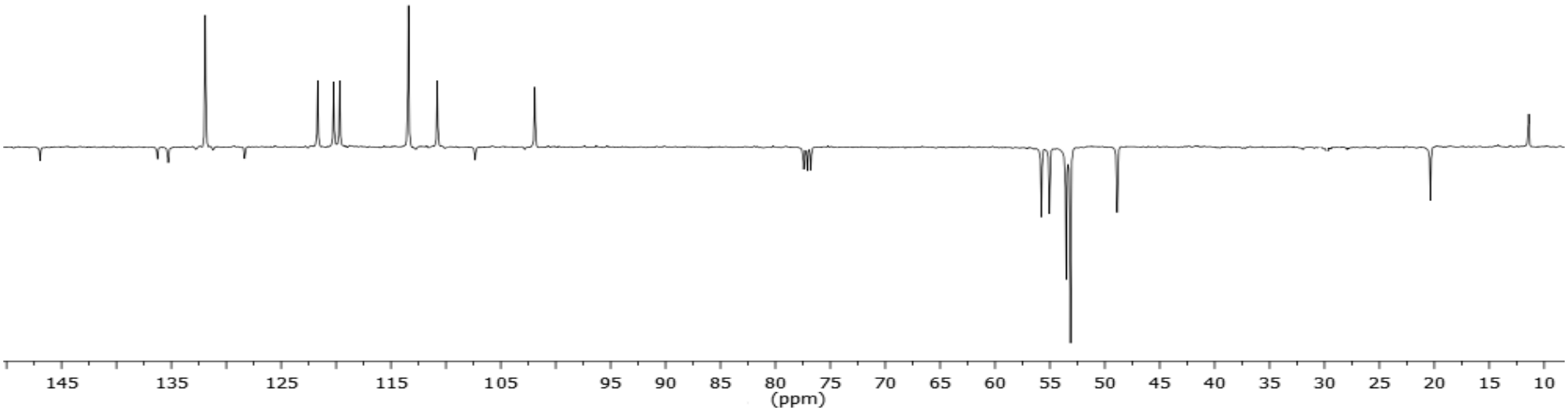

Compound **51**: ^{1}H NMR (400 MHz, $CDCl_3$)

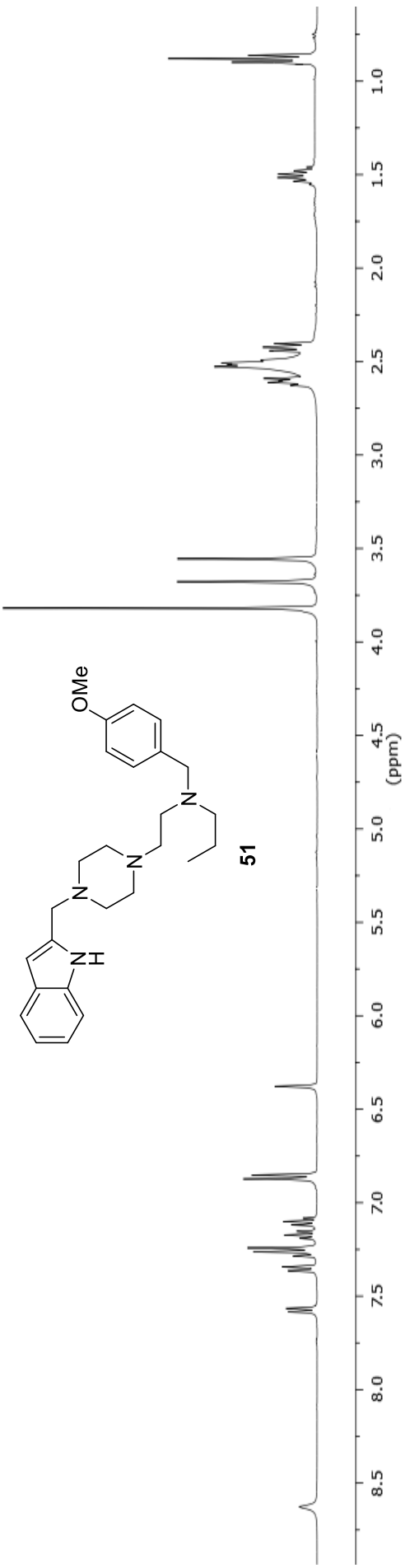

Compound **51**: ^{13}C NMR (100 MHz, $CDCl_3$)

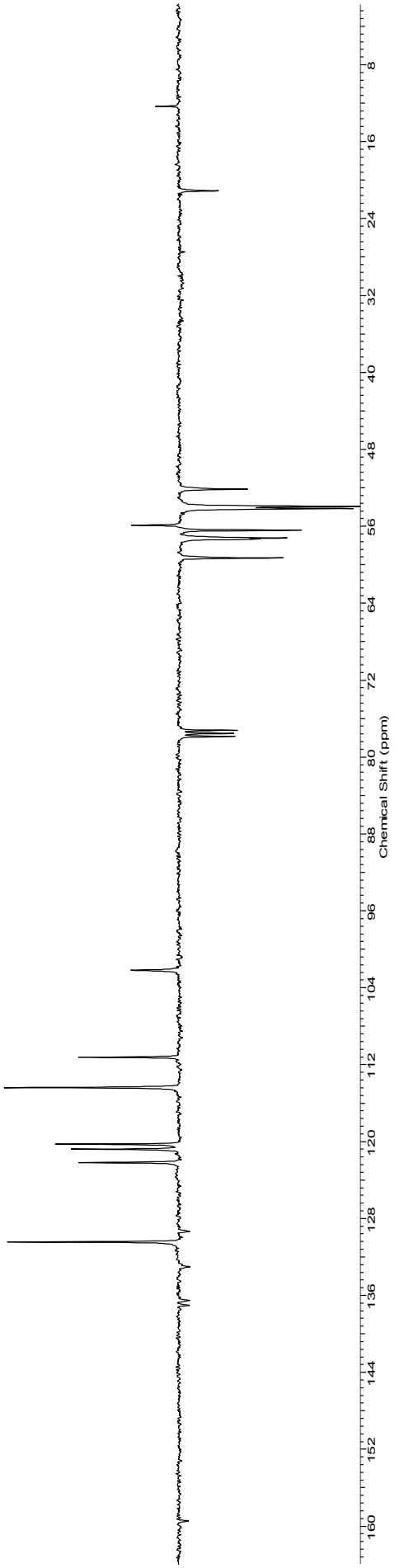

Compound **52**: ^{1}H NMR (400 MHz, $CDCl_3$)

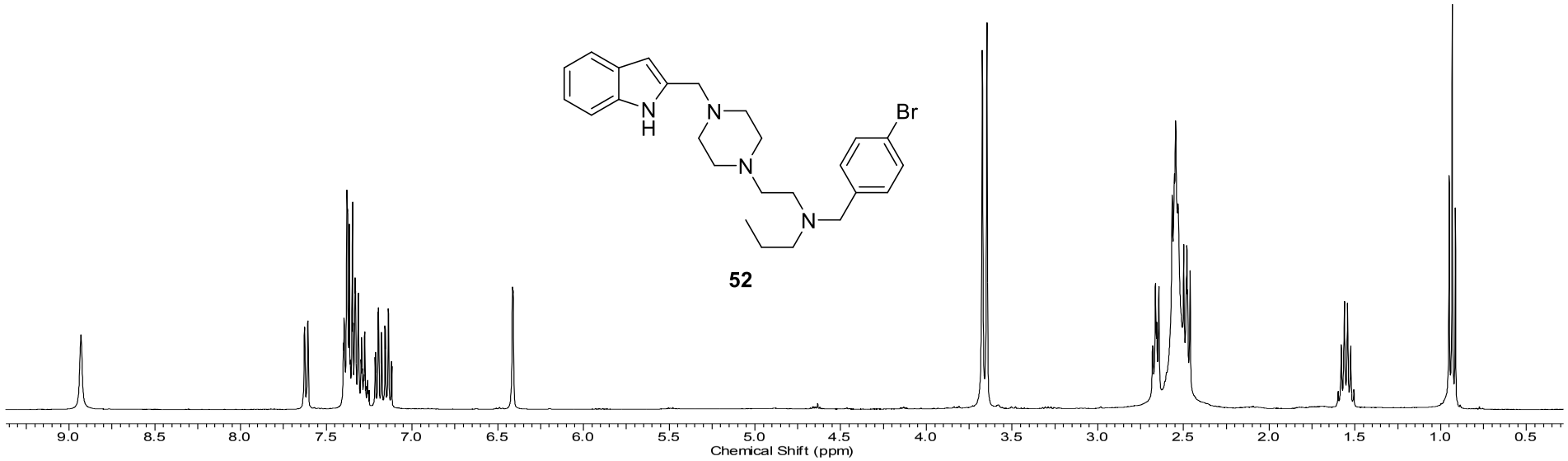

Compound **52**: ^{13}C NMR (100 MHz, $CDCl_3$)

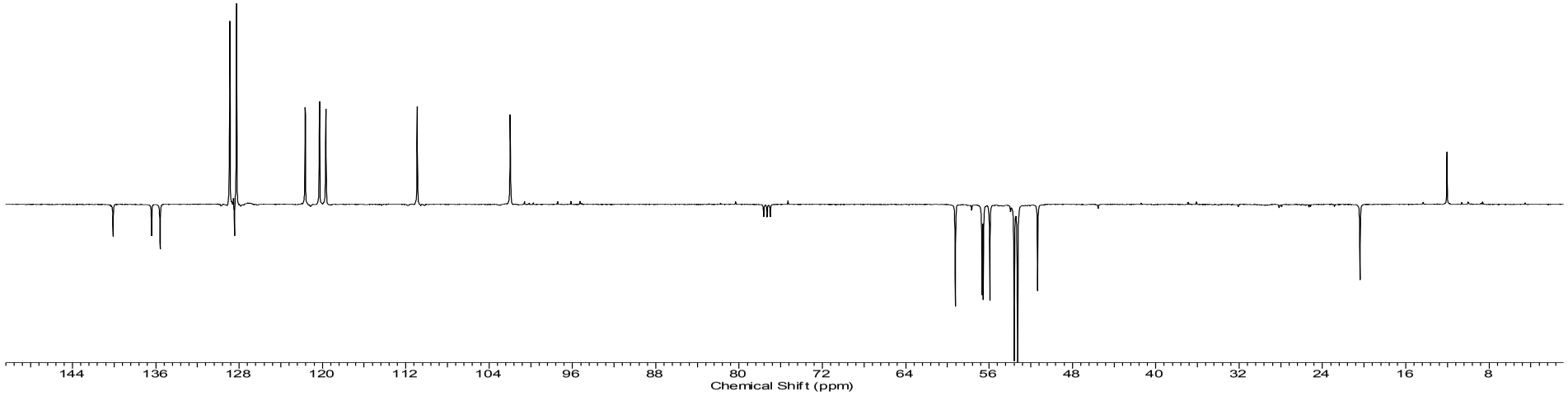

Compound **53**: ^{1}H NMR (400 MHz, $CDCl_3$)

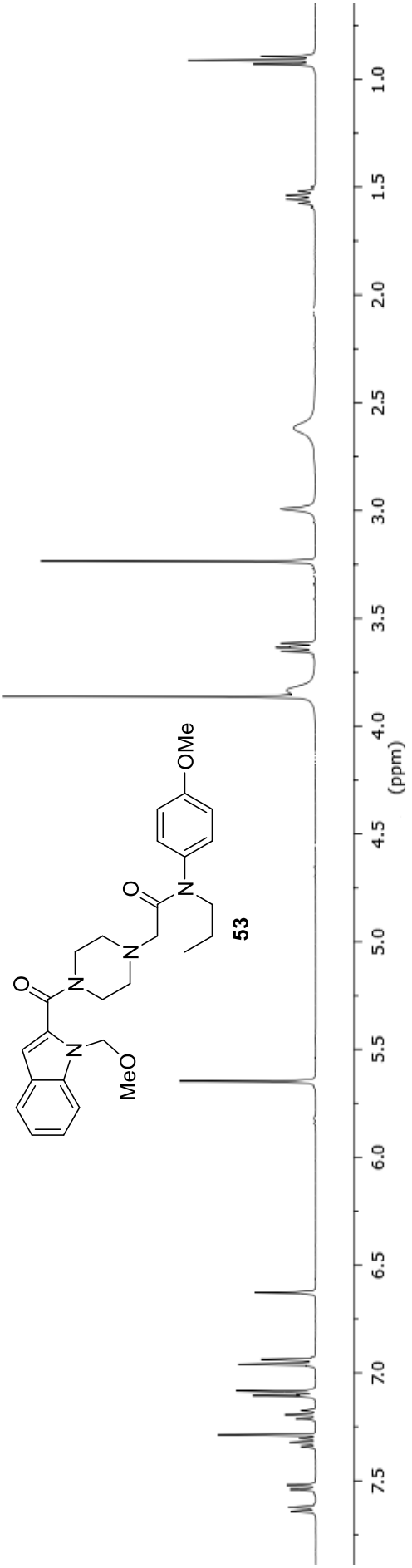

Compound **53**: ^{13}C NMR (100 MHz, $CDCl_3$)

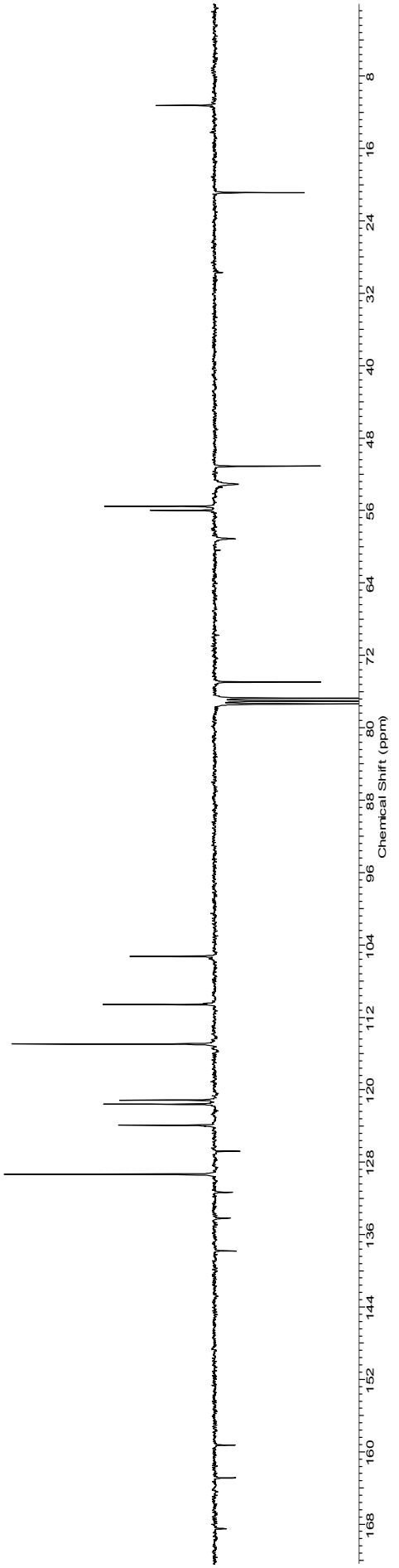

Compound **54**: ^{1}H NMR (400 MHz, $CDCl_3$)

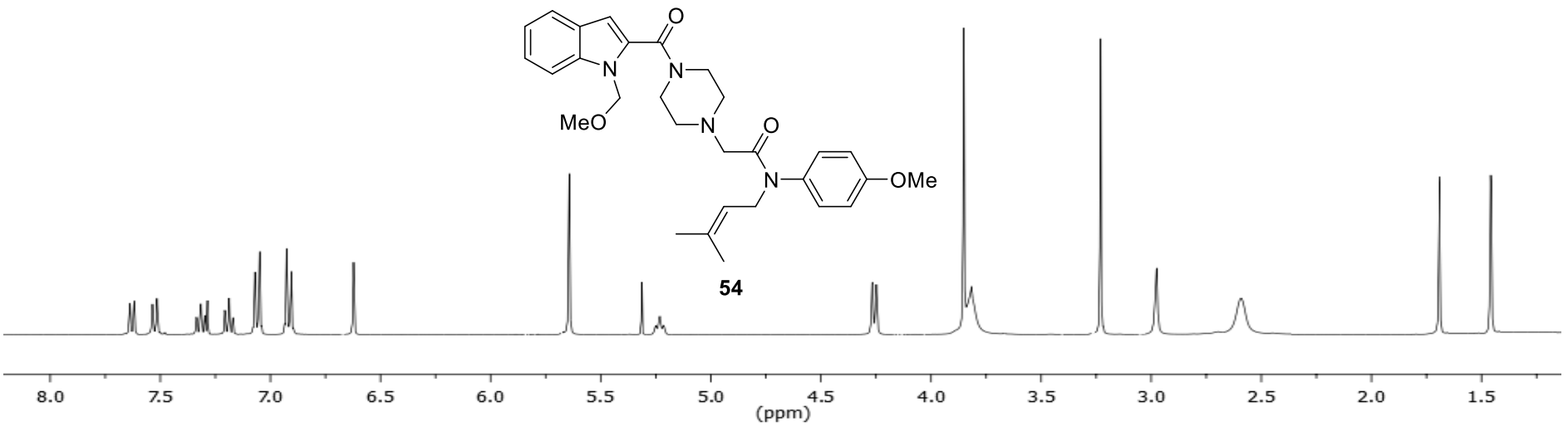

Compound **54**: ^{13}C NMR (100 MHz, $CDCl_3$)

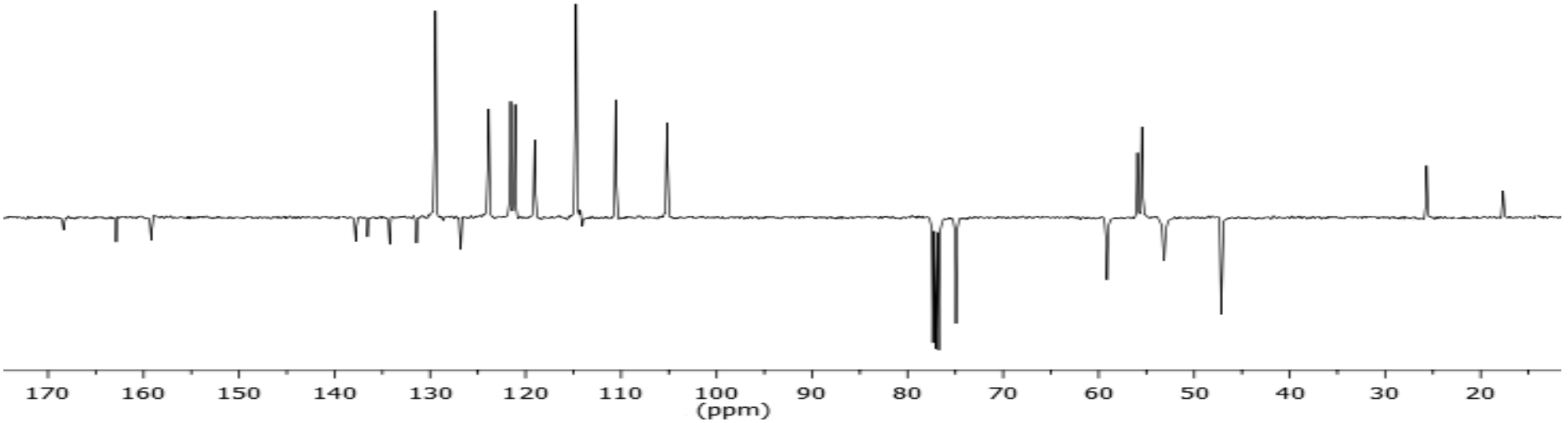

Compound **55**: ^{1}H NMR (300 MHz, $CDCl_3$)

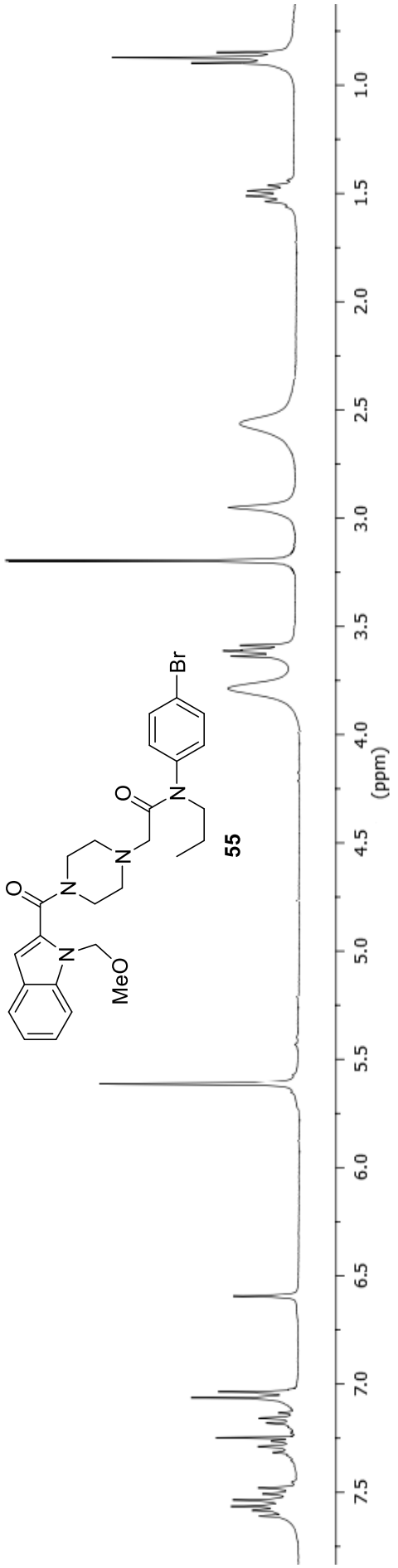

Compound **55**: ^{13}C NMR (75 MHz, $CDCl_3$)

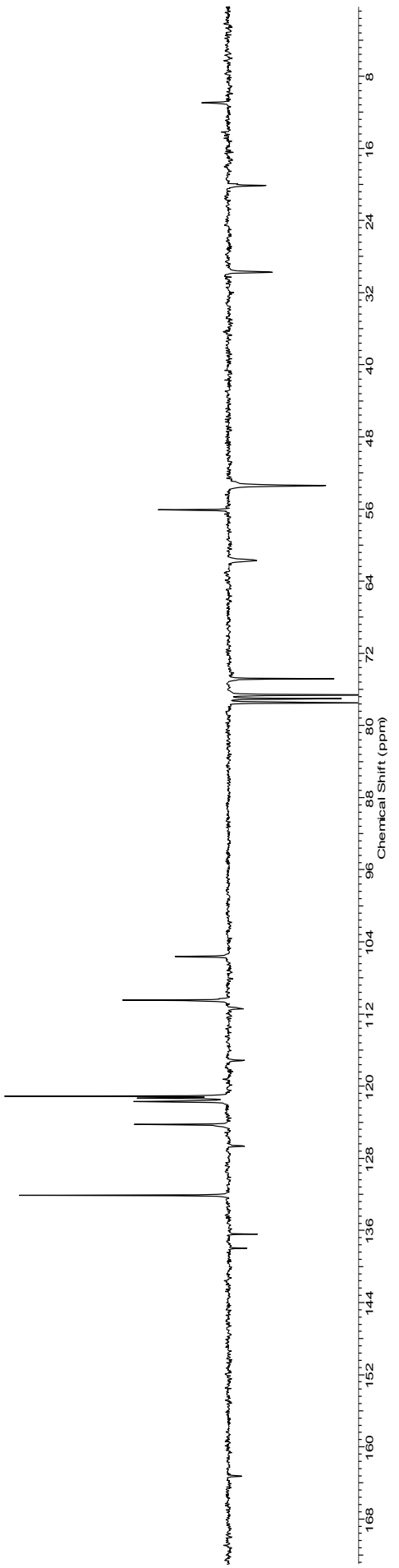

Compound **56**: ^{1}H NMR (300 MHz, $CDCl_3$)

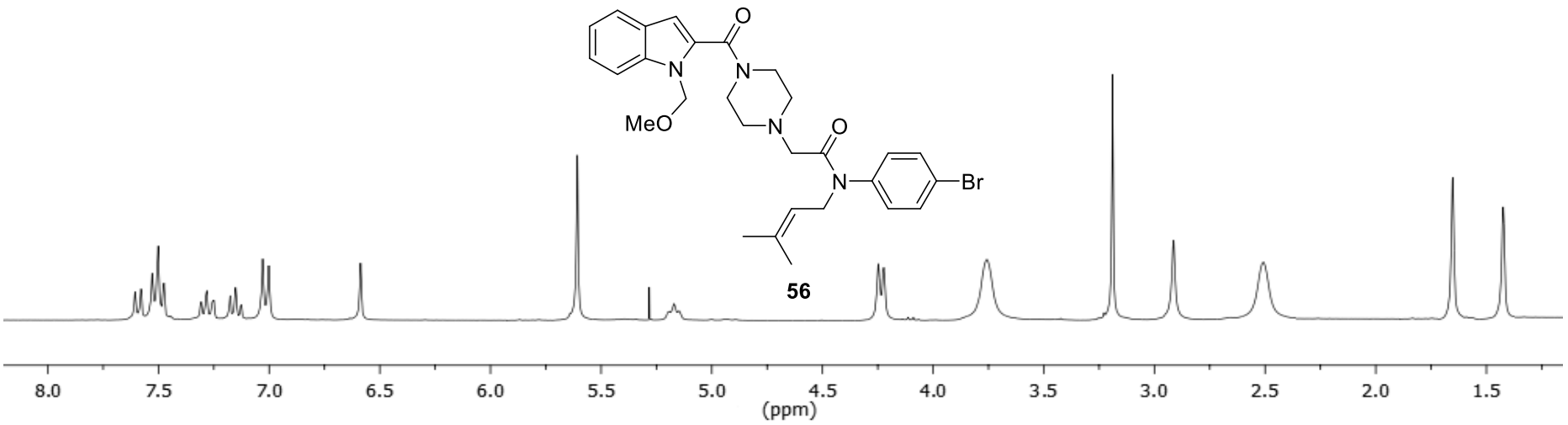

Compound **56**: ^{13}C NMR (75 MHz, $CDCl_3$)

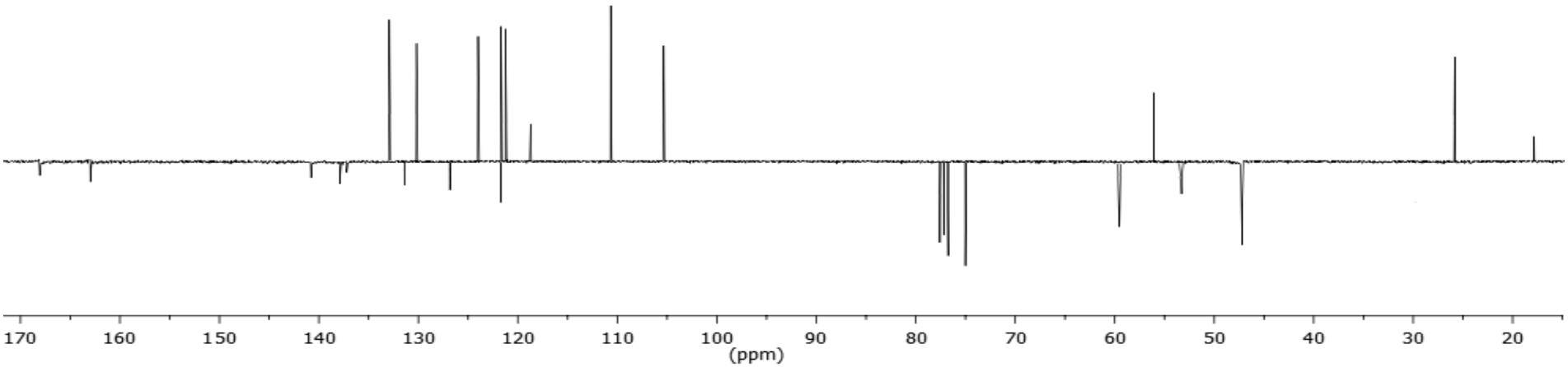

Compound **57**: ^{1}H NMR (300 MHz, $CDCl_3$)

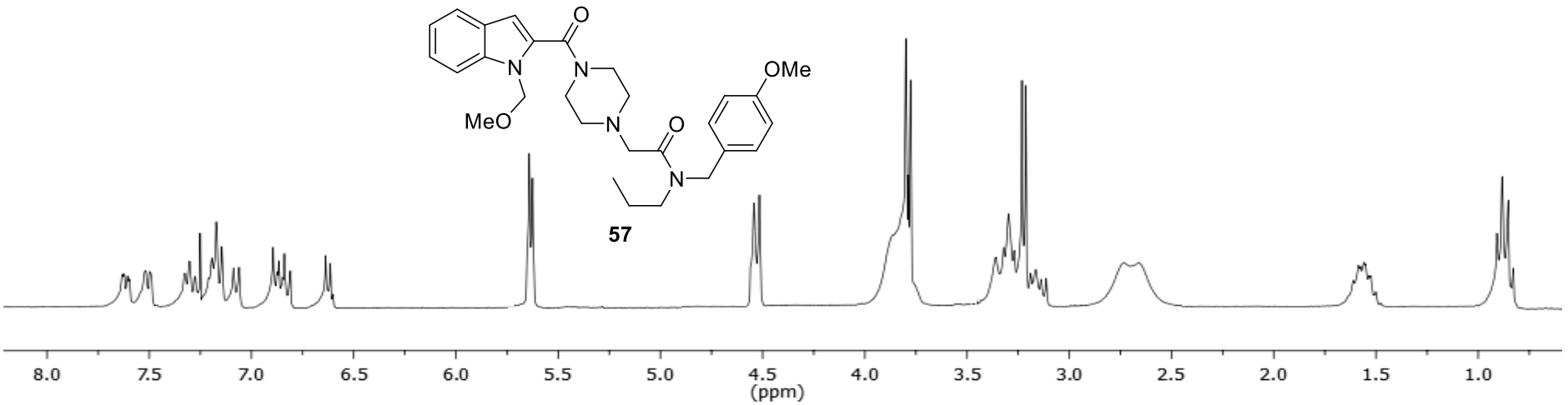

57

Compound **57**: ^{13}C NMR (75 MHz, $CDCl_3$)

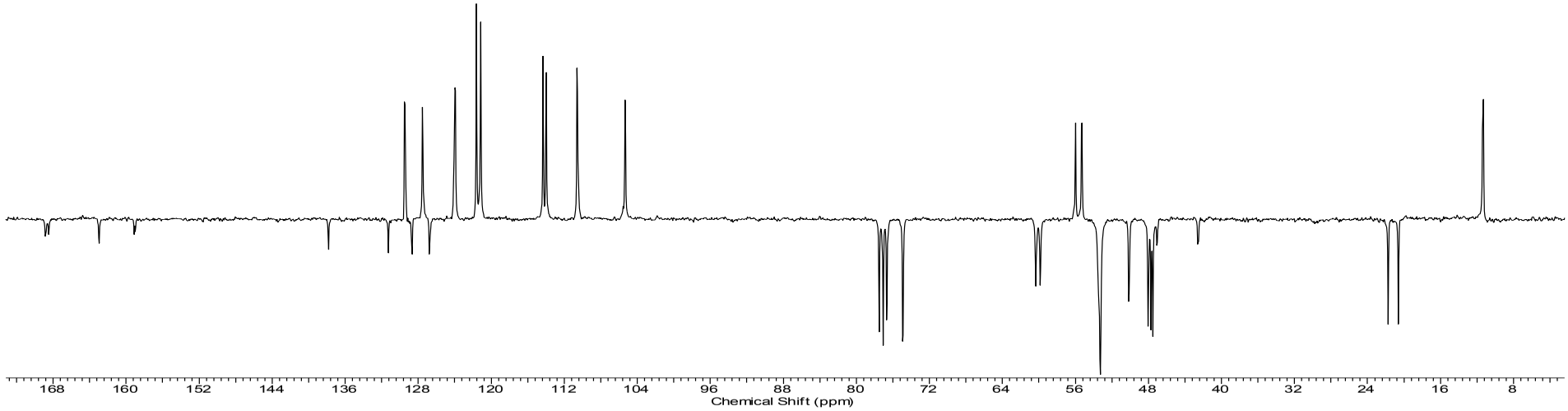

Compound **58**: ^{1}H NMR (300 MHz, $CDCl_3$)

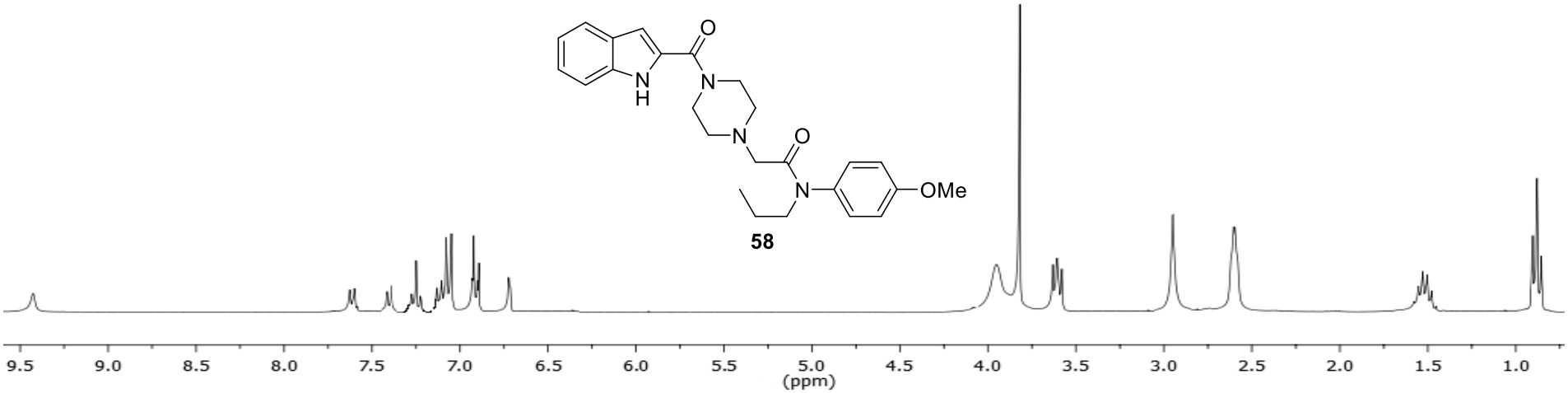

Compound **58**: ^{13}C NMR (75 MHz, $CDCl_3$)

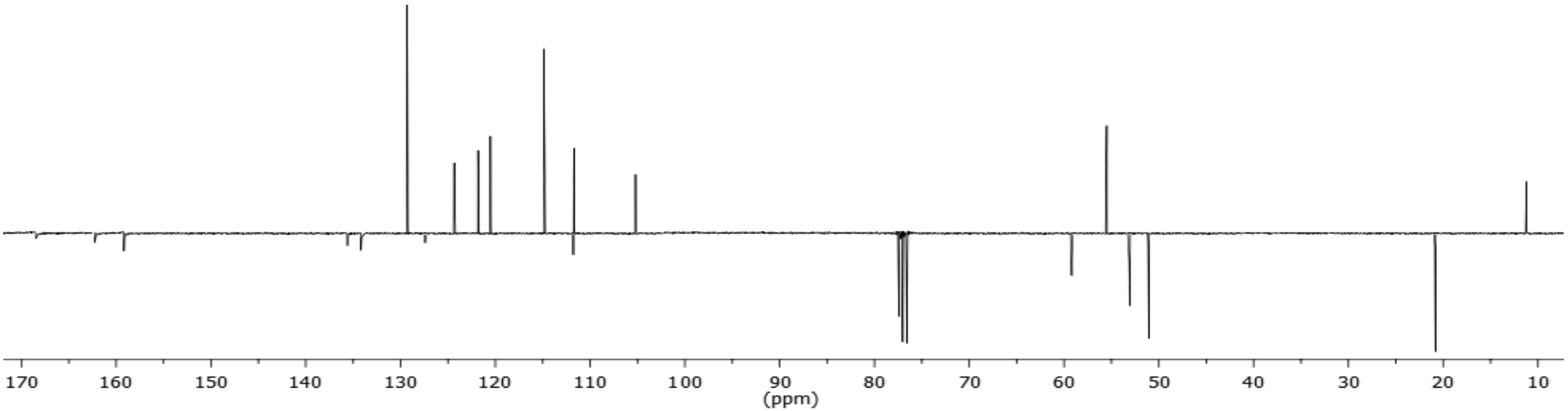

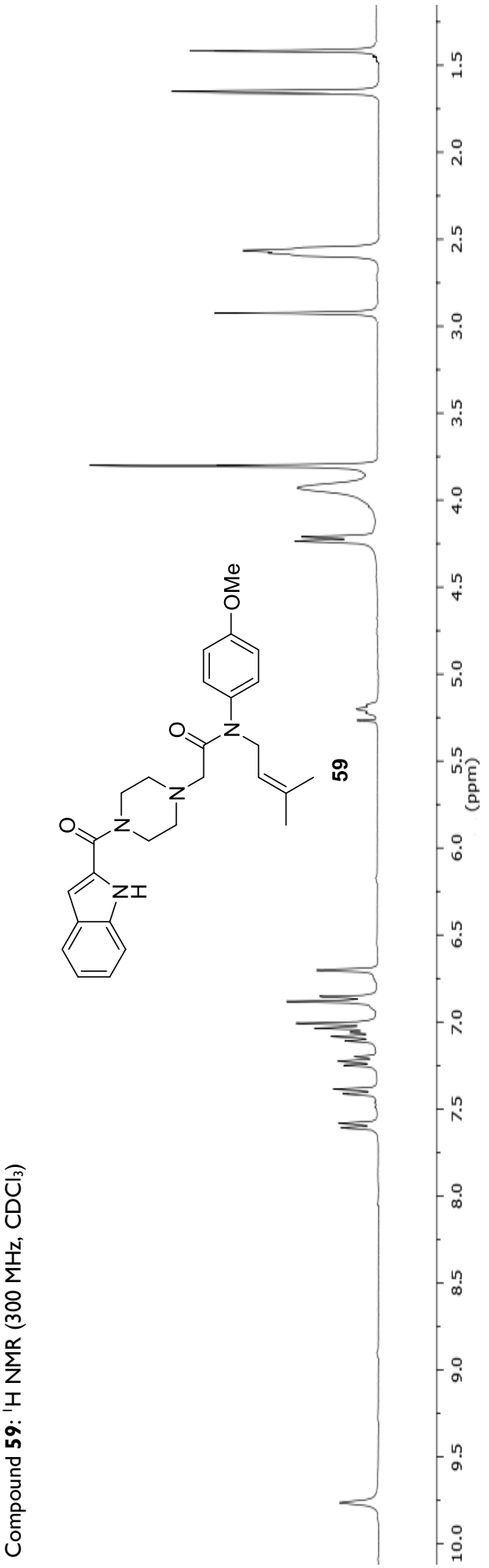

Compound **59**: ^{1}H NMR (300 MHz, $CDCl_3$)

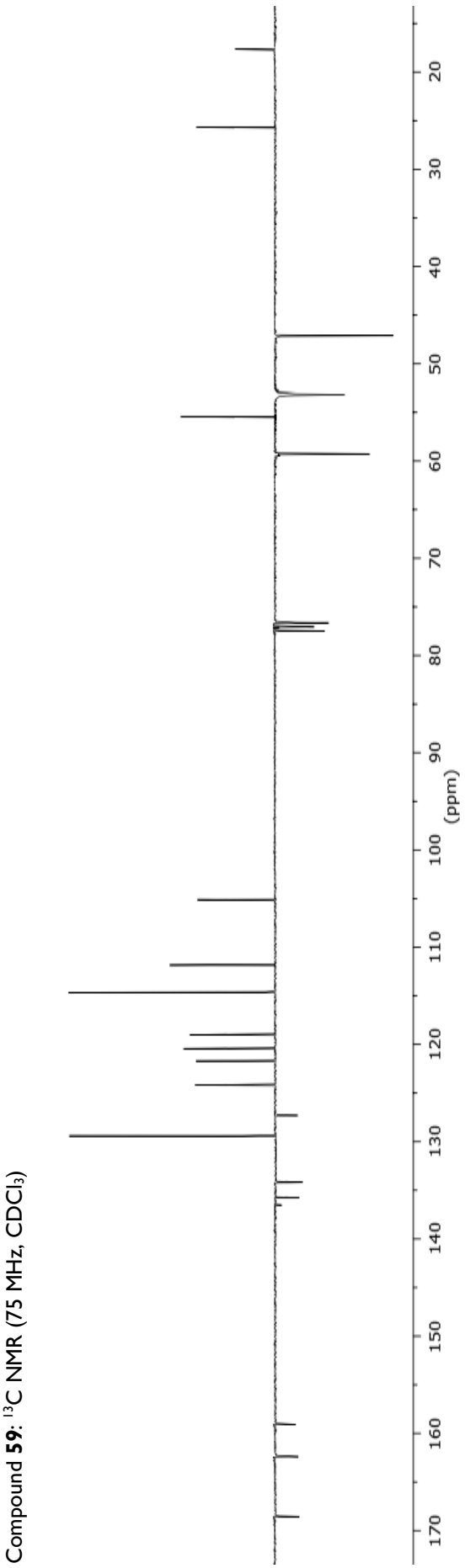

Compound **59**: ^{13}C NMR (75 MHz, $CDCl_3$)

Compound **60**: ^{1}H NMR (300 MHz, $CDCl_3$)

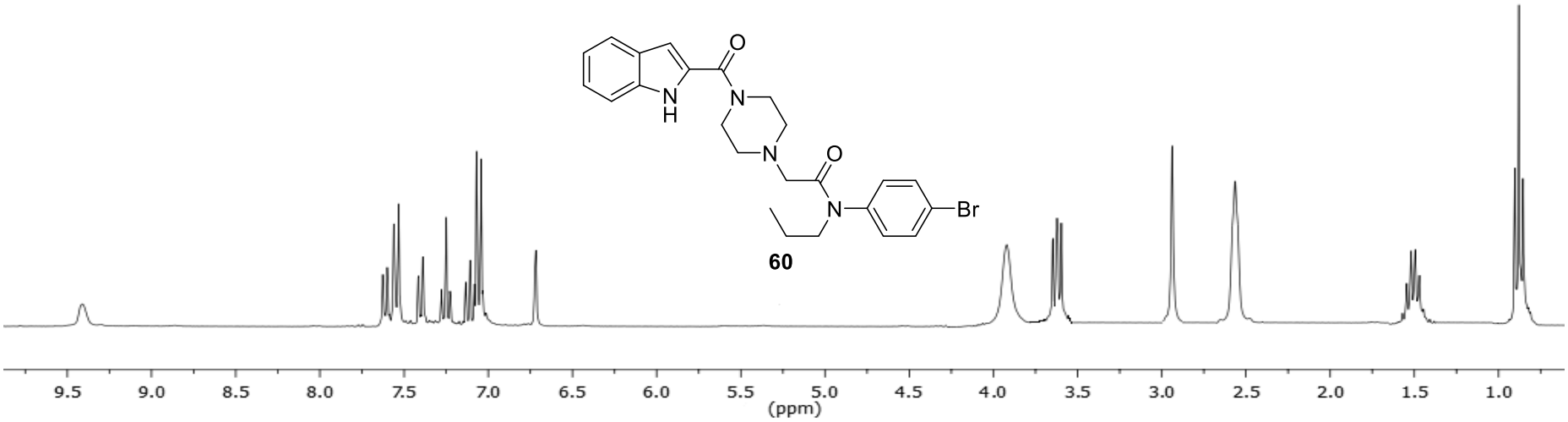

Compound **60**: ^{13}C NMR (75 MHz, $CDCl_3$)

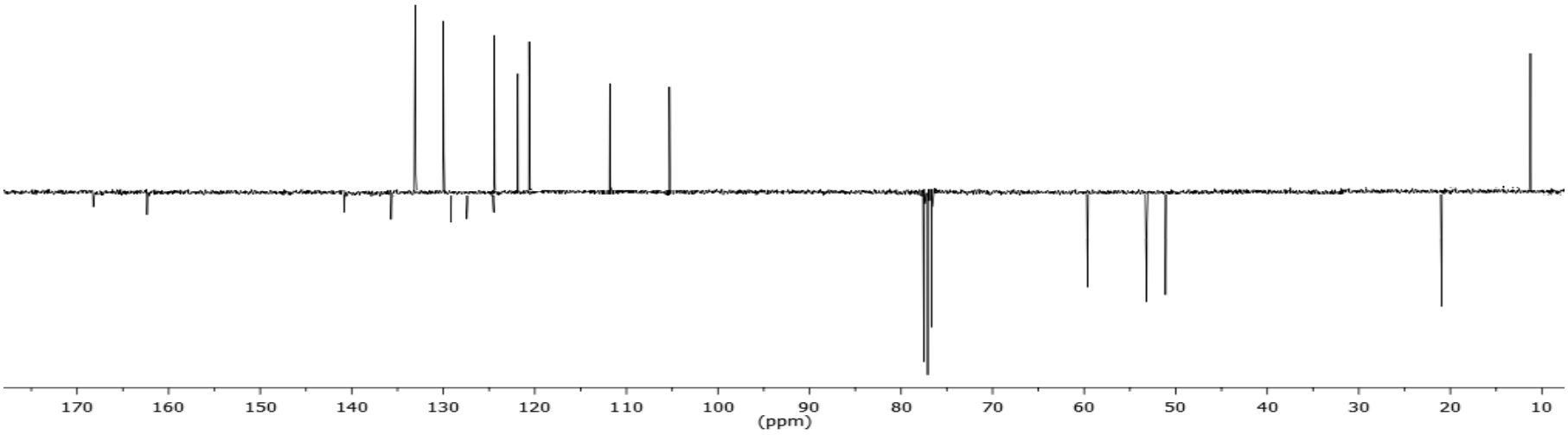

Compound **61**: ^{1}H NMR (300 MHz, $CDCl_3$)

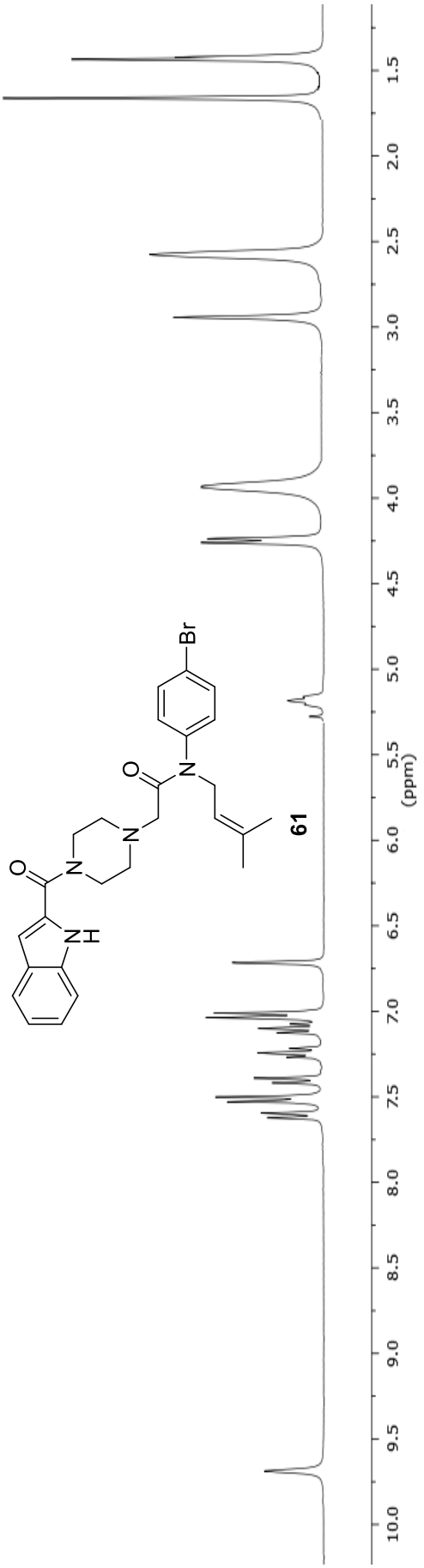

Compound **61**: ^{13}C NMR (75 MHz, $CDCl_3$)

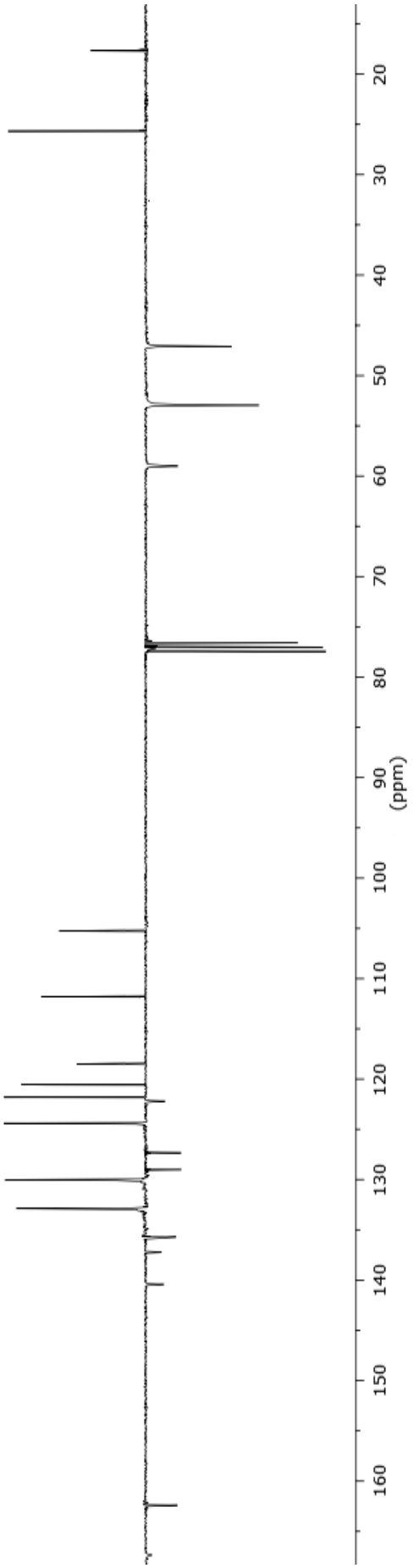

Compound **62**: ^{1}H NMR (400 MHz, $CDCl_3$)

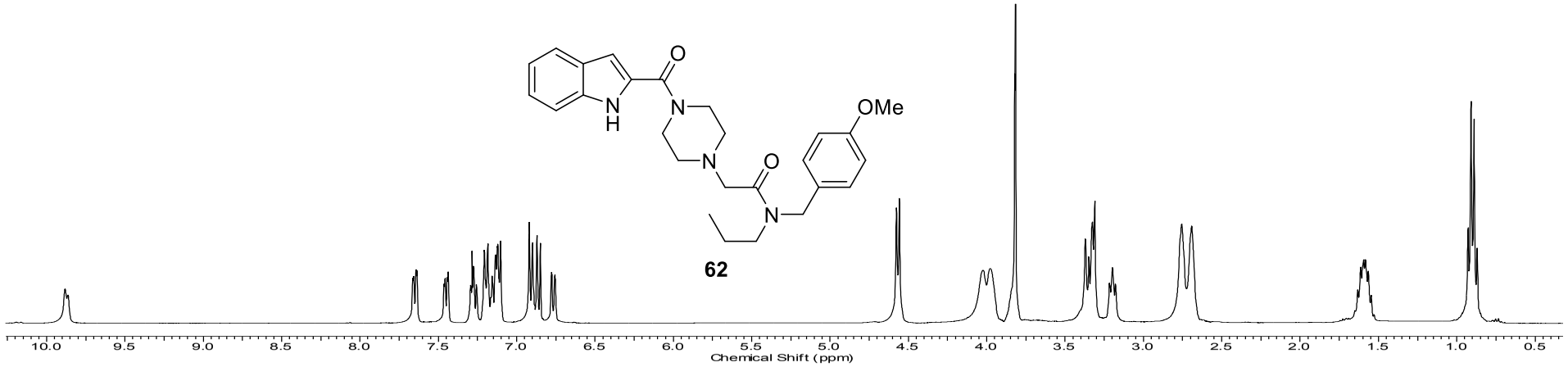

62

Compound **62**: ^{13}C NMR (100 MHz, $CDCl_3$)

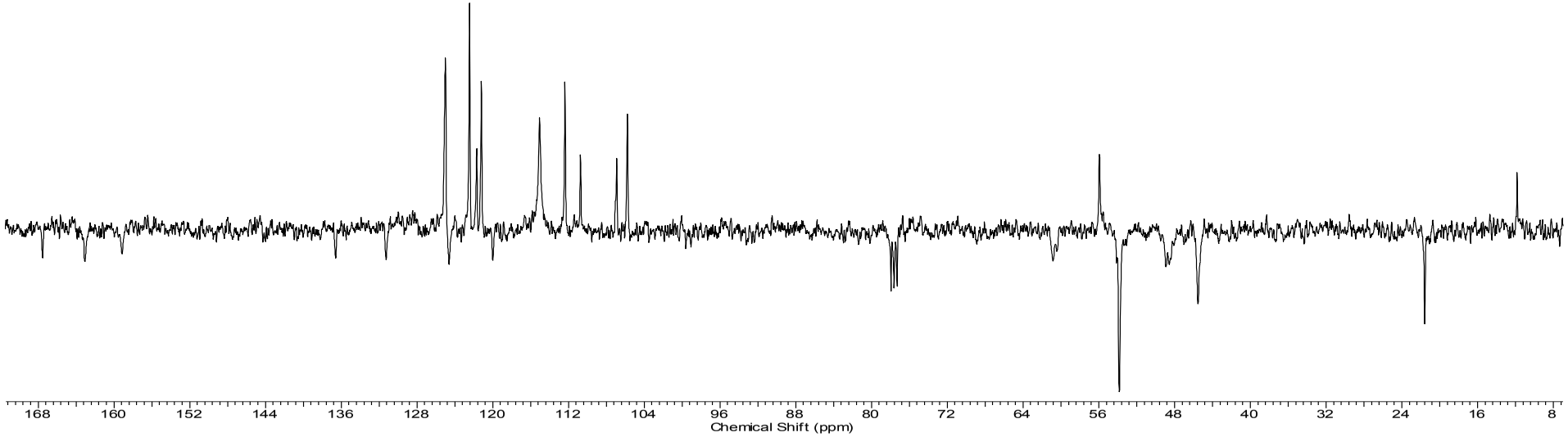

Compound **63**: ^{1}H NMR (300 MHz, $CDCl_3$)

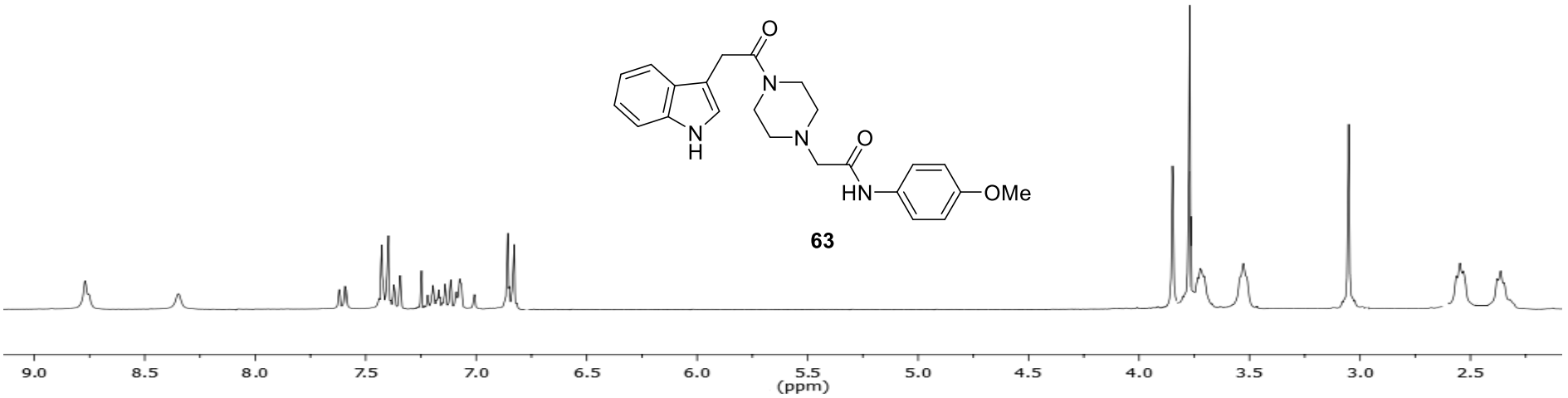

63

Compound **63**: ^{13}C NMR (75 MHz, $CDCl_3$)

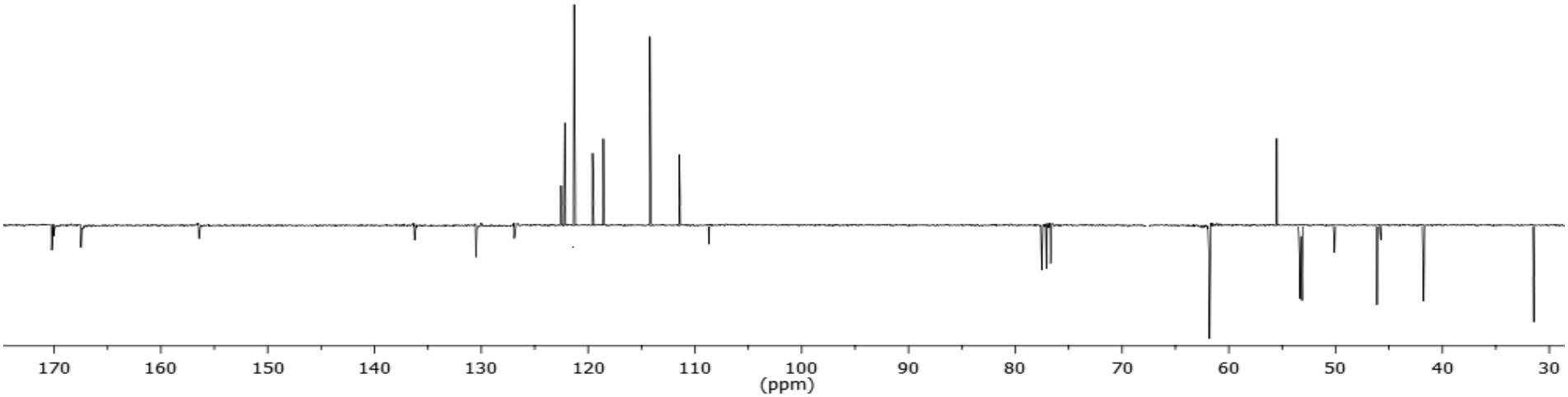

Compound **64**: ^{1}H NMR (300 MHz, $CDCl_3$)

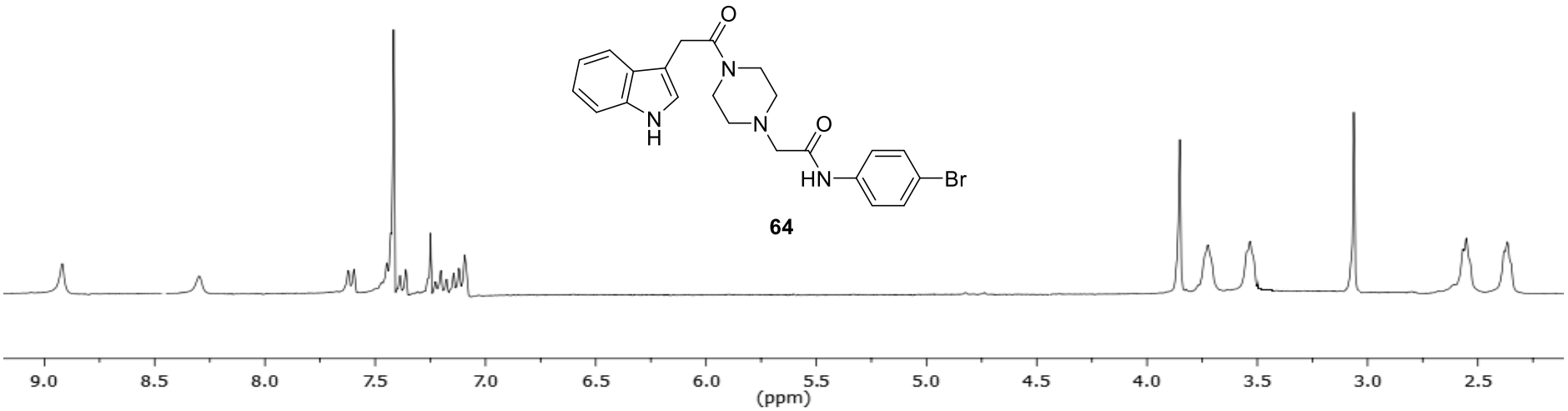

Compound **64**: ^{13}C NMR (75 MHz, $CDCl_3$)

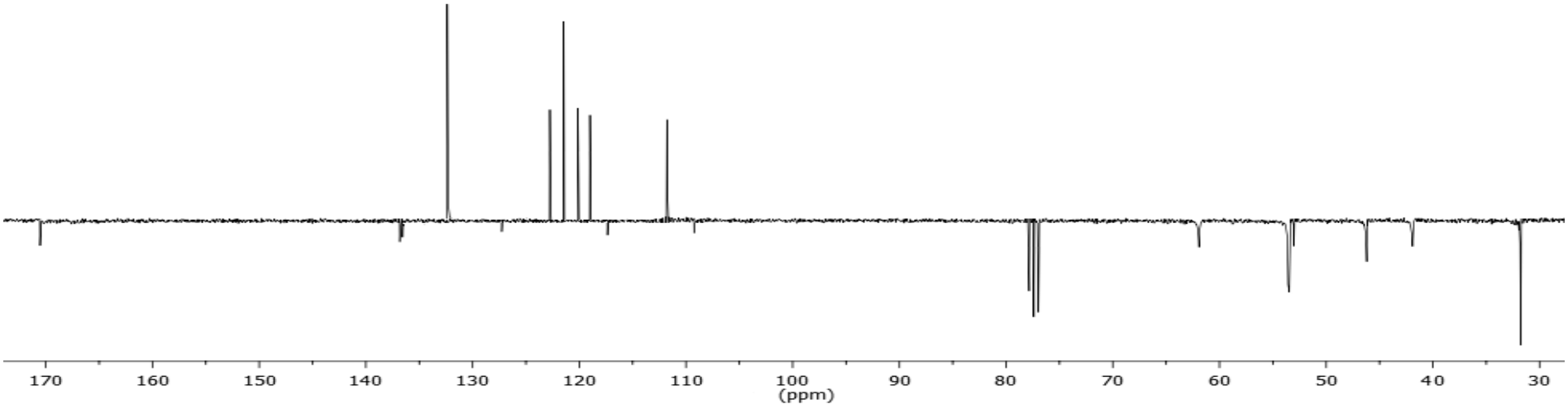

Compound **65**: ^{1}H NMR (300 MHz, $CDCl_3$)

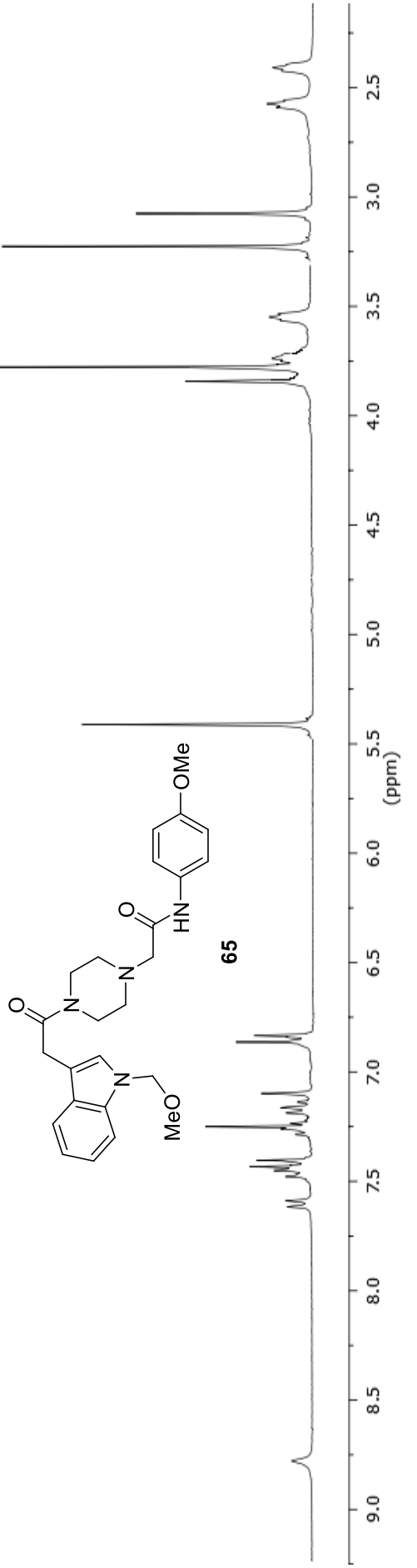

Compound **65**: ^{13}C NMR (75 MHz, $CDCl_3$)

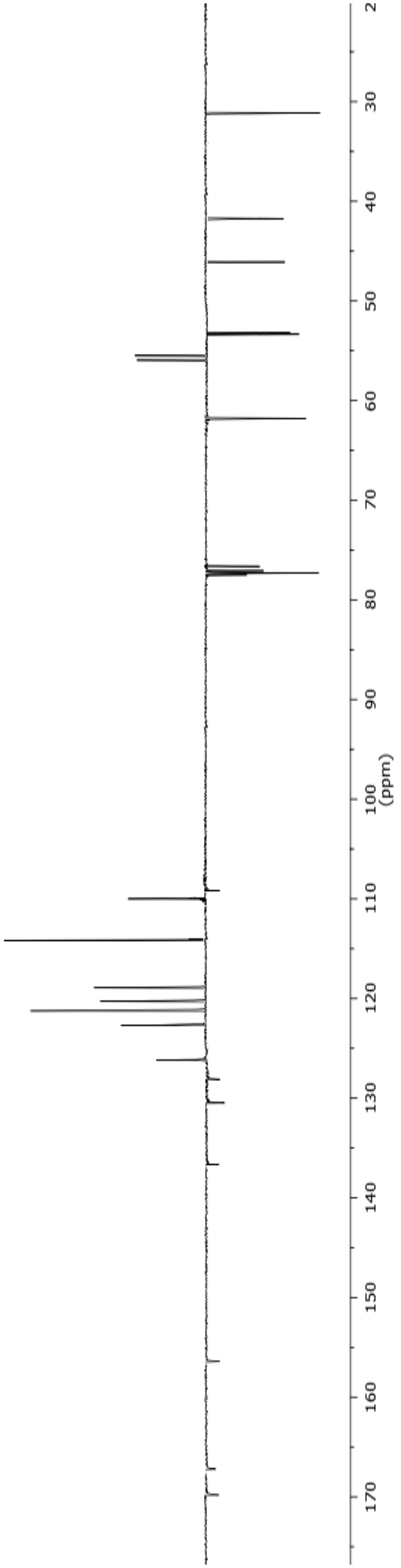

Compound **66**: ^{1}H NMR (300 MHz, $CDCl_3$)

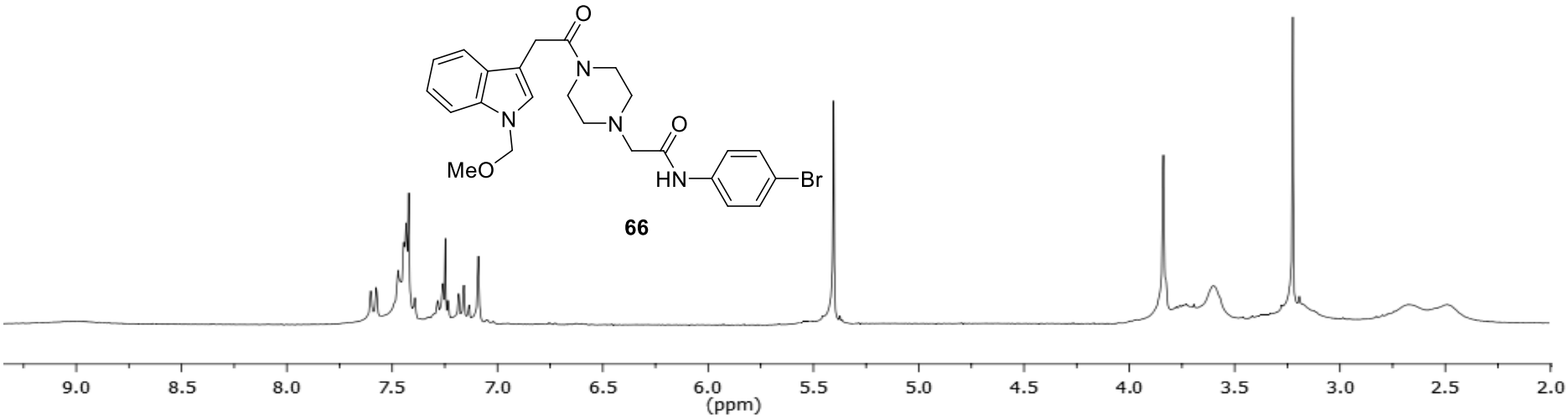

66

Compound **66**: ^{13}C NMR (75 MHz, $CDCl_3$)

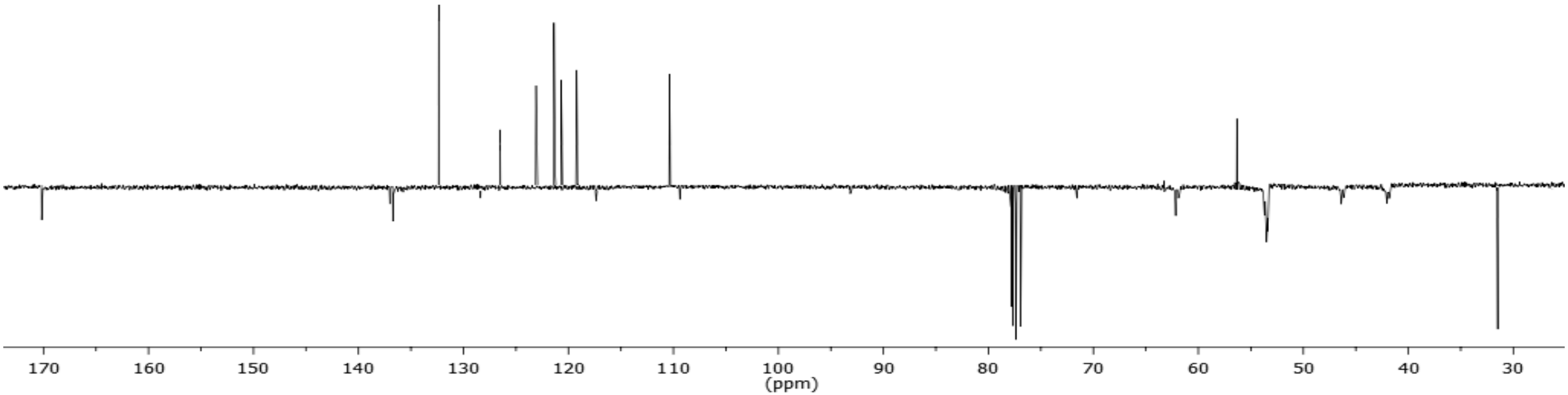

Compound **67**: ^{1}H NMR (300 MHz, $CDCl_3$)

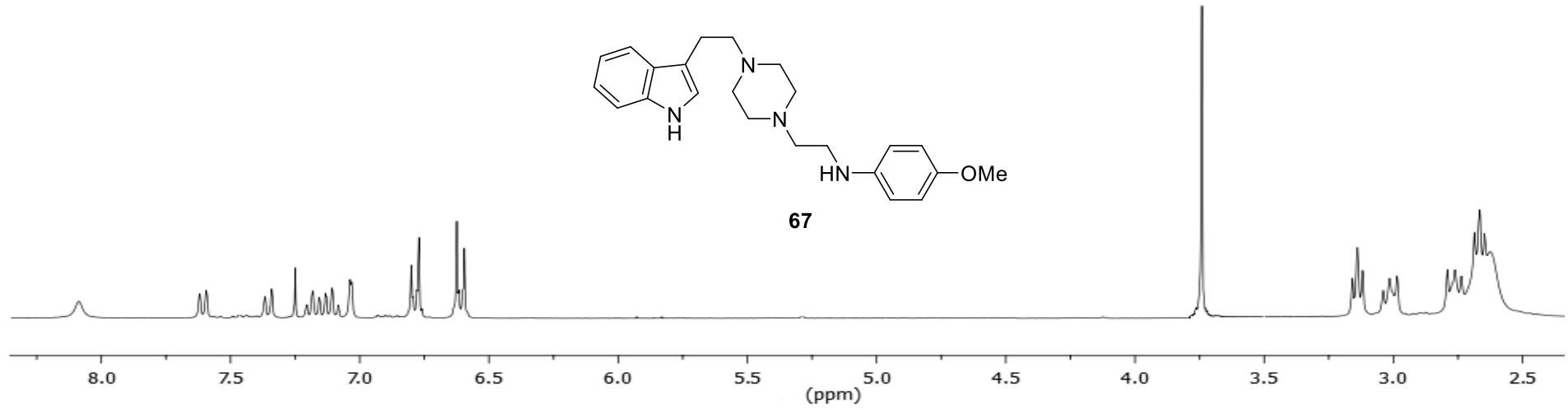

67

Compound **67**: ^{13}C NMR (75 MHz, $CDCl_3$)

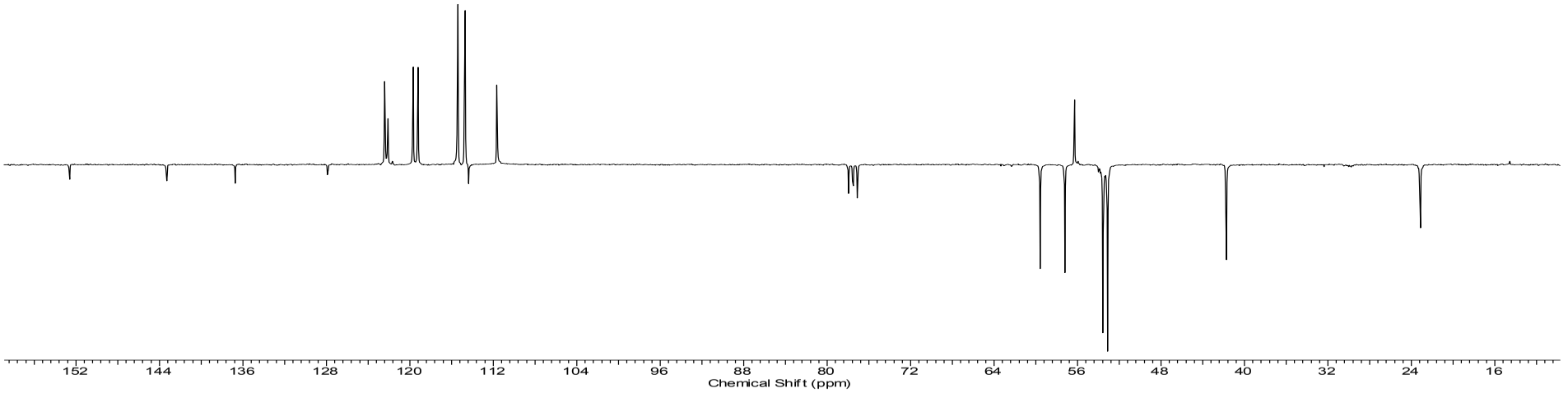

Compound **68**: ^{1}H NMR (300 MHz, $CDCl_3$)

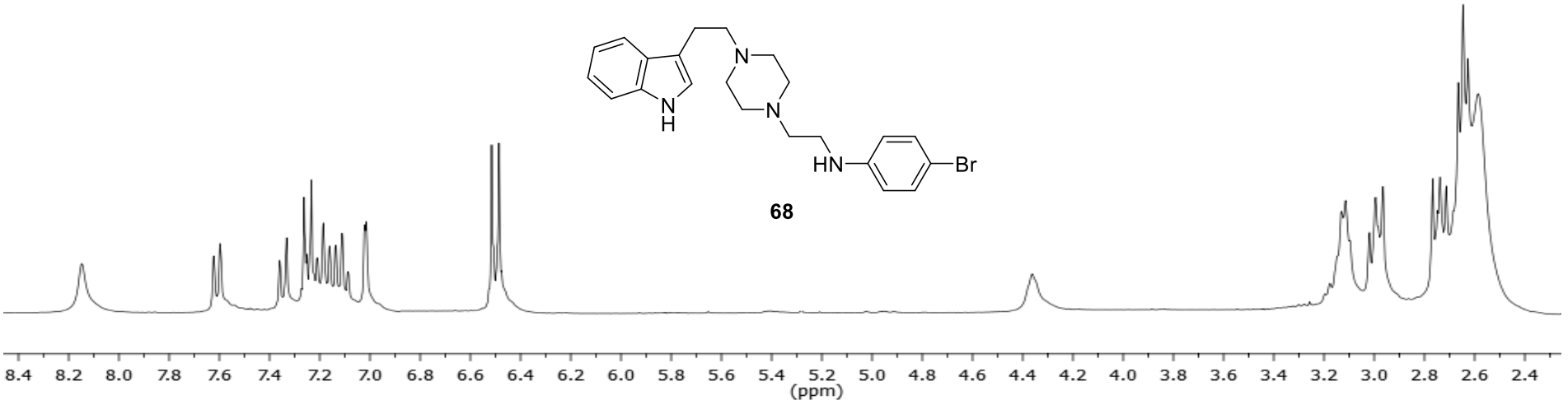

68

Compound **68**: ^{13}C NMR (75 MHz, $CDCl_3$)

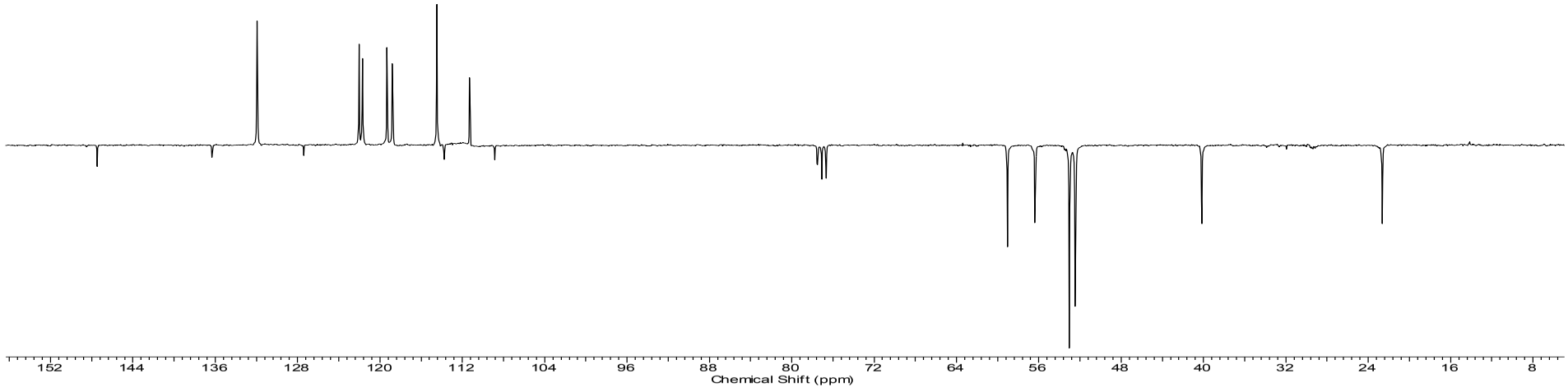

Compound **69**: ^{1}H NMR (400 MHz, $CDCl_3$)

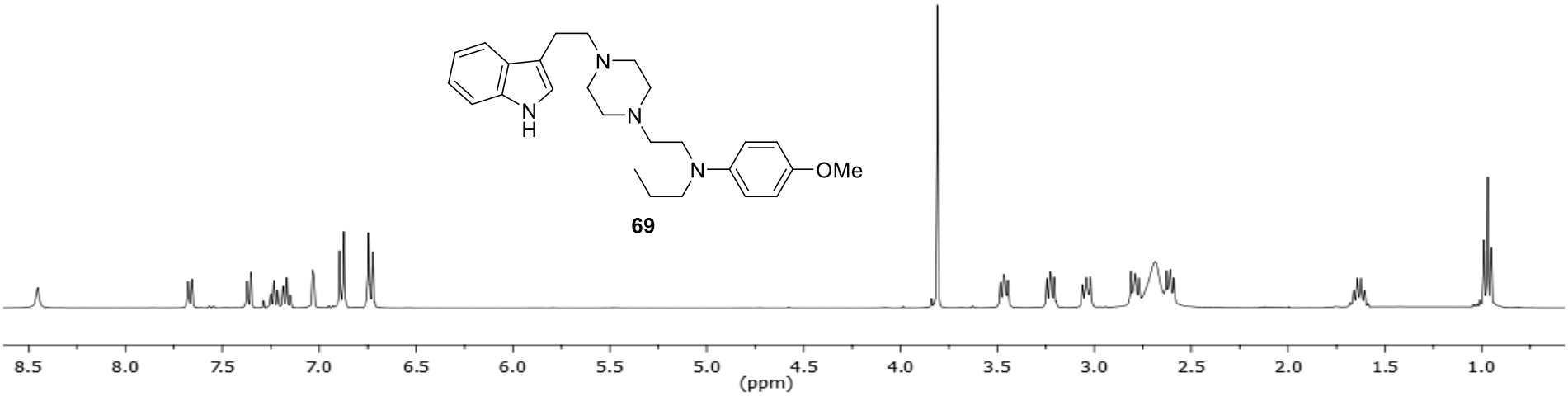

69

Compound **69**: ^{13}C NMR (100 MHz, $CDCl_3$)

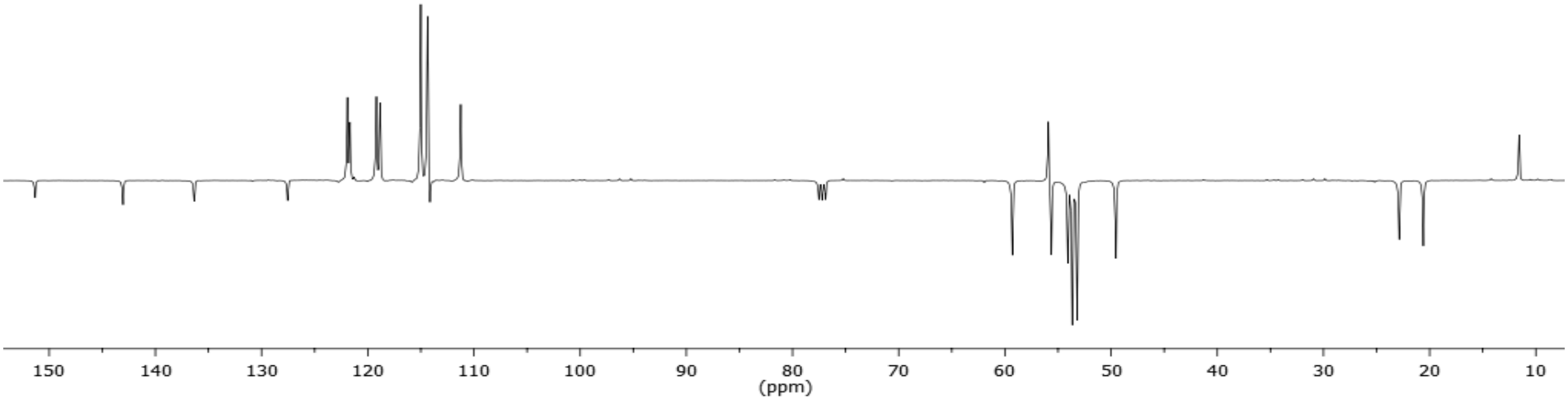

Compound **70**: ^{1}H NMR (300 MHz, $CDCl_3$)

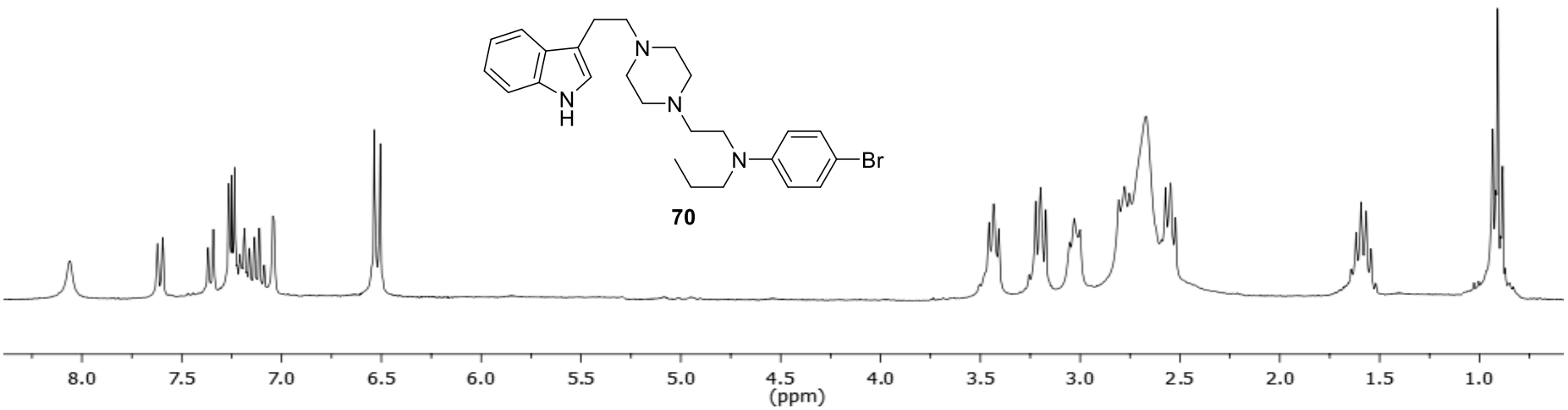

Compound **70**: ^{13}C NMR (75 MHz, $CDCl_3$)

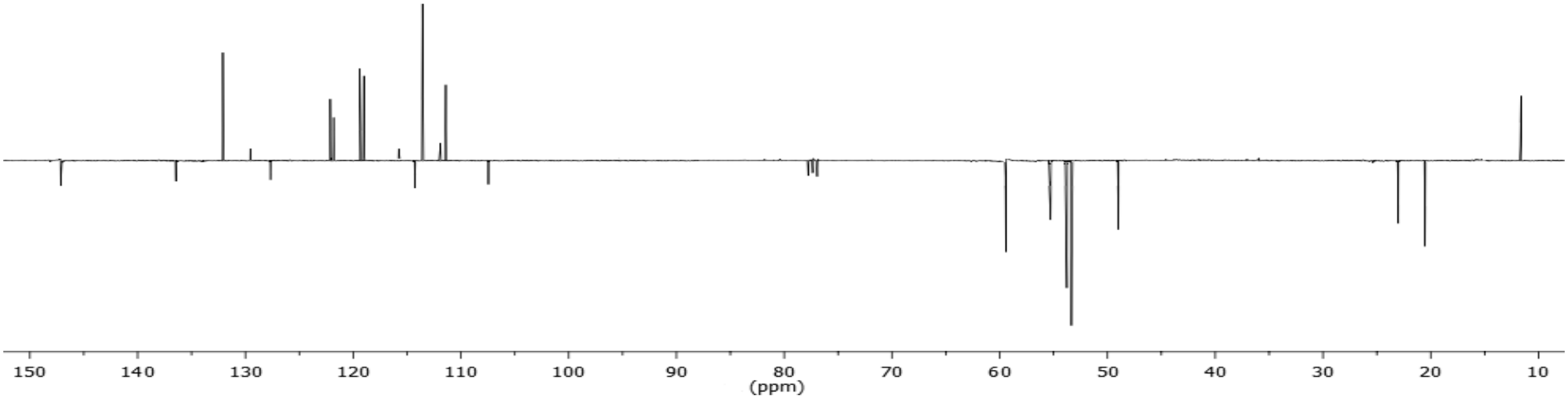

Compound **71**: ^{1}H NMR (400 MHz, $CDCl_3$)

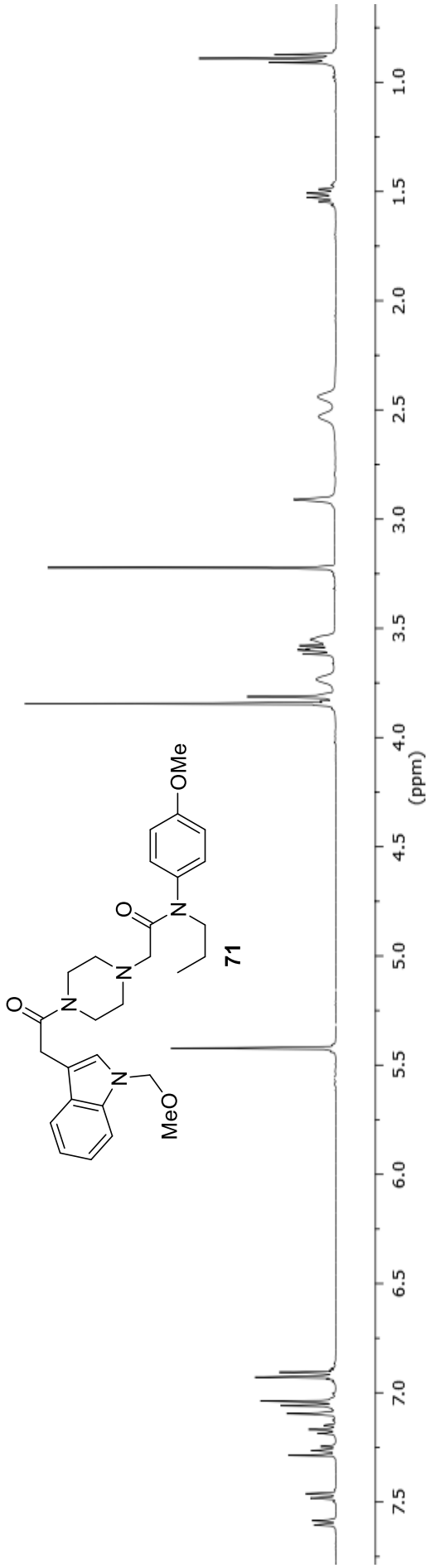

Compound **71**: ^{13}C NMR (100 MHz, $CDCl_3$)

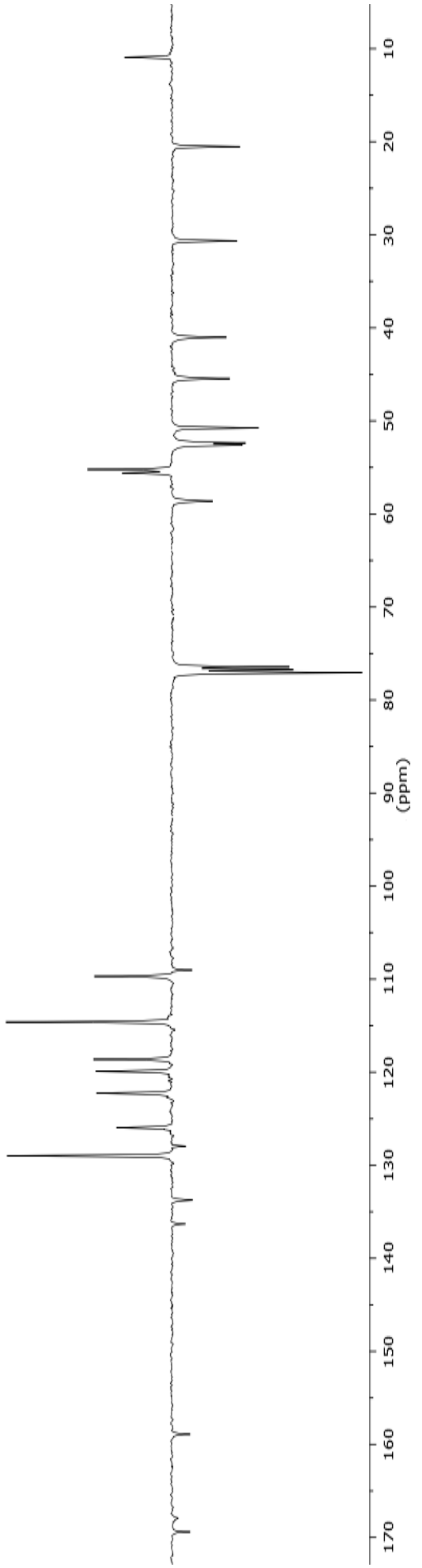

Compound **72**: ^{1}H NMR (400 MHz, $CDCl_3$)

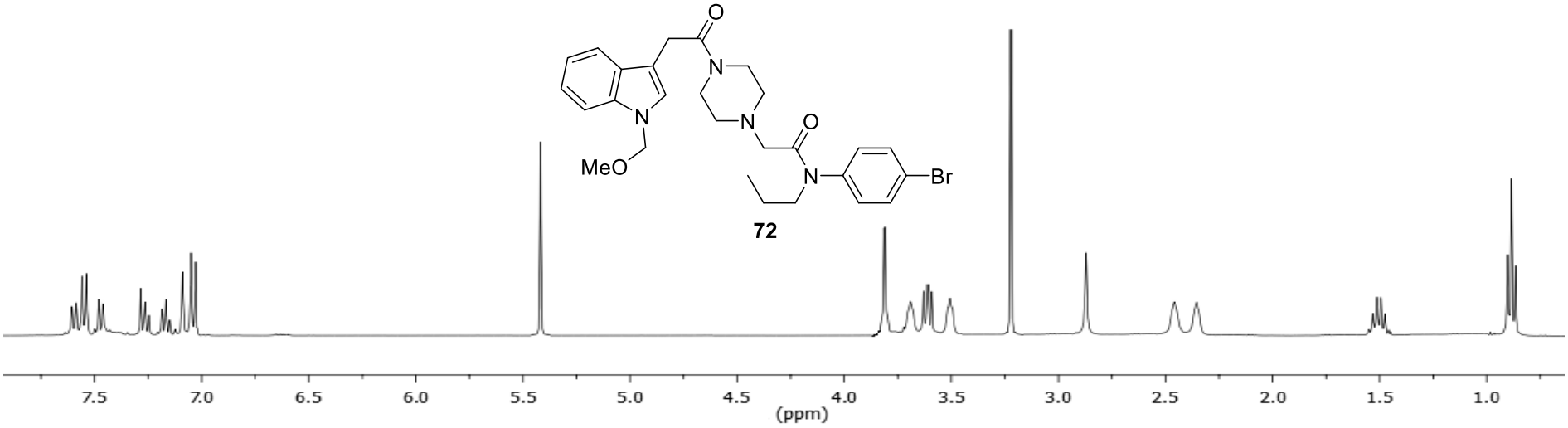

72

Compound **72**: ^{13}C NMR (100 MHz, $CDCl_3$)

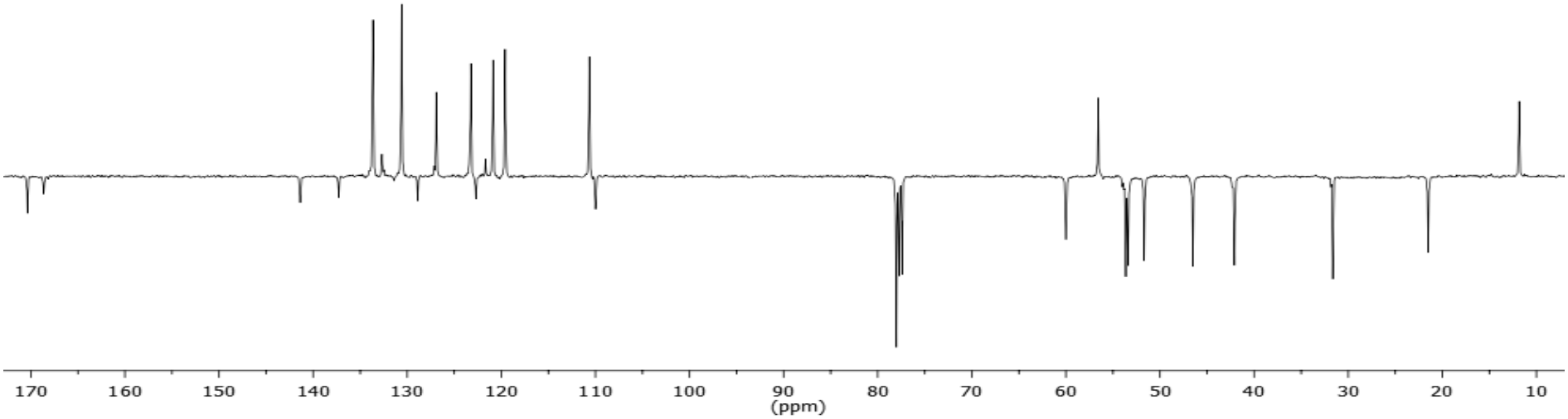

Chapter 4

Compound **75a**: ^{1}H NMR (400 MHz, $CDCl_3$)

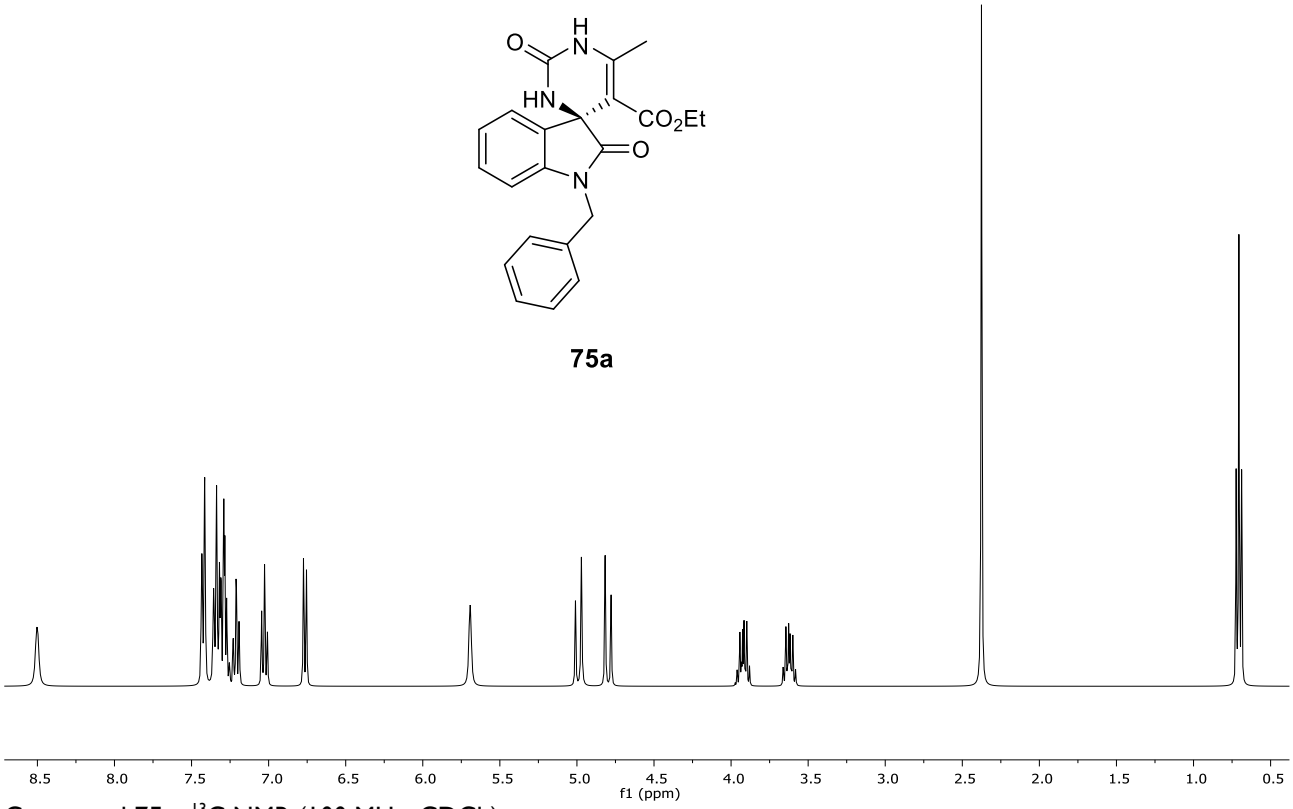

75a

Compound **75a**: ^{13}C NMR (100 MHz, $CDCl_3$)

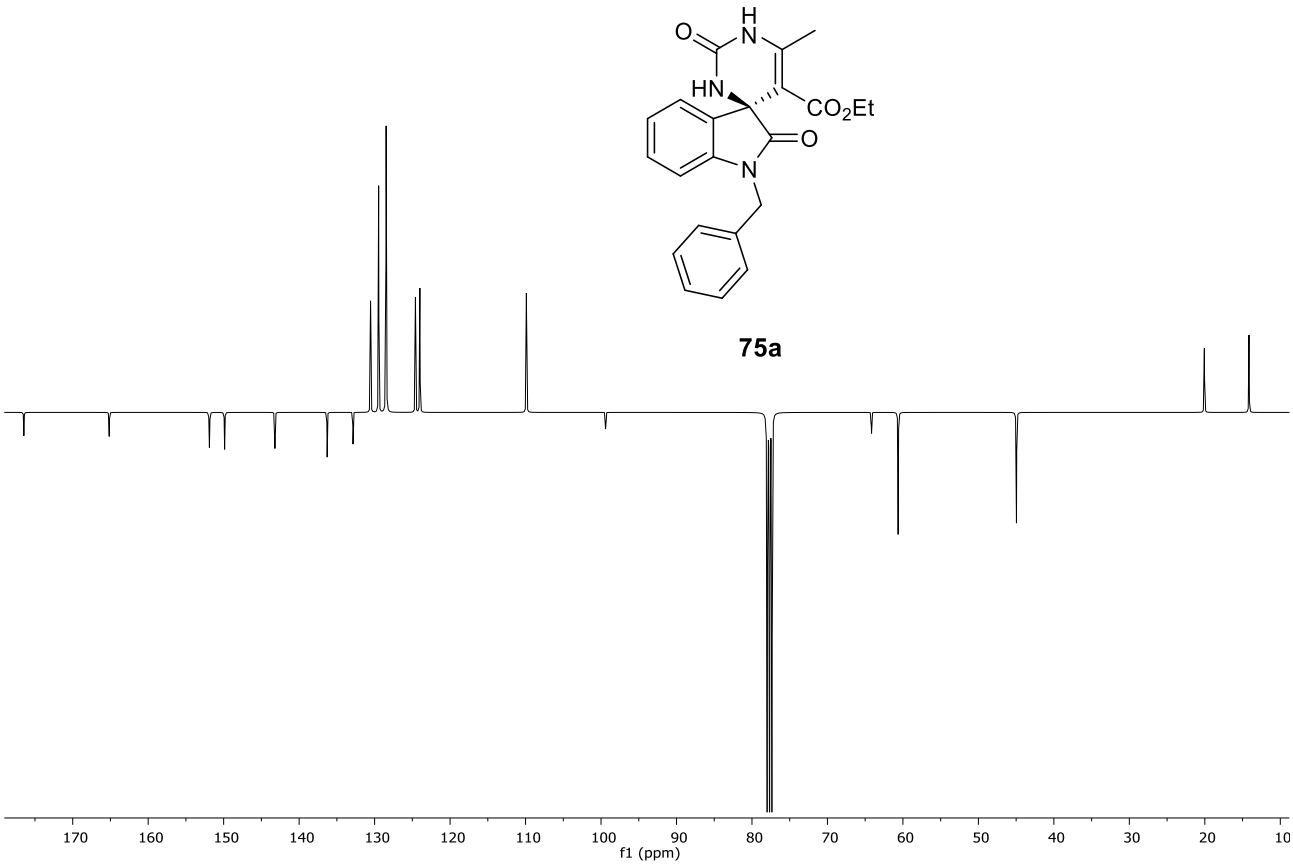

75a

Compound **75b**: ^{1}H NMR (300 MHz, $CDCl_3$)

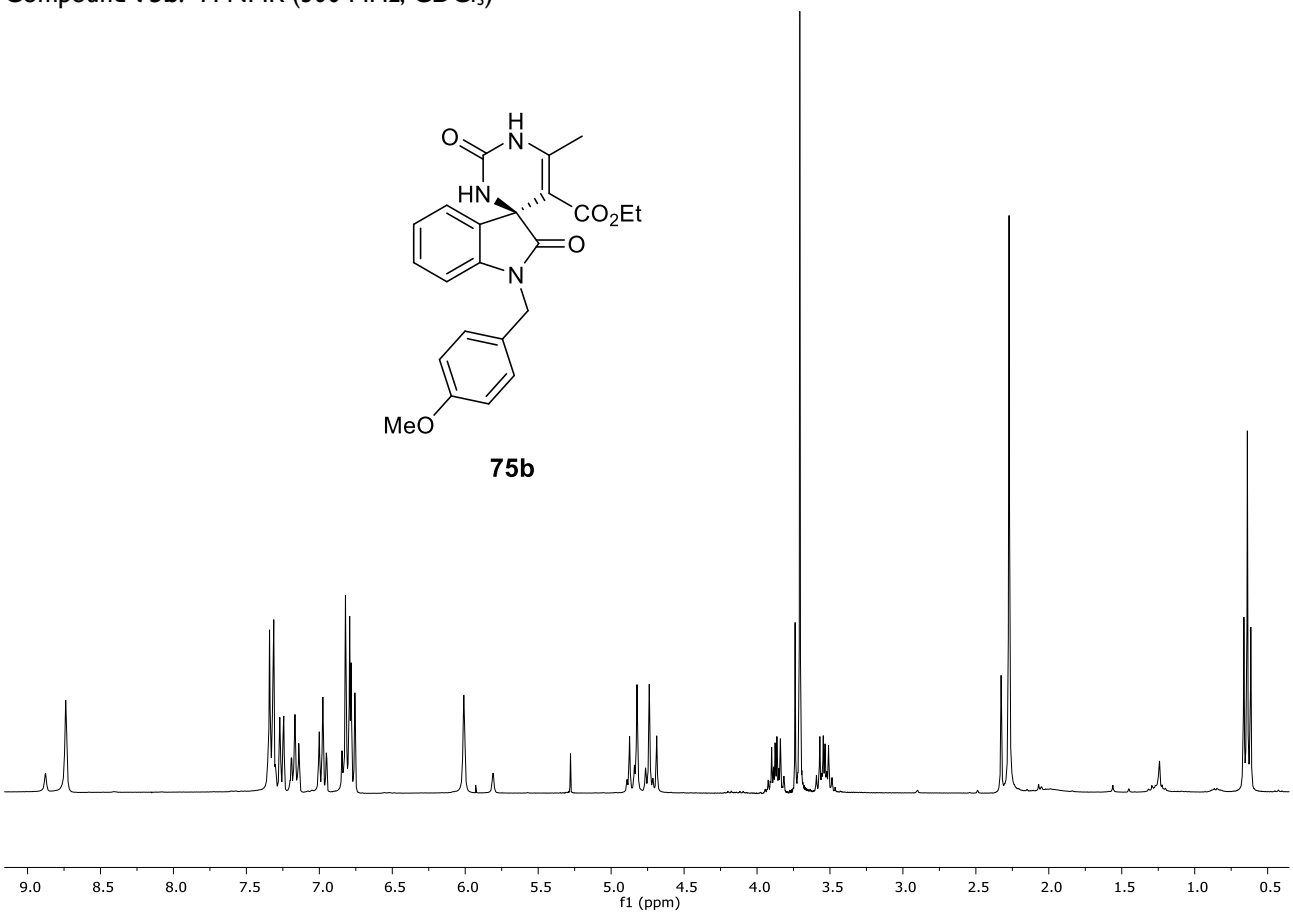

Compound **75b**: ^{13}C NMR (75 MHz, $CDCl_3$)

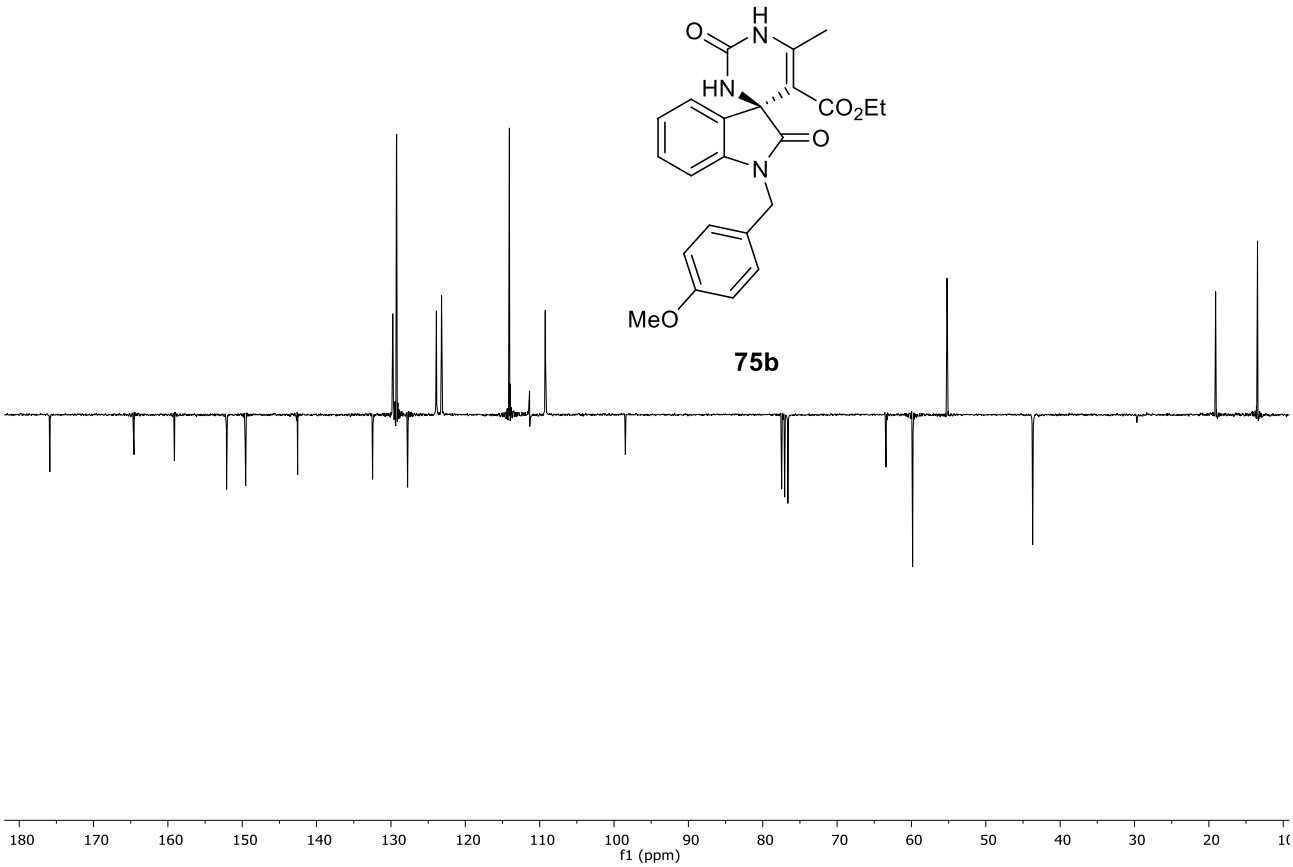

Compound **75c**: ^{1}H NMR (300 MHz, $CDCl_3$)

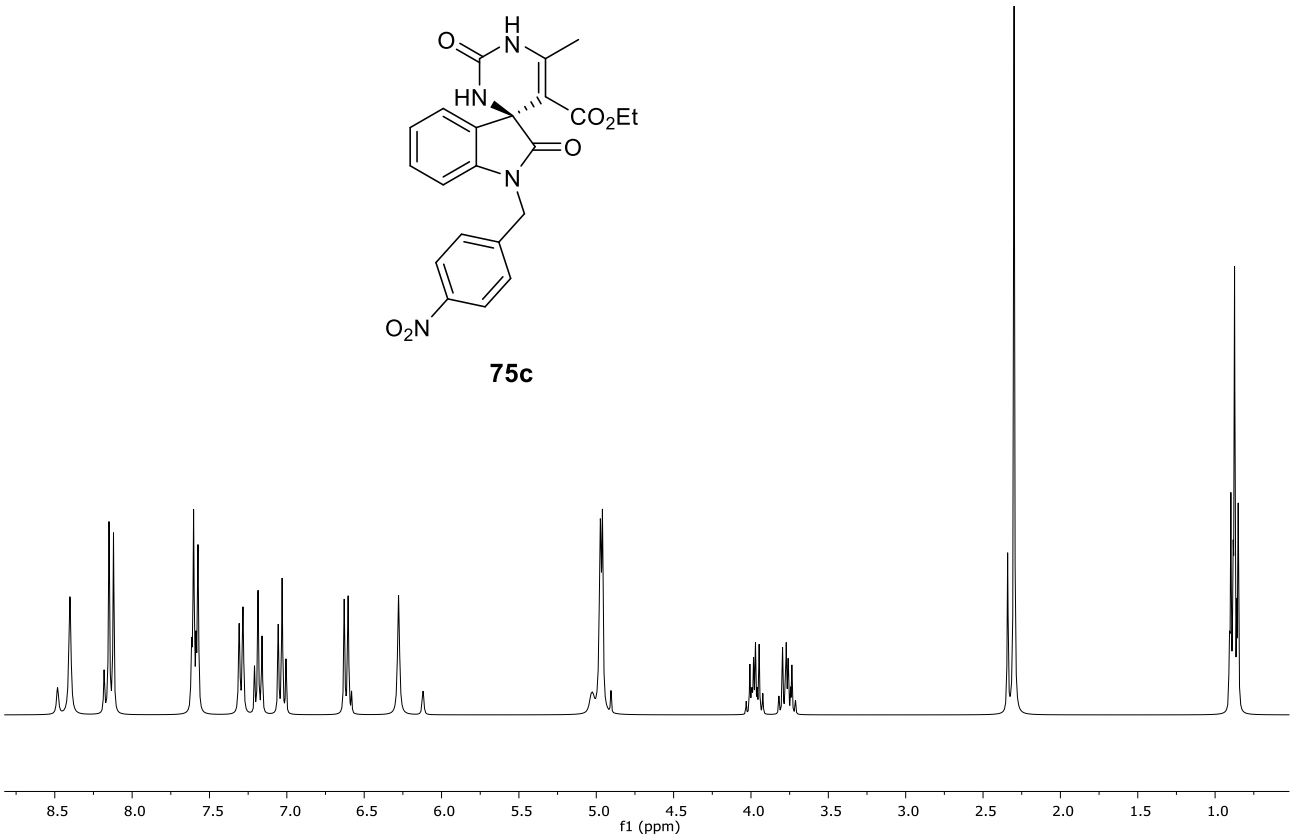

75c

Compound **75c**: ^{13}C NMR (75 MHz, $CDCl_3$)

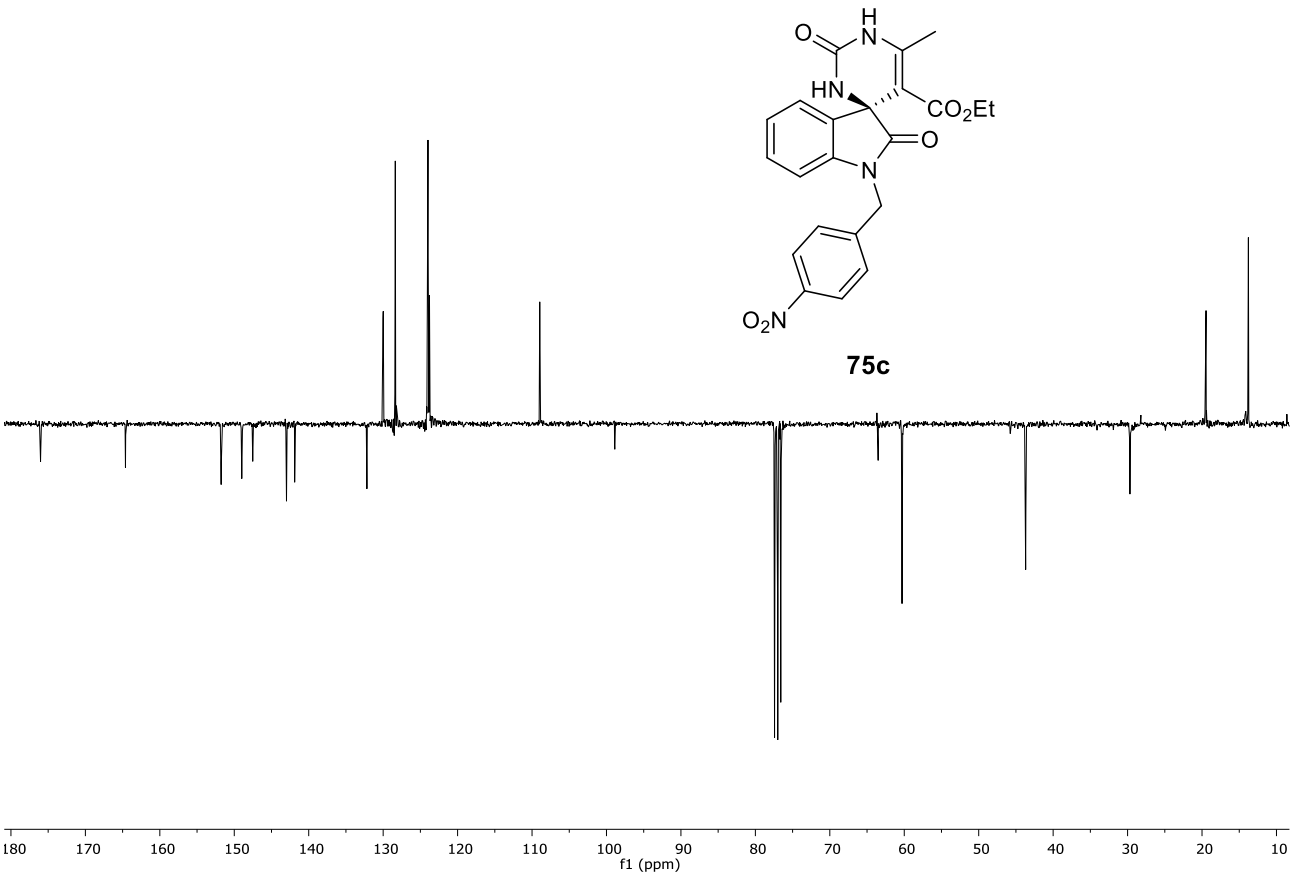

75c

Compound **75d**: ^{1}H NMR (400 MHz, DMSO-d_6)

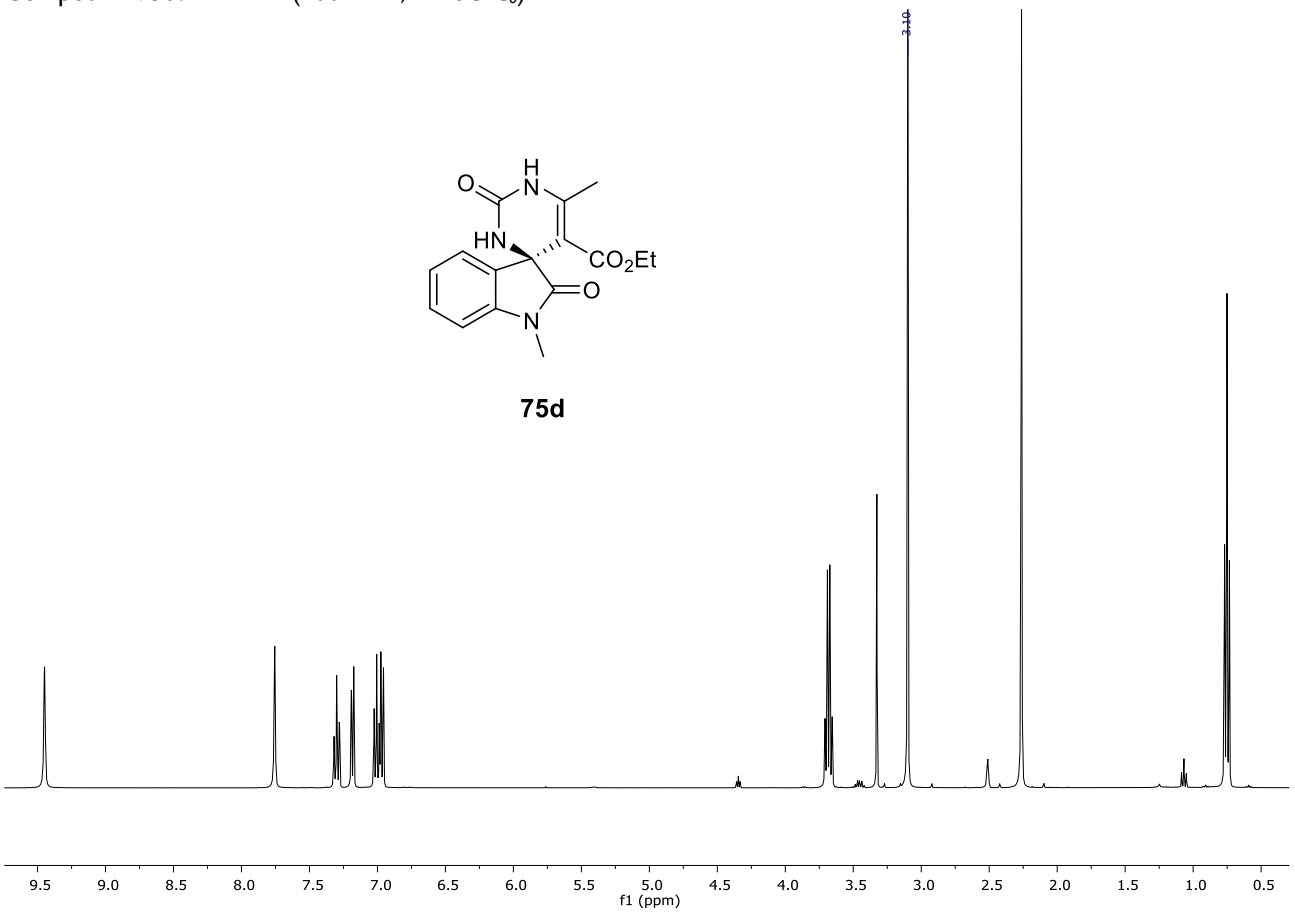

75d

Compound **75d**: ^{13}C NMR (100 MHz, DMSO-d_6)

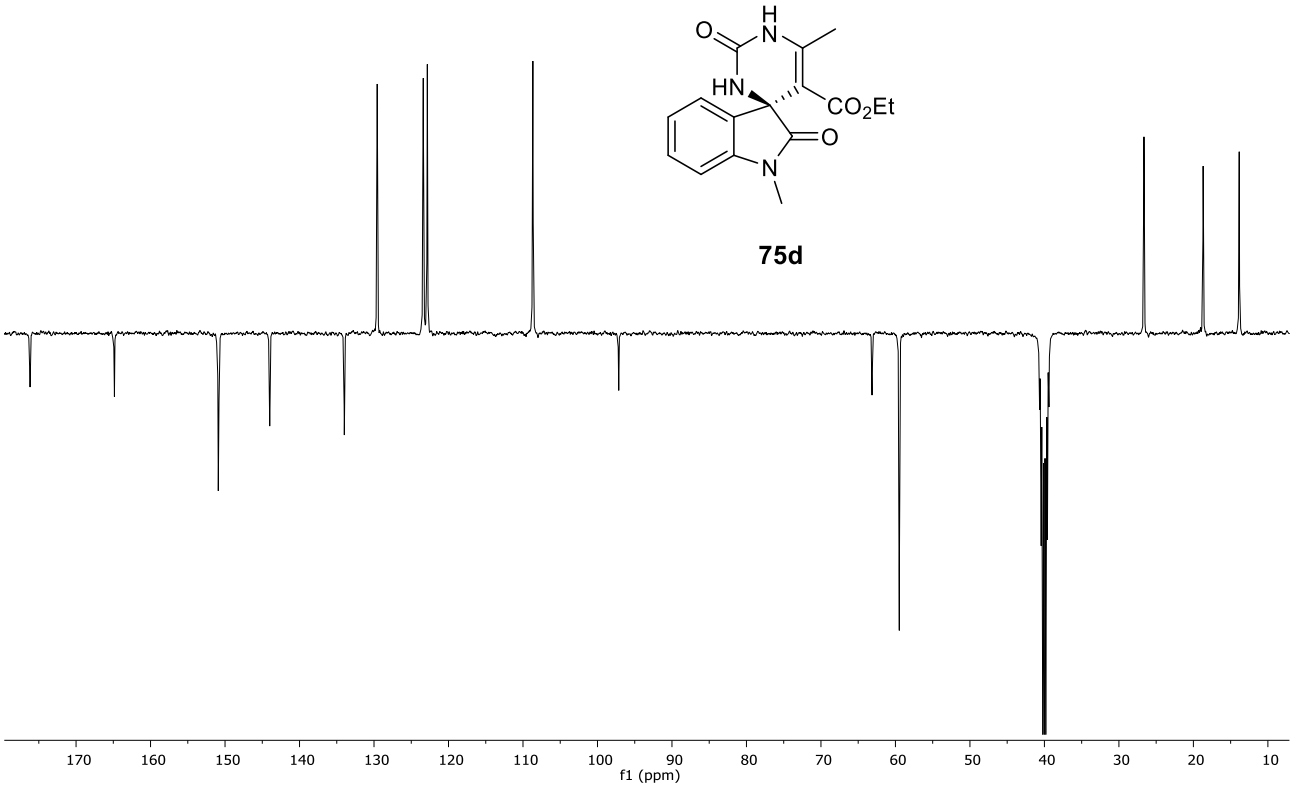

75d

Compound **75e**: ^{1}H NMR (300 MHz, $CDCl_3$)

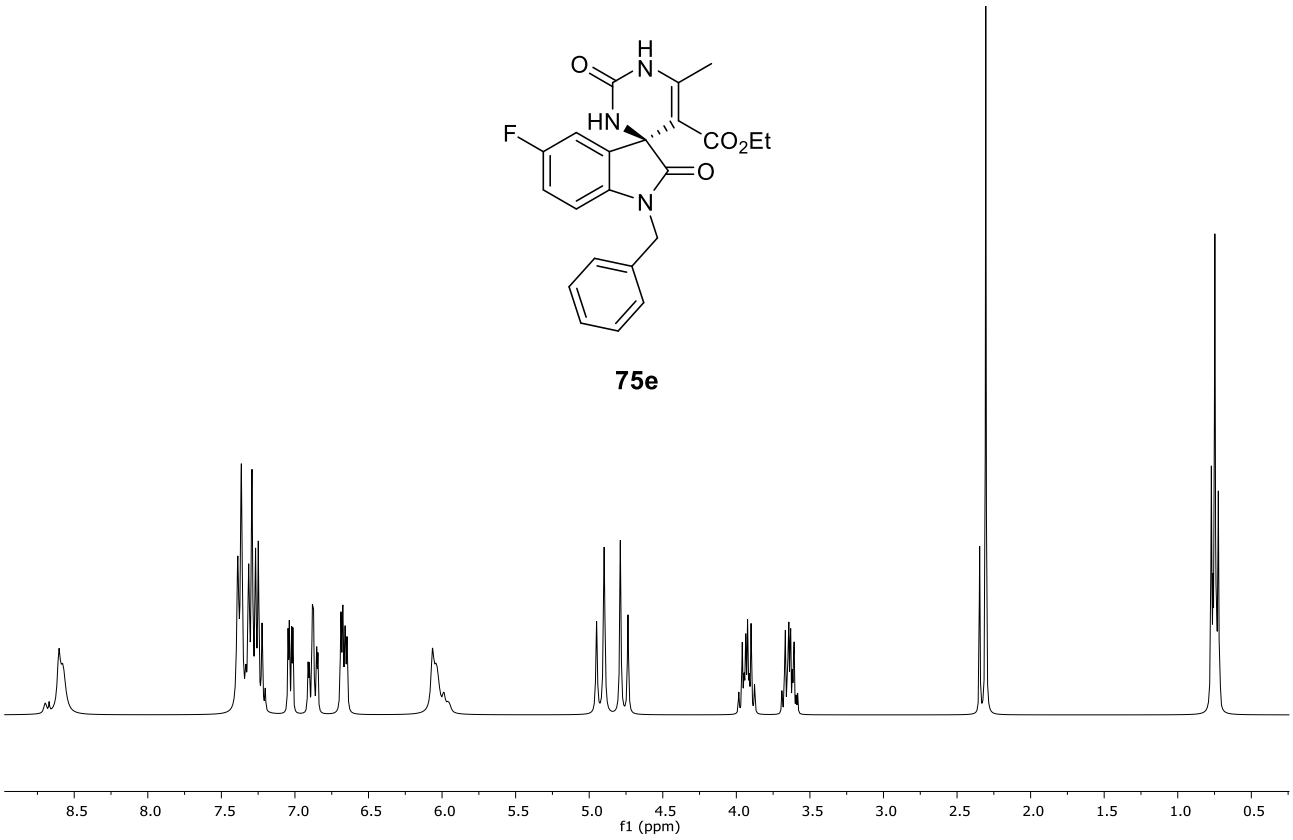

75e

Compound **75e**: ^{13}C NMR (75 MHz, $CDCl_3$)

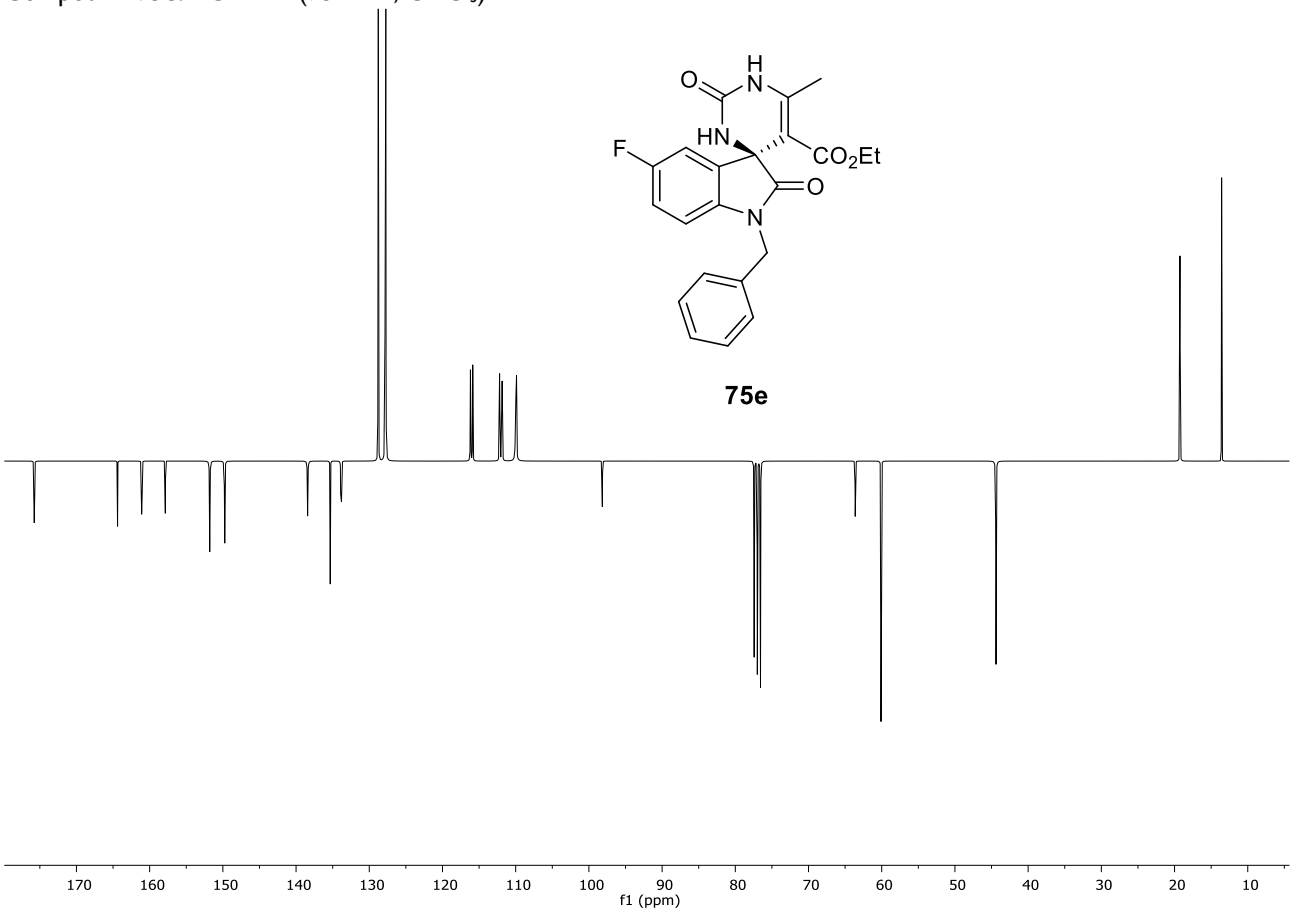

75e

Compound **75f**: ^{1}H NMR (300 MHz, $CDCl_3$)

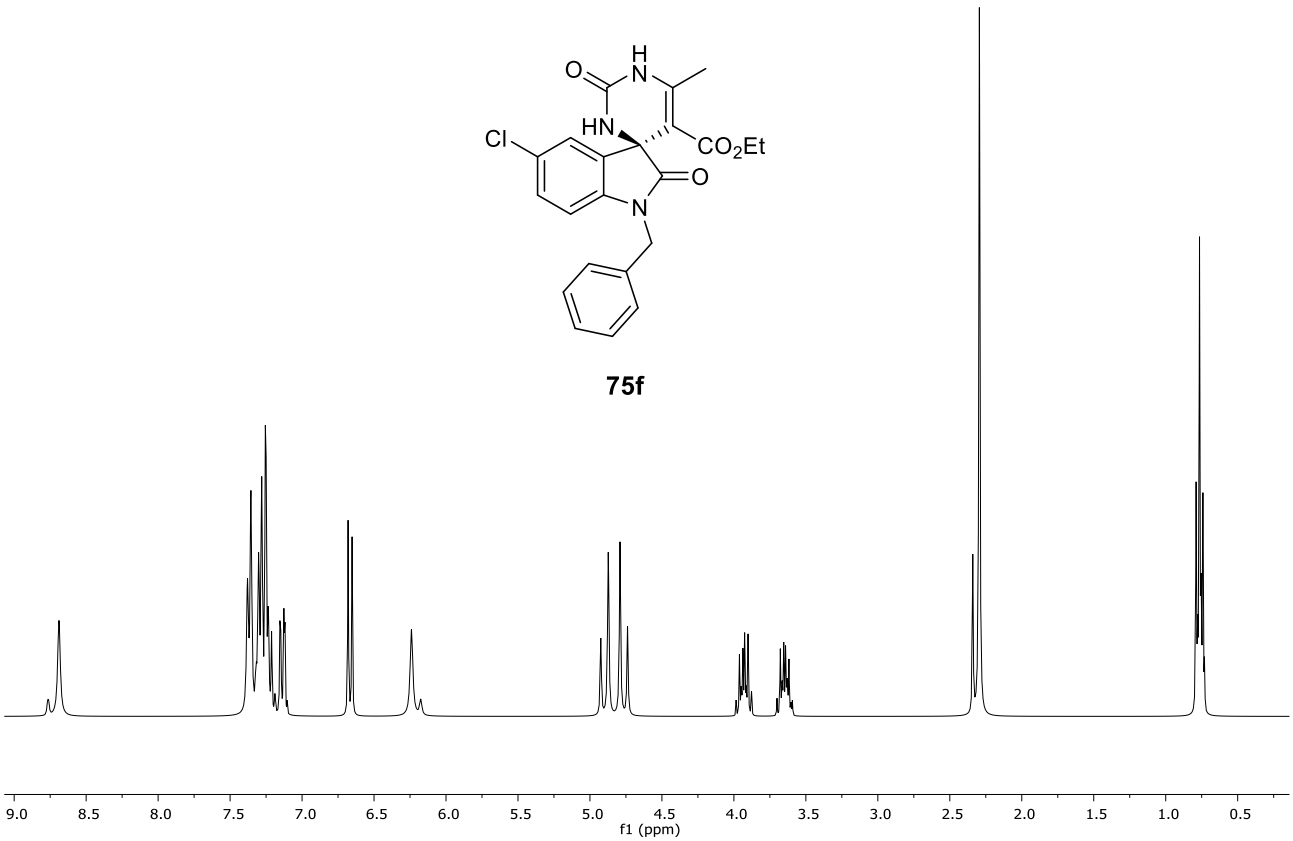

75f

Compound **75f**: ^{13}C NMR (75 MHz, $CDCl_3$)

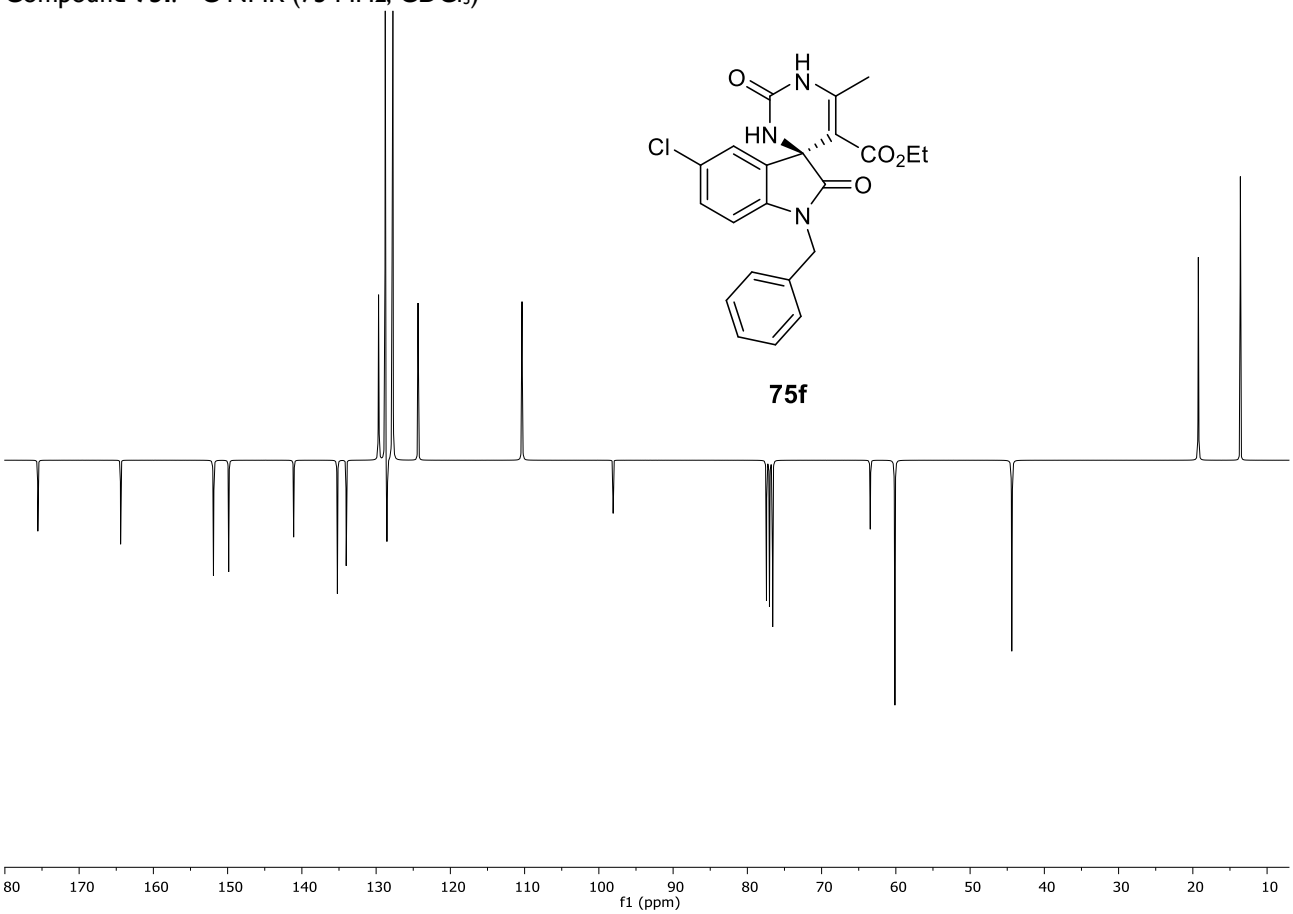

75f

Compound **75g**: ^{1}H NMR (300 MHz, $CDCl_3$)

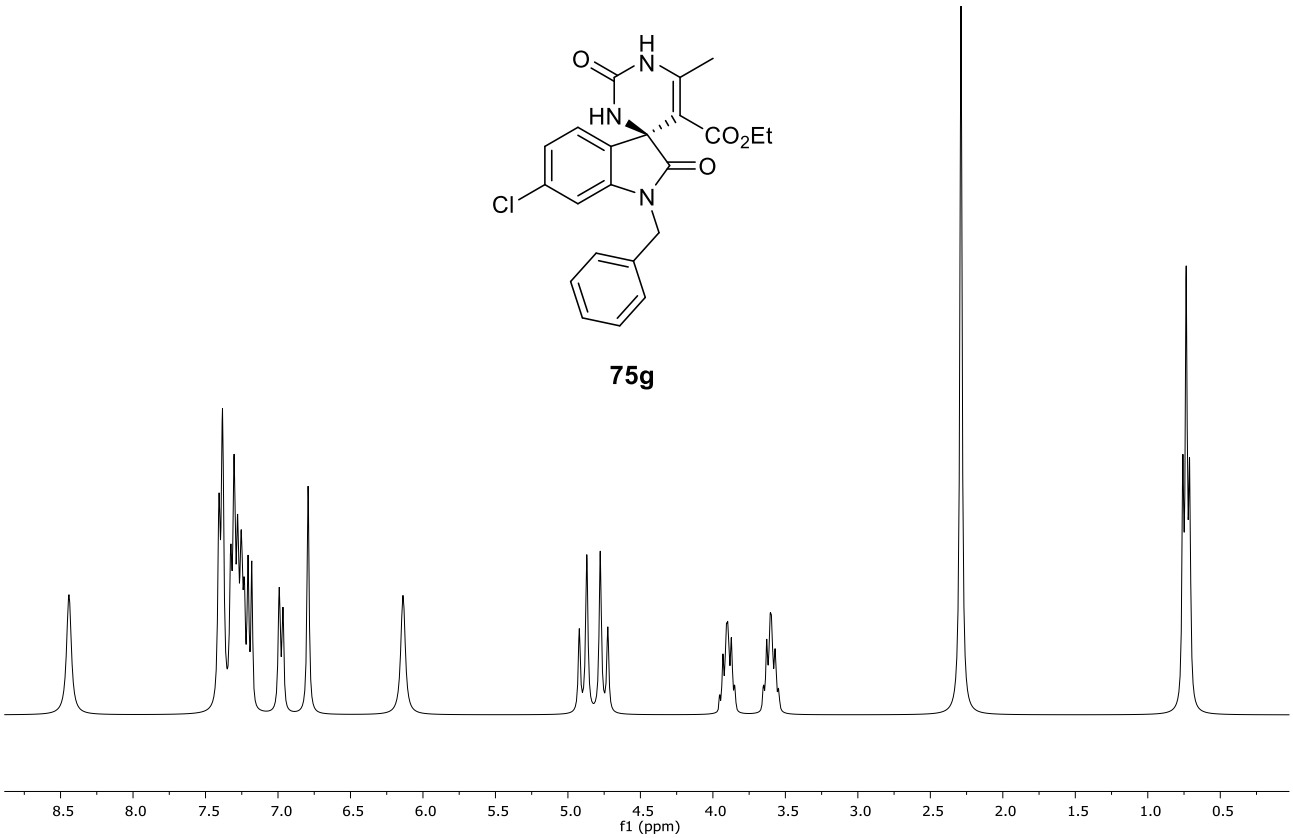

75g

Compound **75g**: ^{13}C NMR (75 MHz, $CDCl_3$)

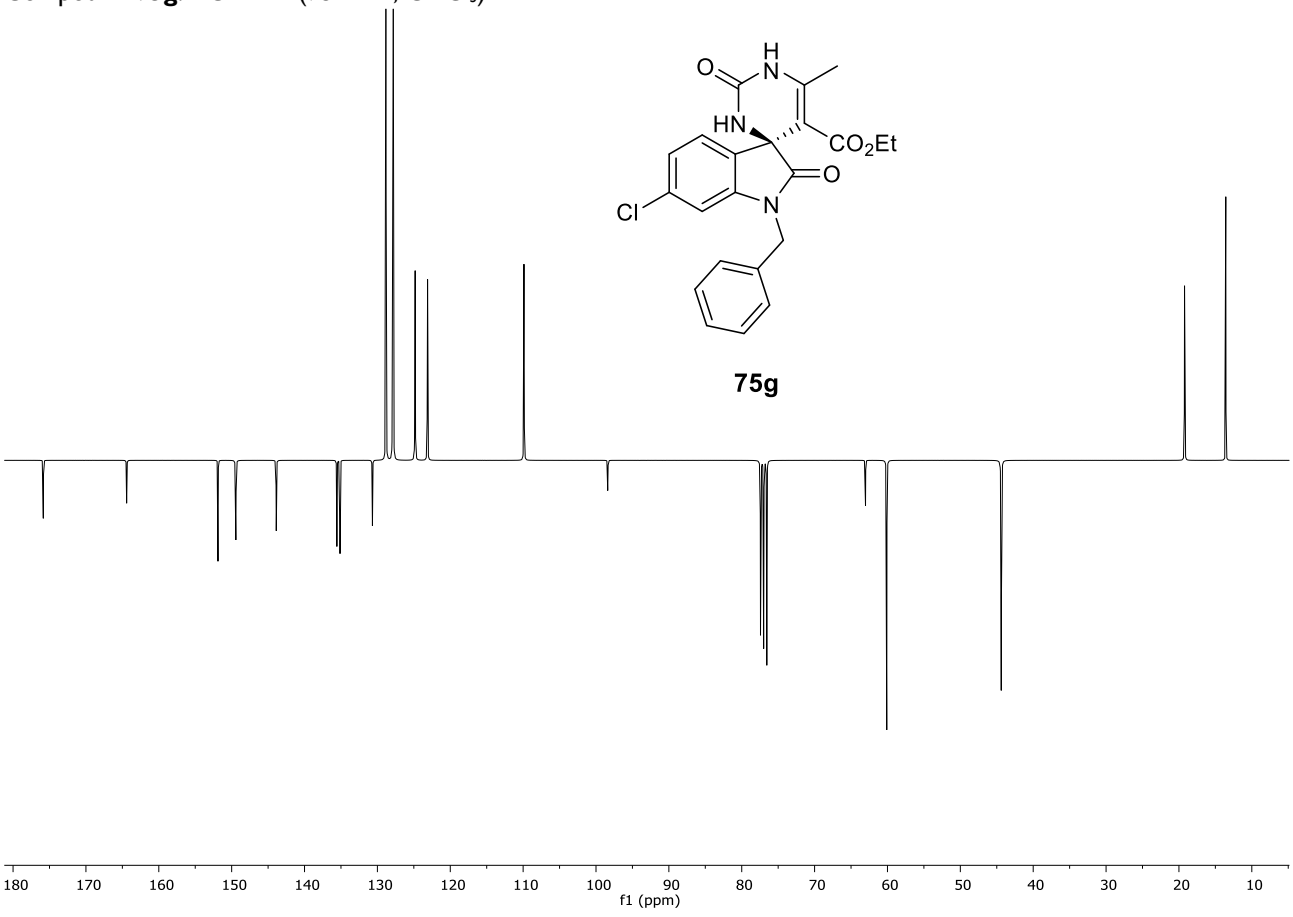

75g

Compound **75h**: ^{1}H NMR (300 MHz, $CDCl_3$)

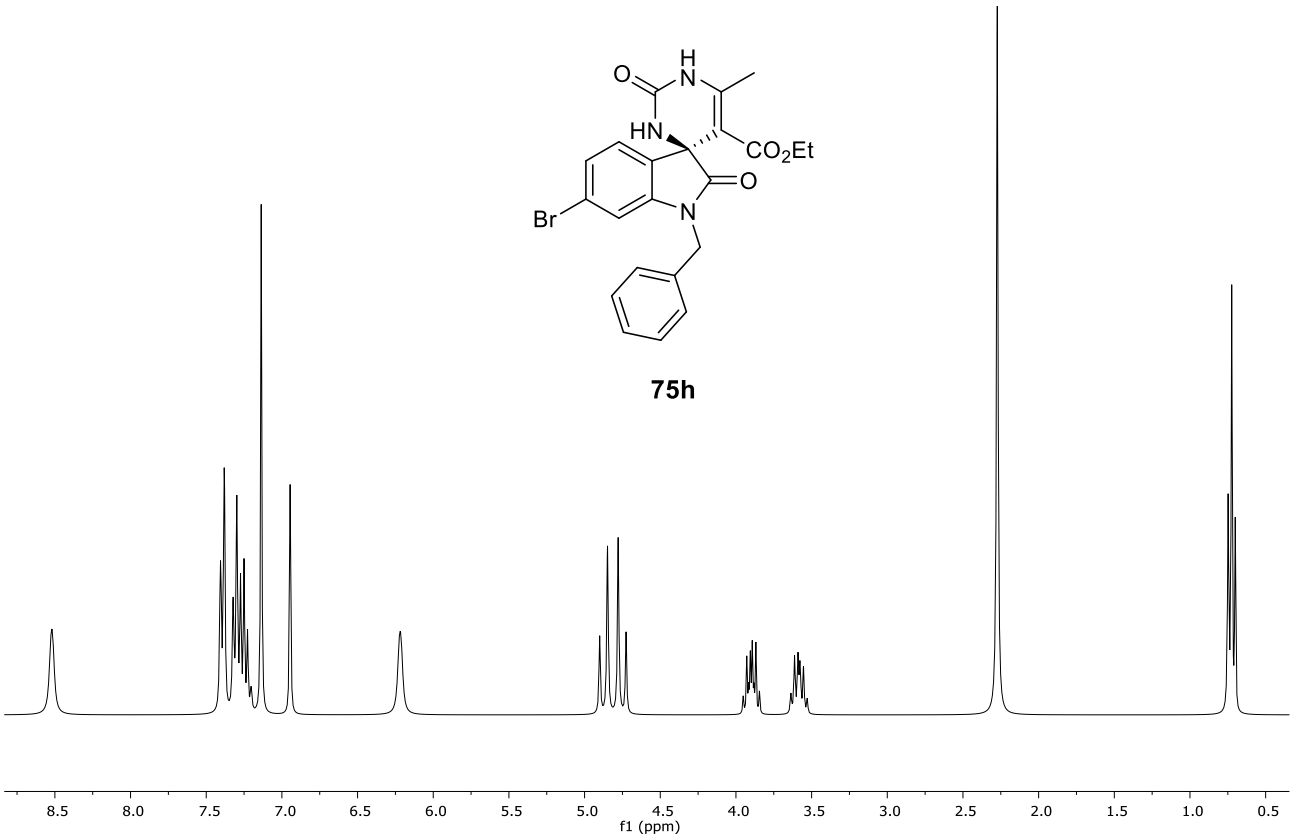

75h

Compound **75h**: ^{13}C NMR (75 MHz, $CDCl_3$)

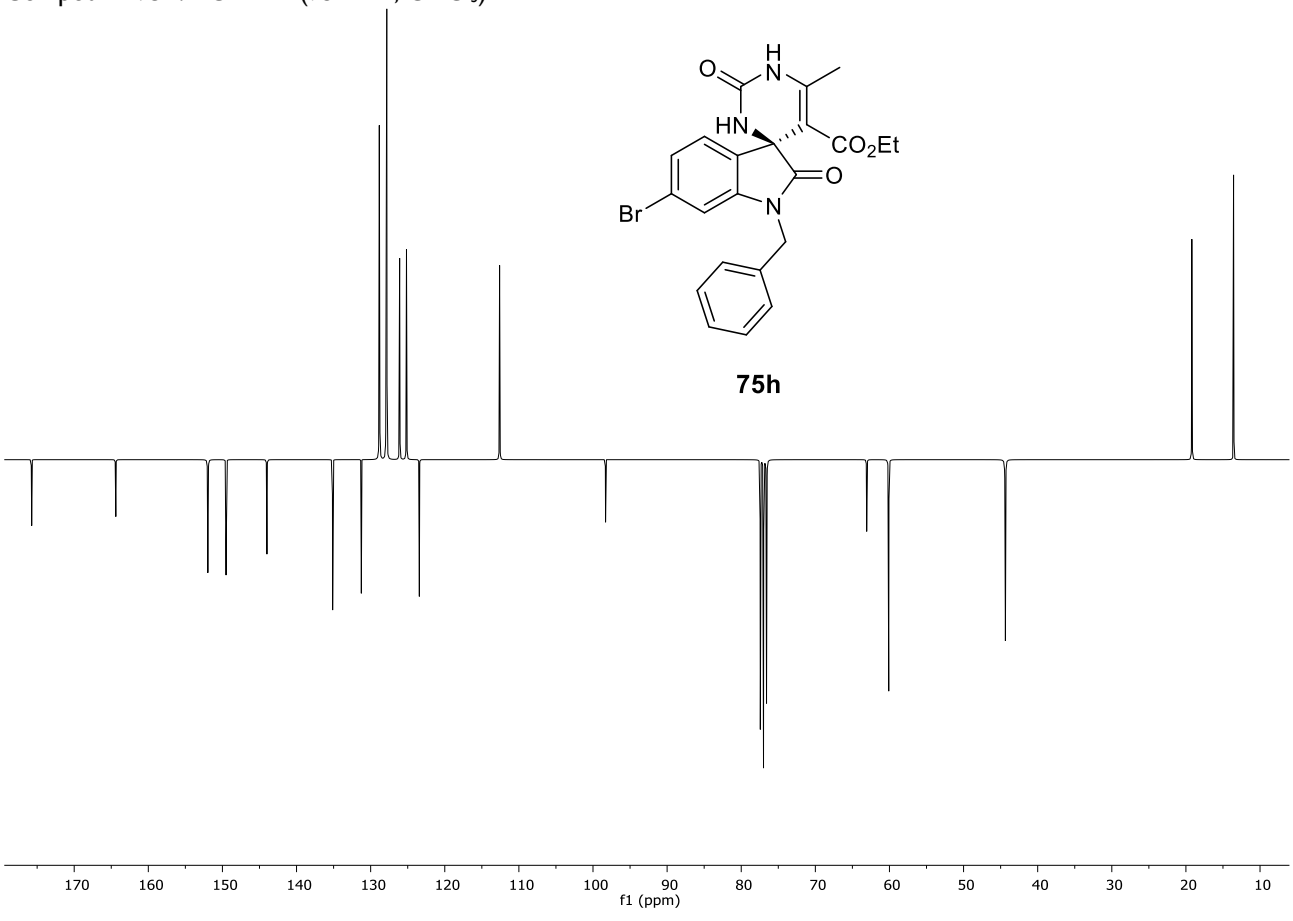

75h

Compound **75i**: ^{1}H NMR (300 MHz, $CDCl_3$)

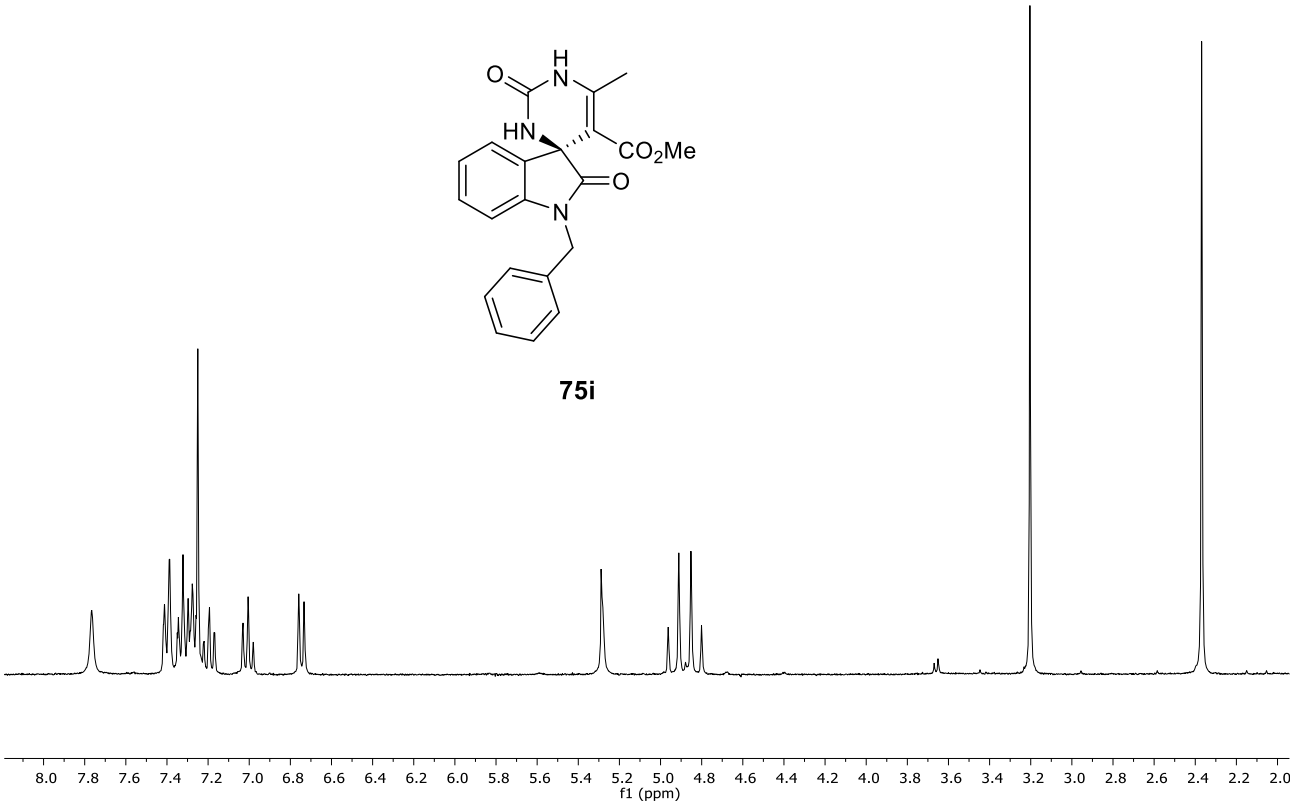

75i

Compound **75i**: ^{13}C NMR (75 MHz, $CDCl_3$)

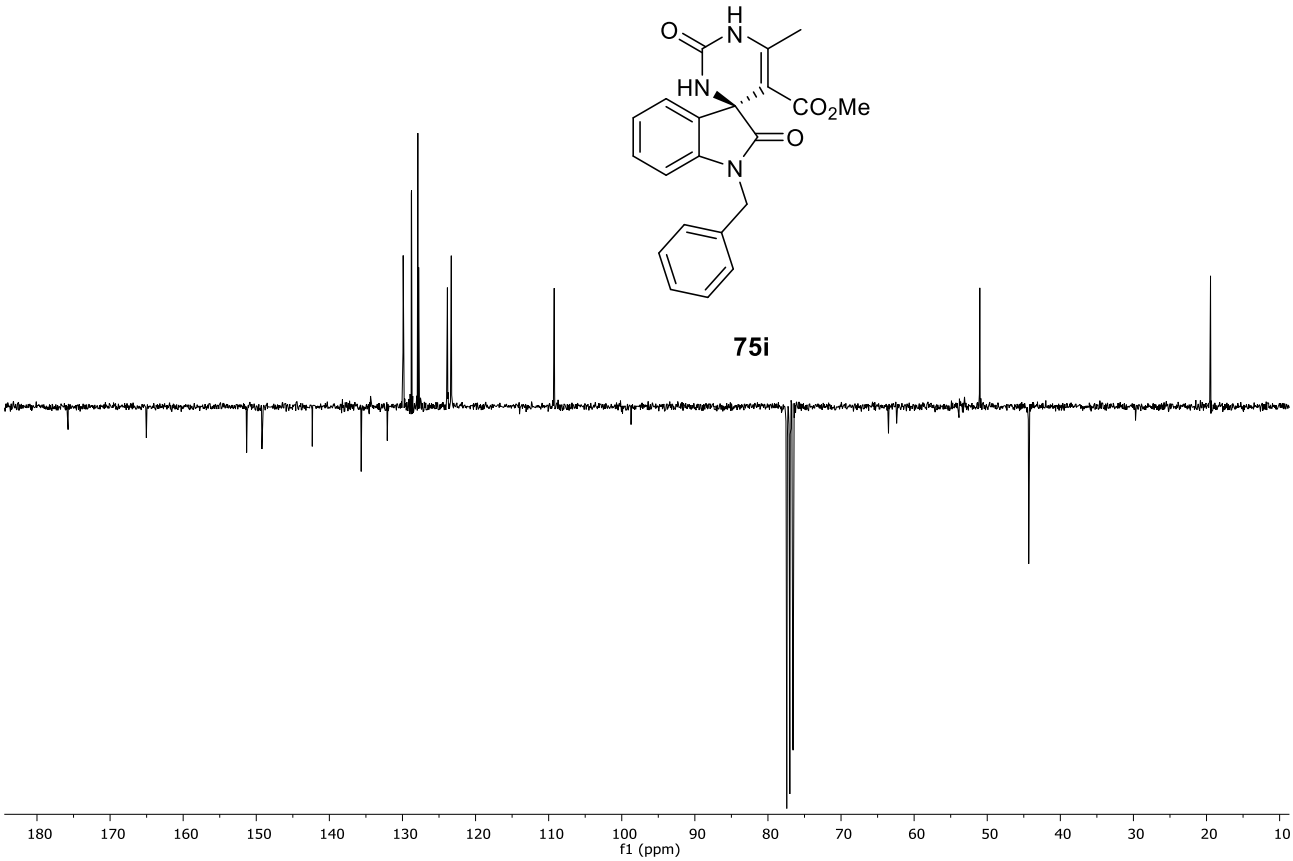

75i

Compound **75j**: ^{1}H NMR (300 MHz, $CDCl_3$)

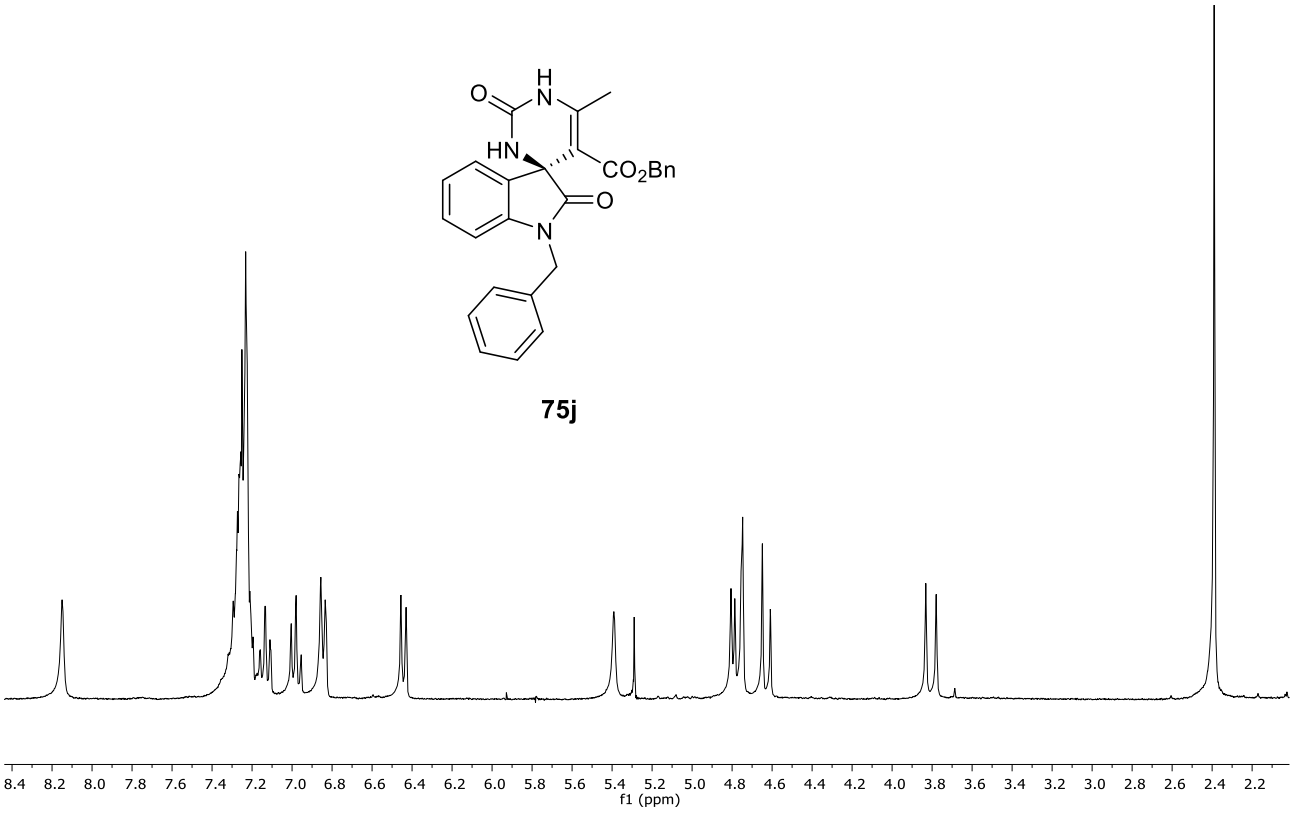

75j

Compound **75j**: ^{13}C NMR (75 MHz, $CDCl_3$)

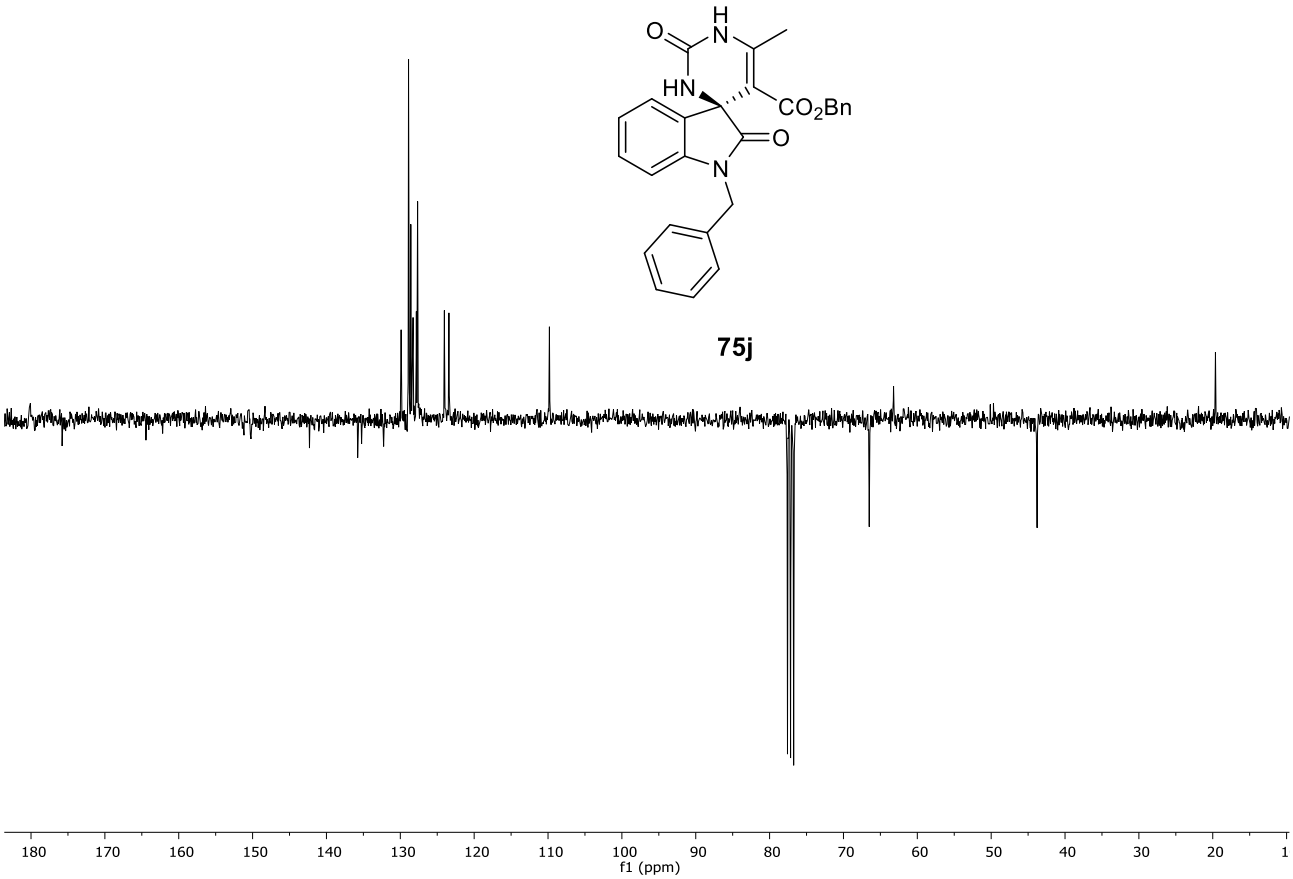

75j

Compound **76**: ^{1}H NMR (300 MHz, $CDCl_3$)

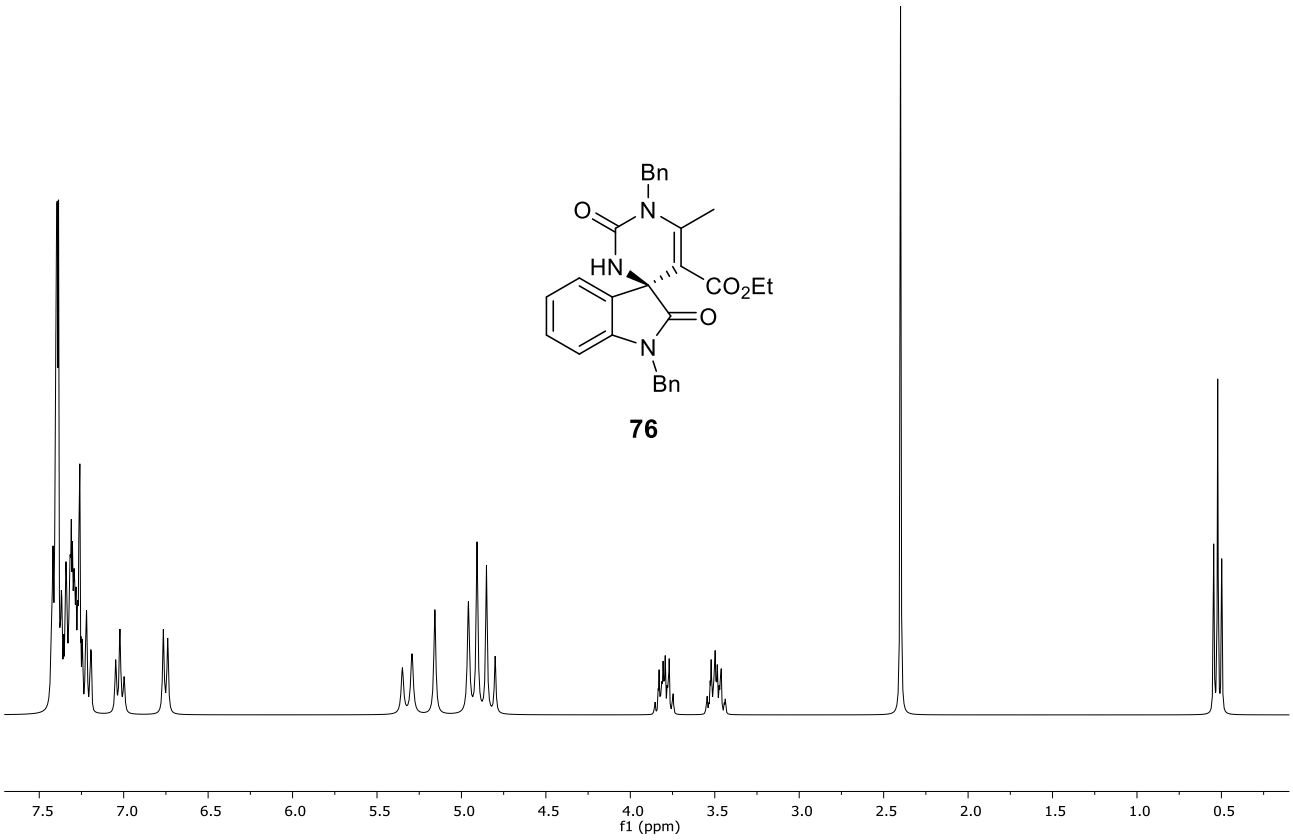

76

Compound **76**: ^{13}C NMR (75 MHz, $CDCl_3$)

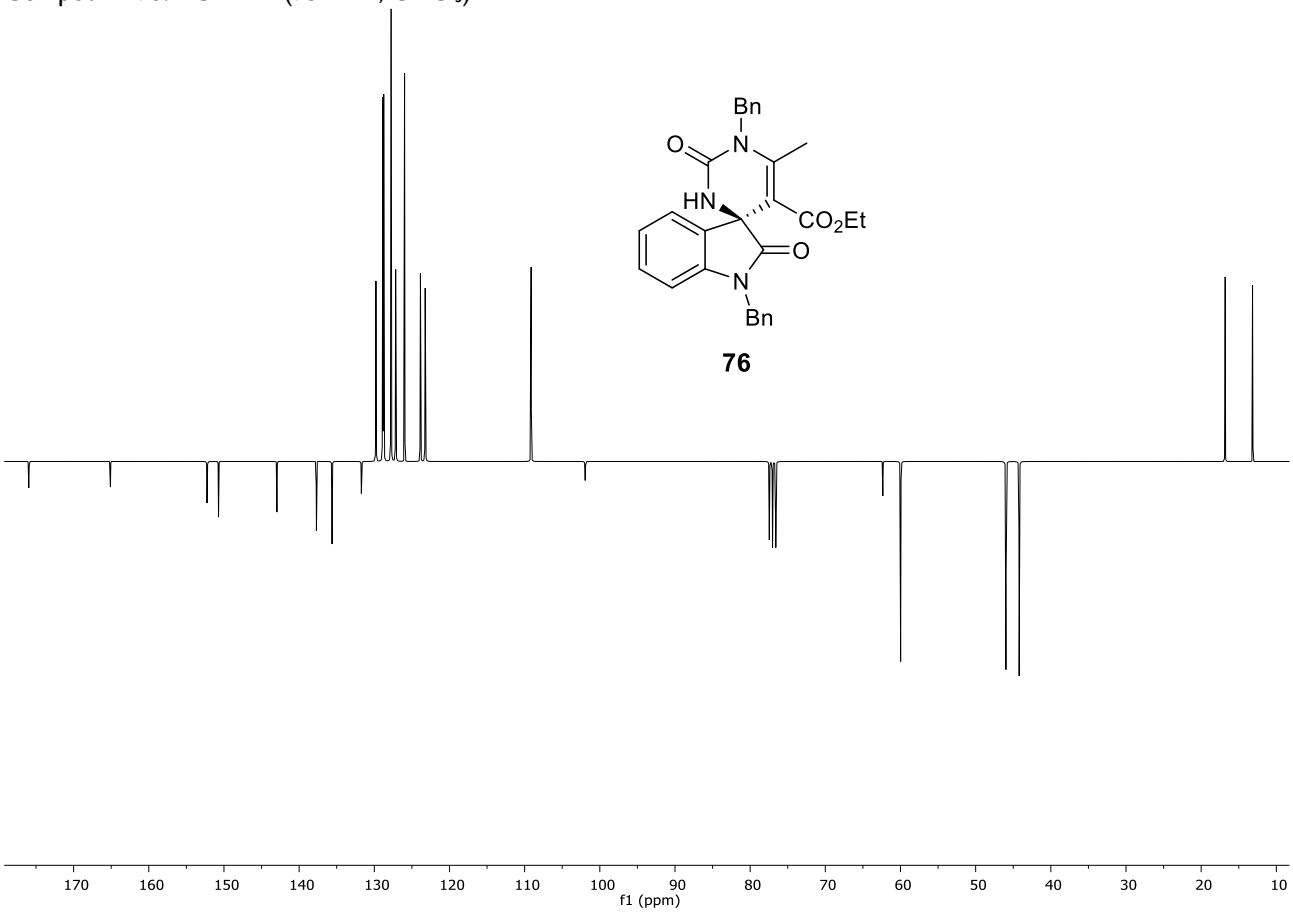

76

Compound **77**: ^{1}H NMR (300 MHz, DMSO-d_6)

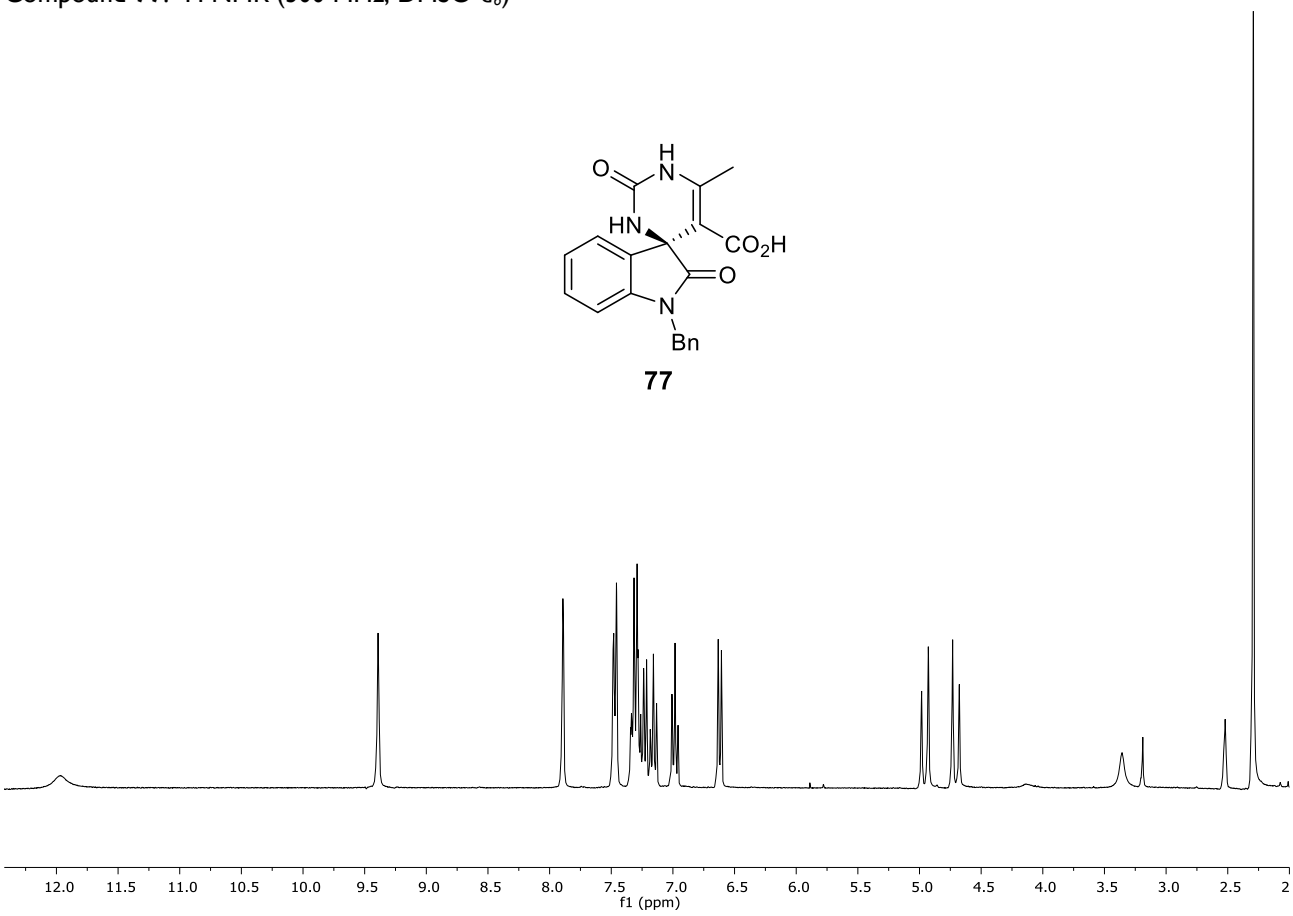

77

Compound **77**: ^{13}C NMR (75 MHz, DMSO-d_6)

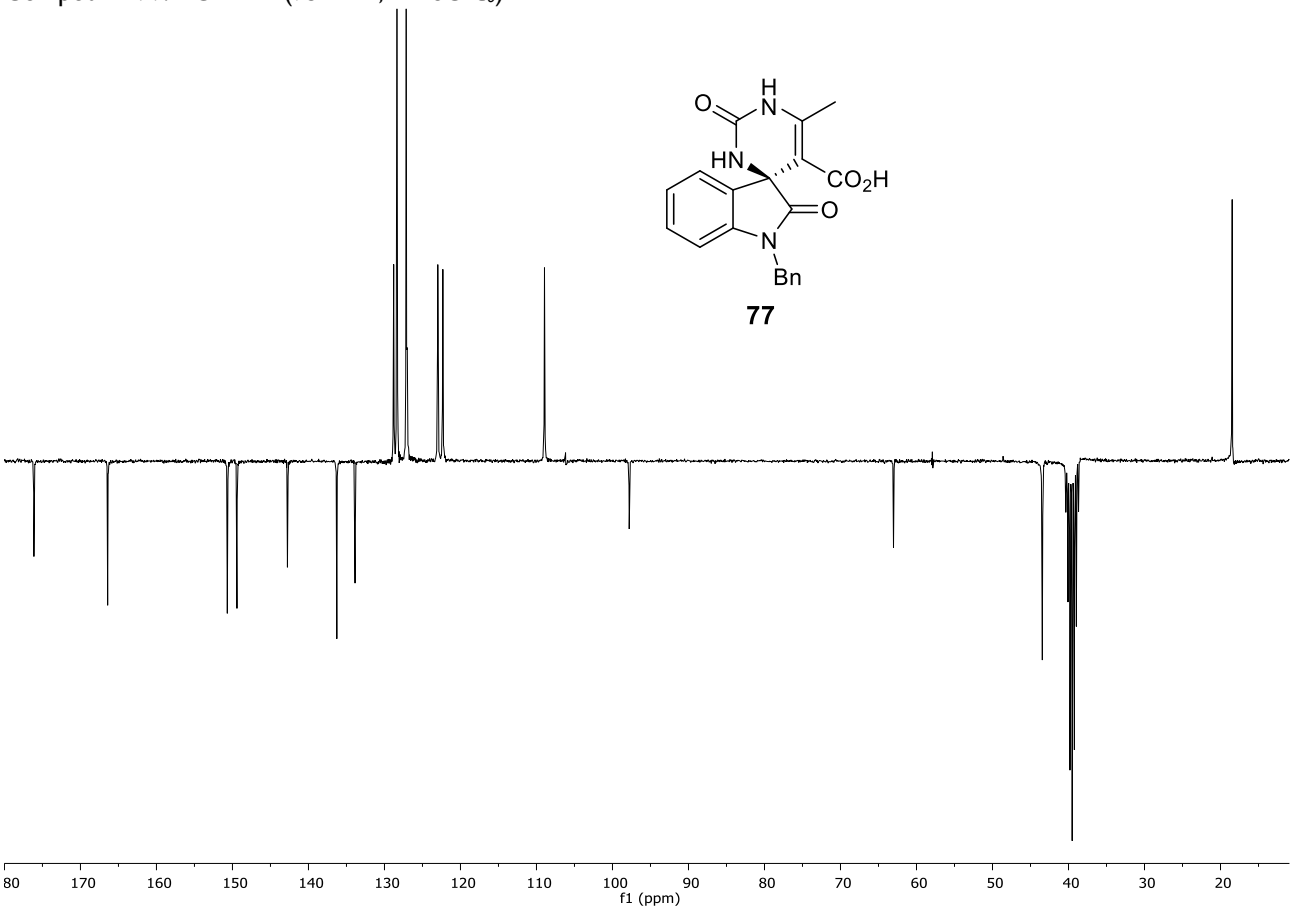

77

Compound **78**: ^{1}H NMR (400 MHz, $CDCl_3$)

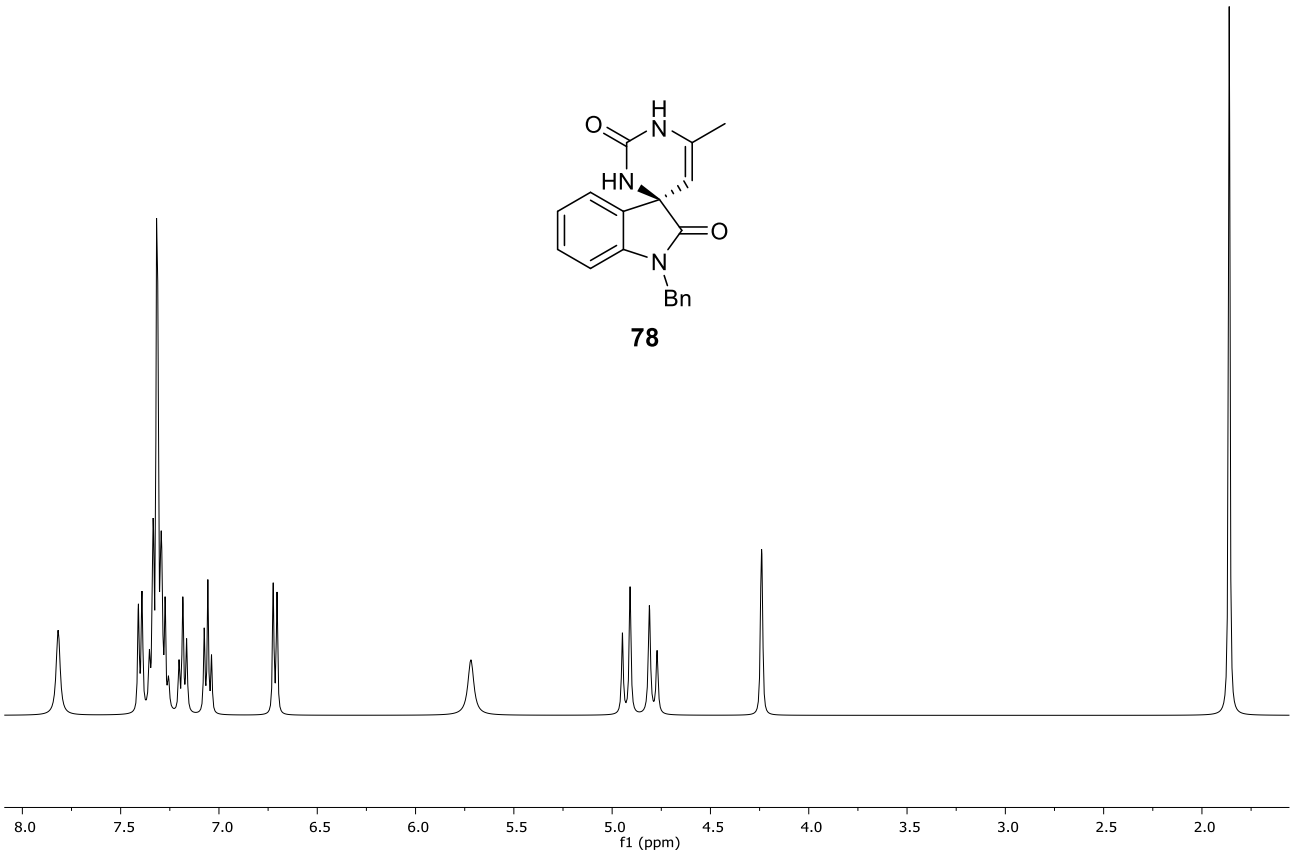

78

Compound **78**: ^{13}C NMR (100 MHz, $CDCl_3$)

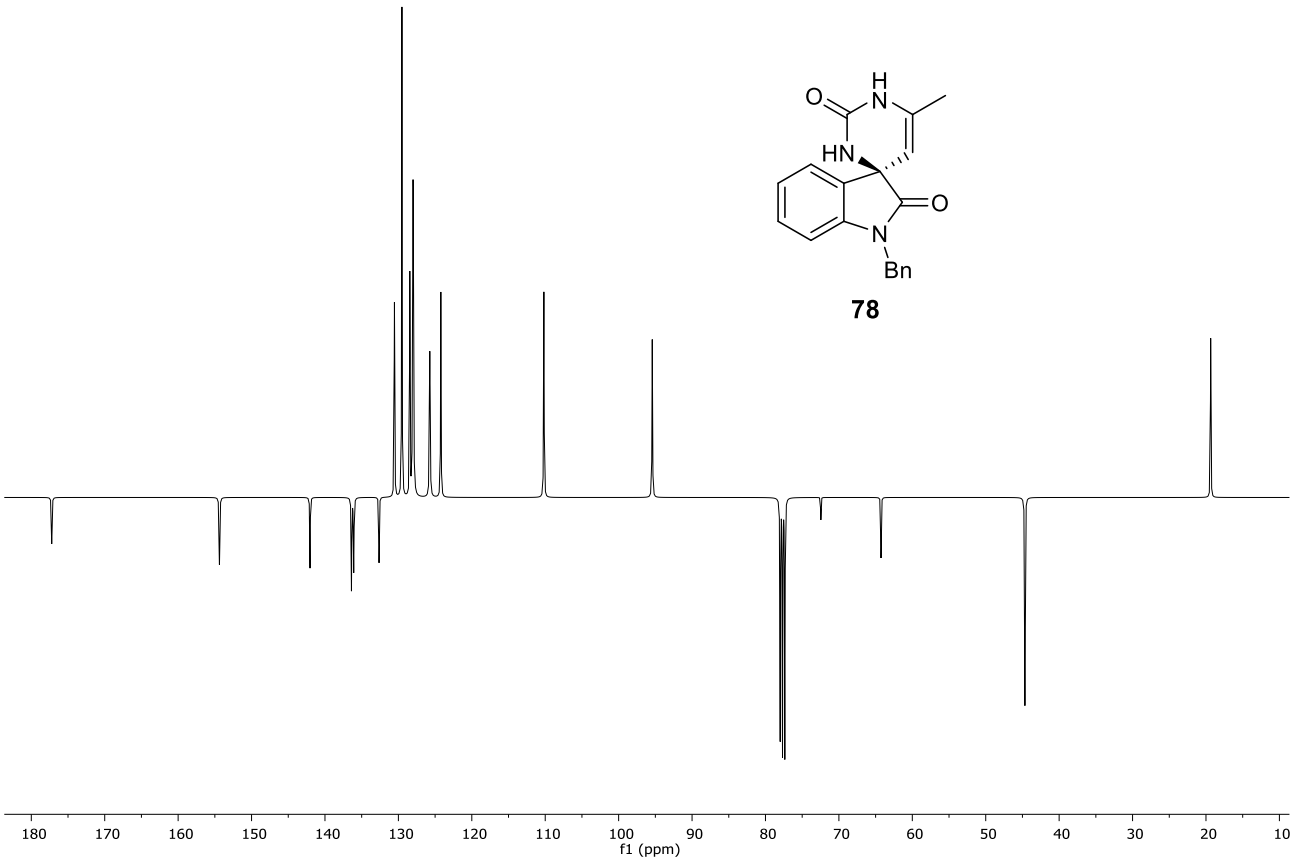

78

Compound **79a**: ^{1}H NMR (400 MHz, DMSO-d_6)

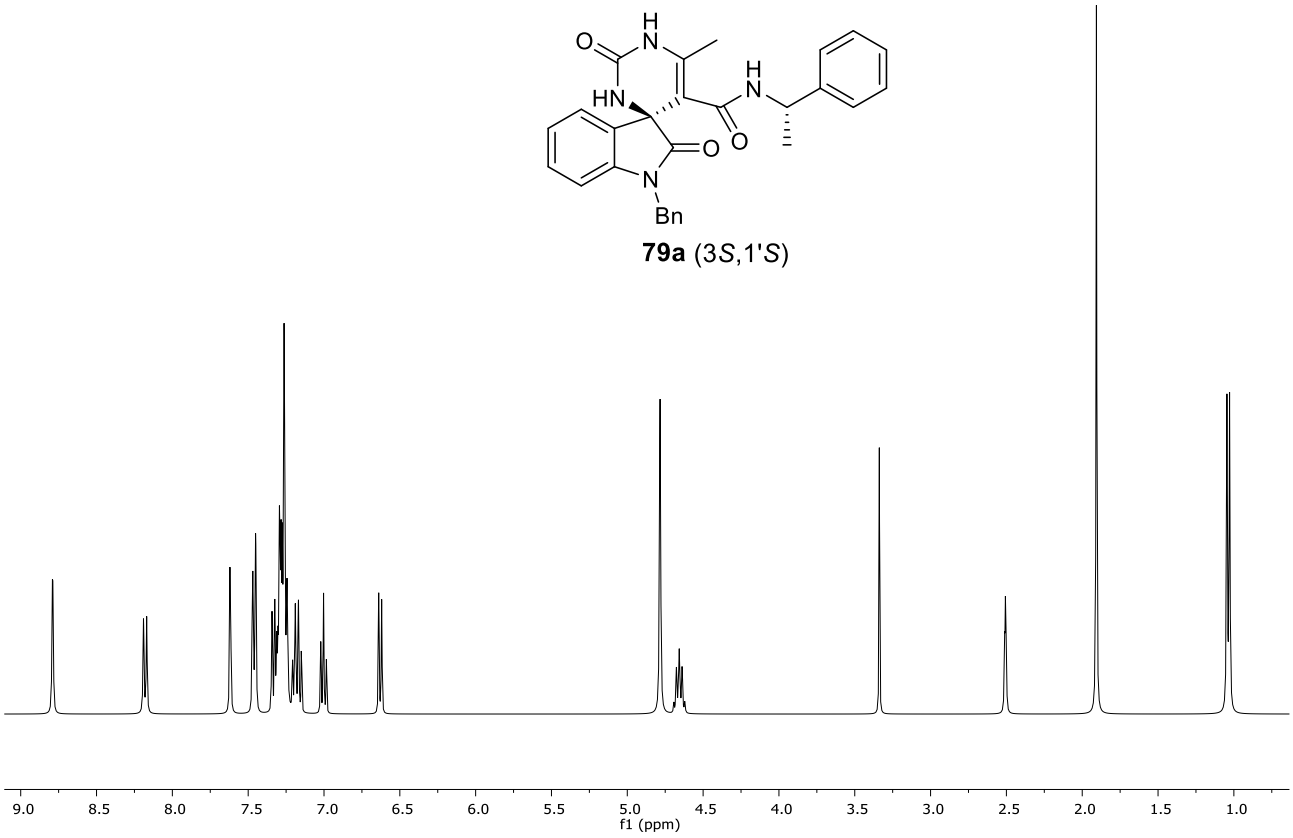

Compound **79a**: ^{13}C NMR (100 MHz, DMSO-d_6)

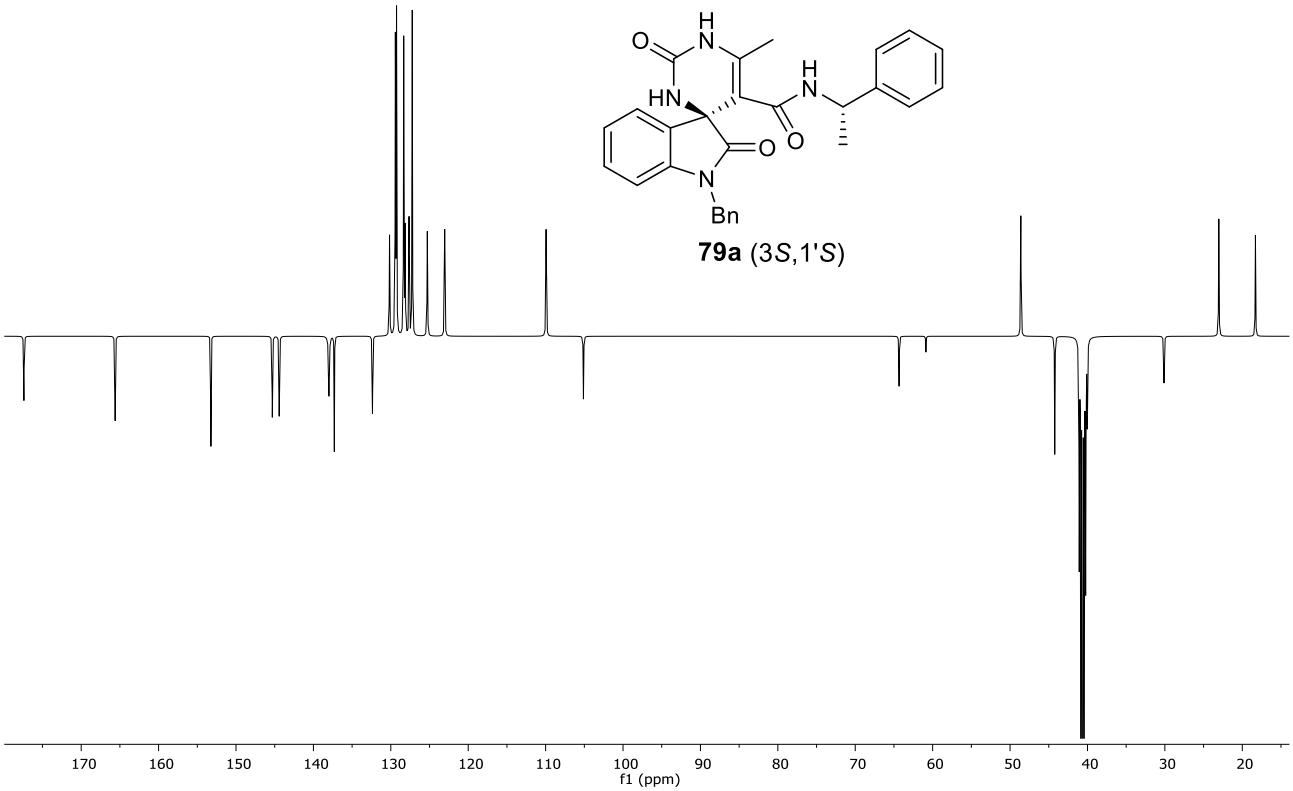

Compound **79b**: ^{1}H NMR (400 MHz, DMSO-d_6)

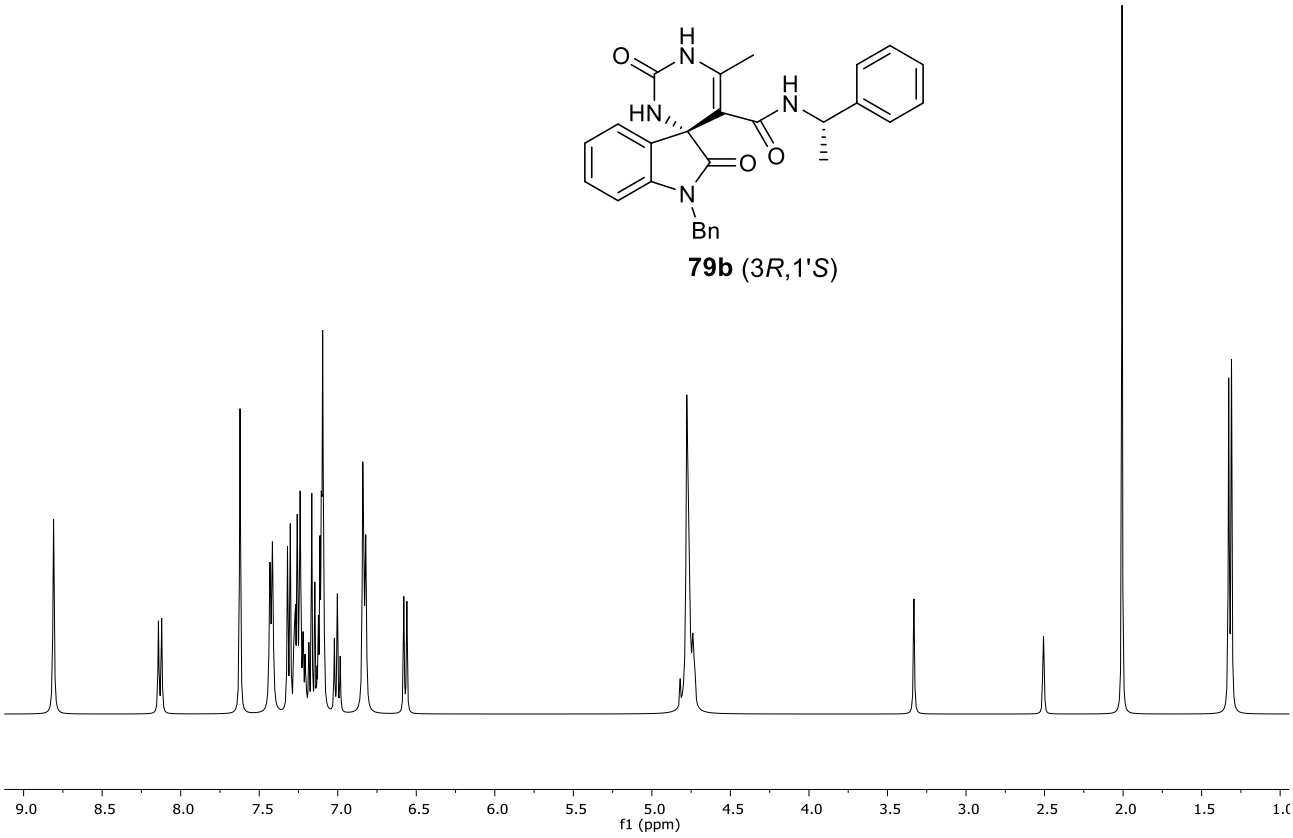

79b (3*R*,1'*S*)

Compound **79b**: ^{13}C NMR (100 MHz, DMSO-d_6)

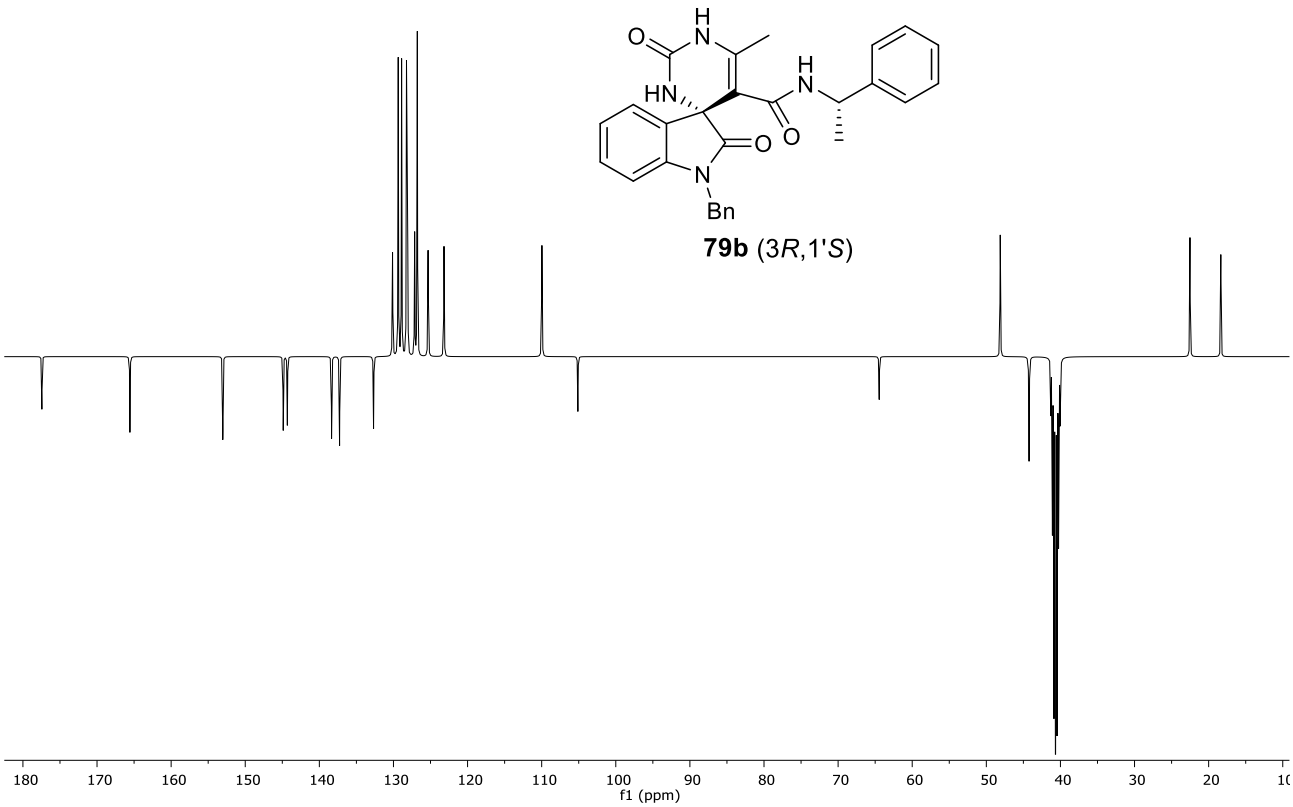

79b (3*R*,1'*S*)

A.2 COMPUTATIONAL DATA

Chapter 2.1

CONFORMATIONAL STUDIES FOR C-2(*S*) AND C-2(*R*) ISOMERS OF COMPOUND **11**:

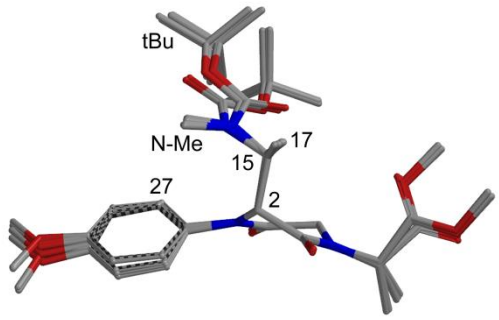

Superposition of the first 8 low-energy structures of isomer C-2(*R*) of compound **11**, calculated at B3LYP/6-31G(d) level.

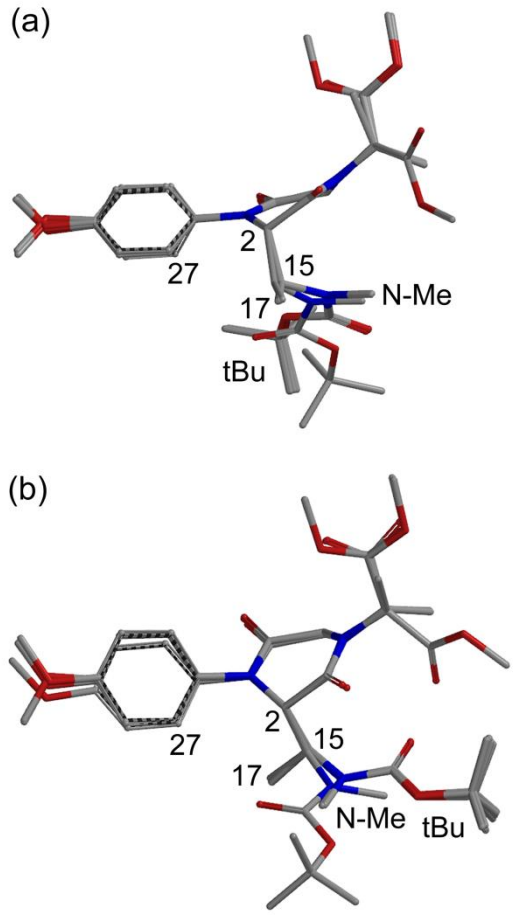

Superposition of the first 9 low-energy structures of isomer C-2(*S*) of compound **11**, calculated at B3LYP/6-31G(d) level (a, more favored; b, less favored)

EXPERIMENTAL AND THEORETICAL CD STUDIES FOR COMPOUND **11**:

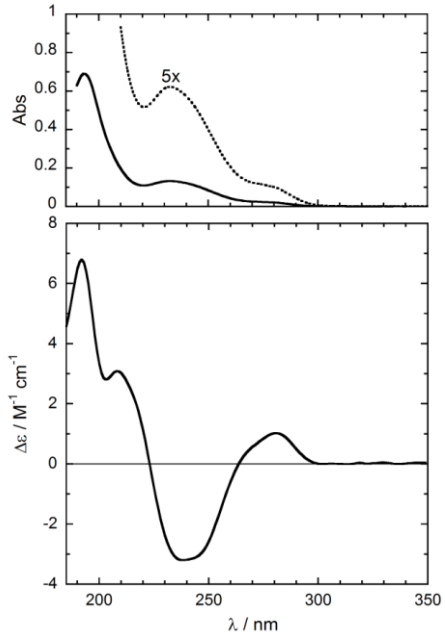

Experimental UV (top) and CD (bottom) spectra of the major diastereoisomer **11b**, measured in acetonitrile solution (2.0 mM). Cell length 0.01 cm and 0.05 cm (expansion).

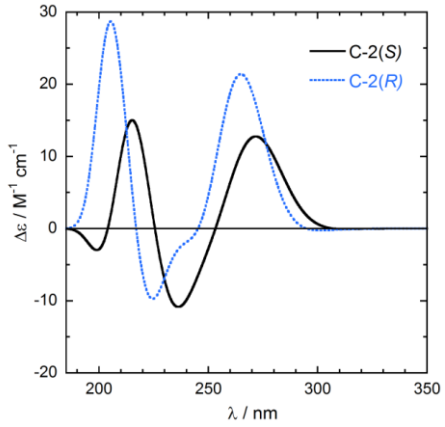

Calculated CD spectra for C-2(*S*) and C-2(*R*) isomers of **11** with CAM-B3LYP/SVP//B3LYP/6-31G(d) method. Boltzmann averages at 300K; Gaussian bandshape with 0.3 eV width; red-shift 30 nm.

Chapter 3

DOCKING STUDIES:

D_2 receptor
Compound **68**. Three clusters were originated:
Clu | Bind.energy |Dissoc. constant | Contacting receptor residues
----+----------+----------+----------
001 | 000011.2300 | 00000000005910.0000 | VAL A 91 LEU A 94 GLU A 95 PHE A 110 VAL A 111 ASP A 114 VAL A 115 CYS A 118 CYS A 182 ILE A 183 ILE A 184 VAL A 190 SER A 193 SER A 194 SER A 197 TRP A 386 PHE A 389 PHE A 390 HIS A 393 TYR A 408 THR A 412 TYR A 416
002 | 000011.0800 | 00000000007530.0000 | LEU A 41 TRP A 90 VAL A 91 LEU A 94 GLU A 95 PHE A 110 VAL A 111 ASP A 114 VAL A 115 CYS A 182 ILE A 183 ILE A 184 VAL A 190 SER A 193 SER A 194 TRP A 386 PHE A 389 PHE A 390 HIS A 393 ILE A 394 TYR A 408 SER A 409 THR A 412 TYR A 416
003 | 000009.1700 | 00000000188850.0000 | LEU A 41 VAL A 91 LEU A 94 GLU A 95 VAL A 97 GLY A 98 PHE A 110 VAL A 111 ASP A 114 VAL A 115 CYS A 182 ILE A 183 ILE A 184 PHE A 389 HIS A 393 TYR A 408 SER A 409 THR A 412 TRP A 413

Compound **70**. Five clusters were originated:
Clu | Bind.energy |Dissoc. constant | Contacting receptor residues
----+----------+----------+----------
001 | 000011.5900 | 00000000003170.0000 | LEU A 41 VAL A 91 LEU A 94 GLU A 95 PHE A 110 VAL A 111 ASP A 114 VAL A 115 CYS A 118 GLU A 181 CYS A 182 ILE A 183 ILE A 184 VAL A 190 SER A 193 SER A 194 SER A 197 TRP A 386 PHE A 389 PHE A 390 HIS A 393 TYR A 408 SER A 409 THR A 412 TRP A 413
002 | 000011.5200 | 00000000003600.0000 | VAL A 91 LEU A 94 VAL A 97 GLY A 98 PHE A 110 VAL A 111 ASP A 114 VAL A 115 CYS A 118 THR A 119 ILE A 122 GLU A 181 CYS A 182 ILE A 183 ILE A 184 VAL A 190 SER A 193 SER A 194 SER A 197 TRP A 386 PHE A 389 PHE A 390 HIS A 393 ILE A 394 TYR A 408 THR A 412 TYR A 416
003 | 000010.0900 | 00000000040030.0000 | LEU A 41 VAL A 87 VAL A 91 LEU A 94 GLU A 95 PHE A 110 VAL A 111 ASP A 114 VAL A 115 CYS A 182 ILE A 183 ILE A 184 VAL A 190 PHE A 389 HIS A 393 TYR A 408 SER A 409 THR A 412 TRP A 413 TYR A 416
004 | 000009.5400 | 00000000102030.0000 | TYR A 34 LEU A 41 VAL A 91 LEU A 94 GLU A 95 VAL A 97 GLY A 98 PHE A 110 VAL A 111 ASP A 114 VAL A 115 CYS A 182 ILE A 183 ILE A 184 PHE A 389 HIS A 393 TYR A 408 SER A 409 THR A 412 TRP A 413
005 | 000008.6100 | 00000000489850.0000 | VAL A 91 LEU A 94 GLU A 95 VAL A 97 GLY A 98 GLU A 99 TRP A 100 PHE A 110 VAL A 111 ASP A 114 VAL A 115 ASN A 180 GLU A 181 CYS A 182 ILE A 183 ILE A 184 TRP A 386 PHE A 389 TYR A 408 SER A 409 THR A 412 TYR A 416

D_3 receptor
Compound **68**. Five clusters were originated:
Clu | Bind.energy |Dissoc. constant | Contacting receptor residues
----+----------+----------+----------
001 | 000011.4600 | 00000000003990.0000 | ARG A 27 TYR A 36 VAL A 86 LEU A 89 GLU A 90 GLY A 94 PHE A 106 VAL A 107 ASP A 110 VAL A 111 CYS A 114 THR A 115 SER A 182 ILE A 183 VAL A 189 SER A 192 SER A 193 SER A 196 TRP A 342 PHE A 345 PHE A 346 HIS A 349 TYR A 365 SER A 366 THR A 369 TRP A 370 TYR A 373
002 | 000011.0500 | 00000000007980.0000 | ARG A 27 TYR A 36 VAL A 86 LEU A 89 GLU A 90 GLY A 94 PHE A 106 VAL A 107 ASP A 110 VAL A 111 CYS A 114 THR A 115 CYS A 181 SER A 182 ILE A 183 VAL A 189 SER A 192 SER A 196 TRP A 342 PHE A 345 PHE A 346 HIS A 349 TYR A 365 SER A 366 THR A 369 TRP A 370 TYR A 373
003 | 000008.8100 | 00000000345950.0000 | TYR A 36 VAL A 86 LEU A 89 GLU A 90 GLY A 94 PHE A 106 VAL A 107 ASP A 110 CYS A 181 SER A 182 ILE A 183 PHE A 345 PRO A 362 TYR A 365 SER A 366 THR A 369 TYR A 373
004 | 000008.6400 | 00000000460910.0000 | ARG A 27 TYR A 32 TYR A 36 VAL A 86 LEU A 89 GLU A 90 GLY A 93 GLY A 94 PHE A 106 VAL A 107 ASP A 110 VAL A 111 CYS A 181 SER A 182 ILE A 183 PHE A 345 HIS A 349 TYR A 365 SER A 366 THR A 369 TYR A 373
005 | 000007.8400 | 00000001800000.0000 | ARG A 27 TYR A 36 VAL A 86 LEU A 89 GLU A 90 THR A 92 GLY A 93 GLY A 94 VAL A 95 VAL A 180 CYS A 181 SER A 182 PRO A 362 TYR A 365 SER A 366 THR A 369 TYR A 373

Compound **70**. Seven clusters were originated:
Clu | Bind.energy |Dissoc. constant | Contacting receptor residues
----+----------+----------+----------
001 | 000011.0600 | 00000000007840.0000 | ARG A 27 TYR A 36 VAL A 86 LEU A 89 GLU A 90 GLY A 94 PHE A 106 VAL A 107 ASP A 110 VAL A 111 CYS A 114 THR A 115 CYS A 181 SER A 182 ILE A 183 VAL A 189 SER A 192 SER A 196 TRP A 342 PHE A 345 PHE A 346 HIS A 349 PRO A 362 TYR A 365 SER A 366 THR A 369 TYR A 373
002 | 000010.5200 | 00000000019370.0000 | ARG A 27 TYR A 36 VAL A 86 LEU A 89 GLU A 90 PHE A 106 VAL A 107 ASP A 110 VAL A 111 CYS A 114 CYS A 181 SER A 182 ILE A 183 VAL A 189 SER A 192 TRP A 342 PHE A 345 PHE A 346 HIS A 349 PRO A 362 TYR A 365 SER A 366 THR A 369 GLY A 372 TYR A 373
003 | 000009.8800 | 00000000057660.0000 | ARG A 27 TYR A 36 VAL A 82 VAL A 86 LEU A 89 GLU A 90 GLY A 94 PHE A 106 VAL A 107 ASP A 110 CYS A 181 SER A 182 ILE A 183 PHE A 345 HIS A 349 PRO A 362 TYR A 365 SER A 366 THR A 369 TYR A 373
004 | 000008.6600 | 00000000451390.0000 | ARG A 27 VAL A 86 LEU A 89 GLU A 90 GLY A 93 GLY A 94 PHE A 106 VAL A 107 ASP A 110 CYS A 181 SER A 182 ILE A 183 PHE A 345 HIS A 349 ASN A 352 VAL A 360 SER A 361 PRO A 362 TYR A 365 SER A 366 THR A 369 TYR A 373
005 | 000008.3000 | 00000000820720.0000 | ARG A 27 TYR A 36 VAL A 86 LEU A 89 GLU A 90 GLY A 94 PHE A 106 VAL A 107 ASP A 110 CYS A 181 SER A 182 PRO A 362 TYR A 365 SER A 366 THR A 369 TRP A 370 TYR A 373
006 | 000008.1400 | 00000001080000.0000 | ARG A 27 TYR A 36 VAL A 86 LEU A 89 GLU A 90 GLY A 94 VAL A 95 TRP A 96 PHE A 106 THR A 179 VAL A 180 CYS A 181 SER A 182 PRO A 362 TYR A 365 SER A 366 THR A 369 TYR A 373
007 | 000007.9100 | 00000001600000.0000 | ARG A 27 TYR A 36 VAL A 86 LEU A 89 GLU A 90 GLY A 93 GLY A 94 PHE A 106 VAL A 107 ASP A 110 CYS A 181 SER A 182 PHE A 345 VAL A 360 SER A 361 PRO A 362 GLU A 363 TYR A 365 SER A 366 THR A 369 TYR A 373

MOLECULAR DYNAMICS STUDIES:

Plots of the energy and the Cα RMSD profiles after MD simulations

D_2 receptor, compound **68**

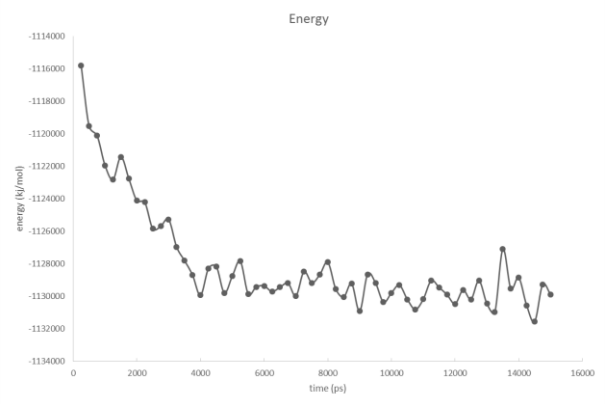

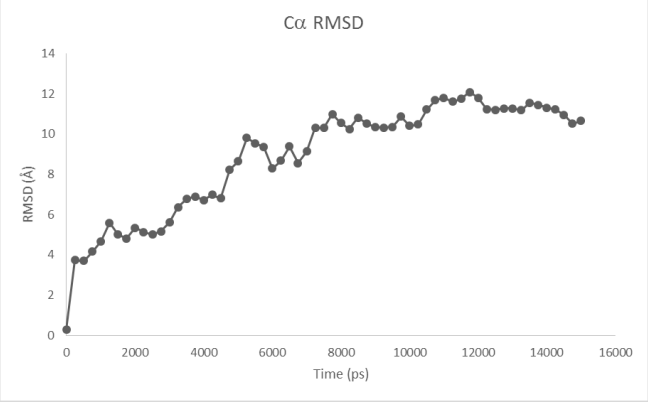

D_2 receptor, compound **70**

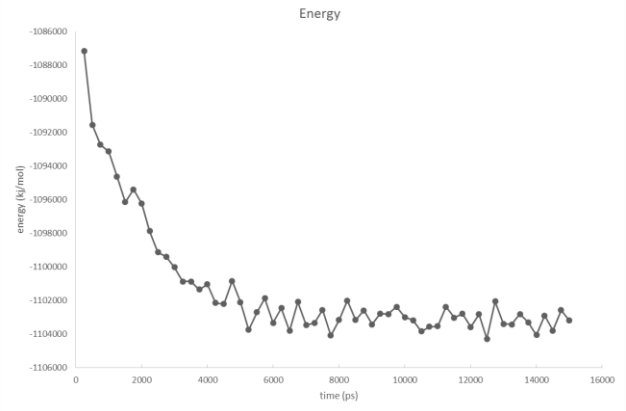

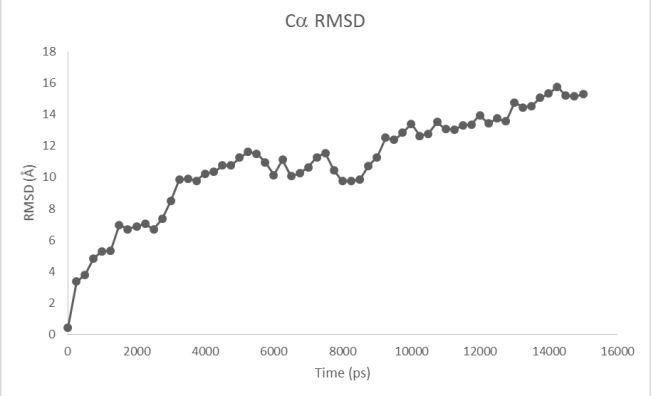

D_3 receptor, compound **68**

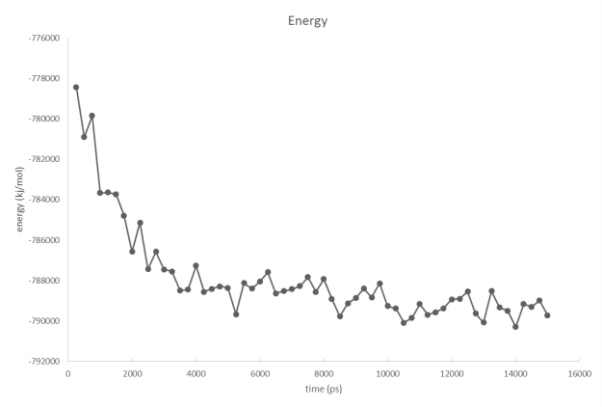

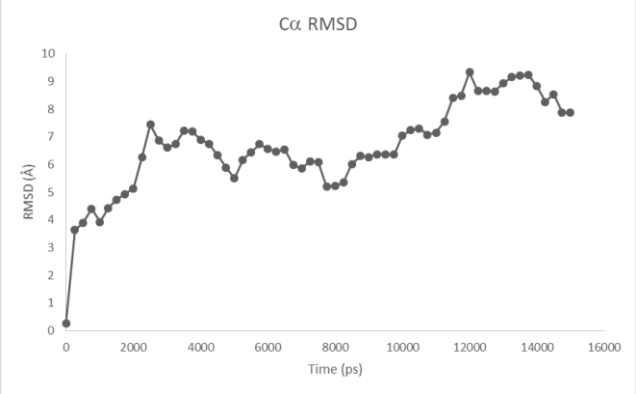

D_3 receptor, compound **70**

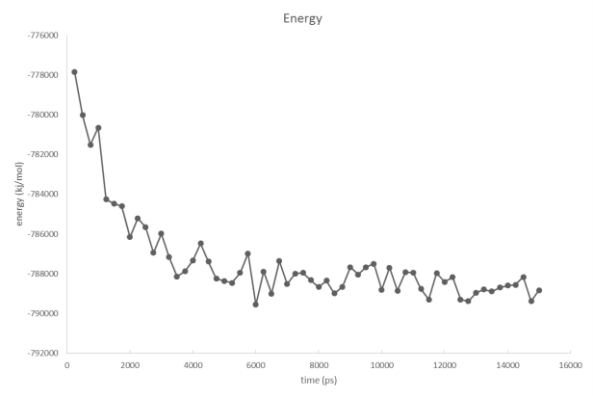

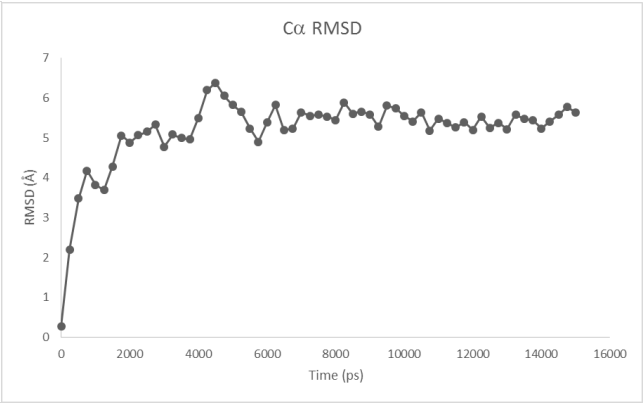

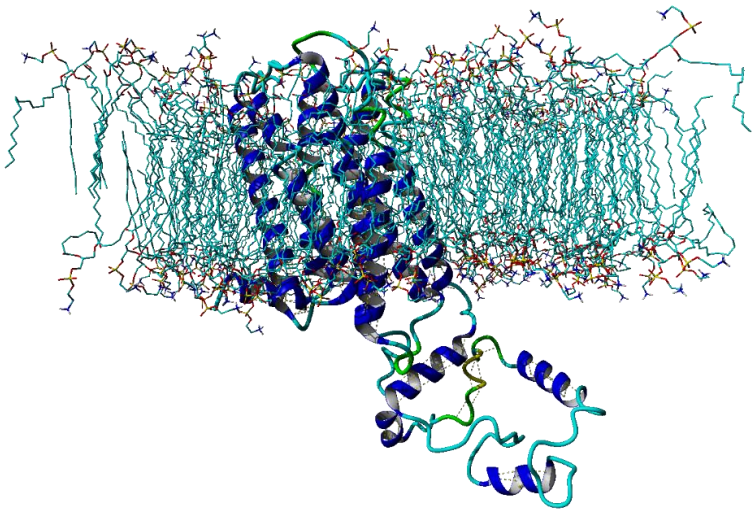

The D_3 receptor embedded in the membrane

For each compound, the lowest energy complex from MD simulations was further minimized with the same force field. The binding energy of the obtained complex was then recalculated with Autodock, giving the following results (binding energy are reported in kcal/mol):

	D_2	D_3
68	10.79	9.30
70	10.66	11.97
69	9.20	8.83
67	9.66	8.50

Chapter 4

COMPUTATIONAL DATA FOR THE TWO TRANSITION STATES **TS-A** AND **TS-B**

TS-A

Cartesian Coordinates (Angstroms)

1	C	-1.8892290	1.7792323	-1.5767275
2	O	-1.9099040	1.3892922	-2.7191745
3	N	-1.8670942	0.8156962	-0.4775048
4	N	-1.7997383	3.0374635	-1.1551571
5	H	-1.8329944	3.7591594	-1.8424761
6	C	-2.8887838	0.3864052	0.2242179
7	H	-1.8601058	3.2953184	-0.1879628
8	C	-3.7709850	2.9042266	1.6067527
9	O	-3.1609968	3.8602303	1.1563790
10	C	-3.2091039	1.6255850	2.0134133
11	H	-3.8742699	0.9906672	2.5626707
12	C	-1.8407773	1.5213665	2.3481786
13	O	-0.9227088	2.2404134	1.9121698
14	H	0.4863183	1.7950655	2.0951394
15	P	1.4975814	0.2367059	0.9733152
16	O	1.3669767	1.2612068	2.0681876
17	O	0.2479051	-0.4901086	0.6081588
18	H	-0.9758390	0.3497510	-0.2809162
19	O	2.1653719	0.9088527	-0.3736185
20	O	2.6414851	-0.8479806	1.4436987
21	C	3.4793745	1.3088645	-0.3576033
22	C	4.4738249	0.3086206	-0.2823161
23	C	3.1983978	-1.6886087	0.5133777
24	C	4.0725981	-1.1197153	-0.4370685
25	C	-4.2780130	0.5947345	-0.3961390
26	C	-3.0154971	-1.0312558	0.7574272
27	C	-4.2921838	-1.5182674	0.4423307
28	N	-5.0334024	-0.5492690	-0.2446699
29	O	-4.6133988	1.6393854	-0.9376629
30	C	-2.1673153	-1.7862926	1.5266990
31	H	-1.2207507	-1.3750714	1.8490764
32	C	-4.7100993	-2.7861951	0.8235505
33	H	-5.6879970	-3.1665981	0.5615406
34	C	-3.8307415	-3.5657177	1.5757999
35	H	-4.1205165	-4.5590134	1.9018997
36	C	-2.5742873	-3.0601655	1.9366622
37	H	-1.8956681	-3.6388924	2.5545045
38	C	5.8342864	0.6978946	-0.0802179
39	C	8.5129522	1.5604550	0.2967438
40	C	6.8911152	-0.2143039	0.1667434
41	C	6.1640407	2.0721529	-0.1116004
42	C	7.4954572	2.4852979	0.0701582
43	C	8.2099514	0.2079731	0.3489551
44	H	6.6817561	-1.2798169	0.2398993
45	H	7.7431242	3.5439276	0.0479613
46	H	8.9877252	-0.5243496	0.5420936
47	H	9.5330454	1.8993094	0.4457855
48	C	4.5437699	-1.9320065	-1.5135754
49	C	5.4680070	-3.6287121	-3.5944840
50	C	5.3031687	-1.4400799	-2.6050714
51	C	4.2340124	-3.3109904	-1.5143331
52	C	4.7062501	-4.1417559	-2.5464417
53	C	5.7631133	-2.2740067	-3.6269537
54	H	5.5255190	-0.3769109	-2.6752246

55	H	4.4645000	-5.2019210	-2.5444193
56	H	6.3381735	-1.8544694	-4.4469483
57	H	5.8118327	-4.2829236	-4.3890750
58	C	5.1588047	3.0237323	-0.3321751
59	H	5.4179786	4.0802784	-0.3710943
60	C	3.8051627	2.6697086	-0.4665060
61	C	3.4540664	-3.8507178	-0.4800880
62	H	3.2499474	-4.9194626	-0.4777129
63	C	2.9099878	-3.0617260	0.5497967
64	O	-5.1412978	2.9330513	1.7698927
65	C	-5.7432007	4.1226198	1.2662198
66	H	-5.4055789	4.9856495	1.8509770
67	H	-5.4824488	4.2647568	0.2110771
68	C	-7.2477355	3.9792765	1.3956200
69	H	-7.5316728	3.8199695	2.4411385
70	H	-7.6010397	3.1084330	0.8332650
71	H	-7.7582750	4.8715805	1.0227852
72	C	-6.3766433	-0.6868792	-0.7254693
73	H	-6.7656873	0.2972868	-1.0136476
74	H	-6.9933618	-1.0380766	0.1109966
75	C	-6.5269602	-1.6097703	-1.9173111
76	C	-6.8707722	-3.2846897	-4.1475700
77	C	-7.6550348	-2.4386889	-2.0237025
78	C	-5.5859495	-1.6181359	-2.9581544
79	C	-5.7534122	-2.4569667	-4.0612412
80	C	-7.8235570	-3.2737747	-3.1306456
81	H	-8.4077628	-2.4395499	-1.2392114
82	H	-4.7037959	-0.9770918	-2.9132388
83	H	-5.0013630	-2.4588944	-4.8463577
84	H	-8.6970461	-3.9157459	-3.1982489
85	H	-6.9952060	-3.9362139	-5.0073081
86	C	2.8220668	3.7321524	-0.7484350
87	C	0.9717824	5.7944104	-1.3024426
88	C	1.7749504	4.0195656	0.1306942
89	C	2.9250739	4.5118245	-1.9166716
90	C	2.0108093	5.5346751	-2.1918748
91	C	0.8536133	5.0338770	-0.1432627
92	H	1.6361609	3.4270533	1.0355368
93	H	3.7133796	4.2998394	-2.6335296
94	H	2.0968038	6.1062277	-3.1094513
95	H	0.0254164	5.1770840	0.5488882
96	H	0.2360398	6.5617198	-1.5162299
97	C	2.1153528	-3.7103866	1.6189545
98	C	0.6846913	-5.0485907	3.6602892
99	C	1.1306233	-4.6683358	1.3159208
100	C	2.3450200	-3.4301366	2.9761523
101	C	1.6350548	-4.0860581	3.9866031
102	C	0.4307720	-5.3397840	2.3233169
103	H	0.8758818	-4.8681635	0.2774993
104	H	3.0676500	-2.6656681	3.2563595
105	H	1.8105637	-3.8136696	5.0228883
106	H	-0.3401559	-6.0546744	2.0549799
107	H	0.1164804	-5.5370571	4.4446620
108	C	-1.5317760	0.6815223	3.6474475
109	H	-1.4319744	1.3617462	4.4996729
110	H	-0.6086860	0.1059486	3.5385628
111	H	-2.3522032	-0.0098574	3.8568810

Translational Enthalpy: 0.889 kcal/mol
Rotational Enthalpy: 0.889 kcal/mol
Vibrational Enthalpy: 583.960 kcal/mol

gas constant (RT): 0.593 kcal/mol
Translational Entropy: 46.298 cal/mol.K
Rotational Entropy: 40.660 cal/mol.K
Vibrational Entropy: 195.074 cal/mol.K
Total Enthalpy: 586.330 kcal/mol
Total Entropy: 282.033 cal/mol.K

TS-B

1	C	-2.426682	-2.408128	0.707203
2	O	-3.554436	-2.830458	0.852490
3	N	-2.185059	-1.004436	0.593342
4	N	-1.288257	-3.099359	0.628425
5	H	-1.327048	-4.093185	0.674452
6	C	-3.153860	-0.135645	0.711594
7	H	-0.408886	-2.619520	0.535719
8	C	-4.165168	1.946489	2.195336
9	O	-3.821716	2.625795	1.235846
10	C	-3.401378	0.875460	2.794472
11	H	-3.918982	0.255830	3.500374
12	C	-2.012392	0.884222	2.876246
13	O	-1.212344	1.591040	2.204959
14	H	0.126850	1.342882	2.228921
15	P	1.546666	0.031600	0.982235
16	O	0.496477	-0.902764	0.476545
17	H	-1.206230	-0.722114	0.483098
18	O	1.126355	0.956156	2.132304
19	O	2.706239	-0.816709	1.303235
20	O	2.189006	1.047592	-0.308464
21	C	3.595844	-1.466715	0.439669
22	C	4.354521	-0.760966	-0.406247
23	C	4.528990	0.671834	-0.319761
24	C	3.504398	1.526216	-0.398939
25	C	5.837748	1.249351	-0.113883
26	C	8.401498	2.449992	0.236915
27	C	7.001656	0.490350	0.179537
28	C	6.013582	2.656493	-0.190085
29	C	7.283583	3.235531	-0.027025
30	C	8.259666	1.076059	0.347346
31	H	6.942713	-0.590977	0.291515
32	H	7.409665	4.314456	-0.093823
33	H	9.122210	0.452142	0.566260
34	H	9.375933	2.912276	0.366790
35	C	3.557890	-2.883824	0.486613
36	C	4.295254	-3.586254	-0.469132
37	C	3.631238	2.929473	-0.504365
38	C	4.909892	3.476290	-0.421681
39	H	5.030562	4.556085	-0.486406
40	C	5.002461	-1.496106	-1.473696
41	C	4.984913	-2.912579	-1.473282
42	H	4.299201	-4.674797	-0.448370
43	C	5.644195	-3.647745	-2.474084
44	C	6.309328	-3.006554	-3.514089
45	C	6.317096	-1.622587	-3.566502
46	H	6.819991	-1.107247	-4.380631
47	C	5.672973	-0.885760	-2.568432
48	H	5.695399	0.198536	-2.666319
49	H	6.808269	-3.586876	-4.285012
50	H	5.633518	-4.735832	-2.457085
51	C	2.462864	3.808408	-0.686721
52	C	0.192292	5.427274	-1.078931
53	C	2.267741	4.496149	-1.895764

54	C	1.504259	3.964903	0.326685
55	C	0.372538	4.759033	0.129361
56	C	1.141996	5.301216	-2.090224
57	H	2.988903	4.391708	-2.703551
58	H	1.624319	3.452219	1.279315
59	H	-0.371820	4.841755	0.918157
60	H	1.001673	5.819184	-3.034989
61	H	-0.692642	6.038967	-1.231701
62	C	2.757054	-3.630792	1.482903
63	C	1.239225	-5.070561	3.378605
64	C	1.878223	-4.654968	1.085895
65	C	2.858856	-3.354550	2.856871
66	C	2.103031	-4.061919	3.795586
67	C	1.129445	-5.371349	2.024132
68	H	1.764966	-4.898763	0.031210
69	H	3.536404	-2.578644	3.209570
70	H	2.194679	-3.824237	4.852239
71	H	0.460705	-6.162581	1.696043
72	H	0.654687	-5.622361	4.109816
73	C	-4.608044	-0.599708	0.539093
74	N	-5.162966	-0.142531	-0.634260
75	C	-4.235505	0.644936	-1.295115
76	C	-2.037330	2.120095	-2.186888
77	C	-3.040757	0.714311	-0.560879
78	C	-4.327822	1.321254	-2.496849
79	C	-3.220895	2.058538	-2.942552
80	C	-1.937501	1.438165	-0.976049
81	H	-5.227356	1.287060	-3.099780
82	H	-3.279045	2.597228	-3.885825
83	H	-1.043714	1.504914	-0.368927
84	H	-1.195389	2.711772	-2.540478
85	C	-6.545504	-0.305145	-1.022866
86	H	-6.977515	0.671626	-1.275931
87	H	-7.142017	-0.682693	-0.181445
88	C	-6.710103	-1.274247	-2.174662
89	C	-7.068131	-3.084759	-4.291845
90	C	-7.433437	-0.902780	-3.318630
91	C	-6.182343	-2.573173	-2.102974
92	C	-6.357044	-3.470473	-3.157649
93	C	-7.607634	-1.802591	-4.372090
94	H	-7.866881	0.091476	-3.399409
95	H	-5.626142	-2.892673	-1.222553
96	H	-5.937132	-4.470703	-3.091143
97	H	-8.166178	-1.504110	-5.255571
98	H	-7.203527	-3.784787	-5.112022
99	C	-1.373461	-0.135542	3.779410
100	H	-0.948741	-0.942938	3.177619
101	H	-2.100332	-0.560725	4.476253
102	H	-0.576946	0.334877	4.362288
103	O	-5.388492	2.091435	2.791034
104	C	-6.213082	3.100195	2.200936
105	H	-6.387711	2.867468	1.144200
106	H	-5.724841	4.077097	2.289937
107	C	-7.536482	3.121191	2.940773
108	H	-8.028303	2.144785	2.878060
109	H	-8.204278	3.880468	2.524348
110	H	-7.380633	3.331673	4.004014
111	O	-5.267656	-1.086902	1.451423

Translational Enthalpy: 0.889 kcal/mol
Rotational Enthalpy: 0.889 kcal/mol

Vibrational Enthalpy: 583.225 kcal/mol
gas constant (RT): 0.593 kcal/mol
Translational Entropy: 46.298 cal/mol.K
Rotational Entropy: 40.707 cal/mol.K
Vibrational Entropy: 185.822 cal/mol.K
Total Enthalpy: 585.595 kcal/mol
Total Entropy: 272.827 cal/mol.K

A.3 BIOLOGICAL DATA

Chapter 2.1

Biological evaluation (cytotoxicities of compounds **11-14**, **19-22** and **23-26**). IC_{50} values in Huh7 and Mahlavu cell lines. Non growth inhibition for compounds **11-13**, **19-22**, **23**, **24**, **25a** and **26**.

Compound	**Huh7**			**MV**		
	IC_{50}(µM)	**R2**	**s.d**	**IC_{50}(µM)**	**R2**	**s.d**
14	15,2	1,0	1,8	11,3	0,9	0,4
25b	16,2	0,9	1,1	30,5	0,8	3,7

Chapter 3

Radioligand binding data for the compounds **38-72** employing the human D_{2L} and D_3 receptors

	K_i ± (SD) [nM][a]				
compd	[^{3}H]spiperone		compd	[^{3}H]spiperone	
	hD_{2L}	hD_3		hD_{2L}	hD_3
38	69000 ± 45000	75000 ± 4200	**57**	60000 ± 2000	82000 ± 18000
39	24000 ± 7800	100000 ± 0	**58**	91000 ± 13000	100000 ± 0
40	44000 ± 17000	72000 ± 29000	**59**	3400 ± 750	2600 ± 0
41	44000 ± 17000	72000 ± 29000	**60**	28000 ± 8500	49000 ± 20000[b]
42	100000 ± 0	87000 ± 8100	**61**	19000 ± 5500	35000 ± 19000
43	11000 ± 0	6600 ± 2300	**62**	33000 ± 1000	48000 ± 3000
44	100000 ± 0	100000 ± 0	**63**	36000 ± 22000	6500 ± 300
45	7500 ± 990	18000 ± 0	**64**	2800 ± 800	4200 ± 150
46	920 ± 49	2300 ± 730	**65**	60000 ± 40000	8000 ± 3100
47	4000 ± 2500	4300 ± 1600	**66**	4200 ± 2500	2600 ± 450
48	5200 ± 1800	1800 ± 640	**67**	430 ± 160	620 ± 65
49	520 ± 150	1300 ± 0	**68**	53 ± 11	200 ± 18
50	220 ± 32	600 ± 100	**69**	120 ± 15	280 ± 38
51	4100 ± 990	4600 ± 570	**70**	58 ± 6.7	89 ± 3.8
52	920 ± 680	930 ± 28	**71**		
53	68000 ± 8000	100000 ± 0	**71**	14000 ± 3000	5600 ± 1000
54	14000 ± 4400	5600 ± 950	**72**	16000 ± 10000	4500 ± 500
55	42000 ± 3000	100000 ± 0	haloperidol	0.96 ± 0.15	6.8 ± 1.3
56	4500 ± 1800	3300 ± 300			

[a] K_i values in nM ± standard deviation (SD) derived from two individual experiments each performed in triplicate. [b] K_i values in nM ± standard error of mean (SEM) derived from 3 individual experiments each performed in triplicate.